U.S. Department
of Commerce

Volume 90
Number 1
January 1992

Fishery Bulletin

U.S. Department of Commerce
Barbara Hackman Franklin
Secretary

National Oceanic and Atmospheric Administration
John A. Knauss
Under Secretary for
Oceans and Atmosphere

National Marine Fisheries Service
William W. Fox Jr.
Assistant Administrator
for Fisheries

Fishery Bulletin

Scientific Editor
Dr. Linda L. Jones
National Marine Mammal Laboratory
National Marine Fisheries Service, NOAA
7600 Sand Point Way NE
Seattle, Washington 98115-0070

Editorial Committee
Dr. Andrew E. Dizon National Marine Fisheries Service
Dr. Charles W. Fowler National Marine Fisheries Service
Dr. Richard D. Methot National Marine Fisheries Service
Dr. Theodore W. Pietsch University of Washington
Dr. Joseph E. Powers National Marine Fisheries Service
Dr. Tim D. Smith National Marine Fisheries Service
Dr. Mia J. Tegner Scripps Institution of Oceanography

Managing Editor
Nancy Peacock
National Marine Fisheries Service
Scientific Publications Office
7600 Sand Point Way NE, BIN C15700
Seattle, Washington 98115-0070

The *Fishery Bulletin* (ISSN 0090-0656) is published quarterly by the Scientific Publications Office, National Marine Fisheries Service, NOAA, 7600 Sand Point Way NE, BIN C15700, Seattle, WA 98115-0070. Second class postage is paid in Seattle, Wash., and additional offices. POSTMASTER send address changes for subscriptions to Fishery Bulletin, Superintendent of Documents, Attn: Chief, Mail List Branch, Mail Stop SSOM, Washington, DC 20402.

Although the contents have not been copyrighted and may be reprinted entirely, reference to source is appreciated.

The Secretary of Commerce has determined that the publication of this periodical is necessary in the transaction of the public business required by law of this Department. Use of funds for printing of this periodical has been approved by the Director of the Office of Management and Budget.

For sale by the Superintendent of Documents, U.S. Government Printing Office, Washington, DC 20402. Subscription price per year: $16.00 domestic and $20.00 foreign. Cost per single issue: $9.00 domestic and $11.25 foreign. **See back page for order form.**

The *Fishery Bulletin* carries original research reports and technical notes on investigations in fishery science, engineering, and economics. The Bulletin of the United States Fish Commission was begun in 1881; it became the Bulletin of the Bureau of Fisheries in 1904 and the Fishery Bulletin of the Fish and Wildlife Service in 1941. Separates were issued as documents through volume 46; the last document was No. 1103. Beginning with volume 47 in 1931 and continuing through volume 62 in 1963, each separate appeared as a numbered bulletin. A new system began in 1963 with volume 63 in which papers are bound together in a single issue of the bulletin. Beginning with volume 70, number 1, January 1972, the *Fishery Bulletin* became a periodical, issued quarterly. In this form, it is available by subscription from the Superintendent of Documents, U.S. Government Printing Office, Washington, DC 20402. It is also available free in limited numbers to libraries, research institutions, State and Federal agencies, and in exchange for other scientific publications.

U.S. Department of Commerce
Seattle, Washington

Volume 90
Number 1
January 1992

Fishery Bulletin

Contents

1 **Buckland, Stephen T., Karen L. Cattanach, and Alejandro A. Anganuzzi**
Estimating trends in abundance of dolphins associated with tuna in the eastern tropical Pacific Ocean, using sightings data collected on commercial tuna vessels

13 **Collette, Bruce B., and Gary B. Gillis**
Morphology, systematics, and biology of the double-lined mackerels (*Grammatorcynus*, Scombridae)

54 **Douglas, Michael E., Gary D. Schnell, Daniel J. Hough, and William F. Perrin**
Geographic variation in cranial morphology of spinner dolphins *Stenella longirostris* in the eastern tropical Pacific Ocean

77 **Gall, Graham A.E., Devin Bartley, Boyd Bentley, Jon Brodziak, Richard Gomulkiewicz, and Marc Mangel**
Geographic variation in population genetic structure of chinook salmon from California and Oregon

101 **Hunter, J. Roe, Beverly J. Macewicz, N. Chyan-huei Lo, and Carol A. Kimbrell**
Fecundity, spawning, and maturity of female dover sole *Microstomus pacificus*, with an evaluation of assumptions and precision

129 **Kendall, Arthur W. Jr., and Toshikuni Nakatani**
Comparisons of early-life-history characteristics of walleye pollock *Theragra chalcogramma* in Shelikof Strait, Gulf of Alaska, and Funka Bay, Hokkaido, Japan

139 **McShane, Paul E.**
Exploitation models and catch statistics on the Victorian fishery for abalone *Haliotis rubra*

147 **Sissenwine, Michael P., and Pamela M. Mace**
ITQs in New Zealand: The era of fixed quota in perpetuity

161 **Stoner, Allan W., Veronique J. Sandt, and Isabelle F. Boidron-Metairon**
Seasonality in reproductive activity and larval abundance of queen conch *Strombus gigas*

171 **Wainwright, Thomas C., David A. Armstrong, Paul A. Dinnel, José M. Orensanz, and Katherine A. McGraw**
Predicting effects of dredging on a crab population: An equivalent adult loss approach

Notes

183 **Chen, Weihzong, John J. Govoni, and Stanley M. Warlen**
Comparison of feeding and growth of larval round herring *Etrumeus teres* and gulf menhaden *Brevoortia patronus*

190 **D'Amours, Denis, and Francois Grégoire**
Analytical correction for oversampled Atlantic mackerel *Scomber scombrus* eggs collected with oblique plankton tows

197 **Rajaguru, Arjuna, and Gopalsamy Shantha**
Association between the sessile barnacle *Xenobalanus globicipitis* (Coronulidae) and the bottlenose dolphin *Tursiops truncatus* (Delphinidae) from the Bay of Bengal, India, with a summary of previous records from cetaceans

203 **Safford, Susan E., and Henry Booke**
Lack of biochemical genetic and morphometric evidence for discrete stocks of Northwest Atlantic herring *Clupea harengus harengus*

211 **Stergiou, Konstantinos I.**
Variability of monthly catches of anchovy *Engraulis encrasicolus* in the Aegean Sea

Abstract.–We summarize the methods for estimating relative abundance of seven dolphin stocks in the eastern tropical Pacific Ocean using sightings data collected on commercial tuna vessels by trained observers, developed by Buckland and Anganuzzi (1988a) and Anganuzzi and Buckland (1989). Their estimates of relative abundance, which may show large year-to-year fluctuations, are smoothed to provide estimates of the underlying trend in dolphin abundance between 1976 and 1988. The bootstrap method provides estimation of precision in a way that allows trend estimates to be used for management purposes, without the need to assume that trends in abundance are linear. Concerns about the validity of the estimates are addressed.

Estimating trends in abundance of dolphins associated with tuna in the eastern tropical Pacific Ocean, using sightings data collected on commercial tuna vessels

Stephen T. Buckland
Karen L. Cattanach
SASS Environmental Modelling Unit, MLURI
Craigiebuckler, Aberdeen AB9 2QJ, United Kingdom

Alejandro A. Anganuzzi
Inter-American Tropical Tuna Commission
8604 La Jolla Shores Drive, La Jolla, California 92093

Manuscript accepted 27 November 1991.
Fishery Bulletin, U.S. 90:1–12 (1992).

Incidental mortality of dolphins in the tuna fishery in the eastern tropical Pacific since 1959 has been sufficient to affect abundance of stocks of at least two species of dolphin: the spotted dolphin *Stenella attenuata* and the spinner dolphin *S. longirostris* (Smith 1983). Although there is less information available on stocks of the common dolphin *Delphinus delphis*, mortality estimates (e.g., Hall and Boyer 1988) suggest that abundance of stocks of this species may also have been reduced. To monitor possible effects of incidental mortality on the size of dolphin stocks, several attempts to estimate abundance have been made, usually applying line-transect methodology to data collected on either commercial tuna vessels ("tuna vessel data") or research vessels ("research vessel data") or both. Holt and Powers (1982) and Holt (1985, 1987) considered analyses of research vessel data alone, and of tuna vessel data combined with research vessel data. More recently, Holt and Sexton (1989, 1990a, b) analyzed data from research vessels alone. Tuna vessel data alone were analyzed by Hammond and Laake (1983), by Polacheck (1987), by Buckland and Anganuzzi (1988a), and by Anganuzzi and Buckland (1989).

The tuna vessel data are collected by scientific technicians placed by two organizations onboard commercial tuna purse seiners. The Inter-American Tropical Tuna Commission (IATTC) places technicians on vessels of the international fleet (including U.S.-registered vessels), and the National Marine Fisheries Service (NMFS) of the United States places technicians on U.S.-registered vessels only. Data were first collected by NMFS in 1974, and by IATTC in 1979.

Tuna vessel data provide a large database, with regular coverage of a substantial portion of the area occupied by the dolphin stocks. However, due to the nature of the fishery operations, the assumptions necessary for line-transect sampling to yield unbiased estimates of absolute abundance are often violated. Therefore, analytic procedures should as far as possible be insensitive to those violations. We summarize here the procedures of Buckland and Anganuzzi (1988a), as modified by Anganuzzi and Buckland (1989). Since these procedures are unlikely to remove all biases, the estimates should

be treated as indices of relative abundance, rather than estimates of absolute abundance of the stocks. The definition of a stock, and its boundaries, is problematic, but we follow the recommendations of Au et al. (1979), for reasons stated by Anganuzzi and Buckland (1989), except in two cases. A more southerly southern boundary was found to be necessary for the southern offshore stock of spotted dolphins (Anganuzzi et al. 1991), and we adopt the recommendation of Perrin et al. (1991) to combine the northern and southern whitebelly stocks of spinner dolphins. We also derive estimates for pooled offshore stocks of spotted dolphins and pooled stocks of common dolphins, since they are not differentiable in the field.

Buckland and Anganuzzi (1988a) provided three types of test for assessing whether abundance of a stock had changed over time. For several stocks, the tests failed to provide a clear indication of recent changes, since the occasional large fluctuation in annual estimates indicated that there were significant changes in abundance that were biologically implausible. We present here a method of smoothing the sequence of estimates of relative abundance. Used in conjunction with the bootstrap, it yields a simple method of assessing change over time which does not require that trends are assumed to be linear, and which does not yield biologically implausible rates of change.

Edwards and Kleiber (1989) have questioned the validity of estimating trends in abundance from sightings data collected on commercial tuna vessels. We carry out a simple simulation study to assess their assertions, and compare the relative abundance estimates calculated from tuna vessel data with those calculated from research vessel data for the years 1986–89, for which data from both sources are available.

Methods

The number of dolphins N in an area for a given stock and year is estimated by

$$\hat{N} = A \cdot \hat{s} \cdot \hat{D}$$

where A is the size of the area,
$\hat{s}$ is the estimated average school size for the stock in area A, and
$\hat{D}$ is the estimated density of schools in area A.

The line-transect method provides the estimate $\hat{D}$ (Burnham et al. 1980). Suppose schools farther than a distance w from the trackline are discarded from the analyses. Then

$$\hat{D} = \frac{n \cdot \hat{f}(0)}{2L} \quad (1)$$

where n is the number of schools detected in the area that are within the truncation distance w,
$\hat{f}(0)$ is the estimated probability density function of the n perpendicular distances, evaluated at perpendicular distance zero, and
L is the total length of transect in nautical miles within the area.

If we define the encounter rate E to be the expected number of sightings detected within w of the trackline per nautical mile of search, then its estimate is given by

$$\hat{E} = n/L.$$

Hence,
$$\hat{D} = \frac{\hat{E} \cdot \hat{f}(0)}{2} \quad (2)$$

and
$$\hat{N} = \frac{\hat{E} \cdot \hat{f}(0) \cdot \hat{s} \cdot A}{2}. \quad (3)$$

If $\hat{D}$ and $\hat{N}$ were estimates of absolute abundance, then the following assumptions would be required:

(i) Within each area or stratum, either the search effort of the tuna vessels is random or the dolphin schools are randomly distributed;
(ii) any movement of schools is slow relative to the speed of the vessel, at least before detection;
(iii) all schools on or close to the trackline are detected and identified;
(iv) sighting distances and angles are measured without error;
(v) sightings of schools are independent events;
(vi) school size is recorded without error, and for mixed schools percent of each species is recorded without error;
(vii) probability of detection of a school is independent of its size, at least out to perpendicular distance w.

If the estimates are used solely as indices of relative abundance, as here, then any or all of the above assumptions may fail without invalidating the estimates, provided that bias arising from the failure of an assumption is consistent across time. Even this proviso may be relaxed when trends in abundance over a long sequence of years are estimated; in this case it is merely necessary to assume that bias shows no trend with time. Catch-per-unit-effort methods for estimating relative abundance are known to show trends in bias over time in some instances, due to increased efficiency of vessels (Cooke 1985). We attempt to avoid such problems by incorporating a parameter that measures the

efficiency of search of the tuna vessels. This parameter, the effective search width, is estimated using line-transect theory. It may be interpreted as twice the distance at which the number of undetected dolphin schools closer to the vessel is equal to the number of detected schools further from the vessel, and is therefore the effective width of the strip of ocean searched by the vessel. As efficiency of the fleet to detect dolphin schools increases (e.g., through the use of helicopters, high-resolution radar, etc.), the effective search width increases, and bias in abundance estimates should remain unaffected.

We adopt a strategy of reducing bias as much as possible, so that the effect of any trend in bias over time on estimated trends in abundance is minimized. To estimate the different components of the estimator of Equation (3), separate stratification schemes are applied for encounter rate, effective search width, and school size. In stratifying for a given component, our aim is to define strata such that each stratum is relatively homogeneous with respect to that component, so that non-random search effort and non-random distribution of schools generate only small bias in any given stratum. Crude encounter rates, average school sizes, and average detection distances are estimated by 1° square. Where data are insufficient, the crude estimates are smoothed, and the same smoothing procedure interpolates for squares in which there was no tuna vessel effort. These estimates are used to allocate 1° squares to strata, yielding the separate stratifications for encounter rate, school size, and effective search width, respectively. Full details are given by Anganuzzi and Buckland (1989).

Thus the problem of abundance estimation has been reduced to three simpler problems: For a random point in the stock area, the expectations of encounter rate, school size, and effective search width are estimated, and the three estimates are multiplied together to obtain the final abundance estimate. Lack of independence between the three estimates does not bias the overall estimate, and independence is not assumed when estimating variance. A nonparametric bootstrap technique is used to obtain variances. The resampling unit in the bootstrap is the individual cruise, and for each bootstrap replicate the full estimation procedure is applied, thus generating bootstrap estimates of abundance. The sample variance of these estimates yields the required variance estimates, and confidence intervals are obtained by the percentile method. (See Buckland and Anganuzzi 1988a, for details.)

Bias arising from rounding errors in the recorded sighting distances r and angles θ is reduced by smearing the data, using the method favored by Buckland and Anganuzzi (1988b). The recorded location of each school relative to the tuna vessel at the time of detection is defined by r and θ, and that location is "smeared" over the sector defined by $r \cdot (1 \pm d)$ and $\theta \pm \phi/2$, to allow for inaccuracy in the recorded values. The smearing parameters d and ϕ are estimated from the data. When a small sighting angle is rounded to zero, the calculated perpendicular distance is zero, giving a spurious spike in the perpendicular distance distribution at zero distance. Smearing yields more robust estimation by removing or reducing this spike.

Here we take the estimates of Anganuzzi and Buckland (1989) and of Anganuzzi et al. (1991) and attempt to estimate the underlying trends in dolphin abundance by smoothing them. Various smoothing methods such as moving averages, running medians, and polynomial regression were investigated (Smith 1988). The chosen method was a compound running median known as "4253H, twice" (Velleman and Hoaglin 1981), which is constructed as follows.

Suppose that $\{X(t)\}$, $t = 1, \ldots, N$, is a time-series of length N, and let $\{S_i(t)\}$ be a smoothed version of it, found by calculating an i-period running median. We can construct compound smoothing methods such as $\{S_{ij}(t)\}$, which is simply $\{S_j(S_i(t))\}$. Thus, a 4253 running median method smooths a time-series using a 4-period running median, which is in turn smoothed by a 2-period running median, smoothed again by a 5-period running median, and then by a 3-period running median (i.e., $\{S_{4253}(t)\} = \{S_3(S_5(S_2(S_4(t))))\}$). Near the endpoints, where there are not enough values surrounding a point to be smoothed using the specified running median, a shorter-period running median may be used. The endpoints of the resultant time-series are calculated by estimating $X(0)$ and $X(N+1)$, the "observed" values at $t = 0$ and $t = N+1$, and then calculating

$$S_{4253}(1) = \text{median } \{\hat{X}(0), X(1), S_{4253}(2)\} \text{ and}$$

$$S_{4253}(N) = \text{median } \{S_{4253}(N-1), X(N), X(N+1)\}.$$

$\hat{X}(0)$ is found by extrapolating from the straight line which passes through the smoothed values at $t = 2$ and $t = 3$, i.e., $\hat{X}(0) = 3 \cdot S_{4253}(2) - 2 \cdot S_{4253}(3)$; similarly, $\hat{X}(N+1) = 3 \cdot S_{4253}(N-1) - 2 \cdot S_{4253}(N-2)$.

The H in "4253H, twice" denotes a linear smoothing method commonly used with running medians, which is known as Hanning. It is a 3-period weighted moving average for $t = 2, \ldots, N-1$, with weights {0.25, 0.5, 0.25}. The endpoints remain unchanged.

The pattern of the time-series may be recovered by calculating the residuals of the series (i.e., the differences between the smoothed and unsmoothed estimates), smoothing the residual series using the same method as for the time-series, and then adding the smoothed values of the residuals to the smoothed

values of the series. This is known as smoothing "twice." For example, if we define the residuals of the time-series smoothed by 4253H to be $\{E(t)\} = \{X(t) - S_{4253}(t)\}$, then the values of the times-series smoothed by "4253H, twice" can be defined by

$$\{S_{4253H,\,twice}(t)\} = \{S_{4253H}(t) + S_{4253H}(E(t))\}.$$

Thus the "4253H, twice" running median method uses a 4253 running median to smooth the time-series, estimates the endpoints of the smoothed series, and then smooths the resultant series by Hanning. The residuals of the series are calculated and are also smoothed, using the same method as above. The smoothed values of the residuals are then added to the smoothed values of the time-series to produce a time-series smoothed by "4253H, twice." The advantage of using running medians is that the magnitude of an extreme estimate does not affect the resultant smoothed time-series. The above method is sufficiently complex that its behavior cannot be readily understood. However, simpler methods were found to suffer from one or more of the following shortcomings: Estimated trends were not always smooth; implausible rates of change were sometimes indicated; trends near the start or end of the sequence of estimates were often poorly estimated.

Nonparametric bootstrap replicates are generated as described by Anganuzzi and Buckland (1989). We select here the bootstrap estimates that correspond to an 85% confidence interval for relative abundance in each year. The rationale for the choice of confidence level is that if two 85% confidence intervals do not overlap, the difference between the corresponding relative abundance estimates is significant at roughly the 5% level ($P \leq 0.05$); whereas if they do, the difference is not significant ($P > 0.05$). If the abundance estimates are assumed to be lognormally distributed, each with the same coefficient of variation, then the exact confidence level that gives this property is 83.4%. If one estimate has twice the coefficient of variation of the other, the confidence level increases slightly to 85.6%. Thus a choice of 85% makes some allowance for variability in the coefficient of variation.

For each abundance estimate, 79 bootstrap replicates are run, so that the 6th smallest and 6th largest bootstrap estimates provide an approximate 85% confidence interval (Buckland 1984). If this procedure is carried out independently for each year, confidence intervals are wide. Provided the assumed stock area spans the whole range of the stock, numbers of dolphins within it are unlikely to vary greatly in successive years, and a procedure that calculates confidence intervals for a given year incorporating information from years immediately preceding and following that year is more informative. For a given stock, we achieve this by carrying out one bootstrap replication for each year that a relative abundance estimate is available. These estimates are smoothed using the routine described above, and the process is repeated 79 times. For each year, the 6th smallest and 6th largest smoothed estimates provide approximate 85% confidence limits. We use the sequence of medians of the smoothed bootstrap estimates (i.e., the 40th estimate of each ordered set of 79) as the "best" indicator of trend, so that it is calculated in a comparable manner to the confidence limits. Larger numbers of bootstrap replicates are preferable, but available computer power was limited. Repeat runs for the northern offshore stock of spotted dolphins were carried out, to assess the Monte Carlo variability.

By using overlapping confidence intervals to test for a difference between years, independence between smoothed estimates for different years is assumed. Given the strong positive correlation in the smoothed estimates between successive years, the test is unlikely to detect a large change between one year and the next, but should be reliable for detecting trends over a period of perhaps five or more years, for which correlations between smoothed estimates are small.

Results

Figures 1–10 show the estimates of underlying trend for each of the main stocks associated with tuna in the eastern tropical Pacific Ocean. Since stock boundaries and stock identity are both uncertain, we also show trend estimates after pooling data from stocks that are not differentiable in the field. The broken horizontal lines in these plots correspond to the upper and lower 85% confidence limits for the 1988 relative abundance estimate. Years for which the entire confidence interval lies outside the region between the broken horizontal lines show a relative abundance significantly different from that for 1988. Because the smoothed estimate for the first or final year of a sequence can be poor, we show the unsmoothed estimate and corresponding 85% confidence limits for the first and last year on each plot.

Figures 1 and 2 show estimated trends for northern offshore spotted dolphins, with and without the abnormally low 1983 estimate, which corresponded with a very strong El Niño event. It is clear that the 1983 estimate affects the smoothed estimate of trend, but its effect is no greater than if it had been just smaller than the 1984 estimate. Thus abnormal estimates may be more safely retained when using this procedure, and subjective decisions of whether to treat an estimate as an outlier are avoided.

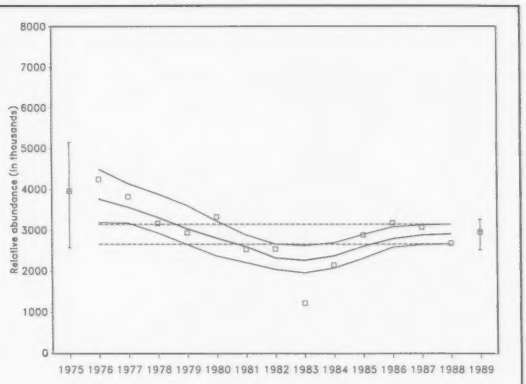

Figure 1

Smoothed abundance trends of northern offshore stock of spotted dolphin *Stenella attenuata* in the eastern tropical Pacific. Broken lines indicate approximate 85% confidence limits. Horizontal lines correspond to 85% confidence limits for the 1988 estimate. If lower limit lies above upper limit for an earlier year, abundance has increased significantly between that year and 1988 ($P<0.05$); if upper limit lies below lower limit for an earlier year, abundance has decreased significantly.

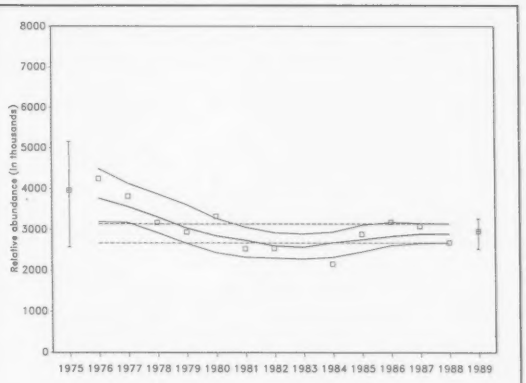

Figure 2

Smoothed abundance trends of northern offshore stock of spotted dolphin *Stenella attenuata* in the eastern tropical Pacific, excluding 1983 estimate. Broken lines indicate approximate 85% confidence limits. See Figure 1 for more details.

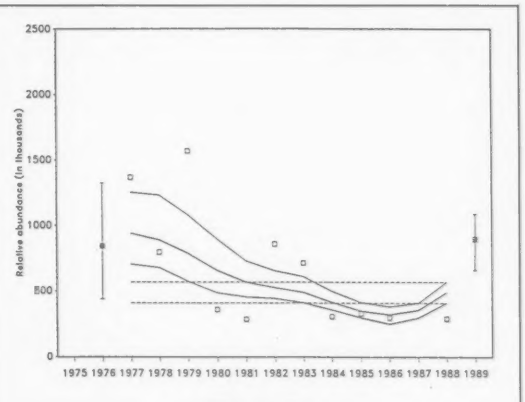

Figure 3

Smoothed abundance trends of southern offshore stock of spotted dolphin *Stenella attenuata* in the eastern tropical Pacific. Broken lines indicate approximate 85% confidence limits. See Figure 1 for more details.

The estimated trend from Figure 1 is downwards until around 1983. Estimated abundance in 1976 and 1977 was significantly higher than in 1988 ($P<0.05$), but there is some evidence of a recovery between 1983 and 1988 ($P<0.05$). Thus northern offshore spotted dolphins appeared to decrease through the 1970s and early 1980s, with numbers remaining stable or increasing since.

Figure 3 suggests there may have been a marked decline in numbers of southern offshore spotted dolphins since the late 1970s. The smoothed 1988 estimate is significantly lower than the smoothed estimates for 1977 and 1978, but there is evidence of an increase since 1986 ($P<0.05$), after a relatively high unsmoothed estimate for 1989. As shown by Anganuzzi et al. (1991), southern offshore spotted dolphins appear to occupy appreciably different regions from one year to another, and the extent of mixing with northern offshore spotted dolphins remains unclear. We therefore believe that trend estimates for this stock are unreliable. The estimated trends obtained by pooling data from the offshore stocks are shown in Figure 4. The estimates are dominated by the data from the larger northern offshore stock, and the plot is similar to Figure 1. The 1988 smoothed relative-abundance estimate is significantly higher than the 1983 and 1984 estimates, and significantly lower than all estimates preceding 1979.

Figure 5 suggests that the eastern spinner dolphin might have had a pattern of change similar to the northern offshore spotted dolphin, although estimated abundance in the late 1980s is roughly equal to that in the mid-1970s, so depletion between 1975 and 1983 may have been less than for northern offshore spotted dolphins. The 1988 smoothed estimate is just significantly higher than the smoothed estimates for 1981 and 1982 ($P<0.05$).

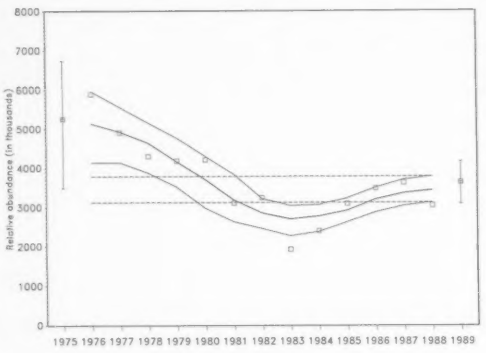

Figure 4
Smoothed abundance trends of pooled northern and southern offshore stocks of spotted dolphin *Stenella attenuata* in the eastern tropical Pacific. Broken lines indicate approximate 85% confidence limits. See Figure 1 for more details.

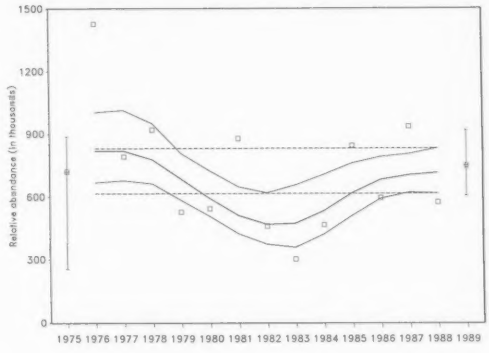

Figure 6
Smoothed abundance trends of whitebelly stock of spinner dolphin *Stenella longirostris* in the eastern tropical Pacific. Broken lines indicate approximate 85% confidence limits. See Figure 1 for more details.

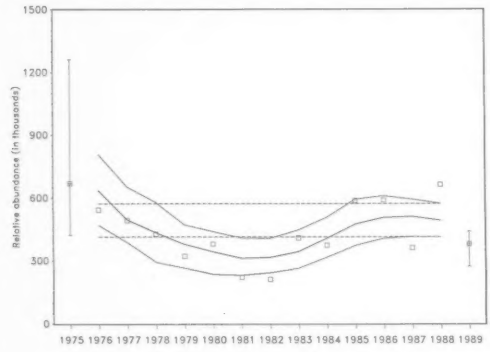

Figure 5
Smoothed abundance trends of eastern stock of spinner dolphin *Stenella longirostris* in the eastern tropical Pacific. Broken lines indicate approximate 85% confidence limits. See Figure 1 for more details.

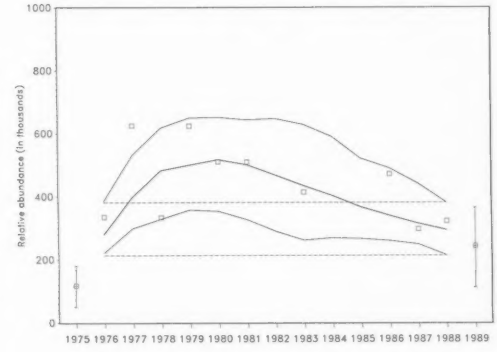

Figure 7
Smoothed abundance trends of northern stock of common dolphin *Delphinus delphis* in the eastern tropical Pacific. Broken lines indicate approximate 85% confidence limits. See Figure 1 for more details.

The estimated trend for whitebelly spinner dolphins (Fig. 6) is similar to that for eastern spinner dolphins and northern offshore spotted dolphins. There is some evidence that abundance in 1988 was higher than in 1982 ($P \cong 0.05$), but no other comparisons with 1988 are significant. The 1982 smoothed estimate is significantly lower than those for 1976–78.

End effects in Figure 7 give rise to an implausible trend in numbers of northern common dolphins during 1975–78. Since 1980, there may have been a decline in this stock, but no smoothed estimates differ significantly. The central stock of common dolphins (Fig. 8) shows evidence of a steep decline from 1977 to 1983, with stability since. The smoothed estimate for 1988 is significantly lower than for all years preceding 1980 ($P < 0.05$), but does not differ significantly from any later estimates. Data on the southern stock of common dolphins are sparse. There may have been a decreasing trend (Fig. 9), but unsmoothed estimates fluctuate widely and no smoothed estimates differ significantly.

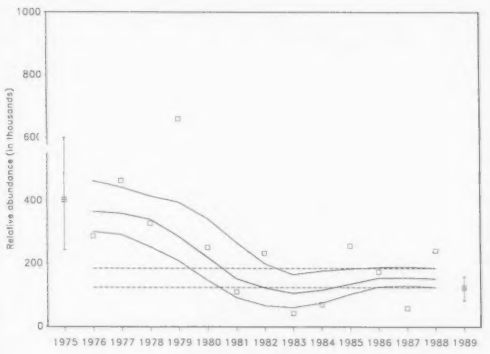

Figure 8
Smoothed abundance trends of central stock of common dolphin *Delphinus delphis* in the eastern tropical Pacific. Broken lines indicate approximate 85% confidence limits. See Figure 1 for more details.

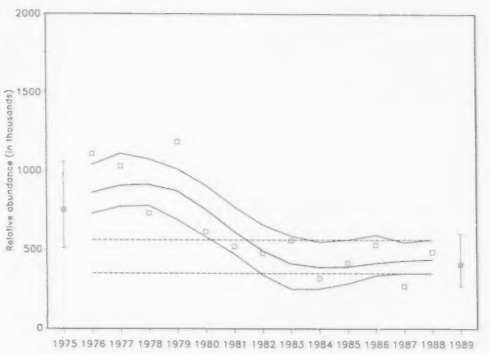

Figure 10
Smoothed abundance trends of pooled northern, central, and southern stocks of common dolphin *Delphinus delphis* in the eastern tropical Pacific. Broken lines indicate approximate 85% confidence limits. See Figure 1 for more details.

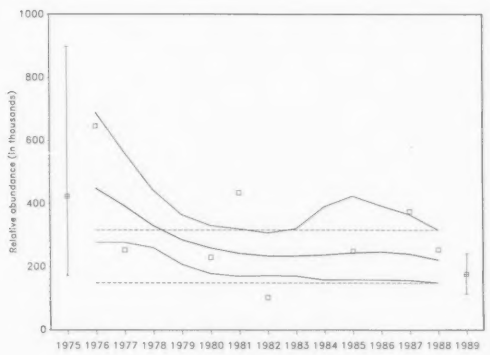

Figure 9
Smoothed abundance trends of southern stock of common dolphin *Delphinus delphis* in the eastern tropical Pacific. Broken lines indicate approximate 85% confidence limits. See Figure 1 for more details.

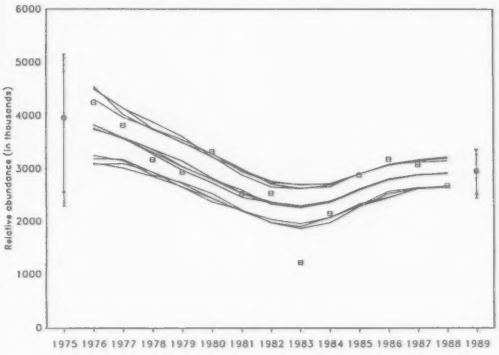

Figure 11
Smoothed abundance trends of northern offshore stock of spotted dolphin *Stenella attenuata* in the eastern tropical Pacific. Broken lines indicate approximate 85% confidence limits. Estimates and limits were determined from four independent sets of 79 bootstrap replicates, so that the plot indicates uncertainty in the estimates arising from Monte Carlo variation.

If data are pooled across stocks of common dolphins (Fig. 10), the 1988 smoothed estimate is significantly lower than all those preceding 1981.

Four independent sets of 79 bootstrap replicates were generated for the northern offshore stock of spotted dolphins. The resulting plots, one of which corresponds exactly to Figure 1, are superimposed in Figure 11. If an infinite number of replicates could be carried out for each set, the four plots would be identical. Thus Figure 11 indicates the uncertainty that can be expected in the median and interval estimates due to Monte Carlo variation.

Discussion

Unsmoothed estimates of relative abundance sometimes show larger year-to-year variation than is

plausible, even if full allowance is made for the precision of the estimates. An example is the 1983 estimate for the northern offshore stock of spotted dolphins, which is significantly lower than either the 1982 or the 1984 estimate. This has been attributed to the strong El Niño event of that year (Buckland and Anganuzzi 1988a). The change in environmental conditions appeared to cause spotted dolphins to split into smaller schools and to disperse more widely than is normal, so that tuna vessels were unable to locate areas of concentration. If, in normal years when concentrations occur in known areas, there is positive bias in the abundance index, then a relatively low estimate might be expected for 1983. This effect would be enhanced if many animals wandered beyond the normal range of the stock, so that the abundance index for 1983 corresponded to only that portion of the stock remaining within its normal bounds. Such effects may be regarded either as bias that fluctuates over time or as an additional source of variability that is unaccounted for in the variances of the abundance indices. Provided the effects are essentially random, and do not exhibit a consistent linear trend over time, the smoothing algorithm described above smooths out the large fluctuations and, in conjunction with the bootstrap, provides variance and interval estimates for the smoothed abundance indices that take full account of variability not allowed for in the variance estimates of the unsmoothed indices.

The validity of estimating trends in dolphin abundance from tuna-vessel sightings data has been questioned by Edwards and Kleiber (1989). They used a simple simulation model of non-random search vessel effort coupled with clustered distributions of dolphin schools to investigate bias. By allowing the clustering of schools to be slight in one year and extreme in the next, they showed that bias in the relative abundance estimates can be inconsistent between years. They define a change estimate as the ratio of relative abundance estimates for the two years. They state, "This two-sample change estimate is only a rough approximation to a trend estimate derived from a series of measurements... However, conclusions about the effects of inconsistent biases on this **change** estimate will be valid for **trend** estimates also, except for the unlikely case in which effects of various inconsistent biases cancel each other out, so that the trend estimate reflects the actual trend, but only fortuitously." (The emphasis on "change" and "trend" is theirs.) They also note that "It is obvious... that even relatively small changes of bias can lead to considerably inaccurate estimates of change and, by implication, estimates of trend." If this is so, there would be little value in estimating trends in abundance from tuna-vessel sightings data. We question whether the simulation model of Edwards and Kleiber (1989), which is a considerable simplification of reality, allows such strong conclusions. However, we use their results to assess the validity of their arguments. We take their worst-case scenario of a static environment, using the stratified and smoothed option, and average across their four replicates for the high-density case. The calculations indicate a downward bias of about 20% for the "simple, gentle" environmental topography of year 1 and an upward bias of about 100% for the "complex, steep" topography of year 2. Thus, if the population comprised 2500 schools (as in their simulations), the expected estimate would be around 2000 schools in the first year and 5000 in the second, a 2.5-fold estimated increase for a population that has constant size. Is this conclusion "valid for **trend** estimates also"? Suppose a population comprised 4 million animals in 1975, and decreased at a rate of 5% per annum until 1989. Suppose we again take an extreme scenario in which the "simple, gentle" environmental topography applied in El Niño years, and the "complex, steep" topography applied in all other years. The expectations of the estimates are shown in Table 1. Also shown are simulated estimates, for which errors were generated from a lognormal distribution which yields a coefficient of variation of 15%, close to that observed for estimates based on tuna vessel data. The errors were then added to the expected estimates. The estimated rate of decrease for the expected estimates is 5.0% per annum (SE 2.5%), and that for the simulated estimates is 4.7% per annum (SE 2.6%). Thus a scenario of extreme and inconsistent

Table 1

Actual abundance (millions), and expected and simulated relative-abundance estimate by year for a hypothetical stock, declining at an annual rate of 5%. Expected abundance is calculated assuming estimates are biased down by 20% in El Niño years (*) and up by 100% in other years.

Year	Actual abundance	Expected estimate	Simulated estimate
1975	4.00	8.00	8.04
1976*	3.80	3.04	3.37
1977	3.61	7.22	6.86
1978	3.43	6.86	5.86
1979	3.26	6.52	6.87
1980	3.10	6.19	8.66
1981	2.94	5.88	6.26
1982*	2.79	2.23	1.97
1983*	2.65	2.12	3.22
1984	2.52	5.04	4.98
1985	2.39	4.79	5.72
1986	2.28	4.55	4.02
1987*	2.16	1.73	1.65
1988	2.05	4.11	4.01
1989	1.95	3.90	4.75

bias does not invalidate the procedures when applied to a long sequence of estimates. In practice, a rate of change in abundance is unlikely to be roughly constant over such a long time-period, yet tests for trend over a short time-period have low power. Figures 1–10 provide a simple method to test for change over longer time-periods without the necessity of assuming the rate of change is constant.

The smoothing procedure used for generating trend estimates can perform poorly at the start (e.g., Fig. 7) or at the end of a sequence of estimates, so that sharp increases or declines during the first or last year or two should be treated with suspicion. The first and last smoothed estimate in a sequence are especially unreliable, and are omitted from Figures 1–10. Thus, changes in abundance are assessed relative to 1988 rather than 1989.

To assess the current status of dolphin stocks, and the effects of recent levels of mortality, it is necessary to determine whether trends in dolphin abundance are best estimated from tuna vessel data or research vessel data, or whether some combination of estimates from both sources is preferable. Given sufficient data and adequate coverage of the entire range of each stock, research-vessel estimates of trend would be preferred, since they are likely to be less biased. However, Holt and Sexton (1989, 1990ab), to exploit fully the small number of research vessel sightings, made assumptions that might be seriously violated. Firstly, data are pooled across all sightings of dolphin schools of at least 15 animals, irrespective of species, to improve precision of effective search-width estimates. This may introduce bias which is not consistent over time, especially if non-target species (those which are seldom associated with tuna, and are therefore seldom encircled by purse seines) have a different effective search width and a different rate of change in abundance than target species. Secondly, although abundance estimates are given by stock, encounter-rate estimates by stock area are ignored for stocks that are not separated in the field. Thus for offshore spotted dolphins, a single abundance estimate per year is generated and then prorated by stock area, to yield separate estimates for the northern and southern offshore stocks. If the southern offshore stock became extinct, and the northern offshore stock increased at a rate that ensured overall abundance remained constant, the expected trend in research vessel estimates would be zero for both stocks. The same applies to common dolphin stocks. The estimates of Holt and Sexton indicate that there are large numbers of common dolphins in the western sector of the eastern tropical Pacific, yet the species is seldom recorded there. Using the estimation methods of Holt and Sexton, valid trend estimates from research vessel data are not available separately for northern and southern offshore stocks of spotted dolphin or for the main stocks of common dolphin.

In Figures 12–15 we show the valid estimates of trend (i.e., those obtained after pooling data from stocks that are not differentiable in the field) from the research-vessel relative abundance estimates for 1986–89, taken from Sexton et al. (1991) and Gerrodette and Wade (1991). Also shown are the corresponding unsmoothed trend estimates from tuna vessel data. Vertical bars show ±2 standard errors. Plots are based on the relative abundance estimates and standard errors of Tables 2 and 3. The research vessel estimates indicate changes in abundance that are biologically implausible, even with full allowance for the estimated precision of the estimates. Thus either the precision of the surveys is appreciably worse than estimated or there is strong and inconsistent bias in the estimates from one year to the next. By contrast, despite the concerns over the validity of tuna vessel estimates, they yield biologically plausible rates of change during 1986–89 when the precision of the estimates is accounted for.

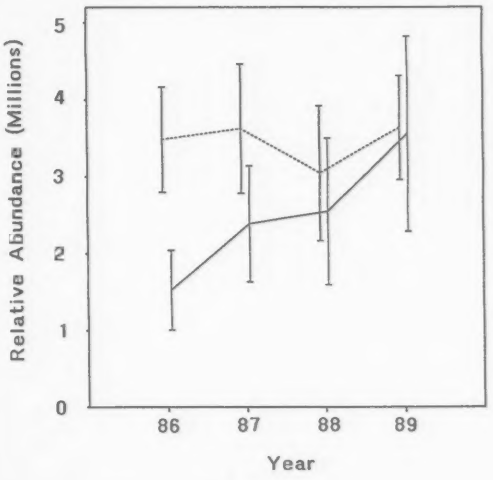

Figure 12
Unsmoothed abundance trends of northern and southern offshore stocks of spotted dolphin *Stenella attenuata* in the eastern tropical Pacific, estimated from research (solid line) and tuna vessel data. Vertical bars are ±2 standard errors.

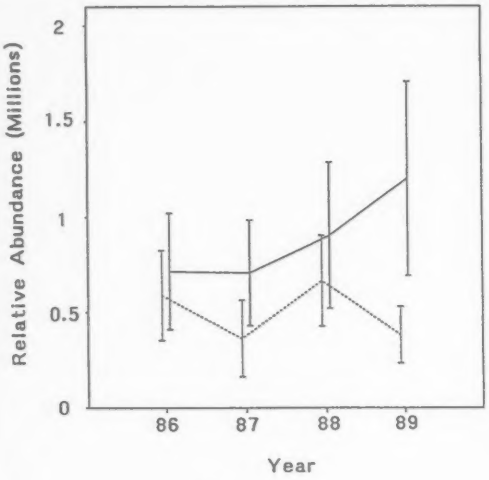

Figure 13
Unsmoothed abundance trends of eastern stock of spinner dolphin *Stenella longirostris* in the eastern tropical Pacific, estimated from research (solid line) and tuna vessel data. Vertical bars are ±2 standard errors.

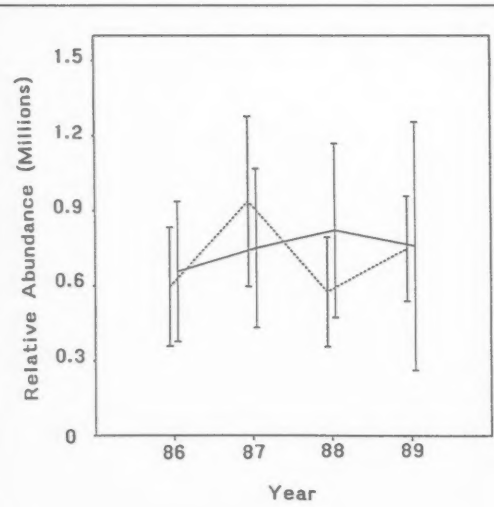

Figure 14
Unsmoothed abundance trends of whitebelly stock of spinner dolphin *Stenella longirostris* in the eastern tropical Pacific, estimated from research (solid line) and tuna vessel data. Vertical bars are ±2 standard errors.

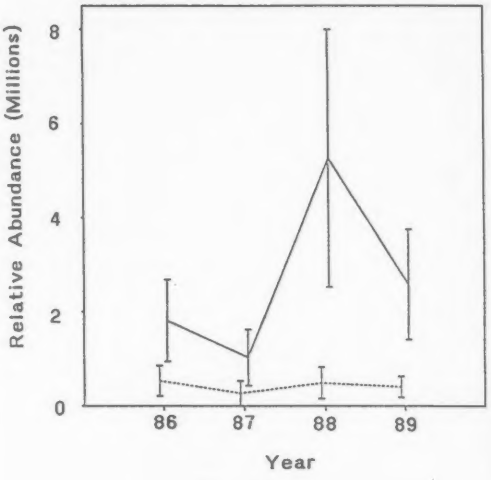

Figure 15
Unsmoothed abundance trends of northern, central, and southern stocks of common dolphin *Delphinus delphis* in the eastern tropical Pacific, estimated from research (solid line) and tuna vessel data. Vertical bars are ±2 standard errors.

Acknowledgments

We are grateful to Dr. J. Joseph, Dr. M. Hall, and Dr. M. Scott for comments on the methods outlined here, and to two reviewers and Dr. L. Jones for their constructive comments and criticisms. We also acknowledge the recent and continuing efforts of the Southwest Fisheries Science Center to evaluate methods for analyzing tuna vessel and research vessel sightings data; their program of work forced us to address more carefully the issue of how to estimate and test for trends in abundance.

Citations

Anganuzzi, A.A., and S.T. Buckland
1989 Reducing bias in estimated trends from dolphin abundance indices derived from tuna vessel data. Rep. Int. Whaling Comm. 39:323–334.

Anganuzzi, A.A., S.T. Buckland, and K.L. Cattanach
1991 Relative abundance of dolphins associated with tuna in the eastern tropical Pacific, estimated from tuna vessel sightings data for 1988 and 1989. Rep. Int. Whaling Comm. 41: 497–506.

Au, D., W.L. Perryman, and W. Perrin
1979 Dolphin distribution and the relationship to environmental features in the eastern tropical Pacific. Admin. Rep. LJ-79-43, Southwest Fish. Sci. Cent., NMFS, NOAA, La Jolla, CA 92038, 59 p.

Table 2

Unsmoothed relative-abundance estimates (standard errors in parentheses) of some stocks of dolphin in the eastern tropical Pacific, calculated from research vessel data collected 1986–89.

Year	Offshore spotted dolphin		Eastern spinner dolphin		Whitebelly spinner dolphin		Common dolphin	
1986	1527	(261)**	716	(152)	657	(140)	1810	(437)*
1987	2388	(377)	707	(138)	750	(159)	1026	(298)‡††
1988	2549	(476)	902	(191)	821	(174)	5263	(1368)*††
1989	3560	(634)**	1200	(254)	759	(248)	2586	(587)‡

*Estimates differ significantly ($P<0.05$)
‡Estimates differ significantly ($P<0.05$)
**Estimates differ significantly ($P<0.01$)
††Estimates differ significantly ($P<0.01$)

Table 3

Unsmoothed relative-abundance estimates (standard errors in parentheses) of some stocks of dolphin in the eastern tropical Pacific, calculated from tuna vessel data collected 1986–89.

Year	Offshore spotted dolphin		Eastern spinner dolphin		Whitebelly spinner dolphin		Common dolphin	
1986	3484	(342)	590	(118)	595	(119)	532	(159)
1987	3627	(420)	363	(100)	937	(170)	271	(132)
1988	3048	(439)	665*	(119)	575	(109)	487	(167)
1989	3640	(337)	381*	(74)	748	(105)	408	(111)

*Estimates differ significantly ($P<0.05$)

Buckland, S.T.
1984 Monte Carlo confidence intervals. Biometrics 40: 811–817.

Buckland, S.T., and A.A. Anganuzzi
1988a Trends in abundance of dolphins associated with tuna in the eastern tropical Pacific. Rep. Int. Whaling Comm. 38: 411–437.
1988b Comparison of smearing methods in the analysis of minke sightings data from IWC/IDCR Antarctic cruises. Rep. Int. Whaling Comm. 38:257–263.

Burnham, K.P., D.R. Anderson, and J.L. Laake
1980 Estimation of density from line transect sampling of biological populations. Wildl. Monogr. 72, 202 p.

Cooke, J.G.
1985 On the relationship between catch per unit effort and whale abundance. Rep. Int. Whaling Comm. 35:511–519.

Edwards, E.F., and P.M. Kleiber
1989 Effects of nonrandomness on line transect estimates of dolphin school abundance. Fish. Bull., U.S. 87:859–876.

Gerrodette, T., and P.R. Wade
1991 Monitoring trends in dolphin abundance in the eastern tropical Pacific using research vessels over a long sampling period: Analysis of 1989 data. Rep. Int. Whaling Comm. 41: 511–515.

Hall, M.A., and S.D. Boyer
1988 Incidental mortality of dolphins in the eastern tropical Pacific. Rep. Int. Whaling Comm. 38:439–441.

Hammond, P.S., and J.L. Laake
1983 Trends in estimates of abundance of dolphins (*Stenella* spp. and *Delphinus delphis*) involved in the purse-seine fishery for tunas in the eastern Pacific Ocean, 1977–81. Rep. Int. Whaling Comm. 33:565–588.

Holt, R.S.
1985 Estimates of abundance of dolphin stocks taken incidentally in the eastern tropical Pacific yellowfin tuna fishery. Admin. Rep. LJ-85-20, Southwest Fish. Sci. Cent., NMFS, NOAA, La Jolla, CA 92038, 32 p.
1987 Estimating density of dolphin schools in the eastern tropical Pacific Ocean by line transect methods. Fish. Bull., U.S. 85:419–434.

Holt, R.S., and J.E. Powers
1982 Abundance estimation of dolphin stocks involved in the eastern tropical Pacific yellowfin tuna fishery determined from aerial and ship surveys to 1979. Tech. Memo. 23, Southwest Fish. Sci. Cent., NMFS, NOAA, La Jolla, CA 92038, 95 p.

Holt, R.S., and S.N. Sexton
1989 Monitoring trends in dolphin abundance in the eastern tropical Pacific using research vessels over a long sampling period: Analyses of 1987 data. Rep. Int. Whaling Comm. 39:347–351.
1990a Monitoring trends in dolphin abundance in the eastern tropical Pacific using research vessels over a long sampling period: Analyses of 1986 data, the first year. Fish. Bull., U.S. 88:105–111.

1990b Monitoring trends in dolphin abundance in the eastern tropical Pacific using research vessels over a long sampling period: Analyses of 1988 data. Rep. Int. Whaling Comm. 40:471–476.

Perrin, W.F., P.A. Akin, and J.V. Kashiwada

1991 Geographic variation in external morphology of the spinner dolphin *Stenella longirostris* in the eastern Pacific and implications for conservation. Fish. Bull., U.S. 89:411–428.

Polacheck, T.

1987 Relative abundance, distribution and inter-specific relationship of cetacean schools in the eastern tropical Pacific. Mar. Mammal Sci. 3:54–77.

Sexton, S.N., R.S. Holt, and D. DeMaster

1991 Investigating parameters affecting relative estimates in dolphin abundance in the eastern tropical Pacific from research vessel surveys in 1986, 1987, and 1988. Rep. Int. Whaling Comm. 41:517–524.

Smith, K.L.

1988 Calibration and smoothing of relative dolphin abundance estimates. MSc. diss., University of Strathclyde.

Smith, T.D.

1983 Changes in sizes of three dolphin (*Stenella* spp.) populations in the eastern tropical Pacific. Fish. Bull., U.S. 81:1–14.

Velleman, P.F., and D.C. Hoaglin

1981 Applications, basics and computing of exploratory data analysis. Duxbury Press, Boston.

Morphology, systematics, and biology of the double-lined mackerels (*Grammatorcynus*, Scombridae)

Bruce B. Collette

Systematics Laboratory, National Marine Fisheries Service, NOAA
National Museum of Natural History, Washington, DC 20560

Gary B. Gillis

Observer Program, Alaska Fisheries Science Center, National Marine Fisheries Service
NOAA, 7600 Sand Point Way NE, Seattle, Washington 98115-0070
Current address: Department of Ecology and Evolutionary Biology
University of California, Irvine, California 92715

Abstract.– Osteological differences confirm the validity of two species of *Grammatorcynus*, *G. bicarinatus* (Quoy and Gaimard 1825) and the long-recognized *G. bilineatus* (Rüppell 1836). In addition to having fewer gill rakers (12–15 vs. 18–24), a smaller eye (3.1–4.6% vs. 4.0–6.0% FL), small black spots on the lower sides of the body, and reaching a larger size (110 cm FL vs. 60 cm), *G. bicarinatus* differs from *G. bilineatus* in having a shorter neurocranium, shorter parasphenoid flanges, lower posterior edge of maxillary shank, shorter quadrate process, narrower first postcleithrum, wider ethmoid, wider vomer, wider lachrymal, longer teeth, wider palatine tooth patch, wider opercle, and a thin posttemporal shelf between the anterior processes. All but one of the 16 osteological differences previously found between *Grammatorcynus bilineatus* and *Scomberomorus* and *Acanthocybium* are confirmed with the inclusion of *G. bicarinatus* in the genus. *Grammatorcynus bilineatus* is widespread in tropical and subtropical waters of the Indo-West Pacific from the Red Sea to Tokelau Islands in Oceania. The range of *G. bicarinatus* is restricted to the western and eastern coasts of Australia and southern Papua New Guinea.

Manuscript accepted 18 December 1991.
Fishery Bulletin, U.S. 90:13–53 (1992).

Until recently, most authors considered the genus *Grammatorcynus* to be monotypic (Fraser-Brunner 1950, Silas 1963, Zharov 1967, Collette 1979). Electrophoretic work (Lewis 1981, Shaklee 1983) indicated there were two species of double-lined mackerels in Australia. This was confirmed by Collette (1983) who showed there are two species: the double-lined mackerel or scad *G. bilineatus*, (Rüppell 1836), widespread in the Indo-West Pacific, with more gill rakers (18–24), a larger eye (4.0–6.0% FL), and a smaller maximum size (60 cm FL); and the shark mackerel *G. bicarinatus* (Quoy and Gaimard 1825), restricted to the waters of northern Australia and southern New Guinea, with fewer gill rakers (12–15), a smaller eye (3.1–4.6% FL), and a larger maximum size (110 cm FL). All morphological information concerning *Grammatorcynus* in Collette (1979) and Collette and Russo (1985b) was based solely on *G. bilineatus*.

The purposes of this paper are to describe osteological differences between the two species of *Grammatorcynus*, redefine the genus and both species, and summarize the literature on both species. The paper is divided into two parts. Part 1, Comparative Morphology, contains descriptions and illustrations of morphometry, meristic characters, soft anatomy, and osteology of the two species of *Grammatorcynus*; comparisons are made with *Scomberomorus* and *Acanthocybium* where appropriate. Part 2, Systematics and Biology, contains a generic description and accounts of both species, including synonymy, types of nominal species, diagnoses (based on characters from the first section), size, biology, interest to fisheries, geographic distribution, and material examined.

Methods and materials

Methods are those used by Collette and Russo (1985b) in a revision of *Scomberomorus*, and by Collette and Chao (1975) in a revision of the bonitos (Sardini).

Material of *Grammatorcynus* is listed at the end of each species account; 80 specimens of *G. bilineatus* and 11 *G. bicarinatus*. Abbreviations of institutions housing the material follow Leviton et al. (1985). Comparative material of *Scomberomorus* and *Acanthocybium* was listed in the species accounts in Collette and Russo (1985b).

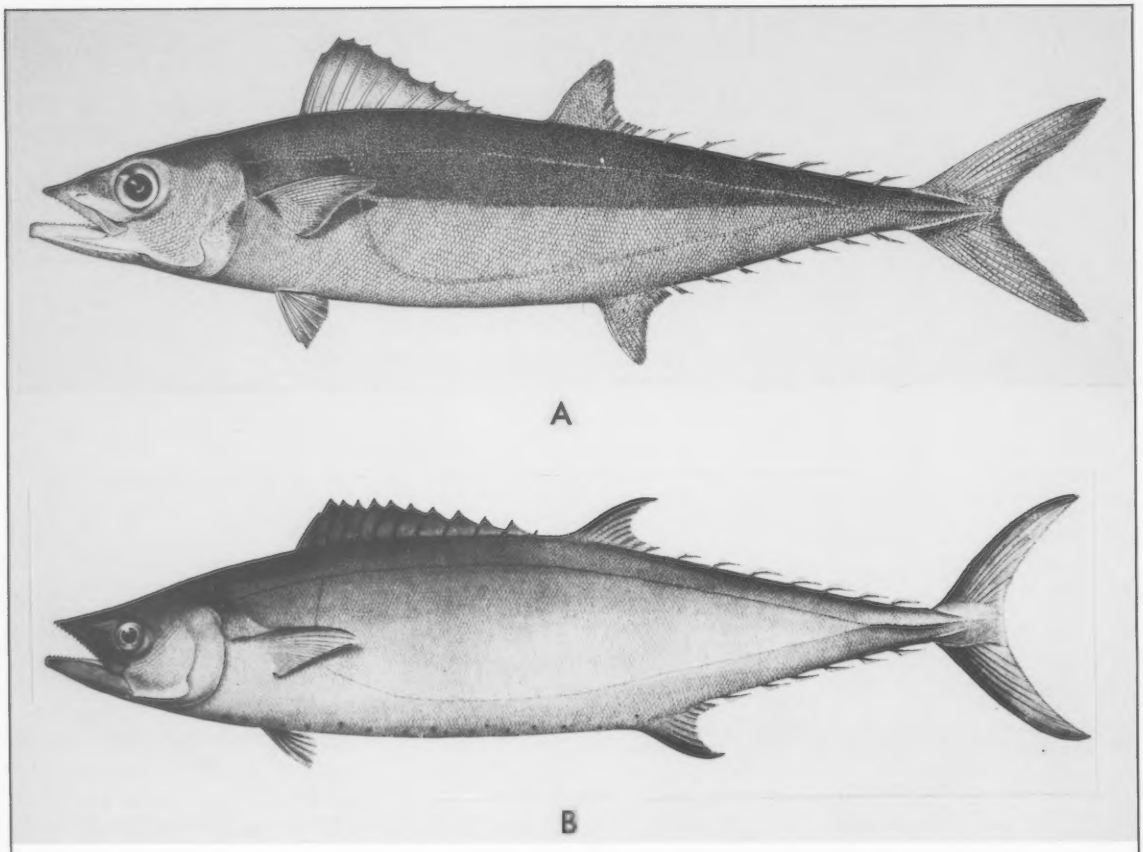

Figure 1
Species of *Grammatorcynus*. (A) *G. bilineatus* (from Evermann and Seale 1907, fig. 3, holotype of *Nesogrammus piersoni*, 372 mm FL, Philippine Is.); (B) *G. bicarinatus* (from McCulloch, 1915, p. 1, fig. 1, 925 mm FL, New South Wales, Australia).

Part 1: Comparative morphology

Morphological characters useful for distinguishing between species of *Grammatorcynus* and for evaluating phylogenetic relationships of the genus are divided into six categories: lateral line, color pattern, morphometry, meristic characters, soft anatomy, and osteology.

Lateral line

The genus *Grammatorcynus* differs from all other genera of Scombridae in having two lateral lines, hence their common name, double-lined mackerels. The dorsal-most lateral line is slightly convex, originates near the dorsal portion of the opercle, and continues posteriorly until it converges with the second lateral line, just anterior to the median caudal keel. The second lateral line originates from the first at a point below the first four spines of the dorsal fin. It starts ventrally, running under, or just posterior to, the pectoral fin, and abruptly turns into a concave line that continues posteriorly until meeting the dorsal lateral line (Fig. 1). The function of this additional lateral line is unknown. The characteristic two lateral lines are discernible in specimens as small as 56.9 mm SL (Nishikawa 1979:133). Anomalies in the pattern of the lateral lines are occasionally found, but none appear to be species specific (Fig. 2; Silas 1963:fig. 3).

Color pattern

Dark spots are usually found on the ventral portion of *G. bicarinatus* (Fig. 1B). The spots are smaller than the pupil, originate near the ventral border of the oper-

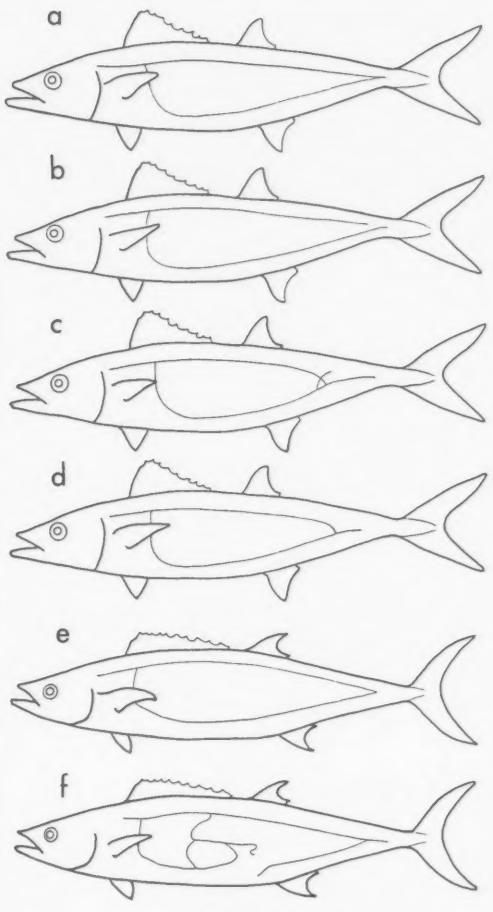

Figure 2
Variations in lateral line pattern in *Grammatorcynus*. (a) Usual pattern in *G. bilineatus*; (b–d) variations in pattern in *G. bilineatus*; (b) Australia, 410 mm FL; (c) Queensland, 416 mm FL; (d) Queensland, 400 mm FL; (e) usual pattern in *G. bicarinatus*; (f) variation in pattern in *G. bicarinatus*, Western Australia, 765 mm FL.

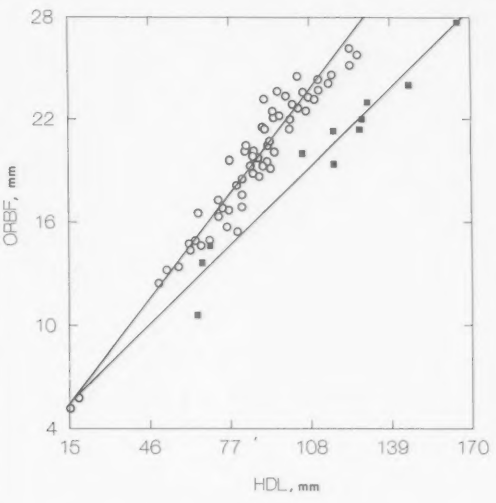

Figure 3
Orbit length (ORBF) compared with head length (HDL) in *Grammatorcynus*. Open circles = *G. bilineatus*, squares = *G. bicarinatus*.

culum, and continue posteriorly to the anal fin. They are found below the ventral lateral line on both sides of the fish. No spots were present in the two smallest specimens examined (AMS IB.5207-8, 306–315 mm FL). Spots are never present in *G. bilineatus* (Fig. 1A).

Morphometric characters

In addition to fork length, 26 measurements were routinely made on all specimens. Several morphometric characters separate the two species. A summary table shows the range and mean of all the characters as thousandths of fork length, and eight of the characters as thousandths of head length (Table 1). Scatter diagrams, with regression lines, show two of the best morphometric characters: *G. bicarinatus* has a smaller orbit (Fig. 3), and a longer first dorsal fin base (Fig. 4).

Meristic characters

Numbers of fin rays (first dorsal spines, second dorsal rays, dorsal finlets, anal rays, anal finlets, and pectoral rays), gill rakers, and teeth on the upper and lower jaws are systematically valuable in *Grammatorcynus*. They are discussed in the relevant osteological sections of the paper.

Soft anatomy

Viscera Emphasis was placed on the appearance of the viscera in ventral view, after removal of an oval segment of the belly wall. Previous descriptions of the viscera of *Grammatorcynus* include Kishinouye (1923), Silas (1963), and Collette and Russo (1985b).

The anterior end of the liver abuts the transverse septum anteriorly in the body cavity. The liver has three lobes. The right and left lobe are longer than the middle lobe, with the right lobe being longest (Fig. 5c–d). The liver is similar in shape in *Scomberomorus*,

Table 1
Morphometric comparison of *Grammatorcynus bilineatus* and *G. bicarinatus*.

	G. bicarinatus					*G. bilineatus*				
Character	*N*	Min	Max	Mean	SD	*N*	Min	Max	Mean	SD
Fork length (thousandths)	10	306	825	551	186	64	226	575	408	77
Snout-A	7	596	626	613	10	61	581	641	606	13
Snout-2D	7	536	558	549	8	61	528	619	547	14
Snout-1D	9	267	301	280	11	64	276	322	295	9
Snout-P2	9	234	272	253	13	63	236	306	258	12
Snout-P1	9	197	230	216	10	63	199	245	226	9
P1-P2	10	91	255	115	49	62	90	135	101	7
Head length	10	191	223	207	9	64	197	236	218	7
Max. body depth	8	177	210	192	13	57	164	234	196	14
Max. body width	8	105	129	115	8	56	91	136	114	9
P1 length	10	118	137	127	5	63	106	142	126	8
P2 length	10	65	81	74	5	63	70	87	77	3
P2 insertion-vent	7	313	345	332	12	62	262	354	328	14
P2 tip-vent	9	238	281	260	15	61	228	275	251	10
Base 1D	9	253	272	264	6	63	207	261	235	11
Height 2D	6	97	111	103	5	54	82	116	98	7
Base 2D	10	76	102	90	8	62	68	118	102	9
Height A	10	94	116	104	8	49	67	114	94	9
Base A	9	66	91	80	8	63	73	105	87	7
Snout (fleshy)	10	77	88	81	4	64	58	90	80	5
Snout (bony)	10	64	76	70	4	64	60	80	72	5
Maxilla length	10	91	110	102	6	63	89	108	98	5
Postorbital	10	87	98	92	3	62	78	98	91	3
Orbit (fleshy)	10	31	46	37	5	64	40	60	49	4
Orbit (bony)	10	48	69	59	8	64	53	88	68	6
Interorbital	9	59	71	64	4	62	56	74	62	3
2D-caudal	9	412	475	454	27	60	427	496	470	13
Head length (thousandths)	11	64	165	112	33	64	50	126	89	17
Snout (fleshy)	11	379	410	393	8	64	248	397	366	21
Snout (bony)	11	313	356	340	16	64	281	357	329	16
Maxilla length	11	475	510	495	12	63	420	480	448	15
Postorbital	11	412	471	446	17	62	350	450	419	15
Orbit (fleshy)	11	164	211	179	16	64	191	257	226	14
Orbit (bony)	11	238	319	282	25	64	252	381	313	24
Interorbit	10	274	322	308	13	62	253	327	283	13

but in *Acanthocybium* the right and left lobes are about the same size. Two efferent vessels lead directly from the anterior surface of the liver into the sinus venosus.

The stomach is sometimes visible in ventral view, partially covered by the liver and caecal mass, but often completely hidden. Stomach contents included crustaceans and small fishes.

The pyloric portion of the intestine arises from the anterior end of the stomach, where the main branches of the pyloric caeca join the intestine. The caeca branch and form a dense dendritic conglomeration, the caecal mass. The intestine continues posteriorly as a simple straight tube to the anus. A straight intestine is also found in *Acanthocybium* (Fig. 5b) and *S. niphonius*, but all other species of *Scomberomorus* have folds (2 or 4) in the intestine (Fig. 5a).

Osteology

The osteological description is divided into five sections: skull, axial skeleton, dorsal and anal fins, pectoral girdle, and pelvic girdle. Osteological terminology and organization generally follow that of Collette and Russo (1985b).

Skull Description of the skull is presented in two sections: neurocranium (Figs. 6–9) and branchiocranium.

Neurocranium Following a general description of the neurocranium, the four major regions are discussed: ethmoid, orbital, otic, and basicranial.

General characteristics In dorsal view (Fig. 6), the neurocranium of *Grammatorcynus* is more or less triangular in shape, narrow at its anterior margin,

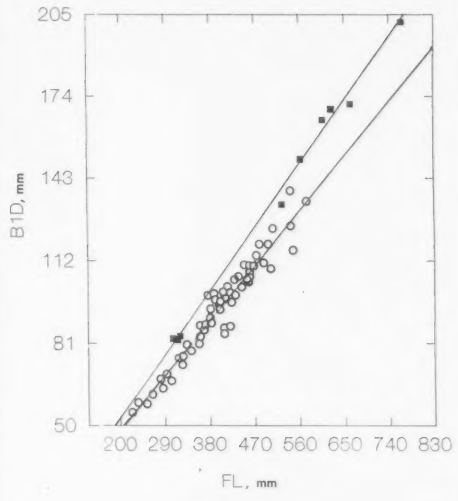

Figure 4
Length of first dorsal fin base (B1D) compared with fork length (FL) in *Grammatorcynus*. Open circles = *G. bilineatus*, squares = *G. bicarinatus*.

widening posteriorly. It is intermediate in shape between the elongate neurocranium of *Acanthocybium*, *Scomber*, and *Rastrelliger*, and the shorter, wider neurocranium of *Thunnus*. The posterodorsal surface is marked by a median ridge (supraoccipital crest), with two parallel ridges on either side. These five thin ridges of bone form six grooves, three on each side: dilator (very shallow), temporal (quite deep), and supratemporal (most easily seen in lateral view) (Allis 1903:49).

The median ridge originates just posterior to the thin, oval pineal foramen located between the posterior, median edges of the frontal bones. This ridge becomes larger posteriorly, and forms the supraoccipital crest. Internal or temporal ridges originate at the posterior portion of the frontals (midlevel of the orbit), continuing posteriorly to the epiotic. External or pterotic ridges also originate near the posterior margin of the frontals, continuing posteriorly to the pterotic.

Neurocrania of the two species of *Grammatorcynus* differ in size, relative to fork length. Length of the neurocranium, measured from the anterior tip of the vomer to the posterior margin of the basioccipital, is slightly longer in *G. bilineatus* (14–16% FL) than in *G. bicarinatus* (13% FL).

Ethmoid region This region is composed of the ethmoid, lateral ethmoid, and vomer. The nasal bone lies lateral to the ethmoid and lateral ethmoid, and, therefore, is included here.

Ethmoid The ethmoid (dermethmoid) has a smooth flat dorsal surface that is partially overlapped by the frontals. It connects ventrally to the vomer, posteriorly to the lateral ethmoids, and anterolaterally to the nasals. Its anterior border is nearly straight, with an anteromedian projection, unlike the relatively smooth, concave border in *Scomberomorus* and *Acanthocybium*. The ethmoid is clearly visible in dorsal view (Fig. 6), and is wider, relative to the length of the neurocranium, in *G. bicarinatus* (width 25–28% of length) than in *G. bilineatus* (19–21%).

Lateral ethmoid The lateral ethmoids (parethmoids) are massive, paired bones that extend downward from the middle region of the frontals and form the anterior margin of the orbit and the posterior and mesial walls of the nasal cavity. The ventral surface of the lateral ethmoid bears an articulating surface for the palatine, and the posterolateral process serves as an articulation surface for the lachrymal. The lateral expansion of the bone is greater in *G. bicarinatus* (45–50% of neurocranium length) than in *G. bilineatus* (39–42%) (Fig. 8).

Vomer The anterior process of the vomer bears a circular or oval patch of fine teeth on its ventral surface. Its pointed posterior end is firmly ankylosed dorsally with the parasphenoid. The anterior process is wider in *G. bicarinatus* (16–18% of neurocranium length) than in *G. bilineatus* (13–15%) (Fig. 8).

Nasal The nasal bones are flat, elongate bones that articulate with the lateral edge of the frontals. They project out beyond the ethmoid and, from a dorsal view, reach about as far anteriorly as the vomer. There is no such projection of the nasal bones in *Scomberomorus* or *Acanthocybium*. Length divided by width is 2.8–3.4 in *Grammatorcynus*, which is intermediate between the ranges of *Scomberomorus* (2.0–3.1) and *Acanthocybium* (3.1–4.2). The anterior end of the bone forms a short, slightly angled arm. No differences were found between the nasals of the two species of *Grammatorcynus*.

Orbital region The orbit (Fig. 7) is surrounded by the posterior wall of the lateral ethmoid, the ventral side of the frontal, the pterosphenoid, sphenotic, prootic, suborbital, and lachrymal bones. The left and right orbits are partially separated by the basisphenoid. The sclerotic bones enclose the eyeballs.

The orbit of *G. bilineatus* is larger than that of *G. bicarinatus* (Fig. 7), reflecting the difference in orbit length (Fig. 3). The maximum height of the orbit measured from the parasphenoid to the pterosphenoid is 24–25% of neurocranium length in *G. bilineatus* vs. 16–17% in *G. bicarinatus*. Orbit length in *G. bilineatus* is 51–54% of neurocranium length vs. 47–49% in *G. bicarinatus*.

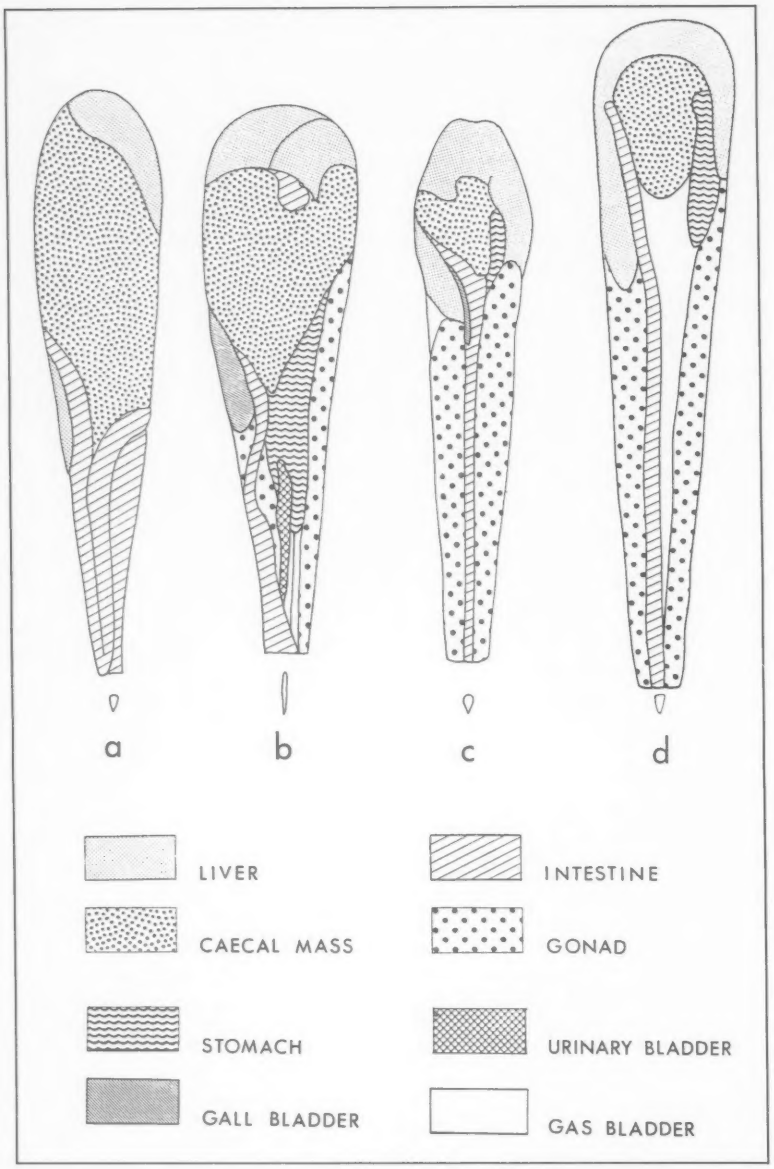

Figure 5
Ventral view of viscera. (a) *Scomberomorus maculatus*, Georgia, 290 mm FL; (b) *Acanthocybium solandri*, Campeche Banks, Mexico, 1280 mm FL; (c) *Grammatorcynus bilineatus*, Marshall Is., 424 mm FL; (d) *G. bicarinatus*, Australia.

Frontal The paired frontals form the largest portion of the dorsal surface of the neurocranium. A small, elongate oval pineal opening is present between the posterior ends of the frontals. A larger and more irregular foramen is present in *Acanthocybium*, but *Scomberomorus* lacks this opening (Collette and Russo 1985b: figs. 11–12).

In *Scomberomorus* and *Acanthocybium*, the frontals form a median ridge that increases in height posteriorly and joins the supraoccipital crest. *Grammatorcynus* lacks this ridge and the supraoccipital crest begins posterior to the pineal opening, giving the top of the skull a much flatter appearance than in the other two genera.

In ventral view (Fig. 8), the left and right frontals articulate with the pterosphenoids at the anterior end of a median opening into the brain cavity. The ridge around the anterior end of this space forms a point and

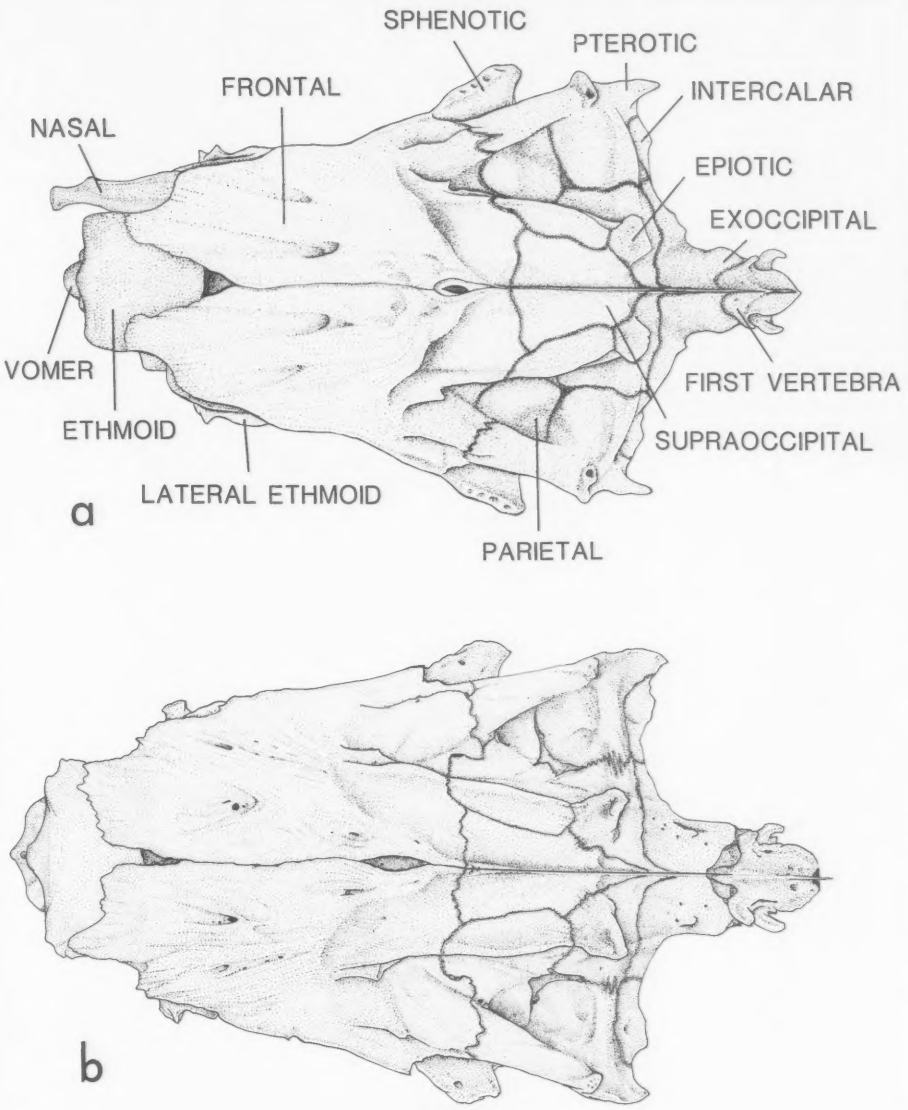

Figure 6

Dorsal view of skulls in *Grammatorcynus*. (a) *G. bilineatus*, Scott Reef, Timor Sea, 453 mm FL; (b) *G. bicarinatus*, Western Australia, Exmouth Gulf, 765 mm FL.

extends almost to the ethmoid in *G. bilineatus*. The ridge curves around the anterior end of the space and ends distinctly more posteriorly in *G. bicarinatus*. This difference cannot be seen in the ventral view of the skulls (Fig. 8) because the median part of the opening is obscured by the parasphenoid, so a separate outline figure has been made (Fig. 9).

Pterosphenoid The pterosphenoids (alisphenoids) form the posterodorsal margin of the orbit. They serve as the base for the median basisphenoid, and abut the prootics posteriorly and the frontals and sphenotics laterally.

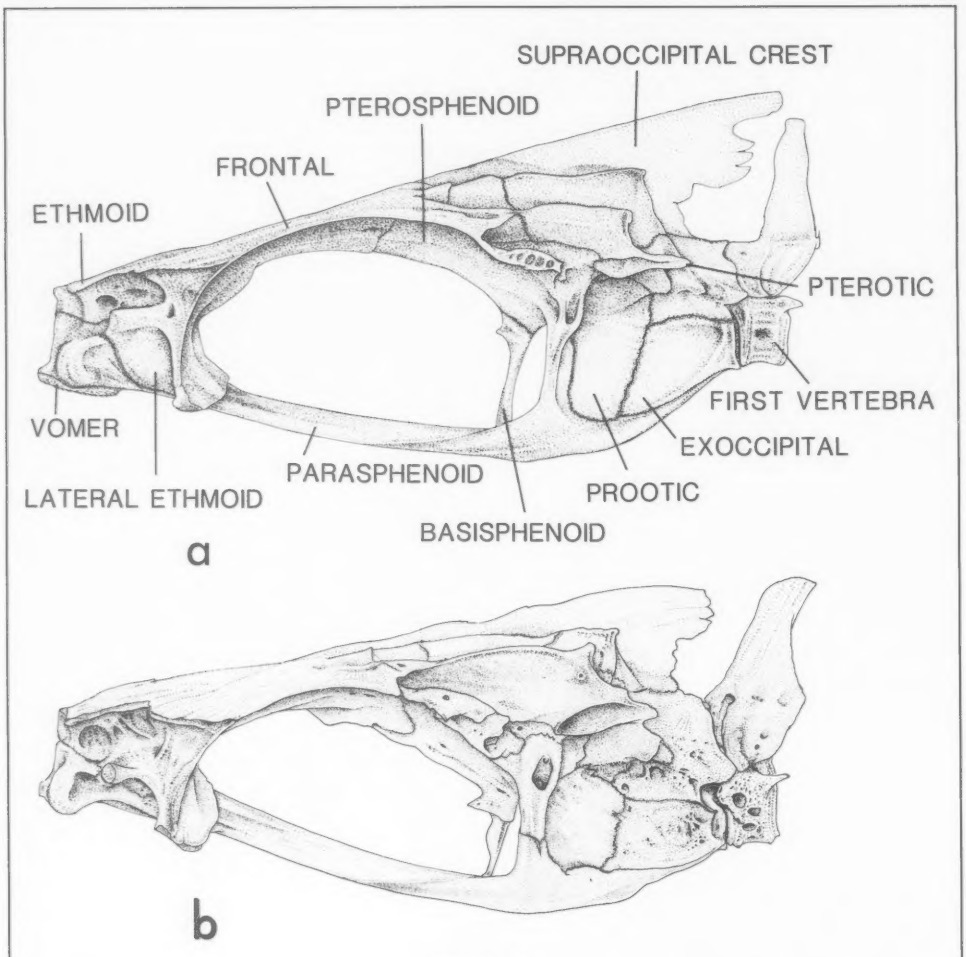

Figure 7

Lateral view of skulls in *Grammatorcynus*. (a) *G. bilineatus*, Scott Reef, Timor Sea, 453 mm FL; (b) *G. bicarinatus*, Western Australia, Exmouth Gulf, 765 mm FL.

Sclerotic The sclerotic bones consist of two thickened, semicircular segments connected by cartilage on the inner surface and by corneal membranes on the outside. The sclerotic bones of *Grammatorcynus* are relatively larger and thinner compared with *Scomberomorus* and *Acanthocybium*.

Basisphenoid The basisphenoid is a small, median, Y-shaped bone that connects the prootics and pterosphenoids dorsally with the parasphenoid ventrally (Fig. 7). The dorsal compressed vertical base bears a slight anterior process, but no posterior process. This is similar to the condition in *Scomberomorus*, but the anterior process is much shorter in *Grammatorcynus*. The basisphenoid is longer in *G. bilineatus* since the height of the orbit is greater in this species compared with *G. bicarinatus*.

Infraorbitals The bones of the infraorbital series (Fig. 10) enclose the infraorbital branch of the lateral sensory canal system. The canal enters the infraorbital series at what is usually considered the last element (dermosphenotic), and continues around the orbit, terminating on the first infraorbital (lachrymal).

The lachrymal, the first and largest element, is elongate with a mesially-directed articular process just anterior to the middle of the bone. It covers part of the maxilla, and articulates with the lateral ethmoid

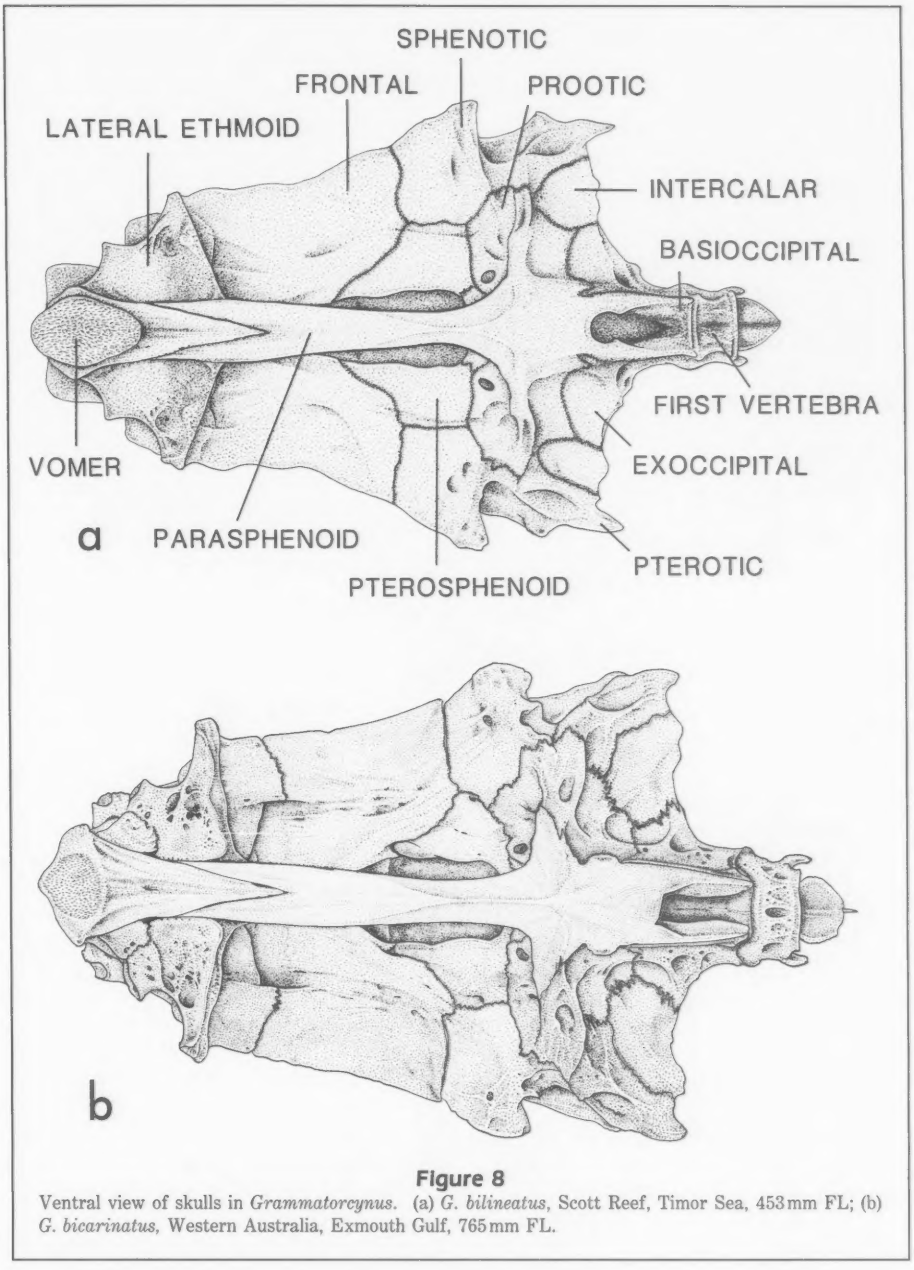

Figure 8

Ventral view of skulls in *Grammatorcynus*. (a) *G. bilineatus*, Scott Reef, Timor Sea, 453 mm FL; (b) *G. bicarinatus*, Western Australia, Exmouth Gulf, 765 mm FL.

dorsally by the articular process. The process is larger in *G. bicarinatus*, making the lachrymal wider (30–35% of total bone length) than in *G. bilineatus* (27–30%). The anterior portion has a small notch in it, much more indistinct than the forked anterior region in *Scomberomorus* (Fig. 10a). The posterior region is distinctly forked, with the ventral arm being wider and longer than the dorsal arm.

The second infraorbital connects to the forked posterior region of the lachrymal. It is a small, elongate bone. The third infraorbital is an elongate, tubular bone that connects to the posterior portion of the second

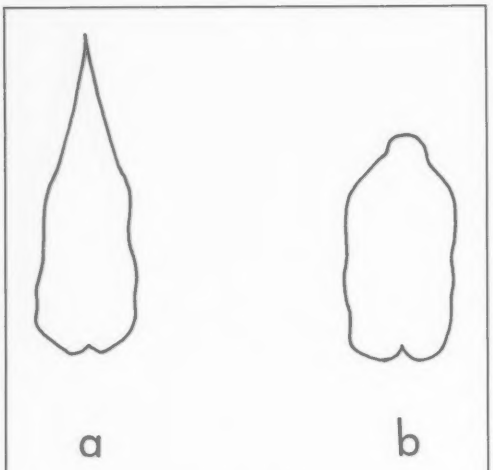

Figure 9
Outline of pterosphenoid opening on ventral side of skull in *Grammatorcynus*. (a) *G. bilineatus*, Scott Reef, Timor Sea, 453 mm FL; (b) *G. bicarinatus*, Western Australia, Exmouth Gulf, 765 mm FL.

infraorbital. It has a large, mesial, shelflike extension (subocular shelf of Smith and Bailey 1962). The fourth through penultimate elements total 13 in a specimen of *G. bilineatus* (Fig. 10c), are small, and are easily lost with cheek scales during dissection. No special effort was made to compare these bones in the two species.

Otic region This region encloses the otic chamber inside the skull, and is formed by the parietal, epiotic, supraoccipital, prootic, pterotic, sphenotic, and intercalar (opisthotic) bones.

Parietals The parietals articulate with the frontals anteriorly, the supraoccipital mesially, the pterotics laterally, sphenotics ventrally, and epiotics posteriorly. There is a short inner lateral crest on the parietals and epiotics, but this crest does not originate on the frontals as it does in *Scomberomorus* and *Acanthocybium*.

Epiotics The epiotics are irregular bones bounded by the parietals anteriorly, the supraoccipital mesially, the exoccipitals posteriorly, and the pterotics laterally. The medial process of the posttemporal bone attaches to a distinct roughened process on the posterior corner of the epiotic. *Scomberomorus* has a roughened area at the posterior end of the fronto-epiotic crest rather than a distinct process.

Supraoccipital The supraoccipital forms the dorsomedian portion of the posterior end of the neurocranium. It bears a well-developed crest that continues forward onto the parietals but stops at the pineal opening instead of extending all the way forward onto the frontals as in *Scomberomorus*. The supraoccipital consists of a thin crest on a roughly hexagonal base. The crest extends down over the exoccipitals along the median line where the dorsal walls of the exoccipitals suture with each other. It extends posteriorly over the first vertebral centrum (Fig. 7).

Prootics In ventral view (Fig. 8), the prootics connect with all the bones in the posterior part of the neurocranium. Each prootic is bordered ventrally by the parasphenoid; posteriorly by the basioccipital, exoccipital, and intercalar; laterally by the pterotic and sphenotic; and anteriorly by the parasphenoid and basisphenoid. The prootics are irregular in shape and meet each other along the ventromedian line of the brain case to form the posterior portion of the myodome.

Pterotics The pterotics form the lateral posterior corners of the neurocranium. Each pterotic is produced posteriorly to form a spine. A pterotic ridge continues anteriorly onto the parietal, but does not extend onto the posterior part of the frontal as it does in *Scomberomorus*. In ventral view (Fig. 8), the pterotics articulate with the sphenotics anteriorly and the prootics and intercalars medially.

Sphenotics The sphenotics form the most posterior dorsolateral part of the roof of the orbit. They continue the outer lateral shelf from the frontals, and articulate with the pterosphenoid medially and the prootic and pterotic posteriorly. A fossa at the juncture of the sphenotic and pterotic receives the anterior condyle of the hyomandibula. In dorsal or ventral view, the distance between the tips of the two sphenotics is the widest portion of the cranium, 60–67% the length of the neurocranium in *Grammatorcynus*.

Intercalars The intercalars (opisthotics) are flat bones that form part of the posterior border of the neurocranium interposed between the pterotics and exoccipitals. The anterior portion on the dorsal surface is concealed by the overlapping pterotic, thus exposing the bone on the dorsal surface less than on the ventral surface (compare in Figures 6 and 8). Each intercalar has a roughened area on its dorsal surface to receive the lateral arm of the posttemporal. There is no posterior projection from the intercalars in *Grammatorcynus* or *Acanthocybium* as there is in eight species of *Scomberomorus*, such as *S. commerson* and *S. concolor* (Collette and Russo 1985b:figs. 11a and 12b).

Basicranial region This region consists of the parasphenoid, basioccipital, and exoccipital bones, and forms the posteroventral base of the skull.

Parasphenoid The parasphenoid is a long, cross-shaped bone. It articulates with the vomer anteriorly and forms the ventral axis of the skull. It also

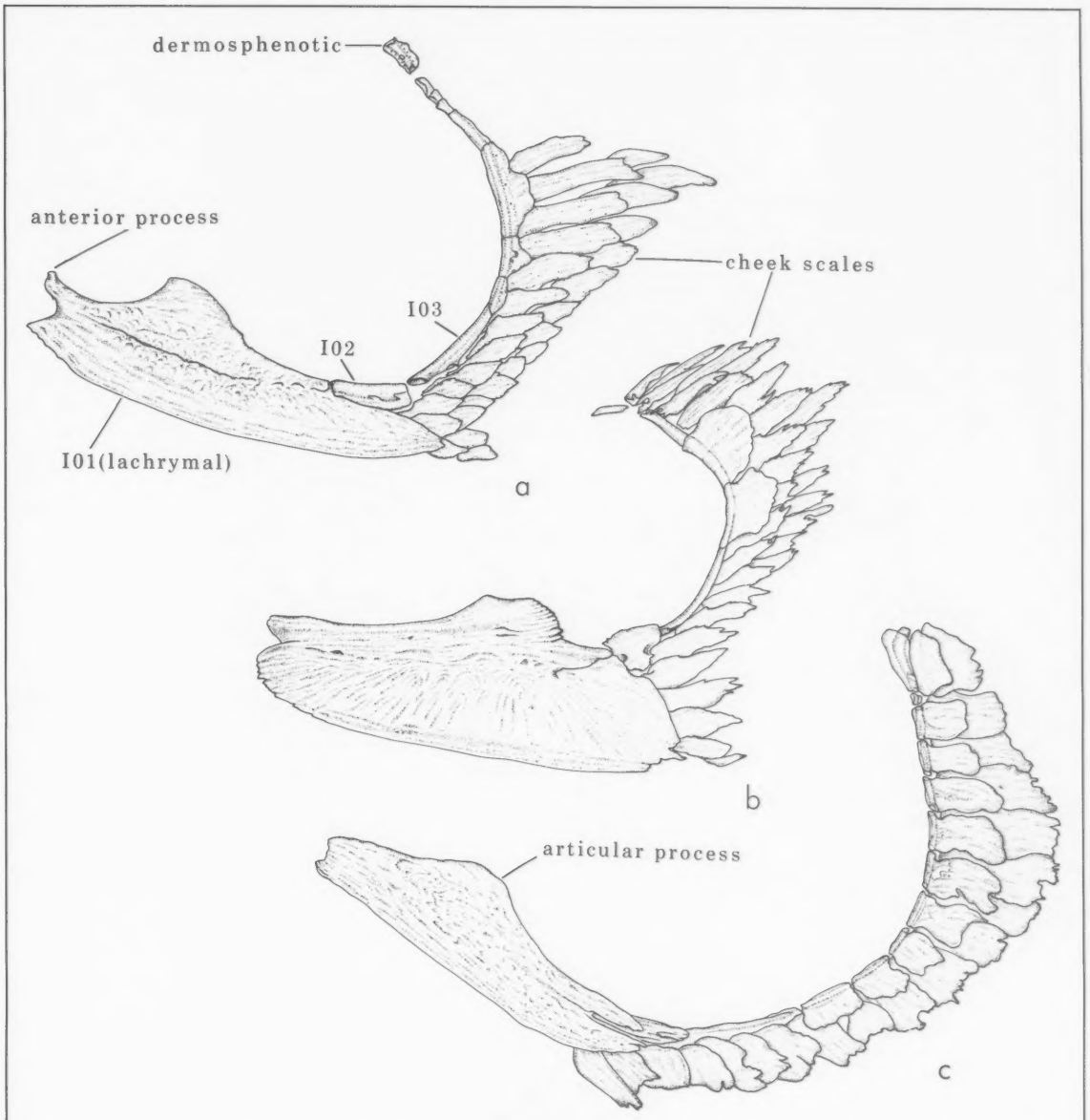

Figure 10

Left infraorbital bones in lateral view. (a) *Scomberomorus maculatus*, Cape Hatteras, NC, 534 mm FL; (b) *Acanthocybium solandri*, Revillagigedos Is., 1068 mm FL; (c) *Grammatocrynus bilineatus*, Timor Sea, 453 mm FL.

forms the ventral border of the orbits and connects with the lateral ethmoids, basisphenoid, prootics, and basioccipital bones dorsally. The lateral wings of the parasphenoid extend dorsolaterally along the ventral ridge of the prootic bones on either side, and have pointed ends which form part of the anteroventral wall of the posterior myodome. Posteriorly, the parasphenoid bifurcates into two lateral flanges that attach dorsally to the corresponding posteroventral flanges of the basioccipital bone, and surround the posterior

opening of the posterior myodome. These flanges are longer in *G. bilineatus* (18–21% of neurocranium length) than in *G. bicarinatus* (14%), making the posterior opening of the posterior myodome larger in *G. bilineatus* (Fig. 8). A ventrally projecting median keel is present in the area anterior to the origin of the lateral flanges. In ventral view, the parasphenoid narrows posteriorly until near the region of the median keel, where it widens slightly before the lateral wings. The anterior portion and the region just anterior to the lateral wings are about equal in width. In *Grammatorcynus*, the shaft of the parasphenoid is narrower than that of *Scomberomorus* and *Acanthocybium*. In *G. bilineatus*, the contour of the parasphenoid is concave, making the orbit larger than in *G. bicarinatus*, in which the parasphenoid is flat (Fig. 7).

Basioccipital The basioccipital has lateral flanges on either side of the skull and forms the roof and lateral walls of the posterior myodome. The lateral flanges expand ventrally to meet the flat posterior flanges of the parasphenoid. Anteriorly, the basioccipital is attached to the prootics and dorsally with the exoccipitals. The first vertebral centrum attaches to the posterior surface of the basioccipital.

Exoccipital The exoccipitals connect the skull with the first vertebra dorsally. The exoccipital articulates with the epiotic and supraoccipital bones anterodorsally, the intercalars laterally, and with the other exoccipital posterodorsally. In ventral view, the exoccipital articulates with the prootic anteriorly, basioccipital ventromedially, and intercalar laterally. In posterior view, the foramen magnum is framed by the exoccipitals.

Branchiocranium The branchiocranium is divided into five sections: mandibular arch, palatine arch, hyoid arch, opercular apparatus, and branchial apparatus.

Mandibular arch The mandibular arch is composed of the upper jaw (premaxilla, maxilla, and supramaxilla) and the lower jaw (dentary, angular, and retroarticular). Teeth are borne on the premaxilla and dentary, and the number of teeth on these bones differs between species.

Dentition Long, thin, slightly laterally compressed teeth are present in a single row in the upper and lower jaws of *Grammatorcynus*. *Scomberomorus* has large, triangular, laterally compressed teeth similar to those of *Acanthocybium*, which are blunter and more tightly compressed. The length of the jaw teeth differs between the species: *G. bicarinatus* has longer teeth than *G. bilineatus* (maximum length 6% vs. 4% dentary length). The number of jaw teeth in *Grammatorcynus* also varies. Teeth are often broken or lost, so the range in mean tooth count may not reflect accurately the actual number of teeth. However, the maximum number of teeth is useful. *Grammatorcynus bicarinatus* has a lower maximum tooth count on its upper jaw than *G. bilineatus* (25 vs. 37), and the same is true of the lower jaw, (23 vs. 32; Table 2). The maximum number of jaw teeth present in *Scomberomorus* is slightly higher than *G. bilineatus* (39, range 5–39 in the upper jaw; and 37, range 4–37 in the lower jaw). Collette and Russo (1985b) noted that in *Scomberomorus*, the species with the fewest teeth has the fewest gill rakers and the species with the most teeth has the most gill rakers. There is a similar correlation in *Grammatorcynus*: *G. bilineatus* also has more gill rakers (18–24 vs. 12–15 in *G. bicarinatus*).

Premaxilla The premaxilla (Fig. 11) is a long, curved bone with an arrowhead-shaped anterior end that extends dorsally and posteriorly as an ascending process. The posterior shank of the premaxilla is elongate and bears a row of 14–37 long, thin teeth on its ventral margin. There are two articular facets for the overlying maxilla at the junction of the posterior margin of the ascending process with the shank portion. Ascending processes of both premaxillae are closely approximated to each other mesially and fit into the median groove of the ethmoid bone. The ascending process forms an angle of 55–67° with the shank: *G. bilineatus* has a slightly larger angle (60–67°, Fig. 11c) than *G. bicarinatus* (55–58°, Fig. 11d). *Grammatorcynus* has a larger angle than any species of *Scomberomorus* except *S. guttatus* (60–61°). The ascending process is 33–40% of the total length of the premax-

Table 2
Number of teeth in upper and lower jaws of *Grammatorcynus*.

Species	Side	Min	Max	$\bar{x}$	Overall $\bar{x}$	N
Upper jaw						
G. bilineatus	L	14	37	23.5	24.0	39
	R	14	36	24.5		
G. bicarinatus	L	14	25	20.5	20.7	8
	R	17	24	20.9		
Lower jaw						
G. bilineatus	L	12	32	18.6	18.8	36
	R	14	30	19.1		
G. bicarinatus	L	16	20	17.5	17.5	7
	R	15	23	17.6		

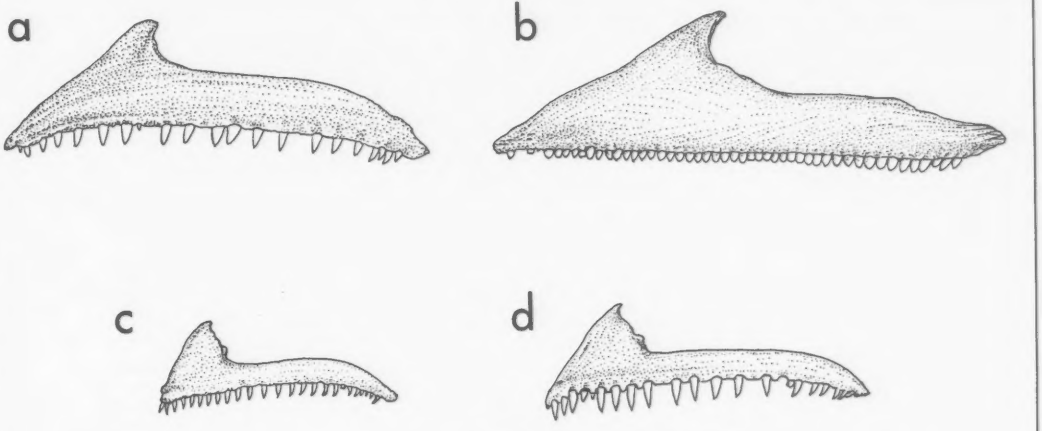

Figure 11
Left premaxillae in lateral view. (a) *Scomberomorus lineolatus*, Cochin, India, 786 mm FL, 2×; (b) *Acanthocybium solandri*, Miami, FL, 1403 mm FL, 1×; (c) *Grammatorcynus bilineatus*, Marshall Is., 424 mm FL, 2×; (d) *G. bicarinatus*, Great Barrier Reef, 563 mm FL.

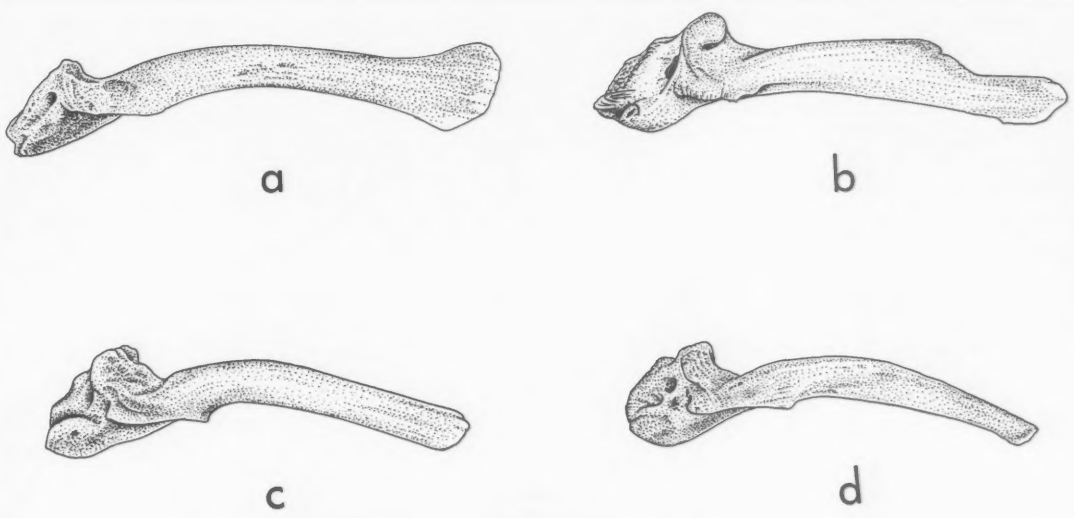

Figure 12
Left maxillae in lateral view. (a) *Scomberomorus munroi*, New Guinea, 512 mm FL, 2×; (b) *Acanthocybium solandri*, Miami, FL, 1403 mm FL, 1×; (c) *Grammatorcynus bilineatus*, Timor Sea, 453 mm FL, 2×; (d) *G. bicarinatus*, Great Barrier Reef, 563 mm FL.

illa. This is a small percentage relative to *Acanthocybium* (50%, Fig. 11b). *Scomberomorus* is intermediate (31–48%, Fig. 11a).

Maxilla The maxilla (Fig. 12) is a long, curved bone surmounting the premaxilla dorsolaterally by means of an anterior head and ventral sulcus. The head consists of a thick, massive inner condyle and a small lateral process. The inner condyle possesses a prominent knob at its dorsolateral aspect that fits into the articular surface of the vomer, and an anterior, deep

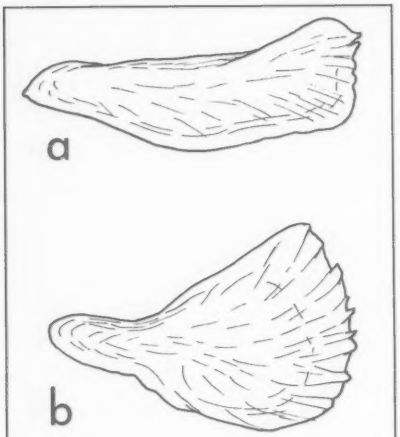

Figure 13
Supramaxillae in lateral view in *Grammatorcynus*. (a) *G. bilineatus*, Western Australia, 460 mm FL; (b) *G. bicarinatus*, Australia, 625 mm FL.

concavity facing the inner wall of the premaxilla. Immediately posterior to the head is a shallow depression that receives the anterior articulating process of the palatine. The shank of the maxilla is narrow and somewhat flattened. It remains at a relatively constant height along its entire length, unlike the shank of *Scomberomorus* (Fig. 12a) in which the posterior end of the shank expands into a flat plate. The posterior end is distinctly thinner than the middle of the shank in *Acanthocybium* (Fig. 12b).

The head of the maxilla is longer (25–29% of total maxilla length) in *Grammatorcynus* than in any species of *Scomberomorus* (18–25%) but shorter than in *Acanthocybium* (33%, Fig. 12b).

The height of the posterior end of the shank, relative to the total length of the maxilla, is less in *G. bicarinatus* (6–8%, Fig. 12d) than in *G. bilineatus* (8–11%, Fig. 12c). *Grammatorcynus bilineatus* is similar to those species of *Scomberomorus* that have the least well-developed (lowest) posterior expansions: *S. multiradiatus* (8–9%) and *S. sinensis* (9–11%). Other species of *Scomberomorus*, such as *S. munroi* (Fig. 12a), have larger posterior expansions (11–15%).

Supramaxilla The supramaxilla (Fig. 13) covers the posterior end of the maxilla. It is a small, flat bone that is expanded posterodorsally. The expansion is much more pronounced in *G. bicarinatus* (59–76% of bone length, Fig. 13b) than in *G. bilineatus* (35–42%, Fig. 13a).

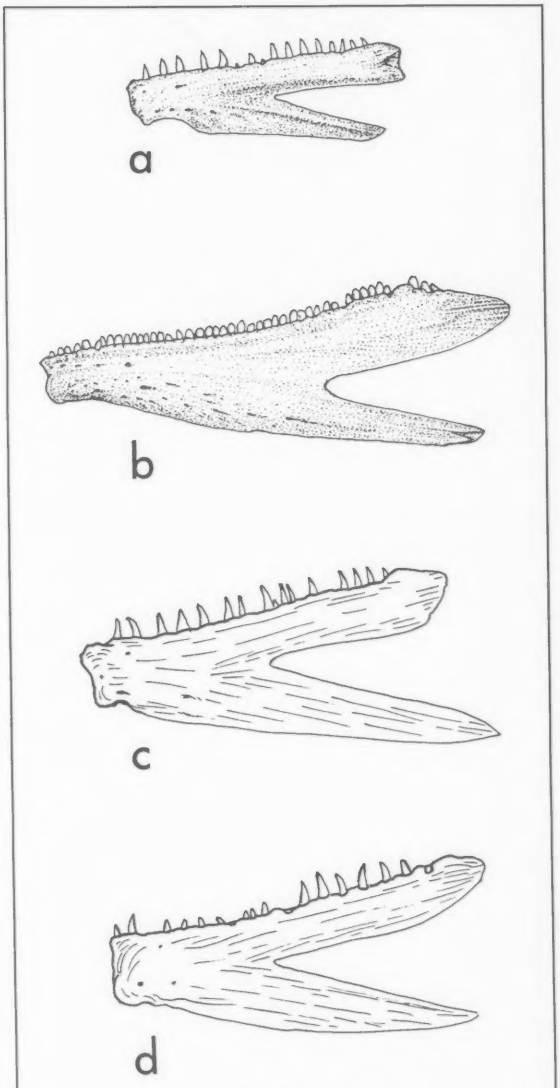

Figure 14
Left dentaries in lateral view. (a) *Scomberomorus semifasciatus*, Port Moresby, New Guinea, 510 mm FL, 2×; (b) *Acanthocybium solandri*, Miami, FL, 1403 mm FL, 1×; (c) *Grammatorcynus bilineatus*, Marshall Is., 424 mm FL; (d) *G. bicarinatus*, Western Australia, 765 mm FL, 1×.

Dentary The dentary (Fig. 14) is laterally flattened and bears a single row of 12–32 long, thin teeth on the dorsal margin. Posteriorly, the dentary has two arms of the same relative width (the ventral arm may be slightly narrower), unlike *Scomberomorus* (Fig. 14a) and *Acanthocybium* (Fig. 14b) where the ventral arm

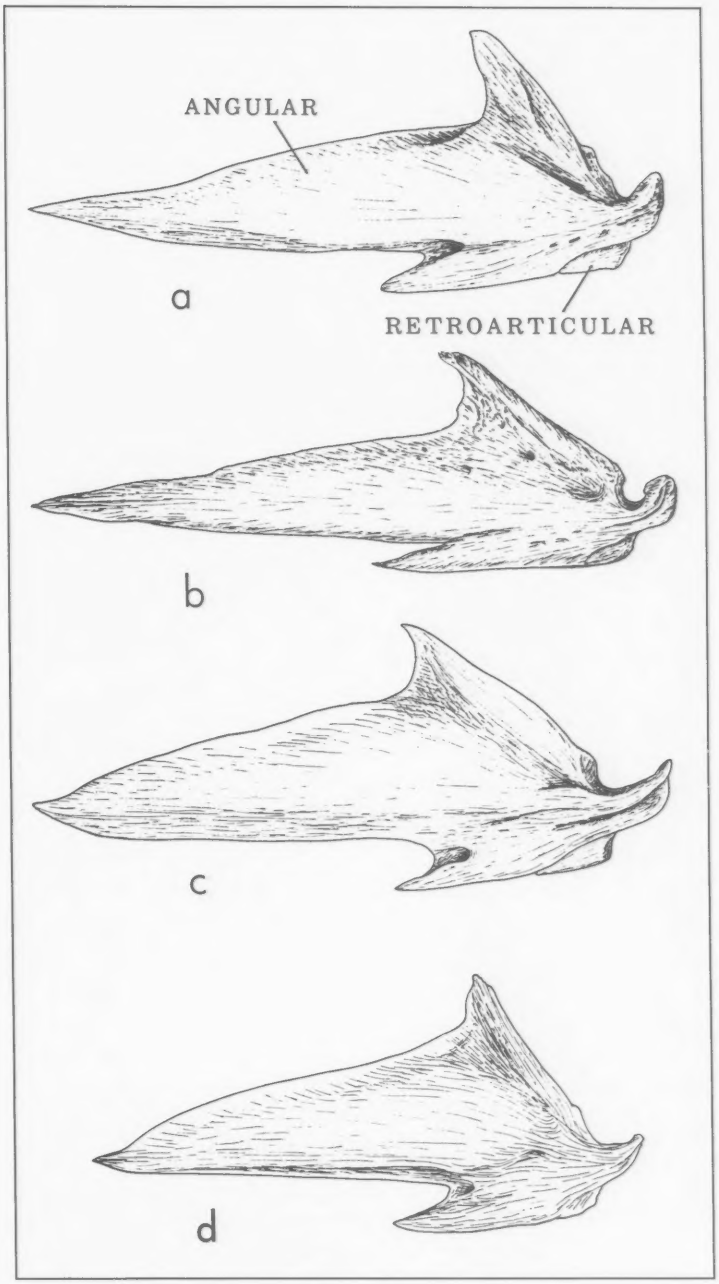

Figure 15
Left angulars and retroarticulars in lateral view. (a) *Scomberomorus semifasciatus*, Port Moresby, New Guinea, 510 mm FL, 3.5×; (b) *Acanthocybium solandri*, Miami, FL, 1403 mm FL, 1×; (c) *Grammatorcynus bilineatus*, Papua New Guinea, 382 mm FL, 4.5×; (d) *G. bicarinatus*, Western Australia, 765 mm FL, 2×.

is much narrower than the dorsal arm. The length of the dentary from its anterior margin to the tip of the ventral arm is 97–109% of the length of the dorsal arm. The ventral arm is longer in *G. bilineatus* (104–109% of dorsal arm length, Fig. 14c) than in *G. bicarinatus* (97–98%, Fig. 14d). The ventral arm is longer in *Grammatorcynus* than it is in *Scomberomorus* (86–97%) and *Acanthocybium* (91–96%). Species of *Grammatorcynus* and *Scomberomorus* have a notch on the anteroventral margin of the dentary that is absent in *Acanthocybium*. *Acanthocybium* has a prominent notch on the anterior margin of the dentary that is indistinct or absent in *Grammatorcynus* and *Scomberomorus*.

Angular (Fig. 15) The triangular anterior end of the angular (frequently called articular) fits into the dentary anteriorly. The posterior end of the angular bears three large processes: the dorsal process, directed forward and upward; the ventral process, directed forward; and the posterior process, directed backward and upward. The posterior process is hooked and carries a transverse articular facet for the quadrate. The length from the tip of the posterior process to the tip of the dorsal process is 40–47% of the total length of the bone. The length from the tip of the posterior process to the tip of the ventral process is slightly longer, 44–52% of bone length. The depth of the angular, measured from the tip of the dorsal process to the tip of the ventral process, is 36–48% of the total length, with the depth of *G. bicarinatus* being greater (44–48%, Fig. 15d) than that of *G. bilineatus* (36–41%, Fig. 15c). The ventral process is approximately as long or longer than the dorsal process in *Grammatorcynus*. In *G. bilineatus*, the ventral process is 84–105% of the length of the dorsal process, and in *G. bicarinatus* the ventral process is longer than the dorsal process (153–200%). Only *Acanthocybium* (99–148%, Fig. 15b), *S. commerson* (99–162%), and *S. queenslandicus* (115–136%) also have a

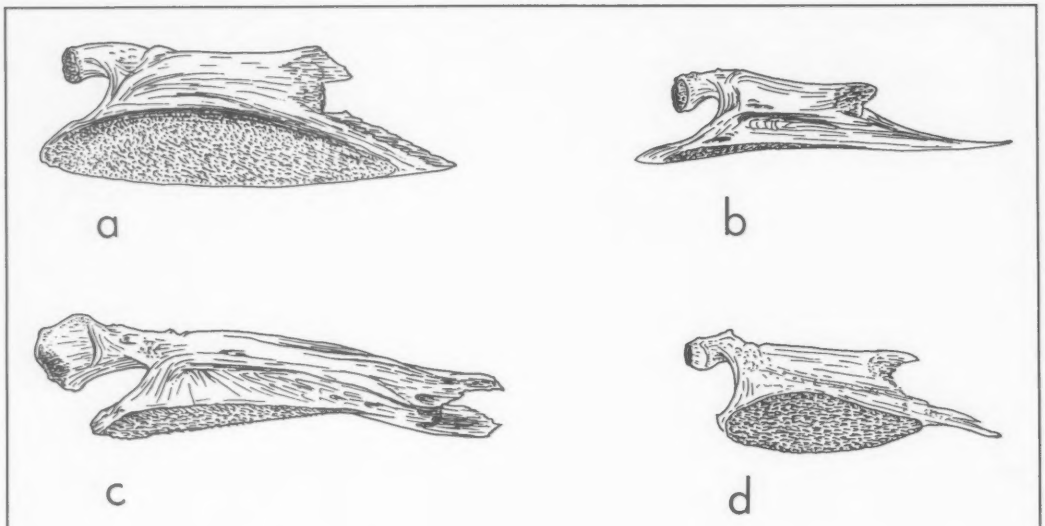

Figure 16
Left palatines in lateral view, slightly rotated to better show tooth patches. (a) *Scomberomorus semifasciatus*, New Guinea, 740 mm FL, 2×; (b) *Scomberomorus commerson*, New South Wales, 1155 mm FL, 1×; (c) *Acanthocybium solandri*, Miami, FL, 1403 mm FL, 1×; (d) *Grammatorcynus bilineatus*, Timor Sea, 453 mm FL, 2×.

ventral process as long or longer than the dorsal process. All other species of *Scomberomorus* (Fig. 15a) have ventral processes that are relatively shorter.

Retroarticular (Fig. 15) The retroarticular bone (frequently called the angular) is rhomboid and attached firmly, but not fused, to the posteroventral margin of the angular. No differences were found between the retroarticulars of the species of *Grammatorcynus*.

Palatine arch The palatine arch consists of four pairs of bones in the roof of the mouth: palatine, ectopterygoid, entopterygoid, and metapterygoid.

Palatine The palatine is forked both posteriorly and anterolaterally (Fig. 16). The dorsal branch of the anterolateral fork is hooked, and its anterior end articulates with a facet on the maxilla, immediately ventral to the nasal. The ventral branch appears almost indistinct in comparison with the longer ventral branch of *Acanthocybium* (Fig. 16c) and the even longer ventral branch of *Scomberomorus* (Fig. 16a–b). In *Scomberomorus*, the ventral branch is longer than the dorsal branch, which is not true of *Grammatorcynus* or *Acanthocybium*. The distance from the anterior end of the ventral branch to the end of the external branch divided by the distance from the tip of the dorsal hook to the end of the external branch is 118–125% in *Grammatorcynus*, 112–121% in *Acanthocybium*, and only 87–107% in *Scomberomorus*. The distance from the tip of the dorsal hook to the tip of the inner branch divided by the distance to the tip of the outer branch is 71–75% in *Grammatorcynus*, 54–84% in *Scomberomorus*, and 97–99% in *Acanthocybium*. Hence, *Acanthocybium* differs from both *Grammatorcynus* and *Scomberomorus* in that its posteriorly directed inner branch is almost as long as the outer branch. The tooth patch is short and wide in *Grammatorcynus* (Fig. 16d), more so in *G. bicarinatus* (width 38–42% of length, Fig. 17b) than in *G. bilineatus* (width 26–32% of length, Fig. 17a), long and narrow in *Acanthocybium*, and between the two extremes in *Scomberomorus*. The teeth are fine in all three genera, but are a little larger in *Grammatorcynus* and *Acanthocybium* than in most species of *Scomberomorus*.

Ectopterygoid The ectopterygoid is a T-shaped bone with the top of the T forming its posterior end. It joins with the entopterygoid dorsolaterally, the palatine laterally and anteriorly, and the quadrate and metapterygoid posteriorly (Fig. 18). Dividing the dorsal distance (from the anterior end of the bone to the tip of the dorsal arm) by the ventral distance (from the anterior end to the tip of the ventral process) results in a number that is greater than 100% in *Grammatorcynus* (107–116%, Fig. 18c) and *Acanthocybium* (103–109%, Fig. 18b), but only 85–100% in *Scombero-*

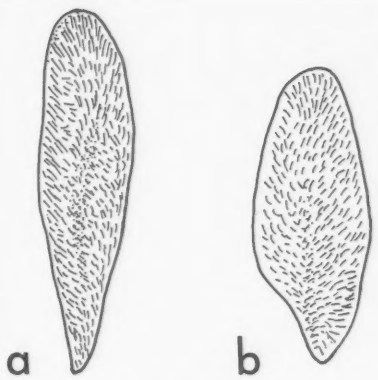

Figure 17
Palatine tooth patches in *Grammatorcynus*. (a) *G. bilineatus*, Queensland, 521 mm FL; (b) *G. bicarinatus*, Western Australia, 765 mm FL.

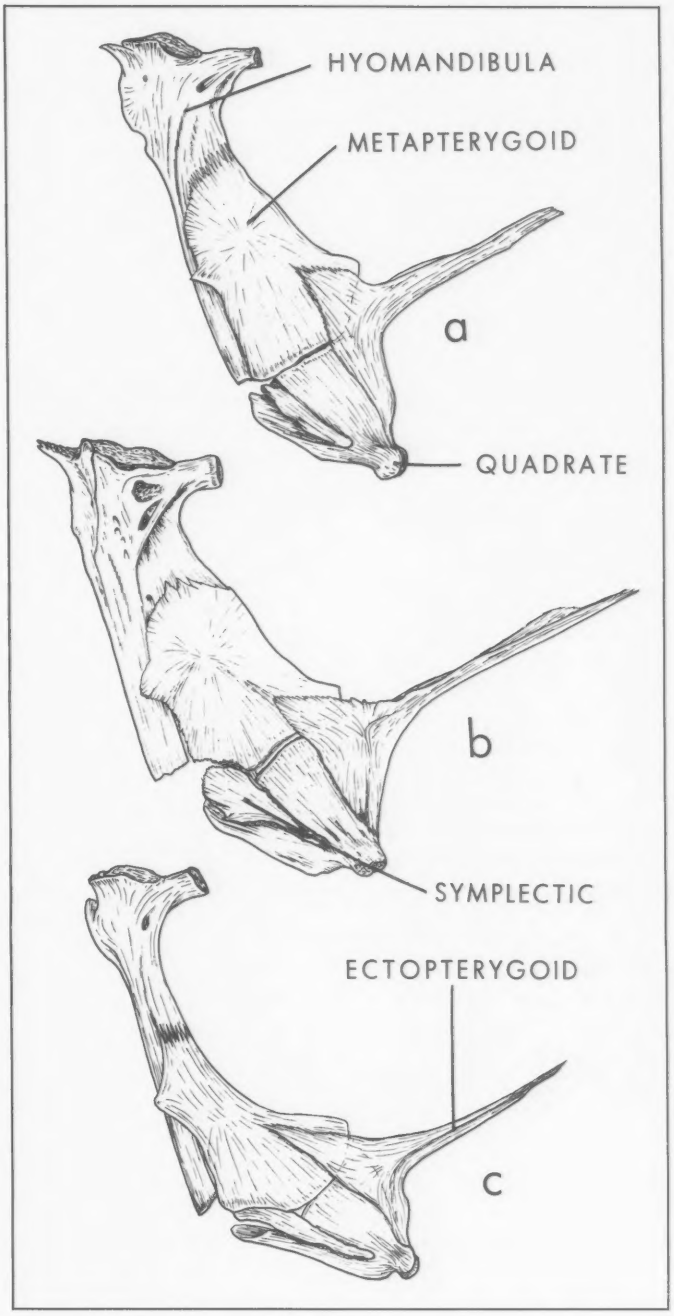

Figure 18 (right)
Left suspensoria in mesial view. (a) *Scomberomorus semifasciatus*, New Guinea, 510 mm FL, 2.5×; (b) *Acanthocybium solandri*, Revillagigedos Is., 1068 mm FL, 1.5×; (c) *Grammatorcynus bilineatus*, Marshall Is., 424 mm FL, 2×.

morus (Fig. 18a). The shank is longer in *Acanthocybium* than in the other two genera. The posterior edge of the ectopterygoid (from the tip of the dorsal process to the tip of the ventral process) relative to the ventral distance is long, 63–72% in *Grammatorcynus*, and relatively shorter in *Acanthocybium* (41–47%) and *Scomberomorus* (43–63%).

Entopterygoid The entopterygoid is elongate and oval in shape (width 35–41% of length, Collette and Russo 1985b: fig. 28). The outer margin of the entopterygoid is the thickest part of the bone and attaches to the inner margin of the ectopterygoid. The entopterygoid also connects with the palatine anteriorly and the metapterygoid posterolaterally. The mesial and posterior borders are free from contact with other bony elements. The dorsal surface is roughly convex. The dorsal surface is similarly convex in *Acanthocybium*, but the dorsal surface in *Scomberomorous* is concave. The ventral surface is convex in all three genera, and it forms the major part of the buccal roof. *Scomberomorus* contains species that have both narrower (*S. commerson*, width

23–28% of length) and wider (*S. maculatus* width 41–42% of length) entopterygoids. The entopterygoid of *Acanthocybium* (30–35%) is slightly narrower than that of *Grammatorcynus* (35–41%).

Metapterygoid The metapterygoid is a flat, quadrangular or somewhat triangular bone (Fig. 18). The posterodorsal margin of this bone is deeply grooved to receive the hyomandibula. The dorsal portion is strongly ankylosed to the lamellar region of the hyomandibula. The ventroposterior margin abuts the lowermost portion of the symplectic process of the hyomandibula, but does not touch the hyomandibula. There is a relatively long slit beween the two bones through which the hyoidean artery passes (Allis 1903). The ventral border is divided into two portions: the horizontal portion in contact with the quadrate and the anterior oblique portion ankylosed to the ectopterygoid. On the mesial surface, the metapterygoid has a triangular-shaped area that forms an interdigitating articulation with the upper arm of the ectopterygoid. The posteroventral margin of the metapterygoid articulates with the dorsal end of the symplectic in *Grammatorcynus* (Fig. 18c) and *Acanthocybium* (Fig. 18b), but does not do so in most species of *Scomberomorus* (Fig. 18a). The posterior, horizontal part of the ventral border is shorter than the anterior oblique part in *Grammatorcynus* (anterior part 132–181% of posterior part) and *Acanthocybium* (188–218%); however, in *Scomberomorus* the posterior part is longer than the anterior part (anterior part 39–86% of posterior part).

Hyoid arch The hyoid arch is composed of the hyomandibula, symplectic, quadrate, hyoid complex (hypohyals, ceratohyal, epihyal, interhyal, and the seven branchiostegal rays), and two median unpaired bones, the glossohyal and urohyal.

Hyomandibula The hyomandibula is an inverted L-shaped bone (Fig. 18) connecting the mandibular suspensorium and opercular bones to the neurocranium. Dorsally, there are three prominent condyles. The long dorsal condyle forms the base of the L and fits into the fossa at the junction of the pterotic and sphenotic bones. The anterior condyle articulates with the ventral fossa of the pterotic, and the lateral process is attached to the inside of the opercle. Anterolaterally, the hyomandibula is drawn out into a lamellar region that joins the metapterygoid. Posterolaterally, it has a long articulation with the preopercle. Ventrally, the hyomandibula has a long symplectic process; at the posterodorsal corner there is a small, sometimes almost indistinct spine. A strong vertical ridge extends from the ventral margin to just below the dorsal border, where it then curves anteriorly to confluence with the anterior condyle. The areas lying anterior and posterior to this ridge are grooved for articulation with the metapterygoid and preopercle, respectively; in situ, only the ridge and a portion of the upper broader surface are visible exteriorly. The upper surface of the symplectic is connected to the ventral border of the hyomandibula by way of a cartilage, best developed in *Acanthocybium*. There is one deep fossa on the inner surface of the hyomandibula in *Grammatorcynus* (Fig. 18c) and *Scomberomorus* (Fig. 18a); there are two such fossae in *Acanthocybium* (Fig. 18b).

The posterodorsal spine, which is quite small in *Grammatorcynus* and in most species of *Scomberomorus*, is best developed in *Acanthocybium*, *S. commerson* (Devaraj 1977), and *S. queenslandicus*. The maximum width (tip of anterior condyle to outer margin of posterior condyle) of the hyomandibula is least relative to the total length (ventral tip to dorsal margin of dorsal condyle) in *Grammatorcynus* (width 34–39% of length) and *S. multiradiatus* (36–39%). The hyomandibula is widest, relative to length in *S. sinensis* (45–52%). *Acanthocybium* and the other species of *Scomberomorus* fall between these two extremes (39–47%).

Symplectic The symplectic is a small bone that fits into a groove on the inner surface of the quadrate (Fig. 18). In *Grammatorcynus* the symplectic is slightly wider than it is in *Scomberomorus*; however, the groove into which the symplectic fits is narrower in *Grammatorcynus* than in *Scomberomorus*, so that the symplectic nearly fills the groove in *Grammatorcynus* and does not fill the groove in *Scomberomorus* (Fig. 18a). The symplectic is greatly expanded at its dorsal end in *Acanthocybium* (Fig. 18b). The symplectics in *Grammatorcynus* and *Acanthocybium* extend well beyond the dorsal margin and even beyond the dorsal end of the posterior process of the quadrate to make contact with the metapterygoids, making them much longer than the symplectics in most species of *Scomberomorus*. The symplectic of *G. bilineatus* (Fig. 19a) is longer than that of *G. bicarinatus* (Fig. 19b).

Quadrate The lower jaw is suspended from the cranium by means of the articulating facet of the ventral surface of the triangular quadrate (Fig. 18). The broad dorsal margin of the quadrate abuts the ventral border of the metapterygoid. There is a strong process on the posterior margin of the quadrate that is attached along the lower anterior arm of the preopercle. This process is quite long in *G. bilineatus* (its length measured from the ventral facet to the tip of the process is 134–145% of the distance from the ventral facet to the dorsal margin; Fig. 19a) and *Acanthocybium*, but shorter in *G. bicarinatus* (122–125%, Fig. 19b) and most species of *Scomberomorus*.

Hyoid complex This complex includes the two hypohyals (basihyal of Mago Leccia 1958), ceratohyal, epihyal, and interhyal bones, and the seven branchiostegal rays (Collette and Russo 1985b:fig. 29). The

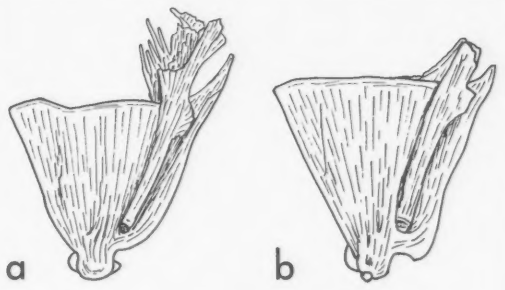

Figure 19
Quadrate and symplectic in *Grammatorcynus*. (a) *G. bilineatus*, Western Australia, 460 mm FL; (b) *G. bicarinatus*, Queensland, 563 mm FL.

hypohyals, ceratohyal, and epihyal are closely associated and form a functional unit.

Hypohyals The hypohyals comprise separate dorsal and ventral elements joined longitudinally. In lateral view, the ventral hypohyal is clearly larger than the dorsal hypohyal in *Grammatorcynus*, but in *Scomberomorus* not quite as large relative to *Grammatorcynus*. In *Acanthocybium* the ventral hypohyal is three times larger than the dorsal hypohyal. Laterally, the suture that runs between the dorsal and ventral hypohyals curves ventrally at various angles in *Grammatorcynus* and *Scomberomorus*, but runs almost horizontally in *Acanthocybium*. Mesially, a pointed lateral process at the anterodorsal end of the dorsal hypohyal forms a symphysis with the glossohyal, urohyal, basibranchial, and the process of the hypohyal from the opposite side in *Grammatorcynus* and *Scomberomorus*. *Acanthocybium* also has a pointed lateral process, but it appears to be further posterior due to also having an anterior pointed end to the hypohyals at the junction of the dorsal and ventral hypohyals. In addition, *Acanthocybium* has a prominent anterolateral process on the ventral hypohyal. The groove for the hyoidean artery runs along the outer surface of the epihyal, ceratohyal, and ventral portion of the dorsal hypohyal. In *Grammatorcynus* the groove in the dorsal hypohyal is relatively short, extending anteriorly 11–39% of the length of the dorsal hypohyal before becoming a covered tunnel leading to the inner side of the dorsal hypohyal. In *Scomberomorus* the groove extends 32–53% before becoming a tunnel to the inner side, and in *Acanthocybium* the groove extends 29–47% before becoming a foramen leading to the inner side. The opening on the inner side appears as a small to moderate pit, usually located in the ventral portion of the dorsal hypohyal in *Grammatorcynus* and *Scomberomorus*.

Ceratohyal The ceratohyal is a long flat bone, broadest at the posterior end, and with an anteroventral projection that articulates with the posteroventral notch of the ventral hypohyal. It is the largest bone of the hyoid complex. Posteriorly, the middle part of the ceratohyal interlocks with the epihyal by means of odontoid processes issuing from both elements (ceratohyal-epihyal suture of McAllister 1968), while the upper and lower portions are joined by cartilage. Four acinaciform branchiostegal rays are attached to the respective articular surfaces along the concave middle portion of the ventral margin in *Grammatorcynus* and *Acanthocybium*. In *Scomberomorus* the fifth branchiostegal ray is also usually attached to the ceratohyal (most posterior part) or on the space between the ceratohyal and epihyal, not on the anterior part of the epihyal. In *Grammatorcynus* and *Acanthocybium* the fifth branchiostegal ray is on the anterior part of the epihyal. The hyoidean groove runs the length of the ceratohyal on its lateral surface. The groove is so deep in 10 species of *Scomberomorus* (*brasiliensis*, *commerson*, *concolor*, *multiradiatus*, *munroi*, *niphonius*, *queenslandicus*, *semifasciatus*, *sierra*, and *tritor*) that it forms a thin slit through the bone, the ceratohyal window or "beryciform" foramen. This slit is rare in *Grammatorcynus* and *Acanthocybium*, and is either rare or occasional in the other eight species of *Scomberomorus*. The dorsal margin of the ceratohyal is usually concave, but sometimes flat in *Grammatorcynus*. It is deeply concave in *Acanthocybium*, and varies from concave to convex in *Scomberomorus*.

Epihyal The epihyal is a triangular bone that interlocks anteriorly with the ceratohyal and has a posterior process that articulates with the interhyal. Three branchiostegal rays articulate with the epihyal in *Grammatorcynus* and *Acanthocybium*. Only two branchiostegal rays are found on the ventral portion of the epihyal in *Scomberomorus*. In *Grammatorcynus* the depth of the epihyal is 66–80% of the length from the smooth anterior margin of the bone to the tip of the posterior process. Epihyal depth is narrowest in *Acanthocybium* (58–62%), and in *Scomberomorus* it varies from 68% in *S. commerson* and *S. cavalla* to 98% in *S. koreanus*, with intermediate values for the other species.

Interhyal The interhyal is a small flattened bone that is attached to the epihyal dorsal to the posterior process. It is directed obliquely upward and links the hyoid complex to the hyomandibula and symplectic. No differences in interhyals were noted.

Glossohyal The glossohyal (basihyal) is a median bone that supports the tongue and overlies the

first basibranchial bone at the anterior end of the branchial arch. In *Grammatorcynus* there is a quadrangular to oval tooth plate fused to and covering the dorsal surface of the glossohyal (Collette and Russo 1985b:fig. 30). No tooth plate is present in *Acanthocybium* or *Scomberomorus*. The glossohyal of *Grammatorcynus* is slightly wider (width 47–55% of length) than the roughly rod-shaped or conical-shaped glossohyal of *Scomberomorus* (35–54%) and the flattened spatulate glossohyal of *Acanthocybium* (42%).

Urohyal The urohyal is a compressed, median, unpaired bone (Fig. 20). The anterior end of this element lies between, and is connected with, the hypohyals of the left and right sides. The most prominent difference in the urohyal of *Grammatorcynus* is that in dorsal view, the posterior end of the dorsal margin is tripartite (Fig. 20c–d) instead of forked, as it is in *Scomberomorus* and *Acanthocybium* (Fig. 20a–b). The dorsal and anterior portions of the ventral margins are thickened in *Grammatorcynus*. The anterior end has an articulation head; the posterior end is deepest in *Scomberomorus*, and much less deep in *Grammatorcynus* due to the convex shape of the ventral margin. The maximum depth of the urohyal in *Grammatorcynus* is 15–20% of the length of the dorsal margin. The maximum depth in *Acanthocybium* is not as great as this (13–15%), and in *Scomberomorus* it is greater (16–24%). In *Grammatorcynus* the ventral margin of the urohyal is relatively short, only 68–71% of the length of the dorsal margin, compared with 80–91% in *Acanthocybium* and *Scomberomorus*.

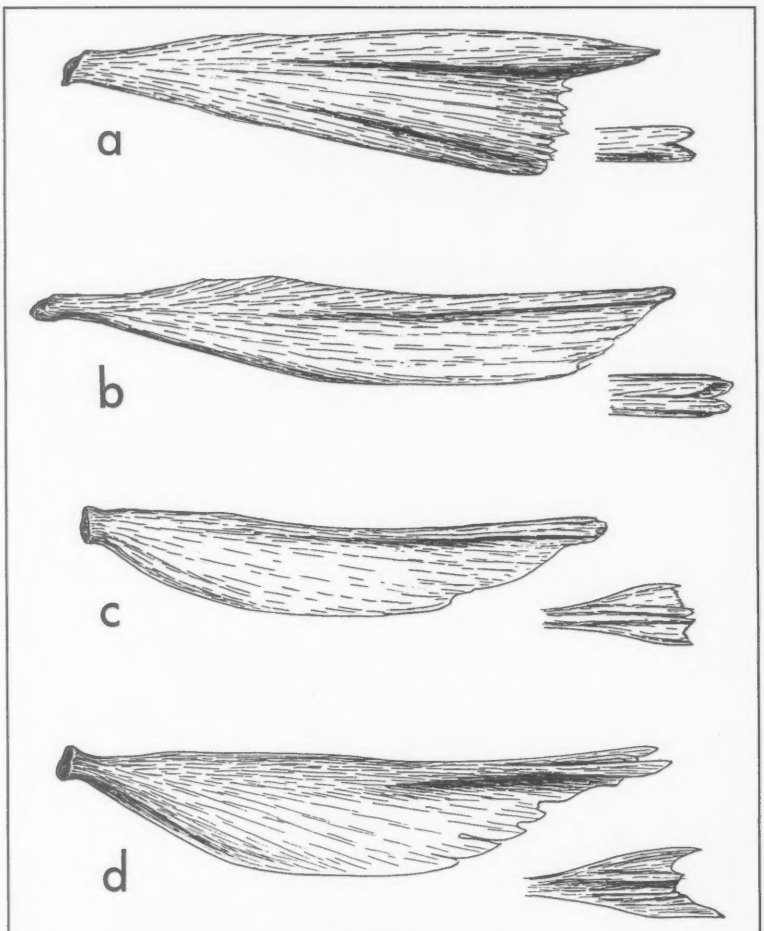

Figure 20

Urohyals in left lateral view. (a) *Scomberomorus queenslandicus*, Queensland, 641 mm FL; (b) *Acanthocybium solandri*, Indian O., 1088 mm FL; (c) *Grammatorcynus bilineatus*, New Guinea, 382 mm FL; (d) *G. bicarinatus*, Australia, 663 mm FL. Fig. (a) drawn twice as large as (b), (c) three times as large. Inset is the posterior end of the dorsal margin, in dorsal view.

Opercular apparatus Four wide, flat bones (opercle, preopercle, subopercle, and interopercle) fit together to form the gill cover.

Opercle The opercle (Fig. 21) is overlapped laterally on its anterior margin by the posterior half of the preopercle. The narrow, elongate, articular facet for the opercular process of the hyomandibula is located on the medial surface of the anterodorsal corner of the opercle. *Grammatorcynus* and most species of *Scomberomorus* have a weak process at the posterodorsal corner. This process is absent in *Acanthocybium*. In *Grammatorcynus* the width of the opercle is 63–79% of the total length of the bone; *G. bicarinatus* has a wider opercle (width 72–79% of length, Fig. 21d) than *G. bilineatus* (63–72%, Fig. 21c). Both species of *Grammatorcynus* have narrow opercles compared with the extremely wide opercles found in *Acanthocybium* (Fig. 21b).

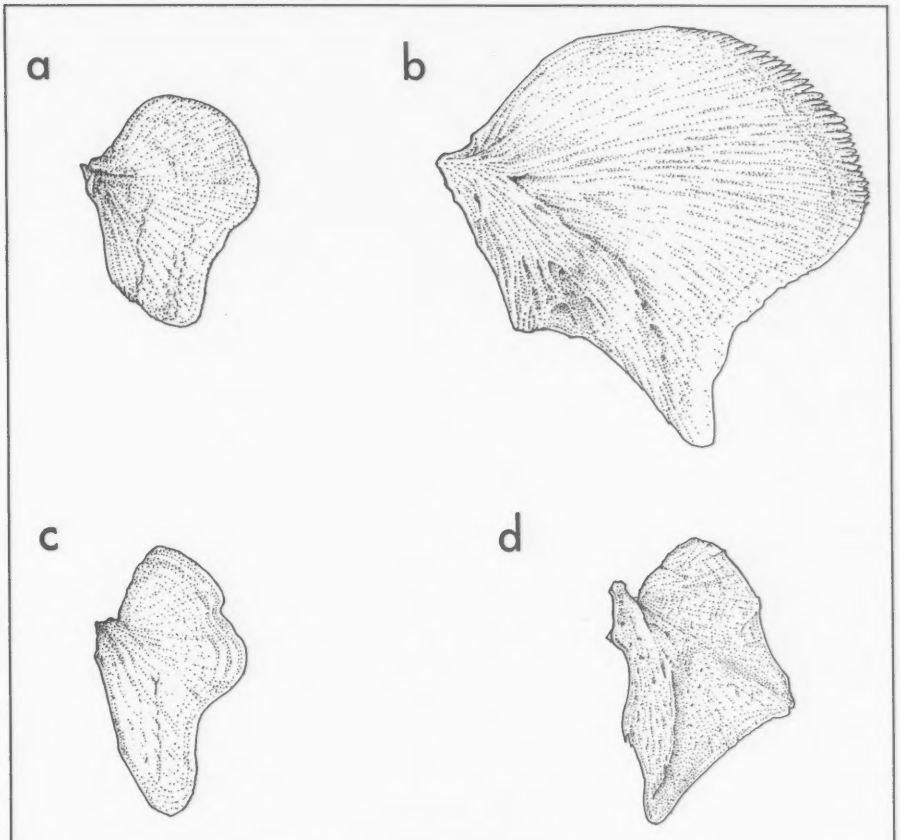

Figure 21
Left opercles in lateral view. (a) *Scomberomorus semifasciatus*, New Guinea, 510 mm FL; (b) *Acanthocybium solandri*, Revillagigedos Is., 1080 mm FL; (c) *Grammatorcynus bilineatus*, Marshall Is., 424 mm FL; (d) *G. bicarinatus*, Great Barrier Reef, 563 mm FL.

Preopercle The preopercle is a large, crescent-shaped flat bone, broadest at the lower posterior angle (Collette and Russo 1985b:fig. 33). The anterior portion of the bone is thickened into a bony ridge. A series of 5–7 pores along the lower margin of the ridge represents the preoperculomandibular canal of the lateral line system which continues onto the dentary. On the mesial side, the bony ridge possesses a groove for attachment to the hyomandibula and the quadrate. There is a shelf mesial to the anteroventral end of the preopercle in *Acanthocybium* that is absent in *Grammatorcynus* and *Scomberomorus*. The canals leading to the preopercular pores are visible through the bone in *G. bilineatus* and all species of *Scomberomorus*, but these canals could not be seen in the specimens of *G. bicarinatus* and *Acanthocybium* due to the thickness of the bone. The posterior margin of the preopercle is distinctly concave in *Grammatorcynus* and most species of *Scomberomorus*. However, it is only slightly concave or flat in *Acanthocybium* and *S. commerson*. In *Grammatorcynus* the distance from the anterior margin of the bony ridge to the posterior end of the lower lobe is 64–75% of the height of the preopercle measured from the ventral margin to the dorsal tip of the bone. In *Scomberomorus* the lower lobe is 69–80% of the height of the preopercle. The anterodorsal margin terminates in a pore similar to the preoperculomandibular lateral-line canal pore at the anteroventral margin of the bone.

Subopercle The subopercle is a flat, roughly triangular bone with a prominent anterior projection (Collette and Russo 1985b:fig. 34). Two ridges

converge posteriorly from the anterior projection on the lateral side of the bone. The upper ridge articulates with the lower posterior projection of the opercle, and the lower ridge connects to the posterodorsal margin of the interopercle. The dorsal ridge is much more prominent than the ventral ridge and extends over the main part of the subopercle as a discrete shelf. The weaker ventral ridge is more difficult to detect in most specimens of *Grammatorcynus*. The angle between the anterior projection and the anterior margin of the subopercle is acute in *Grammatorcynus* and *S. multiradiatus*; however, in *Acanthocybium* and the other species of *Scomberomorus* the angle is close to 90°. The length of the anterior projection in *Grammatorcynus* varies from 23 to 33% of the length of the anterior margin dorsal to the projection. The projection is slightly longer (28–33%) in *G. bicarinatus* than in *G. bilineatus* (23–28%). The projection is longest in *Acanthocybium* (36–45%) and shortest in *S. commerson* (20–25%), with the rest of the species of *Scomberomorus* having projections between 21 and 43%.

Interopercle The interopercle is roughly oval in shape, narrow at the anterior margin and widening posteriorly, with a crest on the superior margin (Collette and Russo 1985b:fig. 35). There is a well-developed facet on the mesial side to receive the articular process of the interhyal. The maximum depth of the interopercle relative to the length of the bone is 35–43% in *Grammatorcynus*. The maximum depth of the interopercle is a little greater in *Acanthocybium* (40–49%), and much greater in the species of *Scomberomorus* (45–61%). Often there is a well-formed notch anterior to the crest on the sloping anterior margin in *Grammatorcynus* and *Scomberomorus*, which is not as well developed in *Acanthocybium*. The posterior margin is rounded in *Grammatorcynus* and *Scomberomorus* but divided into two by a notch in *Acanthocybium*.

Branchial apparatus The branchial apparatus is composed of five pairs of gill arches, gill filaments, gill rakers, pharyngeal tooth patches, and supporting bones. The general arrangement in *Grammatorcynus* is similar to that found in other scombrids such as the Sardini (Collette and Chao 1975), *Thunnus* (Iwai and Nakamura 1964:22, fig. 1; de Sylva 1955:21, fig. 40), *Scomberomorus* (Mago Leccia 1958:327, pl. 12; Collette and Russo 1985b:fig. 36), and *Rastrelliger* (Gnanamuttu 1971:14, fig. 6). Most branchial bones bear patches of tiny teeth.

Basibranchials The three basibranchials form an anteroposterior chain. The first and second are about the same size, and considerably shorter than the third. The first is covered dorsally by the glossohyal.

In lateral view, the first basibranchial is narrowest in the middle. In *Grammatorcynus* and *Acanthocybium* it is elongate. In *Scomberomorus* it is short with a wide base where it joins with the second basibranchial. The second basibranchial has a prominent notch in the ventral margin and a distinct groove laterally that extends from the anteroventral margin to the middorsal region of the bone. This groove accepts the anterior end of the first hypobranchial. The third basibranchial has an expanded anterior end at its junction with the second basibranchial, and then tapers posteriorly. A prominent groove is present anteriorly that accepts the medial anterior end of the second hypobranchial. A section of cartilage extends posteriorly to articulate with the fourth and fifth ceratobranchials.

Hypobranchial Three hypobranchials are present. The first is interposed beween the second basibranchial and the first ceratobranchial. The second is about the same size as the first, fits into a groove on the third basibranchial, and extends to the second ceratobranchial. The third hypobranchial is smaller than the first or second, fits snugly against the posterolateral margin of the third basibranchial, and its posterior end articulates with the third ceratobranchial.

Ceratobranchials The five ceratobranchials are the longest bones in the branchial arches. They have a deep groove ventrally for the branchial arteries and veins. The ceratobranchials support most of the gill filaments and gill rakers. The first three are morphologically similar and articulate with the posterior ends of their respective hypobranchials. The fourth is more irregular and attaches to a cartilage posterior to the third basibranchial. The fifth ceratobranchial is also attached to the cartilage, has a dermal tooth plate fused to its dorsal surface, and the complex is termed the lower pharyngeal bone. It is covered with small conical teeth that are directed slightly posteriad.

Epibranchials The posterolateral end of each of the four epibranchials is attached to the ends of the first four ceratobranchials. Each epibranchial bears a groove posterodorsally for the branchial arteries and veins. The first epibranchial is the longest and bears two processes mesially. The anterior process articulates with the first pharyngobranchial, and the posterior process attaches with the interarcual cartilage. The second epibranchial is similar to the first, but slightly shorter. The anterior end has two processes, an anterior process that attaches to the second pharyngobranchial and a posterior process that is coupled with the third pharyngobranchial by way of an elongate cartilage. This process is relatively elongate in *Grammatorcynus*, but shorter in *Acanthocybium* and *Scomberomorus*. The third epibranchial is the shortest in the series. Laterally, it is attached with the third ceratobranchial; mesially, it is attached with the third pharyngobranchial. An elongate posterodorsal process

is present. This process joins with the fourth epibranchial, which is larger than the third and is interposed between the fourth ceratobranchial and pharyngobranchial. It is a curved bone with the angle formed by the lateral and medial arms being much more acute in *Grammatorcynus* than in *Acanthocybium* and *Scomberomorus*. A dorsal process arises from the middle of the bone and attaches to the third epibranchial.

Pharyngobranchials There are four pharyngobranchials attached basally to the epibranchial of their respective gill arch. The first is long and slender, articulates dorsally with the prootic, and is frequently called the suspensory pharyngeal (Iwai and Nakamura 1964). The elongate second pharyngobranchial bears a patch of teeth. The third is the largest element in the series; it has a broad patch of teeth on its ventral surface, a broad posterior end, and tapers to a narrow anterior end. In *Grammatorcynus* and *Acanthocybium* the third pharyngobranchial is shorter than in *Scomberomorus*. The fourth pharyngobranchial also bears a ventral tooth plate, has a rounded posterior end, and has an elongate strut (pharyngobranchial stay) mesially which overlaps the third pharyngobranchial. This stay is much shorter in *Grammatorcynus* and *Acanthocybium* than in *Scomberomorus*.

Gill rakers The hypobranchial, ceratobranchial, and epibranchial of the first gill arch support a series of slender, rigid gill rakers. The longest gill raker is at or near the junction of the upper and lower arches, between the ceratobranchial and epibranchial. Magnuson and Heitz (1971) have clearly shown that there is a correlation between numbers of gill rakers, gap between gill rakers, and size of food items in a number of species of Scombridae.

The number of gill rakers is easily countable and is an especially useful taxonomic character in differentiating between the two species of *Grammatorcynus*: *G. bilineatus* has more gill rakers (18–24) than *G. bicarinatus* (12–15) (Table 3). *Acanthocybium* differs from all other genera of Scombridae in completely lacking gill rakers. Three species of *Scomberomorus* have greatly reduced numbers of gill rakers: *S. multiradiatus* (1–4 gill rakers), *S. commerson* (1–8), and *S. queenslandicus* (3–9). *Scomberomorus concolor* stands out in having the most gill rakers (21–27). Other species of *Scomberomorus* fall between these extremes. There is a correlation between number of gill rakers and number of jaw teeth in *Grammatorcynus* and *Scomberomorus*. Species with the fewest gill rakers, *G. bicarinatus* and *S. multiradiatus*, also have the fewest jaw teeth, and species with the most gill rakers, *G. bilineatus* and *S. concolor*, have the most teeth.

Axial skeleton This section is divided into four parts: vertebral number, vertebral column, ribs and intermuscular bones, and caudal complex.

Vertebral number Vertebrae may be divided into precaudal (abdominal) and caudal. The first caudal vertebra is defined as the first vertebra that bears a notably elongate haemal spine and lacks pleural ribs. Vertebral counts include the urostyle which bears the hypural plate. *Grammatorcynus* has 31 vertebrae, which is less than *Scomberomorus* (41–56 vertebrae), which in turn is less than *Acanthocybium* (62–64). The same situation also applies to precaudal and caudal vertebrae. Both species of *Grammatorcynus* have 12 precaudal and 19 caudal (except for one specimen of *G. bicarinatus* with 11 plus 20 caudal). *Scomberomorus* has 16–23 precaudal and 20–36 caudal, and *Acanthocybium* has 31–33 precaudal and 31–33 caudal. The presence of only 31 vertebrae in *Grammatorcynus* is a primitive condition agreeing with *Scomber* and *Rastrelliger*, the most primitive members of the Scombrinae. The increased number of vertebrae in *Acanthocybium* is clearly a specialization.

Vertebral column The neural arches and spines are stout and compressed on the first to the fourth vertebra (especially the first 3) in *Grammatorcynus*. They extend farther back, to the fifth or sixth vertebrae, in most species of *Scomberomorus*, and extend farthest, to the seventh vertebra, in *Acanthocybium* and *S. commerson*. Posteriorly, toward the caudal peduncular vertebrae and caudal complex, the neural spines bend abruptly backward and cover most of the neural groove; caudally they merge into the caudal complex as in *Thunnus* (Kishinouye 1923, Gibbs and Collette 1967) and the bonitos (Collette and Chao 1975).

Table 3
Number of gill rakers on first arch in *Grammatorcynus*.

	12	13	14	15	16	17	18	19	20	21	22	23	24	N	$\bar{x}$
G. bilineatus							1	10	15	30	10	5	1	72	20.8
G. bicarinatus	1	—	7	3										11	14.1

The neural prezygapophyses on the first vertebra are modified to articulate with the exoccipital where the vertebral axis is firmly articulated with the skull. Neural postzygapophyses arise posterodorsally from the centrum and overlap prezygapophyses posteriorly. The postzygapophyses progressively merge into the neural spine in the peduncular region to disappear by the last 5–6 vertebrae. The basic structure and elements of the neural arches and neurapophyses are similar to those of other scombrids (Kishinouye 1923, Conrad 1938, Mago Leccia 1958, Nakamura 1965, Gibbs and Collette 1967, Collette and Chao 1975, Potthoff 1975, Collette and Russo 1985b).

Variable characters are found on the haemal arches and haemapophyses. Laterally directed parapophyses, arising from the middle of the centrum, appear on the 4th–6th vertebrae where the intermuscular bones and pleural ribs are encountered (see section on Ribs and Intermuscular Bones). The parapophyses become broader and longer posteriorly and gradually shift to the anteroventral portion of the centra. In lateral view, the first ventrally visible parapophyses are found on the 6th–7th vertebra in *Grammatorcynus*, the 7th–9th in *Scomberomorus* (usually the 8th), and on the 14th–15th in *Acanthocybium*.

Posteriorly, the distal ends of the paired parapophyses meet, forming the first closed haemal arch. The first closed haemal arch is on the 8th vertebra in *Grammatorcynus*, 10th–16th vertebra in *Scomberomorus*, and 25th–28th vertebra in *Acanthocybium*. This location is correlated with the total number of vertebrae. The haemal spines become elongate and point posteriorly until they abruptly become more elongate on the first caudal vertebra. The paired pleural ribs (see section on Ribs and Intermuscular Bones) attach to the distal ends of the parapophyses and arches and extend posteriorly to the last precaudal vertebra. The haemal arches and spines bend posteriorly at the caudal peduncle and then merge into the caudal complex symmetrically with the neural arches and spines on the caudal vertebrae.

Haemapophyses include pre- and postzygapophyses, but their relative positions are different from those of the neurapophyses, and they do not overlap. The first haemal postzygapophyses arise posteroventrally from the 6th–7th centrum in *Grammatorcynus*, the 6th–8th in *Scomberomorus*, and the 9th–10th in *Acanthocybium*. They reach their maximum length at about the junction of the precaudal and caudal vertebrae. The haemal postzygapophyses fuse with the haemal spine or disappear in the caudal peduncle region. The haemal prezygapophyses arise from the anterior base of the haemal arches on the 8th–11th vertebra in *Grammatorcynus*, the 10th–22nd in *Scomberomorus*, and the 23rd–25th in *Acanthocybium*.

Struts between the haemal arch and the centrum form the inferior foramina. Foramina are present from the 17th–19th to the 25th–28th vertebra in *Grammatorcynus*, the 21st–33rd to the 35th–52nd in *Scomberomorus*, and the 49th–51st to the 56th–57th in *Acanthocybium*.

Ribs and intermuscular bones Pleural ribs are present from the second or third vertebra posterior to the 12th–31st vertebra in the three genera. Intermuscular bones start on the back of the skull or the first vertebra and extend to the 10th–30th vertebra.

Correlated with its low number of vertebrae, *Grammatorcynus* has the fewest pleural ribs (10 pairs). *Acanthocybium* has the most pleural ribs (30 pairs) in agreement with its many vertebrae. Species of *Scomberomorus* are intermediate in number of vertebrae and also in number of pleural ribs (15–21). The first pleural rib articulates with the centrum of the third vertebra in *Grammatorcynus* and most species of *Scomberomorus*, and articulates with the centrum of the second vertebra in *Acanthocybium*, as noted by Devaraj (1977:44), and in at least one specimen each of *S. commerson*, *S. maculatus*, and *S. sinensis*. Pleural ribs usually extend posteriorly to about the last precaudal vertebra: 12 in *Grammatorcynus*, 17–23 in *Scomberomorus*, and 31 in *Acanthocybium*.

Intermuscular bones start on the first vertebra in *Grammatorcynus*, *Acanthocybium*, and some species of *Scomberomorus*. In some specimens of at least 13 species of *Scomberomorus*, the first intermuscular bone is attached to the exoccipital on the skull, and in *S. concolor*, *S. koreanus* (also noted by Devaraj 1977), and *S. sierra*, it appears to be the usual condition. *Grammatorcynus* has 19–21 pairs of intermuscular bones, many more than *Acanthocybium* (only 10 pairs, which seems odd given its high number of vertebrae and pleural ribs), but fewer than most species of *Scomberomorus* (20–30 pairs).

Caudal complex Three preural centra support the caudal fin in *Grammatorcynus*. In *Scomberomorus* four or five preural centra support the caudal fin, and in *Acanthocybium* there are five. The urostyle represents a fusion of preural centrum 1 and the ural centrum (Potthoff 1975). The urostyle is fused with the triangular hypural plate posteriorly and articulates with the uroneural dorsally. In *Grammatorcynus* there is very little compression of the preural centra. Preural centrum 4 is not shortened at all, preural centrum 3 is shortened slightly, and preural centrum 2 is shortened slightly more (Collette and Russo 1985b:fig. 39). In *Acanthocybium* and *Scomberomorus*, preural centra 2–4 are compressed more than any of the preural centra in *Grammatorcynus*, but still not as much as the centra in the bonitos and tunas (Collette and Chao

1975, Gibbs and Collette 1967). In *Grammatorcynus* the posterior-most neural and haemal spine bend away from the vertebral axis and parallel the dorsal and ventral edges of the hypural plate. In *Acanthocybium* and *Scomberomorus*, three posterior neural and haemal spines bend away from the vertebral axis more abruptly than in *Grammatorcynus*.

Table 4
Number of dorsal spines, second dorsal fin rays, and dorsal finlets in *Grammatorcynus*.

	Spines			Rays			Finlets		
	11	12	13	10	11	12	6	7	8
G. bilineatus	4	65	1	10	55	4	61	9	
G. bicarinatus		10		10			1	9	1

The triangular hypural plate is composed of 5 fused hypural bones (Potthoff 1975). In some specimens of *Grammatorcynus* (*G. bilineatus* 453 and 521 mm FL, and *G. bicarinatus* 563 mm FL) the dorsalmost (hypural 5) is partially fused with the dorsal part of the hypural plate (hypurals 3–4). However, in smaller specimens (382–424 mm FL) such fusion was absent, as is the case in *Scomberomorus* and *Acanthocybium*. There is a primitive hypural notch present on the middle of the posterior margin of the hypural plate. This notch is a remnant of the fusion of the dorsal part of the hypural plate with the ventral part (hypurals 1–2). The notch is absent in the more advanced bonitos and tunas (Collette and Chao 1975).

The parhypural is separate from the ventral hypural plate in *Grammatorcynus* and *Scomberomorus* but is fused with it in *Acanthocybium*. This fusion was also noted by Conrad (1938), Fierstine and Walters (1968), and Devaraj (1977). The two haemal arches preceding the parhypural are autogenous in the three genera, although Devaraj (1977) stated that they were fused with their centra in *Acanthocybium*.

The parhypural has a strongly-hooked process, the parhypurapophysis (or hypurapophysis), at its proximal end. The parhypurapophysis slopes slightly upwards similarly in *Grammatorcynus* and *Scomberomorus*. In *Acanthocybium* it has a right angle and then a level projection.

There are two epurals as in other scombrids (Potthoff 1975). In shape and size, the anterior epural (1) resembles the neural spine of adjacent preural centrum 3. The smaller, posterior epural (2) is a free splint located between the anterior epural and the uroneural and fifth hypural, which are joined together.

Dorsal and anal fins *Grammatorcynus* usually has 12 dorsal spines, rarely 11 or 13 (Table 4), fewer than either *Scomberomorus* (12–22) or *Acanthocybium* (23–27). Dorsal spine counts are roughly correlated with vertebral number: *Grammatorcynus* has the fewest precaudal, caudal, and total vertebrae, and the fewest dorsal spines, while *Acanthocybium* has the most precaudal and total vertebrae, and the most dorsal spines.

Table 5
Number of anal fin rays and finlets in *Grammatorcynus*.

	Rays			Finlets		
	11	12	13	5	6	7
G. bilineatus	12	42	17	1	61	8
G. bicarinatus	5	3	1		3	7

The range in number of second dorsal fin rays is 10–25 in the three genera. *Grammatorcynus* has 10–12 rays, 10 in *G. bicarinatus* and usually 11 in *G. bilineatus* (Table 4). There are usually more second dorsal rays in *Acanthocybium* (11–16) and *Scomberomorus* (15–25).

Dorsal finlets number 6–11 in the three genera. *Grammatorcynus* has 6–8, usually 7 in *G. bicarinatus*, and usually 6 in *G. bilineatus* (Table 4). *Acanthocybium* has 7–10, and *Scomberomorus* has 6–11. The total number of second dorsal elements is the same in both species of *Grammatorcynus*, 11+6=17 in *G. bilineatus*, 10+7=17 in *G. bicarinatus*.

Anal fin rays show a similar trend to that of dorsal fin rays. The range in the three genera is 11–29. *Grammatorcynus* has 11–13 (Table 5), similar to *Acanthocybium* (11–14), but much fewer than *Scomberomorus* (15–29).

Anal finlets range in number from 5 to 12 in the three genera. *Grammatorcynus* has 5–7, usually 6 in *G. bilineatus*, and usually 7 in *G. bicarinatus* (Table 5), generally fewer than *Acanthocybium* (7–10) or *Scomberomorus* (5–12). Again, the total number of anal elements is the same in both species, 12+6=18 in *G. bilineatus*, 11+7=18 in *G. bicarinatus*.

Pectoral girdle The pectoral girdle consists of the girdle itself (cleithrum, coracoid, and scapula), the radials to which the pectoral fin rays attach, and a chain of bones that connect the girdle to the rear of the skull (posttemporal, supracleithrum, supratemporal, and two postcleithra).

Posttemporal The posttemporal (Fig. 22) is a flat elliptical bone with two sturdy anterior processes that attach the pectoral girdle to the neurocranium. The median (dorsal) process articulates with the dorsal surface of the epiotic. The lateral (ventral) process is shorter, round in cross section, and its hollow anterior end articulates with the dorsal protuberance of the intercalar. There is a thin shelf visible between these two processes in *G. bicarinatus* (Fig. 22d) and *Scomberomorus* (Fig. 22a), but this shelf is hidden behind the flat, posterior portion of the bone in *G. bilineatus* (Fig. 22c) and *Acanthocybium* (Fig. 22b). A variably-sized notch is present at the middle of the posterior edge of the flat body of the bone. *Grammatorcynus* usually has a distinct, variably-sized anteriorly directed spine on the ventral margin of the median process about one-third of the distance from the body of the bone to the anterior tip of the process. In *Acanthocybium*, there is a separate process extending anteriorly from the ventral wall of the median process. This auxillary process (Kishinouye 1923) is as long or almost as long as the median process itself. It ends in a series of several pointed processes. (Both Conrad 1938 and Devaraj 1977 referred to the auxillary process as the median process.) The lengths of the median and lateral processes vary among the species under discussion. The lengths were measured from the midpoint of the shelf that connects the two processes, to the end of the processes. Both the median and lateral processes are longer, relative to the length of the entire bone, in *G. bilineatus* where the shelf is hidden posteriorly (median process is 53–60% length of entire bone, and lateral process is 35–40%) than in *G. bicarinatus* where the shelf is not hidden, and is found more near the midpoint of the bone (median process is 49% and lateral process is 30%). In *Acanthocybium* (shelf hidden) the median process is 56–65% the length of the entire bone, and the lateral process is 27–37%. In *Scomberomorus* (shelf evident) the median process is 36–51% and the lateral process is 15–36%.

Another useful taxonomic character is the presence (if present, shape is important) or absence of a spine or process at the base of the lateral process on the inner surface of the posttemporal. It is present as a wide flap in *Grammatorcynus* (Fig. 22c, d), a blunt process in *Acanthocybium* (Fig. 20b), and as a shelf with a point in *S. commerson*, *S. munroi*, *S. niphonius*, *S. plurilineatus* (Fig. 22a), and sometimes in *S. sinensis*. It is absent or small and inconspicuous in the other 13 species of *Scomberomorus*.

Supracleithrum The supracleithrum is an ovate bone, overlapped dorsolaterally by the posttemporal and overlapping the anterior part of the dorsal wing-like extension of the cleithrum. The anterior border of the bone on the mesial side is thickened into a ridge.

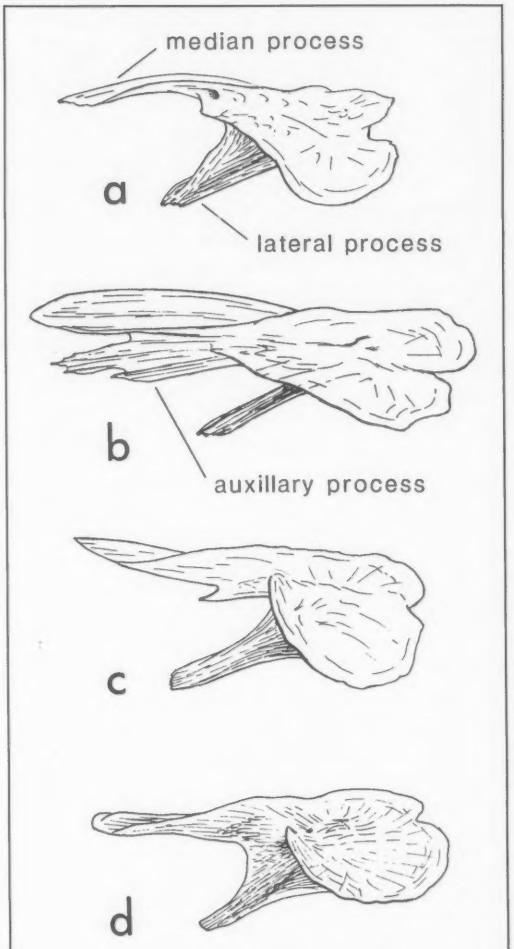

Figure 22
Lateral view of left posttemporals. (a) *Scomberomorus plurilineatus*, South Africa, 910 mm FL, 1×; (b) *Acanthocybium solandri*, Revillagigedos Is., 1068 mm FL, 1×; (c) *Grammatorcynus bilineatus*, Queensland, 521 mm FL, 1.5×; (d) *G. bicarinatus*, Western Australia, 565 mm FL.

Dorsally there is a small handle-shaped process that curves into the posterior margin to end in a notch at the posterodorsal aspect. Both the anterior and posterior borders are extended so that they form humps in *Grammatorcynus* (Collette and Russo 1985b: fig. 41). A branch of the lateralis system extends from the posterior notch of the posttemporal onto the supracleithrum. This short canal lies ventral to the dorsal process of the supracleithrum and extends to the posterior edge of the bone.

The maximum width of the supracleithrum varies from 43 to 75% of the total length of the bone in the three genera. It is widest in *Grammatorcynus*, width 72–82% (89% in one 475 mm FL specimen of *bilineatus*) of length (due to the extensions of anterior and posterior borders). *Scomberomorus* varies in width from 43% in *S. multiradiatus* to 62% in *S. niphonius*. There is no evidence that size is a factor in the size of the supracleithrum in *Grammatorcynus* as was noted by Collette and Russo (1985b) for *Scomberomorus*.

The dorsal process is prominent in *Grammatorcynus*, *S. cavalla*, *S. commerson*, *S. lineolatus*, and especially in *Acanthocybium*. In other species of *Scomberomorus*, it is either small or less sharply set off from the main body of the supracleithrum.

Supratemporal The supratemporal is a thin flat bone having three distinct arms and lying just underneath the skin where its lateral arm articulates with a dorsal articular surface on the pterotic. The anteriormost arm is the longest, while the ventrally directed arm is the shortest. The arm directed posteriorly is intermediate in length. The anterior margin is deeply concave, and the greatly convex posterior margin slightly overlaps the dorsal arm of the posttemporal.

The supratemporal bears a prominent lateral line canal that extends out almost to the tips of all three arms (Collette and Russo 1985b: fig. 42). In these three genera, the canal along the anterior margin of the bone is the longest, and the canal along the lateral side is next longest. In *Grammatorcynus*, the first canal is not branched like it is in most species of *Scomberomorus*, and the second canal is relatively longer.

Cleithrum The main body of the cleithrum is crescent-shaped with an anterodorsal spine and a posteriorly projecting plate at the upper end (Collette and Russo 1985b: fig. 43). The angle between the spine and the plate is much smaller in *Grammatorcynus* and *Scomberomorus* than in *Acanthocybium*. In *Grammatorcynus*, the spine does not extend as far dorsally as the plate. In *Acanthocybium* and most species of *Scomberomorus*, the spine extends about equally as far dorsally as the plate, and in *S. sinensis* the spine extends well beyond the dorsal margin of the plate. In *Grammatorcynus* and most species of *Scomberomorus*, the plate narrows posteriorly. The posterior plate is longer and of uniform width in *Acanthocybium*.

The lower part of the cleithrum is large and folded back upon itself as two walls: one lateral and the other mesial, which meet at their anterior margins and run parallel to each other. The mesial wall of the cleithrum forms a large triangular slit with the coracoid. In *Grammatorcynus* and *Scomberomorus*, the lateral wall of the cleithrum is narrow enough to allow part of the slit to be visible in a lateral view. This slit is hidden in lateral view in the species of *Scomberomorus* because of the great width of the lateral wall of the cleithrum (Devaraj 1977:46, Collette and Russo 1985b: figs. 43a–b).

Coracoid The coracoid is elongate and more or less triangular in shape. It connects with the scapula along its dorsal edge and with the mesial shelf of the cleithrum anterodorsally and anteroventrally. The coracoid is relatively wider in *Grammatorcynus* and *Scomberomorus* than in *Acanthocybium*.

Scapula The anterior margin of the scapula connects to the mesial shelf of the cleithrum. This attachment extends to the posterior projecting plate anterodorsally. The scapula is attached to the coracoid posteriorly and with the first two radials posterodorsally. The posterodorsal margin of the scapula is drawn out into a facet that accepts the most anterior ray of the pectoral fin. The scapula is pierced by a large, usually round, foramen near the lateral margin with the inner shelf of the cleithrum. A prominent suture leads to the dorsal and ventral margin of the scapula from the foramen. The suture is intermediate in size in *Grammatorcynus* relative to the large sutures present in *Acanthocybium*, *S. brasiliensis*, and *S. regalis*, and the small suture in *S. koreanus*.

Radials The four radials differ in size and shape and attach directly to the thickened posterior edges of the scapula and coracoid. The size of the radials increases posteroventrally. Small foramina are located beween the 2nd and 3rd and the 3rd and 4th radials counting posteriorly. In *Grammatorcynus* the first two radials, and sometimes a small portion of the third, attach to the scapula; the second two, sometimes only one and a large portion of the second, attach to the coracoid. In *Acanthocybium* and *Scomberomorus* the upper one-third of the third radial, along with the first two radials, always attaches to the scapula, and the ventral two-thirds of the third radial plus the fourth radial attach to the coracoid. A much larger foramen is present between the largest (fourth) radial and the coracoid. Posteriorly, this foramen is framed by a posterior process of the upper part of the fourth radial meeting an anterior process from the posterior margin of the coracoid. This process is only slightly developed in *Grammatorcynus*. The foramen is about equal in size to, or larger than the scapular foramen in *Grammatorcynus* and *Scomberomorus*, whereas in *Acanthocybium* the scapular foramen is much larger.

Pectoral fin rays The first (uppermost and largest) pectoral fin ray articulates directly with a posterior process of the scapula. The other rays attach to the radials. The number of pectoral rays varies from 19 to 26 in the three genera. *Grammatorcynus* has 21–26

pectoral fin rays, similar to *Acanthocybium* (22–26). *Scombermorus* shows greater variation (19–26) in this character and in most species averages less than either *Grammatorcynus* or *Acanthocybium*. There is a slight difference in number of pectoral fin rays between the species of *Grammatorcynus*: *G. bilineatus* has a range of 22–26, mode 25, $\bar{x}$ 24.4; *G. bicarinatus* 21–24, mode 24, $\bar{x}$ 23.2 (Table 6).

Table 6
Number of pectoral fin rays in *Grammatorcynus*.

	21	22	23	24	25	26	*N*	$\bar{x}$
G. bilineatus		1	11	19	27	4	62	24.4
G. bicarinatus	1	2	2	6			11	23.2

First postcleithrum The posterior projecting plate of the cleithrum has its posterior end attached to the first postcleithrum which connects ventrally to the second postcleithrum. The lamellar first postcleithrum has a narrower upper end and a wider, rounded lower margin (Fig. 23). The upper end is concave in *Grammatorcynus* (Fig. 23c–d) and pointed in both *Scomberomorus* (Fig. 23a) and *Acanthocybium* (Fig. 23b). The width of the postcleithrum varies from 46 to 62% of the length of the bone in *Grammatorcynus*. It is narrower in *G. bicarinatus* (width 46–52% of length, Fig. 23d) than in *G. bilineatus* (55–62%, Fig. 23c). In *Acanthocybium* (47–48%, Fig. 23b) the width is similar to that of *G. bicarinatus*. Species of *Scomberomorus* (Fig. 23a) have narrower postcleithra (24–41%) than the other two genera.

Second postcleithrum The second postcleithrum is broad and lamellar at the upper part with a short pointed ascending process and a long styliform descending process. *Grammatorcynus* (Fig. 24d) differs strikingly from *Acanthocybium* (Fig. 24c) and *Scomberomorus* (Fig. 24a–b) in having a distinct process extending anteriorly from the broad lamellar portion of the bone. The long descending process is so thin in most specimens that an accurate measurement of its length is nearly impossible because some portion of it usually breaks off. No differences were detected in this bone between the two species of *Grammatorcynus*.

Pelvic girdle The pelvic fin rays (I, 5) attach directly to the paired basipterygia that make up the pelvic girdle. The bones are united along the midline and are imbedded in the ventral abdominal wall, free from contact with other bones. Each basipterygium is composed of three main parts: a wide anterodorsal plate, a thin, flat anterior process, and a strong posterior process.

To compare the pelvic girdles, the lengths of the three parts were measured from their bases to their tips. *Grammatorcynus* has the longest anterior process (46–51% of the length of the anterodorsal plate, Fig. 25d), *Acanthocybium* has the next longest (35–47%, Fig. 25c), and *Scomberomorus* the shortest (15–52%, Fig. 25a–b). *Grammatorcynus* (29–33%, Fig. 25d) and *Acanthocybium* (30–39%, Fig. 25c) have shorter posterior processes than the species of *Scomberomorus* (20–90%, Fig. 25a–b).

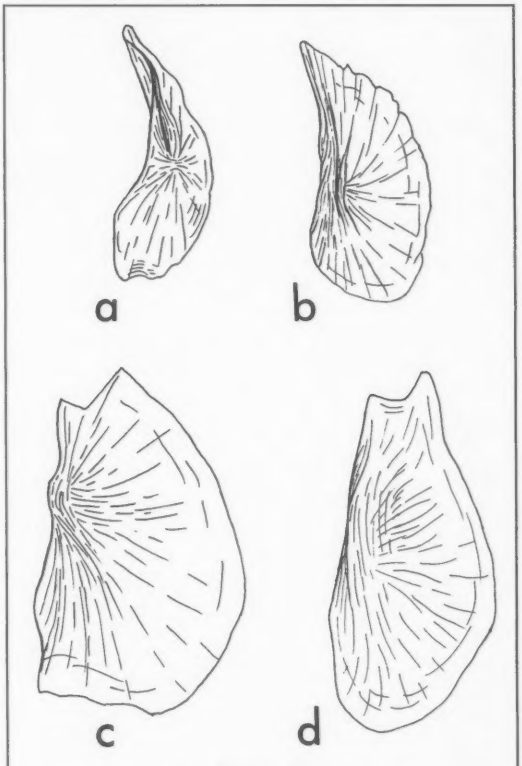

Figure 23
Left first postcleithra in lateral view. (a) *Scomberomorus sinensis*, Hong Kong, 677 mm FL, 1×; (b) *Acanthocybium solandri*, Revillagigedos Is., 1068 mm FL, 1×; (c) *Grammatocynus bilineatus*, Queensland, 521 mm FL, 2×; (d) *G. bicarinatus*, Queensland, 563 mm FL.

Grammatorcynus, some individuals of *Acanthocybium*, and several species of *Scomberomorus* have longer anterior than posterior processes. The lengths of the anterior process as a percentage of the posterior process are: *Grammatorcynus* (154–158%), *Acanthocybium* (91–156%), and *Scomberomorus* species (42–121%).

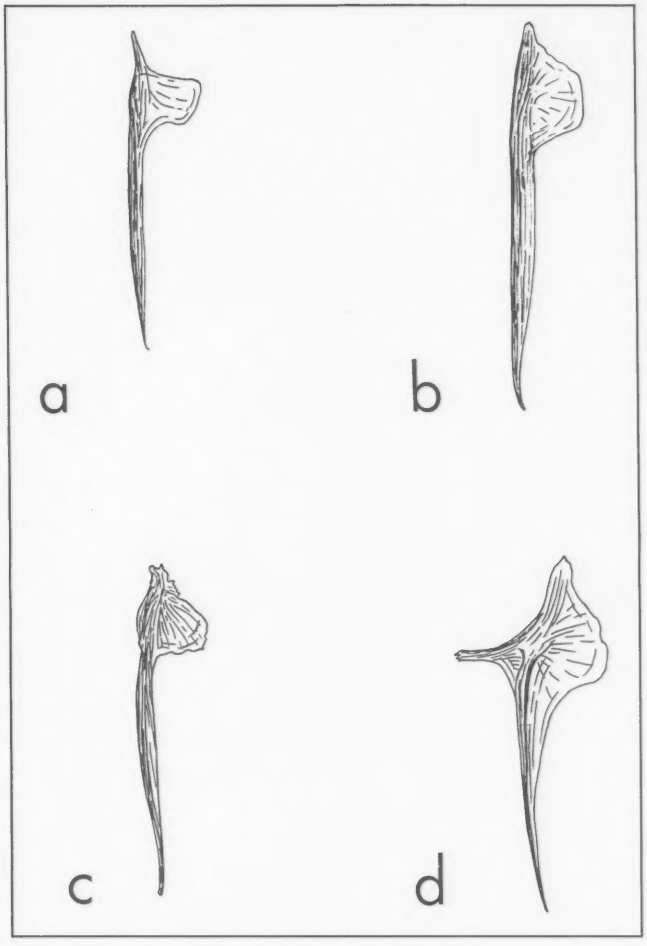

Figure 24
Left second postcleithra in lateral view. (a) *Scomberomorus queenslandicus*, Great Barrier Reef, 641 mm FL, 1×; (b) *S. koreanus*, Indonesia, 480 mm FL, 1.5×; (c) *Acanthocybium solandri*, Revillagigedos Is., 1068 mm FL, 1×; (d) *Grammatorcynus bilineatus*, Queensland, 382 mm FL, 2×.

Grammatorcynus differs from most other scombrids in having a single fleshy interpelvic process. *Auxis* and *Gymnosarda* also have a single interpelvic process; very large in the former, moderate-sized in the latter.

Part 2: Systematics and biology

Grammatorcynus Gill 1862

Grammatorcynus Gill 1862: 125 (original description; type-species *Thynnus bilineatus* Rüppell 1836 by original designation).
Nesogrammus Evermann and Seale 1907: 61 (original description; type-species *Nesogrammus piersoni* Evermann and Seale 1907 by original designation, = *Grammatorcynus bilineatus*).

Figure 25 (below)
Right basipterygia of the pelvic girdle in mesial view. (a) *Scomberomorus regalis*, Miami, FL, 469 mm FL, 1.5×; (b) *S. lineolatus*, Palk Strait, India, 428 mm FL, 2×; (c) *Acanthocybium solandri*, Miami, FL, 1403 mm FL, 1×; (d) *Grammatorcynus bilineatus*, Queensland, 521 mm FL, 1.5×.

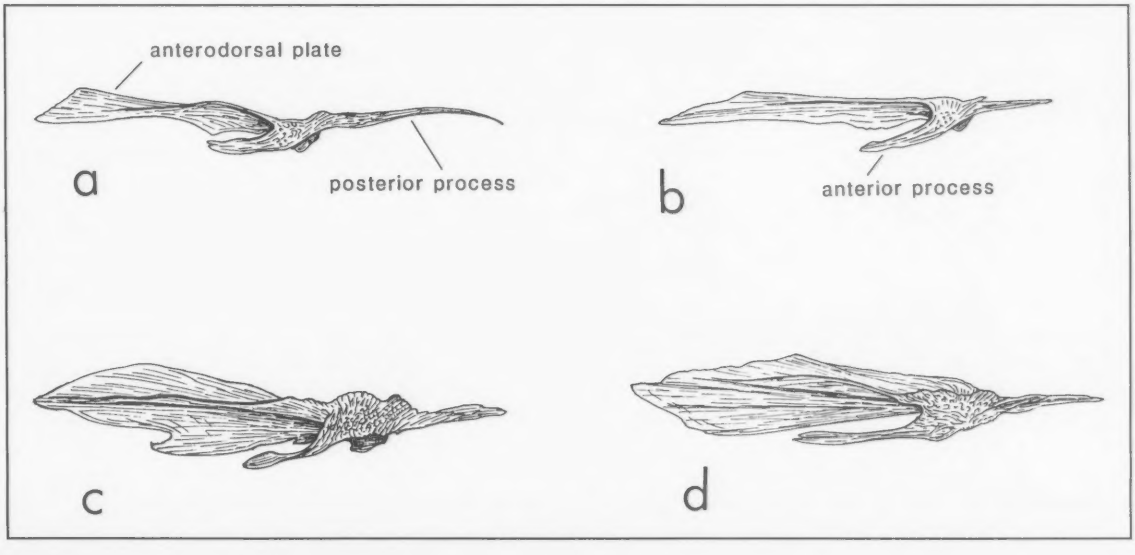

Diagnosis *Grammatorcynus* differs from all other scombrid genera in having a second ventral lateral line, and it differs from all other scombrids and billfishes in lacking a triangular bony stay on the fourth pharyngeal toothplate (Johnson 1986). Like the Scombrini, it has a low number of vertebrae (31) and the caudal fin rays are supported by only the last three vertebrae. Like the Scomberomorini, it has a well-developed median keel on the caudal peduncle, but it lacks the bony support for the keel that is present in bonitos and higher tunas. *Grammatorcynus* differs from *Scomberomorus* in having a pineal window, a single interpelvic process, and large scales.

Collette and Russo (1985b: 612) reported that *Grammatorcynus bilineatus* differed from *Scomberomorus* and *Acanthocybium* in 16 osteological characters. *Grammatorcynus bicarinatus* also differs in 15 of those 16 characters: **(1)** supracleithrum wide, 72–89% of length (narrow, 42–62% in *Scomberomorus* and *Acanthocybium*); **(2)** pores absent along dorsal branch of supratemporal (present); **(3)** nasal bones protrude far beyond ethmoid region (do not protrude far beyond); **(4)** posterior end of urohyal tripartite (forked); **(5)** glossohyal with large tooth patch fused to dorsal surface of bone (no fused tooth patch); **(6)** hyomandibula narrow, 34–39% of length (wide, 39–52%); **(7)** angle of lateral and medial arms of fourth epibranchial more acute (less acute); **(8)** anterior process of second epibranchial elongate (shorter); **(9)** three vertebrae support caudal fin rays (four or five vertebrae); **(10)** distinct anterior process on second postcleithrum (no such process); **(11)** anterior end of first postcleithrum notched (pointed); **(12)** first two pectoral radials attach to scapula (upper one-third of third radial also attaches to scapula); **(13)** jaw teeth conical (compressed and triangular); **(14)** shaft of parasphenoid narrow and concave or flat (wider and convex); and **(16)** posterior edge of ectopterygoid long, 63–72% of ventral distance (short, 41–63%). Unlike *G. bilineatus*, *G. bicarinatus* resembles *Scomberomorus* and *Acanthocybium* in having the upper margin of the dentary longer than the lower margin **(15)**.

Relationships Larval characters of *Grammatorcynus bilineatus* (as described by Wade 1951 from eight specimens 8.5–17.5 mm FL) were used by Okiyama and Ueyanagi (1977, 1978) and Ueyanagi and Okiyama (1979) to construct an "index of primitiveness" that divided the Scombrinae into four groups: mackerels, *Grammatorcynus*, tunas, and Spanish mackerels and bonitos. Nishikawa (1979) expanded the description of larvae based on 62 specimens, 4.75–56.9 mm SL, from Papua New Guinea. Nishikawa (1979) and Jenkins (1989) noted that *Grammatorcynus* larvae have preopercular spines characteristic of higher scombrids but absent in *Scomber* and *Rastrelliger*.

Lewis (1981) examined Australian scombrids electrophoretically and found that the two *Grammatorcynus* species showed fixed differences at 6 (23%) of 26 loci (GPD, ADA, ADH, GDA, PK_2, and PGM_1). Fixed differences were also observed at several other loci not used in his study, namely AD_2 and XO. He analyzed the electrophoretic data phenetically and cladistically. The two most parsimonious Wagner networks involved 308 steps. The species of *Grammatorcynus* were always paired and well-separated from

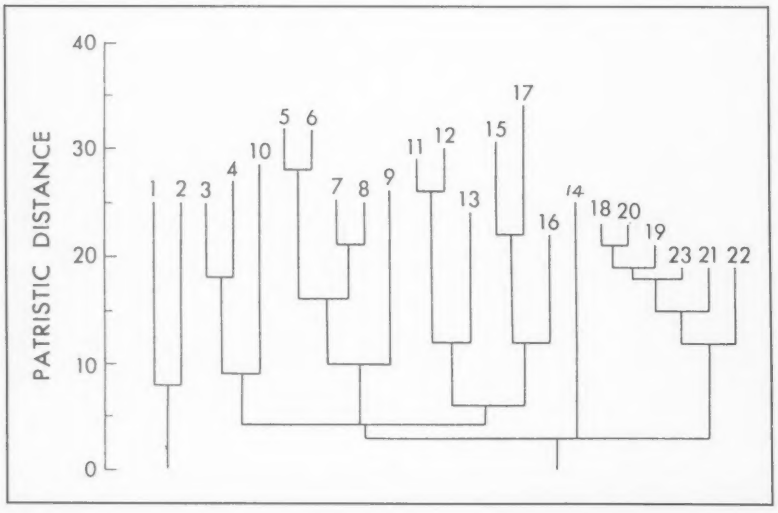

Figure 26
One of two equally parsimonious Wagner networks for 23 Australian species of Scombridae expressed in dendrogram form (from Lewis 1981: fig. 6.4). (1) *Scomber australasicus*, (2) *Rastrelliger kanagurta*, (3) *Grammatorcynus bicarinatus*, (4) *G. bilineatus*, (5) *Scomberomorus commerson*, (6) *S. queenslandicus*, (7) *S. multiradiatus*, (8) *S. semifasciatus*, (9) *S. munroi*, (10) *Acanthocybium solandri*, (11) *Sarda australis*, (12) *S. orientalis*, (13) *Cybiosarda elegans*, (14) *Gymnosarda unicolor*, (15) *Auxis* sp., (16) *Euthynnus affinis*, (17) *Katsuwonus pelamis*, (18) *Thunnus albacares*, (19) *T. tonggol*, (20) *T. obesus*, (21) *T. alalunga*, (22) *T. maccoyii*, (23) *T. thynnus orientalis*.

other Scomberomorini (Fig. 26). They were most often linked with *Acanthocybium* and then with species of *Scomberomorus*.

Based on both adult and larval morphological characters and Lewis' electrophoretic data, *Grammatorcynus* is clearly more advanced than the mackerels (Scombrini) and less advanced than the higher scombrids. Collette et al. (1984: fig. 312) placed it between *Gasterochisma* and the Scombrini on the one hand, and the more advanced Scomberomorini, Sardini, and Thunnini on the other hand. Collette and Russo (1985a, b) used *Grammatorcynus* as the primary outgroup in assessing relationships of the species of *Scomberomorus*. In his reappraisal of scombroid relationships, Johnson (1986: fig. 1 and p. 38–39) placed *Grammatorcynus* in its own tribe, Grammatorcynini, above the Scombrini, as the sister group of higher scombroids, which included the Sardini (including the Thunnini), Scomberomorini, Acanthocybiini, and billfishes.

Grammatorcynus bilineatus (Rüppell, 1836) Double-lined or scad mackerel

Thynnus bilineatus Rüppell 1836:39–40 (original description, Red Sea), pl. 12, fig. 2. Günther 1860: 366–367 (description). Klunzinger 1871:443 (Red Sea). Meyer 1885:270 (Celebes).

Grammatorcynus bilineatus. Gill 1862:125 (*T. bilineatus* type species of new genus). Kishinouye 1923: 413–415 (description, anatomy; Ryukyu and Marshall Is.), fig. 10 (skeleton); pl. 16, fig. 8 (transverse section of vertebrae; pl. 34, fig. 62 (drawing). Hardenberg 1935:137–138 (description; W Java Sea). Okada 1938:170 (E. Indies, Red Sea; nijiyō saba). Morice 1953:36–40 (anatomy; after Kishinouye 1923). Schultz 1960:411–412 (description; Bikini, Marshall Is.). Kuronuma 1961:16 (listed, Vietnam). Lewis 1968:51 (Eniwetok, Marshall Is., infested with parasitic copepod *Caligus asymmetricus*). Collette 1983: 715–716 (distinguished from *G. bicarinatus*), fig. 1A. Collette and Nauen 1983:39–40 (description, range, fig.). Collette et al. 1984:608 (fig. 326, larva after Nishikawa 1979), 618 (larvae). McPherson 1984 (color pattern in Queensland, fig.). Masuda et al. 1984: 224–225 (description); color pl. 220A. Collette and Russo 1985a:141–144 (outgroup for *Scomberomorus*). Collette and Russo 1985b (anatomy, osteology, figures, comparisons with *Scomberomorus*). Allen and Russell 1986:101 (Scott Reef, NW Australia). Grant 1987:362–363 (scad mackerel; Queensland; color photo 769). Allen and Swainston 1988: 144 (Dampier Archipelago northwards, NW Australia), 145 (color painting 966). Bauchot et al. 1989: 657 (large brain, encephalization index of 226). Zug et al. 1989:14 (Rotuma I.). Randall et al. 1990:443 (description, range), color plate VIII-14 (painting).

Nesogrammus piersoni Evermann and Seale 1907 (original description; Bulan, Sorsogon Province, Luzon, Philippine Is.); pl. 1, fig. 3.

Grammatorcynus bicarinatus not of Quoy and Gaimard 1825. Herre 1931:33 (Balabac and Jolo, Philippine Is.). Fraser-Brunner 1950:156 (synonymy), fig. 25. Umali 1950:9 (Zamboanga and Jolo, Philippine Is.). Warfel 1950:18 (Philippine Is.), fig. 13 (drawing of fish, gill arch, and liver). Wade 1951:456–458 (8 larvae, 8.5–17.5 mm; Philippine Is.), fig. 2 (8.5 mm specimen), fig. 3 (17.5 mm specimen). de Beaufort 1951:215–216 (description, synonymy), fig. 36. Herre 1953:248 (synonymy). Dung and Royce 1953: 168–169, table 97 (morphometric data on 17 specimens 408–580 mm FL, western Marshall Is.). Matsubara 1955:519 (2 lateral lines; range), fig. 222B. Munro 1958b:262–263 (New Guinea region records; CSIRO C492, New Hanover, examined). Jones et al. 1960:136 (Ross I., Port Blair, Andaman Is.). Collette and Gibbs 1963a:25 (monotypic genus). Collette and Gibbs 1963b:27 (description), pl. 7. Jones and Silas 1963:1781 (synonymy, Indian Ocean references, range). Silas 1963:811–833 (description, synonymy, synopsis of biological data). Kamohara 1964:34 (Miyako-jima, Ryukyu Is.). Jones and Kumaran 1964:364–365, figs. 70–71 (larvae, after Wade 1951). Jones and Silas 1964a:16, 18 (description, synonymy, range), pl. 4, fig. (449 mm female from Port Blair, Andaman Is.). Jones and Silas 1964b:258 (in key; Andaman Is.). Gorbunova 1965: 55 (references to Wade 1951 and Silas 1963). Tongyai 1966:6 (in key), 17 (pl. 1, outline fig. of specimen from Phuket I.). Kamohara 1967:43 (description). Munro 1967:197–198 (description of *G. bicarinatus*; New Guinea specimens are *G. bilineatus*). Ben-Tuvia 1968:35 (Entedibir Is., Red Sea), fig. 3g. Ben-Yami 1968:40 (schools probably occur in region of Sahlak Archipelago, southern Red Sea). Jones 1968:998 (occur in catches in Andaman area). Jones 1969:26 (Laccadive Archipelago, India). Tongyai 1970:558 (Thai common names; Indian Ocean coast of Thailand). Tongyai 1971:3–5 (description, Thai common names, Thai distribution). Shiino 1972:70 (common names). Richards and Klawe 1972:72 (references to larvae). Gushiken 1973:49 (color photograph of 60 cm specimen from Okinawa). Helfman and Randall 1973:151 (Palau; common names mokorokor and biturturch). Magnuson 1973:350 (correlation of size, pectoral fin length, and presence of swim bladder). Lewis et al. 1974:83, 87 (Bismarck Archipelago, Papua New Guinea). Springer et al. 1974:40 (Indonesia). Romimohtairo et al. 1974:35

(Gamber Bay, Gag I., Indonesia). Gorbunova 1974:26 (fig. 2, after Wade 1951). Orsi 1974:174 (listed, Vietnam). Masuda et al. 1975:256 (color photograph F), 79 (description; Okinawa southward). Cressey 1975: 216 (parasitic copepod *Shiinoa occlusa* from nasal cavity of a specimen from N. Celebes). Kailola 1975:235 (5 collections from Papua New Guinea). Uyeno and Fujii 1975:14 (table 1, comparison of caudal complex with other scombrids). Fourmanoir and Laboute 1976:183 (description; New Caledonia), color photograph. Shiino 1976:229 (common names). Anonymous 1977:15 (table 4, Bagaman I., Louisiade Archipelago, Papua New Guinea). Klawe 1977:2 (table 1, range). Collette 1979:29 (characters, range). Céng and Yāng 1979:472–473 (description; Sisha Is., South China Sea), fig. 335. Yamakawa 1979:43 (Miyako-jima, Ryukyu Is., after Kamohara 1964). Joseph et al. 1979:38 (range, figure). Nishikawa 1979:125–140 (early development; 62 postlarval and juvenile specimens, mostly from Papua New Guinea). Shirai 1980:64 (description, Ryukyu Is.), color photograph. Cressey and Cressey 1980:46 (parasitic copepod fauna: *Shiinoa occlusa* and *Caligus asymmetricus*). Rau and Rau 1980: 512–513 (description, Philippine Is.). Jones and Kumaran 1981:581–582 (description; Laccadive Archipelago), fig. 494. Wang 1981:161 (listed; S. China Sea). Johannes 1981:156–157 (biology, Palau). Lewis 1981:13 (species B, scad; maximum size 60 cm FL, 3 kg), photograph. Kyushin et al. 1982:249 (description, common name nijō-saba), color photograph (specimen from Milne Bay, New Guinea). Cressey et al. 1983:238 (systematic position of genus), 264 (parasitic copepod fauna; 4 species of *Caligus* added). Lewis et al. 1983:7 (table 2, 203 specimens, 380–630 mm FL; Fiji). Wass 1984:31 (Fiji; common name "namuauli"). Masuda et al. 1984:224–225 (description, Japan), pl. 220A. Gillett 1987:20 (caught by Satawal tuna fishermen, central Caroline Is.). Nishikawa and Rimmer 1987:5 (larval description; fig. 5, larva, postlarva, and juvenile from Nishikawa 1979). Dyer et al. 1989:65 (monogenean *Caballerocotyla* sp. from Okinawa specimen). Rivaton et al. 1989:67 (listed, New Caledonia).

Grammatorcynnus (sic) *bicarinatus* not of Quoy and Gaimard 1825. Roux-Estève and Fourmanoir 1955:201 (Abulat I., Red Sea).

Grommatorcynus (sic) *bicarinatus* not of Quoy and Gaimard 1825. Zhang 1981:302 (description of 3 larvae, Sisha Is., South China Sea; fig. 1, 6.4 mm larva).

Grammatorcynos (sic) *bilineatus*. Myers 1988:168 (listed, Mariana Is.). Myers 1989:254 (description; range), underwater photo 134A, 280 (listed; Caroline, Mariana, and Marshall Is.).

Diagnosis *Grammatorcynus bilineatus* has more gill rakers (18–24 vs. 12–15), a larger eye (4.1–6.0% vs. 3.1–4.6% FL), lacks black spots on the lower sides of its body, and does not reach as large a size (max. 600 mm FL) as *G. bicarinatus*.

Description Dorsal spines 11–13, usually 12; rays 10–12, usually 11; finlets 6, rarely 7 (Table 4). Anal fin with one spine, 11–13, usually 12 rays; 6 finlets, rarely 5 or 7 (Table 5). Pectoral fin rays 22–26, usually 24 or 25 (Table 6). Gill rakers on first arch 18–24, usually 21, $\bar{x}$ 20.8 (Table 3). Upper jaw teeth 14–37, $\bar{x}$ 23.5 (left), 24.5 (right) (Table 2); lower jaw teeth 12–32, $\bar{x}$ 18.6 (left), 19.1 (right) (Table 2). Morphometric data summarized in Table 1.

Grammatorcynus bilineatus has a longer neurocranium (14–16% FL vs. 13%), longer parasphenoid flanges (18–21% of neurocranium length vs. 14%), higher maximum number of teeth on the upper (37 vs. 25) and lower (32 vs. 23) jaws, higher posterior expansion of the maxilla (8–11% of maxilla length vs. 6–8%), longer quadrate process (134–145% of quadrate length vs. 122–125%), wider first postcleithrum (55–62% of length vs. 46–52%), narrower ethmoid (19–21% of length vs. 25–28%), narrower vomer (13–15% of length vs. 16–18%), narrower lachrymal (27–30% of length vs. 30–35%), shorter teeth (up to 4% of dentary length vs. up to 6%), narrower palatine tooth patch (26–32% of length vs. 38–42%), narrower opercle (63–72% of length vs. 72–79%), and the shelf between the posttemporal processes is hidden behind the flat posterior portion of the bone.

Color In life, the back is bright pale green, the upper sides and belly silvery, and there are no black spots on the belly as there are in *G. bicarinatus* (Grant 1987: 363). Underwater, it is reported to display a distinctive white patch on the caudal peduncle (McPherson 1984). There are color photographs of fresh specimens from Japan (Masuda et al. 1975:256, Shirai 1980:64), New Caledonia (Fourmanoir and Laboute 1976:183), South China Sea (Kyushin et al. 1982:249), and Australia (Grant 1987: fig. 769). An underwater photograph has been published from Micronesia (Myers 1989: photo 134A). There is a color painting in Randall et al. 1990 (pl. VIII-14).

Size Maximum size is about 63 cm FL, 3.3 kg weight (Lewis et al. 1983). Maturity seems to be attained at about 40–43 cm FL (Silas 1963, Johannes 1981, Lewis et al. 1983).

Biology The best summary of biological information on *G. bilineatus* is Silas (1963). It is an epipelagic species found mostly in shallow reef waters where it

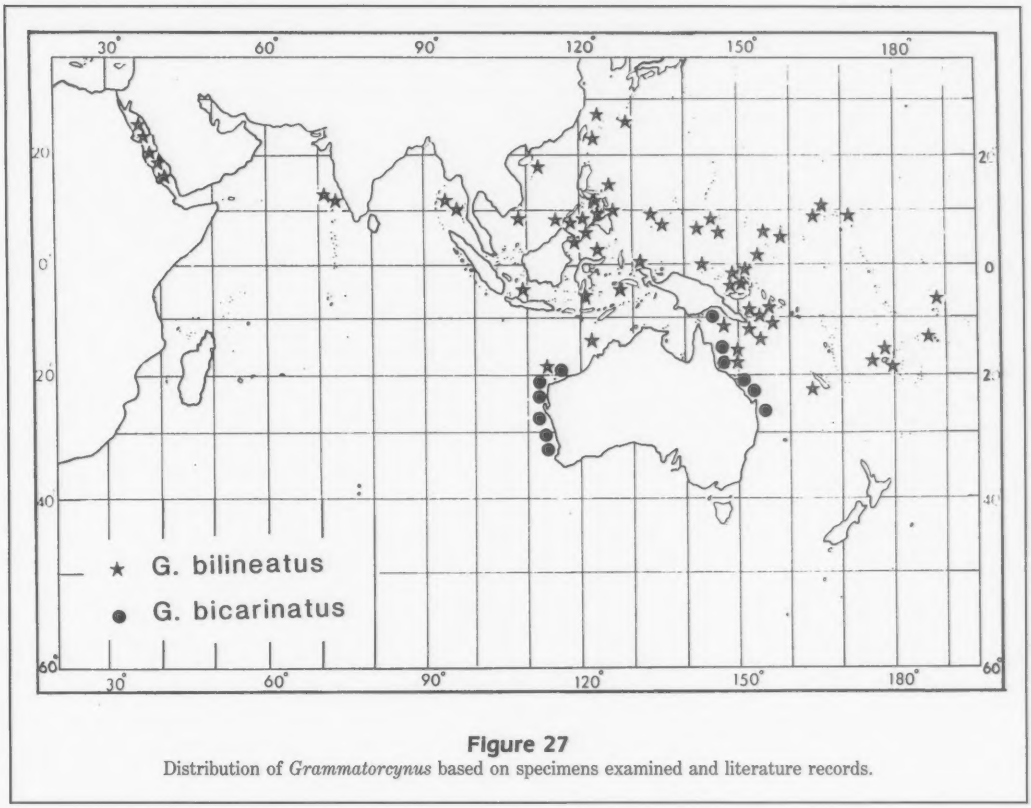

Figure 27
Distribution of *Grammatorcynus* based on specimens examined and literature records.

forms large schools. The spawning season in Fiji extends from October through March (Lewis et al. 1983). Larvae and juveniles have been illustrated from the Philippines (Wade 1951), Papua New Guinea (Nishikawa 1979), and the South China Sea (Zhang 1981). Food includes adult and juveniles of crustaceans and fishes, particularly clupeoids such as *Sardinella* and *Thrissocles*, but also includes other fishes such as *Sphyraena* and *Balistes* (Silas 1963:831).

Parasites Six species of parasitic copepods have been reported from *G. bilineatus* (Cressey and Cressey 1980, Cressey et al. 1983): Shiinoidae: *Shiinoa occlusa* Kabata; Caligidae: *Caligus asymmetricus* Kabata, *C. regalis* Leigh-Sharpe, *C. bonito* Wilson, *C. pelamydis* Krøyer, and *C. productus* Dana. The monogenean *Caballerocotyla* sp. was found on an Okinawan specimen (Dyer et al. 1989).

Interest to fisheries Double-lined mackerel are taken incidentally with hand lines off Port Blair, Andaman Islands (Silas 1963). It is common in the offshore zones of Fiji but is only occasionally seen in Fiji markets (Lewis et al. 1983). The flesh is reported to be mild and pleasantly flavored but it is necessary to remove the kidney tissue before cooking to avoid the ammonia smell. This characteristic has given rise to one of the Palauan names for the species, biturchturch, which means urine (Johannes 1981:187). It is valued for marlin bait in Queensland (McPherson 1984).

Range Widespread near coral reefs in the tropical and subtropical Indo-West Pacific (Fig. 27). Based on literature, specimens examined, and photographs, known from the Red Sea, Andaman Sea, East Indies, Philippines, South China Sea, Ryukyu Islands, New Guinea (New Britain, New Ireland, New Hanover, and the Louisiade Archipelago), Australia (northern Western Australia, from Dampier Archipelago north and Queensland), Solomon Islands, New Caledonia, Caroline Islands, Marshall Islands, Fiji, Tonga, and Tokelau Islands (photograph from Fakaofo Atoll received from Robert Gillett, Regional Fishery Support Programme, Suva, Fiji, Aug. 1985).

Table 7
Morphometric comparison of *Grammatorcynus bilineatus* from the Red Sea and the western Pacific Ocean.

	Red Sea					Western Pacific Ocean				
Character	*N*	Min	Max	Mean	SD	*N*	Min	Max	Mean	SD
Fork length (thousandths)	15	264	432	364	53	44	226	575	430	72
Snout-A	15	592	628	615	11	41	581	641	603	12
Snout-2D	15	534	557	547	7	41	528	619	548	16
Snout-1D	15	287	306	296	7	44	276	322	295	10
Snout-P2	15	249	271	261	7	43	236	306	257	12
Snout-P1	15	220	244	230	7	43	199	245	224	9
P1-P2	15	94	135	105	9	43	90	111	100	5
Head length	15	213	234	220	6	44	197	236	218	8
Max. body depth	13	182	213	201	8	40	164	234	193	15
Max. body width	12	97	122	111	8	40	91	136	115	9
P1 length	14	110	142	122	9	44	106	142	128	7
P2 length	14	74	81	77	2	44	70	87	76	4
P2 insertion-vent	14	312	352	333	12	43	262	354	326	15
P2 tip-vent	13	242	275	256	11	43	228	273	249	9
Base 1D	15	207	246	230	10	43	211	261	236	10
Height 2D	12	88	109	98	6	37	88	116	99	7
Base 2D	14	88	114	102	8	43	79	118	102	8
Height A	11	84	102	93	7	34	82	114	96	7
Base A	14	74	89	84	4	44	73	101	88	7
Snout (fleshy)	15	77	86	81	3	44	58	90	79	5
Snout (bony)	15	71	78	74	3	44	60	80	71	5
Maxilla length	15	95	108	101	4	43	89	107	97	5
Postorbital	15	89	98	93	2	43	78	98	91	4
Orbit (fleshy)	15	44	57	49	4	44	40	60	49	4
Orbit (bony)	15	60	75	68	5	44	53	88	68	7
Interorbital	15	58	67	62	3	43	56	74	62	3
2D-caudal	15	458	475	468	5	41	427	496	471	16
Head length (thousandths)	15	62	94	80	11	44	50	126	94	16
Snout (fleshy)	15	340	384	369	11	44	248	397	365	22
Snout (bony)	15	313	351	336	11	44	281	357	326	18
Maxilla length	15	443	469	459	8	43	420	480	443	14
Postorbital	15	397	433	420	12	43	350	450	419	16
Orbit (fleshy)	15	206	253	222	13	44	191	257	226	15
Orbit (bony)	15	283	336	307	15	44	252	381	313	27
Interorbit	15	268	298	283	9	43	253	327	284	14

Geographic variation The wide range of *G. bilineatus* plus the gaps in distribution due to its preference for coral reef habitats lead to the possibility that some populations differ morphologically from others. However, comparison of frequency distributions by geographic areas of meristic characters summarized in Tables 2–6 showed general uniformity in the range and modes of these characters. The Red Sea population is the most isolated from the rest, but it showed no meristic differentiation. Comparisons of ranges and means of morphometric data showed few differences between the Red Sea and Pacific populations (Table 7).

Dissections 11 (382–521mm FL). USNM 270386 (410), Australia, diss. 1-28-69. USNM 270390 (453), Scott Reef, J. McCosker 73-8, diss. 4-1-76. USNM 270387 (424), Marshall Is., J. E. Randall, diss. 4-29-76. USNM 270384 (382), Kavieng, New Guinea, diss. 10-12-76. USNM 270385 (389), Cairns, Qld., G. McPherson, diss. 3-30-81. USNM 270389 (521), Port Douglas, Qld., diss. 3-31-81. USNM 270388 (416), Cairns, Qld., G. McPherson, diss. 1-5-83. USNM 270383 (475), Scott Reef, J. McCosker 72-18, diss. 1-10-83. USNM 270382 (399), Cairns, Qld., G. McPherson, diss. 1-11-83. USNM 270391 (400), Port Douglas, Qld., diss. 1-13-83. USNM 316130 (460), Scott Reef, J. McCosker 73-8, diss. 7-18-89.

Material examined 80 specimens (23.5–575mm FL) from 58 collections.

Red Sea 16 (264–440) from 10 collections. SMF 2755 (1, 287); Massua; E. Rüppell; holotype of *Thynnus bilineatus*; stuffed. NMW uncat. (5, 362–432); Jambo; 1895–96; I.R.M. Exped. 62c. NMW uncat. (1, 424); Hassani; 1895–96; I.R.M.

Exped. 62b. NMW uncat. (1, 360); Djeddah; 1895–96; I.R.M. Exped. 62. NMW uncat. (2, 264–320); Rothes Meer; 1879–80; Klunzinger. NMW 16825 (2, 304–382); Rothes Meer; Klunzinger. MNHN 52–28 (1, 422); Mer Rouge; "Calypso". USNM 266928 (1, 327); near Entedebir; March 1962; ISRSE 4144. HUJ E62/4399 (1, 368); S Red Sea; March–April 1962; Israel; S Red Sea Exped. BPBM 28388 (1, 440); Saudi Arabia, Jeddah market; 11 May 1982; J.E. Randall.

Andaman Sea 4 (235–294) from 2 collections. MFLB uncat. (2, 282–294); Thailand, Phuket Province; 23 Feb. 1966. MFLB uncat. (2, 235–237); Thailand, Phuket Province; 27 Jan. 1970.

East Indies 4 (108–413) from 4 collections. BMNH 1872. 4.6.25(1, 413); N. Celebes; Meyer. AMNH 17583 (1, 108) Celebes. USNM 213564 (1, 395); Indonesia, Ambon fish market; V.G. Springer; 19 March 1974. USNM 213565 (1, 360); Indonesia, Buton I., Teluk Buton; V.G. Springer and M.F. Gomon; VGS 74-26; 28 March 1974.

Philippine Islands 5 (275–390) from 5 collections. USNM 55899 (1, 372); Luzon, Sorsogon Province, Bulan; C.J. Pierson; holotype of *Nesogrammus piersoni*. USNM 195044 (1, 343); Cebu market; 6 April 1908; Albatross. CAS SU 13575 (1, 275); Balabac I.; A.W.C.T. Herre; 1929. CAS SU 13687 (1, 342); Jolo; A.W.C.T. Herre; 1931. CAS SU 40469 (1, 390); Gulf of Leyte, Leyte; R.F. Annereaux; 12 Sept. 1945.

Okinawa ZUMT 16738 (1, 378); Okinawa. ZUMT 52381 (1, ca. 500); Okinawa, Ishigaki I.; 4 June 1966.

New Guinea 10 (23.5–410) from 6 collections. CSIRO C.492 (1, 226); New Hanover, Drei Inseln Harbor, Kulineva R. USNM 270384, 316162 (2, 363–382); New Ireland, Kavieng; 20 March 1976. DASF 4247 (1, 23.5); New Britain; Borgen Bay; 13 April 1972. DASF 4248 (1, 37.9); New Britain; Tavanatangir; 11 Oct. 1972. DASF 4250 (2, 54.3–65.5); New Britain; Dikarua I.; Cape Lambert; 28 Nov. 1972. USNM 320095 (3, 385–410); Hermit Is., E side Jalun I.; 2 Nov. 1978.

Australia 9 (389–521) from 4 collections. USNM 270383 (1, 475); Western Australia, Scott Reef; J.E. McCosker 72-18. USNM 270390, 316130 (2, 453–460); Western Australia, Scott Reef, 14°05′S, 121°50′E; J.E. McCosker 73-8. USNM 270382, 270385, 270388, 316161 (4, 389–416); Queensland, Cairns; G. McPherson and P. Cooper. USNM 270389, 270391 (2, 400–521); Queensland, off Port Douglas; Sept.–Oct. 1976.

Solomon Islands 2 (275–482) from 2 collections. USNM 205078 (1, 482); New Georgia, Gizo I.; W. Chapman; 30 May 1944. AMS I.19435-020 (1, 275); Solomon Is.; G. Smith.

Caroline Islands 15 (327–575) from 13 collections. CAS GVF 651 (1, 462); Palau Is., Rattakadakoru; Palau 145; 5 Sept. 1955. CAS GVF 933 (1, 439); Palau Is., Velasco Reef; Palau 147; 6 Oct. 1956. CAS GVF 934 (1, 432); Palau Is., Velasco Reef; Palau 148; 6 Oct. 1956. CAS GVF 946 (1, 454); Palau Is., Velasco Reef; Palau 149; 6 Oct. 1956. CAS GVF 1422 (1, 543); Palau Is., Ilruthapel I.; Palau 57–42; 20 Oct. 1957. CAS GVF 1867 (1, 461); Palau Is.; Palau 59–39; 15 April 1959. CAS GVF 1891 (1, 444); Palau Is., Angaur I.; Palau sta. 59-63; 16 June 1959. CAS GVF 1970 (2, 543–575); Palau Is., Kossol Passage, 7°56′18″N, 134°31′55″E; sta. 59-709; 30 July 1959. BPBM 10501 (2, 434–448); Palau; 23 April 1964. USNM 264910 (1, 510); between Ponape and Ant Atoll; R.A. Croft; 1983. CAS GVF (1, 408); Kapingamarangi, 1°6′N, 154°44′W; sta. 108; 4 Aug. 1958. CAS GVF 405 (1, 327); Kapingamarangi; sta. 102; 2 Aug. 1954. CAS GVF 33 (1, 462); Ifaluk; 2 Oct. 1953.

Marshall Islands 9 (254–549) from 7 collections. USNM 140986 (2, 419–468); Bikini Atoll lagoon, V. Brock and J. Marr; 2 April 1946. USNM 142054 (2, 503–549); Bikini Atoll lagoon off Bikini I.; V. Brock and J. Marr; 25 March 1946. USNM 142055 (1, 410) Bikini Atoll, W of Boro I., V. Brock; 6 April 1946. USNM 181932 (1, 382); Majuro Atoll; A.F. Bartsch; 1958. BPBM uncat. (1, 254); Majuro Atoll; P. Shiota; 30 Aug. 1972. USNM 270387 (1, 424); Enewetak Atoll; J.E. Randall; 2 April 1976. BPBM 12800 (1, 330); Enewetak; 4 April 1972; J.E. Randall.

Fiji Islands 2 (335–426) from 2 collections. USNM 176657 (1, 426); S of Suva; J.K. Howard; 4–15 Dec. 1952. USNM 243969 (1, 335); reef NNE Malamala I., V.G. Springer 82-24; 24 May 1982.

Rotuma Island USNM 285517 (396); Rotuma; G.D. Johnson; 14 May 1986.

Samoan Islands USNM 305080 (1, 465); American Samoa, East Bank, 12 mi. off E end of Tutuila; 1 July 1989.

Grammatorcynus bicarinatus (Quoy and Gaimard, 1825) Shark mackerel

Thynnus bicarinatus Quoy and Gaimard 1825:357 (original description; Baie des Chiens-Marins (= Shark Bay), W. Australia), pl. 61, fig. 1.

Grammatorcynus bicarinatus. McCulloch 1915:266–269 (description; off Cook I., near Tweed River Heads, New South Wales; 925 mm FL, 18.75 lbs.), pl. 1, fig. 1. Ogilby 1918:101 (reference to McCulloch 1915; caught off Moreton Bay, Queensland), 105 (30-lb. specimen in Queensland state fish market). McCulloch 1922:106 (New South Wales; rarely captured; to 3 ft.). McCulloch and Whitley 1925:142 (Moreton Bay, Queensland). McCulloch 1929:263–264 (synonymy). Anonymous 1945:7 (listed among marketable fish of Cairns, Queensland area). Whitley 1947:129 (W. Australia). Whitley 1948:24 (listed, W. Australia). Coates 1950:22 (Great Barrier Reef; 25 lbs. maximum; "shark mackerel"), fig. Serventy 1950:20 (common in W. Australia from Geraldton northwards but not extending in waters of the Kimberly Division of W. Australia). Munro 1958a:112 (description; Queensland, N New South Wales, and W. Australia), fig. 748 (after McCulloch). Whitley 1964a:232 (length to 48 in., weight 25 lb.), 239 (fig. 4f, range in Australia only), pl. 4 (fig. b, after McCulloch). Whitley 1964b:48 (listed). Marshall 1964:367 (description, Queensland), color plate 53, fig. 354. Grant 1965:176 (description after Munro 1958a; sought-after market fish in

Queensland), fig. Marshall 1966: 205 (description), color plate 53, fig. 354. Munro 1967:197–198 (text is based on Australian *G. bicarinatus*; New Guinea specimens are *G. bilineatus*), fig. 333. Grant 1972: 107 (same as 1965), fig. Coleman 1974:42 (color, habits), 43 (underwater color photograph, Heron I., Queensland). Grant 1975:165 (same as 1972), fig. Rohde 1976:50 (Lizard I., Queensland). Anonymous 1978:18 (listed among species being investigated by Queensland Fisheries Service). Grant 1978:195 (same as 1975), fig. Hutchins 1979:83 (may visit Rottnest I., W. Australia). Coleman 1981:268 (Australia, habits), color underwater photo (from Coleman 1974). Lewis 1981:12 (species A, shark mackerel; maximum size 110 cm FL, 13.5 kg) photograph. Grant 1982:632 (same as 1978 plus comments on ammonia smell of flesh). Collette 1983:716–718 (distinguished from *G. bilineatus*), fig. 1B. Collette and Nauen 1983:39–40 (description, range, fig.). Hutchins and Thompson 1983:62, 85 (W. Australia), p. 63 (fig. 290). Russell 1983:146 (Heron I., Barrier Reef based on Coleman 1974). McPherson 1984 (color pattern in Queensland, fig.). Collette and Russo 1985b:547 (in key). Hutchins and Swainston 1986: 102 (description, range), 103 (color painting 587), 141 (weight to 11.7 kg). Grant 1987: 362 (shark mackerel; Queensland; color photo 768). Allen and Swainston 1988:144 (Geographe Bay north, Western Australia), 145 (color painting 965). Hutchins 1990:275 (sight record, Shark Bay, Western Australia). Randall et al. 1990:433 (description, range), color plate VII-13 (painting).

Diagnosis *Grammatorcynus bicarinatus* has fewer gill rakers (12–15 vs. 18–24), a smaller eye (3.1–4.6% vs. 4.1–6.0% FL), small black spots on the lower sides of its body, and reaches a larger maximum size (1100 mm FL) than *G. bilineatus*.

Description Dorsal spines 12; rays 10, finlets usually 7, rarely 6 or 8 (Table 4). Anal spines 1, rays 11–13, finlets 6 or 7, usually 7 (Table 5). Pectoral fin rays 21–24, $\bar{x}$ 23.2 (Table 6). Gill rakers on first arch 12–15, $\bar{x}$ 14.1 (Table 3). Upper jaw teeth 14–25, $\bar{x}$ 20.5 (left), 20.9 (right) (Table 2); lower jaw 15–23, $\bar{x}$ 17.5 (left), 17.6 (right) (Table 2). Morphometric data summarized in Table 1.

Grammatorcynus bicarinatus has a shorter neurocranium (13% vs. 14–16% FL), shorter parasphenoid flanges (14% vs. 18–21% neurocranium length), a lower maximum number of teeth on the upper (25 vs. 37) and lower (23 vs. 32) jaws, lower posterior edge of shank of maxilla (6–8% vs. 8–11% maxilla length), shorter quadrate process (122–125% vs. 134–145% quadrate length), narrower first postcleithrum (46–52% vs. 55–62% length), wider ethmoid (25–28% vs. 19–21% length), wider vomer (16–18% vs. 13–15% neurocranium length), wider lachrymal (30–35% vs. 27–30% length), longer teeth (maximum 6% vs. 4% dentary length), wider palatine tooth patch (38–42% vs. 26–32% length), wider opercle (72–79% vs. 63–72% length), and a thin posttemporal shelf between the anterior processes.

Color General color in life is bright, glowing green above, grading into the silver of the sides and belly, which is marked with scattered small black spots that are absent in *G. bilineatus* (Grant 1987:362). Underwater, it is reported to display a dark band along the lower lateral line (McPherson 1984). Color photographs have been published by Marshall (1964 and 1965: pl. 53, fig. 354) and Grant (1987: photo 768), and there are color paintings in Hutchins and Swainston (1986:103), Allen and Swainston (1988:965), and Randall et al. (1990: plate VIII-13). An underwater photograph was published by Coleman (1974:43 and 1981:268).

Size Maximum size is 110–130 cm FL and 11.6–13.5 kg weight (Lewis 1981, Hutchins and Swainston 1986, Allen and Swainston 1988).

Biology Shark mackerel form dense concentrations near individual bays and reefs in Barrier Reef waters. With the rising tide, they move into shallow water over the reef flats, feeding on schools of clupeoid fishes (Grant 1982).

Interest to fisheries Shark mackerel are fished off Western Australia, the Northern Territory, Queensland, and northern New South Wales (Grant 1987). It is regarded as a light-tackle sportsfish with commercial value in Queensland (McPherson 1984). The name shark mackerel comes from the ammonia-like smell noticed when the fish is being filleted. This odor can be masked by brushing the fillets with lemon juice prior to cooking (Grant 1982, 1987).

Range Found over coastal reefs of all Australian warm waters (Grant 1987) with occasional stragglers south to 30° on both east (Cook I., New South Wales) and west (Shark Bay, Western Australia) coasts (Fig. 27) and in the Gulf of Papua (A.D. Lewis, South Pacific Comm., Noumea, pers. commun.). The apparent gap in distribution may be due to ecological reasons, the scarcity of reef habitats along the north coast of Australia, or to historical reasons, as outlined by Springer and Williams (1990).

Dissections 4 specimens (563–765 mm FL). USNM 270392 (563), Cairns, Qld., diss. 1-3-83. USNM 316126 (765),

Exmouth Gulf, WA, B. Hutchins, diss. 1-18-83. USNM 316127-8 (2, 625–663), Australia, diss. 7-5-89.

Material examined 11 specimens (300–765 mm FL) from 8 collections. USNM 316129 (1, 563), Queensland, Fitzroy I. S of Cairns; Jan. 1984. USNM 176832 (1, 525), Great Barrier Reef; J.K. Howard; 8 April–29 May 1952. AMS IB.5207-8 (2, 306–315), Queensland, Gladstone District; P. Gibson. USNM 316126, uncat. (2, 607–765), Western Australia, Exmouth Gulf. WAM-P 27343 (1, 825), Western Australia, N. Muiron I., 21°39′S, 114°22′E. WAM-P 25821 (1, 320), Western Australia, S. Muiron I., 21°39′S, 114°20′E. WAM-P 22974 (head only, 105 mm), Western Australia, Kendrew I., 20°29′S, 116°22′E; 21 Feb. 1973; B. Hutchins. USNM 316127-8 (2, 625–663), Australia.

Acknowledgments

The original impetus for this study came from A.D. Lewis, now with the South Pacific Commission, Noumea, New Caledonia. In the course of his doctoral dissertation on population genetics of Australian scombroids (Lewis 1981), he discovered that there were two species in the genus *Grammatorcynus*, informed us of the problem, and provided us with frozen material needed to do a thorough anatomical study. We are deeply appreciative of his interest and efforts throughout the course of this study. Sally Rothwell spent the month of February 1983 working in the Systematics Laboratory on a Careers in Biology Program from Colgate University. Her efforts made completion of the 1983 preliminary paper possible. Frozen material, vital for this study, was provided through the efforts of A.D. Lewis, J.E. McCosker (CAS), B. Hutchins (WAM), and G. McPherson (Northern Fisheries Research Center, Queensland). Several assistants, students, and colleagues participated in dissections over the years: Linda Pushee Mercer, Frances Matthews Van Dolah, Sally Rothwell, and Joseph Russo. Preserved material was made available by A. Ben-Tuvia (HUJ), B.E. Bookheim (Department of Marine and Wildlife Resources, Pago Pago, American Samoa), W.E. Eschmeyer and P. Sonoda (CAS), R.A. Croft (Ponape State Government), B. Herzig (NMW), W. Klausewitz (SMF), A.D. Lewis (then in Papua New Guinea), G.J. Nelson (AMNH), J.R. Paxton (AMS), J.E. Randall and A.Y. Suzumoto (BPBM), J.B. Hutchins (WAM), and P.J.P. Whitehead (then at BMNH). Assistance with analyzing the morphometric data was provided by Ruth Gibbons. Osteological drawings were painstakingly rendered by Keiko Hiratsuka Moore. The map was produced by Martha S. Nizinski. Participation in this study by the second author was made possible by a Smithsonian Summer Internship in Vertebrate Zoology in the summer of 1989. Drafts of the manuscript were reviewed by G. David Johnson, Thomas A. Munroe, Yosuo Nishikawa, and William Smith-Vaniz.

Citations

Allen, G.R., and B.C. Russell
1986 Part VII. Fishes. *In* Faunal surveys of the Rowley Shoals, Scott Reef and Seringapatam Reef, North-western Australia. Rec. W. Aust. Mus. Suppl. 25:75–103.

Allen, G.R., and R. Swainston
1988 The marine fishes of north-western Australia. West. Aust. Mus., Perth, 201 p.

Allis, E.P. Jr.
1903 The skull, and the cranial and first spinal muscles and nerves in *Scomber scomber*. J. Morphol. 18(1–2):45–328.

Anonymous
1945 Marketable fish of the Cairns Area. N. Queensl. Nat. Club 2, 8 p.
1977 Report on Japan–Papua New Guinea joint skipjack tagging in the PNG area, October–December, 1975 on the R/V *Fuji Maru*. Res. Devel. Div., Fish. Agency Jpn., and Fish. Div., Dep. Primary Ind., Papua New Guinea, 30 p.
1978 Major Queensland bid to track Spanish mackerel. Aust. Fish. 37(3):18–19.

Bauchot, R., J.E. Randall, J.-M. Ridet, and M.-L. Bauchot
1989 Encephalization in tropical teleost fishes and comparison with their mode of life. J. Hirnforsch. 30(6):645–669.

Ben-Tuvia, A.
1968 Report on the fisheries investigations of the Israel South Red Sea Expedition, 1962. Bull. Sea Fish. Res. Stn. Haifa 52:21–25.

Ben-Yami, M.
1968 Observations on the distribution and behaviour of pelagic schooling fish in the southern Red Sea. Bull. Sea Fish. Res. Stn. Haifa 51:31–46.

Céng, B-g., and Y. Yāng
1979 Suborders Scombroidei, Thunnioidei. *In* Fishes of the islands in the South China Sea, p. 470–488. Science Press, Beijing.

Coates, G.
1950 Fishing on the Barrier Reef and inshore. T. Willmett & Sons, Townsville, 72 p.

Coleman, N.
1974 Australian marine fishes in colour. A.H. & A.W. Reed, Sydney, 108 p.
1981 Australian sea fishes north of 30°S. Doubleday, Sydney and Auckland, 297 p.

Collette, B.B.
1979 Adaptations and systematics of the mackerels and tunas. *In* Sharp, G.D., and A.E. Dizon (eds.), The physiological ecology of tunas, p. 7–39. Academic Press, NY.
1983 Recognition of two species of double-lined mackerels (*Grammatorcynus*: Scombridae). Proc. Biol. Soc. Wash. 96(4): 715–718.

Collette, B.B., and L.N. Chao
1975 Systematics and morphology of the bonitos (*Sarda*) and their relatives (Scombridae, Sardini). Fish. Bull., U.S. 73(3): 516–625.

Collette, B.B., and R.H. Gibbs Jr.
1963a A preliminary review of the fishes of the family Scombridae. FAO Fish. Rep. 6(1):23–32.

1963b Preliminary field guide to the mackerel- and tuna-like fishes of the Indian Ocean (Scombridae). Smithson. Inst., Wash. DC, 48 p.

Collette, B.B., and C.E. Nauen
1983 Scombrids of the world. FAO Species Catalogue. FAO Fish. Synop. 125, Vol. 2, 137 p.

Collette, B.B., and J.L. Russo
1985a Interrelationships of the Spanish mackerels (Pisces: Scombridae: *Scomberomorus*) and their copepod parasites. Cladistics 1(2):141–158.
1985b Morphology, systematics, and biology of the Spanish mackerels (*Scomberomorus*, Scombridae). Fish. Bull., U.S. 82(4):545–692.

Collette, B.B., T. Potthoff, W.J. Richards, S. Ueyanagi, J.L. Russo, and Y. Nishikawa
1984 Scombroidei: Development and relationships. *In* Moser, H.G., et al. (eds.), Ontogeny and systematics of fishes, p. 591–620. Spec. Publ. 1, Am. Soc. Ichthyol. Herpetol. Allen Press, Lawrence, KS.

Conrad, G.M.
1938 The osteology and relationships of the wahoo (*Acanthocybium solandri*), a scombrid fish. Am. Mus. Novit. 1000, 32 p.

Cressey, R.F.
1975 A new family of parasitic copepods (Cyclopoida, Shiinoidae). Crustaceana 28(2):211–219.

Cressey, R.F., and H.B. Cressey
1980 Parasitic copepods of mackerel- and tuna-like fishes (Scombridae) of the world. Smithson. Contrib. Zool. 311, 186 p.

Cressey, R.F., B.B. Collette, and J.L. Russo
1983 Copepods and scombrid fishes: A study in host-parasite relationships. Fish. Bull., U.S. 81(2):227–265.

de Beaufort, L.F.
1951 Percomorphi (concluded). *In* The fishes of the Indo-Australian Archipelago 9, p. 1–242. E.J. Brill, Leiden.

de Sylva, D.P.
1955 The osteology and phylogenetic relationships of the blackfin tuna, *Thunnus atlanticus* (Lesson). Bull. Mar. Sci. Gulf Caribb. 5(1):1–41.

Devaraj, M.
1977 Osteology and relationships of the Spanish mackerels and seerfishes of the tribe Scomberomorini. Indian J. Fish. 22(1–2):1–67.

Dung, D.I.Y., and W.F. Royce
1953 Morphometric measurements of Pacific scombrids. U.S. Fish Wildl. Serv. Spec. Sci. Rep. Fish. 95, 170 p.

Dyer, W.G., E.H. Williams Jr., and L.B. Williams
1989 Monogeneans from marine fishes of Okinawa, Japan. Proc. Helminthol. Soc. Wash. 56(1):64–68.

Evermann, B.W., and A. Seale
1907 Fishes of the Philippine Islands. Bull. U.S. Bur. Fish. 26:49–110.

Fierstine, H.L., and V. Walters
1968 Studies in locomotion and anatomy of scombroid fishes. Mem. South. Calif. Acad. Sci. 6:1–31.

Fourmanoir, P., and P. Laboute
1976 Poissons de Nouvelle Calédonie et des Nouvelles Hébrides. Editions Pacifique, Papeete, Tahiti, 376 p.

Fraser-Brunner, A.
1950 The fishes of the family Scombridae. Ann. Mag. Nat. Hist., Ser. 12, 3:131–163.

Gibbs, R.H. Jr., and B.B. Collette
1967 Comparative anatomy and systematics of the tunas, genus *Thunnus*. Fish. Bull., U.S. 66(1):65–130.

Gill, T.N.
1862 On the limits and arrangement of the family of scombroids. Proc. Acad. Nat. Sci. Phila. 14:124–127.

Gillett, R.
1987 Traditional tuna fishing: A study at Satawal, Central Caroline Islands. Bishop Mus. Bull. Anthropol. 1, 48 p.

Gnanamuttu, J.C.
1971 Osteology of the Indian mackerel, *Rastrelliger kanagurta* (Cuvier). Indian J. Fish. 13(1):1–26.

Gorbunova, N.N.
1965 Seasons and conditions of spawning of the scombroid fishes (Pisces, Scombroidei). Tr. Inst. Okeanol. Akad. Nauk SSSR 80:36–61 [in Russ., Engl. summ.].
1974 A review of larvae of scombrid fishes (Scombridae, Pisces). Tr. Inst. Okeanol. Akad. Nauk SSSR 96:23–76 [in Russ., Engl. summ.].

Grant, E.M.
1965 Guide to fishes. Queensl. Dep. Harbours and Marine, Brisbane, 280 p.
1972 Guide to fishes. Queensl. Dep. Primary Ind., Brisbane, 2d ed., 472 p.
1975 Guide to fishes. Coordinator-General's Dep., Brisbane, 3d ed., 640 p.
1978 Guide to fishes. Dep. Harbours and Marine, Brisbane, 4th ed., 768 p.
1982 Guide to fishes. Dep. Harbours and Marine, Brisbane, 5th ed., 896 p.
1987 Fishes of Australia. E.M. Grant Pty Ltd., Queensl., 480 p.

Günther, A.
1860 Catalogue of the acanthopterygian fishes in the collection of the British Museum, Vol. 2. London, 548 p.

Gushiken, S.
1973 Fishes of the Okinawa Islands. Ryukyu Fish. Assoc., Naha, 247 p.

Hardenberg, J.D.F.
1935 Some new or rare fishes of the Indo-Australian Archipelago IV. Treubia 15(2):131–140.

Helfman, G.S., and J.E. Randall
1973 Palauan fish names. Pac. Sci. 27(2):136–153.

Herre, A.W.C.T.
1931 The fishes of the Herre 1931 Philippine Expedition with descriptions of 17 new species. Newspaper Enterprise Ltd., Hong Kong, 106 p. [reprinted by N.K. Gregg, Kentfield, CA].
1953 Check list of Philippine fishes. U.S. Fish Wildl. Serv. Res. Rep. 20, 977 p.

Hutchins, B.
1979 A guide to the marine fishes of Rottnest Island. Creative Research, Perth, 103 p.
1990 Fish survey of South Passage, Shark Bay, Western Australia. *In* Berry, P.F., S.D. Bradshaw, and B.R. Wilson (eds.), Research in Shark Bay, p. 263–278. Rep. France-Aust. Bicent. Exped. Comm., West. Aust. Mus., Perth.

Hutchins, B., and R. Swainston
1986 Sea fishes of southern Australia. Swainston Publ., Perth, 180 p.

Hutchins, B., and M. Thompson
1983 The marine and estuarine fishes of southwestern Australia. A field guide for anglers and divers. West. Aust. Mus., Perth, 103 p.

Iwai, T., and I. Nakamura
1964 Branchial skeleton of the bluefin tuna, with special reference to the gill rays. Bull. Misaki Mar. Biol. Inst., Kyoto Univ. 6:21–25.

Jenkins, G.P.
1989 Scombridae—Mackerels, Spanish mackerels, bonitos, tunas. *In* Leis, J.M., and T. Trnski (eds.), The larvae of Indo-Pacific shorefishes, p. 291–297. New South Wales Univ. Press, Kensington.

Johannes, R.E.
1981 Words of the lagoon. Fishing and marine lore in the Palau District of Micronesia. Univ. Calif. Press, Berkeley, 245 p.

Johnson, G.D.
1986 Scombroid phylogeny: An alternate hypothesis. Bull. Mar. Sci. 39(1):1–41.

Jones, S.
1968 The scombroid fishery of India—present and future. *In* Proc., Symp. Scombroid Fishes, Mar. Biol. Assoc. India, Symp. Ser. 1(3):994–1000.
1969 Catalogue of fishes from the Laccadive Archipelago in the reference collections of the Central Marine Fisheries Research Institute. Bull. Cent. Mar. Fish. Res. Inst. 8, 32 p.

Jones, S., and M. Kumaran
1964 Eggs, larvae and juveniles of Indian scombroid fishes. *In* Proc., Symp. Scombroid Fishes, Mar. Biol. Assoc. India, Symp. Ser. 1(1):343–378.
1981 Fishes of the Laccadive Archipelago. Nature Conserv. and Aquat. Sci. Serv., Trivandrum, 760 p.

Jones, S., and E.G. Silas
1963 Tuna and tuna-like fishes from the Indian Seas. FAO Fish Rep. 3(6):1775–1796.
1964a A systematic review of the scombroid fishes of India. *In* Proc., Symp. Scombroid Fishes, Mar. Biol. Assoc. India, Symp. Ser. 1(1):1–105.
1964b Mackerel from the Andaman Sea. *In* Proc., Symp. Scombroid Fishes, Mar. Biol. Assoc. India, Symp. Ser. 1(1): 255–282.

Jones, S., E.G. Silas, and E. Dawson
1960 New records of scombroid fishes from the Andaman-Nicobar waters. J. Mar. Biol. Assoc. India 2(1):136–137.

Joseph, J., W. Klawe, and P. Murphy
1979 Tuna and billfish–Fish without a country. Inter-Am. Trop. Tuna Comm., La Jolla, 46 p.

Kailola, P.J.
1975 A catalogue of the fish reference collection at the Kanudi Fisheries Research Laboratory, Port Moresby. Dep. Agric., Stock, Fish., Port Moresby, Res. Bull. 16, 277 p.

Kamohara, T.
1964 Fishes obtained in the Okinawa and the Yaeyama Islands. Res. Rep. Kochi Univ. 13(5):31–43 [in Jpn.].
1967 Fishes of Japan in color. Hoikusha Publ. Co., Osaka, 135 p.

Kishinouye, K.
1923 Contributions to the comparative study of the so-called scombroid fishes. J. Coll. Agric. Imp. Univ., Tokyo 8(3): 293–475.

Klawe, W.L.
1977 What is a tuna? Mar. Fish. Rev. 39(11):1–5.

Klunzinger, C.B.
1871 Synopsis der Fische des Rothen Meeres. II. Theil. Verh. Zool. Bot. Ges. Wien 21:441–668.

Kuronuma, K.
1961 A check list of the fishes of Vietnam. Div. Agric., Nat. Res., U.S. Oper. Mission Vietnam, ICA Contract IV-153, 66 p.

Kyushin, K., K. Amaoka, K. Nakaya, H. Ida, Y. Tanino, and T. Senta
1982 Fishes of the South China Sea. Jpn. Mar. Fish. Res. Cent., Tokyo, 333 p.

Leviton, A.E., R.H. Gibbs Jr., E. Heal, and C.E. Dawson
1985 Standards in herpetology and ichthyology: Part I. Standard symbolic codes for institutional resource collections in herpetology and ichthyology. Copeia 1985:802–832.

Lewis, A.D.
1981 Population genetics, ecology and systematics of Indo-Australian scombrid fishes, with particular reference to skipjack tuna (*Katsuwonus pelamis*). Ph.D. thesis, Aust. Natl. Univ. 314 p.

Lewis, A.D., B.R. Smith, and R.E. Kearney
1974 Studies on tunas and baitfish in Papua New Guinea waters—II. Dep. Agric., Stock, Fish, Port Moresby, Res. Bull. 11, 113 p.

Lewis, A.D., L.B. Chapman, and A. Sesewa
1983 Biological notes on coastal pelagic fishes in Fiji. Fish. Div. (MAF) Fiji Tech. Rep. 4:1–68.

Lewis, A.G.
1968 Copepod crustaceans parasitic on fishes of Eniwetok Atoll. Proc. U.S. Natl. Mus. 125(3656):1–78.

Magnuson, J.J.
1973 Comparative study of adaptations for continuous swimming and hydrostatic equilibrium of scombroid and xiphoid fishes. Fish. Bull., U.S. 71(2):337–356.

Magnuson, J.J., and J.G. Heitz
1971 Gill raker apparatus and food selectivity among mackerels, tunas, and dolphins. Fish. Bull., U.S. 69(2):361–370.

Mago Leccia, F.
1958 The comparative osteology of the scombroid fishes of the genus *Scomberomorus* from Florida. Bull. Mar. Sci. Gulf Caribb. 8(4):299–341.

Marshall, T.C.
1964 Fishes of the Great Barrier Reef and coastal waters of Queensland. Angus & Robertson, Sydney, 566 p.
1965 Fishes of the Great Barrier Reef and coastal waters of Queensland. Livingston Publ. Co., Narberth, PA.
1966 Tropical fishes of the Great Barrier Reef. Angus & Robertson, Sydney, 239 p.

Masuda, H., C. Araga, and T. Yoshino
1975 Coastal fishes of southern Japan. Tokai Univ. Press, Tokyo, 379 p.

Masuda, H., K. Amaoka, C. Araga, T. Uyeno, and T. Yoshino (editors)
1984 The fishes of the Japanese Archipelago. Tokai Univ. Press, Tokyo, 437 p.

Matsubara, K.
1955 Fish morphology and hierarchy. Part 1. Ishizaki Shoten, Tokyo, 789 p. [in Jpn.].

McAllister, D.E.
1968 The evolution of branchiostegals and associated opercular, gular, and hyoid bones and the classification of teleostome fishes, living and fossil. Bull. Natl. Mus. Canada 221, 239 p.

McCulloch, A.R.
1915 Notes on, and descriptions of Australian fishes. Proc. Linn. Soc. NSW 40:259–277.
1922 Check list of the fish and fish-like animals of New South Wales. Part 3. Aust. Zool. 2(3):86–130.
1929 A check-list of the fishes recorded from Australia. Aust. Mus. Mem. 5(1):1–144.

McCulloch, A.R., and G.P. Whitley
1925 A list of the fishes recorded from Queensland waters. Mem. Queensl. Mus. 8(2):125–182.

McPherson, G.
1984 Two species of double-lined mackerel (family Scombridae) in Queensland waters. Queensl. Dep. Primary Ind. Leafl., 2 p.

Meyer, A.B.
1885 Catálogo de los peces recolectados en el Archipiélago de las Indias Orientales. Ann. Soc. Espan. Hist. Nat. 14:5–49.
Morice, J.
1953 Essai systématique sur les familles des Cybiidae, Thunnidae et Katsuwonidae, poissons scombroides. Rev. Trav. Inst. Pêches Marit. 18(1):35–63.
Munro, I.S.R.
1958a Families Polynemidae to Scomberomoridae. Handbook of Australian fishes 27:109–112. Aust. Fish. Newsl. 17(10): 17–20.
1958b The fishes of the New Guinea region. Papua New Guinea Agric. J. 10(4):97–369.
1967 The fishes of New Guinea. Dep. Agric., Stock, Fish., Port Moresby, New Guinea, 650 p.
Myers, R.F.
1988 An annotated checklist of the fishes of the Mariana Islands. Micronesica 21(1–2):115–180.
1989 Micronesian reef fishes. Coral Graphics, Guam, 298 p.
Nakamura, I.
1965 Relationships of fishes referable to the subfamily Thunninae on the basis of the axial skeleton. Bull. Misaki Mar. Biol. Inst., Kyoto Univ. 8:7–38.
Nishikawa, Y.
1979 Early development of the double-lined mackerel, *Grammatorcynus bicarinatus* (Quoy and Gaimard), from the western tropical Pacific. Far Seas Fish. Res. Lab., Bull. 17:125–140.
Nishikawa, Y., and D.W. Rimmer
1987 Identification of larval tunas, billfishes and other scombroid fishes (suborder Scombroidei): An illustrated guide. CSIRO Mar. Lab. Rep. 186, 20 p.
Ogilby, J.D.
1918 Ichthyological notes (no. 4). Mem. Queensl. Mus. 6: 97–05.
Okada, Y.
1938 A catalogue of vertebrates of Japan. Maruzen Co., Tokyo, 412 p.
Okiyama, M., and S. Ueyanagi
1977 Larvae and juvenile of the Indo-Pacific dogtooth tuna, *Gymnosarda unicolor* (Rüppell). Bull. Far Seas Fish. Res. Lab., Shimizu 15:35–49.
1978 Interrelationships of scombroid fishes: An aspect from larval morphology. Bull. Far Seas Fish. Res. Lab., Shimizu 16:103–113.
Orsi, J.J.
1974 A check list of the marine and freshwater fishes of Vietnam. Publ. Seto Mar. Biol. Lab. 21(3/4):153–177.
Potthoff, T.
1975 Development and structure of the caudal complex, the vertebral column, and the pterygiophores in the blackfin tuna (*Thunnus atlanticus*, Pisces, Scombridae). Bull. Mar. Sci. 25(2):205–231.
Quoy, J.R.C., and J.P. Gaimard
1824–1825 Voyage autour du Monde,... Exécuté sur les corvettes de S. M. l'Uranie et la Physicienne, pendant les années 1817, 1818, 1819 et 1820. 3, Zoologie, 712 p.
Randall, J.E., G.R. Allen, and R.C. Steene
1990 Fishes of the Great Barrier Reef and Coral Sea. Univ. Hawaii Press, Honolulu, 507 p.
Rau, N., and A. Rau
1980 Commercial marine fishes of the Central Philippines (bony fishes). German Agcy. for Tech. Coop. (GTZ), 629 p.
Richards, W.J., and W.L. Klawe
1972 Indexed bibliography of the eggs and young of tunas and other scombrids (Pisces, Scombridae) 1880–1970. NOAA Tech. Rep. NMFS SSRF-652, 107 p.
Rivaton, J., P. Fourmanoir, P. Bourret, and M. Kulbicki
1989 Catalogue des poissons de Nouvelle-Caledonie. ORSTOM Rapp. Prov., 170 p.
Rohde, K.
1976 Monogenean gill parasites of *Scomberomorus commersoni* Lacépède and other mackerel on the Australian east coast. Z. Parasitenkde. 51:49–69.
Romimohtairo, K., M. Hutomo, and Sumarna
1974 Results of the biological observations in Gamber Bay, Gag Island with a special note on the tuna and skipjack fishing ground in Irian Jaya waters. Oseanol. Indones. 3:29–45.
Roux-Estève, R., and P. Fourmanoir
1955 Poissons capturés par le mission de la *Calypso* en Mer Rouge. Ann. Inst. Oceanogr., Paris 30:195–203.
Rüppell, E.
1836 Neue Wirbelthiere zu der fauna von Abyssinien gehörig. Fische des rothen Meeres. Frankfurt am Main, 148 p. Lfg. 6:29–52.
Russell, B.C.
1983 Annotated checklist of the coral reef fishes in the Capricorn-Bunker Group, Great Barrier Reef Australia. Great Barrier Reef Marine Park Authority, Spec. Publ. Ser. 1, 184 p.
Schultz, L.P.
1960 Suborder Scombrina. Family Scombridae: Tunas. *In* Schultz, L.P., et al., Fishes of the Marshall and Marianas Islands. Bull. U.S. Nat. Mus. 202(2):410–417.
Serventy, D.L.
1950 Tuna survey of north Australia. Aust. Fish. Newsl. 9:18–20.
Shaklee, J.B.
1983 The utilization of isozymes as gene markers in fisheries management and conservation. *In* Isozymes: Current topics in biological and medical research, vol. 11:213–247. Liss, NY.
Shiino, S.M.
1972 List of English names of Japanese fishes with proposition of new names. Sci. Rep. Shima Marineland 1, 210 p. [in Jpn. and Engl.].
1976 List of common names of fishes of the world, those prevailing among English-speaking nations. Sci. Rep. Shima Marineland 4, 262 p.
Shirai, S.
1980 (rev. ed.) Ecological encyclopedia of the marine animals of the Ryukyu Islands in colour. Okinawa Kyoiku Shuppan, 636 p.
Silas, E.G.
1963 Synopsis of biological data on double-lined mackerel *Grammatorcynus bicarinatus* (Quoy and Gaimard) (Indo-Pacific). FAO Fish. Rep. 6, vol. 2:811–833.
Smith, C.L., and R.M. Bailey
1962 The subocular shelf of fishes. J. Morphol. 110(1):1–17.
Springer, V.G., and J.T. Williams
1990 Widely distributed Pacific Plate endemics and lowered sea-level. Bull. Mar. Sci. 46(3):631–640.
Springer, V.G., Burhanuddin, and M.F. Gomon
1974 List of fishes collected during Rumphius Expedition I. Oseanol. Indones. 1:39–45.
Tongyai, M.L.P.
1966 Background notes for Spanish mackerel, (*Scomberomorus* spp.) from Thai waters, studies, 1954–1965. Thai Mar. Fish. Lab., *Scomberomorus* Rep. Paper 1, 25 p.
1970 Plah in-see, *Scomberomorus* spp., of Thailand, 1967. *In* Marr, J.D. (ed.), The Kuroshio—A symposium on the Japan Current, p. 557–564. East-West Center Press, Honolulu.
1971 A taxonomic study of the pla in-si (Pisces: Scombroidei) of Thailand. Div. Mar. Fish. Tech., Dep. Fish., Ministry Agric., Bangkok, 36 p.

Ueyanagi, S., and M. Okiyama
1979 Larval fish characters and phylogeny of scombroid fishes. Kaiyo Kaguku 11(2):93–99 [in Jpn., transl. in NMFS Proc. Rep. 82–14, NMFS, NOAA, Seattle, 24 p.].

Umali, A.F.
1950 Key to the families of common commercial fishes in the Philippines. U.S. Fish Wildl. Serv. Res. Rep. 21, 47 p.

Uyeno, T., and S. Fujii
1975 A fish fossil of the family Scombridae from a Miocene bed in Toyama Prefecture, Japan. Bull. Nat. Sci. Mus. Tokyo, Ser. C (Geol.) 1(1):11–16.

Wade, C.B.
1951 Larvae of tuna and tuna-like fishes from Philippine waters. Fish. Bull., U.S. 51:445–485.

Wang, C.
1981 Studies on the fish fauna of the South China Sea Islands, Guangdong Province, China. Oceanol. Limnol. Sin. (Suppl.) p. 137–165. [in Chinese].

Warfel, H.E.
1950 Outlook for development of a tuna industry in the Philippines. U.S. Fish Wildl. Serv. Res. Rep. 28, 37 p.

Wass, R.C.
1984 An annotated checklist of the fishes of Samoa. NOAA Tech. Rep. NMFS SSRF-781, 43 p.

Whitley, G.P.
1947 New sharks and fishes from Western Australia. Part 3. Aust. Zool. 11(2):129–150.
1948 A list of the fishes of Western Australia. West. Aust. Fish. Dep., Fish. Bull. 2, 35 p.
1964a Scombroid fishes of Australia and New Zealand. *In* Proc., Symp. Scombroid Fishes, Mar. Biol. Assoc. India Symp. Ser. 1(1):221–253.
1964b A survey of Australian ichthyology. Proc. Linnean Soc. NSW 89(1):11–127.

Yamakawa, T.
1979 Studies of the fish fauna around the Nansei Islands, Japan. 1. Check list of fishes collected by Toshiji Kamohara and Takeshi Yamakawa from 1954 to 1971. Rep. Usa Mar. Biol. Stn., Suppl. 1:1–47.

Zhang, R.
1981 On the larvae of tuna-like fishes around waters of Xisha Qundao of the Nan Hai. J. Fish. China 5(4):301–315 [in Chinese, Engl. summ.].

Zharov, V.L.
1967 Classification of the scombroid fishes (suborder Scombroidei, order Perciformes). Vopr. Ikhtiol. 7(2):209–224 [in Russ.].

Zug, G.R., V.G. Springer, J.T. Williams, and G.D. Johnson
1989 The vertebrates of Rotuma and surrounding waters. Atoll Res. Bull. 316, 25 p.

Geographic variation in cranial morphology of spinner dolphins *Stenella longirostris* in the eastern tropical Pacific Ocean

Michael E. Douglas
Oklahoma Biological Survey and Department of Zoology
University of Oklahoma, Norman, Oklahoma 73019
Present address: Department of Zoology and Museum
Arizona State University, Tempe, Arizona 85287

Gary D. Schnell
Daniel J. Hough
Oklahoma Biological Survey and Department of Biology
University of Oklahoma, Norman, Oklahoma 73019

William F. Perrin
Southwest Fisheries Science Center, National Marine Fisheries Service, NOAA
P.O. Box 271, La Jolla, California 92038

Abstract.–The spinner dolphin *Stenella longirostris* is widely distributed in the eastern tropical Pacific Ocean. Geographic patterns in 30 cranial features were determined from 246 museum specimens grouped into 25 5° latitude-longitude blocks. Statistically significant sexual dimorphism was demonstrated for one-half of the cranial characters, with males generally being larger. ANOVAs, as well as principal components, canonical variates, and cluster (UPGMA and function-point) analyses demonstrated geographic variation in all characters. Patterns of geographic variation in morphology were evaluated for all *S. longirostris* specimens using Mantel tests and matrix correlations; 20 of 30 characters showed significant "regional patterning," while most (25 of 30) exhibited "local" patterning. The latitude-longitude block with specimens of *S. l. centroamericana* was distinctive in a number of features. Also, eastern spinner dolphins (*S. l. orientalis*) were smaller than spinners found to the south, southwest, or west. Many of the cranial characters exhibited a concentric pattern of geographic variation similar to that found by previous investigators for several external characters. Hawaiian specimens are the largest incorporated into this study and, typically, are more like those from southern localities than animals from geographically closer blocks. The association between morphological characters and 13 environmental measures was assessed with Mantel tests and product-moment correlations, revealing statistical concordance of morphological patterns for a number of cranial characters with those for water depth, sea surface temperature in January and July, surface salinity, thermocline depth, and surface dissolved oxygen. Several of these environmental variables manifest the same distributional pattern found in many of the cranial features.

Manuscript accepted 9 December 1991.
Fishery Bulletin, U.S. 90:54–76 (1992).

Information on geographic variation of dolphins in the eastern tropical Pacific is of intrinsic scientific interest, but also has practical implications because fishermen in the region kill dolphins in the course of purse-seining for yellowfin tuna (Allen 1985). Tuna in the region associate with schools of dolphins, primarily *Stenella* spp. and *Delphinus delphis*, and the fishermen set their nets on the schools to capture the tuna below them. In the process, many dolphins die, as many as 80,000–125,000 annually in recent years (Hall and Boyer 1988, 1989, 1990). The U.S. Government has used a series of management units, or stocks, in regulating this exploitation of the dolphins by U.S. vessels. For the spinner dolphin, these have been the eastern spinner, Costa Rican spinner, northern whitebelly spinner, and southern whitebelly spinner stocks (Perrin et al. 1985). These divisions are based on morphology, including body length and shape, color pattern, shape of the dorsal fin, and cranial characters. The Costa Rican form occurs close to the coast of Central America and is relatively large, with relatively long beak, erect to forward-canted dorsal fin, and monotonic gray coloration. The eastern form is smaller, with shorter beak; it also has the erect or canted fin and is gray overall, but with light patches in the axillary and genital areas. The whitebelly forms have a tripartite color pattern of dark gray, light gray, and (ventrally) white, and the dorsal fin is highly variable, ranging in adults from falcate to erect. The northern and southern stocks were divided based on modal differences in cranial measurements; the boundary is at the Equator. The eastern spinner and northern whitebelly spinner stocks overlap broadly; overlap between the eastern spinner and southern whitebelly spinner is very slight (Perrin et al. 1985). Dolphins killed in the fishery are identified to stock based on the modal appearance of adults in the school and, in the case of the two whitebelly stocks, location.

Most recently, Perrin (1990) described three subspecies of *Stenella*

longirostris: the pantropical spinner dolphin *S. l. longirostris* occurring in the Central, South, and Western Pacific, Indian, and Atlantic oceans; the Central American spinner *S. l. centroamericana* endemic to the coast of Central America and corresponding to the Costa Rican spinner management stock; and the eastern spinner *S. l. orientalis* endemic to the eastern tropical Pacific off Mexico, Central America, and northern South America and corresponding to the eastern spinner management stock. He concluded that the more offshore whitebelly forms constitute a broad zone of hybridization or intergradation between the eastern and pantropical forms. This view has support from results of a genetic study; Dizon et al. (1991) found no unique haplotypes in a restriction-enzyme examination of mitochondrial DNA of animals of the eastern and whitebelly morphological types.

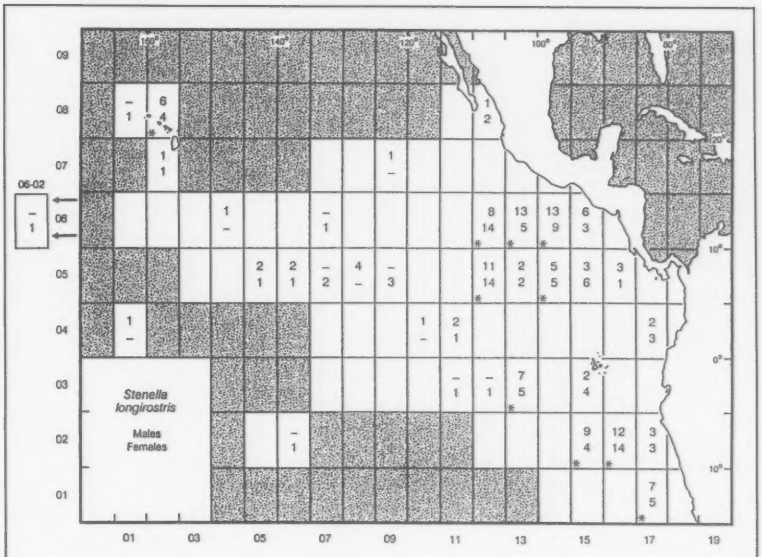

Figure 1

Known range of *Stenella longirostris* in eastern tropical Pacific Ocean (modified from Perrin 1990), with numbers of males (above) and females (below) available for each 5° latitude-longitude block (total of 246 specimens). Asterisks indicate 10 blocks included in analysis of sexual dimorphism. The 25 blocks with two or more specimens used as basis for analyses of geographic variation; for some aspects, the 10 blocks with single specimens projected onto axes based on the 25 blocks. Each block identified by numerical code (numbers on left and bottom margins are combined; e.g., block 0812 is just to east of southern tip of Baja California). One block (i.e., 06-02) is located off map to west (left).

Perrin et al. (1991) reexamined color pattern, body size and shape, and dorsal fin shape without *a priori* assignment of specimens to subspecies or management stock. They compared specimens from 5° geographic blocks. The results of their analyses support the taxonomic treatment by Perrin (1990); the whitebelly forms constitute a complex zone of highly variable animals intermediate between the eastern and pantropical types. Perrin et al. (1991) concluded that the pattern of geographic variation does not justify separation of northern and southern units on morphological grounds alone.

The purpose of the studies reported here was to carry out a parallel analysis of geographical cranial variation in the eastern Pacific, again making no *a priori* assignment of specimens to subspecies or management stock. We also examined relationships between cranial variation and environmental variables, in an effort to better understand the ecologies of the several forms of spinner dolphins.

Materials and methods

Data from 246 adult museum specimens (maturity judged by evaluating fusion of premaxilla with the maxilla at distal end of rostrum; Dailey and Perrin 1973) of spinner dolphins were used in this investigation (Fig. 1). We purposely included all appropriate specimens available, including those from the three named subspecies recognized from the region (Perrin 1990); furthermore, we did not differentiate between those with different color patterns ("eastern" and "whitebelly"; Perrin et al. 1985, 1991), in order to focus simply on cranial features. The animals used included 188 of 199 specimens used in the earlier study of sexual dimorphism (Douglas et al. 1986; the 11 remaining specimens not used had been incorrectly aged or had inadequate locality data) and 58 new specimens.

The first set of specimens was measured by M.E. Douglas and the new specimens by W.F. Perrin. In addition, Perrin remeasured 81 specimens of spinner dolphins and spotted dolphins *S. attenuata* measured by Douglas. This allowed a comparison to determine whether measurements were repeatable. Initially, 36 morphometric and meristic characters were evaluated (illustrations and character definitions given in Schnell et al. 1985a). Comparisons of measurements taken on the same specimens by the two investigators indicated

Table 1

Geographic variation and sexual dimorphism in *Stenella longrirostris* evaluated for 30 characters.

Character[a]	*F*-value[b]		Mean[c]		Correction factor[d]	Percentage difference[e]
	Block	Sex	Male	Female		
1 Condylobasal L.	22.19***	0.05	405.9	404.6	0.22	0.32
2 L. Rostrum (frm.Base)	15.93***	0.50	258.9	259.4	−0.61	−0.21
3 L. Rostrum (frm.Pterygoid)	20.71***	0.01	299.6	299.3	−0.08	−0.11
4 W. Rostrum (at Base)	15.19***	2.88	74.2	73.1	0.37	1.44
5 W. Rostrum (at 1/4 L.)	10.17***	11.82***	52.1	50.6	0.67	2.84
6 W. Rostrum (at 1/2 L.)	9.97***	10.20**	44.2	42.8	0.65	3.16
7 W. Premax. (at 1/2 L.)	5.65***	8.31**	21.4	20.8	0.31	3.02
8 W. Rostrum (at 3/4 L.)	2.92**	24.96***	32.5	30.5	1.01	6.34
9 Preorbital W.	38.05***	8.67**	139.9	137.5	1.00	1.76
10 Postorbital W.	49.34***	8.19**	155.7	153.3	0.93	1.57
11 Skull W. (at Zygomatic P.)	49.11***	14.89***	154.4	151.3	1.27	2.04
12 Skull W. (at Parietals)	6.27***	20.36***	130.1	127.2	0.10	0.52
13 Ht. Braincase	16.56***	15.52***	89.1	87.1	0.89	2.28
14 L. Braincase	18.71***	8.09**	101.7	100.3	0.67	1.47
15 Max. W. Premax.	6.55***	0.22	62.9	62.6	0.04	0.36
16 W. External Nares	3.88***	0.09	41.6	41.5	1.40	2.27
17 L. Temporal Fossa	4.32***	9.27**	50.4	48.7	0.82	3.52
18 W. Temporal Fossa	9.24***	17.82***	40.2	38.2	0.96	5.16
19 Orbital L.	6.56***	0.00	40.7	40.6	−0.01	−0.13
20 L. Antorbital P.	12.41***	11.46***	42.7	41.4	0.67	3.27
21 W. Internal Nares	22.50***	3.85	43.5	42.7	0.31	1.81
22 L. Up. Toothrow	16.23***	1.12	224.3	225.5	−0.82	−0.54
23 No. Teeth (Up.Lf.)	3.39***	3.88	53.2	52.5	0.42	1.30
24 No. Teeth (Up.Rt.)	5.19***	1.15	52.7	52.3	0.21	0.76
25 No. Teeth (Low.Lf.)	2.33*	0.80	51.3	51.1	0.17	0.39
26 No. Teeth (Low.Rt.)	2.61**	0.34	51.0	50.9	0.11	0.29
27 L. Low. Toothrow	13.99***	1.00	218.4	219.5	−0.76	−0.51
28 Ht. Ramus	21.64***	13.02***	55.4	54.1	0.60	2.51
29 Tooth W.	3.74***	13.84***	2.6	2.5	0.07	5.10
30 L. Ramus	18.06***	0.04	346.8	345.6	0.20	0.35

[a] Abbreviations: frm. = from; Ht. = height; L. = length; Lf. = left; Low. = lower; Max. = maximum; No. = number; P. = process; Premax. = premaxillary; Rt. = right; Up. = upper; W. = width.

[b] *F*-values from main effects two-way analysis of variance (5° block vs. sex) involving 10 blocks (*$P<0.05$; **$P<0.01$; ***$P<0.001$). Total of 170 individuals. Degrees of freedom 9 for among-block variation and 1 for between sexes.

[c] Unweighted mean for 10 blocks.

[d] Added to all individual female measurements and subtracted from all individual male measurements to correct for sexual differences.

[e] Difference between sexes (males minus females) multiplied by 100, with the resulting value divided by average of male and female means.

that 6 of the original 36 measurements (i.e., W. Lf. Premax. [at midline of Nares], W. Rt. Premax. [at midline of Nares], Separation of Pterygoids, L. Lf. Tympanic Cavity, L. Rt. Tympanic Cavity, and W. at Pterygobasioocipital Sutures; abbreviations used in these and other character names are listed in footnote a of Table 1) should be deleted, because we were not able consistently to repeat these measurements. For some other measurements, there were differences between investigators, but the differences were consistent (e.g., one obtained measurements that were smaller than those reported by the other). Therefore, we calculated regression equations for each of the remaining characters based on the 81 jointly-measured specimens. These regression equations were used to convert the measurements from the rest of the initial specimens to appropriate values for inclusion with the measurements taken by Perrin. Through these procedures, we developed a data set of 30 characters (listed in Table 1) for 246 specimens.

Only specimens that were largely complete were included in the analysis. Missing values (1.34% of total) were estimated by linear regression ("Missing Data Estimator" program developed by Dennis M. Power, Santa Barbara Mus. Nat. Hist., pers. commun.) onto the character that explained the greatest proportion of the variance for the variable under consideration.

Specimens then were assigned to 5° latitude-longi-

tude blocks, with each geographic block given a numerical code (see Fig. 1). We had specimens from 35 blocks, although 10 were represented by only a single specimen; the other 25 blocks were used as the basis for most analyses of geographic variation. While several of the remaining 25 blocks are represented by relatively small samples, tests for geographic patterning (described below) suggest that, in general, sample values are representative of what would be expected for these blocks based on their geographic positions. The 5° block size was selected, in part, because it was judged that available sample sizes would not permit detailed analysis of smaller geographic units. Furthermore, migratory movements and related factors were less likely to significantly influence results when these relatively large sampling areas were used.

Douglas et al. (1986) showed that *S. longirostris* in the eastern tropical Pacific was sexually dimorphic for 13 of 36 characters. Because some specimens used in that analysis were removed and new specimens added (see above), we reanalyzed the data with a two-way analysis of variance (ANOVA) for block and sex based on specimens in 10 blocks that had at least four of each sex (Fig. 1). We then produced a series of correction terms to adjust measurements of the larger sex downward and the smaller sex upward, thus producing sex-adjusted or "zwitter" measurements (for details on this adjustment, see Schnell et al. 1985a). These corrections enabled us to combine specimens for both sexes in an overall analysis of geographic variation.

Correlation, ordination and clustering

After conversion to zwitters, characters were then standardized so that means for blocks were zeros and standard deviations ones. Product-moment correlations were computed among characters, and the general associations among characters were summarized by clustering characters using the unweighted pair-group method with arithmetic averages (UPGMA).

This type of hierarchical cluster analysis also was performed to summarize average distance coefficients (Sneath and Sokal 1973) calculated for all pairs of blocks based on standardized data. Cophenetic correlation coefficients were computed to indicate the degree to which distances in the resulting dendrogram accurately represented original interblock morphologic distances.

In addition, we analyzed standardized data using a nonhierarchical K-group method called function-point cluster analysis (Katz and Rohlf 1973; described in Rohlf et al. 1979). Blocks are assigned to a series of subgroups at a specified level. The value for the w-parameter used by the function-point clustering method was varied. A hierarchical (but not necessarily non-overlapping) system of clusters can be obtained by conducting the analysis at more than one clustering level. Results are presented in the form of a modified skyline diagram (Wirth et al. 1966) where, for a given w-value, blocks joined in a common line are in the same cluster.

Based on standardized data, we constructed scatter diagrams of blocks projected onto the first two principal components (Sneath and Sokal 1973) extracted from a matrix of correlations among the 30 characters. Canonical variates analysis also was applied to determine the subset of variables that show the greatest degree of geographic variation—in this case, those that provide the greatest interblock separation relative to the degree of intrablock variation (Program P7M of BMDP; Dixon 1990). Plots of the first two canonical variables show the maximum separation of blocks in two-dimensional space. The original variables, which in combination exhibited maximum interblock variability, were then subjected to additional analyses.

Mantel test for geographic patterning

Using a test devised by Mantel (1967) and described by Sokal (1979), we analyzed interlocality variation in each character to determine whether values are geographically patterned, or vary spatially at random. This procedure enabled us to determine whether differences in character values between all pairs of samples are statistically associated in a linear manner with corresponding geographic distances. The observed association between sets of character differences and geographic distances was tested relative to its permutational variance, and the resulting statistic was compared against a Student's t-distribution with infinite degrees of freedom. Computations were performed using GEOVAR, a library of computer programs for geographic variation analysis written by David M. Mallis and furnished by Robert R. Sokal (State University of New York at Stony Brook).

Character differences were compared first with actual geographic distances (in nautical miles) between centers of blocks and then with reciprocals of distances. In evaluations of reciprocals, where distances are scaled in a nonlinear manner, longer distances are considered effectively to be equal, and the portion of the scale involving smaller distances is expanded. Thus, use of reciprocals of distances increases the power of analyses to reveal geographic patterns that are "local" in nature (i.e., involving closely placed blocks), whereas tests involving nautical-mile distances evaluate "regional" trends. Positive associations of character differences and nautical-mile distances are indicated by positive t-values, while negative t-values denote such associations when reciprocals of distances are used.

Table 2
Environmental measurements compiled for each 5° latitude-longitude block.*

1 Sea Current (N., Winter)—Average northern component (in knots) of the surface water current in winter (Innis et al. 1979; their fig. 2.2).
2 Sea Current (W., Winter)—Average western component (in knots) of the surface water current in winter (Innis et al. 1979; fig. 2.3).
3 Water Depth—Average sea depth (in m) (Bartholomew 1975; fig. 122).
4 Solar Insolation (Jan.)—Average incoming solar radiation for January (in gm. · cal/cm^2; Brunt 1934; table 2).
5 Solar Insolation (Annual)—Average annual incoming solar radiation in gm. · cal/cm^2; Brunt 1934; table 2).
6 Sea Surface Temp. (Jan.)—Average January sea surface temperature (in °C; Robinson 1976: fig. 2 north of 5°S; Wyrtki 1974: fig. 2 south of 5°S).
7 Sea Surface Temp. (July)—Average July sea surface temperature (in °C; Robinson 1976: fig. 74 north of 5°S; Wyrtki 1974: fig. 8 south of 5°S).
8 Sea Surface Temp. (Ann. Var.)—Average annual sea surface temperature variation (in °C; Robinson 1976: fig. 148 north of 5°S; Wyrtki 1974: fig. 26 south of 5°S).
9 Oxygen Min. Layer (Depth)—Annual mean depth (in m) of the absolute oxygen minimum surface with respect to the vertical (Levitus 1982: fig. 52).
10 Surface Salinity—Average salinity (‰) of surface sea water (Levitus 1982: microfiche F-02, frames 2–5).
11 Thermocline Depth (Winter)—Mean depths (in m) to the top of the thermocline for January, February, and March (Robinson 1976: figs. 12, 24, and 36 north of 5°S; Cromwell 1958: fig. 1a south of 5°S).
12 Thermocline Depth (Summer)—Mean depths (in m) to the top of the thermocline for July, August, and September (Robinson 1976: figs. 84, 96, and 108 north of 5°S; Cromwell 1958: fig. 1c south of 5°S).
13 Surface Dissolved Oxygen—Annual mean dissolved oxygen (mL/L) of surface sea water (Levitus 1982: microfiche F-03, frames 2–5).

*Abbreviations: Ann. Var. = Annual variation; Jan. = January; Min. = Minimum; N. = North; Temp. = Temperature; W. = West.

As an example of the Mantel procedure, consider the 25 blocks for which two or more specimens were available (Fig. 1). The geographic distances (in nautical miles) between each pair of the 25 blocks (300 pairs total) are computed. We then obtain the mean value for a given morphological character for each block; consider a character with large mean values in northern blocks, a gradual change as one proceeds south, and the smallest means in the most southerly blocks. We calculate the absolute character difference for each pair of blocks (300 difference values); in general, for this hypothetical case, close blocks geographically exhibit small differences in character means, while blocks far apart (e.g., a northern and a southern block) have the largest morphological differences. We and the Mantel test would identify this morphological character as having a strong regional pattern. We also compare reciprocals of geographic distance for each block pair with corresponding morphological differences; this approach indicates whether, in general, geographically close blocks also are similar morphologically (a case of local geographic patterning). The examplar morphological character, thus, would be identified as displaying a strong local pattern (in addition to the strong regional pattern). In general, a character showing a regional pattern (as we have defined it) also will exhibit a local pattern, but the reverse is not necessarily true. For instance, if the morphological character was large in both the north and south, was small for blocks in the middle, and had gradual changes between adjacent blocks, it would have a strong local pattern but no regional pattern (because many distant blocks are nearly identical morphologically). Detailed computational examples of the Mantel test can be found in Douglas and Endler (1982), Schnell et al. (1985b), and Manley (1985).

We also computed matrix correlations (Sneath and Sokal 1973) between character differences and the associated geographic distances or reciprocals of distances between localities. The significance of these coefficients cannot, however, be tested in the conventional way, because all pairs of localities were used and these are not statistically independent. However, the resulting values are useful as descriptive statistics indicating the degree of association of difference values.

Morphological-environmental covariation

Relatively little is known about the relationship (if any) of geographic variation in morphological characteristics of *S. longirostris* to differences in the environment. Therefore, as an initial exploratory analysis of covariation, we have calculated product-moment correlations of block means for morphological characters with environmental variables. Data were available for 13 environmental variables for the eastern tropical Pacific Ocean (Table 2). We also used UPGMA to summarize associations among these environmental variables for 51 blocks with specimens of *S. longirostris* or

S. attenuata or both; since these two dolphin species have broadly overlapping distributions in the eastern tropical Pacific, the blocks used are representative of areas inhabited by *S. longirostris*.

We conducted a principal components analysis of the 13 environmental variables for the 51 blocks in order to obtain summary variables that reflect overall environmental trends. Individual blocks were projected onto the resulting environmental principal components based on standardized data. These block variables were used as composite environmental variables for comparisons with morphological characteristics.

In addition to using matrix correlations and the Mantel procedure to test for local and regional patterning of variation in individual morphological characters, we compared difference patterns of selected morphological measures with those of environmental variables. In these tests, differences between each pair of blocks for a morphological variable were compared with those for an environmental variable.

Sources for environmental data are expanded over those used by Schnell et al. (1986: table 2) so as to accommodate the broader geographic representation resulting from increased numbers of specimens. Values for depth of the oxygen minimum layer were taken for all blocks from Levitus (1982). Data for sea surface temperatures and thermocline depths were not available in the previously used source for blocks west of 120°. Data for these and other blocks north of 5°S were taken from Robinson (1976). Overlapping blocks from the two sources for each environmental variable were used to produce regression equations. Previous data for blocks south of 5°S were converted using these regression equations. Overall, agreement of data for overlapping blocks from the two sources was relatively good. Correlations for sea surface temperatures were: January, 0.956; July, 0.951; annual variation, 0.929. Thermocline depth in winter had a correlation of 0.840, while that for summer values was lower (0.767). All correlations were statistically significant ($P<0.001$), and the associations of values from the two sources were basically linear.

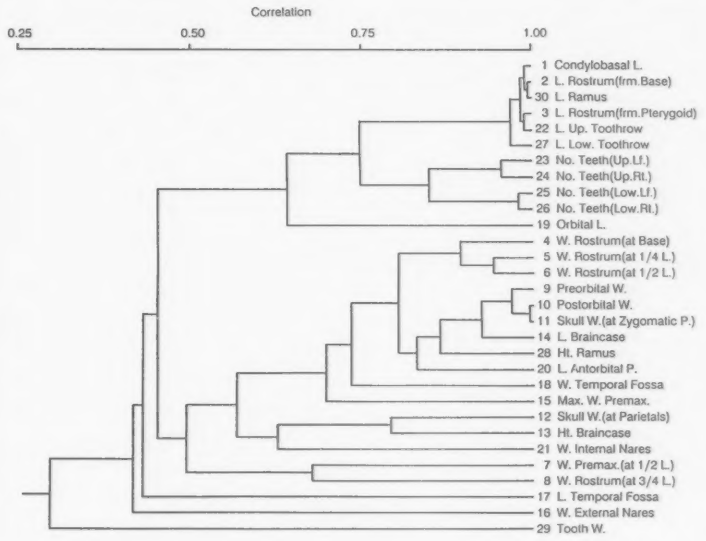

Figure 2

Correlations among characters based on character means for 25 blocks. Clustering performed using UPGMA on absolute correlations among characters (i.e., negative signs removed). Cophenetic correlation coefficient is 0.74.

Results

Sexual dimorphism

In the two-way ANOVA for block and sex, only three measurements showed a significant interaction for block and sex (W. Rostrum [at Base], L. Temporal Fossa and No. Teeth [Up.Lf.]). All characters exhibited significant variation by block (i.e., geographic variation), and 15 of the 30 characters displayed significant sexual dimorphism (Table 1). For most characters, males are larger than females. Character differences between sexes range up to 6.34% (see Table 1), with the most dimorphic character being W. Rostrum (at 3/4 L.).

Correlation, ordination and clustering

Figure 2 summarizes associations among characters based on means for the 25 blocks. Virtually all of the intercharacter correlations were positive in sign; a few indicated weakly negative associations. For the cluster analysis, absolute character correlations were analyzed (i.e., sign of correlation ignored), because we wanted to assess simply the degree of covariation. The character showing the most distinctive pattern relative to

Table 3
Principal component loadings for *Stenella longirostris* involving character means for 25 blocks.

Character	Component* I	Component* II	Character	Component* I	Component* II
1 Condylobasal L.	**0.914**	−0.325	16 W. External Nares	0.573	−0.045
2 L. Rostrum (frm.Base)	**0.872**	−0.397	17 L. Temporal Fossa	0.575	0.040
3 L. Rostrum (frm.Pterygoid)	**0.885**	−0.396	18 W. Temporal Fossa	0.647	0.599
4 W. Rostrum (at Base)	**0.856**	0.083	19 Orbital L.	0.782	−0.064
5 W. Rostrum (at 1/4 L.)	**0.838**	0.242	20 L. Antorbital P.	**0.849**	0.108
6 W. Rostrum (at 1/2 L.)	**0.880**	0.248	21 W. Internal Nares	0.631	0.427
7 W. Premax. (at 1/2 L.)	0.578	0.044	22 L. Up. Toothrow	**0.864**	−0.426
8 W. Rostrum (at 3/4 L.)	0.508	0.504	23 No. Teeth (Up.Lf.)	0.608	**−0.680**
9 Preorbital W.	**0.938**	0.255	24 No. Teeth (Up.Rt.)	0.688	−0.593
10 Postorbital W.	**0.917**	0.344	25 No. Teeth (Low.Lf.)	0.600	**−0.666**
11 Skull W. (at Zygomatic P.)	**0.916**	0.359	26 No. Teeth (Low.Rt.)	0.652	**−0.630**
12 Skull W. (at Parietals)	0.331	**0.659**	27 L. Low. Toothrow	**0.814**	−0.467
13 Ht. Braincase	0.625	**0.719**	28 Ht. Ramus	**0.872**	0.219
14 L. Braincase	**0.881**	0.326	29 Tooth W.	0.216	**0.752**
15 Max. W. Premax.	**0.811**	0.042	30 L. Ramus	**0.877**	−0.366

*Relatively high loadings highlighted in bold as follows: (component I)>|0.8|; (II)>|0.6|.

other morphological characters is Tooth W. In addition, correlations of L. Temporal Fossa and W. External Nares with other characters are relatively low. The rest of the characters are placed in two groups. The first cluster (characters listed between 1 and 19 at top of Fig. 2) includes lengths involving the anterior portion of the skull, tooth numbers, and Orbital L. The second group (characters 4 to 8 as listed in Fig. 2) includes a variety of skull widths, dimensions of the braincase, and Ht. Ramus.

Character loadings of a principal components analysis using 25 blocks are presented in Table 3. The first component explained 57.0% of the total character variance and the second 18.5% (cumulative total of 75.4%). Projections of all blocks onto these components are shown in Figure 3, while Figure 4 is a map summarizing geographically the projections onto the first component. This component, which reflects general skull size, has relatively

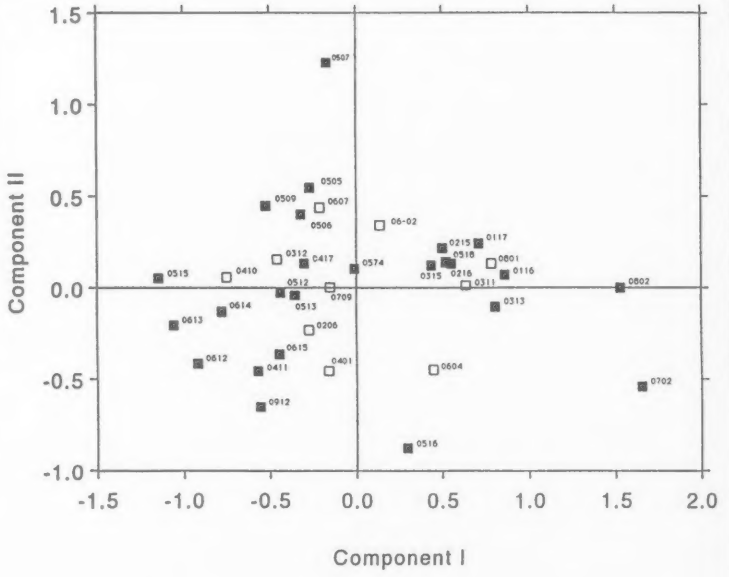

Figure 3
Projections of blocks onto first two principal components based on 30 characters. Solid symbols indicate 25 blocks on which analysis conducted. Open symbols represent blocks with only single specimens, which were projected onto axes generated from 25 blocks with two or more specimens.

high correlations (Table 3) with all characters except Tooth W. and Skull W. (at Parietals). Localities to the right in Figure 3 are from the Hawaiian Island area (0702 and 0802; see Fig. 4), where animals are larger. Specimens from southern blocks (e.g., 0116, 0117, 0313) also are larger than animals from other parts of the range. Blocks to the left in Figure 3, with negative loadings on component I, have smaller individuals. In general, *S. longirostris* from the northeastern blocks were the smallest (e.g., 0515, 0613, 0612).

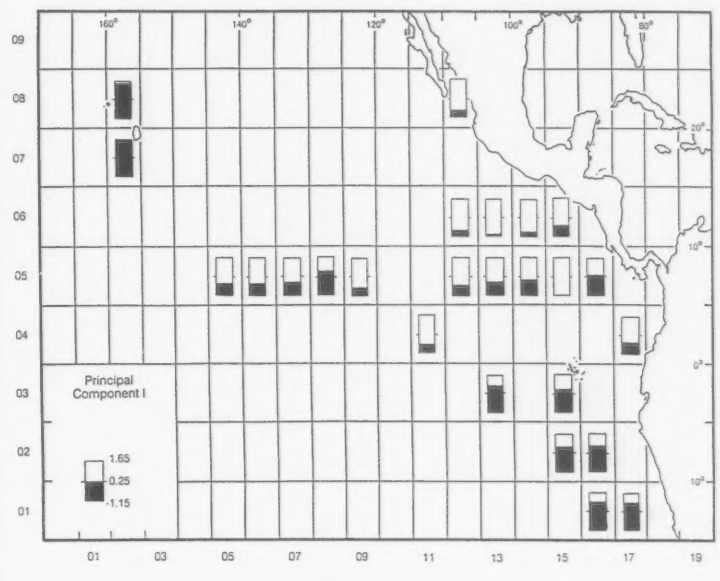

Figure 4
Geographic variation in principal component I. Bar represents range (low to high block values), and midpoint is marked. Darkened part of bar indicates value for particular block.

Component II has its highest positive correlations with Skull W. (at Parietals), Ht. Braincase, and Tooth W.; it has negative associations with characters 23–26, which involve numbers of teeth. Block 0507 is the most extreme, with a positive projection on this component (see Fig. 3); animals from this block have relatively wide skulls and reduced numbers of teeth. In contrast, block 0516 is at the other extreme, with relatively narrow skulls and greater numbers of teeth.

Figure 5 is a dendrogram depicting results from a UPGMA cluster analysis of the 25 geographic blocks. Four main clusters are evident, with block 0702 being the most divergent and in its own cluster. Block 0507 also is in a cluster by itself. The first group in the diagram (i.e., blocks 0116 through 0516 at top of Fig. 5) includes predominantly southern and western localities. Those in the largest cluster (listed from block 0411 to 0509 in Fig. 5) are situated to the north and/or east.

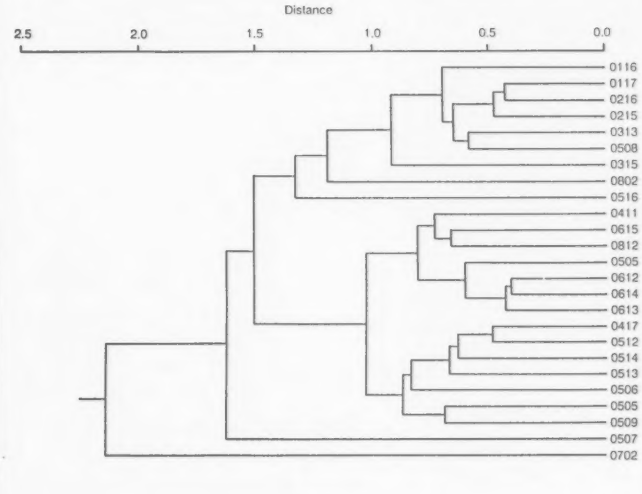

Figure 5
Distance phenogram summarizing UPGMA clustering of 25 blocks based on 30 characters. Cophenetic correlation is 0.80.

A modified skyline diagram (Fig. 6A) resulting from function-point clustering for 25 blocks based on 30 characters indicates an initial separation of block 0702 (which includes part of Hawaii) from the others. At a w-value of 3.50, there are three clusters: (1) block 0702; (2) the southern blocks in addition to blocks 0508 and 0802; and (3) the remaining northern and eastern blocks, including those just north of the Equator. Further subdivision results with smaller w-values (see Fig. 6A).

A similar analysis (Fig. 6B) was conducted using the five characters—Postorbital W., L. Rostrum (frm.

Pterygoid), W. Internal Nares, W. Premax. (at 1/2 L.), and W. Rostrum (at Base)—that, in combination, were best for discriminating among blocks (based on canonical variates analysis reported below). With a w-value of 1.79, block 0702 is separated from the remaining blocks. Note that four groups were formed when using a 1.47 w-value; there are two single-block groups (i.e., 0702 and 0802). When the w-value was lowered to 1.37, the same groups were formed, except that 0315 was in its own group and 0802 joined with a group of predominantly southern localities. With a 1.26 w-value, the clusters are the same except that block 0505 joins the northeastern blocks instead of those from the south. Three groups were formed with a 1.15 w-value: (1) block 0702; (2) a group of eight blocks, including southern blocks in addition to 0508, 0505, and 0802; and (3) the northern and eastern blocks, including 0411 and 0417, as well as 0506, 0507, and 0509. At smaller w-values, there is further subdivision.

A canonical variates analysis, using as initial data the information on all 30 measurements for 25 blocks, incorporated the five characters listed in Table 4. A two-dimensional plot of the 25 block centroids on canonical variables 1 and 2 is included as Figure 7; although not used to generate the axes, 10 blocks with only single specimens also are projected onto these variables. The geographic pattern of canonical variable 1 is depicted in Figure 8B. The eigenvalue for canonical variable 1 is 2.93 and that for the second is 0.55, with the two summarizing 82.0% of the variance for the five characters. These five characters in combination show the

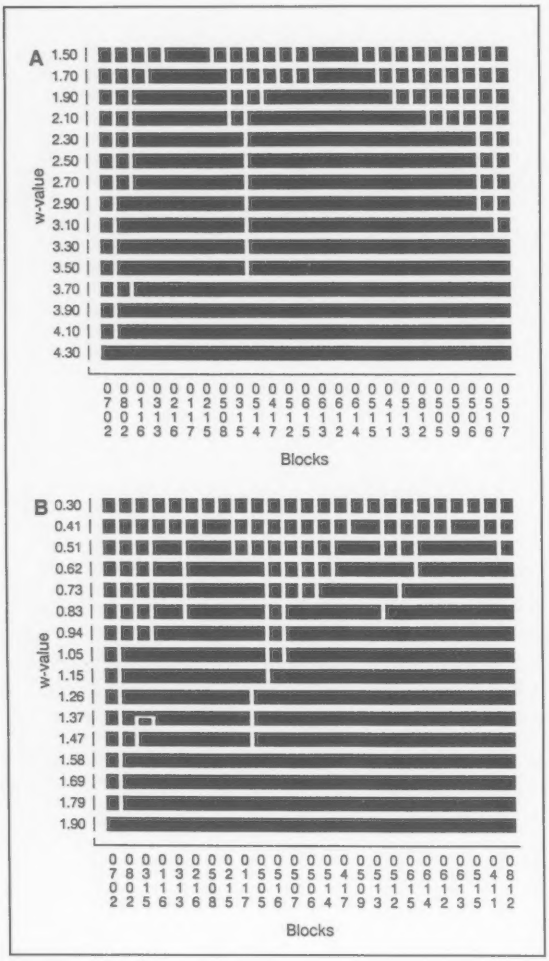

Figure 6

Modified skyline diagrams for 25 blocks, indicating groups formed using function-point clustering procedures and based on: (A) all 30 characters; (B) five characters that, in combination, best discriminate among blocks (Postorbital W., L. Rostrum [frm. Pterygoid], W. Internal Nares, W. Premax. [at 1/2 L.], and W. Rostrum [at Base]). For given w-value (i.e., row), blocks connected in common line are in same cluster.

Table 4

Canonical variates analysis of all specimens from 25 blocks.

Character		F-value to enter	Order of entry	Coefficients* 1	2
3	L. Rostrum (frm.Pterygoid)	4.53	2	0.0242 (0.2830)	−0.0662 (−0.7734)
4	W. Rostrum (at Base)	2.38	5	−0.0603 (−0.1622)	−0.1912 (−0.5145)
7	W. Premax. (at 1/2 L.)	2.30	4	−0.0291 (−0.0393)	0.2419 (0.3273)
10	Postorbital W.	23.21	1	0.2113 (0.8570)	0.0648 (0.2628)
21	W. Internal Nares	2.88	3	0.0958 (0.1870)	0.3324 (0.6489)
	Constant			38.9175	4.4931

*Unstandardized coefficients, with standardized values in parentheses, for canonical variates.

greatest among-group variability relative to that within groups and are used for more detailed comparisons with environmental variables (presented below).

As indicated in Table 4, the first canonical variable is most influenced by Postorbital W. (Fig. 8A). In Figure 7, blocks that are large for this character are to the right, while those that are small are to the left. When considering only those blocks with more than one specimen (i.e., those shown with solid symbols in Fig. 7), the two blocks from the vicinity of the the Hawaiian Islands (0802 and 0702) are to the right, as are blocks predominantly from the southern portion of the range. The blocks with single specimens (which tend to be more westerly) also are to the right. Specimens from blocks to the north and east are smaller; they are depicted to the left in Figure 7. Some west-central blocks group with the southern blocks, while others are intermediate or group with those to the northeast. The second canonical variable contrasts blocks from the Hawaiian Island area (0702, 0802) with the others (see Fig. 7); in the characters reflected by this variable, values of block 0812 (which is northern, but to the east) show some similarities to those for 0702 and 0802.

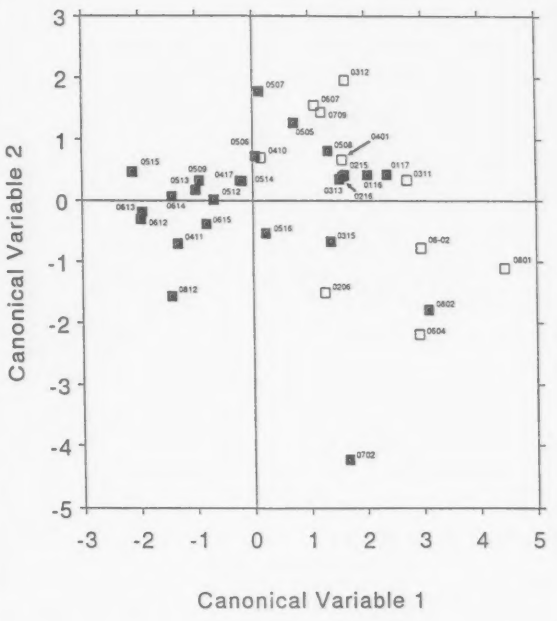

Figure 7

Projections of blocks onto first two canonical variables based on 30 characters. Solid symbols indicate 25 blocks on which analysis conducted. Open symbols represent blocks with only single specimens, which were projected onto axes generated from 25 blocks with two or more specimens.

Mantel test for geographic patterning

Individual characters were evaluated with respect to geographic patterning using Mantel tests, as well as matrix correlations that compare interblock geographic distances (or reciprocals of these distances) and character differences between localities. Of the 30 characters, 66.7% (20) show statistically significant regional patterning indicating that geographic distances (in nautical miles) and interblock character differences are interrelated (Table 5). For measures showing significant t-values the greatest character differences tend to be between blocks that are farthest away from each other, while nearer localities are more similar.

Local patterning, as indicated by a significant negative association of distance reciprocals and character differences, was found in 83.3% (25) of the characters (Table 5). All characters that showed regional patterning also exhibited local patterning.

Principal component projections also were assessed in terms of geographic patterning. As indicated at the bottom of Table 5, component I (Fig. 4) has strong regional and local patterning; component II has significant local patterning. Canonical variables 1 (Fig. 8B) and 2 both exhibit marked regional and local patterning (Table 5).

Morphological-environmental covariation

Figure 9 is a dendrogram indicating absolute correlations among the 13 environmental variables, subdividing them into five clusters. Sea Current (N., Winter) is in a group by itself and quite different from the others. Sea Current (W., Winter) and Oxygen Min. Layer (Depth) are in the second cluster, which joins with a group of five variables involving surface measures of temperature, oxygen, and salinity. The fourth cluster involves two measures of solar insolation, and the fifth reflects aspects of water depth.

The loadings of environmental variables on the first three environmental principal components are given in Table 6. The first component statistically explains 33.0% of the total character variance, the second 23.2%, and the third 15.8% (cumulatively 72.0%). Maps (Fig. 10) depict projections of the 25 blocks with two or more *S. longirostris* onto the first two environmental components. Environmental component I has relatively high values for blocks between 5° and 15°N, with intermediate values to the north and low values south of the Equator (Fig. 10A). Sea Surface Temp. (July)

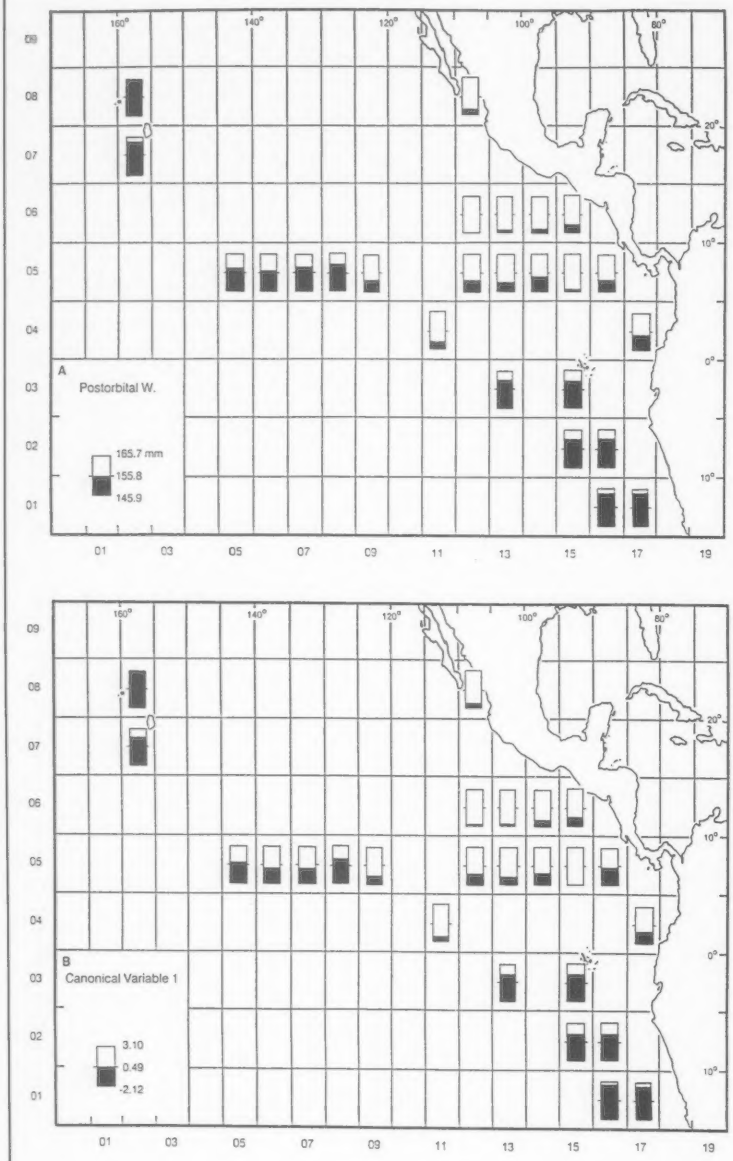

Figure 8
Geographic variation in (A) Postorbital W. and (B) canonical variable 1. Darkened part of bar indicates value for particular block.

has a high positive loading on component I, while that for Sea Surface Temp. (Ann. Var.) is negative. Five other variables have relatively high correlations with this component (Table 6). The second environmental component has high values for the two blocks adjacent to the Hawaiian Islands (Fig. 10B), with intermediate values in other western blocks. Strong negative projections on this component are found for blocks along the coast of South and Central America just north of the Equator. The most substantial loadings on this component are for the two thermocline variables (Table 6), while Water Depth and Surface Salinity also exhibit relatively high positive projections for component II. Environmental component III reflects mainly Solar Insolation (Annual), with Solar Insolation (Jan.) also having a relatively high positive loading (Table 6). The most extreme negative projection for component III is for the northern block near the coast (i.e., 0812), with the highest positive projects for blocks in the west-central portion of the study area (i.e., 0505 through 0509). In general, other blocks have relatively high projection values, except for 0802 (which is somewhat lower). Other components beyond the first three tended to represent only single environmental variables.

Several of the environmental measures showed few or no statistical associations with morphological characters (and resulting principal components or canonical variables), while others exhibited significant covariation (Table 7). The first environmental variable, Sea Current (N., Winter), is not significantly correlated with any of the 30 morphological measures. The other character summarizing sea-current information, Sea Current (W.,Winter), has a geographic pattern showing relatively weak statistical concordance with eight of the morphological characters. Toothrow lengths and three of the four tooth counts are among those with significant associations.

Table 5

Association of interlocality character differences with geographic distances (in nautical miles) and the reciprocals of these distances. Results from Mantel tests (t) and matrix correlations (r) for *Stenella longirostris*.

Character	Distance		Reciprocal of distance	
	t	r	t	r
1 Condylobasal L.	4.49***	0.445	−4.86***	−0.348
2 L. Rostrum (frm.Base)	3.89***	0.395	−4.35***	−0.315
3 L. Rostrum (frm.Pterygoid)	4.26***	0.437	−4.67***	−0.340
4 W. Rostrum (at Base)	3.49***	0.435	−3.86***	−0.316
5 W. Rostrum (at 1/4 L.)	3.16**	0.327	−3.48***	−0.255
6 W. Rostrum (at 1/2 L.)	3.12**	0.297	−3.68***	−0.258
7 W. Premax. (at 1/2 L.)	−0.48	−0.046	0.23	0.017
8 W. Rostrum (at 3/4 L.)	0.33	0.028	−1.98*	−0.132
9 Preorbital W.	4.59***	0.403	−6.36***	−0.429
10 Postorbital W.	3.57***	0.262	−5.97***	−0.373
11 Skull W. (at Zygomatic P.)	3.43***	0.255	−5.98***	−0.357
12 Skull W. (at Parietals)	1.83	0.199	−2.19*	−0.165
13 Ht. Braincase	1.51	0.146	−3.89***	−0.275
14 L. Braincase	3.62***	0.323	−4.85***	−0.329
15 Max. W. Premax.	2.05*	0.209	−3.58***	−0.260
16 W. External Nares	−0.48	−0.047	−0.38	−0.027
17 L. Temporal Fossa	1.87	0.193	−2.74**	−0.201
18 W. Temporal Fossa	3.84***	0.362	−4.69***	−0.327
19 Orbital L.	3.01**	0.325	−3.68***	−0.276
20 L. Antorbital P.	2.93**	0.229	−4.32***	−0.277
21 W. Internal Nares	0.56	0.047	−3.43***	−0.226
22 L. Up. Toothrow	3.96***	0.392	−4.47***	−0.319
23 No. Teeth (Up.Lf.)	3.46***	0.411	−3.61***	−0.286
24 No. Teeth (Up.Rt.)	3.46***	0.434	−3.30***	−0.271
25 No. Teeth (Low.Lf.)	1.62	0.178	−1.38	−0.105
26 No. Teeth (Low.Rt.)	1.52	0.158	−1.28	−0.093
27 L. Low. Toothrow	3.00**	0.285	−3.46***	−0.242
28 Ht. Ramus	3.03**	0.237	−4.77***	−0.306
29 Tooth W.	−0.55	−0.067	−0.13	−0.011
30 L. Ramus	3.91***	0.375	−4.47***	−0.314
Component I	3.77***	0.363	−4.64***	−0.327
Component II	1.13	0.134	−2.72**	−0.214
Canonical Variable 1	2.77**	0.220	−5.08***	−0.327
Canonical Variable 2	4.05***	0.520	−4.12***	−0.343

*$P<0.05$; **$P<0.01$; ***$P<0.001$.

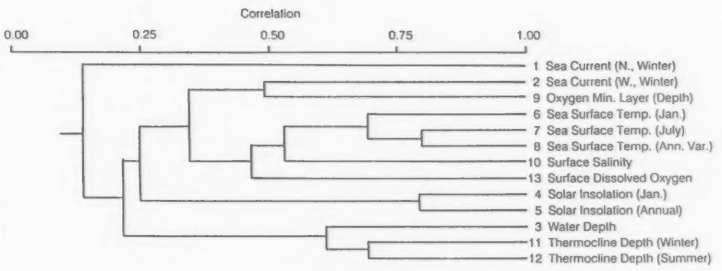

Figure 9

Clustering by UPGMA on absolute correlation values among environmental variables. Cophenetic correlation of 0.75.

Table 6
Principal component loadings for environmental variables.

Environmental variable	Component* I	II	III
1 Sea Current (N.,Winter)	−0.126	0.307	0.431
2 Sea Current (W.,Winter)	−0.495	−0.037	−0.091
3 Water Depth	−0.279	**0.783**	0.279
4 Solar Insolation (Jan.)	−0.683	−0.227	**0.627**
5 Solar Insolation (Ann.)	−0.274	−0.291	**0.872**
6 Sea Surface Temp. (Jan.)	0.768	−0.255	0.380
7 Sea Surface Temp. (July)	**0.942**	0.014	−0.101
8 Sea Surface Temp. (Ann.Var.)	**−0.848**	−0.224	−0.304
9 Oxygen Minimum Layer (Depth)	0.675	0.442	0.157
10 Surface Salinity	−0.608	**0.600**	−0.046
11 Thermocline Depth (Winter)	0.172	**0.888**	−0.269
12 Thermocline Depth (Summer)	−0.044	**0.836**	0.363
13 Surface Dissolved Oxygen	−0.596	0.089	−0.380

*Relatively high loadings highlighted in bold as follows: (component I) > |0.8|; (II and III) > |0.6|.

Table 7
Product-moment correlations of block means for morphological variables and components versus environmental variables and components based on 25 blocks of *Stenella longirostris*.[a]

Character	Environmental variable[b] 1	2	3	4	5	6	7	8	9	10	11	12	13	Environmental component I	II	III
1 Condylobasal L.						−−	−−						++	−		
2 L. Rostrum (frm.Base)						−−	−	+	+				+	−		
3 L. Rostrum (frm.Pterygoid)		+				−−	−−	+	−				++	−		−
4 W. Rostrum (at Base)			++			−−	−			+	+++	++			+++	
5 W. Rostrum (at 1/4 L.)			++			−	−			+	++	++			+++	
6 W. Rostrum (at 1/2 L.)			++				−			+	+	++			++	
7 W. Premax. (at 1/2 L.)													+		++	
8 W. Rostrum (at 3/4 L.)		−	++									++			+	
9 Preorbital W.			++			−−−	−−−			+++	+	++	+	−−	++	
10 Postorbital W.			++			−−	−−−			+++	+	++	+	−−	++	
11 Skull W. (at Zygomatic P.)			++			−−	−−−			+++	+	++	+	−−	++	
12 Skull W. (at Parietals)			+													
13 Ht. Braincase			++			−	−−			+++		++		−	+	
14 L. Braincase			+++			−−−	−−−			+++	+	++	+			
15 Max. W. Premax.					−	−−				+	+					
16 W. External Nares						−	−			++		+++	+	−		
17 L. Temporal Fossa						−	−						+	−		
18 W. Temporal Fossa			+++			−	−			++	++				+++	
19 Orbital L.		+				−−		−					+	−		
20 L. Antorbital P.			+			−−	−−−			++			+	−−		
21 W. Internal Nares			+	++			−−−							−−		
22 L. Up. Toothrow		+			−	−−	−	+	−				++	−		−
23 No. Teeth (Up.Lf.)		+				−−										−
24 No. Teeth (Up.Rt.)		+				−−										−
25 No. Teeth (Low.Lf.)																
26 No. Teeth (Low.Rt.)		+														
27 L. Low. Toothrow		+				−−	−	+	−				+	−	+	
28 Ht. Ramus			++			−	−−			+	+	+	+	−	+	
29 Tooth W.			+													
30 L. Ramus						−−	−	+	−				++	−		
Component I			+			−−−	−−			++	+	+	+	−−	+	
Component II		−−	++									+				+
Canonical Variable 1			++			−−−	−−−	+	−	++		+	++	−−−	+	
Canonical Variable 2		−		++	++						−−					++

Table 7 (continued)

[a] Blanks indicate nonsignificant correlations. Individual symbols refer to significant positive or negative correlations ($P<0.05$; >0.396); double symbols indicate highly significant correlations ($P<0.01$; >0.505); and triple symbols represent very highly significant correlations ($P<0.001$; >0.620).

[b] Environmental variables: (1) Sea Current (N., Winter); (2) Sea Current (W., Winter); (3) Water Depth; (4) Solar Insolation (Jan.); (5) Solar Insolation (Annual); (6) Sea Surface Temp. (Jan.); (7) Sea Surface Temp. (July); (8) Sea Surface Temp. (Ann. Var.); (9) Oxygen Min. Layer (Depth); (10) Surface Salinity; (11) Thermocline Depth (Winter); (12) Thermocline Depth (Summer); and (13) Surface Dissolved Oxygen.

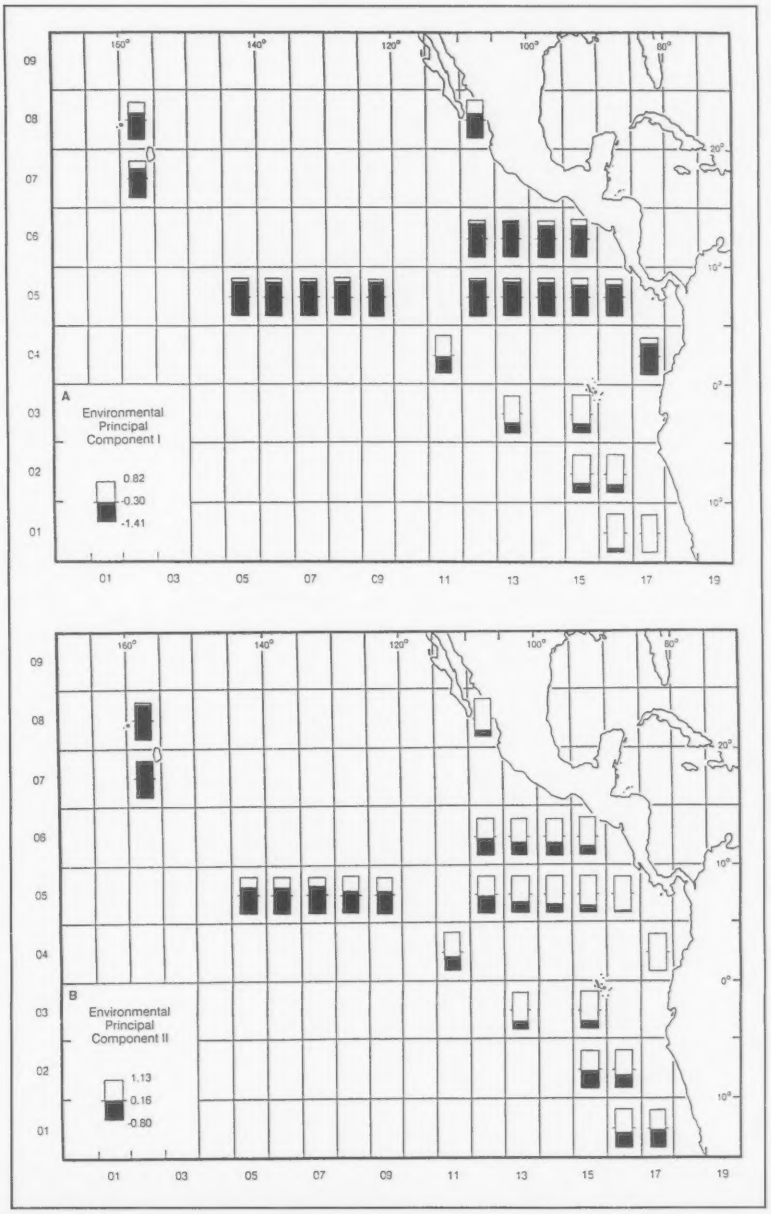

Figure 10
Geographic variation in environmental variables as summarized in (A) principal component I and (B) principal component II. Darkened part of bar indicates value for particular block.

Water Depth (variable 3; Fig. 11B) is positively correlated with 13 morphological measures, two of which (L. Braincase and W. Temporal Fossa) are very highly significant ($P<0.001$). The block values for W. Temporal Fossa (which have a 0.755 correlation with Water Depth values) are shown in Figure 11A. For the 13 variables, relatively large values typically were recorded in block 0117 and those in the vicinity of the Hawaiian Islands (0702 and 0802), all of which have relatively deep waters, while more shallow localities like 0516 and 0812 had individuals that were smaller for these characters.

The fourth environmental measure, Solar Insolation (Jan.), changes from high to low values uniformly from north to south. It is statistically associated with only one character, W. Internal Nares, which has small values for 0812; values tend to get higher as one proceeds south, but there are exceptions (such as 0802, which is relatively high). Canonical variable 2 has a pattern statistically similar to this environmental variable (bottom of Table 7).

Annual solar insolation (variable 5) has high values at the earth's Equator, with decreasing values as one proceeds toward either pole. Only two morphological variables have significant correlations with this environmental factor (Table 7), each of which are negative and relatively weak.

The sixth environmental variable, Sea Surface Temp. (Jan.), has significant negative correlations with 22 morphological characters, as well as principal component I (Fig. 4) and canonical variable 1 (Fig. 8B). Variable 7, which is Sea Surface Temp. (July) (Fig. 12), has a relatively high number (21) of significant negative associations with morphological measures, as well as with principal component I (Fig. 4) and canonical variable 1 (Fig. 8B). Postorbital W. (Fig. 8A) has the strongest correlation (−0.681) of any of the morphological characters with Sea Surface Temp. (July).

The eighth environmental variable, Sea Surface Temp. (Ann. Var.), exhibited relatively weak geographic concordance with six morphological characters, one of which was a negative association (Table 7). Also, only weak negative correlations of five morphological variables were found with depth of the oxygen minimum layer (variable 9).

Fourteen of the 30 morphological measures are significantly correlated with environmental variable 10, Surface Salinity (Fig. 13B). In addition to east-west changes from lower to higher values at a given latitude, salinity also exhibits a north-to-south trend of increasing values (below 15°N). The highest correlation (0.661) is with L. Braincase (Fig. 13A).

Thermocline Depth (Winter), variable 11, was positively associated with 13 morphological variables (Table 8), while Thermocline Depth (Summer), variable 12, has statistically significant positive correlations with 11 morphological traits. The final variable, Surface Dissolved Oxygen, covaries with 16 morphological variables. As suggested in the dendrogram in Figure 9, this environmental variable has a

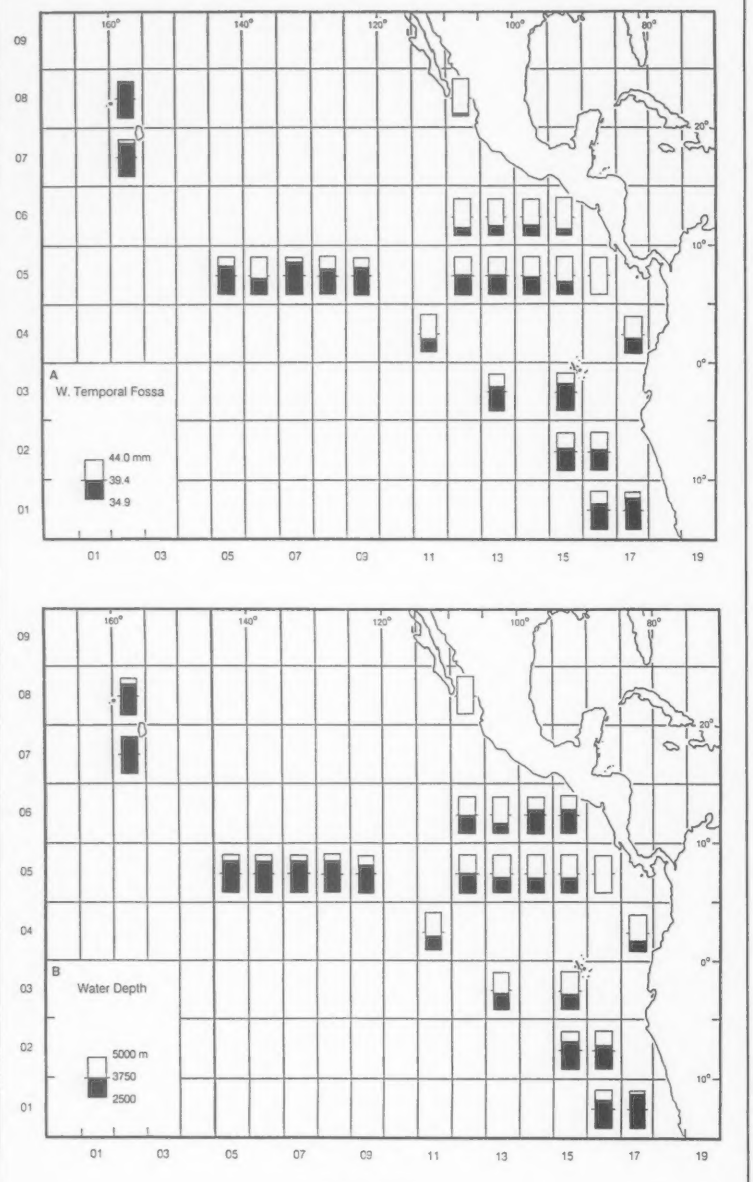

Figure 11
Geographic variation in (A) W. Temporal Fossa and (B) Water Depth. Darkened part of bar indicates value for particular block.

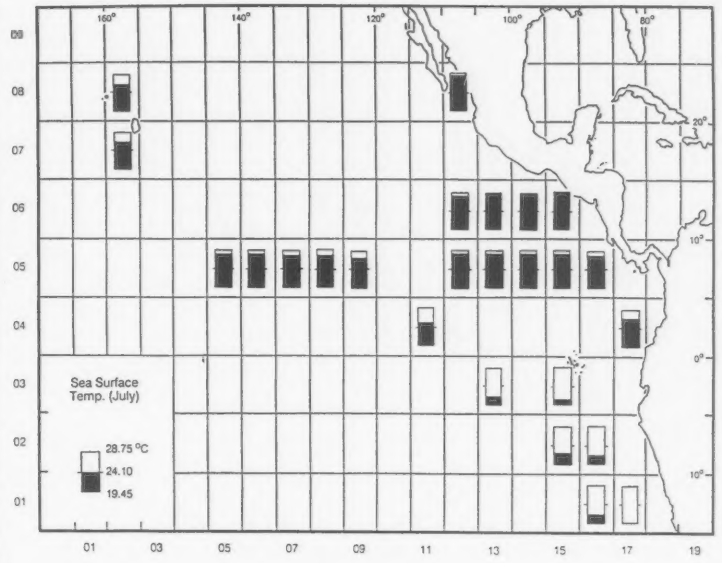

Figure 12
Geographic variation in Sea Surface Temp. (Jul.). Darkened part of bar indicates value for particular block.

pattern with similarities to those for sea surface temperatures.

Table 7 indicates that the pattern of correlations of environmental principal component I with cranial measures is similar to that of Sea Surface Temp. (July) (variable 7), which is expected given the strong loadings of this environmental variable on this component (see Table 6). Environmental principal component II has positive correlations with most skull-width measures (Table 7). The third environmental component has relatively few significant correlations with morphological characters; its strongest association is with one of the summary morphological variables, canonical variable 2.

In Table 8, we have summarized Mantel t-values and matrix correlations between selected

Table 8
Results of Mantel tests (t) and matrix correlations (r) for *Stenella longirostris*. Comparison of interlocality differences for 13 environmental variables and 3 environmental components against those for 5 morphological variables selected in canonical variates analysis.

	Postorbital W.		L. Rostrum (frm.Pterygoid)		W. Internal Nares		W. Premax. (at 1/2 L.)		W. Rostrum (at Base)	
Environmental variable	t	r	t	r	t	r	t	r	t	r
1 Sea Current (N.,Winter)	−0.56	−0.050	−0.59	−0.083	1.99*	0.215	−0.56	−0.073	−0.79	−0.141
2 Sea Current (W.,Winter)	−1.38	−0.092	0.12	0.010	−0.72	−0.053	0.59	0.048	−0.44	−0.044
3 Water Depth	3.23**	0.235	1.27	0.128	2.25*	0.186	−0.76	−0.073	2.22*	0.271
4 Solar Insolation (Jan.)	4.46***	0.339	2.60**	0.283	4.49***	0.393	0.77	0.079	1.81	0.241
5 Solar Insolation (Ann.)	2.14*	0.176	1.95	0.241	1.86	0.180	−0.54	−0.062	1.43	0.219
6 Sea Surface Temp. (Jan.)	5.47***	0.371	3.71***	0.327	3.63***	0.271	0.53	0.045	1.63	0.170
7 Sea Surface Temp. (July)	4.82***	0.353	1.73	0.176	4.65***	0.387	2.55*	0.244	0.64	0.079
8 Sea Surface Temp. (Ann.Var.)	1.64	0.114	1.22	0.113	3.80***	0.294	1.40	0.123	−0.40	−0.044
9 Oxygen Minimum Layer (Depth)	1.22	0.077	2.12*	0.158	3.54***	0.236	1.62	0.116	−0.61	−0.051
10 Surface Salinity	4.57***	0.323	0.37	0.035	1.03	0.082	0.06	0.005	0.62	0.072
11 Thermocline Depth (Winter)	2.92**	0.241	4.42***	0.548	−0.96	−0.093	−0.55	−0.063	3.87***	0.598
12 Thermocline Depth (Summer)	2.52*	0.172	1.63	0.146	−0.15	−0.001	−0.35	−0.030	3.41***	0.362
13 Surface Dissolved Oxygen	2.52*	0.204	1.43	0.172	1.88	0.179	0.93	0.105	−0.18	−0.027
Environmental Component I	3.63***	0.268	1.68	0.174	4.09***	0.345	2.02*	0.197	0.11	0.014
Environmental Component II	2.75**	0.212	3.85***	0.429	−1.11	−0.099	−0.75	−0.078	3.70***	0.508
Environmental Component III	1.39	0.120	1.19	0.160	1.99*	0.207	−0.97	−0.121	0.32	0.054

*$P<0.05$; **$P<0.01$; ***$P<0.001$.

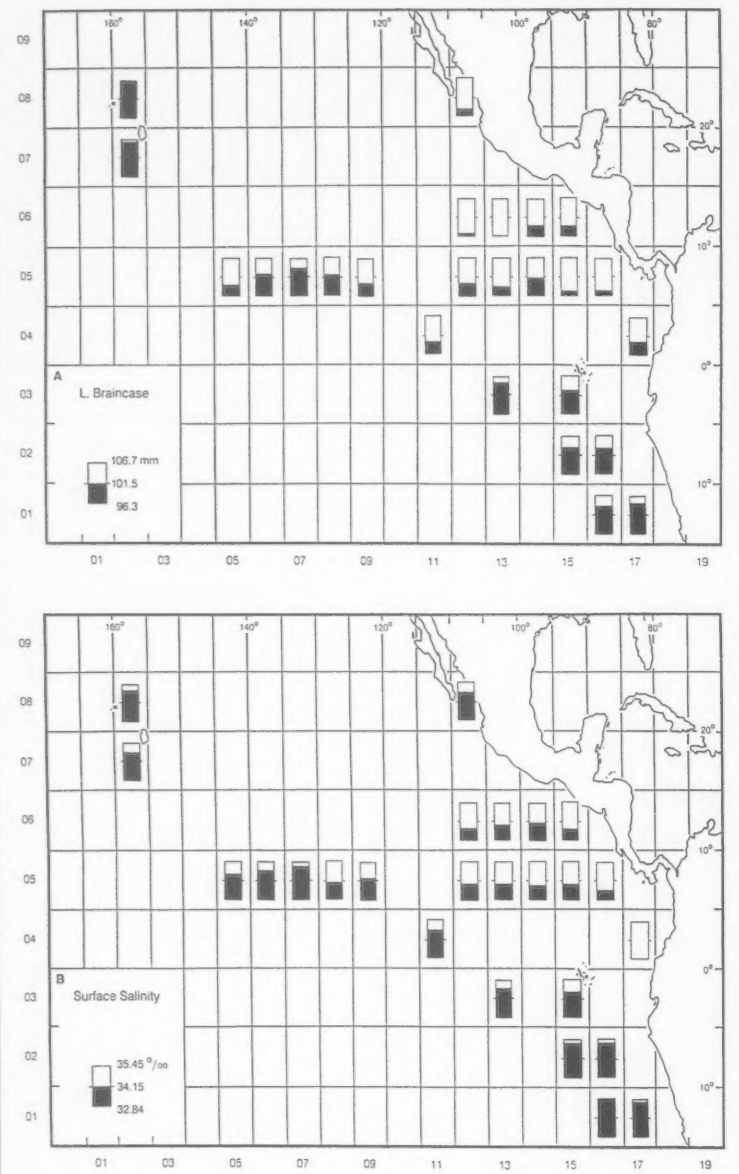

Figure 13
Geographic variation in (A) L. Braincase and (B) Surface Salinity. Darkened part of bar indicates value for particular block.

morphological and environmental variables. Assessing difference matrices using these techniques represents an alternate method with which to evaluate covariation of geographic patterns. For Postorbital W. (Fig. 8A), there are nine significant associations using the Mantel test (Table 8), with Sea Surface Temp. (Jan.) being the highest. The seven environmental variables displaying correlations in Table 7 with Postorbital W. also are judged concordant using the Mantel test. In addition, based on interblock difference values, there are statistically significant associations with the two measures of solar insolation (variables 4 and 5; see Table 8). The concordance with these two environmental variables is primarily on the strength of pattern similarities in the eastern portion of the range. Postorbital W. also shows significant associations with the first two environmental principal components.

Based on correlation tests for block means (Table 7), L. Rostrum (frm.Pterygoid) exhibited a geographic distribution of mean block values that was statistically associated with those for six environmental measures. Four significant associations were identified using the Mantel test (Table 8), only two of which were found by both tests (Sea Surface Temp. [Jan.] and Oxygen Minimum Layer [Depth]). It has a significant association with environmental component II.

In Table 8, a total of seven significant associations of difference values are recorded for W. Internal Nares with environmental variables, including the three listed in Table 7 as having statistically significant associations based on means. Difference values for environmental components I and III significantly covary with those of W. Internal Nares.

Using difference values, W. Premax. (at 1/2 L.) has only a weak correlation with a single environmental variable (Table 8); only a single significant association was found using correlations of mean values, and this was with another environmental variable (see Table 7). W. Premax. (at 1/2 L.) is weakly associated with environmental component I.

The W. Rostrum (at Base) exhibits covariation with three of the environmental variables based on the Mantel test (Table 8), two of which involve thermocline depth. The matrix correlation (Table 8) for W. Rostrum (at Base) with Thermocline Depth (Winter) is substantial (0.598), as it is with environmental component II (0.508). Mean values also showed an association of W. Rostrum (at Base) with the thermocline variables and Water Depth, as well as with three other environmental variables (Table 7).

Discussion

Sexual dimorphism

Our analysis of sexual dimorphism extends the studies of Douglas et al. (1986) in terms of additional specimens and minor adjustments in previously collected data. We found 15 of 30 variables were statistically dimorphic. Douglas et al. (1986) identified 13 of these as showing sexual differences, the increase of two characters (Postorbital W. and Tooth W.) being due primarily to increased numbers of specimens available. In five characters, including two rostral and two toothrow lengths, measurements for females were slightly larger than for males, although the differences were not statistically significant. For all other measures, males are larger than females, including all 15 where statistical significance was found.

Geographic variation

In 1889, when the existence of spinner dolphins in the eastern tropical Pacific was not yet known, True indicated that the absence of adequate samples made very difficult the task of taxonomically evaluating species in the genus *Stenella*. By the 1970s, Perrin (1975b) had available considerably more material for a monographic treatment of *S. attenuata* and *S. longirostris* from the eastern tropical Pacific and was able to make significant advances with respect to our understanding of morphological variation of *Stenella*. However, his work on *S. longirostris* also was hindered by the paucity of skeletal material from parts of the range. For our study, many additional specimens of *S. longirostris* were available. On the whole, our results are strongly supportive of those obtained by Perrin (1975b) for cranial characteristics, but we also have been able to substantially extend his analyses.

Perrin (1972) conducted an initial analysis of geographic variation in color patterns of *S. longirostris* in the eastern Pacific Ocean. He found geographic variation, particularly in the "dorsal field system" of coloration, which overlies a basic general pattern. These and other data suggested differentiation into eastern, whitebelly, and Hawaiian forms. The differences were analyzed further by Perrin (1975a,b), who indicated that the whitebelly form was in some ways similar to the Hawaiian form, but had a proportionately smaller beak. Perrin (1975b) described but did not name four races—the three mentioned above plus a Costa Rican form which occurs off the coast of Central America. Perrin et al. (1979b) evaluated possible differentiation in *S. longirostris* involving animals found south of the Equator in the eastern Pacific Ocean. They concluded that these *S. longirostris* are morphologically distinct from those to the northeast; characteristics showing such a trend include coloration, size, shape, and skeletal measures.

Recently, Perrin (1990) named and described three subspecies: *S. l. longirostris* (Gray's spinner dolphin), *S. l. orientalis* (eastern spinner dolphin), and *S. l. centroamericana* (Central American spinner dolphin). In our geographic variation assessment, we purposely included all adult specimens available, without an attempt *a priori* to differentiate previously described forms. However, the differences among the named forms are reflected in our results for cranial characteristics.

In our analyses, the Central American spinner dolphin of Perrin (1990) is shown to be different from other *S. longirostris* by the positioning of block 0516 on principal component II; it had the lowest value of any of the blocks (see Fig. 3). Three of the four specimens in block 0516 exhibit characteristics of Central American spinners (as does one of the nine from 0615). Character associations with the second principal component—summarized in Table 3—suggest that, after taking into account general size (summarized in and mathematically removed by component I), animals of this subspecies have relatively longer toothrows, greater numbers of teeth, a narrower skull at the parietals, and a shallower braincase than *S. longirostris* from other areas. Perrin (1990: table 2) provided comparative measurements and counts for *S. l. longirostris* and *S. l. centroamericana*, which show the Central American form to have longer toothrows and greater numbers of teeth. He did not include data on Ht. Braincase, but did characterize the Central American form as having a relatively long and narrow skull. While Skull W. (at Parietals) is slightly greater for *S. l. centroamericana* than *S. l. longirostris* (Perrin 1990: table 2), the former has a relatively narrow skull given its considerably greater length. Additional *S. l. centroamericana* specimens are needed, since the diagnosis and understanding of cranial variation in this subspecies still is based on very few animals.

Perrin (1990) suggested the existence of a zone of hybridization/intergradation between *S. l. longirostris*

and *S. l. orientalis* that may be about 2000km wide. *Stenella l. orientalis* is found primarily in the northeastern blocks we assessed. Our analyses confirm that, in general, adult spinner dolphins from this region are smaller than those from areas to the south, southwest, and west (for general trends, refer to block projections onto canonical variable 1 in Fig. 8B). The nominate subspecies, *S. l. longirostris*, of Perrin (1990) subsumes a series of broadly distributed populations. He indicated that *S. l. longirostris* likely includes areal entities (outside the eastern Pacific) worthy of formal taxonomic recognition, but to date these have not been evaluated properly because of a paucity of specimens from major portions of the range.

Extensive data on geographic variation in external morphology of *S. longirostris* in the eastern tropical Pacific were assessed by Perrin et al. (1991). They evaluated color patterns, dorsal-fin shapes, and total lengths for *S. longirostris* from throughout the geographic range covered in our study. Some external characters (e.g., ventral field coloration pattern) exhibited a "radial" or concentric pattern of variation, where spinners to the south, southwest and west were similar, but markedly different from those to the northeast. This pattern also was prevalent among cranial variables (e.g., see values for Postorbital W. [Fig. 8A], canonical variable 1 [Fig. 8B], and L. Braincase [Fig. 13A]).

We were able to incorporate specimens into our analyses from the general vicinity of the Hawaiian Islands. Perrin (1975b) evaluated Hawaiian specimens for cranial features and concluded that, in general, they were strikingly larger than other spinners. However, at the time, few specimens were available from southern localities. When these southern blocks are incorporated into the analysis, the Hawaiian specimens are not quite as extreme, although for most characters the Hawaiian specimens remain the largest (see Postorbital W. [Fig. 8A], W. Temporal Fossa [Fig. 11A] and L. Braincase [Fig. 13A], as well as principal component I [Figs. 3 and 4] and canonical variable 1 [Figs. 7 and 8B]). Also, for many of the characters the Hawaiian specimens are more similar to far-southern ones than to those from geographically closer western blocks located between 5° and 10°N. When evaluating other western single-specimen blocks that are situated closer to the Hawaiian Islands, some analyses (e.g., canonical variates analysis; see Fig. 7) indicate that spinners similar to Hawaiian specimens are present; however, additional specimens will be needed in order to clarify the trends in variation in this part of the Pacific.

In some descriptive analyses (e.g., see Figs. 6 and 7), block 0702 to the south of the Hawaiian Islands is depicted as quite distinct from other blocks, including the adjacent block to the north (0802). This incongruity is likely a statistical aberration related to the small sample size for 0702 (n 2), rather than to a biological difference. Checking the specimens from the two blocks indicated that they were taken in relatively close proximity, but were separated because of where the border between the blocks happened to be located. This apparent anomaly does not detract from the general conclusion that the spinners in the vicinity of the Hawaiian Islands are among the largest found in the overall study region.

Schnell et al. (1986) conducted an extensive analysis of geographic variation of offshore *S. attenuata*, a similar species that broadly overlaps in range with *S. longirostris*. The two species frequently are seen in mixed schools (Au and Perryman 1985, Reilly 1990). Reilly (1990) noted that 73% of the *S. longirostris* sightings from research vessels also included *S. attenuata*; 49% of the records of the more common *S. attenuata* involved schools that also had *S. longirostris*. While detailed comparisons evaluating interspecific geographic covariation in morphology are beyond the scope of this paper, our preliminary findings indicate that about one-half of the individual morphological characters show similar geographic patterns for blocks where both species are represented. However, two characters involving the temporal fossa (variables 17 and 18) exhibit negative correlations (the length correlation is statistically significant and the width nearly so)—localities where the fossa is larger in *S. attenuata*, it is smaller in *S. longirostris*. The temporal fossa reflects the size of muscles involved in the feeding apparatus. Also, the upper tooth counts show pronounced negative correlations interspecifically. Opposite trends in the two similar species for these characters may be an example of ecological character displacement related to differences in feeding and the types of food taken by the two species in given localities (Perrin 1984).

Genetic subdivision, management units, and implications of cranial variation

Considerable attention has been given to definition of stock units with a meaningful biological basis that can be employed to manage *S. longirostris* in the eastern Pacific (Perrin 1975a, b; Perrin et al. 1979b, 1985, 1991). One of the important questions with respect to the effectiveness or relevance of geographic management units is the degree to which the species is genetically subdivided. Perrin et al. (1991) noted a complex patchwork pattern of geographic variation in external and other characteristics in *S. longirostris* suggesting "that there is not a large amount of movement between the various regions." They pointed out that the complex geographic pattern of variation in the

zone of intergradation/hybridization of *S. l. orientalis* with *S. l. longirostris* is consistent with limited data on movements from tag returns (Perrin et al. 1979a), which indicate "a home range of a diameter of hundreds rather than thousands of kilometers."

Our findings strongly support these conclusions. All 30 characters studied showed geographic variation, with two-thirds having demonstrable regional patterning, and 25 of the 30 showing local patterning. These patterns emerge even though data are based on specimens pooled over season and for a number of years; consistent geographic patterns largely would be obscured if animals typically moved long distances within or between years. Clearly, as found by Schnell et al. (1986) for *S. attenuata*, in *S. longirostris* "there are notable patterns of geographic variation. . . indicating that geographic subdivision exists among populations."

We found concordance of geographic patterns in *S. longirostris* for a number of cranial characters as noted by Perrin et al. (1991) for external characters. Yet, some patterns are not concordant; in fact, there is a mosaic of patterns involving different characters and/or character suites. For example, many of the tooth counts, toothrow measurements, and rostrum and ramus lengths show very similar patterns of variation (as indicated in Fig. 2), while other characters like Tooth W. have a pattern among blocks that is not closely related to that of any other character. Not surprisingly, a number of skull widths covary. Overall, the findings for *S. longirostris* parallel the situation typically found in other mammals where geographic variation in morphological characters has been studied. Some observed patterns may be the consequence of action by selective forces, while others simply result from and are maintained because of isolation by distance. The findings are consistent with *S. longirostris* being genetically subdivided, stemming from individual animals or groups of animals having relatively limited home ranges.

For management stocks, Perrin et al. (1991) proposed an alternative management scheme where "an 'eastern spinner conservation zone' could be devised that would offer appropriate and unequivocal protection to the unique and coherent gene pool of the eastern subspecies." For instance, a zone bounded on the south by 10°N and and on the west by 125°W would encompass 84% of the schools that were identified in the field as being composed of "eastern" spinners, and would include very few "whitebelly" animals (Perrin et al. 1991). Based on the cranial measures we employed, spinners from the blocks in this portion of the range are very similar; the blocks typically were closely linked in cluster analyses and ordinations. Blocks from most other parts of the range did not show the same degree of consistency and concordance. Our data also provide additional biological justification for establishing a geographically defined management zone for *S. l. orientalis* that, operationally, would be easily understood and more effective for management purposes.

Perrin et al. (1991) also concluded that data on external characters do not support the division of whitebelly spinners into northern and southern stocks for management purposes. For cranial features, if one considers only eastern blocks, it is possible to achieve a considerable degree of separation between northern and southern whitebelly spinners. However, the situation becomes notably more complex when more westerly blocks are added. For virtually all cranial characters, the western blocks group with the more southerly blocks even though they are at the same latitude as blocks to the east containing northern whitebelly spinners; the only possible exception is W. Internal Nares, which shows a strong north to south gradient involving all blocks except for one in the vicinity of the Hawaiian Islands (i.e., 0802). The addition of cranial specimens from western locations has provided a more sophisticated picture of geographic variation of *S. longirostris* in the region under study.

Morphological-environmental covariation

Considerable heterogeneity exists in environmental parameters over the range of *S. longirostris* in the eastern tropical Pacific (see examples of environmental variation in Figs. 11–13). With two circulatory gyres adjacent to the region, one to the north and the other to the south, the eastern tropical Pacific has an easterly-flowing equatorial counter-current from 3° to 10°N latitude, and a number of fronts and convergences (Wyrtki 1966, 1967). These coupled with latitudinal and other gradients result in substantial spatial differences in environmental characteristics.

Spotted dolphin/environmental comparisons

Schnell et al. (1986) evaluated covariation in a similar suite of environmental and cranial morphological features for offshore *S. attenuata* in the eastern tropical Pacific. The *S. attenuata* investigation was focused in eastern areas (only 1 of 19 blocks was west of 115°W). Our analysis of *S. longirostris* covers considerably more of the ocean, and includes areas around the Hawaiian Islands, which potentially could have substantially different marine environments. The importance of particular environmental variables, of course, could be quite different when different geographic levels and different-sized areas are considered. Furthermore, environmental influence could well vary between species. Yet it can be instructive to compare results of environmental-morphologic patterns for

these two dolphin species with broadly overlapping geographic ranges in the tropical Pacific Ocean.

Sea surface temperatures (variables 6 and 7; July values depicted in Fig. 12) have negative correlations with a large number of morphological features in both studies (Table 7 and Schnell et al. 1986: table 6), indicating a general trend of larger animals in warmer waters. Surface Salinity (Fig. 13B) exhibits relatively strong morphologic correlations in both studies, reflecting a pattern that has both east-west and north-south components. Also, Thermocline Depth (Summer), which has relatively low values in northern localities and higher numbers in blocks as one proceeds to the west and south, is positively associated with a number of morphological measures in *S. longirostris* (Table 7), and covaries with *S. attenuata* cranial features as well.

Solar Insolation (Jan.) registers a north-south gradient. Our *S. longirostris* study produced virtually no significant correlations with this measure, while there were numerous positive correlations in the *S. attenuata* investigation. In the eastern portion of the *S. longirostris* range, a number of cranial features have north-south gradients, but the overall statistical association is negated with the addition of the western blocks, where animals often (irrespective of latitude) exhibit characteristics similar to those found in southern areas. The same findings were obtained for Solar Insolation (Ann.).

Three environmental variables—Water Depth (Fig. 11B), Thermocline Depth (Winter), and Surface Dissolved Oxygen—are positively correlated with cranial measures in *S. longirostris*, but show few of these associations in *S. attenuata*. Again, the differences in findings simply may reflect the inclusion of a wider geographic range of blocks in the *S. longirostris* study.

Schnell et al. (1986) indicated that for *S. attenuata* it would be helpful to have additional samples, particularly from western locations. They suggested that "Such a geographic broadening of representation may enable investigators to separate, at least in part, environmental-morphological correspondences that reflect causal relationships from trends [in morphology] maintained primarily as a result of isolation by distance." For *S. longirostris*, where additional western blocks are now represented (albeit in some cases with very limited samples), it is clear that the gradients in a relatively large number of cranial characteristics are not simply north-south trends, but rather what Perrin et al. (1991) described as a radial pattern. From northeastern blocks, these characters in *S. longirostris* change more-or-less gradually as one moves to the south, the southwest, or the west. There are several environmental variables exhibiting this type of pattern (e.g., Surface Salinity; Fig. 13B). At the same time, the January and July sea surface temperatures (for July values, see Fig. 12) have a predominantly north-south orientation (with the Hawaiian Island blocks being lower than expected, given their latitude) and are correlated with the largest number of cranial characters (see Table 7). When additional specimens of *S. attenuata* become available from westerly blocks not represented in samples available to Schnell et al. (1986), it will be of interest to determine whether patterns of cranial variation (and covariation with environmental measures) in this species will mirror those we have found for *S. longirostris*.

Significance of covariation with environmental measures While previous literature has little information on the relation of environmental and cranial variation in *S. longirostris*, other investigators (Au and Perryman 1985, Reilly 1990) have evaluated physical environmental parameters with respect to distributions of *S. longirostris* and several other species in the eastern tropical Pacific. They pointed out that the highest school densities for *S. longirostris* are in the area off the Mexican coast, which also is the most tropical and least seasonally variable portion of the range. We have demonstrated notable associations of cranial variation with physical environmental characteristics. Analyses involving environmental-cranial correlations, by their very nature, are descriptive and do not provide direct information on causal factors per se. Nevertheless, they clearly indicate that between areas where animals are different cranially, there often are marked habitat differences involving the physical environment.

The first two environmental principal components (Fig. 10) describe independent, orthogonal environmental patterns: component I has a general configuration of high values between 5° and 15°N, slightly lower values further to the north, and low values to the south (Fig. 10A), which is overlain by basically an east-to-west trend summarized in environmental principal component II. The important individual environmental covariates with morphological characters include surface temperatures, salinity, and measures of water depth. The physical environmental differences reflected by the principal components, as well as by individual environmental measures, describe basic habitat differences and likely reflect, indirectly, geographic differences in available prey species and their abundances. Given the marked environmental differences exhibited in the range of *S. longirostris*, the most surprising result would have been if this species had been relatively uniform geographically in cranial features—clearly, this is not the case. Our initial assessment of morphologic-environmental covariation further underscores the appropriateness of treating different parts of the range of *S. longirostris* in the eastern tropical Pacific

separately for management purposes. In particular, a growing base of information suggests giving special attention to the spinners from the relatively uniform area of the Pacific just to the west of the Mexican/Central American coast, and viewing the pattern of morphologic variation as being broadly concentric in nature.

Acknowledgments

S.B. Reilly and A.E. Dizon reviewed the manuscript and provided useful suggestions. We thank J. Gilpatrick and J.V. Kashiwada for preparing and curating some of the specimens, as well as assisting with preparation of data for analysis. Computer programs and assistance were provided by F.J. Rohlf, R.R. Sokal, and M.A. Schene. Support for aspects of this research was received by the University of Oklahoma through Contract 79-ABC-00167 from the U.S. Department of Commerce, National Oceanographic and Atmospheric Administration, and Purchase Orders 84-ABA-02177 and 40JGNF0532 from the National Marine Fisheries Service, Southwest Fisheries Science Center, La Jolla, CA. The following individuals provided access to museum specimens: S. Anderson, G.G. Musser, and D. Russell (American Museum of Natural History, New York, NY); M.C. Sheldrick (British Museum of Natural History, Tring, United Kingdom); S. Bailey, L.C. Binford, and J. Schoenwald (California Academy of Science, San Francisco, CA); P.J.H. van Bree (Instituut voor Taxonomische Zoologie, University of Amsterdam, Amsterdam, The Netherlands); D.R. Patten and J.E. Heyning (Los Angeles County Museum of Natural History, Los Angeles, CA); C.P. Lyman and M. Rutzmoser (Museum of Comparative Zoology, Harvard University, Cambridge, MA); W.Z. Lidicker Jr. (Museum of Vertebrate Zoology, University of California, Berkeley, CA); C.G. van Zyll de Jong (Museum of Natural Sciences, National Museum of Canada, Ottawa, Canada); J.G. Mead and C.W. Potter (National Museum of Natural History, Washington D.C.); D.W. Rice and A.A. Wolman (NOAA Northwest and Alaska Fisheries Science Center, Seattle, WA); L.J. Hansen (NOAA Southwest Fisheries Science Center, La Jolla, CA); G.F. Mees (Rijksmuseum van Natuurlijke Histoire, Leiden, The Netherlands); A. Rea (San Diego Museum of Natural History, San Diego, CA); M.L. Johnson and E. Kritzman (University of Puget Sound, Tacoma, WA); and G.L. Worthen (Utah State University, Logan, UT).

Citations

Allen, R.A.
1985 Dolphins and the purse-seine fishery for yellowfin tuna. *In* Beddington, J.R., R.J.H. Beverton, and D.M. Lavigne (eds.), Marine mammals and fisheries, p. 236–252. Allen and Unwin, London.

Au, D.W.K., and W.L. Perryman
1985 Dolphin habitats in the eastern tropical Pacific. Fish. Bull., U.S. 83:623–643.

Bartholomew, J., and Son
1975 The Times atlas of the world. Comprehensive Edition. Times Books, London, 223 p.

Brunt, D.
1934 Physical and dynamical meteorology. University Press, Cambridge, England, 411 p.

Cromwell, T.
1958 Thermocline topography, horizontal currents and "ridging" in the eastern tropical Pacific. Inter-Am. Trop. Tuna Comm. Bull. 3:135–152.

Dailey, M.D., and W.F. Perrin
1973 Helminth parasites of porpoises of the genus *Stenella* in the eastern tropical Pacific, with descriptions of two new species: *Mastigonema stenellae* gen. et sp. n. (Nematoda: Spiruroidea) and *Zalophotrema pacificum* sp. n. (Trematoda: Digenea). Fish. Bull., U.S. 71:455–471.

Dixon, W.D. (chief editor)
1990 BMDP statistical software, Vol. 1. Univ. Calif. Press, Berkeley.

Dizon, A.E., Ŝ.O. Southern, and W.F. Perrin
1991 Molecular analysis of mtDNA types in exploited populations of spinner dolphins (*Stenella longirostris*). Rep. Int. Whaling Comm. Spec. Issue 13:183–202.

Douglas, M.E., and J.A. Endler
1982 Quantitative matrix comparisons in ecological and evolutionary investigations. J. Theor. Biol. 99:777–795.

Douglas, M.E., G.D. Schnell, and D.J. Hough
1986 Variation in spinner dolphins (*Stenella longirostris*) from the eastern tropical Pacific Ocean: Sexual dimorphism in cranial morphology. J. Mammal. 67:537–544.

Hall, M.A., and S.D. Boyer
1988 Incidental mortality of dolphins in the eastern tropical Pacific tuna fishery in 1986. Rep. Int. Whaling Comm. 38: 439–441.
1989 Estimates of incidental mortality of dolphins in the eastern Pacific fishery for tropical tunas in 1987. Rep. Int. Whaling Comm. 39:321–322.
1990 Incidental mortality of dolphins in the tuna purse-seine fishery in the eastern Pacific Ocean during 1988. Rep. Int. Whaling Comm. 40:461–462.

Innis, G., J. Haefner, G. Worthen, and C. Fowler
1979 ETP ecosystem model documentation. Report for Southwest Fish. Cent., NMFS, NOAA, La Jolla, CA, 277 p.

Katz, J.O., and F.J. Rohlf
1973 Function-point cluster analysis. Syst. Zool. 22:295–301.

Levitus, S.
1982 Climatological atlas of the world ocean. NOAA Prof. Pap. 13, Rockville, MD.

Manley, B.J.F.
1985 The statistics of natural selection on animal populations. Chapman and Hall (Meuthen), NY.

Mantel, N.
1967 The detection of disease clustering and a generalized regression approach. Cancer Res. 27:209–220.

Perrin, W.F.
1972 Color patterns of spinner porpoises (*Stenella* cf. *S. longirostris*) of the eastern Pacific and Hawaii, with comments on delphinid pigmentation. Fish. Bull., U.S. 70:983–1003.
1975a Distribution and differentiation of populations of dolphins of the genus *Stenella* in the eastern tropical Pacific. J. Fish. Res. Board Can. 32:1059–1067.
1975b Variation of spotted and spinner porpoise (genus *Stenella*) in the eastern tropical Pacific and Hawaii. Bull. Scripps Inst. Oceanogr. 21:1-206.
1984 Patterns of geographical variation in small cetaceans. Acta Zool. Fenn. 172:137–140.
1990 Subspecies of *Stenella longirostris* (Mammalia: Cetacea: Delphinidae). Proc. Biol. Soc. Wash. 103:453–463.

Perrin, W.F., W.E. Evans, and D.B. Holt
1979a Movements of pelagic dolphins (*Stenella* spp.) in the eastern tropical Pacific as indicated by results of tagging, with summary of tagging operations, 1969–1976. NOAA Tech. Rep. NMFS SSRF-737, 14 p.

Perrin, W.F., P.A. Sloan, and J.R. Henderson
1979b Taxonomic status of the 'southwestern stocks' of spinner dolphin, *Stenella longirostris*, and spotted dolphin, *S. attenuata*. Rep. Int. Whaling Comm. 29:175–184.

Perrin, W.F., M.D. Scott, G.J. Walker, and V.L. Case
1985 Review of geographical stocks of tropical dolphins (*Stenella* spp. and *Delphinus delphis*) in the eastern Pacific. NOAA Tech. Rep. NMFS 28, 28 p.

Perrin, W.F., P.A. Akin, J.V. Kashiwada
1991 Geographic variation in external morphology of the spinner dolphin *Stenella longirostris* in the eastern Pacific and implications for conservation. Fish. Bull., U.S. 89:411–428.

Reilly, S.B.
1990 Seasonal changes in distribution and habitat differences among dolphins in the eastern tropical Pacific. Mar. Ecol. Prog. Ser. 66:1–11.

Robinson, M.K.
1976 Atlas of north Pacific Ocean monthly mean temperatures and mean salinities of the surface layer. Naval Oceanogr. Office Ref. Publ. 2, Wash. DC.

Rohlf, F.J., J. Kishpaugh, and D. Kirk
1979 NT-SYS. Numerical taxonomy system of multivariate statistical programs. State Univ. New York, Stony Brook.

Schnell, G.D., M.E. Douglas, and D.J. Hough
1985a Sexual dimorphism in spotted dolphins (*Stenella attenuata*) in the eastern tropical Pacific Ocean. Mar. Mammal Sci. 1:1–14.
1986 Geographic patterns of variation in offshore spotted dolphins (*Stenella attenuata*) of the eastern tropical Pacific Ocean. Mar. Mammal Sci. 2:186–213.

Schnell, G.D., D.J. Watt, and M.E. Douglas
1985b Statistical comparison of proximity matrices: Applications in animal behaviour. Anim. Behav. 33:239–253.

Sneath, P.H.A., and R.R. Sokal
1973 Numerical taxonomy. W.H. Freeman, San Francisco.

Sokal, R.R.
1979 Testing statistical significance of geographic variation patterns. Syst. Zool. 28:227–232.

True, F.W.
1889 Contributions to the natural history of the cetaceans, a review of the family Delphinidae. Bull. U.S. Natl. Mus. 36:1–191.

Wirth, M., G.F. Estabrook, and D.F. Rogers
1966 A graph theory model for systematic biology with an example for the Oncidiinae (Orchidaceae). Syst. Zool. 15:59–69.

Wyrtki, K.
1966 Oceanography of the eastern equatorial Pacific Ocean. Oceanogr. Mar. Biol. Annu. Rev. 4:36–68.
1967 Circulation and water masses in the eastern equatorial Pacific Ocean. Int. J. Oceanol. Limnol. 1:117–147.
1974 The dynamic topography of the Pacific Ocean and its fluctuations. Rep. H-16-74-S, Hawaii Inst. Geophysics, 19 p.

Geographic variation in population genetic structure of chinook salmon from California and Oregon

Graham A.E. Gall
Devin Bartley
Boyd Bentley
Department of Animal Science
University of California, Davis, California 95616

Jon Brodziak
Graduate Group in Applied Mathematics and Institute of Theoretical Dynamics
University of California, Davis, California 95616

Richard Gomulkiewicz
Graduate Group in Applied Mathematics and Institute of Theoretical Dynamics
University of California, Davis, California 95616
Present address: Department of Zoology, University of Texas, Austin, Texas 78712

Marc Mangel
Department of Zoology and Center for Population Biology
University of California, Davis, California 95616

Abstract.–We analyzed the protein products of 78 isozyme loci in 37 populations of chinook salmon *Oncorhynchus tshawytscha* from California and Oregon. Allele frequencies at 47 polymorphic loci revealed substantial genetic variability within the study area. The collections of chinook salmon studied could be differentiated into five major groups located in the following geographical areas: (1) Smith River–Southern Oregon area, (2) Middle Oregon Rivers, (3) Klamath–Trinity Basin, (4) Eel River–California Coastal area, and (5) Sacramento–San Joaquin Basin. Average heterozygosity estimates were lowest in collections from the Klamath–Trinity area and highest in the Oregon populations. Gene diversity analysis indicated that differences among fish within samples accounted for 89.4% of the total diversity, whereas intersample differences accounted for 10.6 %. Estimates of the average level of historical gene flow between populations ranged from 15.57 migrants per generation in the Sacramento–San Joaquin River system to 3.97 in the Klamath–Trinity Basin; an overall estimate of number of salmon exchanging genes between populations per generation was 2.11. Although these data appeared to reflect primarily population structures existing prior to the 20th century, evidence of some effects of hatchery management and transplantations was detected.

Manuscript accepted 13 August 1991.
Fishery Bulletin, U.S. 90:77–100 (1992).

Chinook salmon *Oncorhynchus tshawytscha* is the most abundant and commercially important species of Pacific salmon native to California and Oregon (Moyle 1976), but stocks have declined (Netboy 1974), in some cases to near extinction. Efforts to manage and preserve the chinook fishery have involved traditional methods such as tag and recapture estimations and restrictive fishing regulations. Recently, however, population genetic analysis of Pacific salmon has emerged as a major tool in fishery management to estimate population subdivision, migration, gene flow, and stock composition of ocean fisheries (Ryman and Utter 1987).

Genetic studies on chinook salmon have refined our understanding of these populations. Examination of large numbers of polymorphic loci revealed geographic associations among populations of chinook salmon (Gharrett et al. 1987, Utter et al. 1989, Bartley and Gall 1990, Shaklee et al. 1990b). Genetic differences among chinook salmon stocks from different geographic areas are being used to identify the stock composition of mixed ocean salmon fisheries (Pella and Milner 1987, Utter et al. 1987, Shaklee et al. 1990b, Brodziak et al. 1992). In addition, genetic studies have indicated the effects of climate and geological events on the population structure of chinook salmon (Gharrett et al. 1987, Bartley and Gall 1990).

Utter et al. (1989) and Bartley and Gall (1990) recently described California populations of chinook salmon using data sets with 53 isozyme loci for 35 populations, and 25 polymorphic loci for eight populations, respectively. The objectives of the study reported here were to further refine the description of chinook salmon populations in California and southern Oregon, expand the baseline genetic data available for genetic stock-identification studies (Shaklee et al. 1990b, Brodziak et al. 1992),

and provide estimates for heterozygosity, allele frequencies, and genetic identities as used for optimum estimation of stock composition of mixed fisheries.

Materials and methods

Samples

A total 37 samples of juvenile chinook salmon were collected from northern California and southern Oregon during 1987–88 (Fig. 1, Table 1). Fifteen of these samples were from fish hatcheries and pond rearing projects. All the samples represented fall-run fish with the exception of the upper Sacramento sample (#33) which represented winter run salmon. To collect outmigrant chinook salmon from the wild, two fyke nets (1.5×2.1×15m) were placed in a stream approximately 1.6km apart and allowed to set overnight. Juvenile salmon were removed from the nets the following morning and frozen on dry ice. Juvenile chinook from hatcheries were collected with dip nets. A small number of salmon was taken from each raceway that contained salmon until a total of 200 fish was collected. At the laboratory, liver, muscle, heart, and eye tissue were removed from 100 fish from each collection, placed in individual tubes, and stored at −80°C. The remaining 100 salmon were frozen at −80°C in an archival collection.

Electrophoresis

Tissue preparation and horizontal starch-gel electrophoresis followed standard procedures (Aebersold et al. 1987). Gels were made with 12% hydrolyzed potato starch (Connaught Labs.) and one of the following buffer solutions: CAM, an amine citrate buffer from Clayton and Tretiak (1972) adjusted to pH 6.8; TBCL, the discontinuous buffer system of Ridgway et al. (1970) at pH 8.0; TC-4, a Tris citrate buffer of 0.223 M Tris, 0.083 M citric acid pH 5.8 as electrode buffer, and a 3.7% mixture of buffer in distilled water for the gel (Schaal and Anderson 1974); and TG, a Tris glycine buffer of 0.025 Tris and 0.192 glycine pH 8.5 for both gel and electrode buffers (Holmes and Masters 1970). The protein systems analyzed, locus designations, tissue distribution of isozymes, and buffer systems used are presented in Table 2. Because of recent changes in genetic nomenclature (Shaklee et al. 1990a), other locus name synonyms are presented in Table 2 to facilitate comparisons with other studies. Allele designations followed Allendorf and Utter (1979).

Histochemical staining procedures followed Shaw and Prasad (1970) and Harris and Hopkinson (1976). The data set described herein constitutes baseline data

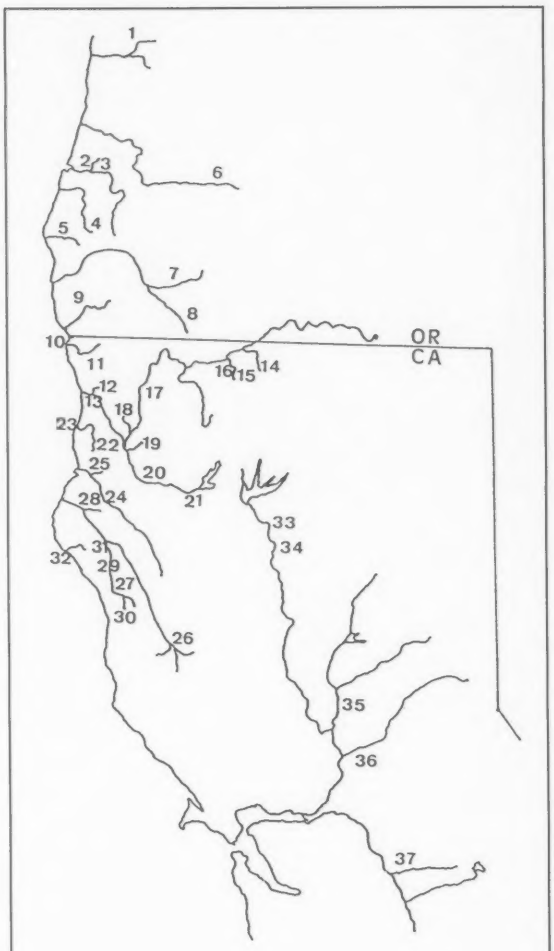

Figure 1
Collection sites of 37 samples of chinook salmon *Oncorhynchus tshawytscha*. Identification numbers are defined in Table 1.

reported in Gall et al. (1989) and used in maximum-likelihood estimates for the California mixed ocean salmon fishery (Brodziak et al. 1992). The duplicated isoloci AAT-1,2, IDH-3,4, MDH-1,2, MDH-3,4, and PGM-3,4 each were treated as two loci. Variant alleles were preferentially assigned to one locus, whereas common alleles were assigned to the other (Gharrett et al. 1987). Variation at the IDH-3,4 isoloci was ascribed to specific loci as described by Shaklee et al. (1990b). Our method of scoring isoloci is not the method of choice for studies of genetic mechanisms, as it may not reflect the true genetic distribution of alleles

Table 1

Thirty-seven collections of juvenile chinook salmon from five areas of California and Oregon. Locations of collections are designated on Figure 1 by identification number (ID#). *N* = number of fish analyzed.

Area	ID#	Collection site	*N*	No. of loci scored	Average heterozygosity (Nei 1973)
Middle Oregon	1	Fall Creek Hatchery	100	78	0.072
	2	Morgan Creek Hatchery	10	78	0.076
	3	Millacoma River	100	78	0.072
	4	Coquille River, South Fork	100	78	0.O73
	5	Elk River Hatchery	100	78	0.076
	6	Rock Creek Hatchery	100	78	0.054
S. Oregon/N. California Coastal	7	Rogue River	100	78	0.052
	8	Applegate River	100	78	0.054
	9	Chetco River Hatchery	100	78	0.063
	10	Rowdy Creek Hatchery	62	77	0.067
	11	Smith River, Middle Fork	99	77	0.059
Klamath–Trinity Basin	12	Blue Creek	100	77	0.059
	13	Omagar Creek Pond-Rearing Facility	100	78	0.064
	14	Irongate Hatchery	99	78	0.031
	15	Bogus Creek	128	77	0.030
	16	Shasta River	100	77	0.028
	17	Salmon River	98	76	0.038
	18	Camp Creek Pond-Rearing Facility	100	77	0.044
	19	Horse Linto Creek	100	77	0.045
	20	Trinity River, South Fork	100	77	0.039
	21	Trinity River Hatchery	120	77	0.030
Eel River–California Coastal	22	Redwood Creek at Orick	95	77	0.050
	23	Redwood Creek Lagoon	100	77	0.054
	24	Mad River Hatchery	99	77	0.045
	25	Mad River, North Fork	61	77	0.054
	26	Eel River, Middle Fork	95	76	0.043
	27	Eel River, South Fork	99	78	0.048
	28	Van Duzen River	100	77	0.050
	29	Redwood Creek, South Fork Eel	93	77	0.046
	30	Hollow Tree Creek	100	78	0.045
	31	Salmon Creek, South Fork Eel	96	77	0.044
	32	Mattole River	100	77	0.049
Sacramento–San Joaquin	33	Upper Sacramento River	94	77	0.059
	34	Coleman Hatchery	100	77	0.063
	35	Feather River Hatchery	100	78	0.061
	36	Nimbus Hatchery	100	78	0.064
	37	Merced River Hatchery	100	78	0.057

(Allendorf and Thorgaard 1984, Waples 1988). However, our method of scoring increases the power of maximum-likelihood estimates of stock composition by equalizing the importance of variant alleles at isoloci and non-duplicated loci. Furthermore, our system was maintained for consistency with other research (Gall et al. 1989, Brodziak et al. 1992).

A missing heteromeric isozyme between GPI-1 and GPI-3 was observed in some fish. We scored this pattern, as described in Bartley and Gall (1990), by assigning variation to an artificial locus named GPI-H and labeling the common and variant alleles *Gpi-H(100)* and *Gpi-H(*)*, respectively. However, Utter et al. (1989) described breeding data that indicated the variation should be assigned to either GPI-1 or GPI-3.

Due to the difficulty of identifying heterozygote banding patterns from GPI-H, LDH-1, and MDHP-2, allele frequencies at these loci were calculated from the square root of the frequency of the alternate homozygote. The frequency of the *Tpi-3(106)* allele also was calculated from the square root of the frequency of the homozygous Tpi-3(106) pattern.

Table 2

Enzyme systems, IUBNC enzyme number, isozyme loci, buffer systems, and tissues used in electrophoretic analyses of chinook salmon. For loci, m = mitochondrial. M = muscle, H = heart, L = liver, E = eye. Buffers explained in the text. Locus designations (synonyms) are locus names used by (1) present study, (2) Bartley and Gall (1990), (3) American Fisheries Society (Shaklee et al. 1990a), and (4) Utter et al. (1989).

Enzyme name	Enzyme no.	Locus designations 1	2	3	4	Tissue	Buffer
Aspartate aminotransferase	2.6.1.1	AAT-1	AAT-1	*sAAT-1,2**	Aat-1,2	M,H	TC-4
		AAT-2	AAT-2			M,H	TC-4
		AAT-3		*sAAT-3**	Aat-3	E	TC-4
		AAT-4	AAT-3	*sAAT-4**		L	TC-4
		mAAT-1		*mAAT-1**		M,H	CAM
		mAAT-2		*mAAT-2**		M,H,L	CAM, TC-4
		mAAT-3		*mAAT-3**		M,H	CAM, TC-4
Acid phosphatase	3.1.3.2	ACP-1		*ACP-1**		M,L	CAM
		ACP-2		*ACP-2**		M	CAM
Adenosine deaminase	3.5.3.3	ADA-1		*ADA-1**		M	TG
		ADA-2		*ADA-2**		M	TG
Alcohol dehydrogenase	1.1.1.1	ADH	ADH	*ADH**		L	TC-4, TBCL
Aconitate hydratase	4.2.1.1	AH-1	AH	*sAH**		L,M,E	CAM, TC-4
		mAH-1		*mAH-1**		E,H	CAM
		mAH-2		*mAH-2**		E,H	CAM
		mAH-3		*mAH-3**		M,H	CAM
		mAH-4		*mAH-4**		M,H	CAM
Alanine aminotransferase	2.6.1.2	ALAT		*ALAT**		M	TG
Creatine kinase	2.7.3.2	CK-1	CK-1	*CK-A1**		M	TBCL, CAM
		CK-2	CK-2	*CK-A2**		M	TBCL, CAM
		CK-4	CK-3	*CK-A2**		E	CAM
Esterase	3.1.1.1	EST-3		*EST-D**		M,E	TG, TBCL
Fructose-biphosphate aldolase	4.1.2.13	FBALD-4	FBA	*FBALD-4**		E	CAM, TC-4
Fumarate hydratase	4.2.1.2	FH	FH	*FH**		M	CAM
Glycerol-3-phosphate dehydrogenase	1.1.1.8	G3PDH-1	GPDH-1	*G3PDH-1**		M	CAM, TC-4
		G3PDH-2	GPDH-2	*G3PDH-2**		M	CAM, TC-4
		G3PDH-3	GPDH-3	*G3PDH-3**		M	CAM, TC-4
		G3PDH-4	GPDH-4	*G3PDH-4**		M	CAM, TC-4
Glyceraldehyde-3-phosphate dehydrogenase	1.2.1.12	GAPDH-5	GAPDH-3	*GAPDH-5**		E	CAM, TC-4
		GAPDH-6	GAPDH-4	*GAPDH-6**		E	CAM, TC-4
Glucose-6-phosphate isomerase	5.3.1.9	GPI-1	GPI-1	*GPI-B1**	Gpi-1	M	TG, TBCL
		GPI-2	GPI-2	*GPI-B2**	Gpi-2	M	TG, TBCL
		GPI-3	GPI-3	*GPI-A**	Gpi-3	M,E	TG, TBCL
		GPI-H	GPI-H	*GPIr**	Gpi-1	M	TG, TBCL
Glutathione reductase	1.6.4.2	GR	GR	*GR**	Gr	M,E,L	TG TBCL
β-Glucuronidase	3.2.1.31	GUS		*GUS**		M	CAM, TC-4
Hydroacylglutathionine hydrolase	3.1.2.6	HAGH		*HAGH**		L,M,E	TG
L-Iditol dehydrogenase	1.1.1.14	IDDH-1	IDDH-1	*IDDH-1**		L	TBCL
		IDDH-2	IDDH-2	*IDDH-2**		L	TBCL
Isocitrate dehydrogenase	1.1.1.42	IDH-1	IDH-1	*mIDHP-1**		M	CAM
		IDH-2	IDH-2	*mIDHP-2**		M	CAM
		IDH-3	IDH-3	*sIDHP-1**	Idh-3,4	M,E,L	CAM, TC-4
		IDH-4	IDH-4	*sIDHP-2**		E,L	CAM, TC-4
L-Lactate dehydrogenase	1.1.1.27	LDH-1	LDH-1	*LDH-A1**		M	TBCL, TC-4
		LDH-2	LDH-2	*LDH-A2**		M	TBCL, TC-4
		LDH-3	LDH-3	*LDH-B1**		H,E	TBCL, TC-4
		LDH-4	LDH-4	*LDH-B2**	Ldh-4	L,E	TC-4
		LDH-5	LDH-5	*LDH-C**	Ldh-5	E	TC-4
α-Mannosidase	3.2.1.24	MAN	MAN	*αMAN**		L	TC-4

Table 2 (continued)

Enzyme name	Enzyme no.	Locus designations 1	2	3	4	Tissue	Buffer
Malate dehydrogenase (NADP)	1.1.1.40	MDHP-1		*sMEP-1**		M	TC-4
		MDHP-2		*sMEP-2**		M, E, L	TC-4
		mMDHP-1		*mMEP**		M	TC-4
Malate dehydrogenase (NAD)	1.1.1.37	MDH-1	MDH-1	*sMDH-A1,2**	Mdh-l, 2	E, M	TC-4
		MDH-2	MDH-2			E, M	TC-4
		MDH-3	MDH-3	*sMDH-B1,2**	Mdh-3, 4	M, E	CAM, TC-4
		MDH-4	MDH-4			M, E	CAM, TC-4
		mMDH-1		*mMDH-1**		M, E	CAM
		mMDH-2		*mMDH-2**		M, H	CAM
Mannose-6-phosphate isomerase	5.3.1.8	MPI	MPI	*MPI**	Mpi	E, M, L	CAM
Phosphogluconate dehydrogenase	1.1.1.44	PGDH	PGDH	*PGDH**		M, E, L	TC-4
Phosphoglucokinase	2.7.2.3	PGK-1		*PGK-1**		L	CAM
		PGK-2	PGK-2	*PGK-2**	Pgk-2	M, E, L	CAM
Phosphoglucosmutase	5.4.2.2	PGM-1	PGM-1	*PGM-1**	Pgm-1, 2	M, E	CAM
		PGM-2	PGM-2	*PGM-2**		M, E, L	TG, TC-4
		PGM-3		*PGM-3,4**		E, L, M	TG, TC-4
		PGM-4				E, L, M	TC-4
Pyruvate kinase	2.1.7.40	PK-1	PK-1	*PK-1**		M	TC-4
		PK-2	PK-2	*PK-2**		M	CAM
Superoxide dismutase	1.15.1.1	SOD-1	SOD-1	*SOD-1**	Sod	L, M	CAM
		mSOD		*mSOD**		H, M, E	TG
Triosphosphate isomerase	5.3. 1.1	TPI-3		*TPI-2.1**		E	TC-4
		TPI-4		*TPI-2.2**		M, E, L, H	TG, TBCl
β-N-Acetyl-D-glucosaminidase	3.2.1.30	a-GA		*βBGLUA**		L	TG, TBCL
Peptidases (substrates)	3.4.*.*						
Glycyl leucine		DPEP-1	PEPA-1	*PEP-A**	Dpep-1	M, E, H	CAM, TG
		DPEP-2	PEPA-2	*PEP-C**	Dpep-2	E	TG, TBCL
Phenylalanyl proline		PDPEP-2	PDPEP-2	*PEP-D2**		M, E	TC-4
Prolyl leucine		PEPLT		*PEP-LT**		M	TG
Leucylglycyl glycine		TAPEP	PEPB	*PEP-B1**	Tapep-1	M, E	TBCL, TG

Analyses

Genetic variability for each collection of salmon was assessed by calculating the frequencies of alleles at each locus and average heterozygosity assuming Hardy-Weinberg proportions (Nei 1973). A locus was considered variable if we observed polymorphism in at least one sample. Analyses were based on a maximum of 78 loci. If a sample was not scored for a particular locus, the locus was retained for analyses involving multiple samples. Deviations from expected Hardy-Weinberg genotypic proportions were tested by chi-square goodness-of-fit tests (Sokal and Rohlf 1981). Variant allele frequencies were pooled so the expected number of genotypes in a given class was always five or greater. Some loci could not be tested for goodness-of-fit because pooling allele frequencies to achieve a minimum class-size reduced the degrees of freedom to zero. In addition, the loci, PGM-3 and PGM-4, were excluded from goodness-of-fit tests due to the arbitrary nature of assigning variation to a specific locus. GPI-H, LDH-1, and MDHP-2 were excluded because of the method of calculating allele frequencies from the frequency of the alternate homozygotes.

Genetic identities (I) were calculated for each pair of samples (Nei 1972) and a dendrogram was constructed from estimates of I using the unweighted pair-group method (UPGMA) (Sneath and Sokal 1973). Total gene diversity (H_T) was partitioned to estimate within-sample (H_S) and between-sample (D_{ST}) components, and to estimate relative gene diversity ($G_{ST} = D_{ST}/H_T$) (Nei 1973, Chakraborty and Leimar 1987). Total gene diversity was partitioned into three hierarchical levels: panmixia (T), area or drainage (D), and sample (S) based on *a priori* geographic considerations (Table 1).

An estimate of average gene flow was calculated from Wright's (1943) fixation index

$$F_{ST} = 1/(4Nm + 1) \quad (1)$$

where Nm is the average number of migrants exchanging genes per generation. Equation (1) was solved for Nm by setting F_{ST} equal to the relative gene diversity appropriate for the hierarchical level of interest. This formulation provided an estimate of the number of migrant fish exchanging genes among samples per generation under the assumptions of selective neutrality of alleles and Wright's (1943) island model of migration. Slatkin and Barton (1989) discussed the sensitivity of equation (1) relative to various methods of estimating F_{ST} in the presence of selection and alternative population structures, and found it to be fairly robust.

Results

A total of 96 isozyme loci were examined. Thirty-one loci were monomorphic, 47 were categorized as polymorphic (Appendix A), whereas variability of an unknown and undefined nature was detected at 18 loci. Details of genetic polymorphisms not described elsewhere are outlined in Appendix B. The enzyme systems involving the 18 loci for which evidence of probable polymorphisms was detected (not listed in Table 2) and warrant further study included: two adenylate kinase loci, creatine kinase, four fructose biphosphate aldolase loci, four glyceraldehyde-3-phosphate dehydrogenase loci, two beta-galactosidase loci, alpha-glucoside, superoxide dismutase, two peptidase loci, and a highly anodal acromatic band. Because of difficulties defining a genetic model of inheritance, poor band resolution, or incomplete data, these 18 loci were not included in the analyses.

Tests of conformance to Hardy Weinberg genotypic proportions revealed 37 out of 462 cases (8%) of disequilibria. For wild samples of chinook salmon, 13 of 252 tests (5%) revealed disequilibrium, whereas in hatchery samples, 24 of 210 tests (11%) showed nonconformance to Hardy-Weinberg expectations. However, in the Klamath Basin, a higher percentage of disequilibrium was found (13 of 97 cases or 13%) in hatchery and wild samples. The proportion of disequilibrium observed in Klamath and non-Klamath samples was found to be significantly different ($P<0.05$) when tested for equality by the generalized likelihood-ratio test for binomial data (Larsen and Marx 1981) . The proportion of disequilibrium observed in hatchery (including pond rearing programs) and wild chinook salmon populations also was significantly different ($P<0.05$). The nature of the observed disequilibrium appeared to be random. That is, we did not observe consistent excesses or deficiencies of heterozygotes, nor did we observe specific loci that consistently deviated from Hardy-Weinberg expectations.

Estimates of average heterozygosity ranged from a low value of 0.028 in Shasta River (#16) to a high of 0.076 in the Morgan Creek (#2) and Elk River (#5) hatcheries. The Middle Oregon samples (#1–6) tended to have high estimates of average heterozygosity, whereas values for the Klamath-Trinity samples (#12–21) tended to be lower (Table 1).

Although genetic identity indices between all pairs of samples were greater than 0.982 (data not shown), the geographic distribution of alleles suggested population subdivision within the study area. For example, we found the *Aat-2(85)*, *Aat-3(90)*, *Aat-4(130)*, and *Iddh-1(0)* alleles predominantly in Oregon and northcoastal California (collections 1–11). The *mAh-4(112)*, *Gpi-H(*)*, and *Pgdh(90)* alleles were present mainly in the Sacramento/San Joaquin system (collections 33–37), whereas *Mdhp-1(92)* and *Gpi-2(60)* were less abundant in the Sacramento Basin compared with more northern areas. *Mdhp-2(78)* was a characteristic of the Klamath–Trinity system and a few coastal samples.

Cluster analysis of genetic identities revealed a strong geographic component to the grouping of chinook salmon samples. Five distinct clusters that reflected geographic areas were evident (Fig. 2): (1) Smith River–Southern Oregon rivers, (2) Klamath–Trinity Rivers, (3) Eel River system–California coastal rivers, (4) Middle Oregon rivers, and (5) Sacramento–San Joaquin system. The Smith River (#11) and the Rowdy Creek Hatchery (#10) samples were the most northern samples collected from California. Therefore, it is reasonable that they would be genetically similar to the southern Oregon samples. The sample from the Fall Creek Hatchery (#1) was the only sample from northern Oregon and therefore, appears as an independent cluster. Three samples, Rock Creek Hatchery (#6, middle Oregon), Blue Creek (#12, Klamath–Trinity Basin), and Omagar Creek (#13, Klamath–Trinity Basin), did not cluster in accordance with their geographic location.

Total gene diversity was 0.0620 (H_T) and average sample diversity was 0.0554 (H_S). Therefore, approximately 89.4% of the total genetic diversity was due to intrasample variability and 10.6% was due to intersample variation (Table 3). Further examination of the intersample diversity showed that genetic differences among samples within the five geographic groups identified from the dendrogram (see Table 1) accounted for about 3.2% of the total variation and 7.4% of the total diversity was due to differences between the major geographic areas. Gene diversity analysis for each geographic area treated separately revealed that although the Klamath–Trinity system possessed the lowest total gene diversity for a given area (H_D), relative gene diversity (G_{SD}) for this drainage was high

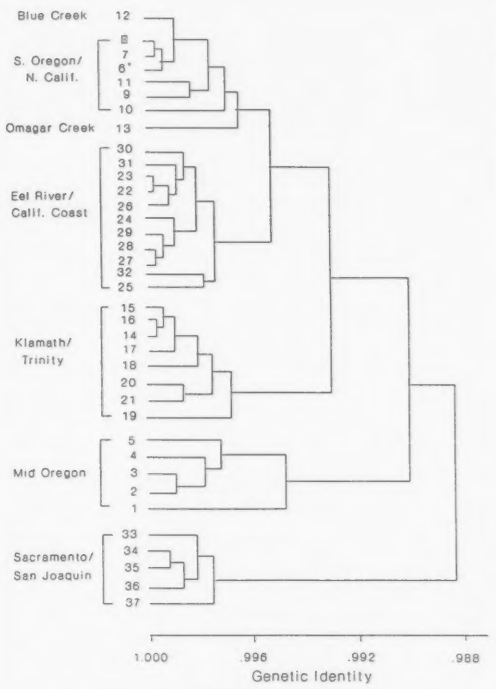

Figure 2

Dendrogram based on UPGMA clustering of genetic identity indices (Nei 1972). Identification numbers are defined in Table 1. Brackets on left side indicate geographic grouping, with Blue Creek and Omagar Creek as outliers (collection #6, indicated as 6*, was from mid-Oregon).

Table 3

Hierarchical gene diversity analyses of 37 samples of chinook salmon from Oregon and California.* H_{SD} = average gene diversity of samples within areas; H_D and G_{SD} = total gene diversity and relative gene diversity for a given area, respectively; Nm = average number of migrants exchanging genes per generation; H_S, H_T, and G_{ST} = within-sample, total, and relative gene diversity, respectively.

Area	H_{SD}	H_D	G_{SD}	Nm
Middle Oregon	0.0704	0.0741	0.0502	4.70
South Oregon/ N. California Coast	0.0586	0.0599	0.0223	10.96
Klamath–Trinity	0.0402	0.0428	0.0592	3.97
Eel River/California Coast	0.0473	0.0486	0.0271	8.98
Sacramento–San Joaquin	0.0607	0.0616	0.0158	15.57

*Total, ignoring subdivisions: H_S 0.0554, H_T 0.0620, G_{ST} 0.106, Nm 2.11

and comparable to the middle Oregon area which shared the highest total gene diversity (Table 3).

Based on an overall estimate of 0.106 for G_{ST} (Table 3), the number of immigrant individuals contributing genes to an average population, Nm, was estimated to be 2.11 individuals per generation. Estimates of gene flow within each geographic cluster were highest in the Sacramento–San Joaquin system (Nm 15.57) and lowest in the Klamath–Trinity drainage (Nm 3.97).

Discussion

The genetic structure of chinook salmon populations reported here appears similar to that reported previously. Distributions of variant alleles at Mdh-4, AH-1 Pgdh, Pgm-2, GPI-H, and Gpi-2 were similar to those reported by Bartley and Gall (1990). However, average heterozygosity estimates for the Klamath–Trinity drainage were somewhat higher than reported by Utter et al. (1989) and Bartley and Gall (1990). Bartley and Gall (1990) observed a range of 0.008–0.016 for this drainage, compared with the range of 0.028 for the Shasta River sample to 0.064 for the sample from Omagar Creek found in the present study. One reason for the higher estimates in the present study was the inclusion of the Mdhp-2 locus, which is highly polymorphic in the Klamath–Trinity drainage (Appendix A); Bartley and Gall (1990) and Utter et al. (1989) did not report data for this locus. Generally, comparisons of heterozygosity estimates between this study and earlier studies are difficult to interpret due to the improved laboratory procedures that have greatly increased the number of isozyme loci available for analysis.

Two samples from the Klamath–Trinity drainage, Blue and Omagar Creeks, were genetically differentiated from other samples from within the basin. For example, Mdhp-2(78) had an average frequency of 0.32 in eight other samples from the drainage, whereas the allele occurred at a frequency of 0.14 in Blue Creek and was not found in the Omagar Creek sample. Furthermore, Omagar and Blue Creeks had higher frequencies of the Tapep-1(130) and mMdh-1(-900) alleles than did other Klamath–Trinity samples. These frequencies indicated that fish from Omagar and Blue Creeks are genetically closer to southern Oregon populations than to Klamath–Trinity populations. This result was unexpected given the pattern of geographic clustering found by Utter et al. (1989) and Bartley and Gall (1990). However, earlier studies did not sample populations near or below the confluence of the Trinity and Klamath Rivers, as was done in the present study.

We do not know if the genetic structure of the Blue and Omagar Creek samples is characteristic of the lower Klamath–Trinity drainage. The Omagar Creek sample consisted of progeny of broodstock captured by instream gill nets at the mouth of Blue Creek and in the main section of the Klamath River; the Blue Creek sample was collected in the main stem of Blue Creek and was presumed to represent progeny of natural spawning. If accurate, our data suggest greater gene exchange between the lower Klamath and coastal populations of northern California–southern Oregon than between the lower and upper Klamath basin. Apparently northern California coastal populations of chinook salmon are genetically similar to southern Oregon populations because the two samples from the Smith River (samples 10 and 11) also clustered with the Oregon populations. This genetic similarity may have resulted from historical gene exchange in the form of transplants into the Klamath basin (Snyder 1931). Chinook salmon in the lower Klamath River are thought to be similar to Oregon populations in other characters, such as timing of spawning migration, fecundity, and size (Snyder 1931; Craig Tuss, U.S. Fish Wildl. Serv., Sacramento, CA 95616, pers. commun., Sept. 1990).

The relatively high incidence of Hardy-Weinberg disequilibria in hatchery and pond rearing programs may be the result of the limited number of broodstock used in production or non-random sampling of a hatchery's production, i.e., only sampling juveniles from a few raceways. For example, the Coleman National Fish Hatchery spawns approximately 10,000 fall-run chinook salmon. It is likely that our sample of 100 juveniles may not be an adequate representation of the hatchery output. The two samples with the highest number of deviations from Hardy-Weinberg expectations were both from pond rearing projects, Omagar and Camp Creeks. These pond rearing projects can serve a useful function by augmenting or establishing runs of chinook salmon in specific streams. However, care must be taken to maximize the effective population size of the broodstock and to prevent changes in the genetic variation.

The large number of significant departures from Hardy-Weinberg expectations for the Klamath samples compared with other samples was due primarily to the samples from Camp Creek and Omagar Creek. These two samples accounted for nine of the 13 significant tests within the Klamath system. Deleting data for these two Creeks from the comparison resulted in 6% (4 of 72) significant deviations for Klamath system samples versus 7% (24 of 349) for non-Klamath samples.

Our results indicate a geographic basis for genetic differentiation and subpopulation structure in chinook salmon populations from California and Oregon. Geographic affinities among chinook salmon populations have now been demonstrated along most of the western coastline of North America (Gharrett et al. 1987, Utter et al. 1989, Bartley and Gall 1990). Bartley and Gall (1990) identified three major clusters of chinook salmon populations in California that corresponded to the three major river drainages: the Sacramento–San Joaquin, the Eel, and the Klamath–Trinity. Utter et al. (1989) identified nine population units of chinook salmon over a large area from British Columbia to California. They found coastal populations from Oregon and Washington to be genetically similar to each other. Our data indicate that some coastal populations in California are differentiated from those in Oregon, but that northern California coastal populations of chinook salmon are similar to southern Oregon populations.

The level of intrasample gene diversity found in the present study, 89.4%, is similar to the values of 82.3 and 87.7% reported by Bartley and Gall (1990) and Utter et al. (1989), respectively. Overall estimates of gene flow of 1.16 (Bartley and Gall 1990) and 2.11 (this study) migrants per generation also are similar. The slightly lower level of population subdivision and therefore, higher level of gene flow found in the present study probably reflect a bias caused by the samples analyzed. Bartley and Gall (1990) analyzed a greater number of inland California populations than the present study. Most of their samples were from the three major drainages within California: the Klamath–Trinity, the Sacramento–San Joaquin, and the Eel. They suggested that straying and gene flow were higher among coastal streams than among separate drainages. Therefore, by including the large number of coastal samples in the present study, slightly higher overall estimates of gene flow and less apparent subdivision were expected. Separate gene diversity analyses of the groups from Oregon and northern California revealed that approximately 6% of the total diversity of the two Oregon groups was due to interpopulation differences compared with 12% for the three California groups. These results further support the expectation of lower levels of population subdivision when analyses involve many coastal samples.

The estimates of gene flow and population subdivision from hierarchical gene-diversity analyses varied among geographic areas. The Klamath–Trinity system would be expected to display lower levels of gene exchange if the lower and upper sections of the Klamath are separate subpopulations. However, deletion of the Blue Creek and Omagar Creek samples from the analysis changed the gene diversity estimates by less than 2%. The high level of estimated gene flow within the Sacramento–San Joaquin system most likely reflects the fact that four of the five samples were from

hatcheries. Although egg and fingerling transfers between areas have been reduced recently, a considerable amount of historical mixing of the hatchery stocks has occurred (Alan Baracco, Calif. Dep. Fish Game, Sacramento, CA 95616, pers. commun. Dec. 1986). Additionally, many salmon from the San Joaquin River stray into the Sacramento River on their spawning migration due to easier access and better water quality in the Sacramento River (Alan Baracco and Forrest Reynolds, Calif. Dep. Fish Game, Sacramento, CA 95616, pers. commun. Dec. 1986).

Independent estimates of straying based on coded-wire tagged fish indicate that chinook salmon in the Sacramento River do stray within the system. Rough estimates are that 2–5% of the Sacramento fall-run fish are from hatcheries in the San Joaquin River system. Approximately 1% of the fall-run chinook salmon returning to the Feather River Hatchery is composed of stray fish from the Nimbus (American River), Mokulumne, and Coleman Hatcheries. Straying also occurs in northern streams because chinook salmon marked on the Rogue River are recovered in the Klamath–Trinity drainage (Fred Meyer, Calif. Dep. Fish Game, Rancho Cordova, CA 95670, pers. commun. Feb. 1991). Therefore, it is not surprising that gene flow estimates for the Sacramento–San Joaquin drainage were high and that southern coastal populations from Oregon should resemble northern California coastal populations.

Stability of allele frequencies over time is often assumed in the methodology of genetic stock identification. Although the present study was not intended to uncover temporal variation of allele frequencies, some samples we examined also had been analyzed earlier. Eighteen locations from the present study were sampled in 1984–86 by Bartley and Gall (1990). For the interstudy comparison, loci chosen had to have a frequency of less than 0.95 for the common allele in at least two populations reported by Bartley and Gall (1990); isoloci were not used. Twelve loci fit the criterion: AH-1, DPEP-1, PDPEP-2, TAPEP, GPI-2, IDDH-2, IDH-2, MPI, PGDH, PGK-2, PGM-2, and SOD-1.

We found 18 instances of significant change in allele frequencies for seven hatchery samples (21.4%), 16 significant results for seven wild populations (19.0%), and five instances of significant change for a pond rearing project (41.7%) based on the G-statistic (Sokal and Rohlf 1981). Interstudy comparisons of the samples from Bogus Creek (= Bogas Creek in Bartley and Gall 1990), Shasta Creek, and the Feather River Fish Hatchery revealed no significant differences in allele frequencies.

Six hatcheries sampled in the present study also had been sampled by Utter et al. (1989). Loci selected to compare allele frequencies for these studies had to have a common allele frequency of less than 0.95 in one of the studies. Eight loci met the frequency criterion: AH, DPEP-1, TAPEP, GPI-2, GR, MPI, PGK-2, and SOD-1. Five of the six hatchery samples displayed significant changes in allele frequency between the two studies. Waples and Teel (1990) also reported significant changes in allele frequencies in hatcheries sampled in different years.

Although we observed differences in allele frequencies between this and earlier studies, we do not know if this represents temporal variation. It is tempting to make statements on the temporal stability or instability of allele frequencies in samples of chinook salmon from a given area, but without estimates of sampling variability for a given year, it is not possible to separate intrasample variation, random sampling error, and temporal variation. Nevertheless, given the presumed constancy of allele frequency data (Allendorf and Utter 1979), the number of significant G statistics uncovered in comparisons between samples in this study and those of Utter et al. (1989) and Bartley and Gall (1990) requires some explanation.

Waples and Teel (1990:149) stated, "tests of the equality of allele frequencies in temporally spaced samples must be interpreted with caution." In addition, Waples and Teel (1990) list inaccurate or artifactual genetic data, nonrandom sampling of fish for genetic analysis, selection, and migration as possible causes of significant change in allele frequencies. For example, large differences in allele frequencies at IDH-3 and IDH-4 between the present study and Bartley and Gall (1990) may be due to banding artifacts associated with tissue breakdown. One of us (Bentley) has observed the increased appearance of variant "alleles" at these loci in samples that were not properly frozen and stored. Therefore, the data for these two loci presented in Bartley and Gall (1990) may be artifactual. In addition, the analyses of Utter et al. (1989), Bartley and Gall (1990), and the present study were done by different personnel in different laboratories. Although standardization was attempted, scoring of gel banding patterns may have been inconsistent.

The level of temporal instability of allele frequencies is an important issue in the use of GSI to manage and conserve chinook salmon populations (Waples 1990, Waples and Teel 1990). However, sampling design should specifically address this question before one draws conclusions concerning wild or hatchery populations. Although we documented differences in allele frequencies between this and earlier studies, the overall association between genetic similarity and geographic location remains constant for populations of chinook salmon in California and Oregon.

Acknowledgments

This research was funded by the California Department of Fish and Game (Interagency Agreement No. C-1335, Genetic Analysis of Chinook and Coho Salmon Populations) and the Institute for Theoretical Dynamics at the University of California, Davis. We gratefully acknowledge the support and assistance of A. Baracco and L.B. Boydstun throughout the study. We thank personnel from the California Department of Fish and Game, the U.S. Fish and Wildlife Service, S. Downey, and W. Shoals for assistance with fish collections. The technical assistance from E. Childs, S. Fox, A. Marshall, C. Panattoni, and C. Qi is also appreciated. The valuable comments of F. Utter and two anonymous referees also are appreciated. We are especially grateful to the Northwest Fisheries Science Center of the National Marine Fisheries Service and the Washington Department of Fisheries Genetic Unit for their contribution to the development of a coastwide program of Genetic Stock Identification.

Citations

Aebersold, P.B., G.A. Winans, D.J. Teel, G.B. Milner, and F.M. Utter
1987 Manual for starch gel electrophoresis: A method for the detection of genetic variation. NOAA Tech. Rep. NMFS 61, 19 p.

Allendorf, F., and G.H. Thorgaard
1984 Tetraploidy and the evolution of salmonid fishes. *In* Turner, B. (ed.), Evolutionary genetics of fishes, p. 1–53. Plenum, NY.

Allendorf, F.W., and F.M. Utter
1979 Population genetics. *In* Hoar, W.J., and D.J. Randall (eds.), Fish physiology, vol. 8, p. 407–454. Academic Press, NY.

Bartley, D.M., and G.A.E. Gall
1990 Genetic structure and gene flow in chinook salmon populations of California. Trans. Am. Fish. Soc. 119:55–71.

Brodziak, J., B. Bentley, D. Bartley, G.A.E. Gall, R. Gomulkiewicz, and M. Mangel
1992 Tests of genetic stock identification using coded-wire tagged fish. Can. J. Fish. Aquat. Sci. (In press).

Chakraborty, R., and O. Leimar
1987 Genetic variation within a subdivided population. *In* Ryman, N., and F. Utter (eds.), Population genetics and fishery management, p. 89–120. Univ. Wash. Press, Seattle.

Clayton, J.W., and D.N. Tretiak
1972 Amine-citrate buffers for pH control in starch gel electrophoresis. J. Fish. Res. Board Can. 29:1169–1172.

Gall, G.A.E., B. Bentley, C. Panattoni, E. Childs, C. Qi, S. Fox, M. Mangel, J. Brodziak, and R. Gomulkiewicz
1989 Genetic stock identification: Chinook mixed fishery project 1986–1989. Rep. to Calif. Dep. Fish Game, Sacramento, by Univ. Calif., Davis, 420 p.

Gharrett, A.J., S.M. Shirley, and G.R. Tromble
1987 Genetic relationships among populations of Alaskan chinook salmon (*Oncorhynchus tshawytscha*). Can. J. Fish. Aquat. Sci. 44:765–774.

Harris, H., and D.A. Hopkinson
1976 Handbook of enzyme electrophoresis in human genetics. North Holland Publ. Co., Amsterdam, var. pag.

Holmes, R.S., and C.J. Masters
1970 Epigenetic interconversions of the multiple forms of mouse liver catalase. FEBS (Fed. Eur. Biochem. Soc.) Lett. 11:45–48.

Larsen, R.J., and M.L. Marx
1981 An introduction to mathematical statistics and its applications. Prentice Hall, Engelwood Cliffs, var. pag.

Moyle, P.B.
1976 Inland fishes of California. Univ. Calif. Press, Berkeley.

Nei, M.
1972 Genetic distance between populations. Am. Nat. 106: 283–292.
1973 Analysis of genediversity in subdivided populations. Proc. Natl. Acad. Sci. USA 70:3321–3323.

Netboy, A.
1974 The salmon: Their fight for survival. Houghton Mifflin, Boston, 613 p.

Pella, J.J., and G.B. Milner
1987 Use of genetic marks in stock composition analysis. *In* Ryman, N., and F. Utter (eds.), Population genetics and fishery management, p. 247–276. Univ. Wash. Press, Seattle.

Ridgway, G.J., S.W. Sherburne, and R.D. Lewis
1970 Polymorphisms in the esterase of Atlantic herring. Trans. Am. Fish. Soc. 99:147–151.

Ryman, N., and F. Utter (editors)
1987 Population genetics and fishery management. Univ. Wash. Press, Seattle, 420 p.

Schaal, B.A., and W.W. Anderson
1974 An outline of techniques for starch gel electrophoresis of enzymes from the America oyster *Crassostrea virginica* Gmelin. Tech. Rep. 74-3, Ga. Mar. Sci. Cent., 18 p.

Shaklee, J.B., R.W. Allendorf,D.C. Morizot, and G.S. Whitt
1990a Gene nomenclature for protein coding loci in fish. Trans. Am. Fish. Soc. 119:2–15.

Shaklee, J.B., C. Busack, A. Marshall, M. Miller, and S.R. Phelps
1990b The electrophoretic analysis of mixed-stock fisheries of Pacific salmon. *In* Ogita, Z-I., and C.L. Markert (eds), Isozymes: Structure, function, and use in biology and medicine, p. 235–265. Wiley-Liss, Inc., NY.

Shaw, C.R., and R. Prasad
1970 Starch gel electrophoresis of enzymes—a compilation of recipes. Biochem. Genet. 4:297–320.

Slatkin, M., and N.H. Baron
1989 A comparison of three indirect methods for estimating average levels of gene flow. Evolution 43:1349–1368.

Sneath, P.H.A., and R.R. Sokal
1973 Numerical taxonomy. W.H. Freeman, San Francisco, 573 p.

Snyder, J.O.
1931 Salmon of the Klamath River, California. Calif. Dep. Fish Game, Fish. Bull. 34:1–130.

Sokal, R.R., and F.J. Rohlf
1981 Biometry. W.H. Freeman, NY, 859 p.

Utter, F.M., D. Teel, G. Milner, and D. McIsaac
1987 Genetic estimates of stock comparisons of 1983 chinook salmon, *Oncorhynchus tshawytscha*, harvests off the Washington coasts and Columbia River. Fish. Bull., U.S. 85:12–23.

Utter, F.M., G. Milner, G. Stahl, and D. Teel
1989 Genetic population structure of chinook salmon, *Oncorhynchus tshawytscha*, in the Pacific Northwest. Fish. Bull., U.S. 87:239–264.
Waples, R.S.
1988 Estimation of allele frequencies at isoloci. Genetics 118: 371–384.
1990 Temporal changes of allele frequency in Pacific salmon: Implications for mixed-stock fishery analysis. Can. J. Fish. Aquat. Sci. 47:968–976.
Waples, R.S., and D.J. Teel
1990 Conservation genetics of Pacific salmon. I. Temporal changes in allele frequency. Conserv. Biol. 4:144–156.
Wright, S.
1943 Isolation by distance. Genetics 28:114–138.

Appendix A

Allele frequencies at 47 variable isozyme loci. Identification numbers (ID#) defined in Table 1 and Figure 1; N = number of fish scored. Allele designations of Bartley and Gall (1990) are included in parentheses.

	AAT-2		Alleles			AAT-3		Alleles		AAT-4		Alleles	
	ID#	N	100 (100)	85 (90)	105	ID#	N	100	90	ID#	N	100	130
Middle Oregon	1	100	0.990	0.010		1	100	1.000		1	100	0.755	0.245
	2	100	0.930	0.070		2	100	0.995	0.005	2	100	0.785	0.215
	3	100	0.890	0.110		3	100	1.000		3	100	0.875	0.125
	4	100	0.920	0.080		4	100	0.995	0.005	4	100	0.835	0.165
	5	100	0.910	0.090		5	100	1.000		5	100	0.880	0.120
	6	100	1.000			6	100	0.975	0.025	6	100	1.000	
S. Oregon/	7	100	1.000			7	100	0.965	0.035	7	100	0.995	0.005
N. California Coastal	8	100	1.000			8	100	0.965	0.035	8	100	1.000	
	9	100	0.995	0.005		9	100	1.000		9	100	1.000	
	10	62	1.000			10	62	0.960	0.040	10	62	1.000	
	11	99	0.970	0.030		11	99	0.990	0.010	11	99	0.995	0.005
Klamath–Trinity Basin	12	100	1.000			12	100	0.990	0.010	12	100	0.975	0.025
	13	100	1.000			13	100	1.000		13	100	0.990	0.010
	14	98	1.000			14	99	1.000		14	98	0.995	0.005
	15	127	1.000			15	128	0.992	0.008	15	121	0.975	0.025
	16	100	1.000			16	100	1.000		16	100	0.970	0.030
	17	98	1.000			17	98	1.000		17	85	0.976	0.024
	18	106	1.000			18	106	1.000		18	106	0.877	0.123
	19	100	1.000			19	100	1.000		19	100	1.000	
	20	100	1.000			20	100	0.985	0.015	20	100	0.970	0.030
	21	120	1.000			21	120	1.000		21	120	0.996	0.004
Eel River–California Coastal	22	95	0.968	0.032		22	95	1.000		22	87	1.000	
	23	100	0.965	0.035		23	100	1.000		23	100	1.000	
	24	99	0.995	0.005		24	99	1.000		24	99	1.000	
	25	61	1.000			25	61	1.000		25	60	1.000	
	26	95	1.000			26	95	1.000		26	95	1.000	
	27	99	1.000			27	99	1.000		27	97	1.000	
	28	100	1.000			28	100	1.000		28	88	0.994	0.006
	29	93	1.000			29	93	1.000		29	93	1.000	
	30	100	0.995		0.005	30	100	1.000		30	94	1.000	
	31	96	1.000			31	96	1.000		31	93	0.984	0.016
	32	100	1.000			32	100	1.000		32	100	1.000	
Sacramento–San Joaquin	33	94	1.000			33	94	1.000		33	94	1.000	
	34	100	1.000			34	100	1.000		34	100	0.995	0.005
	35	100	1.000			35	100	1.000		35	100	1.000	
	36	100	1.000			36	100	1.000		36	100	1.000	
	37	100	1.000			37	100	1.000		37	100	1.000	

Appendix A (continued)

	mAAT-1		Alleles			mAAT-2		Alleles			mAAT-3		Alleles	
	ID#	*N*	−100	−77	−104	ID#	*N*	−100	−125	−90	ID#	*N*	−100	−450
Middle Oregon	1	100	1.000			1	100	0.985	0.015		1	100	1.000	
	2	100	0.970		0.030	2	100	0.960		0.040	2	100	0.965	0.035
	3	100	0.990		0.010	3	100	0.985		0.015	3	100	0.970	0.030
	4	100	1.000			4	100	0.975		0.025	4	100	0.955	0.045
	5	100	0.990		0.010	5	100	1.000			5	100	0.925	0.075
	6	100	0.985		0.015	6	100	0.945		0.055	6	100	1.000	
S. Oregon/	7	100	0.980		0.020	7	100	0.945	0.005	0.050	7	100	1.000	
N. California Coastal	8	100	0.980		0.020	8	100	0.945		0.055	8	100	1.000	
	9	100	0.985		0.015	9	100	0.975		0.025	9	100	0.995	0.005
	10	62	0.984		0.016	10	62	0.911		0.089	10	0		
	11	99	0.955	0.005	0.040	11	70	1.000			11	0		
Klamath–Trinity Basin	12	100	1.000			12	100	0.955		0.045	12	0		
	13	100	1.000			13	100	0.965		0.035	13	100	1.000	
	14	99	1.000			14	59	0.983		0.017	14	59	1.000	
	15	128	1.000			15	49	0.980		0.020	15	0		
	16	100	1.000			16	69	0.993		0.007	16	0		
	17	98	1.000			17	98	0.969		0.031	17	0		
	18	106	1.000			18	106	1.000			18	0		
	19	100	1.000			19	100	1.000			19	0		
	20	100	1.000			20	100	0.970		0.030	20	0		
	21	120	1.000			21	80	0.994		0.006	21	0		
Eel River–California Coastal	22	95	1.000			22	95	1.000			22	0		
	23	100	1.000			23	100	1.000			23	0		
	24	99	0.990	0.010		24	99	0.980	0.020		24	0		
	25	61	1.000			25	61	0.967	0.033		25	0		
	26	95	0.979	0.021		26	95	1.000			26	0		
	27	98	1.000			27	46	0.989		0.011	27	40	1.000	
	28	100	0.995	0.005		28	40	1.000			28	0		
	29	93	1.000			29	93	1.000			29	0		
	30	100	1.000			30	40	1.000			30	40	1.000	
	31	96	1.000			31	96	1.000			31	0		
	32	100	1.000			32	100	0.995		0.005	32	0		
Sacramento–San Joaquin	33	94	0.995		0.005	33	94	1.000			33	0		
	34	100	0.960		0.040	34	100	0.995	0.005		34	0		
	35	100	0.975		0.025	35	100	0.995		0.005	35	100	1.000	
	36	100	1.000			36	100	1.000			36	100	1.000	
	37	100	1.000			37	100	1.000			37	100	1.000	

	ADA-1		Alleles			ADH		Alleles			AH-1		Alleles		
	ID#	*N*	100	83	108	ID#	*N*	−100	−52		ID#	*N*	100 (100)	86 (90)	116 (110)
Middle Oregon	1	100	0.980	0.020		1	100	1.000			1	100	0.855	0.050	0.095
	2	100	0.990	0.010		2	100	0.975	0.025		2	100	0.890	0.095	0.015
	3	100	1.000			3	100	0.995	0.005		3	100	0.875	0.090	0.035
	4	100	0.990	0.010		4	100	1.000			4	100	0.855	0.135	0.010
	5	100	0.995	0.005		5	100	1.000			5	100	0.845	0.145	0.010
	6	100	1.000			6	100	0.990	0.010		6	100	0.890	0.100	0.010
S. Oregon/	7	100	1.000			7	100	1.000			7	100	0.935	0.065	
N. California Coastal	8	100	1.000			8	100	1.000			8	100	0.960	0.040	
	9	100	1.000			9	100	1.000			9	100	0.925	0.075	
	10	62	1.000			10	62	1.000			10	62	0.839	0.161	
	11	99	1.000			11	99	1.000			11	99	0.919	0.076	0.005
Klamath–Trinity Basin	12	100	0.995	0.005		12	100	1.000			12	100	0.940	0.060	
	13	100	1.000			13	100	1.000			13	100	1.000		
	14	99	1.000			14	99	1.000			14	99	0.990	0.005	0.005
	15	128	1.000			15	118	1.000			15	128	1.000		
	16	100	1.000			16	100	1.000			16	100	0.995		0.005
	17	0				17	97	1.000			17	98	1.000		
	18	106	1.000			18	106	1.000			18	106	0.953	0.047	
	19	100	1.000			19	100	1.000			19	100	1.000		

Appendix A (continued)

	ADA-1		Alleles			ADH		Alleles		AH-1		Alleles		
	ID#	*N*	100	83	108	ID#	*N*	−100	−52	ID#	*N*	100 (100)	86 (90)	116 (110)
Klamath–Trinity Basin (continued)	20	100	1.000			20	100	1.000		20	100	1.000		
	21	120	1.000			21	120	1.000		21	120	1.000		
Eel River–California Coastal	22	76	1.000			22	95	1.000		22	95	0.968	0.021	0.011
	23	100	1.000			23	100	1.000		23	100	0.945	0.040	0.015
	24	99	1.000			24	99	0.970	0.030	24	99	1.000		
	25	61	1.000			25	61	1.000		25	61	1.000		
	26	0				26	95	1.000		26	95	0.979	0.021	
	27	99	1.000			27	79	1.000		27	99	0.995	0.005	
	28	100	1.000			28	83	1.000		28	100	1.000		
	29	93	1.000			29	93	1.000		29	93	1.000		
	30	100	1.000			30	100	1.000		30	100	1.000		
	31	23	1.000			31	94	1.000		31	96	1.000		
	32	100	1.000			32	100	1.000		32	100	1.000		
Sacramento–San Joaquin	33	94	1.000			33	94	1.000		33	94	0.862	0.128	0.011
	34	100	1.000			34	100	1.000		34	100	0.775	0.200	0.025
	35	100	0.955		0.045	35	100	1.000		35	100	0.885	0.105	0.010
	36	100	0.960		0.040	36	100	1.000		36	100	0.835	0.130	0.035
	37	100	0.870		0.130	37	100	1.000		37	100	0.765	0.165	0.070

	mAH-1		Alleles		mAH-2		Alleles		mAH-3		Alleles	
	ID#	*N*	100	65	ID#	*N*	100	50	ID#	*N*	100	71
Middle Oregon	1	100	1.000		1	100	1.000		1	100	1.000	
	2	100	1.000		2	100	1.000		2	100	1.000	
	3	100	1.000		3	100	1.000		3	100	1.000	
	4	100	1.000		4	100	0.985	0.015	4	100	1.000	
	5	100	1.000		5	100	0.995	0.005	5	100	1.000	
	6	100	1.000		6	100	1.000		6	100	1.000	
S. Oregon/ N. California Coastal	7	100	1.000		7	100	1.000		7	100	0.995	0.005
	8	100	0.980	0.020	8	100	1.000		8	100	0.995	0.005
	9	100	1.000		9	100	1.000		9	100	1.000	
	10	61	0.992	0.008	10	61	1.000		10	62	1.000	
	11	99	1.000		11	99	1.000		11	99	0.990	0.010
Klamath–Trinity Basin	12	100	0.995	0.005	12	100	1.000		12	100	0.995	0.005
	13	100	1.000		13	100	1.000		13	100	1.000	
	14	99	1.000		14	99	1.000		14	99	1.000	
	15	128	0.980	0.020	15	128	1.000		15	128	1.000	
	16	100	0.990	0.010	16	100	1.000		16	100	1.000	
	17	98	0.995	0.005	17	98	1.000		17	98	1.000	
	18	87	1.000		18	87	1.000		18	106	1.000	
	19	100	1.000		19	100	1.000		19	100	1.000	
	20	100	1.000		20	100	1.000		20	100	1.000	
	21	120	0.975	0.025	21	120	1.000		21	120	1.000	
Eel River–California Coastal	22	95	0.947	0.053	22	95	1.000		22	95	1.000	
	23	100	0.955	0.045	23	100	1.000		23	100	1.000	
	24	99	0.894	0.106	24	99	1.000		24	99	1.000	
	25	61	0.893	0.107	25	61	1.000		25	61	1.000	
	26	95	0.974	0.026	26	95	0.989	0.011	26	95	1.000	
	27	99	0.965	0.035	27	99	1.000		27	99	1.000	
	28	100	0.935	0.065	28	100	1.000		28	100	1.000	
	29	93	0.984	0.016	29	93	1.000		29	93	1.000	
	30	100	0.920	0.080	30	100	1.000		30	100	1.000	
	31	96	0.990	0.010	31	96	0.984	0.016	31	96	1.000	
	32	99	0.909	0.091	32	100	1.000		32	100	1.000	
Sacramento–San Joaquin	33	94	0.973	0.027	33	94	1.000		33	94	1.000	
	34	100	0.975	0.025	34	100	1.000		34	100	1.000	
	35	100	0.995	0.005	35	100	1.000		35	100	1.000	
	36	100	1.000		36	100	1.000		36	100	1.000	
	37	100	1.000		37	100	1.000		37	100	1.000	

Appendix A (continued)

	mAH-4		Alleles				CK-4		Alleles			
	ID#	*N*	100	119	112	123	ID#	*N*	100	105	95	98
Middle Oregon	1	100	1.000				1	100	1.000			
	2	100	1.000				2	100	1.000			
	3	100	0.950	0.050			3	100	1.000			
	4	100	0.975	0.020		0.005	4	100	0.955			0.045
	5	100	0.960	0.010		0.030	5	100	1.000			
	6	100	0.940	0.045		0.015	6	100	1.000			
S. Oregon/N. California Coastal	7	100	0.980	0.015		0.005	7	100	1.000			
	8	100	0.950	0.025		0.025	8	100	1.000			
	9	100	0.915	0.080		0.025	9	100	1.000			
	10	62	0.952	0.008		0.040	10	62	1.000			
	11	99	0.894	0.106			11	99	1.000			
Klamath–Trinity Basin	12	100	0.985			0.015	12	100	0.995	0.005		
	13	100	0.775	0.225			13	80	0.988			0.013
	14	99	0.899	0.101			14	99	1.000			
	15	128	0.938	0.051		0.012	15	118	1.000			
	16	100	0.955	0.030		0.015	16	100	1.000			
	17	98	0.929	0.046	0.005	0.020	17	98	1.000			
	18	106	0.943	0.028		0.028	18	106	1.000			
	19	100	0.905	0.095			19	100	1.000			
	20	100	0.980	0.015		0.005	20	100	1.000			
	21	120	0.942	0.054		0.004	21	120	1.000			
Eel River–California Coastal	22	95	0.874	0.121		0.005	22	95	1.000			
	23	100	0.900	0.100			23	100	1.000			
	24	99	0.924	0.076			24	99	0.985		0.015	
	25	61	0.828	0.172			25	61	1.000			
	26	95	0.868	0.132			26	95	1.000			
	27	99	0.874	0.126			27	99	1.000			
	28	100	0.835	0.165			28	100	1.000			
	29	93	0.871	0.129			29	93	1.000			
	30	99	0.778	0.222			30	100	1.000			
	31	96	0.786	0.214			31	96	1.000			
	32	100	0.900	0.100			32	100	1.000			
Sacramento—San Joaquin	33	94	0.957	0.011	0.032		33	94	1.000			
	34	100	0.925	0.020	0.055		34	100	1.000			
	35	100	0.860	0.035	0.105		35	100	1.000			
	36	100	0.925	0.020	0.055		36	100	1.000			
	37	100	0.905	0.065	0.030		37	100	1.000			

	EST-3		Alleles			GPI-2		Alleles			GPI-H		Alleles	
	ID#	*N*	100	97	107	ID#	*N*	100 (100)	60 (50)	135 (150)	ID#	*N*	100 (common)	* (*)
Middle Oregon	1	100	1.000			1	100	0.315	0.685		1	100	1.000	
	2	100	1.000			2	100	0.585	0.415		2	100	1.000	
	3	100	0.995	0.005		3	100	0.565	0.420	0.015	3	100	1.000	
	4	100	0.985	0.015		4	100	0.335	0.665		4	100	1.000	
	5	100	0.975	0.025		5	100	0.465	0.535		5	100	1.000	
	6	100	1.000			6	100	0.805	0.195		6	100	1.000	
S. Oregon/	7	100	1.000			7	100	0.720	0.280		7	100	1.000	
N. California Coastal	8	100	0.980	0.020		8	100	0.805	0.195		8	100	1.000	
	9	100	0.990	0.010		9	100	0.715	0.265	0.020	9	100	1.000	
	10	62	1.000			10	62	0.750	0.185	0.065	10	62	1.000	
	11	99	0.990	0.010		11	99	0.758	0.227	0.015	11	99	1.000	
Klamath–Trinity Basin	12	100	0.995	0.005		12	100	0.765	0.235		12	100	1.000	
	13	60	0.967	0.033		13	100	0.615	0.385		13	100	1.000	
	14	99	0.980	0.020		14	99	0.949	0.051		14	99	1.000	
	15	58	0.991	0.009		15	128	0.945	0.055		15	128	1.000	
	16	90	0.083	0.017		16	100	0.945	0.055		16	80	1.000	
	17	98	0.995	0.005		17	98	0.888	0.112		17	98	1.000	
	18	106	1.000			18	106	0.769	0.231		18	106	1.000	
	19	100	0.985	0.015		19	100	0.915	0.085		19	100	1.000	

Appendix A (continued)

	EST-3		Alleles			GPI-2		Alleles			GPI-H		Alleles	
	ID#	*N*	100	97	107	ID#	*N*	100 (100)	60 (50)	135 (150)	ID#	*N*	100 (common)	* (*)
Klamath–Trinity Basin	20	100	1.000			20	100	0.885	0.115		20	100	1.000	
(continued)	21	120	1.000			21	120	0.929	0.071		21	120	1.000	
Eel River–California Coastal	22	95	1.000			22	95	0.542	0.458		22	95	1.000	
	23	100	1.000			23	100	0.570	0.430		23	100	1.000	
	24	99	0.995	0.005		24	99	0.556	0.444		24	99	1.000	
	25	61	1.000			25	61	0.484	0.516		25	61	1.000	
	26	95	1.000			26	95	0.432	0.568		26	95	1.000	
	27	99	1.000			27	99	0.535	0.465		27	99	1.000	
	28	100	1.000			28	100	0.570	0.430		28	100	1.000	
	29	93	1.000			29	93	0.586	0.414		29	93	1.000	
	30	100	1.000			30	100	0.545	0.455		30	100	1.000	
	31	96	1.000			31	96	0.693	0.307		31	96	1.000	
	32	100	0.995		0.005	32	100	0.570	0.430		32	100	1.000	
Sacramento–San Joaquin	33	92	0.989	0.011		33	94	0.777	0.064	0.160	33	94	0.643	0.357
	34	100	0.995	0.005		34	100	0.940	0.040	0.020	34	100	0.717	0.283
	35	100	0.995	0.005		35	100	0.925	0.065	0.010	35	100	0.613	0.387
	36	100	1.000			36	100	0.930	0.070		36	100	0.654	0.346
	37	100	1.000			37	100	0.965	0.035		37	100	0.755	0.245

	GR		Alleles		HAGH		Alleles			IDDH-1		Alleles	
	ID#	*N*	100	85	ID#	*N*	100	143	78	ID#	*N*	100	0
Middle Oregon	1	96	1.000		1	100	1.000			1	100	0.950	0.050
	2	100	0.895	0.105	2	100	0.980	0.015	0.005	2	99	0.712	0.288
	3	97	0.943	0.057	3	100	0.985	0.015		3	99	0.864	0.136
	4	99	0.975	0.025	4	100	1.000			4	100	0.710	0.290
	5	80	1.000		5	100	1.000			5	99	0.934	0.066
	6	100	0.995	0.005	6	100	1.000			6	100	0.995	0.005
S Oregon/	7	100	0.995	0.005	7	100	1.000			7	100	1.000	
N. California Coastal	8	100	1.000		8	100	1.000			8	100	0.995	0.005
	9	100	1.000		9	100	1.000			9	99	0.919	0.081
	10	62	0.895	0.105	10	62	1.000			10	62	0.992	0.008
	11	99	0.975	0.025	11	99	1.000			11	99	0.990	0.010
Klamath–Trinity Basin	12	100	0.995	0.005	12	100	1.000			12	100	0.990	0.010
	13	100	1.000		13	100	1.000			13	100	0.995	0.005
	14	99	1.000		14	99	1.000			14	92	1.000	
	15	128	1.000		15	98	1.000			15	128	1.000	
	16	100	0.995	0.005	16	100	1.000			16	100	1.000	
	17	98	1.000		17	98	1.000			17	95	1.000	
	18	106	1.000		18	106	1.000			18	106	1.000	
	19	100	1.000		19	100	1.000			19	100	1.000	
	20	100	1.000		20	100	1.000			20	100	1.000	
	21	120	1.000		21	120	1.000			21	120	1.000	
Eel River–California Coastal	22	95	1.000		22	95	1.000			22	95	0.979	0.021
	23	100	1.000		23	100	1.000			23	100	0.990	0.010
	24	99	0.995	0.005	24	99	1.000			24	99	1.000	
	25	61	1.000		25	45	1.000			25	58	1.000	
	26	95	1.000		26	95	1.000			26	95	1.000	
	27	99	1.000		27	99	1.000			27	97	1.000	
	28	60	1.000		28	54	1.000			28	85	1.000	
	29	93	1.000		29	93	1.000			29	93	1.000	
	30	100	1.000		30	63	1.000			30	73	1.000	
	31	96	1.000		31	96	1.000			31	92	1.000	
	32	100	1.000		32	46	1.000			32	99	1.000	
Sacramento–San Joaquin	33	94	1.000		33	94	1.000			33	93	1.000	
	34	100	1.000		34	100	1.000			34	100	1.000	
	35	100	1.000		35	100	1.000			35	100	1.000	
	36	100	1.000		36	100	0.990		0.010	36	100	1.000	
	37	100	1.000		37	100	1.000			37	100	1.000	

Appendix A (continued)

	IDDH-2 ID#	N	Alleles 100 (100)	61 (50	20
Middle Oregon	1	100	1.000		
	2	99	0.995	0.005	
	3	99	0.990	0.010	
	4	100	0.990	0.010	
	5	99	0.990	0.010	
	6	100	0.940	0.060	
S Oregon/N. California Coastal	7	100	0.975	0.025	
	8	100	0.945	0.055	
	9	99	0.939	0.061	
	10	61	0.861	0.139	
	11	99	0.929	0.071	
Klamath–Trinity Basin	12	100	0.975	0.025	
	13	100	0.925	0.075	
	14	92	0.978	0.022	
	15	128	0.988	0.012	
	16	100	0.985	0.015	
	17	95	0.937	0.063	
	18	104	0.976	0.024	
	19	93	0.892	0.108	
	20	100	0.945	0.055	
	21	120	1.000		
Eel River–California Coastal	22	95	0.974	0.026	
	23	100	0.990	0.010	
	24	99	0.939	0.061	
	25	55	0.945	0.055	
	26	95	0.995	0.005	
	27	97	0.985	0.015	
	28	83	0.982	0.018	
	29	93	0.995	0.005	
	30	73	1.000		
	31	92	1.000		
	32	99	0.909	0.091	
Sacramento–San Joaquin	33	93	0.984		0.016
	34	100	0.990		0.010
	35	100	0.975		0.025
	36	100	0.990		0.010
	37	100	0.990		0.010

	IDH-2 ID#	N	Alleles 100 (100)	154 (120)
	1	100	1.000	
	2	100	1.000	
	3	100	1.000	
	4	100	1.000	
	5	100	1.000	
	6	100	1.000	
	7	100	1.000	
	8	100	1.000	
	9	100	1.000	
	10	62	1.000	
	11	99	1.000	
	12	100	1.000	
	13	100	1.000	
	14	99	1.000	
	15	127	1.000	
	16	100	0.995	0.005
	17	98	0.995	0.005
	18	106	1.000	
	19	100	1.000	
	20	100	1.000	
	21	120	1.000	
	22	95	1.000	
	23	100	1.000	
	24	99	1.000	
	25	61	0.975	0.025
	26	95	0.974	0.026
	27	98	0.990	0.010
	28	100	0.990	0.010
	29	93	1.000	
	30	100	1.000	
	31	96	1.000	
	32	100	1.000	
	33	94	0.941	0.059
	34	100	0.905	0.095
	35	100	0.950	0.050
	36	100	0.830	0.170
	37	100	0.885	0.115

	IDH-3 ID#	N	Alleles 100 (100)	74 (80)	142	94 (80)	83	129 (120)	136
Middle Oregon	1	100	1.000						
	2	100	1.000						
	3	100	0.985					0.015	
	4	100	0.995					0.005	
	5	100	1.000						
	6	100	1.000						
S. Oregon/N. California Coastal	7	100	1.000						
	8	100	0.990					0.010	
	9	100	0.995						0.005
	10	62	1.000						
	11	99	1.000						
Klamath–Trinity Basin	12	100	1.000						
	13	100	1.000						
	14	99	1.000						
	15	124	1.000						
	16	99	1.000						
	17	98	1.000						
	18	106	1.000						
	19	100	1.000						

Appendix A (continued)

	IDH-3 ID#	*N*	Alleles 100 (100)	74 (80)	142	94 (80)	83	129 (120)	136
Klamath–Trinity Basin	20	100	1.000						
(continued)	21	120	0.992				0.008		
Eel River–California Coastal	22	95	0.995					0.005	
	23	100	1.000						
	24	99	1.000						
	25	61	1.000						
	26	95	1.000						
	27	99	1.000						
	28	100	1.000						
	29	93	1.000						
	30	100	1.000						
	31	96	1.000						
	32	100	1.000						
Sacramento–San Joaquin	33	94	0.949	0.005			0.048		
	34	100	0.995		0.005				
	35	100	1.000						
	36	100	0.990			0.010			
	37	100	1.000						

	IDH-4 ID#	*N*	Alleles 100 (100)	127 (120)	50	LDH-1 ID#	*N*	Alleles 100	800	LDH-4 ID#	*N*	Alleles 100 (100)	112 (115)	134	71 (75)
Middle Oregon	1	100	0.935	0.065		1	100	1.000		1	100	1.000			
	2	100	0.995	0.005		2	100	1.000		2	100	0.985		0.015	
	3	100	0.975	0.025		3	100	1.000		3	100	1.000			
	4	100	0.970	0.030		4	100	1.000		4	100	0.990		0.010	
	5	100	0.950	0.050		5	100	0.900	0.100	5	100	0.985			0.015
	6	100	0.930	0.070		6	100	1.000		6	100	1.000			
S. Oregon/	7	100	0.975	0.025		7	100	1.000		7	100	1.000			
N. California Coastal	8	100	0.945	0.055		8	100	1.000		8	100	0.980	0.010	0.010	
	9	100	0.975	0.025		9	100	1.000		9	100	1.000			
	10	62	0.879	0.121		10	62	1.000		10	62	1.000			
	11	99	0.985	0.015		11	99	1.000		11	99	1.000			
Klamath–Trinity Basin	12	100	0.980	0.020		12	100	0.859	0.141	12	100	1.000			
	13	100	0.900	0.100		13	100	1.000		13	100	1.000			
	14	99	1.000			14	99	1.000		14	99	1.000			
	15	128	0.996	0.004		15	127	1.000		15	128	1.000			
	16	99	1.000			16	100	1.000		16	100	1.000			
	17	98	0.980	0.020		17	98	1.000		17	98	1.000			
	18	102	1.000			18	106	1.000		18	106	1.000			
	19	100	0.990	0.010		19	100	1.000		19	100	1.000			
	20	100	0.980	0.020		20	100	1.000		20	100	1.000			
	21	120	1.000			21	120	1.000		21	120	1.000			
Eel River–California Coastal	22	95	0.868	0.132		22	95	0.897	0.103	22	95	1.000			
	23	100	0.845	0.155		23	100	0.900	0.100	23	100	1.000			
	24	99	0.899	0.101		24	99	1.000		24	99	1.000			
	25	61	0.885	0.115		25	61	1.000		25	61	1.000			
	26	95	0.900	0.100		26	95	1.000		26	95	1.000			
	27	99	0.859	0.141		27	99	1.000		27	99	1.000			
	28	100	0.865	0.135		28	100	1.000		28	100	1.000			
	29	93	0.785	0.215		29	93	1.000		29	93	1.000			
	30	100	0.810	0.190		30	100	1.000		30	100	1.000			
	31	96	0.859	0.141		31	96	1.000		31	96	1.000			
	32	100	0.765	0.235		32	100	1.000		32	100	1.000			
Sacramento–San Joaquin	33	94	0.915	0.085		33	94	1.000		33	94	1.000			
	34	100	0.905	0.090	0.005	34	100	1.000		34	100	1.000			
	35	100	0.895	0.105		35	100	1.000		35	100	1.000			
	36	100	0.875	0.125		36	100	1.000		36	100	1.000			
	37	100	0.995	0.005		37	100	1.000		37	100	1.000			

Appendix A (continued)

	LDH-5		Alleles			MDHP-1		Alleles		MDHP-2		Alleles	
	ID#	*N*	100	90	95	ID#	*N*	100	92	ID#	*N*	100	78
Middle Oregon	1	100	1.000			1	100	0.260	0.740	1	100	1.000	
	2	100	0.970	0.030		2	100	0.375	0.625	2	100	1.000	
	3	100	0.975	0.025		3	100	0.470	0.530	3	100	1.000	
	4	100	0.990	0.010		4	100	0.325	0.675	4	100	1.000	
	5	100	1.000			5	100	0.380	0.620	5	100	1.000	
	6	100	0.995	0.005		6	100	0.465	0.535	6	100	1.000	
S Oregon/	7	100	0.975	0.015	0.010	7	100	0.450	0.550	7	100	0.900	0.100
N. California Coastal	8	100	0.990	0.010		8	100	0.415	0.585	8	100	0.900	0.100
	9	100	1.000			9	100	0.325	0.675	9	100	0.900	0.100
	10	62	1.000			10	62	0.282	0.718	10	62	0.746	0.254
	11	99	1.000			11	98	0.362	0.638	11	98	1.000	
Klamath–Trinity Basin	12	100	0.985	0.015		12	100	0.315	0.685	12	100	0.859	0.141
	13	100	0.890	0.110		13	100	0.390	0.610	13	100	1.000	
	14	99	1.000			14	99	0.247	0.753	14	99	0.598	0.402
	15	127	1.000			15	123	0.228	0.772	15	123	0.558	0.442
	16	100	1.000			16	99	0.212	0.788	16	99	0.562	0.438
	17	98	1.000			17	98	0.245	0.755	17	98	0.622	0.378
	18	106	1.000			18	105	0.333	0.667	18	105	0.564	0.436
	19	100	1.000			19	100	0.465	0.535	19	100	0.827	0.173
	20	100	0.975	0.025		20	100	0.330	0.670	20	100	0.859	0.141
	21	120	1.000			21	120	0.150	0.850	21	120	0.726	0.274
Eel River–California Coastal	22	95	1.000			22	95	0.374	0.626	22	95	1.000	
	23	100	1.000			23	100	0.460	0.540	23	100	1.000	
	24	99	1.000			24	99	0.470	0.530	24	99	1.000	
	25	61	1.000			25	60	0.450	0.550	25	60	1.000	
	26	95	1.000			26	95	0.532	0.468	26	95	1.000	
	27	99	1.000			27	79	0.557	0.443	27	79	0.841	0.159
	28	100	1.000			28	100	0.480	0.520	28	100	0.900	0.100
	29	93	1.000			29	93	0.505	0.495	29	93	1.000	
	30	100	1.000			30	100	0.425	0.575	30	100	1.000	
	31	96	1.000			31	96	0.500	0.500	31	96	1.000	
	32	100	1.000			32	100	0.400	0.600	32	100	1.000	
Sacramento–San Joaquin	33	94	1.000			33	94	0.851	0.149	33	94	1.000	
	34	100	1.000			34	100	0.805	0.195	34	100	1.000	
	35	100	1.000			35	100	0.775	0.225	35	100	1.000	
	36	100	1.000			36	100	0.810	0.190	36	100	1.000	
	37	100	1.000			37	100	0.860	0.140	37	100	1.000	

	MDH-2		Alleles				MDH-4		Alleles			
	ID#	*N*	100	120	27	45	ID#	*N*	100 (100)	121 (120)	70 (70)	126
Middle Oregon	1	100	1.000				1	100	1.000			
	2	100	1.000				2	100	0.980	0.020		
	3	100	0.995			0.005	3	100	0.995	0.005		
	4	100	0.995		0.005		4	100	0.995	0.005		
	5	100	0.880		0.075	0.045	5	100	0.980	0.020		
	6	100	1.000				6	100	0.935	0.065		
S Oregon/N. California Coastal	7	100	1.000				7	100	1.000			
	8	100	1.000				8	100	0.975	0.025		
	9	100	0.990	0.005	0.005		9	100	0.950	0.045		0.005
	10	62	1.000				10	62	1.000			
	11	99	1.000				11	99	0.975	0.015	0.010	
Klamath–Trinity Basin	12	100	1.000				12	100	0.985	0.015		
	13	100	1.000				13	100	1.000			
	14	99	1.000				14	99	1.000			
	15	128	1.000				15	128	1.000			
	16	100	0.995			0.005	16	100	1.000			
	17	98	1.000				17	98	1.000			
	18	106	1.000				18	106	1.000			
	19	100	1.000				19	100	1.000			

Appendix A (continued)

	MDH-2		Alleles				MDH-4		Alleles			
	ID#	*N*	100	120	27	45	ID#	*N*	100 (100)	121 (120)	70 (70)	126
Klamath–Trinity Basin (continued)	20	100	1.000				20	100	0.995	0.005		
	21	120	1.000				21	120	1.000			
Eel River–California Coastal	22	95	1.000				22	95	0.995	0.005		
	23	100	0.995			0.005	23	100	0.985	0.015		
	24	99	1.000				24	99	1.000			
	25	61	1.000				25	61	1.000			
	26	95	1.000				26	95	1.000			
	27	99	1.000				27	99	1.000			
	28	100	1.000				28	100	1.000			
	29	93	1.000				29	93	1.000			
	30	100	1.000				30	100	1.000			
	31	96	1.000				31	96	1.000			
	32	100	1.000				32	100	1.000			
Sacramento–San Joaquin	33	94	1.000				33	94	0.979	0.021		
	34	100	1.000				34	100	0.920	0.070		0.010
	35	100	1.000				35	100	0.955	0.045		
	36	100	1.000				36	100	0.905	0.065		0.030
	37	100	1.000				37	100	0.935	0.040	0.025	

	mMDH-1		Alleles		mMDH-2		Alleles		MPI		Alleles	
	ID#	*N*	−100	−900	ID#	*N*	100	200	ID#	*N*	100 (100)	109 (110)
Middle Oregon	1	100	1.000		1	100	1.000		1	99	0.581	0.419
	2	100	0.980	0.020	2	100	0.995	0.005	2	100	0.695	0.305
	3	100	0.990	0.010	3	100	1.000		3	100	0.575	0.425
	4	100	0.995	0.005	4	100	1.000		4	100	0.505	0.495
	5	100	0.960	0.040	5	100	1.000		5	100	0.690	0.310
	6	100	0.915	0.085	6	100	0.995	0.005	6	100	0.900	0.100
S. Oregon/ N. California Coastal	7	100	0.940	0.060	7	100	1.000		7	100	0.890	0.110
	8	100	0.940	0.060	8	100	0.995	0.005	8	99	0.828	0.172
	9	100	0.865	0.135	9	80	1.000		9	100	0.660	0.340
	10	62	0.960	0.040	10	62	1.000		10	62	0.815	0.185
	11	99	0.899	0.101	11	99	1.000		11	99	0.818	0.182
Klamath–Trinity Basin	12	100	0.910	0.090	12	100	0.995	0.005	12	100	0.860	0.140
	13	100	0.795	0.205	13	100	1.000		13	100	0.860	0.140
	14	99	1.000		14	99	1.000		14	99	0.970	0.030
	15	128	0.996	0.004	15	80	1.000		15	128	1.000	
	16	60	1.000		16	60	1.000		16	100	1.000	
	17	98	0.990	0.010	17	98	0.995	0.005	17	98	0.959	0.041
	18	70	1.000		18	106	1.000		18	106	0.953	0.047
	19	100	0.990	0.010	19	100	0.905	0.095	19	100	0.940	0.060
	20	100	0.970	0.030	20	100	1.000		20	100	0.975	0.025
	21	120	1.000		21	120	1.000		21	120	0.992	0.008
Eel River–California Coastal	22	95	0.995	0.005	22	95	0.995	0.005	22	95	0.805	0.195
	23	100	0.990	0.010	23	100	1.000		23	100	0.765	0.235
	24	99	0.995	0.005	24	99	1.000		24	99	0.904	0.096
	25	61	1.000		25	61	1.000		25	61	0.787	0.213
	26	95	0.989	0.011	26	95	1.000		26	95	0.853	0.147
	27	99	1.000		27	99	1.000		27	99	0.818	0.182
	28	100	1.000		28	73	1.000		28	99	0.808	0.192
	29	93	1.000		29	93	1.000		29	93	0.785	0.215
	30	100	1.000		30	100	1.000		30	100	0.800	0.200
	31	96	1.000		31	96	1.000		31	96	0.901	0.099
	32	100	1.000		32	100	1.000		32	100	0.610	0.390
Sacramento–San Joaquin	33	94	1.000		33	94	1.000		33	94	0.617	0.383
	34	100	1.000		34	100	1.000		34	100	0.585	0.415
	35	100	1.000		35	100	1.000		35	100	0.580	0.420
	36	100	1.000		36	100	1.000		36	100	0.545	0.455
	37	100	1.000		37	100	1.000		37	100	0.700	0.300

Appendix A (continued)

	PGDH		Alleles			PGK-2		Alleles		PGM-1		Alleles		
	ID#	*N*	100 (100)	90 (90)	85 (90)	ID#	*N*	100 (100)	90 (90)	ID#	*N*	100	210	50
Middle Oregon	1	100	1.000			1	100	0.660	0.340	1	100	0.855	0.065	0.080
	2	100	1.000			2	100	0.445	0.555	2	100	0.870	0.070	0.060
	3	100	1.000			3	100	0.435	0.565	3	100	0.910	0.070	0.020
	4	100	1.000			4	100	0.355	0.645	4	100	0.870	0.090	0.040
	5	100	1.000			5	100	0.465	0.535	5	100	0.880	0.090	0.030
	6	100	1.000			6	100	0.430	0.570	6	60	1.000		
S. Oregon/	7	100	1.000			7	100	0.395	0.605	7	100	1.000		
N. California Coastal	8	100	0.985		0.015	8	100	0.345	0.655	8	100	1.000		
	9	100	0.990		0.010	9	100	0.515	0.485	9	100	0.980	0.020	
	10	62	1.000			10	62	0.468	0.532	10	62	1.000		
	11	99	1.000			11	98	0.439	0.561	11	99	1.000		
Klamath–Trinity Basin	12	100	1.000			12	100	0.400	0.600	12	80	1.000		
	13	100	0.910		0.090	13	100	0.380	0.620	13	100	1.000		
	14	99	1.000			14	99	0.146	0.854	14	99	1.000		
	15	128	0.996	0.004		15	127	0.185	0.815	15	128	1.000		
	16	100	1.000			16	100	0.155	0.845	16	100	1.000		
	17	98	1.000			17	98	0.189	0.811	17	98	1.000		
	18	106	1.000			18	105	0.186	0.814	18	106	1.000		
	19	100	1.000			19	100	0.380	0.620	19	100	0.950		0.050
	20	100	1.000			20	100	0.320	0.680	20	100	1.000		
	21	120	1.000			21	120	0.292	0.708	21	120	1.000		
Eel River–California Coastal	22	95	1.000			22	95	0.379	0.621	22	95	1.000		
	23	100	1.000			23	100	0.345	0.655	23	80	0.994	0.006	
	24	99	1.000			24	99	0.525	0.475	24	99	1.000		
	25	61	1.000			25	61	0.459	0.541	25	61	1.000		
	26	95	1.000			26	95	0.242	0.758	26	95	1.000		
	27	99	1.000			27	99	0.480	0.520	27	99	1.000		
	28	100	1.000			28	99	0.439	0.561	28	100	1.000		
	29	93	1.000			29	93	0.392	0.608	29	93	1.000		
	30	100	1.000			30	100	0.245	0.755	30	100	1.000		
	31	96	1.000			31	96	0.365	0.635	31	96	1.000		
	32	100	1.000			32	100	0.315	0.685	32	100	1.000		
Sacramento–San Joaquin	33	94	0.979	0.021		33	94	0.590	0.410	33	94	1.000		
	34	100	0.975	0.025		34	100	0.495	0.505	34	100	1.000		
	35	100	0.960	0.040		35	100	0.490	0.510	35	100	1.000		
	36	100	0.920	0.080		36	100	0.605	0.395	36	100	1.000		
	37	100	0.900	0.100		37	100	0.670	0.330	37	100	1.000		

	PGM-2		Alleles 100	166	144	120	PGM-3		Alleles 100	94
	ID#	*N*	(100)	(166)			ID#	*N*		
Middle Oregon	1	100	1.000				1	100	0.710	0.290
	2	100	1.000				2	100	0.945	0.055
	3	100	0.970			0.030	3	100	0.885	0.115
	4	100	0.975			0.025	4	100	0.925	0.075
	5	100	1.000				5	100	0.900	0.100
	6	100	1.000				6	100	0.945	0.055
S. Oregon/N. California Coastal	7	100	0.995	0.005			7	100	0.970	0.030
	8	100	1.000				8	100	0.970	0.030
	9	100	0.965		0.030	0.005	9	100	0.950	0.050
	10	62	0.927		0.073		10	62	0.968	0.032
	11	99	0.995		0.005		11	99	0.934	0.066
Klamath–Trinity Basin	12	100	0.915	0.085			12	100	0.945	0.055
	13	100	0.975	0.025			13	100	0.930	0.070
	14	99	0.929	0.071			14	99	0.980	0.020
	15	128	0.902	0.098			15	114	0.987	0.013
	16	100	0.965	0.035			16	98	0.964	0.036
	17	98	0.964	0.036			17	98	0.923	0.077
	18	106	1.000				18	106	0.981	0.019
	19	100	0.860	0.135	0.005		19	100	0.970	0.030

Appendix A (continued)

	PGM-2		Alleles			
	ID#	*N*	100 (100)	166 (166)	144	120
Klamath–Trinity Basin (continued)	20	100	1.000			
	21	120	1.000			
Eel River–California Coastal	22	95	1.000			
	23	100	1.000			
	24	99	0.970	0.025	0.005	
	25	61	0.967		0.033	
	26	95	1.000			
	27	99	1.000			
	28	100	1.000			
	29	93	1.000			
	30	100	1.000			
	31	96	1.000			
	32	100	0.995	0.005		
Sacramento–San Joaquin	33	94	0.995	0.005		
	34	100	0.990	0.010		
	35	100	0.995	0.005		
	36	100	1.000			
	37	100	1.000			

	PGM-3		Alleles	
	ID#	*N*	100	94
	20	100	0.950	0.050
	21	120	0.900	0.100
	22	95	0.984	0.016
	23	100	0.965	0.035
	24	99	0.995	0.005
	25	61	1.000	
	26	95	1.000	
	27	99	1.000	
	28	100	1.000	
	29	93	1.000	
	30	100	1.000	
	31	96	1.000	
	32	100	1.000	
	33	94	0.995	0.005
	34	100	0.970	0.030
	35	100	0.970	0.030
	36	100	0.980	0.020
	37	100	0.975	0.025

	PGM-4		Alleles					
	ID#	*N*	100	94	108	88	90	97
Middle Oregon	1	100	0.100	0.520	0.015	0.285	0.080	
	2	100	0.325	0.565	0.050	0.010	0.035	0.015
	3	100	0.330	0.610	0.030	0.005	0.020	0.005
	4	100	0.385	0.540	0.055	0.005	0.015	
	5	100	0.265	0.675	0.030	0.030		
	6	100	0.505	0.430	0.055	0.010		
S. Oregon/ N. California Coastal	7	100	0.505	0.435	0.060			
	8	100	0.535	0.415	0.045	0.005		
	9	100	0.370	0.630				
	10	62	0.315	0.685				
	11	98	0.464	0.536				
Klamath–Trinity Basin	12	100	0.490	0.495		0.015		
	13	100	0.565	0.435				
	14	99	0.586	0.414				
	15	114	0.667	0.333				
	16	98	0.592	0.408				
	17	98	0.495	0.505				
	18	106	0.528	0.472				
	19	100	0.665	0.290	0.045			
	20	100	0.505	0.495				
	21	120	0.363	0.638				
Eel River–California Coastal	22	95	0.726	0.268	0.005			
	23	100	0.675	0.325				
	24	99	0.763	0.227		0.010		
	25	61	0.877	0.115		0.008		
	26	95	0.753	0.247				
	27	99	0.813	0.187				
	28	100	0.800	0.200				
	29	93	0.892	0.108				
	30	100	0.855	0.145				
	31	96	0.760	0.240				
	32	100	0.880	0.120				
Sacramento–San Joaquin	33	94	0.500	0.495		0.005		
	34	100	0.555	0.415	0.005	0.025		
	35	100	0.575	0.335		0.090		
	36	100	0.550	0.435		0.015		
	37	100	0.605	0.375		0.005		0.015

	SOD-1		Alleles			
	ID#	*N*	−100 (−100)	−260 (−260)	580 (580)	1260
	1	99	0.788	0.202	0.010	
	2	100	0.770	0.230		
	3	100	0.765	0.230		0.005
	4	100	0.785	0.215		
	5	100	0.570	0.430		
	6	100	0.715	0.270	0.015	
	7	100	0.730	0.255	0.005	0.010
	8	100	0.780	0.210		0.010
	9	100	0.810	0.190		
	10	62	0.782	0.218		
	11	98	0.760	0.240		
	12	100	0.755	0.230		0.015
	13	100	0.815	0.185		
	14	99	0.990	0.010		
	15	128	1.000			
	16	100	1.000			
	17	94	0.968	0.027		0.005
	18	105	0.852	0.148		
	19	99	0.904	0.010		0.086
	20	100	0.845	0.090	0.060	0.005
	21	120	0.917	0.046	0.021	0.017
	22	92	0.750	0.250		
	23	100	0.635	0.365		
	24	99	0.798	0.202		
	25	59	0.636	0.364		
	26	95	0.700	0.300		
	27	99	0.778	0.222		
	28	87	0.793	0.207		
	29	92	0.837	0.163		
	30	99	0.798	0.202		
	31	91	0.714	0.286		
	32	100	0.715	0.270	0.015	
	33	93	0.661	0.339		
	34	100	0.790	0.210		
	35	100	0.755	0.240	0.005	
	36	100	0.690	0.300	0.010	
	37	100	0.715	0.270	0.015	

Appendix A (continued)

	TPI-3		Alleles			TPI-4		Alleles				DPEP-1		Alleles	
	ID#	*N*	100	106	104	ID#	*N*	100	104	102	101	ID#	*N*	100 (100)	90 (90)
Middle Oregon	1	99	0.783		0.217	1	100	1.000				1	100	0.715	0.285
	2	100	0.970		0.030	2	100	1.000				2	100	0.595	0.405
	3	100	0.960		0.040	3	100	1.000				3	100	0.660	0.340
	4	100	0.905		0.095	4	100	1.000				4	100	0.630	0.370
	5	100	0.890		0.110	5	100	1.000				5	100	0.715	0.285
	6	100	0.950		0.050	6	100	0.995	0.005			6	100	0.920	0.080
S. Oregon/	7	100	0.920		0.080	7	100	0.995		0.005		7	100	0.925	0.075
N. California Coastal	8	100	0.890		0.110	8	100	1.000				8	100	0.905	0.095
	9	100	0.840		0.160	9	100	0.975	0.025			9	100	0.810	0.190
	10	62	0.903		0.097	10	62	1.000				10	62	0.871	0.129
	11	99	0.753	0.101	0.146	11	99	0.970	0.030			11	99	0.848	0.152
Klamath–Trinity Basin	12	100	0.865		0.135	12	100	1.000				12	100	0.895	0.105
	13	100	0.965		0.035	13	100	1.000				13	100	0.770	0.230
	14	99	0.970		0.030	14	99	1.000				14	99	0.990	0.010
	15	128	1.000			15	128	1.000				15	128	1.000	
	16	100	1.000			16	100	1.000				16	100	1.000	
	17	98	0.964		0.036	17	98	0.995	0.005			17	98	0.964	0.036
	18	106	0.967		0.033	18	106	1.000				18	105	0.824	0.176
	19	100	0.940		0.060	19	100	1.000				19	100	0.940	0.060
	20	100	0.970		0.030	20	100	1.000				20	100	0.930	0.070
	21	120	0.979		0.021	21	120	1.000				21	120	1.000	
Eel River–California Coastal	22	95	0.984		0.016	22	95	0.989	0.005	0.005		22	95	0.942	0.058
	23	100	0.960		0.040	23	100	0.995	0.005			23	100	0.950	0.050
	24	99	1.000			24	99	0.995	0.005			24	99	0.965	0.035
	25	61	0.714	0.286		25	61	0.959	0.041			25	61	0.967	0.033
	26	95	1.000			26	95	0.968	0.032			26	95	0.963	0.037
	27	99	0.899	0.101		27	99	0.975	0.025			27	99	0.965	0.035
	28	100	0.859	0.141		28	100	0.975	0.025			28	100	0.955	0.045
	29	93	0.805	0.147	0.048	29	93	0.892	0.086	0.022		29	93	0.957	0.043
	30	100	1.000			30	100	0.875	0.125			30	95	0.937	0.063
	31	96	0.995		0.005	31	96	0.974	0.026			31	96	0.880	0.120
	32	100	0.895	0.100	0.005	32	100	0.955	0.045			32	100	1.000	
Sacramento–San Joaquin	33	94	0.936		0.064	33	94	1.000				33	94	0.894	0.106
	34	100	0.945		0.055	34	100	0.930		0.070		34	100	0.810	0.190
	35	100	0.915		0.085	35	100	0.960		0.040		35	100	0.850	0.150
	36	100	0.870		0.130	36	100	0.960		0.035	0.005	36	100	0.875	0.125
	37	100	0.830		0.170	37	100	0.965		0.035		37	100	0.950	0.050

	PDPEP-2		Alleles			PEPLT		Alleles		TAPEP-1		Alleles	
	ID#	*N*	100 (100)	107 (107)	83	ID#	*N*	100	110	ID#	*N*	100 (100)	130 (140)
Middle Oregon	1	100	0.995	0.005		1	100	1.000		1	100	0.725	0.275
	2	100	0.955	0.045		2	100	1.000		2	100	0.865	0.135
	3	100	0.980	0.020		3	100	1.000		3	100	0.880	0.120
	4	100	0.995	0.005		4	100	1.000		4	100	0.945	0.055
	5	100	1.000			5	100	1.000		5	100	0.895	0.105
	6	100	0.990	0.010		6	100	0.945	0.055	6	100	0.950	0.050
S. Oregon/	7	100	0.990	0.005	0.005	7	100	0.965	0.035	7	100	0.925	0.075
N. California Coastal	8	100	0.995	0.005		8	100	0.995	0.005	8	100	0.975	0.025
	9	100	1.000			9	100	1.000		9	100	0.940	0.060
	10	62	1.000			10	62	1.000		10	62	0.847	0.153
	11	99	1.000			11	99	1.000		11	99	0.955	0.045
Klamath–Trinity Basin	12	100	1.000			12	100	0.985	0.015	12	100	0.925	0.075
	13	100	1.000			13	100	1.000		13	100	0.860	0.140
	14	99	1.000			14	99	1.000		14	99	1.000	
	15	128	1.000			15	128	1.000		15	125	0.996	0.004
	16	100	1.000			16	100	1.000		16	100	1.000	
	17	98	1.000			17	98	1.000		17	98	1.000	
	18	106	1.000			18	106	1.000		18	106	1.000	

Appendix A (continued)

	PDPEP-2		Alleles			PEPLT		Alleles		TAPEP-1		Alleles	
	ID#	*N*	100 (100)	107 (107)	83	ID#	*N*	100	110	ID#	*N*	100 (100)	130 (140)
Klamath–Trinity Basin (continued)	19	100	1.000			19	100	1.000		19	100	1.000	
	20	100	1.000			20	60	1.000		20	100	0.980	0.020
	21	120	1.000			21	120	1.000		21	120	1.000	
Eel River–California Coastal	22	95	1.000			22	95	1.000		22	95	0.974	0.026
	23	100	1.000			23	100	1.000		23	100	0.960	0.040
	24	99	1.000			24	99	1.000		24	99	0.985	0.015
	25	61	1.000			25	61	1.000		25	61	0.992	0.008
	26	95	1.000			26	95	1.000		26	95	0.979	0.021
	27	98	1.000			27	60	1.000		27	99	0.965	0.035
	28	100	0.995	0.005		28	100	1.000		28	100	0.995	0.005
	29	93	1.000			29	93	1.000		29	93	1.000	
	30	100	1.000			30	100	1.000		30	100	0.990	0.010
	31	96	1.000			31	96	1.000		31	96	1.000	
	32	100	1.000			32	100	1.000		32	100	1.000	
Sacramento–San Joaquin	33	94	1.000			33	94	1.000		33	94	0.862	0.138
	34	100	0.995	0.005		34	100	1.000		34	100	0.890	0.110
	35	100	1.000			35	100	1.000		35	100	0.950	0.050
	36	100	0.990	0.010		36	100	1.000		36	100	0.940	0.060
	37	100	1.000			37	100	1.000		37	100	0.955	0.045

Appendix B
Recently discovered allozyme variability

Two monomeric mitochondrial loci of aconitate hydratase, mAH-1 and mAH-4, are polymorphic in chinook salmon. The *mAh-1(65)* allele was observed primarily in coastal California samples, although it is also present in the Sacramento system. Three alleles at mAH-4 were important in differentiating coastal and inland samples. Shaklee et al. (Wash. Dep. Fish., Olympia, WA 98504, pers. commun., Feb 1991) have recently performed breeding studies which confirmed the Mendelian model of inheritance for these loci.

Iditol dehydrogenase is coded by two loci in liver tissue. The enzyme is a tetramer for which both loci are assumed to be polymorphic. Variants were assigned to a particular locus based on relative staining intensities. The *Iddh-1(0)* allele was observed in Oregon and coastal northern California populations. The *Iddh-2(61)* allele was observed throughout the study area except in samples from the Sacramento system, whereas the *Iddh-2(20)* allele was only observed in the Sacramento samples.

Variation in NADP-dependent malate dehydrogenase was expressed at two cytosolic loci using chinook salmon muscle and heart tissue. MDHP-2 is also expressed in liver and eye tissue in juvenile fish. MDHP-1 variation has been described by Shaklee et al. (1990b). Due to the low levels of variability found in the Klamath–Trinity system, these MDHP loci wil be extremely important in the identification of fish from this area. The *Mdhp-2(78)* allele has nearly the same mobility as the *Mdhp-1(100)* allele, thus making identification of heterozygous samples difficult.

A duplicated and highly polymorphic monomeric PGM locus was designated by two loci, PGM-3 and PGM-4. These isoloci present particular difficulties when estimating allele and genotypic frequencies (Robin Waples and Paul Aebersold, NMFS Northwest Fish Sci. Cent., Seattle, WA 98115, pers. commun., June 1990). Six alleles have been identified in this system and several individuals with three and four different alleles were observed. Therefore, standards are required for correct analysis of banding patterns. Similar expressions of variants are seen in both liver and eye tissues. Conformance to Hardy-Weinberg proportions at these loci has been found using goodness-of-fit tests of expected and observed genotypes (Waples and Aebersold, pers. commun.) and a protocol for estimating allele frequencies from isoloci was presented by Waples (1988).

Triosphosphate isomerase is coded by four loci in chinook salmon. The products of TPI-1 and TPI-2 migrate cathodally, and those of TPI-3 and TPI-4 migrate anodally. Two variant alleles, *Tpi-3(104)* and *Tpi-3(106)*, were observed from eye tissue, and TPI-4 variation has been described by Shaklee (pers. commun.). Because *Tpi-3(106)* migrates close to *Tpi-4(100)*, only fish homozygous for the *Tpi-3(106)* allele can be

reliably scored. The *Tpi-3(106)* allele was observed in California coastal samples and samples from the Eel River.

The newly discovered alleles, *Ldh-1(800)*, *Mpdh-2(78)*, and *Tpi-3(106)*, could be visualized only in their homozygous form. If these alleles occur at low frequencies in samples of chinook salmon, they may not be detected because of the low probability of sampling the rare homozygote. This may account for the discontinuous distribution observed for some of these alleles (Appendix A). Consequently, *Ldh-1(800)* may be present at low frequency in more than just four samples.

Fecundity, spawning, and maturity of female Dover sole *Microstomus pacificus*, with an evaluation of assumptions and precision

J. Roe Hunter
Beverly J. Macewicz
N. Chyan-huei Lo
Carol A. Kimbrell

Southwest Fisheries Science Center, National Marine Fisheries Service, NOAA
P.O. Box 271, La Jolla, California 92038

Abstract.—The potential annual fecundity of Dover sole becomes fixed before the spawning season when the average diameter of the advanced stock of yolked oocytes exceeds 0.86 mm; hence potential annual fecundity is determinate. More central California females had atretic advanced oocytes than Oregon females, but rates of atresia were not sufficiently high to have an important effect on the potential annual fecundity of the population. A 1-kg female matured about 83,000 advanced yolked oocytes at the beginning of the season. Vitellogenesis continued for the advanced yolked oocytes during most of the spawning season while batches were repetitively matured and spawned. About nine batches were spawned over a six-month spawning season (December–May), and spawning ceased when the standing stock of advanced oocytes was exhausted. A 1-kg female released about 10,000 eggs per spawning, except for the first and last batches which were smaller than the rest. Near the end of the season, females may spawn more frequently than earlier in the year, increasing the daily production of eggs by the population even though fewer females are reproductively active. Annual reproductive effort of Dover sole was equivalent to about 14% of body wet weight per year. Fifty percent of the females had become sexually mature when they reached 332 mm total length.

Various methodological issues were also treated in this paper, including validation of key assumptions underlying estimates of annual fecundity; fecundity sample-size requirements; evaluation of criteria and bias in estimating female sexual maturity; and comparisons of classification by histology and gross anatomy.

Manuscript accepted 15 January 1992.
Fishery Bulletin, U.S. 90:101–128 (1992).

Fecundity and sexual maturity estimates are staples of fishery science. Inevitably, they will be estimated for every species of economic consequence because of their importance in the dynamics of the population. A second reason for studying fecundity is that when fecundity estimates are combined with estimates of the abundance of eggs in the sea, they can be used to estimate the biomass of a stock. Our laboratory is currently evaluating such ichthyoplankton methods for estimating the biomass of Dover sole *Microstomus pacificus*, a large demersal resource occurring along the upper continental slope of the west coast of North America. The fecundity of Dover sole from Oregon has been estimated (Yoklavich and Pikitch 1989), but no estimate exists for the segment of the stock living in central California waters, nor have the assumptions underlying fecundity and sexual maturity assessments been studied with the thoroughness necessary for accurate estimates of adult biomass. Thorough analysis of these assumptions is usually lacking in the fecundity literature.

Our objectives were to describe the reproduction of Dover sole off central California and Oregon, and evaluate the assumptions underlying fecundity and sexual maturity estimates. We describe changes in the reproductive state of female Dover sole during the spawning season, estimate annual fecundity, batch fecundity, rates of atresia, annual rates of spawning, and length at 50% mature (ML_{50}).

Evaluation of the assumptions underlying annual fecundity estimates requires defining six fecundity terms, and those underlying maturity estimates require defining four terms for reproductive state.

Fecundity

Annual fecundity Total number of eggs spawned by a female per year.

Total fecundity Standing stock of advanced yolked oocytes.

Potential annual fecundity Total advanced yolked oocytes matured per year, uncorrected for atretic losses. In species with determinate fecundity, potential annual fecundity is considered to be equivalent to the total fecundity prior to the onset of spawning.

Determinate fecundity Annual fecundity is determinate when the potential annual fecundity becomes fixed prior to the onset of spawning. In fishes with determinate fecundity, total fecundity decreases with each

spawning because the standing stock of advanced yolked oocytes is not replaced during the spawning season.

Indeterminate annual fecundity Annual fecundity is indeterminate when the potential annual fecundity of a female is not fixed prior to the onset of spawning and unyolked oocytes continue to be matured and spawned during the spawning season.

Batch fecundity Number of hydrated oocytes released in one spawning; usually determined by counting the number of hydrated oocytes in the ovary.

Relative fecundity Fecundity divided by female weight.

Reproductive states

Active Females capable of spawning at the time of capture or in the near future (by the end of the survey or of a season, or other temporal end point). Ovaries of active females contain sufficient number of yolked oocytes for a spawning.

Inactive Females not capable of spawning at the time of capture nor in the near future, although some may have been mature in the past.

Mature Females that have spawned in the current reproductive season or can be expected to do so.

Immature Females that have not spawned in the current reproductive season nor can be expected to do so.

The central methodological issue in fishes with determinate fecundity (Hunter and Macewicz 1985a, Horwood and Greer Walker 1990) is to establish that potential annual fecundity is an unbiased estimate of annual fecundity. For this to be true in Dover sole requires four key assumptions. The first and most important assumption is that fecundity is determinate in Dover sole. This means that potential annual fecundity becomes fixed before spawning begins. Estimation of the standing stock of advanced oocytes (total fecundity) is meaningless if, during the spawning season, oocytes are added to that stock.

The second assumption is that the potential annual fecundity is equivalent to annual fecundity. Strictly speaking, this probably never happens because in any fish population some of the females resorb some of their advanced yolked oocytes rather than spawn them, a process known as atresia. If many females resorbed many of their advanced oocytes, potential annual fecundity would be a serious overestimate of annual fecundity in the population. In addition, not all ovulated oocytes are spawned; a few remain in the ovigerous folds of the ovary after spawning and are later resorbed. Retention of ovulated oocytes is probably seldom a serious bias.

The third assumption is that the females used to estimate potential annual fecundity have not spawned during the current reproductive season. Dover sole females that have spawned some of their stock of advanced oocytes cannot always be distinguished from those that have not begun spawning. Inclusion of partially spawned females in an estimate of potential annual fecundity of the population could be a significant bias.

The fourth assumption is that one is able to identify with certainty the oocytes that constitute the potential annual fecundity. An ovary may not be sufficiently developed to identify all of the oocytes destined to be spawned. On the other hand, if the ovary is highly advanced, spawning may have begun and some advanced oocytes lost. Clearly, an optimal range of ovarian development exists where these risks are minimized.

In addition to evaluating the above four assumptions (determinate fecundity, atresia, spawning, and immaturity) we consider several other methodological issues related to assessment of fecundity and female sexual maturity. These issues are (1) validation of our gross anatomical and histological classification of ovaries into active or inactive and mature or immature states; (2) four precision issues related to total fecundity estimates (number of tissue samples per ovary, number of females, location of ovarian tissue samples, and within-trawl and between-trawl variance); and (3) an evaluation of bias in the assessment of female sexual maturity.

Methods

Collections and shipboard measurements

Dover sole were collected along the central California coast (Point Conception to San Francisco Bay) during six research trawl cruises (Table 1). Dover sole were taken off the Oregon coast between Cape Lookout and Heceta Head during two cruises in 1988–89; miscellaneous collections provided by E. Pikitch off the Oregon coast in 1985 and 1986 were also used. Research trawls were one-half hour or one hour long, depending on depth. In central California waters, we used a 400-mesh Eastern trawl (mouth opening ~15 m wide and 1.5 m high; Wathne 1977). In Oregon waters, either an Alaska Fisheries Science Center (AFSC) modified 5-inch mesh, 90/120, high-rise "poly Nor'Eastern" trawl (fishing dimensions ~4.6 m high and 13.5 m wide at wing tips), a 5-inch mesh, 92/83, poly Nor'Eastern trawl, or a 5½-inch mesh, 75/90, high-rise Aberdeen trawl was used. Up to 100 Dover sole from

Table 1

Sources of reproductive data on female Dover sole *Microstomus pacificus*. Number of specimens in three levels of ovarian analysis and number of level-3 females with batch fecundity estimates.

Sampling protocol				Levels of ovarian analysis**				
Date (Begin/End)	State	No. positive trawl collections	Selection of females*	1	2	3	Total	Batch fecundity
				(no. females)				
3 Dec 85 – 12 Dec 85	CA	11	A	–	39	65	104	–
4 Nov 85 – 14 Dec 85	OR	4	Unknown	–	73	–	73	–
6 Feb 86 – 7 Feb 86	OR	3	Unknown	–	37	–	37	–
3 May 86	OR	2	Unknown	–	27	–	34	7
5 Mar 86 – 7 Mar 86	CA	8	A	1	135	3	139	–
2 May 86 – 4 May 86	CA	3	A	–	59	1	60	–
11 Jan 87 – 24 Jan 87	CA	27	B	45	387	103	535	–
5 Feb 87 – 15 Feb 87	CA	22	B	14	391	92	500	3
23 Feb 88 – 9 Apr 88	CA	51	C	1716	120	62	1941	43
28 Nov 88 – 14 Dec 88	OR	53	C	667	620	152	1439	–
21 Feb 89 – 31 Mar 89	OR	21	C	104	151	34	292	3
All Oregon		83		771	908	186	1875	10
All California		122		1776	1131	326	3279	46***
Oregon + California		205		2547	2039	512	5154	56***

*A = Random selection of both females and males until 25 females were collected.
B = Selection stratified by length (N 5) in <275 mm class, 10 in 275–424 mm class, and 10 in ≥425 mm.
C = Random selection of ≤100 fish (either females or males).
**Level 1 = gross anatomical; Level 2 = histological with anatomical; Level 3 = total fecundity with anatomical and histological.
***Five females with hydrated oocytes provided by W.W. Wakefield were included in estimate of batch fecundity.

each trawl haul were measured (total length) to the nearest millimeter, sexed, and their gonads classified; some females immediately after capture were also individually weighed to the nearest gram and their ovaries preserved in 10% neutral buffered formalin. Females selected for ovarian preservation were either taken randomly from the trawl catch or selected by length according to a quota for each of three length classes (<275 mm, 275–424 mm, and ≥425 mm) (see Table 1). The preserved ovaries were used to validate our shipboard classification of ovaries, to estimate fecundity, and to provide material for histological descriptions.

Gross anatomical classification of ovaries

Ovaries that were examined onboard the ship were assigned to one of three classes: no yolked oocytes present; yolked oocytes present; and translucent hydrated oocytes present. Ovaries with hydrated oocytes or other yolked oocytes were considered to be in the active state, while those ovaries in which observers saw no yolked oocytes were considered to be in the inactive state. This simple system based on gross anatomical examination of the ovary is more germane for biomass estimation work than are the more complicated systems which involve many more reproductive stages: for example, the seven-stage scale of Hjort (1910), or the five-stage scale of Hagerman

(1952). Eighty percent of the females that we classified using gross anatomical criteria were also classified as active or inactive using histological criteria. The results were compared to determine the accuracy of identifying active and inactive females by gross anatomical classification.

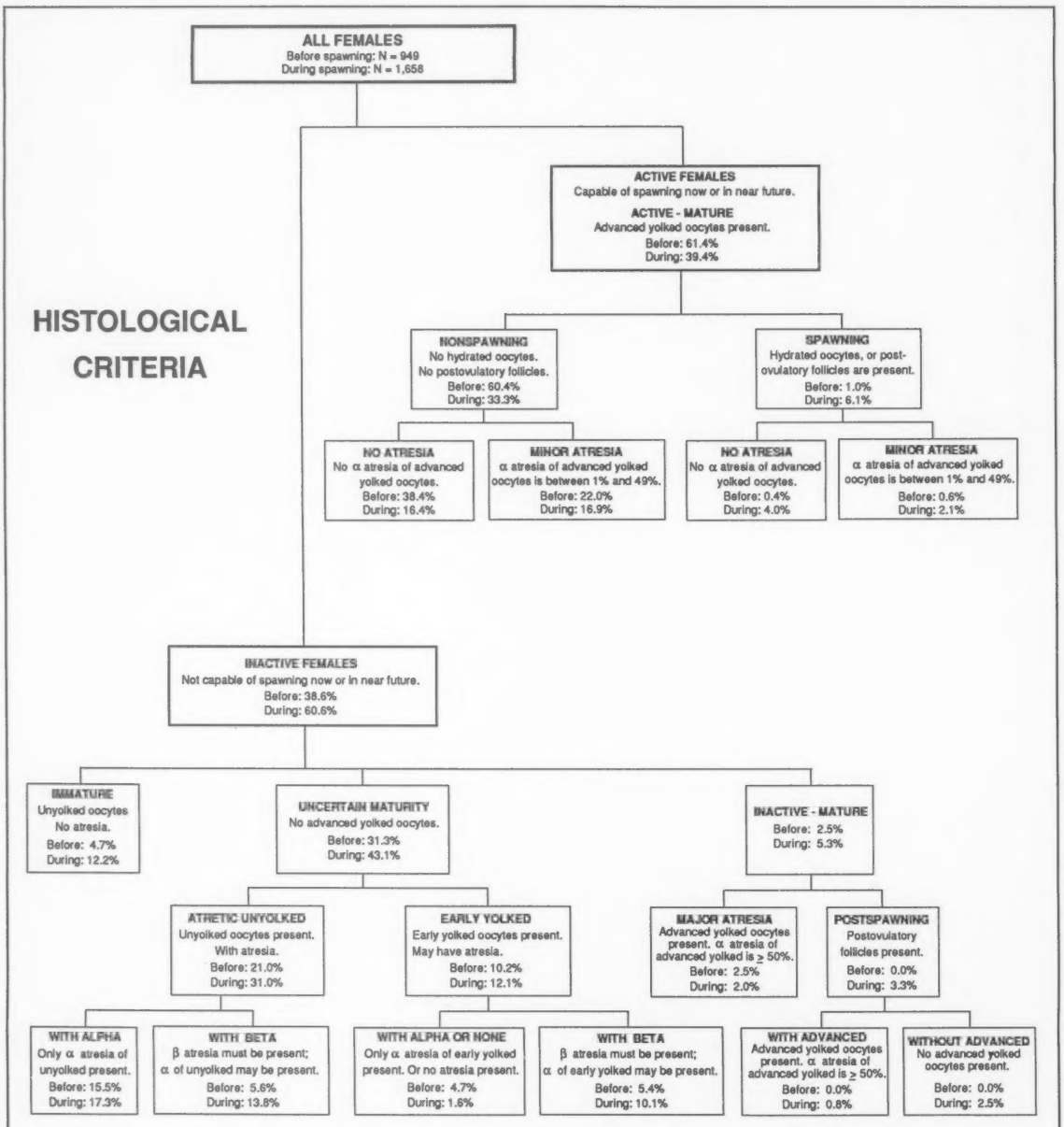

Figure 1

Dendrogram illustrating hierarchial classes of histological criteria of active and inactive ovaries of Dover sole *Microstomus pacificus*. Percentages of females (California and Oregon combined) in each class and subclass taken before (November–December) and during (January–May) the spawning season.

Histological methods

All of the preserved ovaries, regardless of development, had a piece removed for histological analysis. The pieces were dehydrated and then embedded in Paraplast. Subsequently histological sections were cut at 5–6 μm and stained with Harris hematoxylin followed by eosin counterstain (H&E). Each ovary was classified histologically in the manner developed for northern anchovy *Engraulis mordax* by Hunter and Goldberg (1980) and Hunter and Macewicz (1980, 1985ab), with a few modifications appropriate for Dover sole ovarian structure. In the ovary we identified the presence or absence of the following: oocytes that have not begun vitellogenesis; oocytes in the first vitellogenic stages (0.15–0.55 mm diameter); advanced yolked oocytes (0.47–1.4 mm diameter) noting any stages of nucleus migration (precursor to hydration); hydrated oocytes; two stages of postovulatory follicles; and the different stages of atresia. The rate at which postovulatory follicles are resorbed in Dover sole is unknown. Hence no ages were assigned to postovulatory follicles.

Histological classification

We used histological analysis of the ovaries to assess the accuracy of our gross anatomical classification into active and inactive states, to define the optimal criteria for distinguishing mature from immature females, and to calculate various indices of spawning activity and postspawning states. The dendrogram (Fig. 1) indicates the histological characteristics used to classify ovaries into active and inactive states. The dendrogram also gives the frequency of the classes in each state for the prespawning period (November–December) and for the spawning season (January–May) using combined data from California and Oregon. The data are also given by cruise and region in Table 2.

Females were classed as active when histological analysis indicated that the ovary contained the sufficient number of advanced yolked oocytes for one spawning. Active females were then separated into spawning and nonspawning classes using additional histological criteria. Spawning females were those which showed histological evidence of past spawning

Table 2

Numbers of female Dover sole *Microstomus pacificus* in various histological subclasses. Listed by location, before or during the spawning season, and mean cruise date (year and month).

		Inactive										Active				
	Immature	Uncertain maturity							Mature			Mature				
		Atretic unyolked			Early yolked				Major atresia	Postspawning		Nonspawning		Spawning		
		Atresia present			No atresia	Atresia present				Advanced yolk		No atresia	Minor atresia	No atresia	Minor atresia	
Cruise		α only	β only	α and β		α only	β only	α and β		With	Without					All females
Oregon																
Before																
8512	1	4	0	9	0	0	2	9	5	0	0	20	23	0	0	73
8812	32	133	2	37	5	37	4	34	15	0	0	316	150	3	4	772
During																
8602	0	1	0	9	0	0	2	3	4	0	0	6	12	0	0	37
8903	23	70	2	16	1	3	7	18	2	1	3	24	14	3	1	188
8605	1	0	3	4	0	0	5	3	0	4	2	0	0	9	3	34
Total	57	208	7	75	6	40	20	67	26	5	5	366	199	15	8	1104
California																
Before																
8512	12	10	1	4	0	3	0	3	4	0	0	28	36	1	2	104
During																
8701	56	65	11	32	0	7	3	37	11	0	0	115	138	6	9	490
8702	43	99	8	70	2	11	7	36	10	0	1	91	86	12	10	486
8603	38	24	8	40	0	1	7	4	3	3	7	1	2	0	0	138
8803	30	18	4	11	0	4	14	17	3	4	15	31	28	35	11	225
8605	12	9	3	7	2	1	5	0	0	1	13	4	0	2	1	60
Total	191	225	35	164	4	27	36	97	31	8	36	270	290	56	33	1503

(postovulatory follicles present) or imminent spawning (hydrated oocytes or migratory nucleus-stage oocytes present), while the ovaries of nonspawning females showed no evidence of recent or imminent spawning but were capable of spawning in the near future. The fraction of active females classed as spawning was used as a spawning rate index. Spawning performance was also assessed by calculating the mean number of spawning states (postovulatory follicles, hydrated oocytes, migratory nucleus) per female in the spawning class.

Females with ovaries classified as active are considered mature. On the other hand, females with inactive ovaries could be either immature or mature because an ovary may have regressed to an inactive state after the female had attained sexual maturity. We designed our histological classification of inactive ovaries to distinguish as best as possible between mature and immature conditions. Inactive females were grouped into three classes (Fig. 1): immature, uncertain maturity, and inactive-mature. The inactive-mature class included ovaries showing clear histological evidence of past spawning (postspawning subclass) or past maturation of advanced yolked oocytes (major-atresia subclass). Postspawning ovaries contained either postovulatory follicles and no advanced yolked oocytes or postovulatory follicles and mostly atretic advanced yolked oocytes. The fraction of inactive females identified as postspawning was used as an index of the rate at which females passed from the active to the inactive state during the spawning season.

The five major histological classes of active and inactive females were subdivided into atretic subclasses using the first (α) and second (β) stages of resorption as defined by Bretschneider and Duyvene de Wit (1947) and Lambert (1970). One can identify the developmental stage of the oocyte only during the α stage of atresia because the oocyte is completely absorbed by the end of this stage. Subsequent stages (β, γ and δ) involve the resorption of the follicle. Thus, α atresia is of key importance to fecundity studies since the oocyte class can be identified. Subsequent stages may be useful for identifying past spawning activity.

For ovaries containing early yolked or only unyolked oocytes, classification was based solely on presence or absence of the following atresia: β, α of unyolked oocytes, and α of early yolked oocytes (classes immature and uncertain maturity of the inactive females) (Fig. 1).

Ovaries with advanced yolked oocytes were subdivided into two atretic subgroups using the extent of the α atresia of the advanced yolked oocytes: minor atresia, i.e., females with one oocyte to 49% of their advanced yolked oocytes in α; and major atresia, i.e., 50% or more of the advanced yolked oocytes in α. We showed in anchovy that the probability of spawning was very low when more than 50% of the advanced oocytes were atretic (Hunter and Macewicz 1985b). Therefore, ovaries with major atresia of advanced yolked oocytes were considered inactive (inactive-mature class) although the ovary contained some advanced yolked oocytes.

Estimation of total fecundity

We used the gravimetric method to estimate total fecundity of Dover sole. Total fecundity (Y_F) was the standing stock of advanced yolked oocytes in the ovary: $Y_F = Z \cdot C$, where Z is the ovary weight in grams, and C is oocyte density (number of advanced yolked oocytes per gram of ovarian tissue). We also measured diameters of 30 of the advanced yolked oocytes in at least one of the 2–5 tissue samples analyzed for each female for which fecundity was estimated. Advanced yolked oocytes were identified, counted, and measured using a digitizer linked by a video camera system to a dissection microscope.

We used the apparent density of yolk in whole oocytes after preservation, when viewed on the television monitor, to discriminate between developmental stages of yolked oocytes. We defined three stages of yolked oocytes: (1) only an initial layer of yolk along the periphery of the oocyte, appearing as a narrow band but not extending over 20% of the distance between the nucleus and the zona pellucida; (2) lightly-packed yolk possibly extending from the periphery to the nucleus with the nuclear area still evident; and (3) yolk dense enough to occlude the nucleus (Fig. 2) which is histologically equivalent to advanced yolked oocytes. Counts of stage-3 oocytes were used to estimate fecundity and measurements to estimate mean diameter of these advanced yolked oocytes.

Alpha atresia of stage-3 yolked oocytes were distinguished from other whole oocytes viewed on the television screen. The yolk within these α-atretic stage-3 oocytes appeared mottled and lighter due to yolk liquefaction and subsequent resorption, whereas in normal yolked oocytes it appeared dense, dark, and in compact globules (Fig. 2). In addition, the zona radiata (chorion, or membrane layers surrounding the oocyte) of the atretic oocytes was indistinct and irregular in appearance. It was not possible to accurately identify atretic oocytes in frozen, thawed, or poorly preserved ovaries. Atretic oocytes were not included in counts of advanced yolked oocytes used to estimate fecundity. To estimate rates of atresia, we recorded the number of α-atretic yolked oocytes in the random sample of 30 stage-3 oocytes measured. The number of α-atretic advanced yolked oocytes divided by 30 was used as an index of the intensity of atresia in all females used for fecundity estimation.

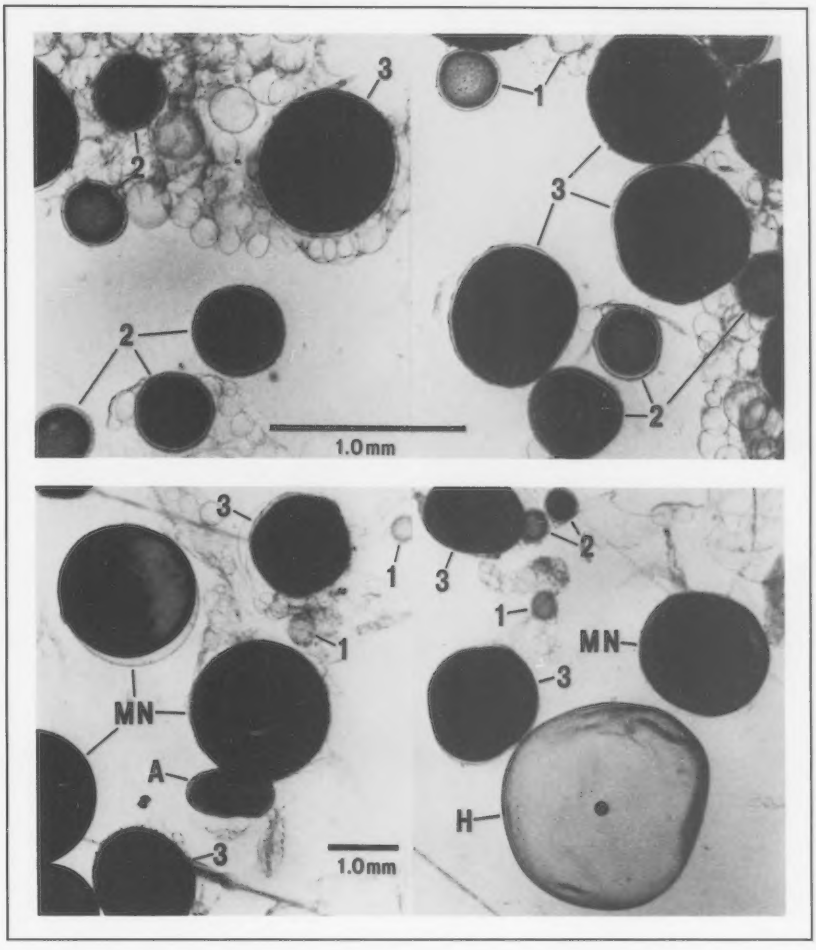

Figure 2
Three stages of preserved whole yolked oocytes of Dover sole *Microstomus pacificus* (stages defined in text). Lower panel also shows migratory nucleus (MN) oocytes, a hydrated (H) oocyte, and an α-atretic advanced yolked oocyte (A). The small air bubble on the hydrated oocyte is an artifact.

Batch fecundity

Batch fecundity was considered to be the number of migratory nucleus-stage oocytes or number of hydrated oocytes in the ovary. We used the gravimetric method to estimate numbers of these oocytes. Migratory nucleus-stage and hydrated oocytes stand out as discrete and easily identified oocyte maturity-classes (Fig. 2). Hydrated ovaries that contained new postovulatory follicles were not used to estimate batch fecundity.

We assigned each spawning batch to one of a possible five batch-order designations [1, 2, $(2<B<U-1)$, $(U-1)$, and U], where B is the batch-order number and U is the total number of spawning batches. The five batch-order designations were defined as follows: first batch (where $B=1$), nonhydrated, advanced yolked oocytes present and postovulatory follicles absent; second batch (where $B=2$), one class of postovulatory follicles and nonhydrated, advanced yolked oocytes present; intermediate batches (where $B>2$ but less than $U-1$), two classes of postovulatory follicles and nonhydrated, advanced yolked oocytes present; the penultimate batch ($U-1$), only two batches were present, one of hydrated and one of migratory nucleus oocytes, with no other advanced yolked oocytes present; and last batch (U), no advanced yolked oocytes present other than a single hydrated batch.

In this classification scheme, we assumed that (1) the presence of a single class of postovulatory follicles indicated one spawning had occurred; (2) the presence of two classes indicated at least two spawnings had occurred; and (3) the absence of postovulatory follicles indicated no spawning had occurred. The assumption of no spawning would not hold if the interval between spawnings was sufficiently long for postovulatory

follicles to be resorbed. We used this batch-order classification system to determine if batch fecundity varied with the order of the spawnings, as it does in some species (Alheit 1986, Hunter et al. 1989).

Estimation of length at 50% mature

We estimated the total length (mm) of female Dover sole when 50% had become mature using histological criteria. The fraction of females considered to be mature was estimated for 10 mm or for 50 mm length-classes, and the data were fit to a logistic curve (Dixon et al. 1988). We estimated the maturity threshold for females taken off central California and off Oregon, before and during the spawning season. In our analysis, we evaluated the extent to which changes in histological criteria affected the maturity estimate using six sets of histological criteria: (1) advanced yolked

Table 3

Conversion equations for Dover sole *Microstomus pacificus* by state, sex, or season.

Frozen to fresh for length and weight

Variable				Linear equation Y = a + bX					
Dependent Y	Independent X	State	Sex	a	b	r^2	F	N	Range of independent variable
Fresh length	Frozen length	Cal	All	9.47	1.01	0.99	25,550	251	196–512 mm
Fresh weight	Frozen weight	Cal	All	0*	1.22	—	10,229	111	54–1551 g
Fresh weight**	Frozen weight**	Cal	F	0*	1.29	—	19,575	147	76–1263 g

Length to weight

Variable				Exponential equation $W = aL^b$					
Dependent W	Independent L	State	Sex	a	SE	b	SE	N	Range of independent variable
Fresh weight (g)	Fresh length (cm)	Cal	F	0.00198	0.00011	3.45	0.016	1245	11.8–54.7 cm
		Cal	M	0.00173	0.00018	3.49	0.029	264	18.5–47.8 cm
		Cal	Unknown					4	12.8–23.5 cm
		Cal	F, M	0.00198	0.00009	3.45	0.013	1509	11.8–54.7 cm
		Ore	F	0.00141	0.00013	3.53	0.026	991	18.8–57.7 cm
		Ore	M	0.00156	0.00015	3.51	0.027	457	20.0–52.2 cm
		Ore	All	0.00159	0.00011	3.50	0.018	1448	18.8–57.7 cm
Fresh weight** (g)	Fresh length (cm)	Cal	F	0.0038	0.00048	3.27	0.033	1198	11.8–54.7 cm
		Ore	F	0.0012	0.00026	3.58	0.056	430	26.8–56.4 cm

Female weight and oocyte volume to ovary weight

Variable				Linear equation $Y = a + bX_1 + cX_2$						
Season	Dependent Y	Independent X_1	Independent X_2	State	a	b	c	r^2	F	N	Range of independent variable
Prespawning	Ovary weight (g)	Fish weight** (g)		Ore	9.07	0.013		0.09	38.9	388	122–2017 g
	Ovary weight (g)	Fish weight** (g)	Spher. vol.*** (mm^3)	Cal	−4.67	0.027	37.7	0.54	17.9	30	202–1124 g 0.33–0.70 mm^3
				Ore	−34.05	0.036	95.3	0.59	45.85	64	236–1816 g 0.33–0.59 mm^3
				Cal+ Ore	−26.06	0.036	76.3	0.59	68.2	94	202–1816 g 0.33–0.70 mm^3
Spawning	Ovary weight (g)	Fish weight** (g)		Cal	−7.05	0.032		0.41	826.7	1198	14–1736 g
				Ore	21.79	0.010		0.07	4.2	42	148–1597 g
				Cal+ Ore	−5.88	0.031		0.39	788.0	1240	14–1736 g

* Intercept not different from 0, line forced through origin.
** Without ovary.
*** Spherical volume = $4/3\pi r^3$; for mean oocyte diameters ≥0.86 mm.

oocytes or postovulatory follicles present; (2) early yolked oocytes with β atresia; (3) early yolked oocytes with only α atresia of the early yolked oocytes or no α or β atresia; (4) unyolked oocytes with β; (5) unyolked oocytes with only α of the unyolked oocytes; and (6) unyolked oocytes with no atresia. The sexual maturity for females identified by criterion 1 is certain, but some females may be excluded if only criterion 1 is used. Criteria 2–5, if added to criterion 1, broaden the maturity definition but increase the risk of misclassification. Criterion 6 is considered by definition to be immature. We evaluated these criteria to determine the optimal histological definition of maturity using a regression analysis of the lengths of females identified by each criterion.

Length, weight, and gonad weight relationships

To enable the reader to convert from one measurement to another, equations are provided to estimate fresh wet weight from frozen wet weight and from length for Dover sole taken in Oregon and central California waters (Table 3). Analysis of covariance indicated that the slope of the regression of the natural logarithms of weight on length did not differ between sexes for either state. The adjusted group mean for males differed from that for females in Oregon (N 1421, $F_{1,1418}$ 64.87, $P<0.005$ for length range 225–522 mm) but not in California. The slope of the regression of the natural logarithms of weight on length did not differ between central California and Oregon females but the adjusted group means were different (N 2215, $F_{1,2212}$ 79.18, $P<0.005$ for length range 188–547 mm). No difference existed between states in the equations for males. We do not attach too much biological importance to these differences; they could be related to differences in the timing of annual reproductive cycle or our sampling of it. Nonetheless, it seemed preferable to use the relationship for a specific sex or region, so all are listed.

An exponential model was fit to these data sets using a statistical program of weighted nonlinear regression (Dixon et al. 1988) where the weighting factor was the inverse of the variance of fish weight because the variance of fish weight increased with fish length. To compute the variance, fish lengths were divided into several segments, chosen so that within each segment the variance of fish weight was homogeneous. We preferred to obtain the estimates of coefficients directly from the nonlinear fitting so that fish weight could be directly estimated from the exponential model (Table 3).

Freezing of Dover sole caused a 9.47 mm shrinkage in total length, independent of fish length (Table 3). A sample of 251 Dover sole was measured just after capture and again, after thawing, four months later. The slope of the regression of fresh total length on frozen total length (after thawing) was not statistically different from 1, but the intercept, 9.47 mm, was significant. Freezing of females, with ovary removed, resulted in about a 22% loss in wet weight ($0.22 = 1 - \frac{1}{1.29}$; see Table 3).

We also provided equations to estimate ovary wet weight (g) from female wet weight (g, without ovary). This conversion is important if one wishes to express fecundity as a function of the total weight of the female, because all fecundity relations in this study are expressed as a function of female weight without an ovary. As ovary weight is a function of the developmental state of the ovary as well as the weight of the female, separate equations are provided for the prespawning period (November–December) when ovaries are less developed and for the spawning season when they are more fully developed. We also provided multiple regression equations to estimate ovary weight from female weight and the spherical volume of the average advanced yolked oocyte (computed from the mean diameter). These equations are used in the discussion to estimate ovary weight when an ovary contains an entire complement of fully matured advanced yolked oocytes.

Reproductive condition

Accuracy of gross anatomical classification

We rarely misclassified inactive ovaries using gross anatomical criteria. Of the 1272 females classified as inactive, only 14 (1.1%) were identified as active using histological criteria. This error rate is so low that differences could be attributable to clerical errors alone. A more common error in gross anatomical classification was to misclassify females as having active ovaries. One hundred and fifty-nine females (11.9%) were visually classified as having advanced yolked oocytes and were believed to be capable of spawning, while histological analysis indicated that their ovaries were inactive and future spawning was unlikely. The 159 females misclassified as active fell predominantly into two classes: females with ovaries in the early stages of vitellogenesis (40.8%), and females with advanced yolked oocytes with high levels of atresia (30.1%) (Table 4).

Misclassification of the early stages of vitellogenesis as active is expected because the gross anatomical criterion, "yolked oocytes visible," is not exact; observers are bound to differ on whether to include or exclude females that fall near the visible threshold

Table 4

Histological classification of female Dover sole *Microstomus pacificus* with inactive ovaries that were misclassified using gross anatomical criteria as having active ovaries. Data from central California and Oregon are combined.

Collection period	Percentage of females misclassified as active per inactive histological class					Total no. misclassed females
	Immature	Unyolk atretic	Early yolked	Major atresia of adv. yolked	Post-spawning	
Nov–Dec	0.0	2.0	48.9	48.9	0.0	49
Jan–May	4.5	23.6	37.2	21.8	12.7	110
Nov–May	3.1	17.0	40.8	30.1	8.8	159

for detection of yolked oocytes in the ovary. An exact criterion, such as oocyte diameter, would be more accurate but would be impractical for production work on the ship. Misclassification of highly atretic ovaries as active is also expected, since α-atretic advanced yolked oocytes are difficult if not impossible to see with the unaided eye. As highly-atretic advanced ovaries were rare in this study, our failure to detect them was a minor systematic error. Under environmental conditions unfavorable to reproduction, however, this could be an error of consequence.

Changes in ovarian condition during the spawning season

The fraction of females anatomically classed with active ovaries

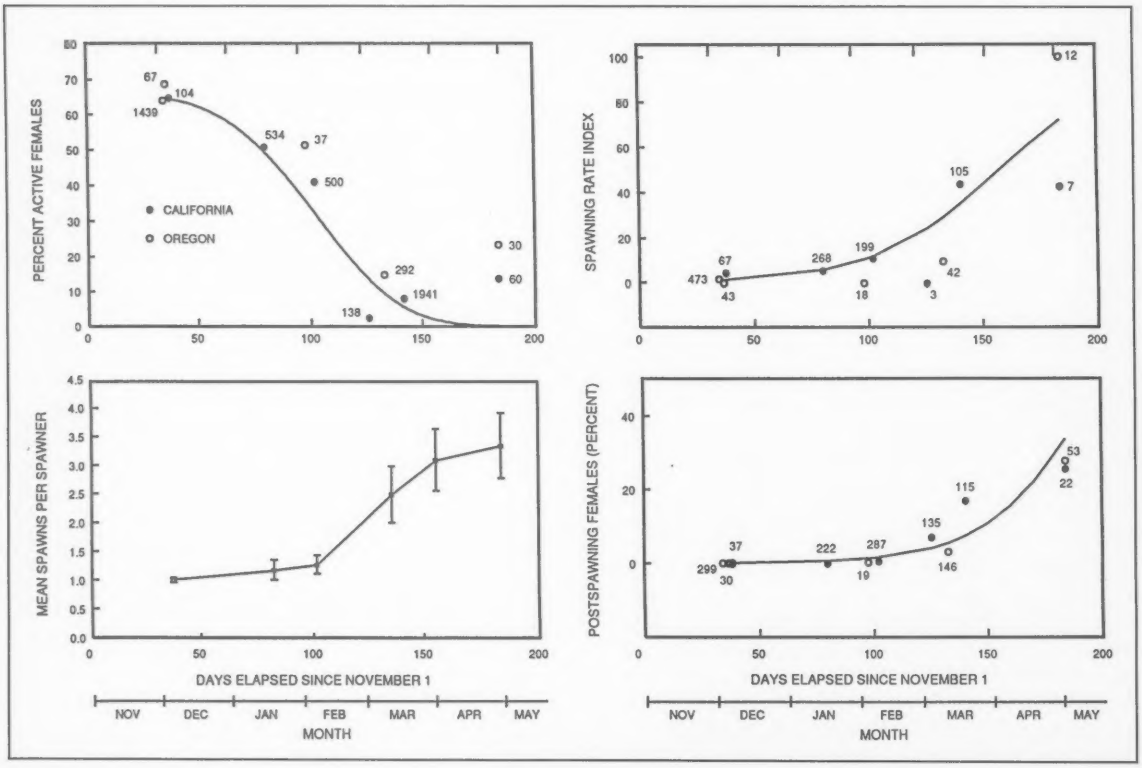

Figure 3 (below)

Seasonal change in four indices of reproduction in Dover sole *Microstomus pacificus*. Indices are plotted as a function of elapsed time since 1 November; data are combined from different years; California (solid circles) and Oregon (open circles) data were combined to fit trend lines; numbers are the sample size of females. (upper left) Percentage of Dover sole with active ovaries; trend line is a weighted Weibull model (see text Eq. 1). (upper right) Percentage of females with active ovaries which had one or more spawning states; trend line is logistic model $P = \frac{e^{a+bL}}{1+e^{a+bL}}$, where a = −5.678 and b = 0.036. (lower left) Mean number of spawning states in active ovaries; bars are two standard errors of the mean. (lower right) Percentage of females with inactive ovaries identified as postspawning; trend line is logistic model where a = 8.495 and b = 0.042.

declined over the spawning season as females expended their stock of advanced yolked oocytes. We fitted a weighted Weibull function to the combined California and Oregon data, yielding the equation

$$P = 0.656\, e^{-\left(\frac{t}{111.5}\right)^{3.76}} \quad \text{(Eq. 1)}$$

where t is days elapsed since 1 November; P, the fraction active, is weighted by $\frac{N}{P(1-P)}$, and pseudo r^2 is 0.96. According to the equation, the percentage of females with active ovaries declined from 65% at the onset of the spawning season (about 6 December) to 40% by the end of January; by the end of February only 18% of the females had active ovaries (Fig. 3, upper left).

In California and Oregon, the mean diameter of the stock of advanced yolked oocytes increased steadily from December through April (Fig. 4). Thus reproductively active females continued vitellogenesis throughout most of the spawning season. By March or April the average advanced yolked oocyte is closer to the minimum size at which hydration begins (diameter 1.35 mm). Thus Dover sole may be able to spawn at a higher rate late in the spawning season, because less yolk would have to be added to the advanced oocytes for them to attain the size at hydration.

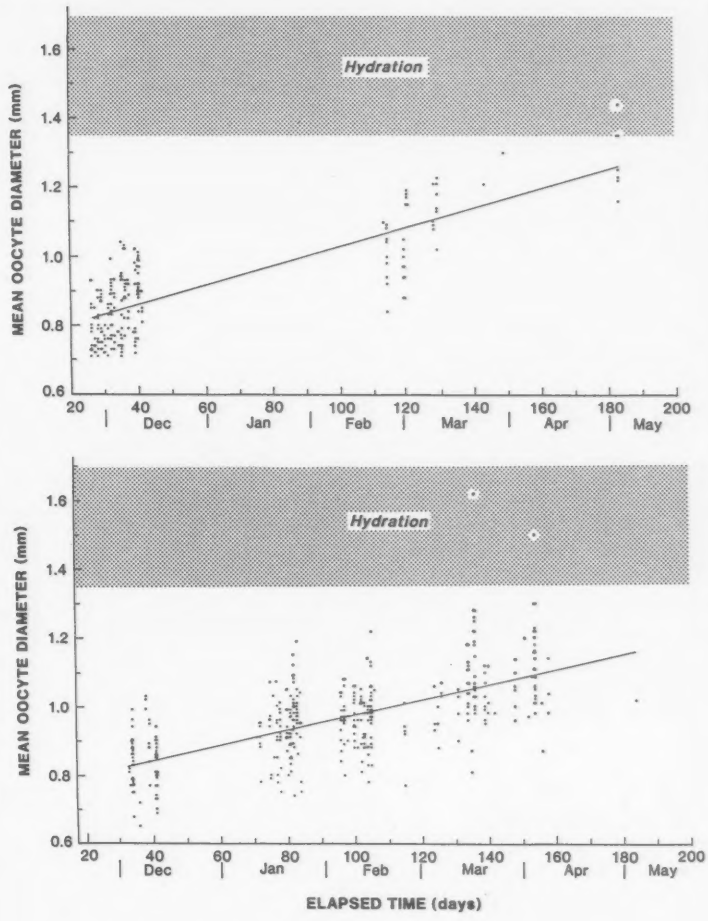

Figure 4

Increase in mean oocyte diameter (D) of the advanced yolked oocytes of Dover sole *Microstomus pacificus* from Oregon (top) and California (bottom) as a function of elapsed time (T) since 1 November. Data from different spawning seasons are combined; shaded area indicates size range of oocytes at the onset of hydration; trend lines are Oregon ($D = 0.742 + 0.00282T$, r^2 0.658, N 195) and California ($D = 0.761 + 0.0022T$, r^2 0.41, N 365).

Only 10 females taken in November–December were classed as spawning on the basis of their ovarian histology (Oregon and California data combined, N 949). They comprised only 1.0% of all females with preserved ovaries taken during this time and only 1.7% of those classed as active. Clearly, spawning is just beginning in November–December in California and Oregon waters. The spawning rate index increased from 1.3% in November–December to 12% by early February; it accelerated at the end of the season with spawning females comprising about 70% of all active females (percent calculated by the trend line in Fig. 3, upper right). Thus at the end of the season, most of the females with active ovaries had spawned recently. We believe this sharp increase in the index near the end of the season is evidence for a seasonal increase in spawning frequency.

A late seasonal increase also existed in the occurrence of multiple spawning stages within the same ovary. As many as five different past or potential spawning stages could be distinguished histologically in the same ovary: two stages of postovulatory folli-

cles, hydrated oocytes, migratory nucleus oocytes, and other advanced yolked oocytes. These data were expressed as the number of spawning states per spawner (spawns per spawner, Fig. 3, lower left). The average number of spawns per spawner increased from about one in mid-March to about three by early April. These data also indicated that spawning frequency may increase near the end of the spawning season.

The fraction of females with inactive ovaries that were classed as postspawning also increased late in the season (Fig. 3, lower right). This index can be considered a measure of the rate females in the population pass from the active to the inactive state. Although the duration of this stage was unknown, we were certain that it was ephemeral because there were always many fewer females classed as postspawning than the cumulative total of females that had passed from the active to inactive state. This index increased sharply in late-March through April, indicating that the rate females passed into the inactive stage accelerated during the last part of the season.

The sharp increases in the three indices described indicated that the daily production of eggs by the population may be higher in March than February even though fewer fish were spawning. For example, by mid-March (13 March), a half to a third as many females had reproductively active ovaries than in mid-February (10 Feb.). On the other hand, in mid-March as compared with mid-February, about twice as many females with active ovaries were classed as spawning, and the ovaries of the spawners contained evidence of about twice as many past or potential spawnings. Thus the reproductive output of the reproductively active females in the population in mid-March might be four times that of the active fish in mid-February. If this is true, half the number of active females could produce twice as many eggs per day. This is, of course, sheer speculation because the duration of these spawning stages is unknown. Nevertheless, the data presented in this section collectively suggest that the daily production of eggs by the population may increase near the end of the season even though fewer females are spawning.

Total fecundity

Location of tissue samples

A key assumption underlying the gravimetric method of fecundity estimation is that oocytes are randomly distributed in the ovary. To determine if advanced yolked oocytes are randomly distributed in the ovary, we compared the densities of advanced yolked oocytes in tissue samples taken from five different locations in the ovary of ten females. The location of a tissue sample within the ovary was defined in terms of three characteristics: longitudinal plane of the ovary (anterior end, middle, and posterior end); cross-sectional plane (interior near the lumen, exterior near the ovarian wall, or interior and exterior combined); and right and left lobes of the ovary. The characteristics of the five ovarian locations along with the mean oocyte density of each location are indicated in Table 5.

Initially we tested the overall effect of location of the tissue sample on oocyte density using two-way ANOVA; the effect of position was insignificant at the 5% level of significance (Table 5, lower). We also tested for possible differences between pairs of location characteristics: posterior end vs. middle; posterior vs. anterior ends of the ovary; right vs. left lobes of the ovary; and interior and exterior sections of the ovary. No significant differences were detectable between any of

Table 5

Effect of location of tissue samples within the ovary of Dover sole *Microstomus pacificus* on oocyte density (number of advanced yolked oocytes per unit sample weight) with mean and standard deviation (SD) and, below, two-way analysis of variance on results.

Position no.	Location in ovary of sample*			Oocyte density		
		Plane of section				
	Lobe	Long.	Cross.	*N*	Mean	SD
1	Rt	Post	Int & Ext	10	1803.7	468.1
2	Rt	Mid	Ext	10	1801.1	532.0
3	Rt	Mid	Int	10	1754.1	488.6
4	Rt	Ant	Ext	10	1886.1	440.2
5	Lt	Mid	Int	10	1839.3	537.6

Analysis of variance on five locations

Source	DF	SS	MS	*F*
Fish	9	10,379,034	1,153,226	
Position	4	96,638	24,160	1.373
Error	36	633,493	17,597	
Total	49	11,109,165		

*Long. = longitudinal, Rt = right lobe, Lt = left lobe, Post = posterior end, Mid = middle, Ant = anterior end, Int = internal, and Ext = external.

these four comparisons; F values ranged from 0.01 to 0.14, with the degrees of freedom being 1 and 45 for each comparison. Thus the advanced yolked oocytes in Dover sole are randomly distributed within the ovary, and tissue samples can be taken from any location or lobe without bias.

Optimal number of tissue samples

To develop a procedure for estimating the number of tissue samples needed for estimating total fecundity, we first considered the general fecundity model. The true total fecundity (Y_F) is the condition where all the advanced yolked oocytes in the ovary are counted, and the relation between female weight (W) and fecundity is defined as

$$Y_F = f(W) + A \qquad \text{(Eq. 2)}$$

where $f(W) = a+bW$, and A is the error term. The variance of A, σ^2_A, measures the deviation of the data set (Y_F, W) to the model f(W). As it was impractical to count all advanced yolked oocytes in the ovary, Y_F is estimated from counts of oocytes in weighed tissue samples, expressed as oocytes per gram of tissue or oocyte density. The precision of a fecundity estimate can be increased by increasing the number of tissue samples taken per female. On the other hand, if the amount of labor for fecundity work is fixed, then increasing the number of tissue samples per fish would reduce the number of fish that can be sampled. Thus we needed to know the minimum number of tissue samples necessary to guarantee a goodness-of-fit of the model to the data set.

We determined the optimum number of tissue samples by minimizing the variance of sample variance of A ($\sigma^2(s^2_A)$). This procedure led to using the ratio of the variance of oocyte counts between tissue samples within fish (σ^2_e) to the variance around the regression line (σ^2_A), i.e., $\theta = \sigma^2_e/\sigma^2_A$. The smaller the θ, the fewer tissue samples are needed.

Let's denote for the ith fish, $i = 1,..,n$,

W_i = fish weight,

Y_{Fi} = total number of advanced yolked oocytes in the ovary,

y_{ij} = advanced yolked oocyte count in the jth tissue sample, $j = 1,..,m$,

z_{ij} = weight of the jth tissue sample,

Z_i = formalin wet weight of ovary,

m = number of tissue samples from an ovary,

M_i = maximum number of tissue samples in an ovary,

$\hat{Y}_{Fij}$ = estimate of total number of advanced yolked oocytes in the ovary from the jth tissue sample $\left(\frac{y_{ij}}{z_{ij}}\right) Z_i$,

$\hat{Y}_{Fi}$ = estimated total number of advanced yolked oocytes in the ovary and is used for all analyses in fish fecundity in later sections $= \frac{\sum_{j=1}^{m} \hat{Y}_{Fij}}{m}$, and

$\tilde{Y}_{Fi}$ = estimate of total fecundity from the regression model.

We write $\hat{Y}_{Fij}$ as

$$\hat{Y}_{Fij} = Y_{Fi} + (\hat{Y}_{Fij} - Y_{Fi})$$

$$= f(W_i) + A_i + e_{ij} \qquad \text{(Eq. 3)}$$

where $e_{ij} = \hat{Y}_{Fij} - Y_{Fi}$. The estimated total number of advanced yolked oocytes in the ovary is

$$\hat{Y}_{Fi} = \frac{\sum_{j=1}^{m} \hat{Y}_{Fij}}{m} = f(W) + A_i + e_i$$

$$= f(W) + \xi \qquad \text{(Eq. 4)}$$

and

$$\sigma^2_\xi = \sigma^2_A + \frac{\left(\frac{M-m}{M}\right)\sigma^2_e}{m}. \qquad \text{(Eq. 5)}$$

Thus the variance around the regression line σ^2_ξ based upon the data set $(\hat{Y}_{Fi}, W_i)$ is composed of two variance components: one is σ^2_A and the other is σ^2_e. The sample counterparts for σ^2_ξ and σ^2_e are s^2_ξ and s^2_e:

$$s^2_\xi = \frac{[\hat{Y}_F - f(W)]^2}{n-q} \qquad \text{(Eq. 6)}$$

is the mean square error from a regression analysis on $(\hat{Y}_{Fi}, W_i)$ where q is the number of regression coefficients and n is the number of fish, and

$$s^2_e = \frac{\sum_{i=1}^{n}\sum_{j=1}^{m} (\hat{Y}_{Fij} - \hat{Y}_{Fi})^2}{n(m-1)} \qquad \text{(Eq. 7)}$$

is the within-sample variance (Hunter et al. 1985). The estimate (s^2_A) of the variance around f(W) when Y_F is known (σ^2_A) can be estimated by subtraction:

$$s^2_A = s^2_\xi - \frac{\left(\frac{M-m}{M}\right) s^2_e}{m}. \qquad \text{(Eq. 8)}$$

According to Hunter et al. (1985), the optimum number of tissue samples can be determined for a given θ ($= s^2_e/s^2_A$), the cost of processing a tissue sample, and the cost of processing a fish. The ratio, $K = s^2_\xi/s^2_A$, measured the excess variance which is contributed by taking tissue samples rather than counting every advanced oocyte in the ovary.

We used Dover sole collected during January–February 1987 to determine the optimal number of tissue samples. Two tissue samples were taken from the ovaries of 99 Dover sole. The within-sample variance of oocyte density ($s^2_e = 1053 \times 10^4$) was obtained from an ANOVA, and the linear regression of $\hat{Y}_F$ on W ($\hat{Y}_F = 20{,}255 + 40.54W$) gave the MSE ($s^2_\xi = 18{,}469 \times 10^4$) (Table 6; Fig. 5, lower middle). Thus θ is 0.058 when calculated from equations (7 and 8) where m = 2. Because M was large (range 200–700), $\frac{M-m}{M}$ was assumed to equal 1, and s^2_A was computed as $s^2_\xi - (s^2_e/2) = 17{,}942 \times 10^4$. Hence when two tissue samples are used, the variance within tissue samples is only 5.8% of the variance around the fecundity-fish weight regression line. To quantify the excess variance due to subsampling, we computed $K = s^2_\xi/s^2_A = 1.03$. This means the variance around the regression line which was based on two tissue samples per fish (Eq. 4) is about 1.03 times that of an equation based on counts of all advanced yolked oocytes in the ovary (Eq. 2). Although the within-ovary variance was small, we recommend counting two tissue samples per female because the cost of processing the second sample was minimal.

Optimal number of females

In addition to the sample allocation based on cost of processing fish and cost of processing tissue samples, the number of females needed for a regression estimate of total fecundity was determined by modifying a procedure suggested by Thigpen (1987) to the 1987 fecundity data for Dover sole. The equation for determining the sample size (n) for a linear regression was

$$n - 1 = \frac{\left(\frac{1-r^2}{r^2}\right)}{CV(b)^2} \qquad \text{(Eq. 9)}$$

Table 6

Within-sample variance ($s^2_e \times 10^{-4}$) from ANOVA and the MSE ($s^2_\xi \times 10^{-4}$) from the regression analysis of fecundity ($Y \times 10^{-2}$) and weight of Dover sole *Microstomus pacificus*. California females taken January–February 1987.

Analysis of variance on total fecundity

Source	DF	SS	MS
Fish	98	8,559,008	87,337
Error	99	104,201	1,053
Total	197	8,663,209	

Analysis of variance on linear regression

Source	DF	SS	MS	F
Regression	1	2,488,019	2,488,019	134.72
Residual	97	1,791,468	18,469	

Predictor	Coeff.	SD	t
Constant	202.55	32.03	6.32
Fish wt.	40.54	3.49	11.61

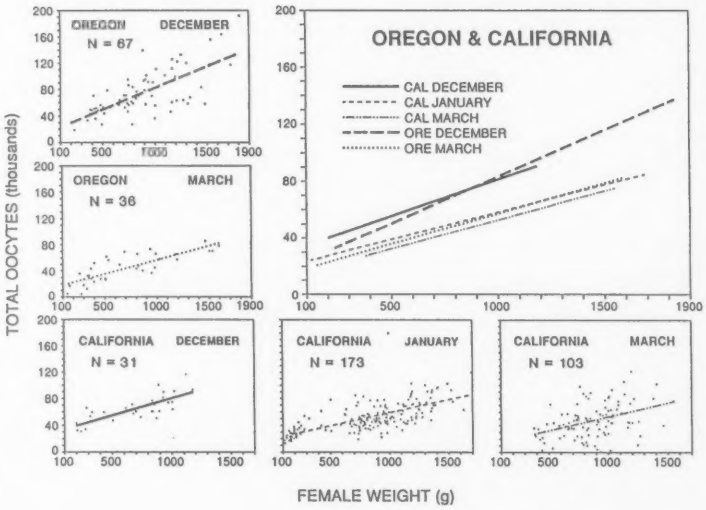

Figure 5

Total fecundity of Dover sole *Microstomus pacificus* as a function of female wet weight in grams (without ovary) for various months taken in central California and Oregon. Each point represents a single female; equations are given in Table 9.

where r^2 is the coefficient of determination, and CV(b) is the coefficient of variation for the regression coefficient (b). The coefficient of determination (r^2) for Dover sole total fecundity and fish weight was 0.58. Thus 73 females are required for a CV(b) = 0.10. In conclusion, two tissue samples from each of 70–80 Dover sole females were adequate for expressing the relation between weight and total fecundity, if a CV(b) of about 0.10 is desired.

Relation to ovarian development

The optimum time for estimating potential annual fecundity is early in the spawning season when the probability of spawning is low. Estimates taken in this period may be biased because all oocytes may not have been recruited into the advanced stock of yolked oocytes. In this section, we use Oregon Dover sole taken in November–December to examine the recruitment of oocytes into the advanced stock of yolked oocytes.

If substantial numbers of oocytes are maturing from early-yolked to more advanced stages, one would expect an overlap in the size distributions of oocytes in different development stages. When vitellogenesis of the early yolked oocytes does not continue, one would expect that a gap would develop between the less-advanced and the most-advanced oocytes as the yolked oocytes continued their maturation. In Dover sole, the diameter distributions of stage-1, -2, and -3 oocytes broadly overlap when the mean diameter of the advanced yolked oocytes (stage 3) is less than 0.7 mm (Fig. 6). The extent of overlap declines as the stage-3 oocytes grow from 0.7 mm to 0.8 mm. Separation of the advanced stock (stage 3) from the other vitellogenic stages (1 and 2) becomes complete as the advanced stock grows from 0.8 to 0.9 mm. It appears from this qualitative analysis that recruitment of stage-2 oocytes into the advanced stock probably ends when the mean diameter of stage 3 is between 0.8 and 0.9 mm.

We conducted a stepwise multiple regression analysis of total fecundity ($\hat{Y}_F$) on mean diameter of the advanced oocytes (D) and female weight (W) for females taken off Oregon in November–December. The coeffi-

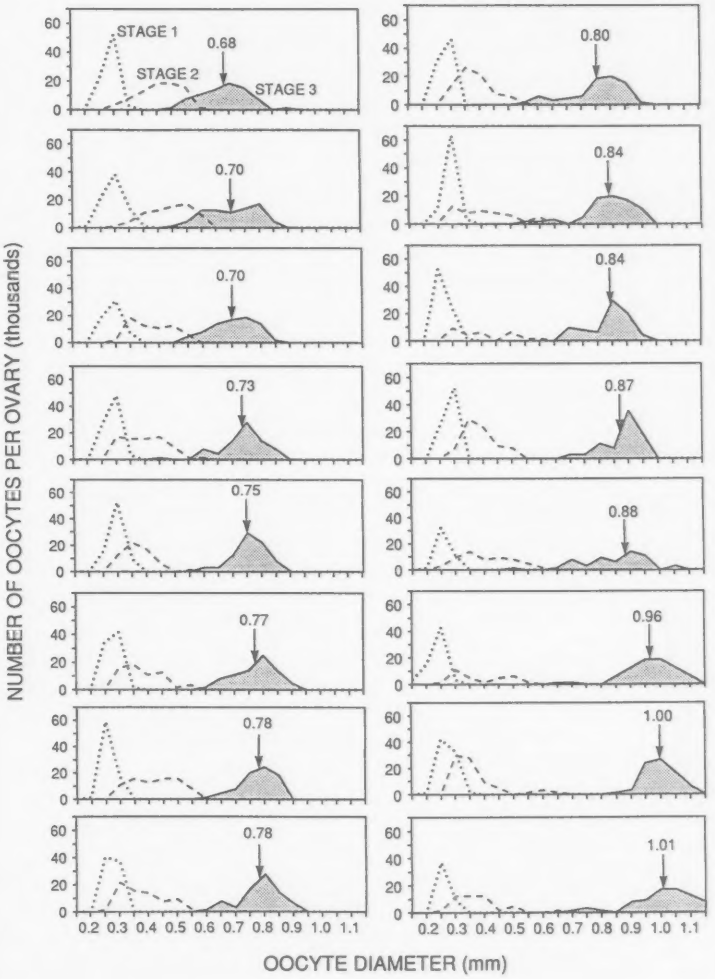

Figure 6

Frequency distribution of oocyte diameter of three vitellogenic oocyte stages in ovaries of Dover sole *Microstomus pacificus*. Each panel represents the ovary from one female. Fish arranged in order of the mean diameter of the advanced yolked oocytes, stage 3 (which is shaded); numbers and arrows indicate mean diameter of stage-3 oocytes. Mean total length was 420 mm and mean ovary-free weight of the females was 868 g. Fish were taken November–December 1988 along the Oregon coastline.

Table 7

Analysis of the relation between total fecundity ($\hat{Y}_F$) of Dover sole *Microstomus pacificus* and gonad-free body weight (W) and the average diameter of the advanced oocytes (D) using stepwise regression with analysis of variance. Specimens from Oregon in November–December 1988.

Stepwise regression		
Step	1	2
Constant	22,398	−88,768
Weight (W)	45.4	47.8
t*	7.56	8.80
Diameter (D)		129,893
t*		6.01
S	25,654	23,096
R^2	27.58	41.69

Analysis of variance					
Source	DF	SS	MS	F	P
Regression	2	5.68×10^{10}	2.84×10^{10}	53.27	<0.000
Error	149	7.95×10^{10}	5.33×10^{10}		
Total	151	1.36×10^{10}			
Source	DF	Sequential SS			
Weight	1	3.76×10^{10}			
Egg diameter	1	1.92×10^{10}			

*For $P = 0.05$, $1.96 < t < 1.98$., df ≥ 120.

cient for diameter, as well as the one for weight, was positive and significant (Table 7). Thus the potential annual fecundity was not fully recruited as stage-3 oocytes in some of the Oregon Dover sole taken in November–December, since total fecundity increased with the mean diameter of the oocytes used to estimate total fecundity.

To determine the level of ovarian development (oocyte diameter) at which the full complement of oocytes was recruited into the advanced yolked oocyte class (stage 3), we conducted a series of stepwise multiple regression analyses by successively removing the data by 0.01 mm decrements from the lowermost oocyte diameter class starting at 0.71 mm. This analysis indicated that the threshold for a significant effect of oocyte diameter on total fecundity was between mean diameters of 0.85 and 0.86 mm (Table 8). The multiple regression coefficient for oocyte diameter was significant and positive when females with oocyte diameter

Table 8

Results of stepwise multiple regression of the total fecundity ($\hat{Y}_F$) of Dover sole *Microstomus pacificus* on gonad-free body weight (W) and mean oocyte diameter (D) for a succession of oocyte diameter-classes using the model $\hat{Y}_F = a + b_1 W + b_2 D$. Specimens taken along Oregon coast November–December 1988. Line separates oocyte diameter-classes where diameter is a significant variable, from those where it is not.

Oocyte diameter class (mm)	Constants		Multiple regression coefficients and their t-ratios for: Fish weight		Oocyte diameter		
	N	a	b_1	t	b_2	t*	r^2
0.71–1.04	152	−88,768	47.8	8.80	129,893	6.01	0.417
0.72–1.04	148	−90,147	48.3	8.90	130,860	5.87	0.424
0.74–1.04	133	−94,375	49.6	8.34	134,295	5.14	0.415
0.76–1.04	119	−90,710	51.3	7.98	128,688	4.17	0.407
0.78–1.04	105	−83,087	53.4	7.53	118,385	3.16	0.396
0.80–1.04	91	−90,344	55.9	7.29	123,891	2.60	0.400
0.82–1.04	85	−87,274	59.2	7.34	117,459	2.20	0.405
0.83–1.04	81	−111,317	56.9	7.44	145,193	2.77	0.440
0.84–1.04	77	−103,009	58.7	7.55	134,678	2.42	0.460
0.85–1.04	72	−90,464	60.1	7.33	120,166	1.95	0.457
0.86–1.04	67	−38,172	65.3	7.96	60,555	0.94	0.502
0.87–1.04	64	−33,982	63.5	7.30	57,891	0.87	0.482
0.88–1.04	60	−15,721	69.4	7.63	33,456	0.48	0.514
0.90–1.04	46	45,073	82.0	7.92	−40,601	−0.47	0.594
0.92–1.04	34	60,339	84.0	6.92	−58,185	−0.49	0.616

*For $P = 0.05$, t is 1.98 for df = 120, 2.00 for df = 60, and 2.06 for df = 25.

equal to or less than 0.86 mm were included, but was insignificant when only those having a diameter greater than 0.86 mm were considered. We concluded that ovaries in which the advanced stock of yolked oocytes has an average diameter of 0.85 mm or less are not sufficiently developed to be certain that the annual stock is fully recruited. Consequently, to estimate the potential annual fecundity, we used only females in which the average oocyte diameter of the advanced stock exceeded 0.85 mm.

No relationship between oocyte diameter and total fecundity was detected in the females taken off central California during November–December. Oocyte diameter may not have been a significant variable in central California because fewer females were examined and their ovaries were more advanced. In 48% of females from California, advanced yolked oocytes averaged more than 0.85 mm in diameter (N 65), whereas only 34% of the fish taken off Oregon had oocytes that did so (N 128).

Seasonal variation in total fecundity

Total fecundity of Dover sole decreased during the spawning season off both central California and Oregon (Fig. 5). Analysis of covariance indicated that equations expressing the relation between female weight and fecundity differed within the spawning season (Table 9). The total fecundity for a 1 kg female declined from about 80,000 advanced oocytes in December to about 50–60,000 during the spawning season (Table 9).

To further describe the decline in total fecundity over the season, we also regressed fecundity on female weight and elapsed time since 1 November. In both central California and Oregon the negative coefficients for elapsed time were significant, indicating that total fecundity declined with elapsed time (Table 9). Analysis of covariance indicated that multiple regression equations for California and Oregon were not different (analysis over a similar weight range of 174–1542 g; $F_{1,388}$ 1.59, P 0.208; adjusted mean fecundity for Oregon 57,849, SE 2092; adjusted mean fecundity for California 54,733, SE 1152). When we combined data for the two regions, we found that total fecundity declined on the average about 12% per month. This computation underestimated the actual rate of decline, since it did not take into account females that had spawned all of their advanced yolked oocytes.

Potential annual fecundity

Potential annual fecundity was considered to be equivalent to the standing stock of advanced yolked oocytes in fully developed, prespawning females. We consider

Table 9

Linear regression coefficients, confidence intervals, and estimates for the relationship between female weight (W, ovary-free, in g) and total fecundity ($\hat{Y}_F$) of Dover sole *Microstomus pacificus* from California and Oregon. Analysis of covariance for the effect of season on the relation between total fecundity and weight. Multiple regression coefficients are also given for the effect of elapsed time (T; days since 1 Nov.) and female weight on total fecundity.

Linear regression by month and state

State	Mean date of cruise	Linear equation $\hat{Y}_F = a + bW$ a	95% CI	b	95% CI	r^2	F	N	Regression estimate for 1 kg female	Analysis of covariance for effect of month with weight ranges similar Variables	df	F	P
Oregon	7 Dec 88	17,640	±15,460	65.5	±16.4	0.49	63.9	67	83,140	Weight	1	67.85	<0.005
	3 Mar 89	14,492	±8,530	42.9	±10.6	0.66	67.9	36	57,392	Month	1	20.06	<0.005
										Error	95		
										Total	97		
Central California	8 Dec 85	29,497	±6,121	51.6	±16.1	0.58	42.9	31	81,097	Weight	1	25.20	<0.005
	31 Jan 87	20,154	±6,344	38.9	±6.8	0.42	127.0	173	59,022	Month	2	18.91	<0.005
	23 Mar 88	12,072	±16,924	40.7	±18.6	0.15	18.9	103	52,772	Error	217		
										Total	220		

Multiple regression of total fecundity on weight and days elapsed since 1 November

State	Multiple regression equation $\hat{Y}_F = a + b_1W + b_2T$ a	95% CI	b_1	95% CI	b_2	95% CI	r^2	F	N	W_{min} (g)	W_{max} (g)	T_{min} (d)	T_{max} (d)
Oregon	35,162	±13,378	55.2	±11.2	−237	±104	0.59	74.9	103	147.7	1815.9	33	151
Central California	41,552	±8,142	40.3	±6.4	−224	±63	0.37	92.3	307	120.0	1690.3	34	160

Table 10

Relationship between total fecundity ($\hat{Y}_F$) and gonad-free body weight (g) or total length (mm) for California and Oregon Dover sole *Microstomus pacificus* females meeting specifications for potential annual fecundity estimation (females taken in November–December with average oocyte diameter >0.85 mm and no evidence of past or imminent spawning). Data are compared with Yoklavich and Pikitch (1989) estimates for Oregon.

Fecundity and weight

	Linear equation $\hat{Y}_F = a + bW$							Estimate for	Gonad-free weight (g)	
State	a	95% CI	b	95% CI	r^2	F	N	1 kg female	Mean	Range
Oregon	17,640	±15,453	65.5	±16.4	0.488	63.86	67	83,140	870.5	236.0–1815.9
California	29,871	±12,996	50.9	±17.1	0.544	37.06	30	80,771	704.7	202.1–1124.2
Oregon + California	21,124	±9,248	62.0	±10.4	0.504	98.42	97	83,124	819.2	202.1–1815.9

Fecundity and length

	Exponential equation $\hat{Y}_F = aL^b$							Estimate for	Total length (mm)	
State	a	95% CI	b	95% CI	Pseudo r^2	F	N	453 mm female*	Mean	Range
Oregon	$5.667 \cdot 10^{-6}$	$\pm 1.943 \cdot 10^{-5}$	3.806	±0.713	0.431	47.03	64	72,856	436	298–551
California	$6.101 \cdot 10^{-4}$	$\pm 5.042 \cdot 10^{-3}$	3.020	±1.380	0.084	2.57	30	64,094	423	296–526
Yoklavich & Pikitch**	$1.637 \cdot 10^{-6}$	$\pm 6.928 \cdot 10^{-6}$	4.021	±0.684	0.818	135.13	32	78,382	448	358–550

*Weight is about 1000 g using equation in Table 3.
**Estimated from Yoklavich and Pikitch (1989) original data.

Dover sole to be developed when the average diameter of the advanced oocytes (stage 3) exceeds 0.85 mm; prespawning females are those taken in November–December which show no histological evidence of recent past or of imminent spawning (no postovulatory follicles nor hydrated oocytes present).

Using only specimens that met these specifications, we regressed total fecundity on female weight (without ovary) for females taken in central California and Oregon. The two regression equations were quite similar; when the data are truncated so that the ranges of female weights were equal, no statistical difference existed between California and Oregon. Combining all data, we obtained the general equation

$$\tilde{Y}_F = 21{,}124 + 62.0\,W \quad \text{(Eq. 10)}$$

where $\tilde{Y}_F$ is estimated total fecundity from the regression line, and W is ovary-free female weight in grams. Therefore, the potential annual fecundity for a 1 kg Dover sole is about 83,000 oocytes (Table 10).

Fecundity of Dover sole was estimated recently by Yoklavich

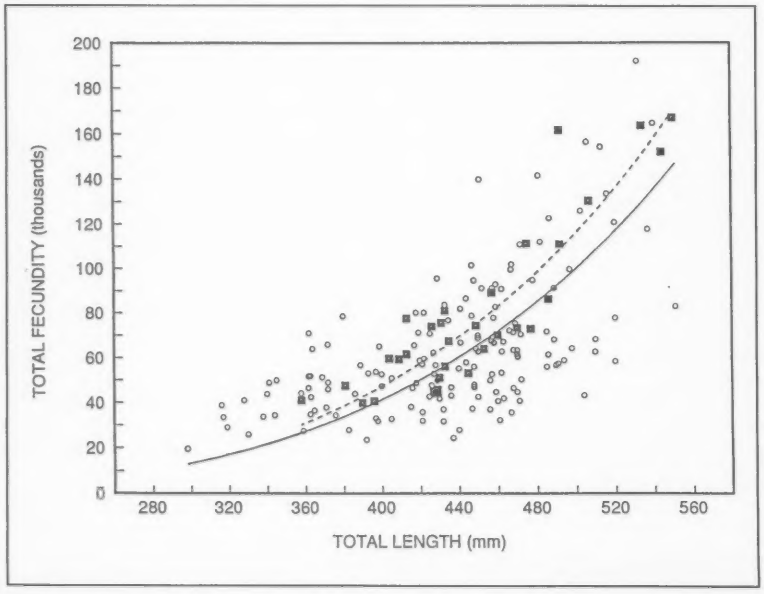

Figure 7

Total fecundity as a function of total length of Dover sole along the Oregon coast for our November–December 1988 data (open circles and solid line) and for data given by Yoklavich and Pikitch (1989) (filled squares and dashed line). Equations are given in Table 10.

Figure 8

Relative frequency distribution of the fraction of the random sample of advanced yolked oocytes measured that were atretic (α stage) from the Dover sole *Microstomus pacificus* females used in estimates of total fecundity shown by state: Oregon females, N 189; California females, N 361.

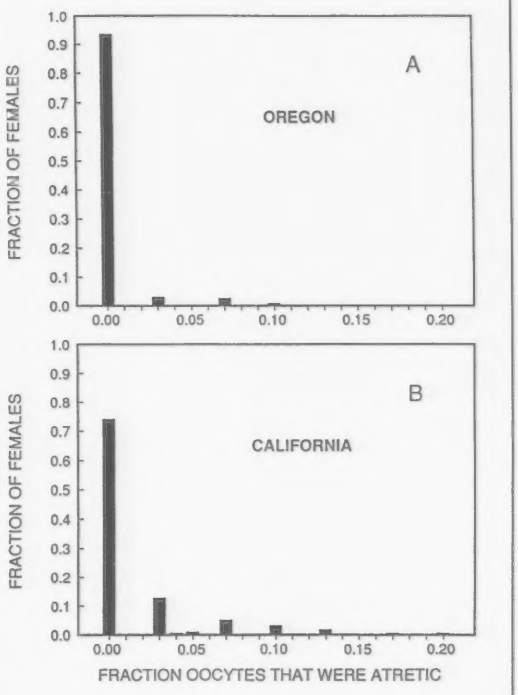

and Pikitch (1989) for females caught along the Oregon coast. Those authors used an exponential model and expressed annual fecundity as a function of length. The distribution of points in our data broadly overlapped the data of Yoklavich and Pikitch (1989) (Fig. 7). To compare our Oregon data with theirs, we truncated ours so that the length ranges of the two sets coincided and applied an analysis of covariance to log-transformed data. Analysis of covariance indicated that no significant difference existed between the two equations ($F_{1, 81}$ 2.03, P 0.158). In Table 10, the exponential equation for fecundity as a function of length is given for our data (not truncated) and for that of Yoklavich and Pikitch (1989). In summary, we found no statistical difference between California and Oregon, nor between our Oregon data and that of Yoklavich and Pikitch (1989).

Atretic losses

In fishes with determinate fecundity, a key question is whether atretic losses during a season constitute an important fraction of the potential annual fecundity. We identified whole atretic oocytes under a microscope while doing our fecundity work. To measure atretic losses, we counted the number of atretic oocytes (α advanced yolked oocytes) occurring in a random sample of 30 advanced yolked oocytes for each of the females used to estimate total fecundity (N 550).

In the fish used to estimate fecundity, the average fraction of advanced yolked oocytes that were atretic was low with the mean 0.015 (SD 0.032, N 361) in California, and even lower in Oregon females (mean 0.0033, SD 0.014, N 189). Atretic oocytes were observed in only 26% of California females and in only 6% of Oregon females (Fig. 8).

The total fecundity of California females was negatively correlated with the fraction of oocytes in the ovary that were atretic. A stepwise multiple regression of female weight, elapsed time, and fraction atretic on total fecundity (Table 11) indicated that the coefficient for the fraction

Table 11

Analysis of the relation between total fecundity ($\hat{Y}_F$) of Dover sole *Microstomus pacificus* ovary-free body weight, elapsed days since 1 November, and fraction of atretic oocytes using stepwise regression. Specimens from California.

Stepwise regression			
Step	1	2	3
Constant	23,335	40,296	40,976
Weight	37.7	40.8	41.4
t*	2.11	14.03	14.23
Elapsed days		−205	−206
t		−7.85	−7.94
Fraction atretic			−63,278
t			−2.17
S	19,317	17,868	17,776
r^2	28.99	39.41	40.20

Analysis of variance					
Source	DF	SS	MS	F	P
Regression	3	7.58×10^{10}	2.53×10^{10}	79.99	<0.001
Error	357	1.13×10^{11}	3.16×10^{8}		
Total	360	1.89×10^{11}			

Source	DF	Sequential SS
Weight	1	6.28×10^{10}
Elapsed days	1	1.15×10^{10}
Fraction atretic	1	1.49×10^{9}

*For P = 0.05, t 1.97.

of oocytes that were atretic was significant and negative. According to the equation, when 10% of the advanced oocytes were atretic, total fecundity in a 1 kg female was about 8% lower than when no advanced yolked oocytes were atretic. This analysis indicated that atretic losses of potential annual fecundity occurred, but on a population basis such losses were negligible. No relation between fecundity and atresia existed for Oregon females, probably because atresia was less prevalent in Oregon, with only 6% of females effected compared with 26% in central California.

The ovaries of many more females were examined histologically for atresia (N 2607) than were examined using the anatomical method, because we restricted the anatomical work to the fish used to measure total fecundity. Only 2% of all females examined histologically (Table 2) had ovaries in which 50% or more of the advanced yolked oocytes were in α atresia, but minor atresia was more common. Minor atresia occurred in 52% of the nonspawning California females and in 35% of the nonspawning Oregon females (Table 2).

The histological method was more sensitive than the anatomical one. Alpha atresia of advanced yolked oocytes was detected at least twice as frequently using histological techniques. The histological method was more sensitive because we could detect more subtle changes in oocyte structure and because we scanned about 150 oocytes per ovary, compared with 30 oocytes in the anatomical method. Despite the lack of sensitivity, the anatomical method was valuable because the standing stock of atretic oocytes could be easily estimated and directly related to total fecundity.

The histological evidence indicated that females with α-atretic advanced yolked oocytes were more common in central California waters than off Oregon. However, season and locality were confounded because most females from Oregon were taken prior to the spawning season while most females from California were taken during the season. To determine if either season or locality affected the relative frequency of atretic females, we combined the minor-atresia and major-atresia classes for California and Oregon and fit the stepwise logistic model

$$P = \frac{e^{\beta_0+\beta_1 X_1+\beta_2 X_2}}{1+e^{\beta_0+\beta_1 X_1+\beta_2 X_2}} \qquad \text{(Eq. 11)}$$

to the data (Table 12), where P is the fraction of females with atretic oocytes. The independent variables for location (X_1) are -1 for California and 1 for Oregon, and for season (X_2) are -1 for prespawning and 1 for during spawning. The estimates of coefficients for the equation are $\beta_0 = -0.183$ (SE 0.056) and $\beta_1 = -0.288$ (SE 0.056) (β_2 is not given because effect of season was not significant in an early regression analysis); the estimate of the atresia rate P for California is 0.525 (95% CI 0.479–0.572; Carter et al. 1986) and for Oregon is 0.384 (95% CI 0.338–0.433).

Table 12

Histological determination of number of Dover sole *Microstomus pacificus*, with α atresia of advanced yolked oocytes expressed as a percentage of all females with advanced yolked oocytes taken in central California and in Oregon, beginning (November–December) and during (January–May) the spawning season.

	Spawning season						
	Beginning		During		Beginning + During		
State	%	*N*	%	*N*	%	95% CI	*N*
Central California	59.2	71	51.9	617	52.5	47.9–57.2	688
Oregon	36.8	536	49.4	83	38.4	33.8–43.3	619

Table 13

Mean relative batch fecundity for five batch-order numbers (B), from the first batch to the last batch.

Batch-order no.[a] (B)	No. of females	Relative batch fecundity (oocytes/female wt(g))	
		Mean	SD
1	4	2.421	3.810
2	12	11.661	4.410
2<B<U-1	19	10.489	3.184
U-1	11	12.378	8.035
U	9	7.835	5.723

Analysis of variance on five batch orders

Source	DF	SS	MS	*F*	*P*
Batch order	4	371.2	92.8	3.44	0.015
Contrast[b]	1	352.6	352.6	13.08	0.001
Error	50	1347.6	27.0		
Total	54	1718.8			

[a] First batch spawned, B = 1; last batch spawned, B = U; penultimate batch, B = U-1.
[b] Comparison of relative fecundity of the first and last batch to the other batches.

Table 14

Comparison of fecundity between the penultimate batch and the last batch within the same Dover sole *Microstomus pacificus* female.

	Female weight (g)	Batch fecundity* (no. of oocytes)	
		Penultimate	Last
	270.00	4634	2121
	270.00	3716	323
	324.50	9374	1025
	539.00	11445	2903
	703.86	3906	411
	713.24	12213	6455
	752.11	2843	124
	793.54	6134	5856
	824.66	7022	3820
	1017.70	3621	29
	1247.82	11047	250
Mean	677.9	6905	2120
SD	309.8	3525	2355

*Paired t-test: t 4.99, df 10, P 0.0005.

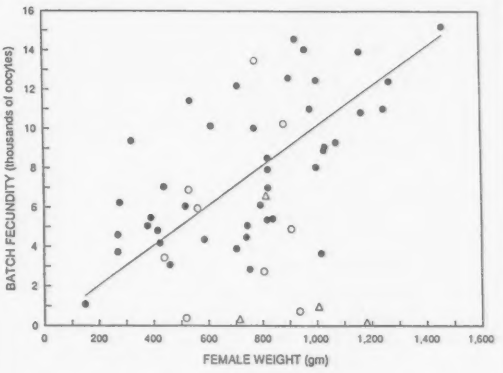

Figure 9

Batch fecundity of Dover sole *Microstomus pacificus* as a function of female weight (without ovary). Line is $\hat{Y}_B = 10.1W$ for the second through the penultimate spawning batches (filled circles); triangles = first spawning batch; open circles = last spawning batch.

This computation indicated that the occurrence of females with α atresia of advanced oocytes was significantly affected by locality of the samples but not by season. In short, more California females had one or more α-atretic advanced oocytes in their ovary than did Oregon females.

Batch fecundity

The first step in our analysis of batch fecundity ($\hat{Y}_B$) was to determine if the batch size varied with the order of spawning. Analysis of variance indicated that a significant batch-order effect existed (Table 13). The mean relative fecundity of the first (1) and last spawning batch (U) were significantly lower than the other batches (Table 13).

In eleven females, the only advanced oocytes left in the ovary were two "hydrated" spawning batches (Table 14). Each was in a different stage of development: one was fully hydrated (last batch), and the other was in the migratory nucleus stage (penultimate batch). In all of the eleven females, the last batch was always lower than the penultimate batch. The t-test for paired differences confirmed the effect of batch order on fecundity indicated by the ANOVA. The t-test also had less potential for bias because we used absolute rather than relative batch fecundity. The t-test indicated that the fecundity of the last batch differed from the penultimate batch (t 4.99, df 10, P 0.0005). We concluded that the batch size of a female Dover sole did change over the spawning season, with the last and the first batch being lower than the rest.

We determined the relation between batch fecundity and weight using regression analysis. We did not use the first and last batches since they were lower than the rest. The intercept for the regression of batch fecundity on female weight did not differ from zero (a 2142; t 1.87, df 40, P 0.07). Therefore we forced the regression line through 0, yielding the relationship $\hat{Y}_B = 10.1W$, where female weight ranged from 148 to 1464 g (Fig. 9). This analysis indicated that the relative batch fecundity of Dover sole is about 10 oocytes per gram ovary-free female weight, except for the first and last batch. The relative fecundity for the first and last batches combined was also about 10 oocytes per gram (1 and U in Table 13). Thus the number of potential spawnings (S) per year can be calculated using $S = (\tilde{Y}_{FR}/10) + 1$, where $\tilde{Y}_{FR}$ is the relative potential annual fecundity ($\tilde{Y}_F/W$; $\tilde{Y}_F$ from Eq. 10). This means that the average 1 kg female spawns its 83,000 advanced yolked oocytes in about nine batches.

Sexual maturity

To determine the optimal criteria for sexual maturity in female Dover sole, we established six sets of histological criteria for maturity (Table 15). The first set of criteria selects females with either advanced yolked

Table 15

Six sets of histological criteria for female sexual maturity in Dover sole *Microstomus pacificus*, with the mean length of the females in each set. (o) not present; (+) present; (–) not considered.

Criteria set no.	Certainty	Advanced yolked oocytes: with α atresia	Advanced yolked oocytes: no α atresia	Post-ovulatory follicles	Early yolked oocytes: with β atresia	Early yolked oocytes: only α atresia or none	Unyolked oocytes: with β atresia	Unyolked oocytes: only α atresia	Unyolked oocytes: no atresia	Mean length (mm): $\bar{x}$	Mean length (mm): ±2 SE	No. of females Calif. + Oregon (*N* 2595): No. in class	No. of females Calif. + Oregon (*N* 2595): Cumulative percent
1	Certain maturity	+	+	+	–	–	–	–	–	434	±3	1343	52
2	Uncertain	o	o	o	+	–	–	–	–	414	±7	218	60
3	Uncertain	o	o	o	o	+	–	–	–	397	±11	77	63
4	Uncertain	o	o	o	o	o	+	–	–	379	±6	279	74
5	Uncertain	o	o	o	o	o	o	+	–	350	±5	432	90
6	Certain immaturity*	o	o	o	o	o	o	o	+	297	±10	246	100

*Defined as certain immaturity because no histological evidence exists for maturity.

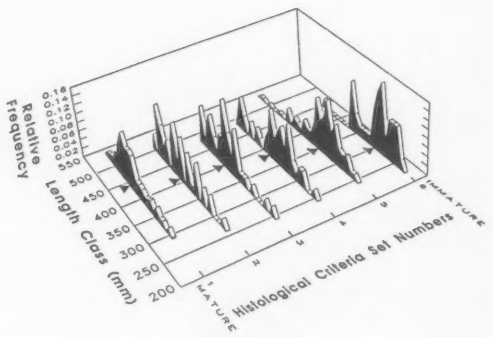

Figure 10

Length distribution of female Dover sole *Microstomus pacificus* identified by six sets of histological maturity criteria, ranging from criteria set 1 where maturity is certain, to set 6 where all females are considered to be immature (see Table 15). Females captured in November–December in California and Oregon; filled triangles indicate mean length of females.

oocytes or postovulatory follicles. The sexual maturity of these females is certain, but some mature females may be excluded if only the first set of criteria are used. Criteria sets 2 to 5, if added to the first set, broaden the maturity definition to include females having ovaries in the earliest stages of vitellogenesis and those showing possible signs of past reproductive activity (β- or α-stage atresia). Each additional criteria set that one might add to the first set increases the risk that immature fish will be classed as mature. Females in set 6 are considered to be immature because they have none of the characteristics mentioned in the other five sets.

Use of β atresia as a possible sign of past reproductive activity seems justified. Females with early yolked oocytes and β atresia (set 2) were larger on the average than those with no β atresia (set 3; t 2.45, P 0.015, df 293); and females with unyolked oocytes and β atresia (set 4) were larger than those with only α atresia of the unyolked (set 5; t 7.69, $P<0.001$, df 709). In addition, the ranking of criteria sets based on our intuitive appraisal of the risk of classification error is largely borne out by the length distributions of the females identified by the criteria set, since mean length decreased with criteria set number (Fig. 10).

To estimate the length at which 50% of the Dover sole are mature (ML_{50}) using all six histological criteria sets, we first used a maturity algorithm to estimate the fraction of fish that were mature in a given length-class. This algorithm is a regression method similar to those used to construct age-length keys (Bartoo and Parker 1983, Kimura and Chikuni 1987).

This analysis was based on two equations. The first equation was

$$q_{j|i} = q_{m|i}\, q_{j|m} + (1 - q_{m|i})\, q_{j|im} \qquad \text{(Eq. 12)}$$

where $q_{j|i}$ is the fraction of fish of length-class j in the ith criteria set; $q_{j|m} = q_{j|1}$ and $q_{j|im} = q_{j|6}$ because the criteria set 1 consists of all mature (m) fish and the criteria set 6 consists of all immature (im) fish; and $q_{m|i}$ the overall fraction of mature fish in the ith cri-

teria set. The second equation assumed that $q_{m|i}$ changed linearly with criteria set number i:

$$\hat{q}_{m|i} = b_1 + b_2 i. \quad \text{(Eq. 13)}$$

Combining equations (12) and (13) results in the final equation

$$y_{ij} = b_1 x_{1j} + b_2 x_{2j} \quad \text{(Eq. 14)}$$

where $y_{ij} = q_{j|i} - q_{j|im}$,
$x_{1j} = q_{j|m} - q_{j|im}$, and
$x_{2j} = i(q_{j|m} - q_{j|im})$.

For each criteria set i, we obtained the estimate of the fraction of mature fish ($q_{m|j|i}$) in each length-class j as

$$\hat{q}_{m|j|i} = \hat{q}_{m,j|i} / \hat{q}_{j|i} = [\hat{q}_{m|i} q_{j|m}] / \hat{q}_{j|i}.$$

We then obtained the estimated number of mature fish of length-class j in the criteria set i ($\hat{N}_{m|j|i}$) as the product of the total number of fish at length-class j ($N_{j|i}$) and the estimated fraction of mature fish at length-class j ($\hat{q}_{m|j|i}$):

$$\hat{N}_{m|j|i} = N_{j|i}\, \hat{q}_{m|j|i}.$$

The summation of $\hat{N}_{m|j|i}$ over all criteria (i) is the total number of mature fish at length-class j ($\hat{N}_{m|j} = \Sigma_i \hat{N}_{m|j|i}$). The total number of fish in length-class j ($N_j = \Sigma_i N_{j|i}$) and the number of mature fish ($\hat{N}_{m|j}$) were used to estimate ML_{50} for all females taken before the onset of spawning (California and Oregon data combined) using BMDPLR (Dixon et al. 1988).

We compared the above estimate with the ML_{50} for each of the five maturity definitions created by including progressively more criteria sets (Table 16). When the definition of sexual maturity is expanded by progressively adding criteria sets 2 to 5 to the definition, the ML_{50} decreased for each additional set of criteria added. Our estimate of ML_{50} from the model was 332 mm and is most similar to maturity definition IV in Table 16. Thus, definition IV is the preferred histological definition of maturity because it is probably the least biased.

Inspection of Table 16 also indicated that the ML_{50} is always greater when measurements are made during the reproductive season than before it begins, regardless of the number of criteria sets used to define sexual maturity. This implied that during the spawning season the ovaries of some postspawning females are reabsorbed to the extent that they become indistinguishable from females defined as immature. Thus maturity should be estimated prior to the onset of spawning, and the definition of maturity should be broader than definition I.

We believe the preferable estimate of ML_{50} is one based on the maturity algorithm because it uses all the histological data, while those based on definitions use only a portion of it. The maturity algorithm should be applied only to data taken before the spawning season, since data collected later in the season will be biased. This method demands detailed histological classification which may be too costly for many purposes. Definition III could be used if tissue were examined microscopically or with a powerful hand lens, and it gives an ML_{50} value close to that provided by the model.

Table 16

Estimated length at which 50% of Dover sole females are sexually mature, using six histological definitions of ovarian maturity and a maturity algorithm that uses all data. California and Oregon data are combined; length at 50% mature estimated using logistic model (Dixon et al. 1988).

		Before spawning (*N* 854 females)			During spawning (*N* 1321 females)		
			No. of mature females			No. of mature females	
Definition no.	Histological criteria sets incl. in maturity definition[a]	Length at 50% mature (mm)	*N*	% of females	Length at 50% mature (mm)	*N*	% of females
I	1	373	541	63	419	568	43
II	1, 2	361	582	68	396	692	52
III	1, 2, 3	348	626	73	391	720	54
IV	1, 2, 3, 4	332	669	78	348	917	69
V	1, 2, 3, 4, 5	258	810	95	255	1184	90
Maturity algorithm	1, 2, 3, 4, 5, 6	332	691[b]	81[b]	389	742[b]	56[b]

[a]From Table 15.
[b]Estimated from maturity algorithm.

Table 17

Final maturity thresholds and logistic model parameters* for female Dover sole *Microstomus pacificus*, taken before the spawning season in California, Oregon, and the two states combined.

Region	Maturity definition	50% mature	95% CI	a	SE	b	SE	*N*
California	IV	298	215–391	−14.412	4.374	0.0483	0.0149	104
Oregon	IV	336	322–351	−9.268	0.806	0.0276	0.0022	750
California + Oregon	Maturity algorithm	332	305–367	−14.960	1.239	0.0450	0.0036	854

*$P = \frac{e^{a+bL}}{1+e^{a+bL}}$

We combined data from Oregon and California in this analysis because sample sizes (before spawning) were inadequate for application of the model separately. However, in Table 17 we provide estimates and fitting parameters based on definition IV for each region as well as those based on the model using the combined data. The ML_{50} estimated for definition IV was lower in California than in Oregon. However, analysis of covariance of the log transformation of fraction mature, $\mathrm{Ln}\left(\frac{q_m}{1-q_m} + 1\right)$, on length and locality indicated that the difference between states was not significant (P 0.625, F 0.26). Thus our ML_{50} estimate for Dover sole along the California and Oregon coasts is 332 mm with 95% CI of 315–349 mm (Carter et al. 1986; Fig. 11). The ML_{50} we estimated from data in Hagerman (1952) for Dover sole from the Eureka California fishery is high (363 mm) compared with our final estimate for Oregon and California coasts (Fig. 11). However, Hagerman collected his specimens during the spawning season, and his estimate is similar to the ML_{50} for females taken during the spawning season (Definition IV, Table 16).

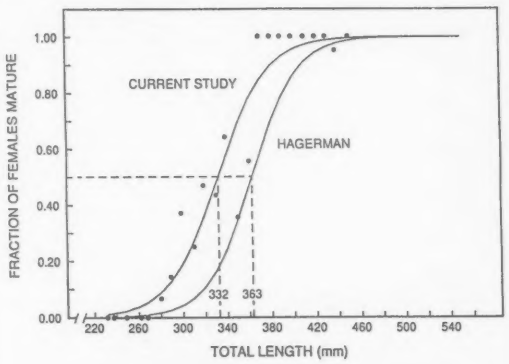

Figure 11

Fraction of female Dover sole *Microstomus pacificus* that were sexually mature as a function of total length. Points are for 10 mm length-class intervals; the fraction mature per length-class was assigned using maturity algorithm; data were from California and Oregon in November–December; logistic parameters are in Table 17. Present study is compared with Hagerman (1952), line only (logistic curve parameters, a −17.854, b 0.0450).

Discussion

Validation of fecundity assumptions

In the Introduction, we specified four assumptions required for an unbiased estimate of annual fecundity in Dover sole. These assumptions were that (1) fecundity was determinate; (2) potential annual fecundity was equivalent to actual fecundity; (3) females used to estimate annual fecundity had not spawned; and (4) recruitment of oocytes into the advanced stock of yolked oocytes had ceased for the season. The following is a review of the evidence for the four assumptions.

Five lines of evidence support the assumption of determinate fecundity for Dover sole: (1) in mature ovaries (mean diameter of advanced oocytes >0.85 mm), a hiatus existed between the advanced stock of mature oocytes and smaller, less mature oocytes; (2) total fecundity declined over the spawning season; (3) total fecundity was lower in females having postovulatory follicles; (4) the mean diameter of the advanced oocytes increased over the spawning season; and (5) our analysis of the order of spawning batches was consistent with the determinate fecundity assumption.

The second assumption, lack of significant atresia, also was supported by our analysis. Overall, atretic losses of advanced oocytes were negligible during the years of our study. Multiple regression analysis indicated that atresia had a small but significant effect on total fecundity of the California females that had

atretic oocytes. A few females suffered substantial losses in total fecundity, but such fish were rare and they had little effect on population means. Histological and anatomical evidence indicated that females with α-atretic advanced yolked oocytes were more common in central California than in Oregon waters. Atresia might be more common in central California Dover sole because bottom sediments are contaminated. Alternatively, females with atretic ovaries may be more common in central California waters because they are living near the southern end of their range where food supply and other habitat conditions may be less than optimal. Both explanations seem equally plausible at present.

The third assumption, that females used to estimate potential annual fecundity have not spawned in the current reproductive year, would be rejected for females taken in January through May. The assumption probably held for the females used to estimate annual fecundity in November–December because only 2.9% of the females from California and only 1% of the females in Oregon showed any histological signs of past or imminent spawning. The few females that showed histological signs of spawning were not used, of course, to estimate annual fecundity. Spawning may have gone undetected in some of the females used to estimate fecundity since postovulatory follicles are eventually resorbed. This does not seem likely for the November–December case because the spawning season had just begun and resorption is probably slow at the low temperatures of Dover sole spawning habitat.

Our fourth assumption, that all the oocytes that constitute the potential annual fecundity were included in our oocyte counts, is supported by two lines of evidence. The first is that no positive correlation existed between the mean diameter of the advanced oocytes and total fecundity. Such positive correlations were eliminated by excluding all ovaries in which the mean diameter of the advanced oocytes was less than 0.86 mm. A positive correlation between diameter and fecundity existed when all ovaries were considered (range in mean diameter of the advanced oocytes, 0.71–1.04 mm). This is evidence that recruitment of oocytes into the advanced class continued until the advanced stock was well separated from early vitellogenic oocytes (stages 1 and 2, Fig. 6). The second source of evidence is the form of the oocyte size-frequency distribution. A prominent gap between stage-2 and stage-3 oocytes existed when the mean diameter of stage-3 oocytes was between 0.84 and 0.96 mm (Fig. 6). The absence of significant numbers of oocytes in the intervening diameter classes (0.55–0.65 mm) indicates maturation of oocytes across this range either had ceased or was proceeding at a very slow pace. We conclude that recruitment of significant numbers of oocytes into the advanced stock probably ceases in Dover sole when the mean diameter of the advanced stock is between 0.86 and 0.96 mm.

Some authors working with other species (Hislop and Hall 1974 on *Melangius merlangus* (L.), Horwood and Greer Walker 1990 on *Solea solea*) consider all yolking oocytes to comprise the potential annual fecundity. In Dover sole this would mean that in addition to stage 3, the most advanced yolked oocytes, stages 1 and 2 would also be used to estimate annual fecundity. Such broad criteria are acceptable if all oocytes that began vitellogenesis ultimately become a part of the mature stock of oocytes that are spawned. This was not the case in Dover sole because oocytes in the early stages of vitellogenesis (stages 1 and 2) occurred in nearly all mature ovaries, including those in which some of the batches had already been spawned. The fate and dynamics of these small partially-yolked oocytes in advanced ovaries is uncertain; their numbers might either decrease due to resorption, increase and become part of next year's production, or remain in stable numbers until later in the year. It would seem impractical to adjust estimates of potential annual fecundity based on all vitellogenic oocytes for the fraction of those oocytes which do not continue vitellogenesis. Therefore, we believe use of the more mature yolked oocytes for estimating the potential annual fecundity is preferable.

An important implication of our discussions of the third and fourth assumptions is that timing the sampling of females is a critical element in estimating potential annual fecundity: Sample too early in the reproductive cycle and the ovaries are not sufficiently mature; sample too late and spawning is prevalent. The optimal time to sample Dover sole ovaries is when the average diameter of the advanced stock is between 0.86 and 1.1 mm (Fig. 12). When the diameter is less than 0.86 mm, the numbers of advanced oocytes are still increasing (indicated by the t value for the diameter coefficient in the fecundity equation, Fig. 12). When the diameter exceeds 1.1 mm, 20% or more of the females show histological signs of past or imminent spawning, and the assumption of no spawning cannot be safely made.

Spawning rates and reproductive energetics

The spawning season of Dover sole was protracted with postovulatory follicles occurring as early as December and hydrated oocytes as late as May, indicating a season of six months. This is a long season for a fish of determinate fecundity, since typically they are high-latitude species with short, 1–2 month spawning seasons. Batch fecundity was low, averaging about 10 oocytes per gram female weight, except for the first and last batch which average about 5 oocytes per gram. Dover sole spawn about nine times during their

protracted spawning season. Vitellogenesis does not cease when spawning begins, but rather it continues throughout most of the season as the advanced stocks of yolked oocytes are matured and spawned. Spawning frequency appears to increase near the end of the season. This may cause a higher daily production of eggs by the population in late-March or April than in February, even though fewer females have active ovaries in April.

To estimate reproductive effort of Dover sole, we calculated the hypothetical weight of the ovary when the entire advanced stock of oocytes had completed vitellogenesis and hydration had begun. The weight is hypothetical because a Dover sole ovary never contains a full complement of completely yolked oocytes, since vitellogenesis of the smaller advanced yolked oocytes continues after a female begins spawning. To compute the hypothetical weight, we assumed that all oocytes completed vitellogenesis when their average diameter was 1.5 mm. Hydration begins when the advanced yolked oocytes have a mean diameter of 1.3–1.7 mm. We estimated the gonad weight of a 1000 g female with oocytes having a mean diameter of 1.5 mm, using an equation in which gonad weight was expressed as a function of fish weight and volume of the average advanced oocyte (1.5 mm diameter has a volume of 1.77 mm^3; California plus Oregon data; Table 3). The ovary was estimated to weigh 144 g, or about 14% of the body weight. In other words, the annual reproductive effort of Dover sole was about 14% per year, and this effort was distributed over about nine spawnings averaging about 1.6% of their body weight per spawning. Gonad weight was considered to be a measure of reproductive effort by Gunderson and Dygert (1988); but they did not adjust the gonad weight for the full complement of yolk, and consequently their estimates are not comparable to these.

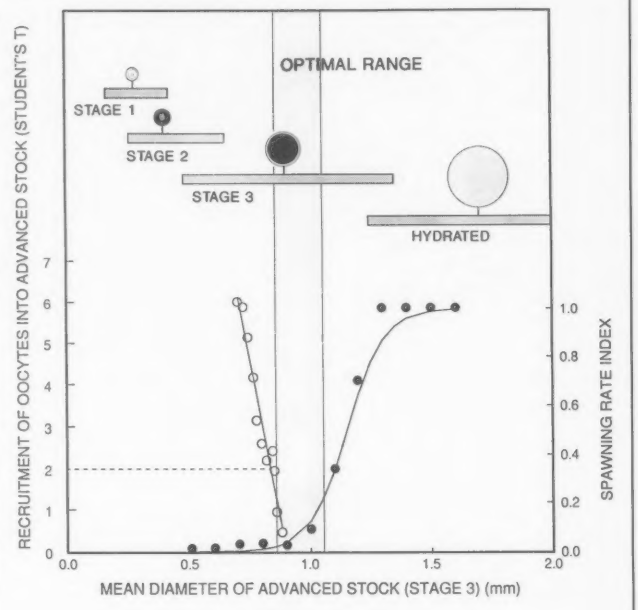

Figure 12

Optimal range of mean diameter of advanced yolked oocytes (stage 3) for determining potential annual fecundity of Dover sole (shaded area, 0.86–1.1 mm). Open circles, Student's t as a function of the minimum mean diameter of stage-3 oocytes included in the fecundity data set: when $t \geq 2$ (P 0.05), the mean oocyte diameter had a positive correlation with fecundity, indicating the stock of yolked oocytes for the season was not fully recruited into stage 3. Spawning rate index (filled circles) for females used in fecundity estimates; index = 0 when no females show signs of past or imminent spawning, and index = 1 when all females have postovulatory follicles or hydrated oocytes. Upper panel indicates diameter range of oocytes in three yolked oocyte stages and hydrated oocytes. Only stage-3 oocytes were used to estimate potential annual fecundity.

Assessment of sexual maturity

Our estimates of length at 50% mature (ML_{50}) were higher when females were taken during the spawning season than when they were sampled before spawning began, regardless of the histological criteria used. Thus, during the spawning season ovaries of some postspawning females had regressed far enough that they were histologically indistinguishable from immature females. This finding has two important implications: First, it indicates that even the broadest histological criteria, based on analysis of H&E sections, will not identify all postspawning females; second, it means that estimates of length or age at first maturity should always be conducted prior to the onset of spawning, when postspawning females with highly regressed ovaries are rare.

Another limit to our ability to assess sexual maturity is that we do not know how many of the females that begin vitellogenesis actually complete it during the current reproductive season. Dover sole ovaries with oocytes in the early vitellogenic stage occurred throughout the spawning season as well as before it began, indicating some females that begin vitellogenesis may not reach sexual maturity in the current

season. At this time, it is an arbitrary choice to consider as mature all females with vitellogenic ovaries or only those with advanced yolked oocytes. Our analysis showed that this arbitrary decision had a pronounced effect on ML_{50} estimates. Thus the criteria for maturity estimates should be precisely specified. It is particularly important to specify the minimum level of oocyte development necessary for a female to be considered as mature. Our preferred definition of maturity included females in the early stages of vitellogenesis with yolked oocytes as small as 0.18 mm diameter, and also included some females without vitellogenic oocytes (maturity IV, Table 16). Those females without vitellogenic oocytes had β atresia in the ovary. We believe that the presence of some β atresia is an inevitable consequence of the resorption of an active ovary or ovulation.

No discussion of sexual maturity would be complete without mentioning the gross anatomical systems used to classify ovaries, because they are the chief method used by fishery biologists to measure sexual maturity in marine fishes. Using gross anatomical criteria, we accurately separated active ovaries (advanced yolked oocytes present) from inactive ovaries (no advanced oocytes) with classification errors of 1–12%. Determining sexual maturity is a far more difficult task, however. Identification of mature females using gross anatomical methods has the same problems with postspawning and early vitellogenesis criteria as histological methods, but the potential for bias is greater. Anatomical criteria are less accurate and may be detectable for shorter periods than histological ones. For these reasons, differences between maturity studies should be interpreted with caution, especially when done by different observers, or with different methods, or when sampling at different times of the year. Many investigators have not been particularly careful to restrict sampling to early in the spawning season. The tendency will be to overestimate the ML_{50} using anatomical methods, especially when samples are taken midseason.

In an earlier paper on Dover sole, Hunter et al. (1990) concluded that size at 50% mature in Dover sole from central California in the 1980s differed from that of Dover sole in northern California in the late 1940s as determined by Hagerman (1952). Although a statistical difference existed between these two data sets, we are inclined to dismiss this difference, since it could be due to differences in criteria and sampling times. Similarly, Yoklavitch and Pikitch (1989) speculated that size at 50% maturity of Oregon Dover sole has changed because their estimate of maturity differed from Harry (1959). We believe that this difference also could easily be due to differences in criteria and timing of sampling. Our analysis of histological criteria for maturity clearly shows that differences in criteria or timing of sampling can produce differences in the ML_{50} as large as any of those seen in the Dover sole literature.

Acknowledgments

We appreciate and thank M. Yoklavich and E. Pikitch for providing original data and supplying some specimens, and W.W. Wakefield for providing some specimens. We thank all on shipboard who helped collect Dover sole ovaries: E. Lynn, W. Flerx, R. Dotson, R. Leong, E. Acuna, and D. Squires. We thank all others who served on the scientific crews and the crews of NOAA ships *David Starr Jordan* and *Miller Freeman*; they contributed greatly to the success of the cruises. Processing of laboratory specimens and estimation of fecundities were assisted by W. Kicklighter, M. Drawbridge, R. Leong, E. Lynn, D. Ramon, and S. Swailes. Computer programs were written by C. Vedovato, R. Young, and J. Butler. L. Jacobson provided suggestions on the modeling of sexual maturity. Illustrations were produced by R. Allen and H. Orr. K. Schaefer, J. Zeldis, and an anonymous reviewer reviewed the manuscript.

Citations

Alheit, J.
1986 Reproductive biology of sprat, *Sprattus sprattus*: Factors determining annual egg production. ICES CM 1986/H:58, 16 p.

Bartoo, N.W., and K.R. Parker
1983 Stochastic age-frequency estimation using the von Bertalanffy growth equation. Fish. Bull., U.S. 81:91–96.

Bretschneider, L.H., and J.J. Duyvene de Wit
1947 Sexual endocrinology of non-mammalian vertebrates. Monogr. Prog. Res., Vol. II. Elsevier, NY.

Carter, W.H. Jr., V.M. Chinchilli, J.D. Wilson, E.D. Campbell, F.K. Kessler, and R.A. Carchman
1986 An asymptotic confidence region for the ED_{100p} from the logistic response surface for a combination of agents. Am. Stat. 40:124–128.

Dixon, W.J., M.B. Brown, L. Engelman, M.A. Hill, and R.I. Jennrich
1988 BMDP statistical software manual, Vol 2. Univ. Calif. Press, Los Angeles, 1234 p.

Gunderson, D.R., and P.H. Dygert
1988 Reproductive effort as a predictor of natural mortality rate. J. Cons. Cons. Int. Explor. Mer 44:200–209.

Hagerman, F.B.
1952 The biology of the Dover sole, *Microstomus pacificus* (Lockington). Calif. Fish Game, Fish Bull. 85:1–48.

Harry, G.Y.
1959 Time of spawning, length at maturity, and fecundity of the English, petrale, and Dover soles (*Parophrys vetulaus*, *Eopsetta jordani*, and *Microstomus pacificus*, respectively). Fish Comm. Oreg. Res. Briefs 7:5–13.

Hislop, J.R.G., and W.B. Hall
1974 The fecundity of whiting, *Merlangius merlangus* (L.) in the North Sea, the Minch and at Iceland. J. Cons. Cons. Int. Explor. Mer 36:42–49.

Hjort, J.
1910 Report on herring investigations until January 1910. Publ. Circ. Cons. Explor. Mer 53.

Horwood, J.W., and M. Greer Walker
1990 Determinacy of fecundity in sole (*Solea solea*) from the Bristol Channel. J. Mar. Biol. Assoc. U.K. 70:803–813.

Hunter, J.R., and S.R. Goldberg
1980 Spawning incidence and batch fecundity in northern anchovy, *Engraulis mordax*. Fish. Bull., U.S. 77:641–652.

Hunter, J.R., and B.J. Macewicz
1980 Sexual maturity, batch fecundity, spawning frequency, and temporal pattern of spawning for the northern anchovy, *Engraulis mordax*, during the 1979 spawning season. Calif. Coop. Oceanic Fish. Invest. Rep. 21:139–149.
1985a Measurement of spawning frequency in multiple spawning fishes. *In* Lasker, R. (ed.), An egg production method for estimating spawning biomass of pelagic fish: Application to the northern anchovy, *Engraulis mordax*, p. 79–94. NOAA Tech. Rep. NMFS 36.
1985b Rates of atresia in the ovary of captive and wild northern anchovy, *Engraulis mordax*. Fish Bull., U.S. 83:119–136.

Hunter, J.R., N.C.H. Lo, and R.J. Leong
1985 Batch fecundity in multiple spawning fishes. *In* Lasker, R. (ed.), An egg production method for estimating spawning biomass of pelagic fish: Application to the northern anchovy, *Engraulis mordax*, p. 67–78. NOAA Tech. Rep. NMFS 36.

Hunter, J.R., B.J. Macewicz, and C.A. Kimbrell
1989 Fecundity and other aspects of the reproduction of sablefish, *Anoplopoma fimbria*, in Central California waters. Calif. Coop. Oceanic Fish. Invest. Rep. 30:61–72.

Hunter, J.R., J.L. Butler, C. Kimbrell, and E.A. Lynn
1990 Bathymetric patterns in size, age, sexual maturity, water content, and caloric density of Dover sole, *Microstomus pacificus*. Calif. Coop. Oceanic Fish. Invest. Rep. 31:132–144.

Kimura, D.K., and S. Chikuni
1987 Mixtures of empirical distributions: An iterative application of the age-length key. Biometrics 43:23–25.

Lambert, J.G.D.
1970 The ovary of the guppy *Poesilia reticulata*. The atretic follicle, a *Corpus atreticum* or a *Corpus luteum praeovulationis*. Z. Zellforsh. 107:54–67.

Thigpen, C.C.
1987 A sample size problem in simple linear regression. Am. Stat. 41:214–215.

Wathne, F.
1977 Performance of trawls used in resource assessment. Mar. Fish. Rev. 39(6):16–23.

Yoklavich, M.M., and E.K. Pikitch
1989 Reproductive status of Dover sole, *Microstomus pacificus*, off northern Oregon. Fish. Bull., U.S. 87:988–955.

Comparisons of early-life-history characteristics of walleye pollock *Theragra chalcogramma* in Shelikof Strait, Gulf of Alaska, and Funka Bay, Hokkaido, Japan*

Arthur W. Kendall Jr.

Alaska Fisheries Science Center, National Marine Fisheries Service, NOAA
7600 Sand Point Way NE, Seattle, Washington 98115-0070

Toshikuni Nakatani

Laboratory of Principles of Fishing Grounds, Faculty of Fisheries
Hokkaido University, Hakodate, Japan 041

Abstract.–Over the past several years researchers in Japan and the United States have independently been conducting extensive studies on the early life history of two discrete populations of walleye pollock *Theragra chalcogramma*, trying to understand recruitment variation. The population of interest to Japanese researchers spawns near Funka Bay, Hokkaido, Japan, while the population of interest to American researchers spawns in Shelikof Strait, Gulf of Alaska. This paper summarizes and compares characteristics of spawning and ecology of eggs, larvae, and early juveniles of the species in these two areas. Although the species has apparently adapted its early-life-history pattern to environmental differences in the two areas, some underlying similarities exist. The adults mainly spawn at a particular time of year following a spawning migration to a specific location so that the eggs and larvae can reach specific areas for subsequent development. In both areas oceanographic conditions are favorable for larval food production (copepod nauplii) when the walleye pollock larvae are present. Drift of the eggs into the bay, where copepod production is enhanced, seems important in Funka Bay, and drift of the larvae toward juvenile nursery grounds on the continental shelf as opposed to being swept offshore, seems important in Shelikof Strait. Interannual differences in larval drift and food production because of varying oceanographic conditions may contribute significantly to variations in year-class size.

Manuscript accepted 27 November 1991.
Fishery Bulletin, U.S. 90:129–138 (1992).

Walleye pollock *Theragra chalcogramma* is a dominant fish in the North Pacific Ocean and in the Bering Sea, both in terms of population size and importance to commercial fisheries. It is a major fishery resource in the Funka Bay area on the Pacific Ocean side of Hokkaido, Japan, and in Shelikof Strait, Gulf of Alaska. In both areas, most fishing is done just prior to and during the spawning season. In Funka Bay, walleye pollock are caught in bottom gillnets, while in Shelikof Strait midwater trawls are used. In Funka Bay the catch varied from about 4.3×10^4 metric tons (t) to about 10.7×10^4 t from 1976 to 1986. In Shelikof Strait, an intense fishery on the spawners existed from 1981 through 1988, although harvest has been severely restricted since 1986 because of reduced abundance of the population (Megrey 1989). The harvest in Shelikof Strait peaked in 1984 at about 31×10^4 t.

There is a growing interest in understanding recruitment in this species, and considerable work has been conducted independently by Japanese researchers in Funka Bay and by U.S. researchers in Shelikof Strait over the past several years. This paper compares the results of these studies (Table 1). While these studies reveal that the early-life-history strategy of walleye pollock allows this species to adapt to different environments, they also indicate that underlying similarities exist between populations. Although understanding causes of recruitment variation in either area is a distant goal, testable hypotheses have been developed in both areas. The comparisons presented in this paper may help researchers in both areas focus their studies toward an understanding of the recruitment process. They may also guide future studies of the species in other areas such as the Bering Sea.

Environmental comparisons

Physical setting

Funka Bay is located in the southern part of Hokkaido, Japan, at about 42°N (Fig. 1). Depths within the bay are generally less than 80 m, although there is a small area of water deeper than 100 m in the center of the bay. Immediately outside the bay the bottom slopes evenly to 500 m within 45 km. The area of the bay is 2270 km^2.

* Contribution FOCI-138 to Fisheries Oceanography Coordinated Investigations, NOAA.

Shelikof Strait is located in the northern Gulf of Alaska between the Alaska Peninsula and the Kodiak Archipelago at about 57°N (Fig. 1). Water depths within Shelikof Strait exceed 300 m in some areas. At the northeast and southwest ends of the strait there are sill depths of about 200 m. Depths of greater than 500 m are reached on the continental slope immediately beyond the southwestern sill. The southern part of the strait and waters to the south comprising about 12,450 km^2, are the areas occupied by eggs and larvae of walleye pollock originating in Shelikof Strait.

Table 1

Comparisons of early-life-history characteristics of walleye pollock *Theragra chalcogramma* and their spawning environments in Funka Bay, Japan, and Shelikof Strait, Gulf of Alaska.

	Funka Bay	Shelikof Strait
Latitude	45°50′–42°35′N	56°00′–59°00′N
Area	2270 km^2	12,450 km^2
Nominal annual catch	[a]70,000 t	[b]100,000 t
Spawning season	[c]Dec.–Mar.	[d]Early April
Spawning depth	[e]100–120 m	[d]200–300 m
Temperature at spawning depth	[e]2–6°C	[f]5.5°C
Depth of maximum egg concentrations	[e]0–40 m	[f]150–200 m
Egg specific gravity	[e]1.020–1.026 g/cm^3	[f]1.024–1.031 g/cm^3
Depth of maximum larval occurrence	[g]10–20 m	[h]15–50 m
Length of larvae when copepod nauplii are predominant components of diet	[e]<7–8 mm	[h]<11 mm
Larval growth rate	—	[h]0.21 mm/day

[a]Nakayama et al. 1987, [b]Megrey 1989, [c]Maeda et al. 1976, [d]Kendall and Picquelle 1990, [e]Nakatani 1988, [f]Kendall and Kim 1989, [g]Kamba 1977, [h]Kendall et al. 1987.

Physical oceanography

The water of Funka Bay originates from the seasonal influx of two water masses: The Tsugaru Warm Water and the Oyashio Water. Tsugaru Warm Water enters the Bay in late-summer when surface waters exceed 15°C and there is a strong thermocline in the upper 20 m (Nakatani 1988). Autumnal cooling produces isothermal conditions and cooling to about 4°C (Winter Funka Bay Water: Ohtani and Kido 1980). In late-winter or early-spring, the cold (<2°C), less saline (<33.0‰) Oyashio Water usually intrudes into the Bay above the Winter Funka Bay Water, producing a stratified condition with a temperature inversion. In late-spring and early-summer, seasonal warming of surface waters occurs and a thermocline develops. Throughout the year, bottom temperatures remain at 3–6°C.

Shelikof Strait has an estuarine type circulation, with less seasonal variation than Funka Bay. In its upper layers, the Alaska Coastal Current (ACC) flows to the southwest and is particularly pronounced on the Alaska Peninsula side of the Strait. During runoff seasons (late-spring to early-fall), substantial amounts of freshwater enter the strait, primarily from Cook Inlet, and flow along the Peninsula until thoroughly mixed with the ACC. From approximately 150 m to the bottom, more saline water flows into the strait over the sill to the southwest (Kim 1987). During April and May (when walleye pollock eggs and larvae are present), near-surface water temperatures in the ACC are generally 0–4°C, warming to 7°C by late May, while the deeper waters are generally 4–5.5°C. Salinity varies from about 31 to 33.5‰.

In Funka Bay there is considerable interannual variation in the date when the Oyashio Water intrudes and in the length of time that surface temperatures remain cold (<3°C). In Shelikof Strait, interannual variation in the frequency, intensity, and track of storms affects water properties and transport.

Biological comparisons

Spawning

In Funka Bay, adult walleye pollock mature and spawn from November to March, with peak spawning activity occurring in January and February (Maeda et al. 1976 and 1981, Yoon 1981), whereas in Shelikof Strait most fish mature in February and March and spawning peaks in early April (Kim 1989, Kendall and Picquelle 1990). Pelagic eggs are present in Funka Bay from December until March, and in Shelikof Strait eggs are present mainly in April. There is some interannual variation in time of spawning in Funka Bay, and eggs have even been collected in November and April (Maeda et al. 1980). Thus the spawning season seems to occur earlier in the year and lasts longer in Funka Bay than in Shelikof Strait. Spawning occurs mainly at depths of 100–120 m near the entrance of Funka Bay (Maeda et al. 1976, Nakatani 1988, Nakatani and Maeda 1989). In Shelikof Strait, spawning is concen-

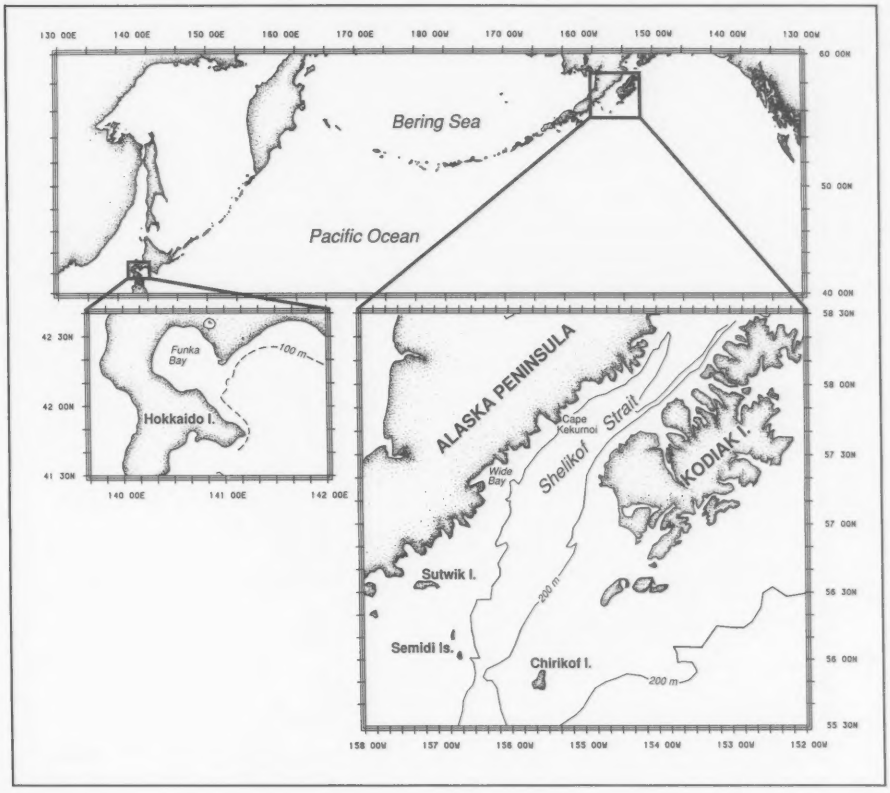

Figure 1
Location of Funka Bay, Japan, and Shelikof Strait, Gulf of Alaska. Insets are enlargements of the areas with pertinent bathymetry.

trated in a small area of deep water (>250 m) near Cape Kekurnoi (Fig. 1) (Kendall and Picquelle 1990).

Field surveys of adult walleye pollock in Funka Bay and Shelikof Strait show that fish congregate and migrate to a particular part of their range just prior to the spawning season. Final migration to a restricted spawning area takes place quickly. In Shelikof Strait, hydroacoustic surveys show that the fish separate into vertical strata, presumably by sex (females below males) and readiness to spawn (Muigwa 1989).

Although the fish move to the spawning area as a large group, spawning itself is by pairs. Behavior of spawning walleye pollock has been investigated using captive fish from Funka Bay (Sakurai 1982, 1989), as well as from Puget Sound, Washington (Baird and Olla 1991). The shallow tanks used by Sakurai (1989) may have prevented some of the vertical aspects of spawning behavior observed by Baird and Olla (1991). Although no such studies have been conducted on fish from Shelikof Strait, similarities between the behavior of fish from near the eastern (Puget Sound) and western (Funka Bay) extremes of the species distribution may indicate that spawning behavior varies little geographically. In experimental tanks, the fish form loose aggregations near the surface. Males frequently follow other males and females. Sakurai (1989) related male–male interaction to the agonistic behaviors associated with dominance; Baird and Olla (1991) considered the male's following behavior as a searching behavior for potential mates. Sakurai (1989) also observed courtship displays by males toward prospective mates. At the onset of a spawning, a female would swim down with a male following her. The male then made contact with her by rubbing his ventral surface first against her dorsum or side and then he swam beneath her, with their two vents in contact. Other males occasionally followed the pair closely and also made contact with the female. During vent-to-vent contact, the male rubbed his body rapidly against the female's abdomen, and presumably gametes were released at this time (they could not be seen in the water, but were found in the tank overflow within an hour). Most spawning took place in evening or morning twilight (Baird and Olla 1991).

Female walleye pollock characteristically spawn a number of batches of eggs over a fairly short period

each year. The interval between batches is a few days. The number of eggs per batch and size of eggs decrease with successive batches. These patterns have been observed both in Funka Bay (Sakurai 1982) and Shelikof Strait (Hinckley 1990).

Fecundity

Miller et al. (1986) related fecundity of walleye pollock from Shelikof Strait to gutted weight and fork length, while Sakurai (1982) related fecundity of walleye pollock from Funka Bay to whole weight and body length. Conversions were applied here to the Funka Bay length and weight data so fecundity could be compared with Shelikof Strait values based on

$$Y = 0.7634X + 23.4472 \ (r^2\ 0.96628,\ N\ 40)$$

where X = body weight and Y = gutted weight (Y. Sakurai, unpubl.); and

$$Y = 1.0659X + 4.050 \ (r^2\ 0.9959,\ N\ 53)$$

where X = body length and Y = fork length (T. Maeda, unpubl.).

The relative fecundity of Funka Bay fish is represented by the relationship $F = 8.73 \times 10^{-6} L^{3.98}$ and $F = 106.2 W^{1.21}$, where L = body length in mm and W = body weight in grams (N 94) (Sakurai 1982); therefore a 300 g (gutted weight) fish produces 129,000 eggs and a 1000 g fish yields 589,000 eggs. In Shelikof Strait, the relationship was found to be $F = 1.2604 L^{3.2169}$ and $F = 387.4551 W^{1.0160}$ (N 60), where L = fork length in cm and W = gutted weight in grams; this yields 127,000 eggs for a 300 g fish and 433,000 eggs for a 1000 g fish (Miller et al. 1986). Thus small fish from Funka Bay have about the same number of eggs, but larger fish have more eggs than those from Shelikof Strait (Fig. 2).

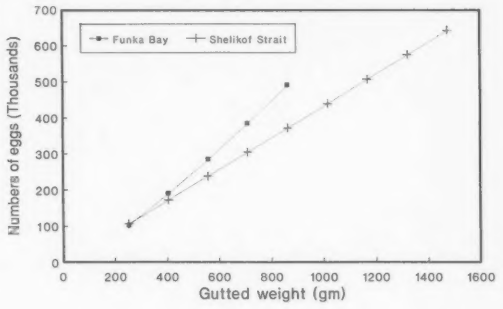

Figure 2
Fecundity-weight relationship for walleye pollock in Funka Bay, Japan (based on Sakurai 1982), and Shelikof Strait, Gulf of Alaska (based on Miller et al. 1986).

Eggs

Development Eggs from Funka Bay are more variable in size and slightly larger than those from Shelikof Strait. In Funka Bay, eggs are 1.15–1.68 mm ($\bar{x}$ 1.46 mm) in diameter (Nakatani and Maeda 1984, T. Nakatani, unpubl.). In Shelikof Strait, egg diameter ranges from 1.30 to 1.41 mm, and egg size has been shown to vary interannually and decrease during the spawning season (Hinckley 1990).

Eggs from Funka Bay develop at a rate dependent on temperature according to the relationship

$$D = 31.70 \exp(-0.12T),$$

where D is days to 50% hatch and T is temperature (°C). Thus 50% hatch times are 22.1 days at 3°C, 17.4 days at 5°C, and 15.4 days at 6°C (Nakatani and Maeda 1984). No measurements of incubation time are available for eggs from Shelikof Strait; however, reared eggs from Auke Bay in southeast Alaska (58°20′N) required 19.2 days at 3°C, 14.1 days at 5°C, and 12.2 days at 6°C for 50% hatch (Haynes and Ignell 1983). Thus eggs from southeast Alaska developed to hatching more quickly, by about 2–3 days, than those from Funka Bay (Fig. 3).

Vertical distribution The vertical distribution and buoyancy of eggs have been investigated in both Funka Bay and Shelikof Strait. In Funka Bay, eggs rise in the water column as they develop. Stage-1 (fertilization to morula) eggs were found at a depth of roughly 30 m (10–40 m), whereas Stage-5 (embryo more than three-fourths yolk circumference) eggs were mainly at depths of 10–20 m (Nakatani 1988). The specific gravity of Funka Bay eggs throughout development was within a range of 1.020–1.025 g/cm^3 ($\bar{x}$ 1.0226 g/cm^3). This resulted in an upward velocity of 4.9 m/h in ambient water through the homogenized water column early in the spawning season (σ^t 26.41–27.17), and is consistent with field observations of shallower depths for older eggs compared with those recently spawned (Nakatani and Maeda 1984, Nakatani 1988).

In Shelikof Strait, the vertical distribution of eggs changes during development in response to their changing specific gravity. Newly spawned eggs are positively buoyant, and thus rise from the deep locations where they are spawned. In middle stages of development, the eggs become heavier and sink until just before hatching when they again rise toward the surface (Kendall and Kim 1989). The specific gravity

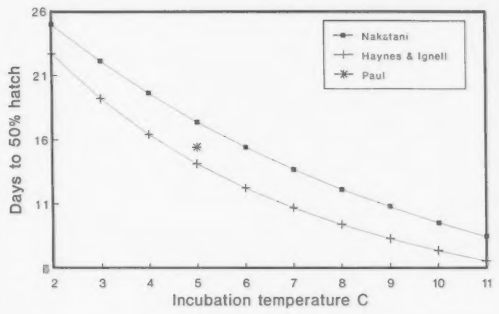

Figure 3
Incubation period of walleye pollock eggs from Funka Bay, Japan (based on Nakatani 1988); Resurrection Bay (based on A.J. Paul, Univ. Alaska, Seward, pers. commun.) and Auke Bay, Alaska (based on Haynes and Ignell 1983).

of eggs from Shelikof Strait varied from 1.0243 to 1.031 g/cm^3, whereas the water density varied from 1.0256 to 1.0259 g/cm^3 (in 1985). Less than 20% of eggs of all ages occurred above 162 m in Shelikof Strait. Over 80% of early- (fertilization to morula) and late-stage eggs (embryo more than one-half circumference of yolk to hatching) occurred between 216 and 277 m (near bottom), while over 60% of middle-stage eggs (gastrula) occurred between 162 and 216 m (Kendall and Kim 1989). Thus eggs in Shelikof Strait are heavier and occur deeper than those in Funka Bay.

Horizontal distribution The horizontal distribution pattern of eggs in Funka Bay was fairly consistent among the 3 years (1977, 1978, and 1987) for which data are presented (Nakatani 1988, Nakatani and Maeda 1981 and 1989). Younger eggs are mainly found just outside the entrance to the bay and older eggs are found inside the bay, indicating that spawning occurs outside the bay and the eggs drift into the bay as they develop. During the period 24 January to 11 February 1978, egg abundance reached 13,424 Stage-4 eggs/m^2 at a station just south of the entrance to the bay where large numbers of Stage 2–5 eggs were also present, producing a total of 23,817 eggs/m^2.

The egg distribution pattern in Shelikof Strait was most intensively examined in 1981; however, sampling in other years (1978–86) indicates similar patterns. The first appearance of low numbers of eggs occurs in March and early April, mainly in the southern part of the strait (Kendall and Picquelle 1990). The highest concentrations of eggs occur off Cape Kekurnoi in early April, where abundances of Stage-2 and -3 eggs exceeded 1000/m^2 in 1981. The combined abundance for all stages was 350,000 eggs/m^2 in the area of maximum concentration; about 15 times the maximum abundance observed in Funka Bay. By late April, egg abundance is reduced as eggs are spread more evenly throughout the southern two-thirds of the strait and the area immediately to the southwest of the strait. By late May, egg abundance is further reduced, but the area of occurrence is still similar to that seen in late April. As opposed to Funka Bay, there is little evidence of drift of eggs in Shelikof Strait. It appears that the adults spawn some eggs in the southwestern part of the strait as they move toward the main spawning area off Cape Kekurnoi. Later spawning in late April and May seems to be dispersed throughout the strait and occurs at a much reduced level. Measurements of currents in Shelikof Strait also indicate that little drift would be expected in the deep waters (>150 m) where most eggs occur (Kendall and Kim 1989).

Larvae*

Vertical distribution The ecology of walleye pollock larvae has been investigated in both Funka Bay and Shelikof Strait. In both areas most larvae occur above 50 m in the water column and exhibit limited diel vertical migration (Kamba 1977, Kendall et al. 1987). Few larvae are collected at the surface, but some larvae move up to 10–20 m depth in the evening. At night they are fairly evenly distributed throughout the upper 50 m, and in the early morning they are again concentrated above 20 m. During midday they are most abundant at 20 m and deeper to 50 m. The larvae sampled by Kendall et al. (1987) in Shelikof Strait averaged 11.0 mm (SD 1.7 mm), while those in Funka Bay sampled by Kamba (1977) had a wide range of lengths from 4.6 to 26.4 mm, although most were 4.6–12.8 mm. Kamba (1977) indicated that larger larvae (>13.7 mm) were more often collected in shallow tows at night and in deep tows during the day, suggesting that either the larger larvae migrated more than the smaller ones or that the larger larvae were more successful at avoiding the shallow nets during the day. No large larvae were collected by Kendall et al. (1987). Kamba (1977) concluded that the diel vertical movements of pollock larvae in Funka Bay corresponded to those of their zooplankton prey. Both Kamba (1977) and Kendall et al. (1987) found a diel pattern in gut fullness, with little food found in guts at night and most food found in guts during the day.

* Lengths of larvae and juveniles are reported here as standard length (SL, from the tip of the snout to the end of the notochord or base of the hypural plate), although in the Japanese literature they were given as total length (TL). Conversion from TL to SL is based on our paired measurements of 1048 fish (4.2–103 mm SL) which resulted in the relationship: SL(mm) = 0.108 + 0.907 TL(mm).

Horizontal distribution In the Funka Bay region, walleye pollock larvae are generally concentrated inside the bay from late January through early April (Nakatani 1988, Nakatani and Maeda 1989). Their abundance decreases during this time from >5000 larvae/m^2 in the area of maximum concentration in late January to 200–400 larvae/m^2 in early April. In many cases, surveys have disclosed more than one area of abundance within the bay. Their occurrence generally overlaps that of the Oyashio Water. For example, in 1980 the Tsugaru Warm Water remained in the bay longer than usual, and the Oyashio Water did not enter the bay until mid-March; before then, the larvae were concentrated at the mouth of the bay. It is possible that larvae entering the bay before the invasion of the Oyashio Water would experience low survival because of inadequate prey production.

In Shelikof Strait, most larvae are concentrated in one large patch that can be followed as it drifts to the southwest with the prevailing currents from April through May (Kendall et al. 1987). The velocity of drift may vary interannually and depend on weather patterns in the area as well as the strength of the ACC. In some years, it appears that most of the larvae drift out of the strait within 2–4 weeks after hatching, but in other years they remain for several more weeks because of the influence of nearshore eddies (Incze et al. 1989). There is considerable cross-strait shear in the current, so the drift of larvae is influenced by where they reach the surface layer from their deep incubation area (Kim and Kendall 1989). Larval abundances as high as 10,000/m^2 were observed in the patch in late April 1981, and by late May abundances of 2400/m^2 were present (Bates and Clark 1983).

Feeding Copepod nauplii, which were not identified to species, are the major prey item of first-feeding walleye pollock larvae (Kamba 1977, Kendall et al. 1987, Nakatani and Maeda 1983). Copepodids are the most important prey item in the diet of 11 mm larvae in Shelikof Strait and 8 mm larvae in Funka Bay. Copepod eggs were more prevalent in guts of larvae in Funka Bay than in Shelikof Strait (Nakatani and Maeda 1983, Kendall et al. 1987). Their digestibility and nutritional value for walleye pollock larvae are unknown. *Pseudocalanus* spp. was the most abundant copepod taxon in the water column in Shelikof Strait and Funka Bay when larvae were present (Kendall et al. 1987, Nakatani 1988). The nauplii in the guts of small larvae were probably mostly *Pseudocalanus* spp. and *Oithona* spp., and most of the copepodids in larger larvae were *Pseudocalanus* spp. Copepodids of *Pseudocalanus minutus* and *Oithona similis* were most abundant in larger larvae up to 30 mm in Funka Bay (Nakatani and Maeda 1983). The maximum prey size increases with growth of the larvae, but the minimum size remains fairly constant through fish up to about 73 mm (Kamba 1977).

Based on laboratory and field studies, naupliar abundances of about 10 per liter seem to be required to support growth of small (<8 mm) walleye pollock larvae (Paul 1983, Dagg et al. 1984). Prey densities above this threshold have been observed associated with the larval patch in Shelikof Strait before and during a storm (Incze et al. 1990). Naupliar abundances below this threshold were seen in Funka Bay throughout most of the larval period in 1987, but they were above 10 per liter in several other years (Nakatani and Maeda 1989). However, naupliar densities were probably underestimated, since they were collected on 100 μm sieves. Availability of smaller nauplii as larval food will require further observations.

Age and growth Daily growth increments on otoliths have been used to determine the age of larvae and early juveniles from both Shelikof Strait and Funka Bay. Based on a series of 109 larvae (6.0–14.6 mm SL) collected in Shelikof Strait in May 1983, the linear growth equation $SL = 4.29\,mm + 0.21\,d$ (r^2 0.75), where d = age in days, was fit (Kendall et al. 1987). Growth based on 357 larvae and early juveniles 3.9–30.0 mm SL from the Shelikof spawning collected May through July 1987 fit a Laird-Gompertz function: SL at age t = 4.505 ($e^{7.854(1-e^{-0.004t})}$), where t = days after hatch (Yoklavich and Bailey 1989). The growth of larvae and juveniles from Funka Bay fit the function: $TL = 121.5/(1 + e^{-0.026(t-124.511)})$, with TL in mm (Nishimura and Yamada 1984). Thus larvae 50 days old from Funka Bay were about 14.0 mm SL (see footnote) while those from Shelikof Strait would range from 14.8 mm SL (Kendall et al. 1987) to 18.7 mm SL (Yoklavich and Bailey 1989) (Fig. 4).

Larval population length-frequency distributions depend on time of spawning, mortality of larvae, growth of larvae, and sampling bias. Except for sampling bias, these factors represent population processes occurring to the annual cohort of larvae. In Funka Bay, even though spawning takes place over a protracted period, larval survival appears low except during periods when adequate food is present. Mortality due to starvation is high for larvae that hatch before the spring increase of nauplii in Funka Bay (Nakatani and Maeda 1989, Nakatani 1991). Thus variations in size of larvae may depend more on differences in the birth dates of surviving larvae than on differences in growth rates.

In Shelikof Strait, spawning peaked during the first week of April in several years. By the end of April 1981, most larvae were about 4.8 mm. By the third week in May 1981, they were mostly 7–8 mm (Dunn et al. 1984), as they were in 1982 (Kendall et al. 1987).

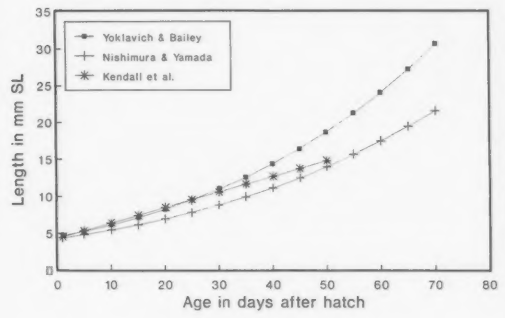

Figure 4
Growth of walleye pollock larvae and juveniles from Funka Bay, Japan (Nishimura and Yamada 1984), and larvae from Shelikof Strait, Gulf of Alaska (Kendall et al. 1987, Yoklavich and Bailey 1989).

However, in 1983 larvae averaged 11.23 mm in late May (Kendall et al. 1987). No interannual differences in larval growth rates were discerned for larvae collected in Shelikof Strait in late May 1983, 1985, 1986, or 1987. Because larvae were larger in late May 1983 than in 1985, 1986, or 1987, they may have been survivors of an earlier spawning than those observed in the other years (Yoklavich and Bailey 1989).

Early juveniles

Young-of-the-year juvenile walleye pollock (18–73 mm) have been sampled extensively in Funka Bay using midwater and bottom trawl nets (Nakatani and Maeda 1987). The juveniles are about 34 mm in late May, 36 mm in June, and 55–80 mm in late July. In June, juveniles (22–66 mm) are found mainly at 25–30 m at night and at 10–15 m during the day (Nakatani and Maeda 1987). The juveniles move deeper in the water column in May and June, and by late July most are on the bottom (Nakatani and Maeda 1987). In July, larger fish are caught in bottom trawls while smaller fish are still in the water column. As the juveniles grow and move toward deeper water and the bottom, they also move from inside the bay toward the entrance (in June) and to the shelf (100–300 m) just outside the bay (by August) (Nakatani and Maeda 1987).

Some variation in size-at-date of juveniles among years has been observed (Fukuchi 1976, Nakatani and Maeda 1987), which may be due to interannual differences in growth rates, or differences in hatch dates of surviving juveniles.

Food organisms changed during juvenile growth with *Neocalanus plumchrus* being most important in fish >27 mm long in midwater. Juveniles collected on the bottom fed on large-sized copepodids of *Neocalanus cristatus* and *Eucalanus bungii*, *Euphausia pacifica* (a euphausid), and *Parathemisto japonica* (an amphipod) (Nakatani and Maeda 1987).

Young-of-the-year juveniles from the Shelikof Strait spawning were sampled with a Methot midwater frame trawl (Methot 1986) in June and July 1987 (Hinckley et al. 1989), and by small-mesh midwater and bottom trawl surveys in late-summer of several years (Bailey and Spring, in review). Data from these studies have not yet been completely analyzed. However, in June and July the early juveniles (mainly 20–30 mm) were found on the shelf along the Alaska Peninsula. As with the eggs and larvae, they formed a large discrete patch surrounded by a large area with lower abundances. From their pattern of distribution, it appears that at this size and time of year they still inhabit midwater depths and are not schooling (Hinckley et al. 1989). Fish were found to feed mainly on various life stages of *Pseudocalanus* spp., smaller fish ate primarily nauplii and copepodids, while adults became more important in larger fish. Differences in diet between fish sampled at different locations indicated that the food organisms were patchily distributed (Grover 1990).

Sampling in late-summer has concentrated mainly on the bays around Kodiak Island and along the Alaska Peninsula. Considerable interannual variation in sampling and pattern of distribution of juveniles characterized these surveys. In 1987, when the sampling area in late-summer included the shelf west of the Shumagin Islands, a concentrated patch of juveniles was found that was likely the product of the Shelikof Strait spawning, i.e., the eggs and larvae that had been followed through the spring during their drift to the southwest from Shelikof Strait (Bailey and Spring, in review).

Year-class determinants

Studies of walleye pollock early life history in both Funka Bay and Shelikof Strait have been designed to determine causes of year-class fluctuations. The basic premise is that these fluctuations result from events during early life history and have little relation to the abundance or other characteristics of the spawning population. The influence of hydrography and its effect on larval food supply has been the most intensively studied factor in both areas, but predation has also been considered in Shelikof Strait research.

In Funka Bay, walleye pollock early life history seems to be closely tied to the timing and extent of the influx of Oyashio Water (Nakatani 1984). This cold, low-salinity water carries *Pseudocalanus minutus* into the bay where they produce nauplii, the primary diet of small larvae in nearsurface waters. Walleye

pollock spawning seems to be timed and positioned to correspond to this influx. In years when this influx is delayed or absent, survival of larvae may be reduced (Nakatani and Maeda 1989). Years with an early invasion of the Oyashio Water have resulted in large year-classes of walleye pollock (Nakatani 1988). However, a strong year-class was also observed in 1980 when there was a late invasion (Nakatani and Maeda 1983, Nakayama et al. 1987). To predict population size fluctuations will require further studies on the causes of larval mortality.

Besides factors influencing larval food production in Shelikof Strait (Incze et al. 1990), the complex dynamics of the ACC as it exits the strait seem important in determining the rate of drift of the larval patch and its resultant position when the larvae are ready to settle (Reed et al. 1989). If the larvae are in the center of the ACC as it exits the strait, they may be carried quickly offshore through the sea valley between the Semidi Islands and Chirikof Island, as apparently happened in 1985 (Incze et al. 1989). Some of these larvae may remain offshore where larval feeding conditions are probably not ideal. The return of offshore larvae to the shelf for demersal settlement is also problematical. If the larvae are on the Alaska Peninsula side of the core of the ACC as it exits the strait, their drift will be slower, and they should remain in the coastal region where food production is probably enhanced. Their trajectory should carry them west along the Alaska Peninsula to shelf areas suitable for demersal settlement.

Storm winds blowing offshore from Wide Bay may displace the ACC as it exits the strait, and eddies have been observed in this area. The influence of such factors on the larval patch and larval food production may be important in determining the numbers of larvae reaching the juvenile stage.

Conclusions

It appears that within large areas of distribution, walleye pollock populations have evolved to spawn in very specific areas and during brief times of the year. Adults migrate to these areas annually for spawning. This spawning pattern produces concentrations of planktonic eggs and larvae that far exceed those reported for any other fish (>20,000 eggs/m^2; <5000 larvae/m^2). These spawnings are such that the eggs and larvae find themselves in areas where suitable food is abundant and where currents later carry larvae to suitable nursery areas. It appears that interannual variations in oceanographic conditions responsible for food production and larval drift impact larval survival, and hence year-class strength. Although there are marked differences in the geography and oceanography of Shelikof Strait and Funka Bay, walleye pollock have adapted to reproduce successfully in both areas. Adaptations in the early life history of walleye pollock to these differences in environment include timing and duration of the spawning season, specific gravity of the eggs, and differences in prey size in relation to larval size.

Time of spawning in both areas corresponds to seasonal transitions in hydrographic conditions (Nakatani 1988, Kim 1987). The spawning season is several months long in the lower-latitude Funka Bay area where there is considerable interannual variation in timing of the intrusion of the cold Oyashio Water, which increases copepod naupliar production. The Shelikof Strait area spawning is very peaked, taking place mainly over a few weeks and during the same time each year, early April. This is the time when currents are at an annual minimum due to reduced precipitation and weak winds. We do not know if low current strength is the seasonal signal that fish respond to, but presumably the signal is less variable than the intrusion of Oyashio Water.

Eggs are less dense in Funka Bay where water depths are only about one-third those of Shelikof Strait. In Funka Bay, the eggs rise in the water column after spawning and drift into the inner part of the bay. In Shelikof Strait, the eggs remain in the nearbottom water where they are spawned and show no appreciable drift. This difference in transport of eggs may relate to the desired location of hatching. Copepod production is enhanced when Oyashio Water enters Funka Bay and the egg drift pattern enables the eggs to hatch there. In Shelikof Strait, the upper layers of water during the spawning season are moving to the southwest at a rate that would flush eggs in surface waters out of the strait and into the offshore Alaska Stream in a few weeks. By remaining in the sluggish bottom waters, hatching is more likely to occur in southwest Shelikof Strait where larval prey may be more abundant. Interannual variations in storms in this area may effect copepod production and thereby larval condition.

In both areas, nauplii of species of small copepods, *Pseudocalanus* and *Oithona*, are dominant in the diet of first-feeding larvae. Eating small prey is energetically costly for larger larvae, so it may be critical for them to encounter more advanced stages of copepods (Incze et al. 1984). This may be more important in Shelikof Strait than in Funka Bay because larvae in Funka Bay start eating larger prey at a smaller size than do larvae in Shelikof Strait.

Drift of larvae to nursery grounds is more important in Shelikof Strait than it is in Funka Bay. It appears that most juveniles that result from spawning in Shelikof Strait inhabit shelf and nearshore areas 100–200 km from the spawning location by the age of 4 months

(Hinckley et al. 1989). Juveniles from the Funka Bay spawning are mostly found in waters just outside the bay during their first summer (Nakatani 1988). In the following winter, some of them remain in the center of the bay (T. Maeda and T. Nakatani, unpubl. data).

Acknowledgments

Many investigators in Japan and the United States are studying the early life history of walleye pollock. Many have generously shared ideas and data with us and we thank them. In particular, Dr. Kevin Bailey, AFSC, and Dr. Jim Schumacher, PMEL, reviewed early drafts of this manuscript and gave numerous helpful suggestions, as well as Dr. Tatsuaki Maeda who conducted many of the Funka Bay studies that formed the basis for this paper with Dr. Toshikuni Nakatani. Dr. Lew Haldorson, University of Alaska, and Dr. Svein Sundby, Institute of Marine Research, Norway, provided valuable reviews of an earlier draft.

Citations

Bailey, K., and S. Spring
In review Comparison of larval, age-0 juvenile, and age-2 recruit abundance indices of walleye pollock *Theragra chalcogramma* in the western Gulf of Alaska. ICES J. Mar. Sci.

Baird, T.A., and B.L. Olla
1991 Social and reproductive behavior of walleye pollock *Theragra chalcogramma* of a captive group. Environ. Biol. Fish. 30:295–301.

Bates, R.D., and J. Clark
1983 Ichthyoplankton off Kodiak Island and the Alaskan Peninsula during spring 1981. NWAFC Proc. Rep. 83-89, Northwest & Alaska Fish. Cent., NMFS, NOAA, Seattle, WA 98115-0070, 105 p.

Dagg, M.J., M.E. Clarke, T. Nishiyama, and S.L. Smith
1984 Production and standing stock of copepod nauplii, food items for larvae of walleye pollock *Theragra chalcogramma* in the southeastern Bering Sea. Mar. Ecol. Prog. Ser. 19: 7–16.

Dunn, J.R., A.W. Kendall Jr., and R.D. Bates
1984 Distribution and abundance patterns of eggs and larvae of walleye pollock (*Theragra chalcogramma*) in the western Gulf of Alaska. NWAFC Proc. Rep. 84-10, Northwest & Alaska Fish. Cent., NMFS, NOAA, Seattle, WA 98115-0070, 66 p.

Fukuchi, M.
1976 Some aspects of bioenergetics of walleye pollock (*Theragra chalcogramma* Pallas) at early life stages. Ph.D. thesis, Univ. Hokkaido, Hokkaido, Japan.

Grover, J.J.
1990 Feeding ecology of late-larval and early-juvenile walleye pollock *Theragra chalcogramma* from the Gulf of Alaska in 1987. Fish. Bull., U.S. 88:463–470.

Haynes, E.B., and S.E. Ignell
1983 Effect of temperature on rate of embryonic development of walleye pollock, *Theragra chalcogramma*. Fish. Bull., U.S. 81:890–894.

Hinckley, S.
1990 Variation in egg size of walleye pollock (*Theragra chalcogramma*) with a preliminary examination of the effect of egg size on larval size. Fish. Bull., U.S. 88:471–483.

Hinckley, S., K. Bailey, J. Schumacher, S. Picquelle, and P. Stabeno
1989 Preliminary results of a survey for late stage larval walleye pollock and observations on larval drift in the western Gulf of Alaska, 1987. *In* Proc., Int. symp. on biology and management of walleye pollock, p. 297–306. Alaska Sea Grant Rep. 89-1, Univ. Alaska, Fairbanks.

Incze, L.S., M.E. Clarke, J.J. Goering, T. Nishiyama, and A.J. Paul
1984 Eggs and larvae of walleye pollock and relationships to the planktonic environment. *In* Ito, D.H. (ed.), Proceedings of the workshop on walleye pollock and its ecosystem in the eastern Bering Sea, p. 109–159. NOAA Tech. Memo. NMFS-F/NWC-62, Northwest & Alaska Fish. Cent., NMFS, Seattle, WA 98115-0070.

Incze, L.S., A.W. Kendall Jr., J.D. Schumacher, and R.K. Reed
1989 Interactions of a mesoscale patch of larval fish (*Theragra chalcogramma*) with the Alaska Coastal Current. Continental Shelf Res. 9:269–284.

Incze, L.S., P.B. Ortner, and J.D. Schumacher
1990 Microzooplankton, vertical mixing and advection in a larval fish patch. J. Plankton Res. 12:365–379.

Kamba, M.
1977 Feeding habits and vertical distribution of walleye pollock, *Theragra chalcogramma* (Pallas), in early life stage in Uchiura Bay, Hokkaido. Res. Inst. N. Pac. Fish., Hokkaido Univ., Spec. Vol., p. 175–197.

Kendall, A.W. Jr., and S. Kim
1989 Buoyancy of walleye pollock (*Theragra chalcogramma*) eggs in relation to water properties and movement in Shelikof Strait, Gulf of Alaska. *In* Beamish, R.J., and G.A. McFarlane (eds.), Effects of ocean variability on recruitment and evaluation of parameters used in stock assessment models, p. 169–180. Can. Spec. Publ. Fish Aquat. Sci. 108.

Kendall, A.W. Jr., and S.J. Picquelle
1990 Egg and larval distributions of walleye pollock, *Theragra chalcogramma*, in Shelikof Strait, Gulf of Alaska. Fish. Bull., U.S. 88:133–154.

Kendall, A.W. Jr., M.E. Clarke, M.M. Yoklavich, and G.W. Boehlert
1987 Distribution, feeding, and growth of larval walleye pollock, *Theragra chalcogramma*, from Shelikof Strait, Gulf of Alaska. Fish. Bull., U.S. 85:499–521.

Kim, S.
1987 Spawning behavior and early life history of walleye pollock, *Theragra chalcogramma*, in Shelikof Strait, Gulf of Alaska, in relation to oceanographic features. Ph.D. diss. Univ. Wash., Seattle, 221 p.
1989 Early life history of walleye pollock, *Theragra chalcogramma*, in the Gulf of Alaska. *In* Proc., Int. symp. on biology and management of walleye pollock, p. 117–139. Alaska Sea Grant Rep. 89-1, Univ. Alaska, Fairbanks.

Kim, S., and A.W. Kendall Jr.
1989 Distribution and transport of larval walleye pollock (*Theragra chalcogramma*) in Shelikof Strait, Gulf of Alaska, in relation to water movement. Rapp. P.-V. Reun. Cons. Int. Explor. Mer 191:127–136.

Maeda, T., T. Takahashi, M. Ijichi, H. Hirakawa, and M. Ueno
1976 Ecological studies on the Alaska pollock in the adjacent waters of the Funka Bay, Hokkaido-II spawning season. Bull. Jpn. Soc. Sci. Fish. 42:1213–1222 [in Jpn., Engl. abstr.].

Maeda, T., T. Nakatani, T. Takahashi, and M. Ueno
1980 On the population and developmental fluctuations of the Alaska pollock at the southern area off the Hokkaido in the Pacific Ocean. Bull. Jpn. Soc. Fish. Oceanogr. 37:29–33 [in Jpn.].

Maeda, T., T. Takahashi, and M. Ueno
1981 Annual life period of the adult Alaska pollock in the adjacent waters of the Funka Bay, Hokkaido. Bull. Jpn. Soc. Sci. Fish. 47:741–746 [in Jpn., Engl. abstr.].

Megrey, B.A.
1989 Exploitation of walleye pollock resources in the Gulf of Alaska, 1964–88: Portrait of a fishery in transition. *In* Proc., Int. symp. on biology and management of walleye pollock, p. 33–58. Alaska Sea Grant Rep. 89-1, Univ. Alaska, Fairbanks.

Methot, R.D.
1986 Frame trawl for sampling pelagic juvenile fish. Calif. Coop. Oceanic Fish. Invest. Rep. 27:267–278.

Miller, B.S., D.R. Gunderson, D. Glass, D.B. Powell, and B.A. Megrey
1986 Fecundity of walleye pollock (*Theragra chalcogramma*) from the Shelikof Strait, Gulf of Alaska. FRI-UW-8608, Coll. Fish., Univ. Wash., Seattle, 40 p.

Muigwa, N.M.
1989 Vertical distribution patterns of prespawning and spawning pollock (*Theragra chalcogramma*) in Shelikof Strait. *In* Proc., Int. symp. on biology and management of walleye pollock, p. 403–432. Alaska Sea Grant Rep. 89-1, Univ. Alaska, Fairbanks.

Nakatani, T.
1984 The early life history of walleye pollock *Theragra chalcogramma* (Pallas) in Funka Bay and the adjacent waters, Hokkaido. Aquabiology 34:341-347 [in Jpn., Engl. abstr.].
1988 Studies on the early life history of walleye pollock in Funka Bay and vicinity, Hokkaido. Mem. Fac. Fish., Hokkaido Univ. 35:1–46.
1991 Copepod nauplii as food of walleye pollock larvae (Pisces: Gadidae) in Funka Bay, Japan. Proc., Fourth int. conf. copepoda. Bull. Plankton Soc. Jpn., Spec. Vol., p. 515–525.

Nakatani, T., and T. Maeda
1981 Transport process of the Alaska pollack eggs in Funka Bay and the adjacent waters, Hokkaido. Bull. Jpn. Soc. Sci. Fish. 47:1115–1118.
1983 Distribution of walleye pollock larvae and their food supply in Funka Bay and the adjacent waters, Hokkaido. Bull. Jpn. Soc. Sci. Fish. 49:183–187 [in Jpn., Engl. abstr.].
1984 Thermal effect on the development of walleye pollock eggs and their upward speed to the surface. Bull. Jpn. Soc. Sci. Fish. 50:937–942 [in Jpn., Engl. abstr.].
1987 Distribution and movement of walleye pollock larvae *Theragra chalcogramma* in Funka Bay and the adjacent waters, Hokkaido. Bull. Jpn. Soc. Sci. Fish. 53:1585–1591 [in Jpn., Engl. abstr.; Engl. transl. avail. Alaska Fish. Sci. Cent., NMFS, NOAA, Seattle, WA 98115-0070].
1989 Distribution of copepod nauplii during the early life stages of walleye pollock in Funka Bay and vicinity, Hokkaido. *In* Proc., Int. symp. on biology and management of walleye pollock, p. 217–240. Alaska Sea Grant Rep. 89-1, Univ. Alaska, Fairbanks.

Nakayama, N., Y. Watanabe, H. Ida, and K. Nagasawa
1987 Observation report of walleye pollock fishery in the south region of Hokkaido, the Pacific Ocean, 1987, no. 1, p. 1–13 [in Jpn.].

Nishimura, A., and J. Yamada
1984 Age and growth of larval and juvenile walleye pollock, *Theragra chalcogramma* (Pallas), as determined by otolith daily growth increments. J. Exp. Mar. Biol. Ecol. 82:191–205.

Ohtani, K., and K. Kido
1980 Oceanographic structure in Funka Bay. Bull. Fac. Fish., Hokkaido Univ. 31:84–114 [in Jpn., Engl. abstr.].

Paul, A.J.
1983 Light, temperature, nauplii concentrations, and prey capture by first feeding pollock larvae, *Theragra chalcogramma*. Mar. Ecol. Prog. Ser. 13:175–179.

Reed, R.K., L.S. Incze, and J.D. Schumacher
1989 Estimation of the effects of the flow on dispersion of larval pollock, *Theragra chalcogramma*, in Shelikof Strait, Alaska. *In* Beamish, R.J., and G.A. McFarlane (eds.), Effects of ocean variability on recruitment and evaluation of parameters used in stock assessment models, p. 239–246. Can. Publ. Fish. Aquat. Sci. 108.

Sakurai, T.
1982 Reproductive ecology of walleye pollock *Theragra chalcogramma* (Pallas). Ph.D. diss., Hokkaido Univ., 178 p. [Engl. transl. avail. Alaska Fish. Sci. Cent., NMFS, NOAA, Seattle, WA 98115-0070.
1989 Reproductive characteristics of walleye pollock with special reference to the ovarian development, fecundity and social behavior. *In* Proc., Int. symp. on biology and management of walleye pollock, p. 97–115. Alaska Sea Grant Rep. 89-1, Univ. Alaska, Fairbanks.

Yoklavich, M.M., and K. Bailey
1989 Growth of larval and juvenile walleye pollock from Shelikof Strait, Gulf of Alaska, as determined from daily increments in otoliths. *In* Proc., Int. symp. on biology and management of walleye pollock, p. 241–251. Alaska Sea Grant Rep. 89-1, Univ. Alaska, Fairbanks.

Yoon, T.
1981 Reproductive cycle of female walleye pollock *Theragra chalcogramma* (Pallas), in the adjacent waters of Funka Bay, Hokkaido. Bull. Fac. Fish. Hokkaido Univ. 32:22–38 [in Jpn., Engl. abstr.].

Abstract.–Catch and effort data for the abalone *Haliotis rubra* fishery off Victoria, Australia, revealed that catches were allied to incentive (price); annual catch was proportional to effort. The robustness of the fishery can be attributed to low fishing mortality (F around 0.1) and a relatively high minimum length of capture (120 mm). Exploitation models showed that egg production was at least 50% that of unfished stocks. The analyses also showed that egg production was sensitive to variation in the growth parameters; fast-growing populations were more vulnerable to recruitment overfishing than slow-growing populations. For slow-growing populations, yields could be considerably increased without endangering recruitment. It is suggested, from the available evidence, that overfishing has been overemphasized in the collapse of abalone fisheries.

Manuscript accepted 18 December 1991.
Fishery Bulletin, U.S. 90:139–146 (1992).

Exploitation models and catch statistics of the Victorian fishery for abalone *Haliotis rubra*

Paul E. McShane

Marine Science Laboratories, Fisheries Division, Ministry for Conservation and Environment
P.O. Box 114, Queenscliff, Victoria 3225, Australia
Present address: Fisheries Research Division, Ministry of Agriculture and Fisheries
P.O. Box 297, Wellington, New Zealand

Recent and comprehensive descriptions of the state of the world's abalone (*Haliotis* spp.) fisheries include reviews of the abalone fisheries in California (Tegner 1989, Tegner et al. 1989 and 1992), British Columbia (Breen 1986, Sloan and Breen 1988), Australia (Prince and Shepherd 1992), Mexico (Guzman del Proo 1992) and Japan (Mottet 1978). A unifying theme of these reviews is that abalone fisheries are characterised by initial high productivity followed by irreversible decline. Australia has developed an abalone fishery only recently by world standards. In Victoria, the fishery for the abalone *Haliotis rubra* is productive, valuable, and apparently stable (McShane 1990). The government limits the number of operators in the fishery (71), the annual catch (1460 metric tons) since 1988, and minimum length of capture (120 mm).

A fundamental objective of fisheries science is to predict the production from a fishery under varying management strategies. A common approach is to consider the yield from an individual or year-class of individuals under different fishing conditions (Beverton and Holt 1957, Ricker 1975, Gulland 1988, Megrey and Wespestad 1988). Such exploitation models treat populations as the sum total of their individual members; yield is expressed as yield-per-recruit because the absolute level of recruitment is rarely known. Yield-per-recruit models have been applied to several abalone fisheries including those for *H. discus discus* (Ishibashi and Kojima 1979), *H. iris* (Sainsbury 1982a), *H. laevigata* (Sluczanowski 1984), *H. kamtschatkana* (Breen 1986, Sloan and Breen 1988), *H. rufescens* and *H. corrugata* (Tegner et al. 1989), and the Tasmanian fishery for *H. rubra* (Nash 1992).

Although yield-per-recruit models can provide information on appropriate harvest strategies to maximize yield, the results provide no indication of the sustainability of a particular harvest regime. Because of the historical tendency of abalone fisheries to collapse, increasing attention has been focused on management strategies which maintain egg production as well as yield (Sluczanowski 1984 and 1986, Breen 1986, Sloan and Breen 1988, Tegner et al. 1989, Nash 1992).

In the present paper, the productivity of the fishery for abalone *Haliotis rubra* off Victoria, Australia, is described. To investigate the effect of growth rate, the relative yields of weight and eggs for two hypothetical populations of *H. rubra*, fast- and slow-growing, are examined. Management implications of my results are discussed for *H. rubra* as well as for other abalone species generally.

Materials and methods

Fishery statistics

Data on annual catch, effort, and price (whole weight) for the Victorian abalone fishery were obtained from

fishermen's returns and unpublished information supplied by the Victorian Fisheries Division. Information on the history of the Victorian abalone fishery was extracted from unpublished records supplied by the Victorian Fisheries Division (Dep. Conserv. Environ., 240 Victoria Pde, Melbourne 3002; see also McShane 1990).

Table 1
Estimates of rates of natural mortality (M) for *Haliotis rubra*.

Reference	Location	M(yr^{-1})
Beinssen and Powell (1979)	northeast Victoria	0.20
Nash (1992)	northern Tasmania	0.24–0.29
Shepherd et al. (1982)	South Australia	0.21–0.36
Prince et al. (1988)	southeast Tasmania	0.1–0.7

Yield-per-recruit

Generalised fisheries exploitation models such as yield-per-recruit rely heavily on several assumptions. For any "unit stock":

1 Growth rates do not vary with time or density of the exploitable stock. Thus growth can be modeled with one set of parameters, e.g., the von Bertalanffy growth equation (Ricker 1975). Departures from these assumptions are known for abalone (e.g., Newman 1968, Sloan and Breen 1988, Day and Fleming 1992). However, for stocks of *H. rubra* the assumptions are reasonable (McShane et al. 1988a).

2 The rate of natural mortality is known and does not vary with age, time or density of the stock. Natural mortality is an important parameter in yield-per-recruit models, yet it is often the most difficult to estimate accurately. Natural mortality of *H. rubra* is constant with age after the first year (Shepherd et al. 1982, McShane 1991, Shepherd and Breen 1992). Estimates of natural mortality are in Table 1.

3 Fishing (F) and natural (M) mortality are independent of each other. For abalone fisheries, fishing mortality cannot be considered applicable to the entire fishery. Individual exploitation rates are applied to substocks opportunistically according to weather and incentive (Sluczanowski 1984, McShane and Smith 1989a). Incidental mortality can be caused by fishing, for example, wounding of undersize individuals (Sloan and Breen 1988, Tegner 1989, Shepherd and Breen 1992).

4 Recruitment is constant. Recruitment measured as the density of post-settlement individuals is highly variable for *H. rubra* (McShane et al. 1988b, McShane and Smith 1991). However, variation in growth rates of prerecruit individuals within a population acts to smooth out year-to-year variation in those *H. rubra* reaching harvestable size (McShane 1991).

5 Individuals of the same age have the same weight and susceptibility to capture. Individual variation in the relationships of weight to length and length to age has been demonstrated for *H. rubra*, but reasonable generalizations of these relationships can be made for the stock (McShane et al. 1988a, McShane and Smith 1992).

To investigate the effects of various rates of fishing, the yield-per-recruit equation of Ricker (1975:237) was used. The increase in length with age of *H. rubra* was computed using the von Bertalanffy growth equation

$$L_t = L_\infty(1 - e^{-Kt-t_0})$$

where L_t is the shell length in mm of *H. rubra* at age t years, L_∞ is the hypothetical maximum length, K is the Brody growth constant, and t_0 is the hypothetical age when length is zero.

In calculating the yield-per-recruit of *H. rubra* at various ages, I assumed that individuals were recruited in the year corresponding to the minimum length at capture. The biomass of an individual of age t years, W_t (g), was assumed to be $0.00016L_t^3$, where L_t is in mm (McShane et al. 1988a).

Egg-per-recruit

A simple age-structured model was used in which the relative abundance of females of age t years (N_t) was computed as

$$N_t = N_0 e^{-Zt}$$

where Z is total mortality (F + M). The egg production of a female of age t years (E_t) has a linear relationship with length (L_t) for *H. rubra* (McShane et al. 1988b) such that

$$E_t = 0.03\ L_t - 2.4$$

where E is fecundity in millions of eggs, and L is shell length in mm; L_t is derived from the von Bertalanffy growth equation.

Total egg production (E_{tot}) is given by

$$E_{tot} = \sum_{t=0}^{t=25} N_t \cdot E_t$$

where t = 25 years is assumed to be the maximum age

Table 2

Parameters used in computations of yield and egg-per-recruit. Values for slow- and fast-growing populations of *Haliotis rubra* are derived from mark-recapture studies in Victoria, Australia (McShane 1990). Estimates provided are the von Bertalanffy growth parameters (see text for details).

Parameter	Fast	Slow
L_∞	152.1	139.7
K	0.37	0.20
t_0	−0.01	−0.12

(McShane et al. 1988a). Egg production under various combinations of F, M, and minimum length-at-capture was compared with egg production of an unfished population (F = 0).

Fast- and slow-growing populations of *H. rubra* were modeled. The generalised growth parameters (Table 2) were based on empirical estimates (McShane et al. 1988a, McShane 1990, McShane and Smith 1992). Both yield and egg-per-recruit were expressed graphically as a function of minimum length-at-capture (i.e., length-at-recruitment) and F, using two rates of natural mortality estimated for *H. rubra* (M = 0.1 and 0.2, Table 1). Length-at-recruitment was varied (in 10 mm increments) from 100 mm to 140 mm for fast-growing populations and from 70 mm to 130 mm for slow-growing populations. The value of F was varied from 0.1 to 1.5. A smooth surface was interpolated through points in 3-dimensional plots of yield and egg-per-recruit, following the method of McLain (1974) in which negative exponential weights are computed from distances between points in a regular grid and the irregularly spaced data points in the X–Y plane (Wilkinson 1990).

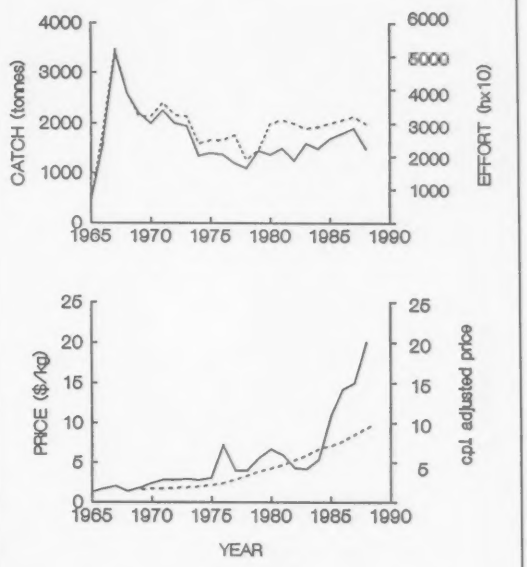

Figure 1

Comparison of (upper) annual catch and effort (dashed line), and (lower) actual price and CPI adjusted price (dashed line) of abalone *Haliotis rubra* in the fishery off Victoria, Australia, 1965–88.

Results

Fishery statistics

Annual variations in catch, effort, and value of the Victorian abalone fishery are described in Figure 1. Catch is highly correlated with effort (r 0.98, n 25, $P<0.001$). Although the catch rose in 1965–66 (accompanying development of export markets), the trend in both catch and effort is one of a slight but unalarming decrease followed by a slight increase during the 1980s. The introduction of catch quotas in 1988 is reflected in the decrease in catch in that year (Fig. 1). It is noteworthy that prior to 1988, price of abalone is a significant factor influencing the catch of the Victorian abalone fishery. Allowing for inflationary increases, the price of abalone doubled between 1967 and 1976–77 accompanying development of Japanese markets. Four exceptions to the steady rise in price have occurred. In 1967–68, a slight fall in price resulted from shipments of poor-quality abalone. Processing techniques were, at the time, in a developmental phase. Second, in 1976 an increase in price occurred concomitant with high demand by export markets and increased competition between processors for supply. The introduction of a competitive product, the Chilean "loco" *Concholepas concholepas*, on Asian markets coupled with buyer resistance to elevated prices of Australian abalone resulted in a decrease in price during 1977 (Stanistreet 1978). Note that there is a lag between price variation and catch and effort; the relative decrease in catch and effort in 1978 reflects the price drop in 1977 (Fig. 1). Buyer resistance also affected the price of abalone in 1981–82 and led to a decrease in effort and catch during this period.

More recently, the collapse of the large Mexican abalone fishery and the imposition of catch quotas on the Tasmanian and South Australian abalone fisheries (Prince and Shepherd 1992) decreased the world supply of abalone and increased the competitiveness of Victorian suppliers (McShane 1990). This and a decrease in the relative value of the Australian currency against

that of export markets resulted in a rapid increase in price of abalone during the 1980s.

Exploitation models

The yield and egg-production-per-recruit for individuals of various lengths under various levels of exploitation are shown for fast-growing (Fig. 2) and slow-growing (Fig. 3) populations of *H. rubra*. It can be seen that the relative yield-per-recruit is greater for fast-growing compared with slow-growing populations of *H. rubra*. The minimum lengths producing maximum yield-per-recruit are 130 mm for fast-growing populations and 120 mm for slow-growing populations. These maxima occurred at high exploitation rates (F~1) and were independent of the natural mortality rates applied to the model (0.1, 0.2). Natural mortality had an obvious effect on the decline of yield-per-recruit with minimum length. For M = 0.2, yield-per-recruit was less sensitive to variation in minimum length compared with M = 0.1. Note that at realistic levels of F (0.1, McShane and Smith 1989a), yield-per-recruit is comparatively low (Figs. 2 and 3). For such low rates of exploitation, the model shows that for fast-growing (in contrast to slow-growing) populations, yield-per-recruit is relatively insensitive to variation in the minimum length-at-capture. Similar results were obtained from yield-per-recruit analyses of other species of abalone, provided that rates of fishing mortality are relatively low (F < 0.3) (Ishibashi and Kojima 1979, Sainsbury 1982a, Sluczanowski 1984, Breen 1986, Sloan and Breen 1988, Tegner et al. 1989, Nash 1992).

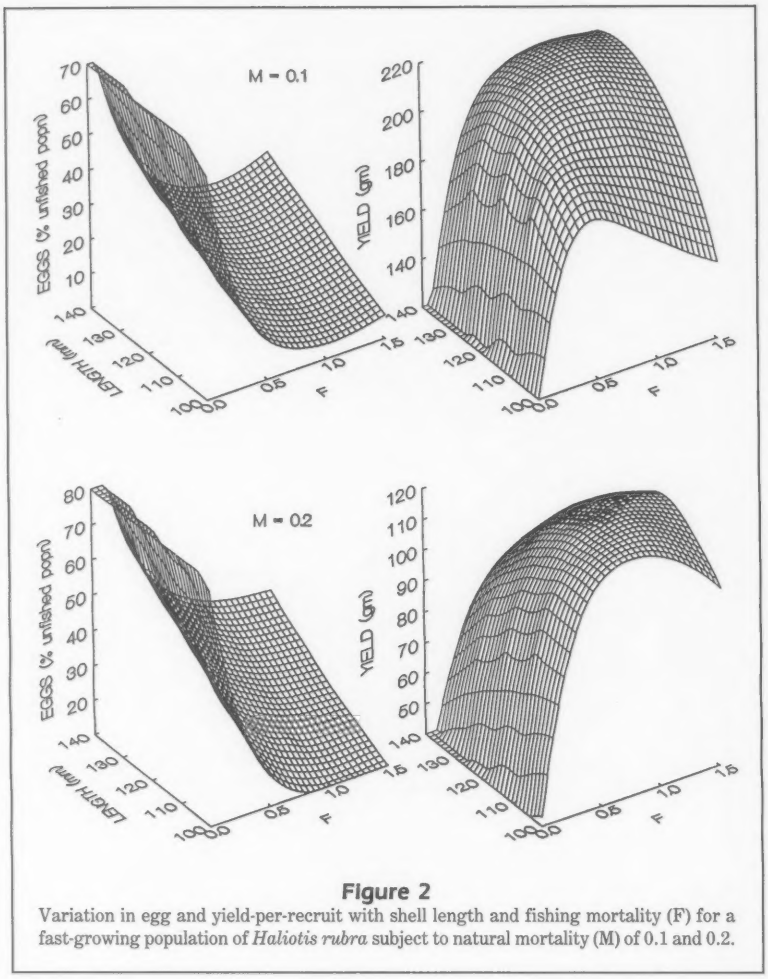

Figure 2
Variation in egg and yield-per-recruit with shell length and fishing mortality (F) for a fast-growing population of *Haliotis rubra* subject to natural mortality (M) of 0.1 and 0.2.

For fast-growing populations, exploitation rates producing maximum yield-per-recruit are associated with minimum egg production. Indeed, values of F > 0.3 are associated with egg production of less than 50% of an unfished population. Low egg production may cause recruitment failure in abalone stocks (Sloan and Breen 1988, Tegner et al. 1989). Egg production increases with minimum length; results of other studies show that fecundity of *H. rubra* is directly related to length (McShane et al. 1988b, Prince et al. 1988).

Egg production is less sensitive to variation in fishing mortality in slow-growing than in fast-growing populations of *H. rubra*. For minimum lengths over 120 mm, egg production rates are over 50% of an unfished population. At F = 0.1, egg production is over 60% of that of an unfished population for both M = 0.1 and 0.2.

Discussion

Catch levels for the Victorian abalone fishery suggest a robust fishery. But catch data are poor indicators of the stock abundance of abalone because fishermen can maintain catch rates by exploiting substocks (Breen

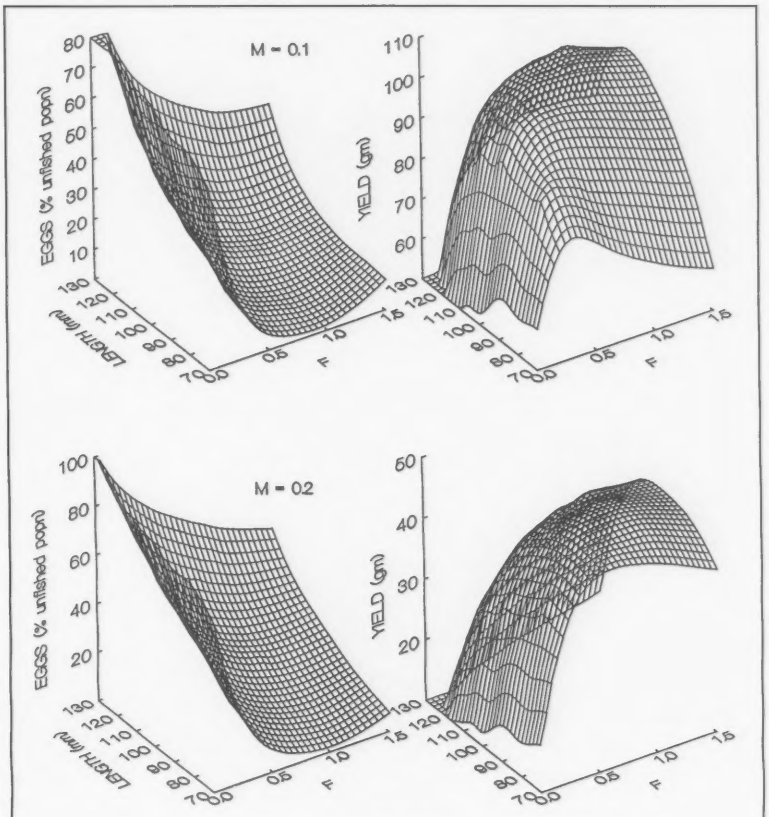

Figure 3
Variation in egg and yield-per-recruit with shell length and fishing mortality (F) for a slow-growing population of *Haliotis rubra* subject to natural mortality (M) of 0.1 and 0.2.

1980, Sloan and Breen 1988, McShane and Smith 1989a). Yet the available evidence is that the fishery is underexploited (McShane and Smith 1989ab; McShane 1990). Catches of *H. rubra* can be adjusted opportunistically by increasing effort when incentive (price) is high. Although Victorian abalone fishermen have the capacity to serially deplete substocks, rates of exploitation of *H. rubra* are generally low (see McShane and Smith 1989a). A surplus of harvestable individuals is maintained in substocks by the conservative fishing practices employed by Victorian abalone fishermen (McShane and Smith 1989a). With low exploitation rates ($F<0.3$), the egg-per-recruit model shows that there is adequate egg production by individuals above the present legal minimum length of 120 mm. However, as a consequence of reaching harvestable size in about 4 years, prerecruit individuals from fast-growing populations have fewer years of egg production than those *H. rubra* from slow-growing populations which reach harvestable size in about 10 years. Fast-growing populations of *H. rubra* are therefore vulnerable to recruitment overfishing should exploitation rates increase ($F>0.3$). This is unlikely in the Victorian abalone fishery because both the number of operators and the annual catch are controlled.

Most abalone fisheries are generally subject to pulse fishing. Substocks are fished, then left to recover (Sluczanowski 1984, McShane and Smith 1989a). Fast-growing populations are important in this regard because they can be fished at a higher frequency than slow-growing populations (Sluczanowski 1984). Thus fast-growing populations are subject to higher exploitation rates than slow-growing populations. Slow-growing populations are often characterised by large accumulations of prerecruit abalone which are food-limited (Sloan and Breen 1988, McShane 1990). Egg-per-recruit analysis shows that even at extraordinarily high rates of fishing mortality ($F>1$) egg production in slow-growing populations of *H. rubra* is above the assumed "safe" level of 50% of an unfished population (Sloan and Breen 1988, Tegner et al. 1989). The model shows that slow-growing populations could be "fished down" at a reduced size limit and high exploitation rate without endangering egg production. Such a harvesting strategy could reduce the abundance of the accumulated stock to a level where food is no longer a limiting factor (McShane and Smith 1989b). To date in Victoria, such slow-growing stocks are rarely fished because of a paucity of abalone of harvestable size (McShane and Smith 1989b).

Why is the Victorian fishery for *H. rubra* apparently robust in contrast to other abalone fisheries? The viability of the Victorian fishery can be attributed to a relatively low number of operators (limited entry has operated in Victoria since 1968) and an associated low exploitation rate (see McShane and Smith 1989a). A minimum length that maintains a safe level of egg production provides further safeguards against recruit-

ment overfishing, as does an annual catch quota. However, size limits introduced to the California abalone fishery were also conservative but failed to arrest the decline of the fishery (Tegner 1989, Tegner et al. 1992). The combination of high commercial effort and intense recreational and illegal harvest resulted in a removal of surplus stocks in the California (Tegner et al. 1992) and Mexican (Guzman del Proo 1992) abalone fisheries. Unrestrained recreational and illegal harvest remains a threat to the Victorian fishery, but with a comparatively low human population and a relatively inaccessible coastline the Victorian abalone fishery is less vulnerable to noncommercial overfishing than the California or Mexican abalone fisheries (McShane 1990).

While fishing can deplete stocks, there are a multitude of other factors that affect the abundance of abalone. For example, overfishing could not explain the recruitment failure which occurred in the abalone fishery of British Columbia (Breen 1986, Sloan and Breen 1988). Recruitment failure in various species of abalone has been attributed to sea temperature anomalies (Hayashi 1980, Forster et al. 1982, Shepherd et al. 1985) or natural variation (Sainsbury 1982b; see also McShane and Smith 1991). The collapse of the California abalone fishery for *H. rufescens* coincided with predator release (Lowry and Pearse 1973, Hines and Pearse 1982, Tegner 1989, Tegner et al. 1989, 1992). The importance of predation in controling abalone abundance is further exemplified by the recovery of stocks of *H. cracherodii* concomitant with a reduction in the abundance of major predators (Davis et al. 1992). The decrease in abundance of some California populations of abalone (*H. rufescens*, *H. cracherodii*) was attributed to low food availability caused by El Niño events (Tegner and Dayton 1987, Tegner et al. 1989), competition with other herbivores, and kelp harvest (Davis et al. 1992). Starvation in abalone causes a decrease in reproductive effort (Cox 1962) and an increased susceptibility to disease, both of which can cause a severe decline in stocks (Haaker et al. 1992, Tissot 1992). A major factor in the reduced abundance of abalone stocks in Japan is nearshore pollution (I. Hayashi, Igarashi-Jutaku 2-205, Niigata, Japan, pers. commun. 1990), a factor also implicated in the decline of California abalone stocks (see Tegner et al. 1992).

Variation in abiotic factors such as temperature have demonstrable effects on the survival and growth of exploited species (Cushing 1988). Such factors, apart from seasonal variation, vary stochastically and introduce uncertainty in fisheries management (Megrey and Wespestad 1988, Walters and Collie 1988). Faced with this uncertainty, fishery managers must proceed cautiously and gain a better understanding of the ecology of exploitable species, particularly of abalone which have a history of unexplained stock collapse.

Acknowledgments

I thank Dr. Paul Breen for helpful discussion and constructive comments on the manuscript. Drs. Linda Jones and Scoresby Shepherd offered helpful suggestions as did an anonymous reviewer.

Citations

Beinssen, K., and D. Powell
1979 Measurement of natural mortality in a population of blacklip abalone, *Notohaliotis ruber*. Rapp. P.-V. Reun. Cons. Int. Explor. Mer 175:23–26.

Beverton, R.J.H., and S.J. Holt
1957 On the dynamics of exploited fish populations. Fish. Invest. Ser. II Mar. Fish. G.B. Minist. Agric. Fish. Food 19, 533 p.

Breen, P.A.
1980 Measuring fishing intensity and annual production in the abalone fishery of British Columbia. Fish. Res. Board Can. Tech. Rep. 947, 49 p.
1986 Management of the British Columbia fishery for northern abalone (*Haliotis kamschatkana*). *In* Jameison, G.S., and N. Bourne (eds.), North Pacific workshop on stock assessment and management of invertebrates, p. 300–312. Can. Spec. Publ. Fish. Aquat. Sci. 92.

Cox, K.W.
1962 California abalones, family Haliotidae. Calif. Fish Game, Fish Bull. 118, 138 p.

Cushing, D.H.
1988 The study of stock and recruitment. *In* Gulland, J.A. (ed.), Fish population dynamics, 2d ed., p. 105–128. Wiley, NY.

Davis, G.E., D.V. Richards, P.L. Haaker, and D.O. Parker
1992 Mass mortality and fishery management of black abalone, *Haliotis cracherodii*, in Southern California. *In* Shepherd, S.A., M.J. Tegner, and S.A. Guzman del Proo (eds.), Abalone of the world: Biology, fisheries and culture. Blackwells, Oxford (in press).

Day, R.W., and A. Fleming
1992 The determinants and measurement of abalone growth. *In* Shepherd, S.A., M.J. Tegner, and S.A. Guzman del Proo (eds.), Abalone of the world: Biology, fisheries and culture. Blackwells, Oxford (in press).

Forster, G.R., G.W. Potts, and R. Swinfen
1982 Changes in the ormer populations of Guernsey and Jersey. J. Mar. Biol. Assoc. U.K. 62:717–727.

Gulland, J.A.
1988 Fish population dynamics, 2d ed. Wiley-Interscience, NY.

Guzman del Proo, S.A.
1992 Una revision sobre la biologia y pesqueria del abulon (*Haliotis* spp.) en Mexico. *In* Shepherd, S.A., M.J. Tegner, and S.A. Guzman del Proo (eds.), Abalone of the world: Biology, fisheries and culture. Blackwells, Oxford (in press).

Haaker, P.L., D.V. Richards, C. Friedman, G. Davis, D.O. Parker, and H. Togstad
1992 Abalone withering syndrome and mass mortality of black abalone, *Haliotis cracherodii*, in California. *In* Shepherd, S.A., M.J. Tegner, and S.A. Guzman del Proo (eds.), Abalone of the world: Biology, fisheries and culture. Blackwells, Oxford (in press).

Hayashi, I.
1980 Structure and growth of a shore population of the ormer, *Haliotis tuberculata*. J. Mar. Biol. Assoc. U.K. 60:431–437.

Hines, A.H., and J.S. Pearse
1982 Abalones, shells and sea otters: Dynamics of prey populations in central California. Ecology 63:1547–1560.

Ishibashi, K., and H. Kojima
1979 A study on the stock of Japanese black abalone, *Haliotis discus discus* in Tokushima Prefecture—III. Analysis on abalone fisheries management. Bull. Tokai Reg. Fish. Res. Lab. 98:65–75.

Lowry, L.F., and J.S. Pearse
1973 Abalone and sea urchins in an area inhabited by sea otters. Mar. Biol. (Berl.) 23:213–219.

McLain, D.H.
1974 Drawing contours from arbitrary data points. Computer J. 17:318–324.

McShane, P.E.
1990 The fisheries ecology of Victorian abalone. Ph.D. thesis, La Trobe Univ, Melbourne, 364 p.
1991 Density dependent mortality of the abalone *Haliotis rubra* (Mollusca:Gastropoda). Mar. Biol. (Berl.) 110:385–389.

McShane, P.E., and M.G. Smith
1989a Direct measurement of fishing mortality in abalone (*Haliotis rubra*) off southeastern Australia. Fish. Res. 8: 93–102.
1989b Victorian abalone fishery in good shape. Aust. Fish. 48:20–25.
1991 Recruitment variation in sympatric populations of the abalone *Haliotis rubra* (Mollusca:Gastropoda). Mar. Ecol. Prog. Ser. 73:203–210.
1992 Shell growth checks are unreliable indicators of age of the abalone *Haliotis rubra* (Mollusca:Gastropoda). Aust. J. Mar. Freshwater Res. (in press).

McShane, P.E., M.G. Smith, and K.H.H. Beinssen
1988a Growth and morphometry in abalone (*Haliotis rubra*) from Victoria. Aust. J. Mar. Freshwater Res. 39:161–6.

McShane, P.E., K.P. Black, and M.G. Smith
1988b Recruitment processes in *Haliotis rubra* (Mollusca: Gastropoda) and regional hydrodynamics in southeast Australia imply localised dispersal of larvae. J. Exp. Mar. Biol. Ecol. 124:175–203.

Megrey, B.A., and V.G. Wespestad
1988 A review of biological assumptions underlying fishery assessment models. *In* Wooster, W.S. (ed.), Fishery science and management—Objectives and limitations, p. 31–74. Lect. Notes Coastal Estuarine Stud. 28.

Mottett, M.G.
1978 A review of the fishery biology of abalones. Wash. Dep. Fish. Tech. Rep. 37, 78 p.

Nash, W.J.
1992 Determination of appropriate size limits by egg-per-recruit analysis, with an assessment of size limits as a management tool for blacklip abalone (*Haliotis rubra*) in Tasmania. *In* Shepherd, S.A., M.J. Tegner, and S.A. Guzman del Proo (eds.), Abalone of the world: Biology, fisheries and culture. Blackwells, Oxford (in press).

Newman, G.G.
1968 Growth of the South African abalone *Haliotis midae*. S. Afr. Div. Sea Fish. Invest. Rep. 67:1–24.

Prince, J.D., and S.A. Shepherd
1992 Australian fisheries for abalone and their management. *In* Shepherd, S.A., M.J. Tegner, and S.A. Guzman del Proo (eds.), Abalone of the world: Biology, fisheries and culture. Blackwells, Oxford (in press).

Prince, J.D., T.L. Sellers, W.B. Ford, and S.R. Talbot
1988 Recruitment, growth, mortality and population structure in a southern Australian population of *Haliotis rubra* (Mollusca: Gastropoda). Mar. Biol. (Berl.) 100:75–82.

Ricker, W.E.
1975 Computation and interpretation of biological statistics of fish populations. Bull. Fish. Res. Board Can. 191, 382 p.

Sainsbury, K.J.
1982a Population dynamics and fishery management of the paua, *Haliotis iris*. 2. Dynamics and management as examined using a size class population model. N.Z. J. Mar. Freshwater Res. 16:163–173.
1982b Population dynamics and fishery management of the paua, *Haliotis iris*. 1. Population structure, growth, reproduction and mortality. N.Z. J. Mar. Freshwater Res. 16:147–161.

Shepherd, S.A., and P.A. Breen
1992 Mortality in abalone: Its estimation, variability and causes. *In* Shepherd, S.A., M.J. Tegner, and S.A. Guzman del Proo (eds.), Abalone of the world: Biology, fisheries and culture. Blackwells, Oxford (in press).

Shepherd, S.A., G.P. Kirkwood, and R.L. Sandland
1982 Studies on southern Australian abalone (genus *Haliotis*). III. Mortality of *H. laevigata* and *H. ruber*. Aust. J. Mar. Freshwater Res. 33:265–272.

Shepherd, S.A., P.S. Clarkson, and J.A. Turner
1985 Studies on southern Australian abalone (genus *Haliotis*). V. Spawning, settlement and early growth of *H. scalaris*. Trans. R. Soc. S. Aust. 109:61–62.

Sloan, N.A., and P.A. Breen
1988 Northern abalone, *Haliotis kamtschatkana*, in British Columbia: Fisheries and synopsis of life history information. Can. Spec. Publ. Fish. Aquat. Sci. 103, 46 p.

Sluczanowski, P.R.
1984 A management oriented model of an abalone fishery whose substocks are subject to pulse fishing. Can. J. Fish. Aquat. Sci. 41:1008–1014.
1986 A disaggregate model for sedentary stocks: The case of South Australian abalone. *In* Jamieson, G.S., and N. Bourne (eds.), North Pacific workshop on stock assessment and management of invertebrates, p. 393–401. Can. Spec. Publ. Fish. Aquat. Sci. 92.

Stanistreet, K.
1978 Abalone sales prospects may be on the mend. Aust. Fish. 37:29–30.

Tegner, M.J.
1989 The California abalone fishery: Production, ecological interactions, and prospects for the future. *In* Caddy, J.F. (ed.), Scientific approaches to management of invertebrate stocks, p. 401–420. J. Wiley & Sons, NY.

Tegner, M.J., and P.K. Dayton
1987 El Niño effects on southern California kelp forest communities. Adv. Ecol. Res. 17:243–279.

Tegner M.J., P.A. Breen, and C.E. Lenner
1989 Population biology of red abalones, *Haliotis rufescens*, in southern California and management of the red and pink, *H. corrugata*, abalone fisheries. Fish. Bull., U.S. 87:313–339.

Tegner, M.J., J.D. DeMartini, and K.A. Karpov
1992 The California red abalone fishery: A case study in complexity. *In* Shepherd, S.A., M.J. Tegner, and S.A. Guzman del Proo (eds.), Abalone of the world: Biology, fisheries and culture. Blackwells, Oxford (in press).

Tissot, B.N.
1992 Mass mortality of the black abalone (*Haliotis cracherodii*) in the California Channel Islands. *In* Shepherd, S.A., M.J. Tegner, and S.A. Guzman del Proo (eds.), Abalone of the world: Biology, fisheries and culture. Blackwells, Oxford (in press).

Walters, C.J., and J.S. Collie
1988 Is research on environmental factors useful to fisheries management? Can. J. Fish. Aquat. Sci. 45:1848–1854.

Wilkinson, L.
1990 SYGRAPH: The system for graphics. SYSTAT, Inc., Evanston, IL.

ITQs in New Zealand: The era of fixed quota in perpetuity

Michael P. Sissenwine

Headquarters, National Marine Fisheries Service, NOAA, Silver Spring, Maryland 20910

Pamela M. Mace

P.O. Box 7357, Silver Spring, Maryland 20907

Abstract.–On 1 October 1986, New Zealand introduced Individual Transferrable Quota (ITQ) management for most of its fisheries. ITQ management was implemented to address overfishing, overcapitalization, and excess government regulation. Quotas were based on catch histories, with a quota "buyback" (costing $42.4 million NZ) and prorated cuts to achieve total allowable catch (TAC) levels indicated by preliminary stock assessments. Fixed amounts of quota (defined by weight) were issued in perpetuity. Annual stock assessments are conducted. Government stated that it would buy or sell quota at market-determined prices in order to adjust TACs. On 1 April 1990, ITQs were redefined as proportions of annual TACs (known as "proportional ITQs"). Government extracts resource rent.

To date, there is little evidence of improvement in the condition of the fisheries resources. It is difficult to determine the economic effects of ITQ management; however, economic conditions have worsened due to factors which are unrelated to ITQ management. Revenues to government from the ITQ system have exceeded total costs, but there would have been a deficit if government had purchased quota to reduce TACs to the levels indicated by stock assessments. Government regulation has not been reduced.

Although there is general support for ITQ management in New Zealand, many problems have been encountered: quota overruns resulting from bycatch; inadequate stock assessment capability; disagreement over the level of resource rentals; and failure of government to enter the marketplace to reduce TACs when necessary.

Manuscript accepted 16 December 1991.
Fishery Bulletin, U.S. 90:147–160 (1992).

The idea of managing fisheries by Individual Transferable Quotas (ITQs) is not new. Christy (1973) suggested the method, and Maloney and Pearce (1979) provided the economic rationale for it. Until recently, there were only a few applications of ITQ management (e.g., southern bluefin tuna, Geen and Nayar 1988; Lake Erie freshwater fisheries, Muse and Schelle 1989). One application that has received considerable attention is the ITQ management of fisheries in New Zealand. Two reasons for this attention are that (1) New Zealand is applying ITQ management on a more comprehensive national scale than ever before, and (2) New Zealand officials have done a good job of describing their ITQ system to the rest of the world (e.g., Clark et al. 1988, Crothers 1988). New Zealand's early experience with ITQ management is of interest to the United States because ITQ management is being planned or discussed for several fisheries (e.g., Pacific sablefish and halibut, South Atlantic wreckfish, and East Bering Sea groundfish). It has recently been implemented for Mid-Atlantic surf clams and ocean quahogs. This paper reviews the potential benefits and problems of New Zealand's ITQ management system based on firsthand observations of the authors.[1] The main body of the paper was completed in mid-1990. A postscript has been added to reflect more recent events through 1991.

Before describing the fisheries management situation in New Zealand, the authors want to caution that by pointing out problems, they are not condemning the ITQ system. Despite problems, there seems to be a general acceptance that ITQs are the way New Zealand fisheries will be managed. There is no widespread sentiment, either within government or the industry, to repeal ITQs. A regional poll conducted shortly after implementation of the ITQ system (Dewees 1989) found that the majority of the fishing industry favored it. It would be interesting to repeat the poll nationwide now. The authors are of the opinion that the industry would not want to return to the fisheries management situation (or lack thereof) that preceded ITQs.

New Zealand fisheries setting

Fisheries have always been important to New Zealand. Legend has it that a Maori (the native people of New Zealand) pulled up the North Island of New Zealand from the sea on a hook-and-line while fishing. Fishing was so important that the

[1] The authors of this paper were fortunate to have the opportunity to observe ITQ management in New Zealand firsthand. The first author made six trips to New Zealand during the first three and a half years of ITQ management, including approximately seven months employed by the New Zealand Fisheries Research Centre. The second author was employed by the New Zealand Fisheries Research Centre from August 1986 until May 1989. Both authors maintain contact with the fisheries management situation in New Zealand through their previous affiliations.

Treaty of Waitangi between the Maoris and the British, signed in 1840, deeds the Maoris' rights to their traditional fisheries.[2]

Although New Zealand is a small nation in terms of population and land area, its Exclusive Economic Zone (EEZ) of 1.3 million nm^2 (more than 15 times the land mass) is the fourth largest in the world. Most of the EEZ is deep; 72% of the zone has waters deeper than 1000 m, so it is difficult to judge the total potential yield.

Historically, New Zealand fisheries were restricted to coastal waters (<200 m in depth) and yielded less than 50,000 tons annually (Fig. 1). Deepwater fisheries (to 1500 m) developed during the 1970s, and the yield increased rapidly to a peak of about 500,000 tons in 1977. Most of the increase was due to foreign fishing. In 1978, New Zealand extended its jurisdiction to 200 miles. The yield decreased sharply for a few years, but it has since returned to about 500,000 tons. Since extended jurisdiction, domestic fishing has replaced almost all of the foreign fishing. However, it should be noted that much of the catch recorded as domestic is actually taken by foreign vessels and foreign crews under contract to New Zealand firms. In 1987, the first sale value of the catch was about $350 million NZ.[3] The export value of New Zealand fisheries products increased from $50 million NZ in 1977 to $676 million NZ in 1987. The 1987 figure represented about 6% of New Zealand's total exports (Bevin et al. 1989).

Fisheries management began with the Fisheries Act of 1908 which established authority for input controls, such as limited entry licensing, closed areas and seasons, controls on minimum fish sizes, and requirements for vessels to land at specific ports. The actual basis for the number of licenses allowed in the fisheries is unclear. Restrictive licensing was repealed in 1963.

New Zealand established authority for output controls (i.e., total allowable catches, or TACs) in 1978 when it extended jurisdiction. At the same time, a moratorium was placed on new fishing permits for rock lobsters and scallops. In 1980 the moratorium was extended to finfish permits. In 1983, a Deepwater Enterprise Allocation system was established. Deepwater Enterprise Allocations were a forerunner of ITQs. Quota for each of the species fished in deep water (below about 200 m) was allocated to nine companies which had already invested in deepwater harvesting and shoreside processing capability. The motivation for the Deepwater Enterprise Allocations was not overfishing or overcapitalization. It was intended to prevent these ills from occurring (Clark et. al. 1988) Presumably, it also encouraged investment in the deepwater fisheries and hastened the replacement of foreign fishing activity by domestic fishing. The quotas were initially awarded for a period of ten years, but were made permanent in 1985. Although the government had no authority to make quotas transferable, there was considerable de facto trading and leasing of shares among the nine companies.

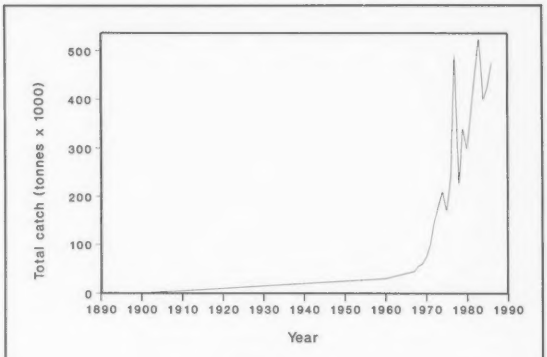

Figure 1
Annual yields from New Zealand EEZ, 1890–1990.

New Zealand implemented ITQs for most of its fisheries in October 1986. The Government gave several reasons for introducing ITQs. According to Crothers (1988), "Fishery managers were faced with an open access inshore fishery under severe biological and economic pressure... many of the prime species were experiencing growth and probably recruitment overfishing... and the industry was overcapitalized, crippled by excessive government management intervention, and rapidly declining economic performance." A government publication titled "Inshore Finfish Fisheries: Proposed Policy for Future Management" (Anonymous 1984) stated that "... a broad description of the problem of the inshore fishery is that the major fish stocks are too low as a result of overfishing... there has been a moratorium on new entries to the inshore... part-time fisherman were removed administratively... this had a negligible effect on fishing effort or catch... the harvesting sector remains overcapitalized."[4] In summary, the government turned to

[2] The fishing heritage of the Maori people and the Treaty of Waitangi are more than a matter of passing interest. As will be discussed later in the paper, the Treaty of Waitangi has complicated implementation of ITQ management.

[3] Economic values are expressed in New Zealand dollars which equal about $0.58 U.S.

[4] While the removal of part-time fishermen may have had a negligible effect on fishing effort or catch, it did have social ramifications. Many of the part-time fishermen were Maoris. It could be argued that their removal was one of the factors that stimulated them to attempt to regain access to the fisheries through the courts under the Treaty of Waitangi.

ITQs because of perceived overfishing, overcapitalization, and crippling excess regulation.

Undoubtedly, the success of the Deepwater Enterprise Allocation system contributed to the decision to use ITQs to solve the perceived problems in the inshore fisheries. Clark et. al. (1988) labeled it as a model for inshore fisheries management. There was also a belief that problems could be solved only by applying some form of output controls (Sandrey and O'Donnell 1985), and that input controls had already been attempted and had failed (Crothers 1988). In fact, it is unclear how seriously input controls had been attempted, or how severely the fisheries were overfished or overcapitalized.[5] Of course, the failures of input controls or overfishing and overcapitalization are not prerequisites for ITQ management. It is better to put in place a property rights system, such as ITQs, before problems occur.

Implementation of ITQ management in New Zealand

The idea behind ITQ management of fisheries is quite simple. ITQs are intended to conserve the fisheries resource by setting a TAC. They increase economic efficiency by assigning ownership of portions of the TAC, thus eliminating competition between harvesters to obtain the largest possible share of the TAC. By making quota transferable, ownership should eventually rest with the most efficient harvesters, since they should be able to afford to pay the highest price to purchase quota. Excess capital is likely to be removed from the fishery as more efficient operators buy up enough quota to make optimal use of the capital that remains in the fishery.

In New Zealand, implementation of the ITQ management system began with stock assessments of all of the fisheries resources to be managed. Initially, this involved assessments of 153 management units, composed of 26 species-groups in up to 10 management areas per species-group. By April 1990, there were 169 management units, composed of 29 species-groups (45 species) and 10 major management areas. Forty-seven of these management units are of minor importance (in terms of amount of quota) with TACs established for administrative purposes only. There are insufficient data to conduct meaningful assessments for most management units. Initially, most of the TACs were based on one of two methods of estimation: (1) They were equated to landings in the most recent year(s) for which information was available, or (2) they were equated to the product of a trawl-survey biomass estimate and a stock productivity value in the range 0.05–0.15. The first method probably produced overly-optimistic estimates of sustainable yields since recent landings were often the highest on record. On the other hand, the second method may have resulted in overly-conservative estimates, since biomass estimates were conservative (due to conservative assumptions about the vulnerability of fish to trawl gear) and a maximum productivity level of 0.15 is low (although there are notable exceptions such as orange roughy). Other methods used to estimate a few of the initial TACs may have produced reasonable results. These included use of tagging data, yield-per-recruit analysis, and stock reduction analysis.

For the deepwater fisheries, TACs generally matched the sum of quota allocations under the Deepwater Enterprise Allocation system. These Deepwater Enterprise Allocations were converted directly to ITQs. In the inshore, a provisional maximum allocation was determined separately for each fishing permit holder as the average catch of that individual's best two out of the three fishing years of October–September 1981–82, 1982–83, and 1983–84. These catch histories were the basis for the initial allocation of quota defined in fixed amounts by weight. Since the allocations were based on the average of the best two-out-of-three years, it was likely that the "Sum of Catch Histories" (SCH) would exceed the maximum annual catch that had occurred during the base period. In addition, fishermen were given the right to appeal their allocations if they felt it did not represent their true share of the fisheries. Of the 1800 fishermen notified of their catch histories, about 1400 appealed, and many of these have subsequently increased their allocations. The appeals process is still ongoing even though the ITQ system has been fully implemented for more than three years.

If the SCH was equal to or less than the TAC, permit holders were allocated their catch histories as ITQ in perpetuity. TACs in excess of the SCHs were offered for sale. When the SCH exceeded the TAC, there was

[5] It is interesting that there were virtually no input controls on New Zealand fisheries during 1963–78 for rock lobsters and scallops and 1963–80 for finfish. Even after moratoria on new licenses were implemented in 1978 and 1980, there were no additional direct controls on fishing effort (e.g., limits on the number of days that could be fished), although there were some indirect controls (e.g., closed areas).

With regard to overcapitalization, the government estimated that the harvesting sector was overcapitalized by $28 million NZ in 1983, although details of how overcapitalization was defined and how it was estimated are lacking (Anonymous 1984). Investment (book value) in the harvesting sector in 1983 was estimated as $142 million NZ (Bevin et al. 1989). This indicates that the harvesting sector was overcapitalized by about 20%, which is almost certainly less than some North American fisheries (e.g., Mid-Atlantic surf clams, New England groundfish, Pacific halibut).

Clearly some inshore resources were overfished (e.g., snapper), but it is difficult to evaluate how serious the overfishing problem was in general. Stock assessment information is quite limited, as will be discussed later in this paper.

a Government buyback of quota. Crothers (1988) indicates that the buyback was to facilitate an orderly "rationalization" of the industry, and to help create a climate of support for ITQ management. Clark et al. (1988) indicates the buyback was to reduce the mismatch of fleet capacity to available catch. If the Government was not able to buy back as much quota as was necessary, prorated cuts in quota were made. This threat of proration probably encouraged permit holders to be more reasonable in determining the selling price of their provisional allocation of quota.

The buyback cost the Government $42.4 million NZ to purchase 15,700 tons of quota (the annual amount the owners would have been entitled to catch in perpetuity). Prorated cuts were made to reduce quota by an additional 9500 tons. Presumably, the Government felt that the potential increase in value of the fishery when overfished stocks recovered merited the cost of the buyback and the short-term losses that resulted from prorated cuts.

Relatively few stocks accounted for most of the cost of the buyback. Table 1 indicates that more than 85% of funds spent on the buyback were used to buy quota for four species (mostly in one management area where traditional inshore fisheries are prosecuted). Nearly 50% were used for the snapper fisheries. The total reduction from SCHs to TACs for the 1986–87 fishing year (which began 1 October 1986) was 6%. For the 21 species that were involved in the buyback and prorated cuts, the reduction was about 24%. For the four primary species involved, the reduction was 54%.

Table 2 gives detailed information for the four primary species affected by the buyback and prorated costs. It is noteworthy that, in all cases, the SCH greatly exceeded the actual catch in the year just prior to ITQs (1985–86). This means that a portion of the quota that was bought back probably would not have been caught. In fact, in all cases the actual catch in the first year of the ITQ system (1986–87) was lower than the TAC. This suggests there may have been a declining trend in the resource condition from the base period when SCHs were established to the point in time when ITQs were implemented. It also seems likely, in the authors opinion, that SCHs were inflated by the industry (i.e., a moral hazard phenomenon) in anticipation of ITQs. As a result, the government may have spent much of the $42.4 million NZ to buy back quota which would not have been caught; therefore, the buyback may have had relatively little effect on fishing mortality rates.

Since ITQ management was implemented in 1986, stock assessments have been conducted annually for each management unit, to the extent that the available data allow. These assessments are conducted in Fisheries Assessment Meetings (FAMs) during the middle of the fishing year (April or May) in order to recommend TAC adjustments for the next fishing year (beginning in October). New Zealand law requires that the TAC be set to produce the maximum sustainable yield (MSY), as qualified by relevant factors including economic and environmental considerations and regional or global standards. Methods for estimating yields have been refined since 1985 when the initial TACs were calculated. New Zealand scientists now interpret MSY in two alternative ways: a static interpretation in which MSY is the maximum constant yield (MCY) that can be taken year after year from a fishery, and a dynamic interpretation in which MSY is the maximum average yield (MAY) that can be attained by varying the current annual yield (CAY) in response to fluctuations in stock size (Annala 1989 and 1990, Mace and Sissenwine 1989). MCY estimates are based on historic estimates of stock biomass from resource surveys, stock production models, or landings statistics. CAY estimates are generally based on recent estimates

Table 1

Buybacks and prorated cuts for implementation of New Zealand ITQ management.

Species	Tons reduced (1000s)	Payments ($NZ millions)	% Total $
Snapper	5.7	19.4	45.7
Rig	3.0	7.7	18.1
School shark	3.7	4.3	10.0
Hapuku bass	1.7	5.1	12.0
17 other	11.0	5.9	14.2
Total	25.1	42.4	100.0

Table 2

Relevant information for the four main species included in the buyback and prorated cuts under New Zealand ITQ management. Values in thousands of tons or $millions NZ.

	Hapuku bass	Rig	School shark	Snapper
Tons reduced	1.7	3.0	3.7	5.7
Cost of buyback	5.1	7.7	4.3	19.4
SCH (sum of catch histories)	3.3	4.4	6.0	12.2
TAC 1986–87 (total allowable catch)	1.7	1.4	2.4	6.5
Catch 1985–86	1.7	2.9	3.7	8.6
Catch 1986–87	1.1*	1.1*	1.9*	5.4*

*Provisional

of stock biomass and a target level of fishing mortality which is expected to produce MAY. Although the dynamic (CAY) strategy leads to higher average yields, the static (MCY) option has received the most attention for two reasons. First, the ITQ system was initially specified in terms of fixed weights of quota, valid in perpetuity. In practice, most TACs were constant. Second, the facilities for fisheries research are inadequate for providing frequent updates of stock status for all but a few of the more important fish stocks.

It should be recognized that FAMs are only part of the process of determining the level of TACs. The actual advice to the Minister of Fisheries on the setting of TACs is given by senior government officials who integrate stock assessment information with other considerations, including an evaluation of the risk to the resource of not adjusting a TAC. But the authors consider FAMs the best source of information on the condition of the fisheries resources, since they are open scientific meetings which formally document their deliberations and conclusions.

When ITQ management was implemented, the government stated that it would adjust the TAC by entering the market to buy or sell quota at market-determined prices. Government also reserved the option to make prorated cuts in quota. During the first three years of ITQ management, government either sold quota in perpetuity or leased annual quota for barracuda, hake, ling, orange roughy, hoki, and stargazer (Table 3). Most transactions were in the first year. A total of $84.2 million NZ was collected in quota sales and lease fees. But since the initial buyback when ITQs were implemented, government has not entered the marketplace to reduce any TACs,[6] despite the fact that the need for reductions has been indicated by several stock assessments (Annala 1989 and 1990; see next section).

Since ITQ management should increase resource rent, government charges an annual royalty (known as a resource rental) on quota holdings. In order to discourage speculation on quota (i.e., owning it without using it), resource rentals are charged on quota holdings rather than landings. This practice is an implied guarantee that fish are abundant enough for all quota to be caught without dissipating rent, which may not be the case due to assessment errors, failure to adjust TACs when assessments indicate TACs are too high, and because of varying economic conditions.

Gilbert (1988) estimated that the ITQ system could result in resource rents (referred to as surpluses in his paper) of 15–45% of the first sale value of the catch, depending on the species. His estimates reflect only the benefits of reducing effort relative to the open-access equilibrium (although the validity of an open-access equilibrium baseline is questionable for some of New Zealand's fisheries). They do not include the benefits of eliminating competition for shares of an overall TAC. If the average rent is 25% of the first sale value of the fishing, then there is the potential for government to extract at least $90 million NZ annually (i.e., 25% of the 1987 first sale) as resource rentals. Resource rentals averaged about $20 million NZ annually during the first three years of ITQ management.

Table 3
Revenues from sale/lease of quota under New Zealand ITQ management, 1986–89.

Species	Tons (1000s)	$NZ (millions)	% Total $
Barracuda	1.7	1.7	2.0
Hake	1.3	2.2	2.6
Ling	2.1	2.2	2.7
Orange roughy	7.8	23.4	27.8
Hoki	131.0	53.2	63.2
Stargazer	1.8	1.5	1.8
Total	145.7	84.2	100.1

On 1 April 1990, ITQs were redefined as portions of annual TACs. This eliminated the need for government to adjust TACs by entering the marketplace to buy and sell quota, and makes it more practical to vary TACs in response to the inherent variability in fisheries resources, and other factors (e.g., new scientific information). The change to proportional ITQs came at a time when government was facing a large liability (discussed further below) to buy quota to adjust TACs. Therefore, government agreed to freeze the rate of resource rentals for five years and redistribute the resource rentals to industry as compensation for TAC reductions.

What has happened under ITQ management

It is probably too early to conduct a formal evaluation of ITQ management in New Zealand. A transition period of 3–5 years, or longer, is to be expected. Many of the species in New Zealand are long-lived, and it is likely that adjustments in the condition of the resource, which ultimately affect the economic benefits, will be protracted. However, since some authors have already declared New Zealand's ITQ management a success

[6] The TAC for orange roughy on the Chatham Rise was reduced by exchanging quota in that area for quota on the Challenger Plateau. This was a temporary reduction for 1988–89, although stock assessments indicated that a permanent reduction was necessary.

(Clark et al. 1988), it is worth considering what has happened to date, to the extent this is possible given limitations in available information. As discussed earlier, government authors and government publications indicate that the ITQ system was put in place to address three problems: (1) conservation, (2) economic performance, and (3) government intervention. The initial effects of the ITQ system with respect to these problems are discussed below.

Conservation

There is little evidence of improvement in the condition of fisheries resources; but since stock assessment information is limited, it is difficult to know. The increase in TACs that lead to the revenues reported in Table 3 resulted from a reassessment of the stocks, and not an increase in abundance.[7] There is evidence that some stocks have declined, most notably orange roughy, which has been found to be much less productive than previously believed (Mace et al. 1990). The current TAC for the largest stock of orange roughy exceeds even the most optimistic estimates of long-term sustainable yield by a factor of three. ITQs are not responsible for the problem, but have done little to resolve it.

There are several species in addition to orange roughy in need of TAC reductions. There is accumulating evidence that TACs are too high in the long term for valuable species such as hoki, squid, paua, and rock lobster (Annala 1990). At the 1989 FAM (Annala 1989), MCY was estimated for 110 management units. Twenty-one of the estimates were within 10% of the TACs, 82 were less than 90% of the TAC, and only 7 were greater than 110% of the TAC. CAY was estimated for nine management units. One estimate was within 10% of the TAC, seven were less than 90% of the TAC, and one was greater than 110% of the TAC. In 36 cases, yield estimates were less than 50% of the TAC. Reductions in TACs, either immediate or gradually toward MCY or CAY estimates, were recommended for several species. In other cases, reductions were not recommended because of uncertainty in MCY or CAY estimates, because accumulated biomass was still being fished down (in new or developing fisheries), or because recent catches indicated it was unlikely the TAC would be reached. It should also be noted that "actual" TACs are now almost invariably higher than "official" TACs, mostly as a result of successful appeals to the Quota Appeals Authority. Some of the differences are trivial, but a comparison between actual and official TACs from Annala (1989) indicates that of the 122 scientifically-based TACs (i.e., excluding the 47 administrative TACs), 25% of the actual TACs exceeded the official TACs by more than 10%, and 6% were higher by more than 20%.

There are also many species for which the TAC greatly exceeds the catch. For example, in the 1987–88 fishing year, the TAC was undercaught by more than 10% in 122 (out of 169) management units (including 47 "administrative" management units that have TACs of only 10–30 tons), and by more than 20% in 104 management units (Annala et al. 1991). For the 1988–89 fishing year, the total catch for all management units was 66% of the sum of the actual TACs. In situations in which TACs are nonrestrictive, they have little conservation benefit. In these cases, the stocks are either being overfished (because TACs are too high), or they would not be overfished without the ITQ system. There are other cases in which TACs have been overrun (17 of the 169 management units exceeded the TAC by more than 10% in the 1987–88 fishing year; Annala et al. 1991). There are a number of mechanisms by which fishermen can legally exceed their quota. Most of these mechanisms were established in order to deal with bycatch in multispecies trawl fisheries.

The general conclusion is that TACs are not closely tied to the best available assessments of the fisheries resources, nor are catches strongly controled by the TACs. Some valuable stocks have probably declined in abundance. To date, the track record of ITQ management with respect to conservation is not good.

Economic effects

There is even less information on the economic effects of ITQ management. ITQ management could increase economic benefits through several mechanisms: (1) Conservation could lead to an increase in resource abundance and a decrease in harvesting costs; (2) the initial buyback of quota and prorated cuts might have caused some excess capital and labor to move to segments of the economy where they could add production; (3) transfer of quota might have led to consolidation of ownership by the most efficient operators, and resulted in some excess capital being removed from the fishery; and (4) elimination of competition for TACs might have resulted in a more efficient harvest and an increase in the value of product.

As discussed earlier, it is unlikely that ITQ management has resulted in an increase in population

[7] In the case of hoki, the increase in TAC from 100,000 tons in 1985–86 to 250,000 tons in 1986–87 was controversial. Some components of industry were skeptical of the assessment which was in part based on a single hydroacoustics survey. The hydroacoustics survey results were later found to be gross overestimates. So far, the hoki resource has sustained the increase in TAC, but stock assessment results (Annala 1990) suggest that a catch of 250,000 tons may not be sustainable over the longer term. Government is giving high priority to monitoring the stock.

abundance. On the other hand, the decline in the abundance of orange roughy probably has not increased harvesting costs so far. Although orange roughy abundance has decreased considerably, the catch has been stable. Since orange roughy are fished in dense, spatially and temporally predictable aggregations, the catch rate is probably relatively insensitive to overall population size (see Paloheimo and Dickie 1964, for a general discussion of the phenomenon).

It is difficult to determine whether the initial buyback of quota and prorated cuts reduced excess capital, but it seems unlikely. As noted earlier, it probably did not reduce fishing mortality in most cases because the quota that was bought back would probably not have been caught. Fishing mortality is a function of capital investment in the harvesting sector (e.g., number of vessels), labor inputs (e.g., number of days the vessels are operated), and technology. It seems unlikely that capital would have been removed from the fishery unless fishing mortality were reduced.

There is evidence that quota holdings have been consolidated, presumably to more efficient owners.[8] During the period October 1986–April 1988, there were 15,580 quota sales involving 453,000 tons, and 3417 leases of quota involving 253,000 tons, the sum of which exceeds the total amount of quotas (494,000 tons owned privately and 64,000 owned by government); therefore, some quota was involved in multiple transactions (Muse and Schelle 1988). According to Bevin et al. (1989), the total number of quota holders decreased by 5.7% during the first two years of ITQ management. The amount of quota held by the top ten quota owners increased from 57% to 80% of the total. The number of quota holders with more than 50 tons decreased by 37%. This consolidation in ownership of quota does not necessarily mean that vessel ownership has also been consolidated. Apparently, a number of vessel owners who have sold their ITQ allotments to fishing companies have also entered contracts to fish that quota for periods of several years.

Unfortunately, the authors have not been able to obtain reliable data on the number of vessels in the fishery prior to and since ITQ management. There are some data available (e.g., Anonymous 1987, Bevin et al. 1989), but the information is inconsistent. There are data that indicate a slight decrease in investment in the harvesting sector in 1987, after several years of steady growth (Bevin et al. 1989). On the other hand, the data indicate that employment and investment in the fisheries increased steadily through 1987 (Table 4).[9]

Table 4

Investment and employment (in harvesting sector and total; processing-sector values can be obtained by difference) in New Zealand fisheries, 1983–87 (from Bevin et al. 1989). Values are in $millions NZ (book-value) and numbers of employees.

	1983	1984	1985	1986	1987
Investment					
Harvesting	142	170	182	223	213
Total	353	405	437	510	550
Employment					
Harvesting	3700	4000	4450	3800	4240
Total	7500	8000	8650	9200	10240

It is also difficult to evaluate the effects of eliminating competition for TACs, but there are some positive signs. In informal discussions with members of the fishing industry, the authors have been told that harvesters have modified their fishing practices to reduce costs and/or increase the market value of their catches.

At this stage, it is unclear what economic effects ITQ management has had. But, all other things being equal, it seems reasonable that ITQ management should have increased economic benefits. Unfortunately, all other things are not equal.

Two events unrelated to ITQ management have adversely affected the economic condition of the New Zealand fishing industry. They are a weakening of the price of product in export markets (particularly orange roughy in the USA) and unfavorable exchange rates. As a result, the industry had only a 4.3% return on investment (before income taxes) during the one-year period beginning 1 April 1987 (Bevin et al. 1989).[10]

While the overall economic benefit of ITQ management to New Zealand is unclear so far, it was profitable for the government. As noted earlier, the government's revenues from sale or lease of quota was $84.2 million NZ. It also collected about $60 million dollars in

[8] There is a legal limit to how much consolidation can occur. It is illegal for a company to own more than 35% of the quota for a species in any management area, or more than 20% of the quota for a species overall. It is interesting that some segments of the fishing industry have viewed the potential of consolidation of ownership of quota negatively, while government fisheries managers have generally viewed it as part of the process of increasing economic efficiency (i.e., efficient harvesters can afford to buy quota from less efficient harvesters). New Zealand government officials also note that consolidation should reduce the cost of managing the ITQ system.

[9] Note that there was a high rate of inflation during this period (3.6, 9.4, 15.3, 18.2, and 9.6% in 1983–87, respectively, or 69% overall) which approximately offsets the increase in nominal value of capital investment.

[10] It should be recognized that the economic condition of the New Zealand industry is a controversial matter because of resource rentals and fuel excise taxes. Bevin et al. (1989) indicate that in 1987 the industry paid $55 million NZ in resource rentals and fuel excise taxes which reduced the rate of return on investment from 16.2% to 4.3% (before income taxes).

resource rentals during the first three years of ITQ management. This income exceeds the cost of the buyback ($42.4 million NZ) and the entire cost of the government's fisheries research, management, and enforcement programs (about $30 million NZ per year). And there is the potential for resource rentals to increase substantially (see previous discussion). On the other hand, the authors are of the opinion that government should increase fisheries research considerably if it is to produce adequate stock assessments to support ITQ management (i.e., to conserve without being too restrictive). Furthermore, if government had entered the marketplace and purchased quota to implement the reductions suggested by yield calculations performed at the 1989 Fisheries Assessment Meetings (Annala 1989), the cost would have far exceeded the revenue from the ITQ system (e.g., the reductions for orange roughy alone would have cost in the range of $60–150 million NZ).

Government intervention

The third problem that ITQ management was intended to solve was excess government intervention. To date, it has not reduced government intervention except by removing the moratorium on new licenses. The moratorium was replaced by the requirement to own quota. In addition, there are new recordkeeping/reporting requirements and complicated rules that are intended to cope with bycatch (Annala et al. 1991).

One form of government intervention that probably hampered the fishing industry was restrictions on the port at which harvesters were allowed to land their catch. However, this restriction was removed prior to ITQ management. Other forms of input controls, such as minimum fish size restrictions and closed areas or seasons, have usually not been removed. Some of these restrictions are necessary, in addition to a quota, in order to conserve the fisheries resources and to prevent potential yield from being wasted.[11] In other cases, regulations were put in place to aid one segment of the fishing industry relative to another. For example, large factory trawlers are restricted from fishing within 25 miles of the coast, which reduces direct competition with smaller vessels.

General reaction

It is not surprising that implementation of ITQs in New Zealand has been accompanied by controversy. The newspapers report numerous charges by the industry against the government. The industry is upset about the level of resource rentals. There are complaints about the fairness of the Quota Appeals Authority. There were complaints that government had overestimated the productivity of the hoki resource when it sold quota, and there are complaints that it has overestimated the severity of the problem with orange roughy now that it is attempting to reduce the quota. Although there is strong support from industry and government for ITQ management, many specific aspects of implementation are unpopular. This is probably unavoidable for a system that is relatively complex and so radically different from previous management.

Potential problems

From a theoretical perspective, ITQ management is an ideal method which generates maximum net economic returns, under some simplifying assumptions; but as Copes (1986) points out, there are many potential problems. Instead of reviewing Copes' list of potential problems that apply to ITQ management in general, this paper reviews actual and potential problems that apply specifically to New Zealand. They are (1) problems arising from redefinition of quota ownership, (2) implications of the Treaty of Waitangi, (3) inadequacy of the scientific basis of TACs, (4) bycatch, (5) high-grading, (6) enforcement, and (7) an adequate basis for setting resource rentals.

Redefinition of quota ownership

The need to redefine ITQs from fixed quantities in weight to proportions of the TAC resulted from government's failure to enter the marketplace to reduce TACs when necessary. Early versions of the proposed ITQ system included a "revolving fund" that would be administered by the New Zealand Treasury. Resource rentals and revenues from the sale of quota would have gone into the fund which could then be used to buy back quota as necessary. In fact, Crothers (1988) actually reported that the revolving fund existed. However, the fund never materialized and revenues paid to government by the fishing industry were used for other government functions. When faced with the overwhelming cost of buying back quota to reduce the TAC for orange roughy, the government announced its intention to change the ITQ system from fixed to proportional ITQ. The authors were surprised at how rapidly government was able to obtain the legal authority from Parliament to make such a fundamental, and economically significant, change in the system. It took approximately one year from the time that

[11] Fisheries management needs to consider two control variables: the fishing mortality rate which can be regulated by a quota, and the age- or size-at-first-capture which can be regulated by gear restrictions, area/season closures, or minimum fish size (Sissenwine and Shepherd 1987).

government announced its intentions to convert the system to proportional ITQs until the change became effective on 1 April 1990.

The actual details of how the conversion will be implemented had not been determined at the time this paper was written, but some difficulties are almost certain to be encountered. In order to gain industry acceptance of the change, government agreed to freeze resource rental rates for five years, and redistribute these funds to compensate industry for quota reductions. Industry may have misjudged the amount of compensation it will receive, since several of the species that are most likely to have large quota reductions are also the species that generate most of the resource rentals (e.g., orange roughy, hoki, squid). Therefore, the greater the reductions, the smaller the pool of funds available for compensation.

One implication of converting from ITQ in fixed amounts to proportional ITQ is that there will be pressure to change the method of yield estimation from an MCY strategy to a CAY strategy, with consequent increases in the amount and variety of assessment information required. With quota as a fixed amount, there was little change in TACs from year to year. With ITQs as a proportion of the TAC, there will be greater pressure from the industry to change TACs (particularly to increase them when stock size is perceived to be high).

Treaty of Waitangi

The Maori people have sued for rights to the fisheries under the terms of the Treaty of Waitangi. There are several related cases which had not been settled at the time this paper was written, but it appears that the Maori people are entitled to a significant amount of quota. Prior to the ITQ system, when there was no ownership of the fisheries, there was less incentive for the Maoris to exercise provisions of the Treaty of Waitangi. But when property rights were established, and many Maoris were excluded from the system because they were part-time fish harvesters who had already been removed from the fishery, it was inevitable that a controversy would follow. Bevin et al. (1989) reported that industry has delayed major investments in the fisheries because of uncertainty about Maori fishing rights. Industry is concerned that the eventual settlement with the Maoris will be at their expense (i.e., they will not be compensated for quota that is transferred to Maori ownership). The dispute over the Treaty of Waitangi has also caused government to delay adding important species into the ITQ system.

Stock assessments

The scientific basis for assessing fish stocks, setting TACs, and evaluating the overall performance of the ITQ system is generally inadequate. New Zealand had relatively little need for stock assessment capability prior to ITQs. For the most part, their fisheries management was laissez-faire. In the case of data for assessing deepwater species, New Zealand relied heavily on foreign research vessels. When ITQs were implemented, they were ill-prepared, in the opinion of the authors, to conduct stock assessments for all of the management units included in the system. The situation has improved since the implementation of ITQ management as New Zealand scientists have developed and refined the scientific basis for stock assessments, but they have had inadequate support (e.g., research vessels, data collection systems, and personnel). Inadequate assessment databases mean that the ITQ system is operating under high levels of uncertainty. The price of uncertainty is either conservative quotas or a high risk of stock collapses.

Bycatch

Some bycatch is inevitable in multispecies fisheries. This means harvesters will catch some fish for which they do not own quota. New Zealand planned to manage bycatch with a taxation scheme (referred to as surrendering catch to the government or "Crown"), which was intended to produce a neutral incentive for bycatch. The tax was supposed to be high enough so that harvesters would have no incentive to catch species for which they did not hold quota, but if they caught them as bycatch, it would be worth their while to land them for sale. The problem is knowing what the proper tax level is in order to result in a neutral incentive. In some cases, even taxing 100% of the ex-vessel value does not discourage fishing for species for which harvesters do not hold quota. This is because of vertical integration in the fishing industry and a very high value added during processing.

There are several other provisions for dealing with bycatch. Quota holders may overcatch by up to 10% in exchange for next year's quota. They may trade retrospectively for quota to cover catch they have already taken. They may trade quota of certain species to cover bycatch of certain other species (for specified combinations of species, often involving one-way trades only).

Another aspect of the bycatch problem is that it is difficult to distinguish between bycatch problems that are a conservation threat to the bycatch species and those that result from setting the wrong TAC, as a result of imprecise assessments. Regardless of whether

it is a conservation problem or not, bycatch constitutes a management problem. It also constitutes a problem for members of the fishing industry when they try to adjust their portfolios of quota holdings to match their landings. In theory, this can be done by buying and selling quota, assuming that the overall TACs match the relative catch rates experienced by the fishing industry in aggregate; but this may not be so.

Annala et al. (1991) reviewed the bycatch situation in detail. In the 1987–88 fishing year, the quota was overcaught for 33 (out of 169) management units, by up to 74%. Nine management units were overcaught by more than 20%. The frequency and magnitude of overcatching increased from 1986–87 to 1987–88.

Highgrading

Highgrading is the discarding or dumping of a lower valued size or species of fish, in favor of keeping more valuable fish. Although highgrading is illegal under the New Zealand ITQ system, it is known to occur (Annala et al. 1991). For example, it probably occurs in the snapper fishery where there is a premium paid for high quality fish for the Japanese "iki jime" (killed by spiking the brain) market, and in the oreo dory fishery where three species (spiky, and black and smooth oreo dory) with significantly different values are managed by a combined TAC. The amount of highgrading in New Zealand fisheries has not been quantified.

Clark and Duncan (1986) felt that highgrading would be "...a short term, transitional problem and should disappear once the fishery recovers and product value differential within the same stock diminish..." There is little evidence that the fishery has recovered. Nor should recovery of the fishery eliminate the incentive for highgrading, unless the ITQ system is administered such that TACs do not limit catch. If so, then other advantages of ITQ management would be undetermined. Nor are the authors aware of reasons why ITQ management should reduce value differences between species or levels of quality.

Enforcement

ITQ management is potentially difficult to enforce. New Zealand has some advantages over the United States when it comes to enforcement. First, the population is small, and therefore there is less scope for the development of a domestic black market, although black markets may be significant for some inshore species consumed domestically. Second, the country is remote, so that it is difficult to smuggle fish elsewhere. Third, most fish are exported, which involves recordkeeping that helps to check the accuracy of quota reports. Finally, fisheries enforcement is carried out entirely by a single, coordinated agency.

New Zealand placed a high priority on establishing enforcement capability when it implemented ITQs. It reoriented enforcement from at-sea operations to shoreside investigations. The emphasis moved from conservation officers to accountants and investigators and "electronic surveillance" (computerized data recording). The industry is required to maintain and submit several different types of records that are necessary for monitoring catch and product flow. Penalties for quota violations are heavy. They may involve forfeiture of catch, vessel, and quota holdings, in addition to fines of up to $10,000 NZ. A second offense within seven years may result in prohibition from participation in any aspect of the fishing industry for up to three years. In addition, the fisheries enforcement agency passes information on to the tax department, which may then be used in income tax prosecutions. It is difficult to assess how well this enforcement approach is working.

Resource rentals

The New Zealand fishing industry is concerned about the basis of setting resource rentals, although it does not seem to dispute them in principle. The government planned to gradually increase resource rentals[12] until the fair market value of quota was reduced to approximately zero. In theory, government is extracting all of the resource rent from the fisheries at the point in time that there is no longer incentive to enter the fisheries. The industry argued that not all of the resource rent should be extracted, since investment in fishing is inherently risky.

It is arguable whether the market value of quota reflects resource rent in the fisheries. The price paid for quota should reflect the buyer's estimate of its net present value. However, the buyer's estimate may be incorrect (i.e., a bad investment). Even if the price paid for quota is correct, it may not reflect rent in a particular year. In practice, the price paid for quota has been extremely variable (e.g., from $13 per ton to $16,500 per ton for snapper; Bevin et al. 1989) for a variety of reasons (e.g., imperfect knowledge, inclusion of other assets in the price of quota, different discount rates, noncompetitive price setting). This makes it difficult to use the sales price of quota as a criterion for setting resource rentals.

[12] The law limits increases in resource rental rates to 20% per year.

Table 5
Problems and benefits of fisheries management by input controls, quotas (Q), and ITQs. The symbol "0" is used as the standard. The symbol "+" means a more difficult problem or greater benefit than "0." The symbol "++" means even greater problems or more benefit than "+."

	Type of management		
	Input	TACs	ITQs
Problems			
Stock assessments	0	+	+
Catch statistics	0	+	++
Enforcement	0	+	++
Bycatch	0	+	++
Benefits			
Conservation	0	0	0(+)
Economics	0	0	+

General issues

Many potential problems of ITQ management are problems associated with TAC management in general. In some cases they are exacerbated by individual quotas. Table 5 compares the problems and benefits associated with input controls (e.g., effort limits, closed areas or seasons), TACs, and ITQs. TAC management requires more frequent and timely stock assessments than management by most input controls (Sissenwine and Kirkley 1982). The problem is particularly severe for short-lived species (Copes 1986). The problem of providing stock assessments for ITQ management is about the same as that for TAC management. Catch statistics are one component of stock assessments. The need for catch statistics is generally greater for TAC management than for management by input controls. The need is even greater for ITQs because statistics on individual quota holders are the basis of management. Both TAC and ITQ management encourages "data fouling" or misreporting (Copes 1986), although the incentive is greater for ITQs. Similarly, enforcement is generally more of a problem for TAC management (although this is not universally true) because the catch has to be accurately enumerated. For ITQs, it must be accurately enumerated for individual quota owners, some of whom may have developed successful methods for circumventing the system. The bycatch problem is more difficult for TAC management than for input controls. For ITQs, the bycatch problem is even more difficult because individual quota owners must adjust their portfolios to match their multispecies catch rates.

In terms of the conservation benefits, input controls, TACs, and ITQs are all potentially effective (Sissenwine and Kirkley 1982). ITQs may have a potential advantage over TAC management because, with ownership, there should be greater incentive for the industry to cooperate. But limited-entry licensing (a form of input control) also conveys privileges that may encourage industry cooperation. In terms of economic benefits, ITQs are superior in theory. Both input controls and TAC management eventually allow dissipation of resource rent. For both forms of management, there is an incentive for fishermen to increase their cost of fishing, in order to gain a larger share of the resource, until the rent is dissipated. In practice, the actual economic benefits of input controls, TACs, and ITQs are probably fishery-specific.

Learning from New Zealand's experience

There is much to be learned from New Zealand's experience with ITQ management. New Zealand took a systems approach. Comprehensive new legislation was introduced. Enforcement needs, penalty schedules, reporting and recordkeeping requirements (including wholesalers and retailers), a quota trading system, a process for appealing initial allocations, a buyback scheme for "rationalization" of some fisheries, mechanisms for controling bycatch, the principle of resource rentals, and public and fishery industry education were all considered. New Zealand made some mistakes, but it would have probably made more if its approach had been piecemeal.

The authors are of the opinion that one mistake made by New Zealand fisheries managers was to establish ITQs in fixed amounts, valid in perpetuity. This method was used because it was thought that ITQs in fixed amounts would create a more certain environment for industry; they would provide a mechanism for government revenue-raising, since government believed TACs were conservative and future quota sales were likely; and the trading price for fixed amounts of quota would be the most effective method to obtain information to set resource rentals (Clark et. al. 1988).

Apparently, the government did not recognize how uncertain TACs might be (due, for example, to errors in stock assessments) or how often TACs might need to be adjusted (due, for example, to the inherent variability in the size of fish stocks) by entering the market to buy and sell quota, since the revolving fund (or some other method) was not established. It is also possible government did not expect the price of quota to be so high as to make it prohibitively expensive for the government to buy it to reduce quotas. In fact, the sales price of quota may not have been economically rational, in which case government would not want

to overpay to adjust TACs downward. But it should be noted that the Government did sell quota for similarly high prices. In any case, it seems more practical to define quota as a portion of the TAC, in an uncertain and dynamic environment.

In the authors' opinion, New Zealand fisheries managers underestimated the complexity of the bycatch problem. In a multispecies setting, the apparent independent fluctuations of each species complicate the bycatch problem. In general, insufficient information, variability between harvesters, and the complex organization of fisheries mean that it will be difficult to solve the bycatch problem by adjusting a tax on bycatch. Many fisheries are essentially single-species (e.g., surf clams, herring, scallops, lobsters). These are the best candidates for ITQ management with respect to bycatch. If ITQ management is to be applied to multispecies fisheries (e.g., New England groundfish), it might be better to exclude some of the minor species from the scheme, or to recognize that they may need to be "sacrificed" in order to optimize fishing on the more valuable species.

New Zealand lacked adequate stock assessment data for a quota-based management system such as ITQs. And, unfortunately, it will take time to develop appropriate time-series of data. In addition, there is much that needs to be learned about the basic biology of the deepwater species, many of which have only recently been discovered in commercially viable quantities. The basis for stock assessments is better in some other places (e.g., throughout North America and Europe), but the expectations for a high degree of precision may still make stock assessment capability problematic.

ITQ management requires adequate monitoring and enforcement capability to track individual catches. New Zealand's enforcement of ITQs is geared towards investigations by accountants and auditors, instead of traditional fisheries officers. In order for these investigators to be effective, the New Zealand fishing industry is required to maintain detailed "paper trails" for products. Penalties for violations are severe. It is too early to say whether this scheme is working, but it is obvious that it will be necessary to impose additional recordkeeping to enforce ITQs in most cases in the United States.

It is unclear how serious the overcapitalization problem was in New Zealand, but there are U.S. fisheries that are severely overcapitalized (e.g., New England groundfish). The buyback scheme in New Zealand probably did little to reduce overcapitalization. If a buyback scheme is intended to reduce overcapitalization, funds should be used to reduce capital, and not hypothetical catches that might not have been taken anyway.

A positive lesson that should be learned from New Zealand is the need to be clear about objectives when applying an ITQ system. Clearly, one of the intentions of New Zealand's fisheries managers was to increase resource rent in the fisheries and to extract the rent (through annual royalty payments[13]) for the general benefit of the country. What will be the objective for applying ITQ management elsewhere? If the objective is conservation, then quota management (or other forms of management) is sufficient in theory, although pressure from an overcapitalized fishing industry may prevent TACs from being set conservatively enough. If the objective is economic efficiency, then it is important to address distributional issues (resource rents, producer surplus, and consumer surplus).

There is a great potential for ITQ management, but it is not a panacea. When ITQ management is applied, it is important that it be approached with realism and based on adequate experience and data.

Postscript

Approximately 20 months have passed since New Zealand converted its ITQ program from one of fixed quota valid in perpetuity to one based on quota specified as a proportion of an annual TAC (also referred to as a percentage ITQ system in New Zealand or a percentage quota share system in the United States). As predicted in this paper, the transition has been controversial, in part because compensation available to the industry in the form of resource rentals has not been as large as anticipated. As a result, the fishing industry filed a $150 million NZ court action against the government. The lawsuit has since been settled out of court.

In spite of the change from fixed to variable quota, most TACs have remained unchanged from one year to the next. This is partly a result of inadequate information for stock assessments. However, there have been three notable reductions in TACs. The total hoki TAC has been reduced from 250,000 to 200,000 tons, Challenger orange roughy from 12,000 to 1900 tons, and Chatham Rise orange roughy from 32,800 to 23,800 tons. The reduction in hoki quota was a reflection of new stock assessment results suggesting that then-current TACs were unlikely to be sustainable; the reductions in orange roughy TACs resulted from assessment results suggesting that stock collapse was imminent.

The anticipated need for large reductions in the Chatham Rise orange roughy TAC was one of the

[13] At present, a legal basis for resource rentals in an ITQ system is lacking in the Unites States.

major factors that precipitated the change from fixed to variable ITQs, since it could have cost the government more than $100 million NZ to buy back sufficient quota to reduce the TAC to the estimated long-term sustainable level. After the change, it was agreed that the quota would be reduced at the rate of 5000 tons per year to the sustainable level, the latter being recalculated periodically as new data became available. Recent assessments (Francis and Robertson 1991) indicate a sustainable level of 7000–9000 tons and show that the risks of stock collapse under the proposed reduction schedule have increased due to the accumulation of new data which has resulted in a decrease in the point estimates of stock size and a decrease in uncertainty of the estimates. The results clearly indicate the need for a faster rate of reduction. However, the fishing industry continues to oppose quota reductions, and at this point in time the government has postponed the 5000-ton reduction schedule. The discovery of new orange roughy aggregations in the southern portion of the management area may alleviate the problem in the short term, but the low productivity of orange roughy stocks means that any accumulated biomass can be quickly fished down. Long-term sustainable yields from orange roughy stocks are estimated to be only about 1.5–2.5% of the recruited virgin biomass.

The problem of not reducing quotas when reductions are indicated by assessments is exacerbated by widespread rumors of quota busting, in spite of New Zealand's efforts to tailor enforcement to ITQ management. Some of these rumors have been confirmed by government sources.

New Zealand is now considering further evolution in its fisheries management system towards a form of comanagement. Topics being debated include the need to incorporate recreational fisheries into the management system, the need to include all remaining exploited species-stocks, and the pros and cons of eliminating the current limits on aggregation of quota (Pearse 1991). One objective is to transfer the costs of management and responsibility for the resource to the users of the resource, under the assumption that with ownership comes motivation for conservation. Stay tuned.

Citations

Annala, J.H.
1989 Report from the Fishery Assessment Plenary, May 1989: Stock Assessments and Yield Estimates. Fish. Res. Cent., N.Z. Minist. Agric. Fish., Wellington, 158 p.
1990 Report from the Fishery Assessment Plenary, April–May 1990: Stock Assessments and Yield Estimates. Fish. Res. Cent., N.Z. Minist. Agric. Fish., Wellington, 165 p.

Annala, J.H., K.J. Sullivan, and A. Hore
1991 Management of multispecies fisheries in New Zealand by individual transferable quotas. *In* Daan, N., and M.P. Sissenwine (eds.), Multispecies models for management of living resources. ICES Mar. Sci. Symp. 193:321–330.

Anonymous
1984 Inshore finfish fisheries: Proposed policy for future management. N.Z. Minist. Agric. Fish., Wellington, 31 p.
1987 Economic review of New Zealand fishing industry, 1986–1987. N.Z. Fish. Ind. Board, Wellington, 56 p.

Bevin, G., P. Maloney, and P. Roberts
1989 Economic review of the New Zealand fishing industry, 1987–1988. N.Z. Fish. Ind. Board, Wellington, 56 p.

Christy, F.T.
1973 Fishermen quotas: A tentative suggestion for domestic management. Occas. Pap. 19, Law of the Sea Inst., Univ. R.I., Narragansett.

Clark, I.N., and A.J. Duncan
1986 New Zealand's fisheries management policies—Past, present and future: The implementation of an ITQ based management system. *In* Fishery assess control programs worldwide, p. 107–141. Alaska Sea Grant Rep. 86-4, Univ. Alaska, Fairbanks.

Clark, I.N., P.J. Major, and N. Mollet
1988 Development and implementation of New Zealand's ITQ management system. Mar. Resour. Econ. 5:325–349.

Copes, P.
1986 A critical review of the individual quotas as a device in fisheries management. Land Econ. 62(3):278–291.

Crothers, S.
1988 Individual transferable quotas: The New Zealand experience. Fisheries (Bethesda) 13(1):10–12.

Dewees, C.M.
1989 Assessment of the implementation of individual transferable quotas in New Zealand's inshore fishery. N. Am. J. Fish. Manage. 9:131–139.

Francis, R.I.C.C., and D.A. Robertson
1991 Assessment of the Chatham Rise (ORH 3B) orange roughy fishery for the 1991/92 season. N.Z. Fish. Assess. Res. Doc. 91/3, N.Z. Minist. Agric. Fish., Wellington, 36 p.

Geen, G., and M. Nayar
1988 Individual transferable quotas in the southern bluefin tuna fishery: An economic appraisal. Mar. Resour. Econ. 5: 365–388.

Gilbert, D.J.
1988 Use of a simple age structured bioeconomic model to estimate optimal long run surpluses. Mar. Resour. Econ. 5:23–42.

Mace, P.M., and M.P. Sissenwine
1989 Biological reference points for New Zealand fisheries assessments. N.Z. Fish. Assess. Res. Doc. 89/11, N.Z. Minist. Agric. Fish., Wellington, 10 p.

Mace, P.M., J.M. Fenaughty, R.P. Coburn, and I.J. Doonan
1990 Growth and productivity of orange roughy (*Hoplostethus atlanticus*) on the north Chatham Rise. N.Z. J. Mar. Freshwater Res. 24:105–119.

Maloney, D.G., and P.H. Pearce
1979 Quantitative rights as an instrument for regulating commercial fisheries. J. Fish. Res. Board Can. 36:859–866.

Muse, B., and K. Schelle
1988 New Zealand's ITQ Program. Alaska Commer. Fish. Entry Comm. (CFEC 88-3), Juneau, 47 p.
1989 Individual fisherman's quotas: A preliminary review of some recent programs. Alaska Commer. Fish. Entry Comm. (CFEC 89-1), Juneau.

Paloheimo, J.E., and L.M. Dickie
1964 Abundance and fishing success. Rapp. P.-V Reun. Cons. Int. Explor. Mer 155:152–163.
Pearse, P.H.
1991 Building on progress: Fisheries policy development in New Zealand. Unpubl. rep. prepared for Minist. Agric. Fish., Wellington, NZ.
Sandrey, R.A., and D.K. O'Donnell
1985 New Zealand's inshore fishery: A perspective on the current debate. Agric. Econ. Res. Unit Res. Rep. 164, Lincoln College, Canterbury, NZ, 46 p.
Sissenwine, M.P., and J.E. Kirkley
1982 Fishery management techniques: Practical aspects and limitations. Mar. Policy 6:43–58.
Sissenwine, M.P., and J. Shepherd
1987 An alternative perspective on biological reference points and recruitment overfishing. Can. J. Fish. Aquat. Sci. 44: 913–918.

Seasonality in reproductive activity and larval abundance of queen conch *Strombus gigas*

Allan W. Stoner
Veronique J. Sandt
Isabelle F. Boidron-Metairon
Caribbean Marine Research Center
805 46th Place East, Vero Beach, Florida 32963

Abstract.–Reproductive behavior and larval abundance of queen conch *Strombus gigas* L. were investigated near Lee Stocking Island, Bahamas, with the primary purpose of determining relationships between physical variables, spawning frequency, and larval abundance. Monthly observations made by divers at the offshore spawning site showed that copulation increased as a linear function of bottom water temperature from April until the end of July, when maximum summer temperature was reached. Pairing, copulation, and egg-laying were all positively correlated with photoperiod throughout the study period. The last pairing and copulating conch were observed in the middle of the warmest period in August suggesting that stimuli other than temperature, such as declining photoperiod, induce the end of reproductive activity. The last egg mass was found in early October.

There was a significant correlation between spawning activity at the offshore reproductive site and larval abundance in the adjacent downcurrent inlet. The first conch veligers were found in plankton tows made in early June, five weeks after the first egg masses were observed at the end of April. High larval density was confined to July and August. Advanced-stage larvae, close to metamorphosis, were found only in the vicinity of a shallow, benthic nursery habitat. Comparison of reproductive season in queen conch populations of the Caribbean region showed no latitudinal trend. In all areas, reproduction was associated with long days and warm temperatures. Production of conch larvae at the time of high water temperature and steady trade wind conditions may promote rapid larval development and facilitate transport of the veligers to inshore nursery habitats.

Manuscript accepted 31 January 1992.
Fishery Bulletin, U.S. 90:161–170 (1992).

The queen conch *Strombus gigas* L. is the second most important fisheries species in the Caribbean region, after spiny lobster *Panulirus argus* (Brownell and Stevely 1981). Consequently, its general life history is well known (Randall 1964, Brownell and Stevely 1981, Berg and Olsen 1989). Sexes are separate and sexual maturity occurs at about 3½ years of age, a few months after the flared lip is formed (Egan 1985, Wilkins et al. 1987, Appeldoorn 1990). Fertilization is internal and copulation may precede spawning by several weeks (D'Asaro 1965). An individual female may spawn six to eight times during a single reproductive season (Davis and Hesse 1983). An egg mass, usually laid on clean, coral sand, takes 24–36 hours to produce and consists of a single continuous egg-filled tube folded upon itself to form a kidney-shaped aggregate of eggs and sand about 15 cm in length. Robertson (1959) estimated that between 385,000 and 430,000 eggs were laid in a single egg mass. Eggs hatch after 5–6 days; pelagic veligers remain in the water column for 18–40 days prior to metamorphosis (Randall 1964, D'Asaro 1965, Brownell 1977, Davis et al. 1987, Boidron-Metairon 1988, Mianmanus 1988).

Reproductive seasonality in queen conch has been reported for different sites within the Caribbean region (see Fig. 6), but the mechanisms which regulate reproductive behavior are poorly known. In this study, we provide the first report on abundance and seasonality of queen conch veligers in the field, and examine relationships between adult habitat, reproductive activity, temperature, photoperiod, and larval abundance.

Methods and materials

Study site

This study was conducted near Lee Stocking Island (southern Exuma Cays), Bahamas, an area known for high abundance of queen conch (Fig. 1). The islands and cays of the Exuma chain are bordered on the west by the shallow Great Bahama Bank (mean depth ~3 m) and on the east by the deep Exuma Sound. Waters from the Exuma Sound flow onto the Bank through numerous passes on the flood tide and are mixed with Bank water by wind-driven circulation. Surface drogue studies (N.P. Smith, Harbor Branch Oceanogr. Inst., Fort Pierce, FL 34946, unpubl. data) indicate that at the north end of Lee Stocking Island, water flows through Adderley Cay cut toward Shark Rock. At the south end of the Island, water flows through Rat Cay cut to the west between Barraterre Island and Children's Bay Cay. Most juvenile queen conch are located in shallow seagrass habitats on the Exuma Bank; largest populations are found near Shark Rock and southwest of Children's Bay Cay.

In Exuma Sound, approximately 1 km to the east of Lee Stocking

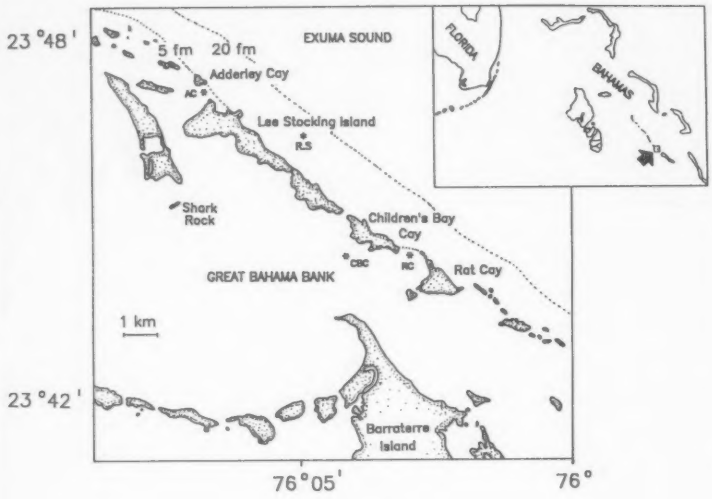

Figure 1

Map of the Lee Stocking Island, Bahamas, study site showing plankton sampling stations (*). RS = location of the Reproductive Site, where observations and plankton collections were made; RC = Rat Cay cut; AC = Adderley Cay cut; CBC = Children's Bay Cay nursery site.

Island, there is a coral ledge at which depths increase rapidly from 10 to 18m. Beyond the ledge is a 1km-wide platform with a gradual slope from 18 to 24m. Seaward from the platform, depth increases rapidly to the deep basin of Exuma Sound. This geomorphology is typical of the western side of the Exuma Sound. Highest number and density of adult *S. gigas* occur on the 18m-deep platform, which is beyond the normal free-diving range of conch fishermen. In this area, more than 99% of the conch are sexually mature (Stoner and Sandt 1992). In the colder months, the conch are found on algae-covered hardbottom; they move to sand for mating and egg-laying in the summer.

A study site of approximately 12 ha surface area on the 18m platform was chosen for the investigation of reproductive behavior and habitat association in adult conch (Fig. 2). The particular location, north of the 10m coral ledge, was selected because of an abundance of adult conch and close proximity of feeding and spawning habitats (Stoner and Sandt 1992). A scale map of the site was constructed from compass bearings and distances measured by scuba divers along the sides of primary habitat features or boundaries. Figure 2 shows all prominent features between the coral ledge and the 23m isobath.

Observations on reproductive behavior were made in three habitat types (1) Five hard-bottom domes (called "mounds"), each surrounded completely by bare sand, were examined. All of the mounds (designated with the letter "M" in Fig. 2) were located at depths of 18m at the base with tops between depths of 12 and 14m. (2) Sand habitats were divided into two major regions. S1 is the extensive sand flat between the 10m reef front and the mound zone. S2 is the sand area within the mound zone. (3) Rubble and boulder areas are found at the base of the 10m reef in a narrow band, with an extensive boulder field (B1) at the southeast end of the study site. The mounds and rubble, particularly in the B1 area, are covered with a turf of green algae (primarily *Cladophoropsis* spp.), plus abundant erect forms such as *Halimeda* spp. An area of mixed hardground, sand, and coral heads (H1) extends to the north and east of the study site.

Reproductive activity

Reproductive behavior was surveyed for 14 months, on a monthly basis during the period of highest activity (March–October 1988) and at 6–8 week intervals during January–February 1988 and November 1988–February 1989. Longer sampling intervals were used in the winter because preliminary observations near Lee Stocking Island in previous years indicated that no reproductive behavior occurs between November and March. During each survey, spanning 5–15 days, a scuba diver search for adult conch was made on mounds M1, M3, M4, and M5, in the boulder area (B1), in the rubble area (at the base of the coral ledge), and in both sand zones S1 and S2. During each survey period, all conch were counted on each of the mounds and at least one-half of the B1 area was examined. Very few conch were found on M2 and this mound was abandoned early in the study. After determining that most reproductive activity occurred on sand and not on hardground or rubble (Table 1), the sampling protocol was modified to locate at least 100 individuals on sand for each survey. During winter months, less than 100 conch were located on sand in several days searching; however, 100–300 animals were observed per month during most of the reproductive season.

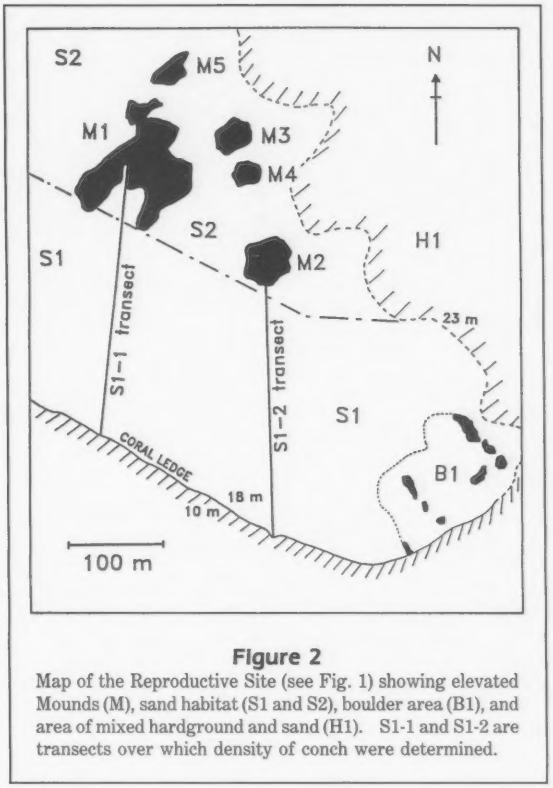

Figure 2
Map of the Reproductive Site (see Fig. 1) showing elevated Mounds (M), sand habitat (S1 and S2), boulder area (B1), and area of mixed hardground and sand (H1). S1-1 and S1-2 are transects over which density of conch were determined.

Table 1
Numbers and (percentages) of queen conch engaged in reproductive activity on three substratum types near Lee Stocking Island, Bahamas, 1988. Values for pairing and copulating represent number of male/female pairs.

	Behavioral type		
Substratum	Pairing	Copulating	Egg-laying
Sand	51 (94.4)	28 (84.4)	148 (99.3)
Rubble	0 (0.0)	2 (6.1)	0 (0.0)
Hardground	3 (5.6)	3 (9.1)	1 (0.7)

Each individual conch was classified in one of the following reproductive categories. (1) Pairing: Two conch were aligned, with the anterior part of the shell of one animal overlapping the posterior part of the shell of the other; but copulation was not observed. (2) Copulating: Animals were engaged in copulation, with the verge of the male beneath the mantle of the female. (3) Egg-laying: A female was actively laying an egg mass. (4) Non-reproductive: Conch was not engaged in reproductive behavior.

Seasonality in reproductive behavior was quantified by recording the percentage of total animals on sand in each behavioral category. Notes were made on the locations and substratum types (sand, rubble, hardground) where pairing, copulating, and egg-laying conch were found. Conch were measured for total shell length (spire to siphonal groove) and greatest shell lip thickness (approximately two-thirds of the distance posterior from the siphonal groove). Shell measurements were made to the nearest mm.

To estimate seasonal abundance of conch on sand, two quantitative transects across the S1 sand area (transects S1-1 and S1-2; Fig. 2) were examined each survey period. The transect surveys were made by a scuba diver who counted all adult conch within a known range while being towed 5 m above the sediment. High water transparency resulted in a mean transect width of 29 m (SD 6; range 20–40 m), which was measured with a tape on each survey date. The total survey area for each transect was calculated on the basis of horizontal visibility and the fixed distance of each transect line. For additional information on the abundance of queen conch on sand during the reproductive season, all adult conch were counted in circles of 20 m radii at locations of highest conch density in August 1987 (n 7 circles), and in June (n 2) and July 1988 (n 2).

Physical measurements

To provide information on sediment grain-size and organic content in the spawning habitat, sediment samples were taken from the surface adjacent to females laying eggs in August. Only eight samples were collected; however, the sediment in sand areas S1 and S2 appeared to be of uniform grain size. An effort was made to collect sediment samples from throughout the study site. Sediments were frozen until laboratory analysis. Organic content was determined by drying a subsample (~100 g wet wt) at 80°C to constant weight and incinerating at 500°C for 4 hours. Organic content was quantified as the percent difference between dry weight and ash-free dry weight. Another subsample (~50 g wet wt) was examined for granulometric properties. The sample was washed to remove salts and extract the silt-clay fraction (<62 μm). Silt-clay was analyzed with standard pipette procedures (Galehouse 1971), and the sand fraction with standard dry sieve procedures (Folk 1966).

Bottom-water temperature was recorded with a Ryan Instruments Temp Mentor placed at 17 m depth, near the base of the coral ledge. The thermograph recorded temperature with a precision of 0.2°C every

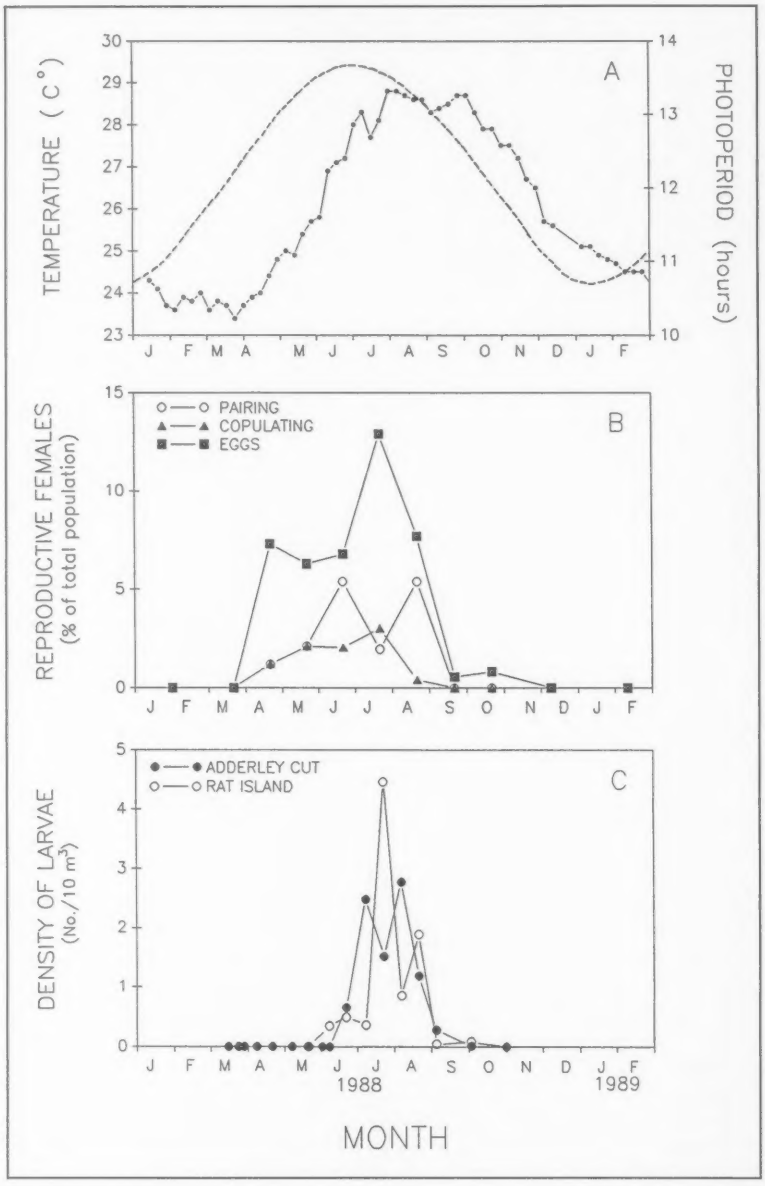

Figure 3
(A) Bottom-water temperature at 17 m depth with 7-day averages (solid line) and photoperiod in number of hours between sunrise and sunset (dashed line). (B) Number of queen conch *Strombus gigas* females on sand engaged in various reproductive activities. (C) Number of conch larvae in Rat Cay and Adderley Cay passes, January 1988–February 1989.

30 minutes; 7-day averages were generated and plotted (Fig. 3A). Surface-water temperature and weather conditions were recorded each time that plankton was collected.

To examine potential correlation between reproductive seasonality and photoperiod, a year-long photoperiod curve (Fig. 3A) was constructed for the study site. Numbers of hours and minutes between sunrise and sunset were calculated for local latitude at 9-day intervals using the Nautical Almanac.

Plankton collections

Daytime plankton collections were made for queen conch veligers from mid-March to October 1988. For seasonal analysis of larval abundance, collections were made every 2 to 3 weeks in the pass between Lee Stocking Island and Adderley Cay (Adderley Cay cut) and in the pass between Rat Cay and Children's Bay Cay (Rat Cay cut) (Fig. 1). Additionally, collections were made over the area surveyed for reproductive activity (Reproductive Site) with the primary purpose of detecting low densities of conch larvae at the onset and end of the reproductive season. Collections were not made at the Reproductive Site during peak reproduction, between July and mid-August. To examine densities and size-frequency of larvae on Exuma Bank, four collections were made over a known nursery for *S. gigas*, west of Children's Bay Cay (Fig. 1). This site is approximately 3.4 m deep and vegetated with the seagrass *Thalassia testudinum*.

In the passes, plankton were sampled during the first 2 hours of the flood tide; on the bank, tows were scheduled during the last 2 hours of flood tide. Plankton collections were made by towing a 0.5 m diameter conical net, 5 m long, with 202 μm mesh. Two tows were made at each site. Because the location of larvae in the water column was unknown, collections at the Reproductive Site were made by towing the net at 9 m depth (midwater column) for 10 minutes, then raised near

the surface at 1.5 m depth for another 10 minutes. At the other three sites where there was considerable vertical mixing and shallow depth, the net was towed for 20 minutes in the upper 1.5 m of the water column. Water volume sampled was calculated using a calibrated General Oceanics flowmeter, and larval abundance was expressed in numbers of veligers per $10\,m^3$.

To identify larvae, samples were refrigerated, sorted live (within 4 hours), and compared with laboratory-cultured larvae of the two most abundant *Strombus* spp. in the central Bahamas, *S. gigas* and *S. costatus*. Two other strombids occur in the Lee Stocking Island area (*S. gallus* and *S. raninus*); however, both are very rare relative to *S. gigas* and neither has been observed on the windward side of the island or in the inlets. Shell length, shell width, and shape of the shell tip were the principle criteria used to identify early-stage larvae. Number and shape of shell whorls and other shell characteristics were used to identify advanced larval stages. Measurement of shell length, from apex to siphonal edge, was made with an ocular micrometer and reported in microns for all intact shells.

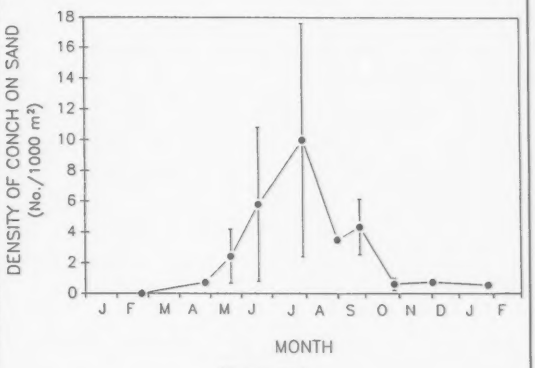

Figure 4

Density of queen conch *Strombus gigas* on sand at the Reproductive Site, off Lee Stocking Island, Bahamas, January 1988–February 1989. Values are mean ±SE for two transects.

Results

Conch reproduction

The reproductive season for *Strombus gigas* at Lee Stocking Island extended from mid-April to early October. The beginning of the season was marked by a massive migration of conch from hardground (mounds, rubble, and boulder areas) to sand habitats (Fig. 4) where first copulation, pairing, and spawning were observed on 14, 15, and 25 April 1988, respectively. In subsequent months, virtually all reproductive behavior occurred on sand (see later). The number of females engaged in reproductive activity increased gradually from April (9.7% of total sampled population) to July (18%) (Fig. 3B). In August, 13.8% of the population were reproductively active females; the percentage declined to less than 1.0% in September and October. Last copulation and pairing were seen in August, but egg-laying was observed through September. The last egg mass was discovered on 5 October 1988.

The number of reproductive conch increased with conch density on sand (Fig. 4) from January and February (0 conch/$1000\,m^2$) to July (10 conch/$1000\,m^2$). Density decreased after the beginning of August and was 0.61 conch/$1000\,m^2$ in October. Conch were aggregated on some dates and not distributed evenly along the transect lines. Large error bars in Figure 4 show that the two transect lines frequently had different densities of conch during the primary reproductive season. In August 1987, measurements in areas with high conch densities ranged from 11.1 to 20.7 conch/$1000\,m^2$. Values as high as 29.7 conch/$1000\,m^2$ (SE 2.0) were found in June 1988.

Low bottom-water temperatures were observed from early March to early April 1988 (near 23.6°C) (Fig. 3A). First pairing and copulating conch were seen at a temperature of 24°C in mid-April, and the first egg-laying female was found at 24.5°C. The number of copulating females increased as a linear function of bottom water temperature until the reproductive maximum (r 0.916, F 15.726, p 0.029; March through July 1988). There was no significant correlation between egg-laying and temperature (p 0.061) and pairing and temperature (p 0.285). Bottom temperature was relatively constant (28.3–28.8°C) from the end of July through September; the last pairing and copulating conch were observed during this period. Temperature decreased rapidly after September, and the last egg mass was found on 5 October. Water temperature was 26.5°C by late November 1988, decreasing to 25.1°C in late December.

All pairing and copulation were confined to the season with photoperiod greater than 12 hours, while egg-laying was observed until day length declined to 11 hours (Fig. 3A,B). Highest correlation occurred between length of day and copulation (r 0.870, F 24.838, p 0.001), but significant correlations were also found between photoperiod and both pairing (r 0.709, F 8.064, p 0.022) and egg-laying (r 0.838, F 18.896, p 0.002).

A few conch were buried partially in sand in mid-October 1987 and again in January and early February 1988. Burrowing was not seen again until mid-September 1988. In November, a few conch were buried

Table 2

Density of queen conch larvae at the Reproductive Site offshore from Lee Stocking Island, Bahamas, and at the nursery site near Children's Bay Cay on Exuma Bank, 1988. Values are numbers of conch larvae/10m³ ± SD (*n* 2).

	Location	
Date	Reproductive Site	Children's Bay Cay
15 March	0±0	—
28 March	0±0	—
7 April	0±0	—
20 April	0±0	—
19 May	0±0	—
2 June	0.26±0.11	—
6 June	0.04±0.03	—
16 June	0.99±0.25	—
29 June	0.30±0.09	—
13 July	—	0.82±0.23
28 July	—	1.35±0.47
12 August	—	0.77±0.41
23 August	0.77±0.32	—
14 September	—	0.17±0.10
23 September	0±0	—
6 October	0±0	—

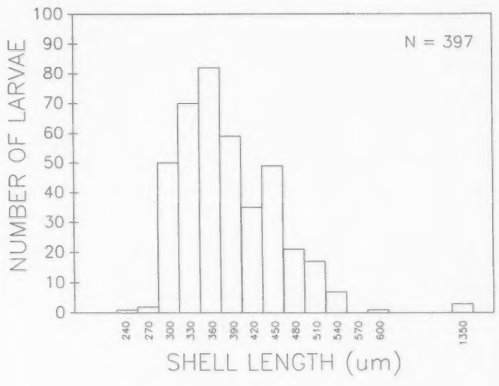

Figure 5

Length-frequency distribution for veligers collected near Lee Stocking Island, Bahamas, May–September 1988 (*n* 397).

in sand-filled depressions on the mounds. Some were almost entirely covered with sand and the shells were devoid of algae. It is possible that conch in the sand habitat were underestimated during winter months because of burial behavior; however, tag return data (Stoner and Sandt 1992) suggest that most adult conch move to hardground or rubble for the winter months.

The mean shell length of pairing, copulating, and egg-laying females ($\bar{x}$ 226mm, SD 23.6, *n* 180) was 2.3% larger than that for males in reproductive behavior ($\bar{x}$ 221mm, SD 17.4, *n* 180). However, pairwise ANOVA, using female-male pairs as statistical blocks, indicated no significant differences in shell length among pairs (F 1.155, p 0.358), or between females and males (F 0.847, p 0.366). Results were similar in the case of copulating conch (among pairs, F 1.105, p 0.430; between females and males, F 0.112, p 0.743).

Reproductive activity in *Strombus gigas* was rare on hardbottom substrata (i.e., mounds, rubble and boulder areas). Ninety-four percent of the pairing conch were observed on sand, none were observed on rubble, and only 5.6% were found on hardbottom (Table 1). Eighty-five percent of copulating conch were found on sand, with small percentages found on rubble and hardbottom.

A total of 149 egg-laying females were observed between April and October 1988; except for one female found laying eggs on hardbottom in area B1, all were found spawning on sand (Table 1). Nine observations of simultaneous pairing and egg-laying were made; only one simultaneous copulation and egg-laying was observed. All 148 females on sand were oriented perpendicular to sand waves, with the anterior end of the shell elevated near the crest of the wave and the egg mass near the trough. Mean grain size of sediments collected immediately adjacent to egg-laying females was 0.389 θ (774μm) (SD 0.248, *n* 8), which is in the coarse-sand classification. Sediments were poorly sorted as indicated by a mean sorting coefficient of 0.967 θ (SD 0.302, *n* 8). Organic content was 3.45% of dry weight (SD 0.69, *n* 8).

Larval abundance

Conch larvae were first collected at the Reproductive Site on 2 June 1988 at a density of 0.26 larvae/10m³ (Table 2), 5 weeks after the first egg mass was discovered (Fig. 3B). Surface- and bottom-water temperatures were 27.5°C and 25.8°C, respectively. Veliger density at the Reproductive Site ranged from 0.04 larvae/10m³ on 6 June to 0.99 larvae/10m³ on 16 June. No plankton collections were made at this site between 29 June (0.30 larvae/10m³) and 23 August (0.77/10m³); during this interval, emphasis was shifted to the Children's Bay Cay site on Exuma Bank.

Larvae were not found until 6 June in Rat Cay cut and 20 June in Adderley Cay cut (Fig. 3C). By the end of June, surface-water temperature was near maximum (29.5°C and 29°C) in the two inlets. Highest density in the tidal passes was 4.46 larvae/10m³ on 21 July at the Rat Cay cut, concurrent with maximum egg-laying frequency (13%) and surface and bottom temperatures

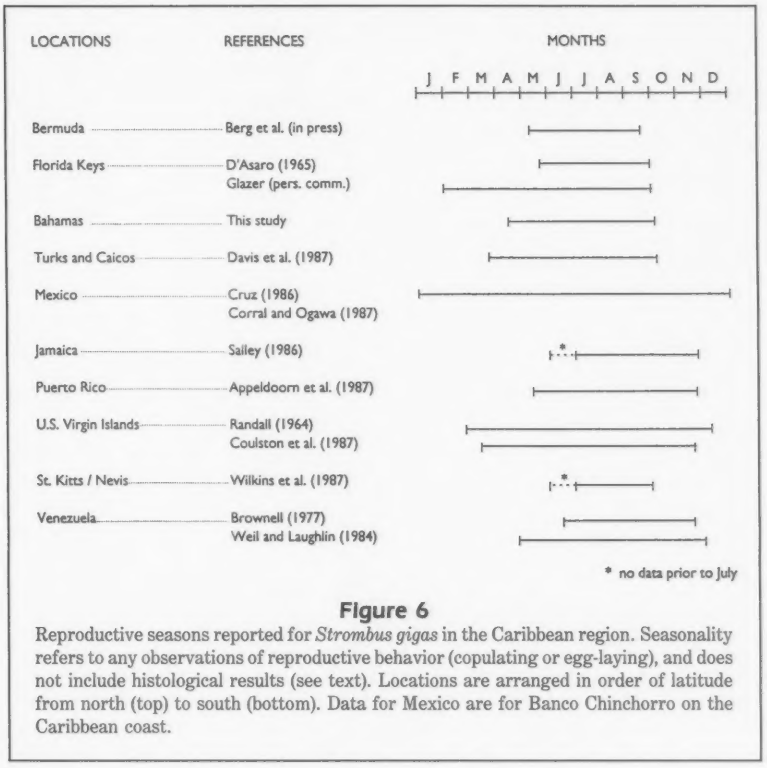

Figure 6

Reproductive seasons reported for *Strombus gigas* in the Caribbean region. Seasonality refers to any observations of reproductive behavior (copulating or egg-laying), and does not include histological results (see text). Locations are arranged in order of latitude from north (top) to south (bottom). Data for Mexico are for Banco Chinchorro on the Caribbean coast.

of 29.8°C and 28.1°C, respectively. Larvae continued to be found at the pass sites until the end of September, but were not present at the Reproductive Site after 23 August. No veligers were collected at any of the sites in October, concurrent with observation of the last egg mass. At this time, surface-water temperature had declined to 27.2°C and bottom temperature was 27.5°C.

Density of larvae at the Adderley Cay cut site showed a direct correlation with the percentage of females copulating (r 0.952, F 68.312, $p<0.0001$) and egg-laying (r 0.860, F 19.889, p 0.003). Densities of larvae at the Reproductive Site and the Rat Cay cut site were not correlated with copulation or egg-laying ($p>0.05$). Maxima in larval abundance occurred during months with highest water temperature, but there was no significant correlation between abundance of larvae and surface-water temperature at Adderley Cay cut (F 5.232, p 0.056) or Rat Cay cut (F 0.514, p 0.494) during the reproductive season (June–October). Log-transformation of the data did not improve the correlation coefficients.

Plankton collections over the nursery area, west of Children's Bay Cay, were begun on 13 July 1988; larval density was 0.82/10 m^3 (Table 2) and surface-water temperature was 31°C. Highest density at this site (1.35 larvae/10 m^3) occurred on 28 July, when numbers of copulating and spawning females were highest at the Reproductive Site. On 12 August, larval density declined to 0.77 larvae/10 m^3, concurrent with declines in reproductive activity. Larvae were last collected over the nursery area on 14 September at a density of 0.17 larvae/10 m^3; at this time, surface-water temperature on the Exuma Bank was 30°C and reproductive activity was near zero.

During the reproductive season, all but three of the conch veligers collected were between 340 and 600 μm in shell length ($\bar{x}$ 384 μm, SD 64, n 394) (Fig. 5). The largest three larvae (1350 μm) were removed alive from samples collected at the bank site in mid-July. Metamorphosis occurred within 24 hours in all three larvae.

Discussion

At Lee Stocking Island, the reproductive season for queen conch began in April and ended in early October. Although differences by a few months were found in the occurrence of reproductive behavior, there was no apparent trend related to latitude in beginning, end, or length of reproductive season in queen conch from Bermuda to Venezuela (Fig. 6).* The longest reproductive season was reported for the Caribbean coast of Mexico (Banco Chinchorro) (Cruz 1986, Corral and Ogawa 1987), where egg masses were found year-round. One of the shortest reproductive seasons was reported by D'Asaro (1965) for the Florida Keys, but more recent, intensive observations have shown that queen conch may spawn over at least a 9-month period in Florida (R. Glazer, Dep. Nat. Resour., Marathon, FL 33050, pers. commun., Sept. 1990).

* For geographic comparison, "reproductive seasonality" refers to any reported observation of pairing, copulation, or egg-laying in queen conch, except where noted in the text. Histological data are not included.

Geographic comparisons of seasonality in reproduction must be interpreted cautiously due to different methods, frequency and number of observations, annual variation, and different habitat types. For example, Brownell (1977) found that egg-laying in Los Roques, Venezuela, extended later into the season in deep water than in shallow water. Quantitative measures of reproductive activity provide a basis for examining mechanisms of seasonality, which is more useful than records of reproductive occurrence. In all studies that present seasonal curves for reproductive behavior or numbers of egg masses (e.g., Davis et al. 1984, Weil and Laughlin 1984, Corral and Ogawa 1987, and this study), maximum reproductive activity was reported during the warmest months of the year.

Control of gametogenesis and the physiology of egg production are still unknown for *S. gigas*, but histological studies of queen conch from Belize showed that mature eggs and sperm were in the gonads year-round (Egan 1985). External factors, therefore, are likely to mediate seasonality in the intensity of reproductive behavior and egg-laying.

Emphasis in the past has been placed on the potential role of water temperature in reproductive activity. Similar to observations in Los Roques, Venezuela (Brownell 1977, Weil and Laughlin 1984), reproductive activity at Lee Stocking Island began with rise in temperature. At both locations, reproductive activity intensified with increasing temperature to reach its maximum during the warmest period. Brownell (1977) suggested that a sharp temperature decline of 1.1°C from November to December was responsible for the termination of queen conch egg-laying in Los Roques. Similarly, egg-laying at Lee Stocking Island ended as bottom-water temperature began to decline steadily from 28.6°C in late September to 25.1°C in December. On the other hand, pairing, copulation, and egg-laying all decreased suddenly between August and September, during a period of high and relatively-stable water temperature, near 28.5°C.

Unlike the partial (early summer) correlation between reproductive behavior and temperature, pairing, copulation, and egg laying were all positively correlated with length of day throughout the year. Photoperiod, therefore, may be one of the important environmental variables which mediates the timing and length of reproductive season. Synergistic interaction between photoperiod and water temperature is possible.

In addition to decreasing length of day in late summer, increasing frequency and intensity of winds from the northeast produce a surge reaching the bottom at the Lee Stocking Island study site in the fall (Caribb. Mar. Res. Cent., Vero Beach, FL 32963, unpubl. data). The significance of wave disturbance is suggested by our own anecdotal observations of short-term decreases in reproductive activity concurrent with 1–2 day periods of reduced temperature and increased surge which occurred during the survey periods in early summer. Reductions in reproductive activity with increasing water turbulence have been noted for queen conch in the Caicos Islands (Davis et al. 1984) and for milk conch *Strombus costatus* in Puerto Rico (R.S. Appeldoorn, Dep. Mar. Sci., Univ. Puerto Rico, Mayaguez, PR 00709, pers. commun., May 1990).

As with temperature, photoperiod may influence the production of mature gametes or have a direct effect on the behavior of conch. It is likely that the combination of increasing water temperature, coupled with increasing length of day, triggers the mass migration of adult conch from hardground to sand habitats and to search for mates. Decreasing length of day and increasing wave surge appear to provide the best explanation for termination of the reproductive season, as pairing and copulation ended while bottom-water temperature was high. Experimental analysis will be required to determine the mechanisms involved in seasonal reproductive rates. Temperature, rates of temperature change, photoperiod, physical turbulence, and other seasonally variable environmental factors will need to be considered.

Similar to the findings of several others (D'Asaro 1965, Robertson 1959, Brownell 1977), egg-laying occurred primarily on clean coral sand with coarse grain size. Davis et al. (1984) noted that this type substrate may be critical for reproductive activity. Copulation and spawning stopped when they placed conch on a bottom type other than coral sand. At Lee Stocking Island, mating on hardbottom was observed, but was rare. Given that only one egg mass was found on substrate other than coral sand, it is clear that this is the preferred, if not critical, substrate for egg-laying.

This study provides the first report on abundance and distribution of queen conch veligers in the field. Veligers were present in the water column from 2 June to the end of September, in concordance with relatively constant rates of egg-laying from April through August. Despite a spawning season spanning 7 months, high numbers of larvae were present in the two inlets only during a 2-month period (July and August).

Although mechanisms involved in seasonality of larval production and survival are unknown as yet, it is clear that larvae were most abundant during the period of warmest water conditions. Summer spawning in Exuma Sound has adaptive significance. First, high temperatures are associated with higher developmental rates in pelagic larvae (Thorson 1950, McEdwards 1985, Boidron-Metairon 1987), decreasing the time larvae spend in the plankton and probably reducing larval mortality (Strathmann 1980). However, increase in temperature needs to be coupled with a food

supply sufficient to provide for higher feeding and metabolic rates (Scheltema and Williams 1982). Second, midsummer months are characterized by prevailing tradewind conditions (i.e., relatively constant winds and moderate seas from the southeast) in the Exuma Cays. General circulation over the reproductive site during this period was to the northwest, parallel to the Exuma island chain (N.P. Smith, Harbor Branch Oceanogr. Inst., Fort Pierce, FL 34946, unpubl. data). This would facilitate transport of pelagic larvae past the numerous inlets which veligers must enter to reach primary nursery habitats on Exuma Bank. As veligers are carried alongshore on the island shelf, they would readily be drawn through the inlets on flood tides. Northwest drift over the reproductive site may, in fact, explain the close correlation between larval abundance in Adderley Cay cut and reproductive activity occurring upcurrent. Winter weather patterns, with frequent passage of cold fronts and shifting winds and currents, would be less favorable for transport of conch larvae to the Exuma Bank nurseries.

On the basis of laboratory growth curves (Boidron-Metairon, unpubl. data), all but the three largest larvae collected in this study were less than approximately 2 weeks old in a larval life stage near 30 days. There are several possible explanations for the scarcity of advanced stage larvae: Late stages occupy habitats different from those of early-stage larvae (on or near the bottom), the abundance of older stages in the water column is reduced due to natural mortality, and/or the late stages are advected to different locations. Virtually nothing is known about transport or behavior of queen conch larvae in the field. Given the great significance of recruitment processes to management of this rapidly depleted fishery species, future research should include studies of larval transport and settlement.

In summary, highest reproductive activity occurred near Lee Stocking Island at a time of stable circulation patterns, high temperature (28–30°C), and long photoperiod. Maximum larval abundance in July and August placed high numbers of veligers in the water column at a time favorable for both high rates of development and transport to nursery habitats. Proximal mechanisms affecting short-term and seasonal variation in reproduction in queen conch may include temperature, rates of temperature change, photoperiod, wave-induced turbulence, and other variables associated primarily with season.

Acknowledgments

This research was supported by a grant from the Undersea Research Program of the National Oceanic and Atmospheric Administration (U.S. Department of Commerce) to the Caribbean Marine Research Center. We thank R.I. Wicklund, Director of the Caribbean Marine Research Center, for providing bottom-water temperature data for the reproductive site. Thanks to P. Bergman, N. Christie, K. McCarthy, O. Monterrosa and E. Wishinski for assistance in the field. R. Appeldoorn, P. Colin, L. Jones, J. Shenker, J.-P. Thonney, and anonymous reviewers provided helpful comments on the manuscript.

Citations

Appledoorn, R.S.
1990 Fishing pressure and reproductive potential in strombid conchs: Is there a critical stock density for reproduction? Mem. Soc. Cienc. Nat. La Salle (In press).

Appeldoorn, R.S., G.D. Dennis, and O. Monterrosa Lopez
1987 Review of shared demersal resources of Puerto Rico and the Lesser Antilles region. *In* Mahon, R. (ed.), Report and proceedings of the expert consultation on shared Fishery resources of the Lesser Antilles region. FAO Fish. Rep. 383: 36–57.

Berg, C.J. Jr., and D.A. Olsen
1989 Conservation and management of queen conch (*Strombus gigas*) fisheries in the Caribbean. *In* Caddy, J.F. (ed.), Marine invertebrate fisheries: Their assessment and management, p. 421–442. Wiley, NY.

Berg, C.J. Jr., J. Ward, B. Luckhurst, K. Nisbet, and F. Couper
In press Observations of breeding aggregations of the queen conch, *Strombus gigas*, in Bermuda. Proc. Gulf Caribb. Fish. Inst.

Boidron-Metairon, I.F.
1987 Effet de la temperature sur la duree des periodes larvaires de quatre especes d'Echinides des Caraibes. Bull. Soc. Sci. Nat. Ouest Fr. H.S:75–79.
1988 A new approach to comparative studies of *Strombus gigas* L. (Gastropoda: Strombidae) larvae at the developmental and nutritional levels. Proc. Gulf Caribb. Fish. Inst. (In press).

Brownell, W.N.
1977 Reproduction, laboratory culture and growth of *Strombus gigas*, *S. costatus*, and *S. pugilis* in Los Roques, Venezuela. Bull. Mar. Sci. 27:668–680.

Brownell, W.N., and J.M. Stevely
1981 The biology, fisheries, and management of the queen conch, *Strombus gigas*. Mar. Fish. Rev. 43(7):1–12.

Corral, J.L., and J. Ogawa
1987 Cultivo masivo de larva de caracol *Strombus gigas* en estanques de concreto. Proc. Gulf Caribb. Fish. Inst. 38: 345–352.

Coulston, M.L., R.W. Berey, A.C. Dempsey, and P. Odum
1987 Assessment of queen conch (*Strombus gigas*). Population and predation studies of hatchery reared juveniles in Salt River Canyon, St. Croix, U.S. Virgin Islands. Proc. Gulf Caribb. Fish. Inst. 38:294–306.

Cruz, R.S.
1986 Avances en la experimentacion de produccion massiva de caracol en Quintana Roo, Mexico. Proc. Gulf Caribb. Fish. Inst. 37:12–20.

D'Asaro, C.N.
1965 Organogenesis, development and metamorphosis in the queen conch, *Strombus gigas*, with notes on breeding habits. Bull. Mar. Sci. 15:359–416.

Davis, M., and C. Hesse
1983 Third world level conch mariculture in the Turks and Caicos Islands. Proc. Gulf Caribb. Fish. Inst. 35:73–82.

Davis, M., B.A. Mitchell, and J.L. Brown
1984 Breeding behavior of the queen conch *Strombus gigas* Linne, held in a natural enclosed habitat. J. Shellfish Res. 4:17–21.

Davis, M., C. Hesse, and G. Hodgkins
1987 Commercial hatchery produced queen conch, *Strombus gigas*, seed for research and grow-out market. Proc. Gulf Caribb. Fish. Inst. 38:326–335.

Egan, B.D.
1985 Aspects of the reproductive biology of *Strombus gigas*. M.S. thesis, Univ. British Columbia, Vancouver, 147 p.

Folk, R.L.
1966 A review of grain-size parameters. Sedimentology 6: 73–93.

Galehouse, J.S.
1971 Sediment analysis. *In* Carver, R.E. (ed.), Procedures in sedimentology petrology, p. 69–94. Wiley, NY.

McEdwards, L.R.
1985 Effects of temperature on the body form, growth, electron transport system activity, and development rate of an echinopluteus. J. Exp. Mar. Biol. Ecol. 93:169–181.

Mianmanus, R.T.
1988 Induction of settlement and metamorphosis in larvae of *Aplysia brasiliana* and *Strombus gigas* (Mollusca: Gastropoda). Ph.D. diss., Univ. Miami, Coral Gables, 171 p.

Randall, J.E.
1964 Contributions to the biology of the queen conch, *Strombus gigas*. Bull. Mar. Sci. 14:246–295.

Robertson, R.
1959 Observations on the spawn and veligers of conchs (*Strombus*) in the Bahamas. Proc. Malacol. Soc. 33:164–171.

Salley, S.
1986 Development of the statocyst of the queen conch larva, *Strombus gigas* L. (Gastropoda: Prosobranchia). M.S. thesis, McGill Univ., Montreal, 116 p.

Scheltema, R.S., and I.P. Williams
1982 Significance of temperature to larval survival and length of development in *Balanus eburneus* (Crustacea: Cirripedia). Mar. Ecol. Prog. Ser. 9:43–49.

Stoner, A.W., and V.J. Sandt
1992 Population structure and seasonal movements in deep-water queen conch, *Strombus gigas*. Bull. Mar. Sci. 51 (In press).

Strathmann, R.R.
1980 Why does a larva swim so long? Paleobiology 6:373–376.

Thorson, G.
1950 Reproductive and larval ecology of marine bottom invertebrates. Biol. Rev. 25:1–45.

Weil, E., and R. Laughlin
1984 Biology, population dynamics, and reproduction of the queen conch, *Strombus gigas* Linne, in the Archipielago de Los Roques National Park. J. Shellfish Res. 4:45–62.

Wilkins, R.M., M.H. Goodwin, and D.M. Reid
1987 Research applied to conch resource management in St. Kitts/Nevis. Proc. Gulf Caribb. Fish. Inst. 38:370–375.

Predicting effects of dredging on a crab population: An equivalent adult loss approach

Thomas C. Wainwright
David A. Armstrong
Paul A. Dinnel
José M. Orensanz
Katherine A. McGraw

School of Fisheries, WH-10
University of Washington, Seattle, Washington 98195

Abstract.—The effect of benthic dredging on coastal fisheries has been of concern for several decades, but little work quantifying direct population impacts has been published. Modeling approaches have been used extensively to assess effects of power plant entrainment on fishery stocks. Several important differences between power plant and dredge operations prevent direct application of these models to dredge problems: Entrainment by dredges is short-term, has a moving intake, and affects all age-classes of the population. We present an equivalent adult loss model of impacts to the Washington coast Dungeness crab *Cancer magister* Dana fishery from dredging of a navigation channel in Grays Harbor, Washington. The model is driven by empirical population data to account for spatial and temporal variation in abundance and age-class structure. Results show that impacts are quite sensitive to the type of dredge used and the season in which dredging occurs. Contrary to initial expectations, the 0+ age-group loss was unimportant relative to losses from older age-classes. Despite many limitations, the model has proven useful for focusing impact assessment work, as a basis for scheduling construction to reduce impacts, and as a basis for scaling mitigation projects.

Manuscript accepted 17 January 1992.
Fishery Bulletin, U.S. 90:171–182 (1992).

The effect of dredging on marine organisms has been an issue of environmental concern for several decades. Most studies on the impact of dredging and disposal of dredged material are concerned with changes in infaunal species assemblages and community characteristics, and generally measure effects by pre- and post-dredging comparisons. Very little work has been done on the direct effects of entrainment on populations of mobile epibenthic invertebrates or demersal fish, in part because such species are difficult to quantify. The reviews by Morton (1977) and Poiner and Kennedy (1984) indicate a strong research emphasis on habitat modification (by either dredging or disposal of sediments) and water column effects (turbidity, release of chemical pollutants) during dredging operations. Water column effects were also the focus of a workshop on anadromous fish and dredging (Simenstad 1990). Virtually no published works report on direct population losses due to entrainment or burial during dredging, except Stevens (1981) and Armstrong et al. (1982). There are few predictive models of dredging impacts other than that of Bella and Williamson (1980), who developed a model of dredging effects in Coos Bay, Oregon. Their model focused on water chemistry and sediments, but also gave some consideration to broad categories of animals.

In sharp contrast, power plant entrainment and impingement of fish has generated a large quantitative modeling literature (e.g. van Winkle 1977). Among the methods used in power plant assessments, the "equivalent adult loss" (Horst 1975, Goodyear 1977) and "production foregone" (Rago 1984) approaches are transferable to dredging operations, if sufficient biological and operational data are available. There are, however, several noteworthy differences between power plant and dredging operations which require different considerations in their analyses. Firstly, power plant water intakes operate continuously at a fixed location, while dredging operations are generally short-term, with a moving intake. This means that continuous, equilibrium approaches (e.g., MacCall et al. 1982) are not appropriate for dredging. Secondly, mobile benthic invertebrate populations are characterized by spatial aggregations and seasonal shifts in distribution which must be taken into account in estimating entrainment by a moving dredge. Finally, power plant entrainment is usually restricted to a single age-class (larvae or early juveniles), whereas dredging removes all age-classes present in the dredged habitat, but may kill age-classes at different rates.

The work we describe here applies an equivalent adult loss model (the "Dredge Impact Model" or "DIM") to assessing entrainment loss to the Dungeness crab *Cancer magister* Dana fishery in and around Grays Harbor, Washington. The Grays Harbor navigation channel (Fig. 1) extends from the harbor mouth to the city of Aberdeen, a distance of about 25 km. The U.S. Army Corps of Engineers currently removes an average of 1.2 million m^3 of sediment annually from the channel during maintenance dredging. To improve accessibility for deep draft vessels, the Corps planned to widen and deepen the channel by removing about 8.7 million m^3 of material over a two-year period (McGraw et al. 1988). Based on results and predictions of DIM, the Corps changed their original dredging program by modifying gear, volume dredged, and location/season combinations to minimize impact on crab within operational constraints (including weather and protection of other resources). Project construction took place throughout 1990, ending in January 1991. This paper extends an initial analysis (Armstrong et al. 1987), incorporating two additional years of biological data and providing a more thorough analysis of year-to-year variation. The study was undertaken in response to concerns of crab fishermen and resource managers that Grays Harbor is important as a juvenile crab nursery.

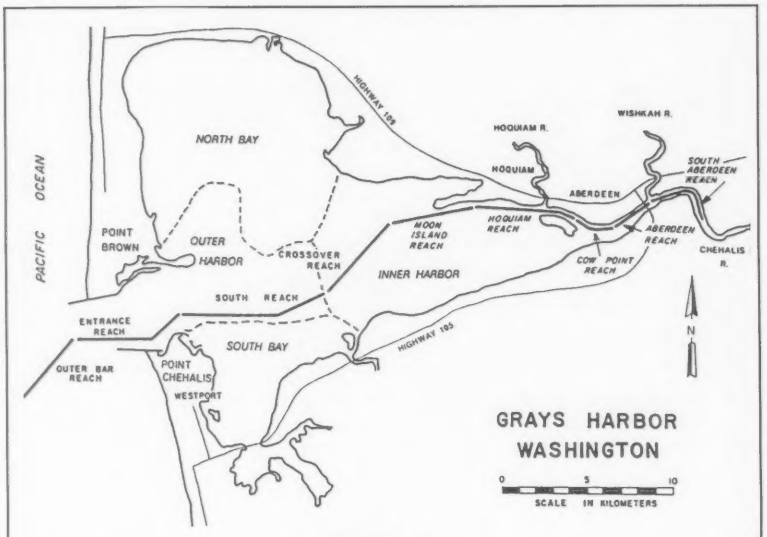

Figure 1
Map of Grays Harbor, Washington, showing existing navigation channel (heavy solid line) and sampling strata (separated by dashed lines).

Dungeness crab provide major fisheries along the west coast of North America, from central California to southern Alaska (Botsford et al. 1989). Since 1945, annual Washington coast crab landings have fluctuated between 1.2 and 9.5 thousand metric tons per year (Fig. 2). The general life-history pattern of Dungeness crab along the Washington coast is as follows (Gunderson et al. 1990, Jamieson and Armstrong 1991). Females molt to maturity along the open coast, generally in the spring. Mating occurs at this time, but eggs are not extruded until the following winter. Eggs generally hatch between December and March, and larvae remain in the water column for a few months. Late-stage larvae are found onshore in late-spring and summer, where they settle to the bottom and metamorphose. Settlement occurs both in nearshore coastal waters and in estuaries; within estuaries, crab settle in both subtidal and intertidal habitats. Crab settling in intertidal areas may remain there during their first summer, but move into the subtidal zone in fall. Few older crab are resident in the intertidal, but move on and off the tidal flats with the tides (Stevens et al. 1984). Crab settling in nearshore waters may remain there for life, but there is evidence of some migration into the estuary between their first and second summers. Crab remain in estuarine subtidal areas for up to two years, but late-juvenile and early-adult crab leave the estuary before reproduction, which occurs mainly along the open coast. Both female and male crab reach sexual maturity at about 2 years of age, but males may not breed until age-3 or older (Butler 1960 and 1961, Hankin et al. 1989).

Methods

Model structure

The calculation of crab loss is driven by two variables: crab abundance (uncontrolled) and volume dredged (controlled). Both of these vary in both space and time. The two types of data are related through an entrainment function that describes the number of crab entrained by each type of dredging gear as a function of local crab density and volume dredged. Not all crab entrained are killed, so a second relationship describes the number killed as a function of crab age and dredge type. To apply the model, crab abundance is measured

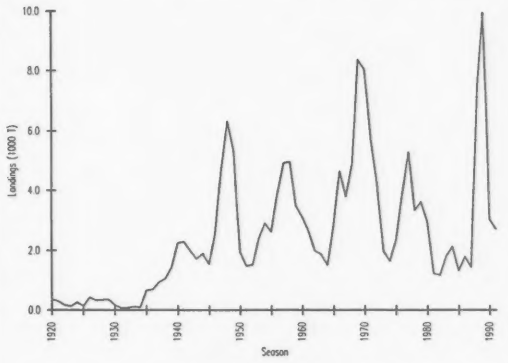

Figure 2

Historical landings in the Washington coastal Dungeness crab fishery. Sources: 1920–47, Cleaver (1949); 1948–50, Wash. Dep. Fish. (1951); 1951–87, Pac. Mar. Fish. Comm. (1989); 1988–91 are preliminary estimates (S. Barry, Wash. Dep. Fish., Olympia, pers. commun.).

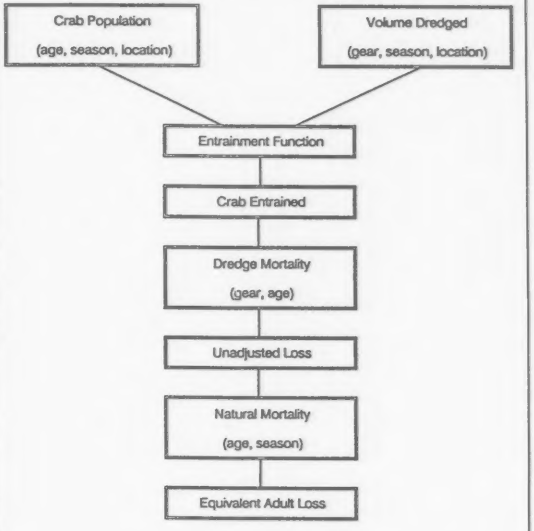

Figure 3

Flowchart of Dungeness crab adult loss model, showing main variables and structural categories (in parentheses).

as density stratified by age, season, and location. Dredging is described as the volume dredged by a particular gear in a location during a given season. Unadjusted loss figures are converted to equivalent adult loss by multiplying by the expected survival of crab from a certain age-class and season to adulthood. This approach is shown schematically in Figure 3, and described in detail below. Because we could not resolve older age-classes within our survey data, a crab was considered to reach adulthood in winter of its age 2+ year (i.e., approaching the end of its third year post-settlement).

Calculating losses in this manner requires an underlying concept of population dynamics and several simplifying assumptions. Creating a detailed model of local dynamics for a mobile benthic animal is difficult; there is continuous mortality and migration among habitats, the rates of which may vary with season, age, and locality. This may be summarized by the usual mass-balance equation for change in the population in a local area over a discrete time period:

$$N(t_1) = N(t_0) + R - M - E + I, \qquad (1)$$

where N is population abundance, t_0 and t_1 are two times, R is recruitment to the population (settlement), M is mortality, E is emigration, and I is immigration.

Mortality and migration rates are rarely known accurately (certainly not in our problem), so we have taken an empirical approach to defining population abundance. The approach is similar to, but simpler than, that taken by Boreman et al. (1981) for power plant entrainment in an estuary. The model is a discrete time, discrete age-population model with discrete habitat structure. To allow for seasonal changes in abundance or population structure, the year is subdivided into four seasons. Thus the population can be described as the numbers in various age-classes present in various habitat areas during particular seasons. In our model, abundance of any age-class in an area during a single time-step is taken to be the average abundance estimated from field surveys. We assume that all changes in abundance (i.e., mortality or migration) occur between time-steps, so that populations are constant throughout a step. This assumption introduces little error if the change during a step is small (less than about 10%), which will be true if time steps are relatively short and rates of change are relatively low. To meet this assumption in our application, we defined variable-length seasons of relatively constant population structure (see Data and Estimation section below).

The starting point for our calculations is estimated total crab density (D) for locations (l) and seasons (s), combined with age-class proportions (P). (Variables are fully defined in Table 1.) The second set of information needed for the calculation is the dredging schedule, expressed as volume dredged (V) by a specific gear type (g) in a specific location and season. For planning

Table 1
Model notation.

	Symbol	Description
Subscripts	a	age-class
	l	location
	s	season
	g	dredge gear
Population	D_{ls}	density
	P_{als}	age class proportions
	S_{as}	natural survival to adulthood
Dredging	V_{lsg}	volume dredged
Entrainment	e_g	entrainment rate
	m_{asg}	dredge-induced mortality proportion
Loss	E_{lsg}	total entrainment
	L_{alsg}	unadjusted loss
	EAL_{alsg}	equivalent adult loss

purposes, volume was measured as thousands of cubic yards (kcy) of dredged material (1 kcy = 765 m^3).

To obtain crab loss due to dredging from these two sets of information, we require crab entrainment rates (e), measured as numbers of crab entrained per unit volume dredged. Total entrainment (E) is

$$E_{lsg} = D_{ls} \cdot e_g \cdot V_{lsg}. \quad (2)$$

Postentrainment mortality (m), expressed as a proportion of those entrained, varies with gear type, age, and season. Age-specific loss (L) of crab in a single season, location, and gear combination will be

$$L_{alsg} = E_{lsg} \cdot P_{als} \cdot m_{asg}. \quad (3)$$

To compare the relative importance of losses from different age-classes, equivalent adult loss (EAL) for any season-location-gear combination is calculated as

$$EAL_{lsg} = \sum_{a} L_{alsg} \cdot S_{as}, \quad (4)$$

where S_{as} is the total natural survival to adulthood from age-class i in season k (assumed equal in all habitats). Total loss for the project is then

$$EAL_{tot} = \sum_{lsg} EAL_{lsg}. \quad (5)$$

Data and estimation

Population abundance Crab population surveys were conducted over a six-year period (1983–88) in Grays Harbor and along the adjacent coast. Stratified random sampling was done with a small beam trawl at biweekly or monthly intervals during spring and summer (May–September) with occasional sampling during fall and winter. From these surveys, crab densities were estimated for each stratum, and total population estimates were computed separately for Grays Harbor and the adjacent coast using the National Marine Fisheries Service BIOMASS program (Alaska Fish. Sci. Cent., 7600 Sand Point Way NE, Seattle, WA 98115), which uses standard stratified random survey statistical methods (Cochran 1962). Details of the survey design and population estimates can be found in Armstrong and Gunderson (1985) and Gunderson et al. (1990). In addition to the trawl surveys, intertidal crab were sampled in 0.25 m^2 quadrats at several locations within the harbor, and total intertidal population was estimated as described by Dumbauld and Armstrong (1987).

Growth and age-classes In general, age-class identification is difficult in crustaceans (Hartnoll 1982). The lack of retained hard parts prohibits direct aging techniques (such as scale analysis in fish), so age must be estimated from size. We relied on visual separations of age-classes in size-frequency plots from the population surveys, but molting and individual variability in growth obscure age-class modes except for young, rapidly growing crab. In all cases, young-of-the-year (age 0+) crab were easily identifiable as a separate size-group. Age 1+ size distributions sometimes overlapped older ages; in these cases, visual estimates of the separation point were supplemented by projecting growth from earlier observations. No reasonable separations could be made for older ages. For this reason, our analysis uses three age-classes: 0+, 1+, and >1+. Within Grays Harbor, we believe that most crab leave the estuary before their third year, so that almost all crab within the estuary identified as >1+ are actually age 2+, and this assumption is made in our analysis. Proportions in each age-class were then calculated from the total size-frequency distribution of each sampling stratum.

Definition of model seasons Seasons were defined to reflect important biological processes and major changes in crab abundance through the year. The spring season (April and May) reflects the start of settlement of the 0+ age-class and a period of migration into the estuary by age 1+ coastal crab; summer (June–September) is a period of continued settlement,

rapid growth, and steady mortality for 0+ crab and relative stability for older age-classes. Fall (October–December) and winter (January–March) are periods for which we have little sampling data, but both are periods of general population decline, migration from intertidal to subtidal areas within the estuary by 0+ crab, and emigration from the estuary by older age-classes. Where data were lacking during fall and winter, values were projected from late-summer populations according to the trends in numbers observed in years for which winter data were available.

Definition of geographic strata The population survey design had four strata within Grays Harbor: Outer Harbor, North Bay, South Bay, and Inner Harbor (Fig. 1). The navigation channel passes through two of these (Inner and Outer Harbor), and crab densities within various reaches of the channel were assumed to be the average densities for the corresponding sampling strata. In fact, crab densities estimated within the channel during entrainment studies are quite comparable with those estimated from the corresponding strata of the regular surveys (Dinnel et al. 1986, Dumbauld et al. 1988, Wainwright et al. 1990). Thus calculations for Bar, Entrance, and South Reaches used crab densities for the Outer Harbor, while Inner Harbor values were used from Crossover Reach to Aberdeen Reach. Crab densities decline upriver, and South Aberdeen Reach was assumed to have no crab.

Mortality Mortality estimates were calculated by regressing logarithm of population abundance on age. This method was applied separately for early juveniles (age 0+) and for older juveniles and adults (age 1+ and older). Because substantial migration of 0+ crab to or from the estuary does not occur, mortality rates specific to Grays Harbor could be calculated for this age-group. To estimate mortality, total estuarine 0+ and 1+ populations were calculated from the six years of trawl survey data. Estimates for 0+ subtidal populations were supplemented with intertidal estimates to provide a complete representation of the estuarine population. Direct calculation of mortality requires analysis of a population with no recruitment or migration. Settlement had essentially ended by July of each year, so we chose July of the 0+ year as the starting point for calculations. During the 1+ year, migration begins near the end of the summer as crab leave the estuary. Because of this, we chose June of the 1+ year as the endpoint for estimating first-year survival. First-year mortality estimates were calculated for each of five cohorts (1983–87 year-classes).

Estimation of mortality for older ages is more difficult for two reasons: age-class separation is difficult and inaccurate, and migration to and from the estuary occurs. Because of these problems, a different approach was used. To reduce problems of migration, population estimates for the estuary and adjacent coast were combined. Age-class separations were made using an instar analysis technique (Armstrong et al. 1987, Orensanz and Gallucci 1988) to identify instar composition of the population. Instar abundances were then assigned to year-classes. To reduce errors from sampling and age-class identification, monthly abundance estimates were averaged over all year-classes, then averaged over months within each survey season to give a single estimate for each age-class (a):

$$N_a = \text{mean}(N_{amy}), \tag{6}$$

where N_{amy} is the abundance estimate for age a in month m of sample year y. Then survival from age a to a+1 was calculated as

$$S_{a,a+1} = \frac{\bar{N}_{a+1}}{N_a}. \tag{7}$$

Because a single strong year-class biases estimates calculated in this way, the very strong 1984 year-class was excluded. The calculated age-specific natural mortality rates were then combined to produce the survival schedule (S_{as} in Eq. 4) used to calculate equivalent adult loss from unadjusted loss.

Estimating entrainment rate Numerous studies have been conducted to estimate the rate of entrainment of crab by various kinds of dredges, and the subsequent damage and mortality to entrained crab (McGraw et al. 1988). Entrainment and subsequent mortality are discussed separately below.

A regression relationship was used to predict the entrainment rate (crab entrained/kcy dredged; e in Eq. 2) from trawl-based density estimates (crab/ha). This approach was used by Armstrong et al. (1987) and McGraw et al. (1988) to estimate entrainment rates for a hopper dredge. More data have been collected since those studies, so a new relationship has been calculated. Sampling during the entrainment surveys consisted of two parts: sampling of the dredged material stream aboard a hopper dredge, and concurrent trawl surveys within the channel section being dredged. During each survey, sampling occurred over a two- to three-day period and covered several stations within the navigation channel. For each survey, mean entrainment (crab per kcy dredged) and mean density (crab per ha) were calculated over all samples within each station. This provided a total of 14 points which were used to calculate the regression. Details of survey methods are given in McGraw et al. (1988).

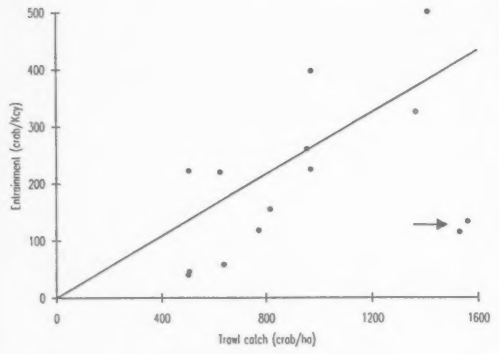

Figure 4
Relationship between trawl catch and entrainment of Dungeness crab by a hopper dredge. The line was fit by least-squares and non-parametric regression. Arrow indicates two outliers which were excluded from the least-squares regression.

To relate crab entrainment to crab density, several regression models were tried. The selection of a final model was based on both statistical measures of fit and biological reasonableness (i.e., an expectation that entrainment should increase with increasing crab density). First, a test for linearity ("XLOF" in the Minitab package; Minitab Inc., University Park, PA) was performed, and no significant nonlinearity was detected ($p>0.10$). Second, a linear least-squares regression was calculated; neither the slope nor the intercept were significantly different from zero for this model. However, this relationship was heavily influenced ("Cook's Distance Measure"; Weisberg 1985) by two points. When these two points were excluded, the best least-squares model was (Fig. 4)

$$Y = 0.27X, \quad (8)$$

where Y is entrainment by the dredge (crab/kcy), and X is trawl-estimated density (crab/ha). Finally, a non-parametric median-slope regression (Conover 1980) was calculated using all 14 data points. This method returned the same slope as the 12-point least-squares regression.

Entrainment for the other dredge types was calculated from this model based on relative entrainment factors given by Stevens (1981); entrainment by a pipeline dredge is assumed to be 100% of the hopper dredge value (this value is controversial, but is conservative), while a clamshell dredge entrains only about 5% of the hopper dredge value.

Table 2
Postentrainment mortality rates for Dungeness crab by age, season, and dredge type.

Dredge type	Age-class	Season	Size range (mm)	Mortality (%)
Hopper	0+	Apr–May	7–10	5
		Jun–Sep	11–30	10
		Oct–Dec	31–40	20
		Jan–Mar	41–50	40
	1+	Apr–Sep	51–75	60
		Oct–Mar	>75	86
	>1+	All	>75	86
Clamshell	All	All	All	10
Pipeline	All	All	All	100

Postentrainment mortality After entrainment, crab may be killed due to physical trauma during transport through pipes and pumps, burial under excessive sediment weight, or confined disposal in landfill by a pipeline dredge. Several estimates of postentrainment mortality (m in Eq. 3) have been made. For a hopper dredge, Stevens (1981) reported approximately 75% mortality, all sizes of crab combined. Armstrong et al. (1982) reported mortality rates by crab size for a hopper dredge, with 86% mortality for crab larger than 50 mm carapace width (CW) and 46% mortality for those smaller than 50 mm CW. Other studies indicate that hopper dredge mortality rates for small (<10 mm) 0+ age-class crab range from 1% to 5% (K. Larson, Portland Dist., U.S. Army Corps of Eng., pers. commun., 1987). Gross mortality observations were also made during later entrainment studies (McGraw et al. 1988, Wainwright et al. 1990), but these recorded only obvious mutilations and so underestimate total mortality. We adopted a set of size-dependent mortality rates for a hopper dredge based on these studies (Table 2).

Little information is available concerning mortality of crab entrained by a clamshell dredge. Stevens (1981) reported an overall mortality rate of less than 10%, which seems reasonable considering the operation of the gear. We have used a 10% mortality rate for a clamshell dredge for all age-classes. Because its effluent goes to confined upland disposal, 100% mortality was assumed for all crab entrained by the pipeline dredge.

Simulations Scheduling of dredge operations was based on engineering constraints, weather limitations, avoidance of salmon migration periods, and avoidance of seasons and areas with high predicted crab loss. To help in this planning process, loss rates (expressed as crab per volume dredged) were calculated for each area and each season, based on average seasonal crab densities and age-class composition.

Table 3
Hypothetical project scenarios for Grays Harbor, WA, showing volume to be dredged by each dredge type in each area and season.

Harbor section	Season	Dredge	Volume (kcy)
Scenario 1: Full confined disposal			
Outer	Jan–Mar	Hopper	1698
Outer	Apr–May	Hopper	1132
Outer	Apr–May	Hopper	330
Outer	Jun–Sep	Hopper	2800
Inner	Jun–Sep	Hopper	1000
Inner	Jun–Sep	Pipeline	434
Inner	Oct–Dec	Hopper	2036
Inner	Oct–Dec	Pipeline	2224
Inner	Jan–Mar	Hopper	1714
Inner	Jan–Mar	Pipeline	670
		Total	14,038
Scenario 2: Limited confined disposal			
Outer	Apr–May	Hopper	1462
Outer	Jun–Sep	Hopper	2800
Outer	Jan–Mar	Hopper	1698
Inner	Apr–May	Clamshell	771
Inner	Jun–Sep	Hopper	1000
Inner	Jun–Sep	Clamshell	579
Inner	Oct–Dec	Hopper	2036
Inner	Oct–Dec	Clamshell	778
Inner	Oct–Dec	Pipeline	374
Inner	Jan–Mar	Hopper	1714
Inner	Jan–Mar	Clamshell	826
		Total	14,038

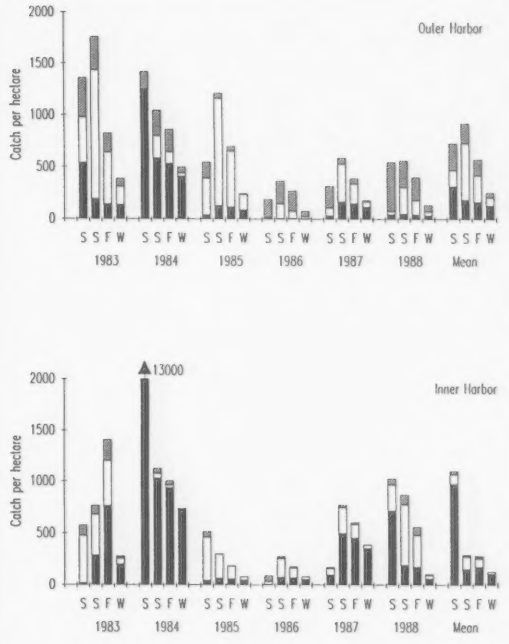

Figure 5
Seasonal abundance (catch per hectare) of Dungeness crab in the Outer and Inner Harbor strata of Grays Harbor, Washington, by age-class. Solid bars, age 0+; white, age 1+; hatching, age >1+.

Once project scheduling was determined, predictions of total crab loss were needed, which we calculated by simulating entrainment for planned construction scenarios. The scenarios we have used for calculating crab losses reflect the project as planned in 1987 (Table 3). There was some conflict between project costs and crab protection, particularly regarding the tradeoff between using gear that is economically efficient (hopper and pipeline) and that which minimizes loss (clamshell). Throughout most of the estuary, the efficiency of the hopper dredge makes alternatives uneconomic. In certain areas of the Inner Harbor, the pipeline dredge is economically most efficient but results in high post-entrainment mortality. The alternative dredge in those areas is a clamshell, which is generally more costly. To better evaluate this tradeoff, two scenarios are contrasted. Scenario 1 includes full use of a pipeline dredge where it is most effective; in Scenario 2, a clamshell dredge is substituted where feasible. Table 3 shows volumes dredged under each scenario by gear type, location, and season.

As initially planned, construction was to occur over two calendar years, extending through seven seasons. To simplify calculations, we compressed the project into a single model year (from spring of a given calendar year through winter of the next), and calculated entrainment and losses for each scenario separately based on each of the six years of survey-based crab abundance estimates. This produced a set of 12 (six years by two construction scenarios) model runs.

Because the project was revised in several ways since these calculations were made, results presented here do not reflect actual expected losses resulting from the project, and are presented only to illustrate the method.

Results

Population parameters

Age-class abundance Densities of crab in the Inner and Outer Harbor strata varied considerably among years and seasons (Fig. 5). Average seasonal total density ranged from 73 ha^{-1} to 13,000 ha^{-1}. Age 0+ crab were most abundant in 1984, and were usually more abundant in the Inner Harbor. Older crab were more

Table 4
Estimates of instantaneous mortality (Z) and annual survival (S) for age 0+ Dungeness crab, Grays Harbor, WA.

Year-class	Z (yr^{-1})	S (%)
83	3.4	3.4
84	2.2	11.5
85	3.5	3.0
86	1.6	19.8
87	1.9	15.2
Average	2.5	8.1

Table 5
Estimates of instantaneous mortality (Z) and annual survival (S) for older age-classes of Dungeness crab, Grays Harbor, WA, and adjacent coast combined. Estimates are for July–July, average for several years.

Age	Z (yr^{-1})	S (%)
1+ – 2+	1.6	19.5
2+ – 3+	0.8	45.0
3+ – 4+	1.0	38.0

Table 6
Survival schedule: percent of Dungeness crab surviving from each season to midwinter (15 Feb.) of the 2+ year.

		Age-class		
Season	Midpoint	0+	1+	2+
Apr–May	30 Apr	0.87	10.7	53.2
Jun–Sep	31 Jul	1.65	16.0	64.9
Oct–Dec	15 Nov	3.40	25.5	81.9
Jan–Mar	15 Feb	6.35	38.0	100.0

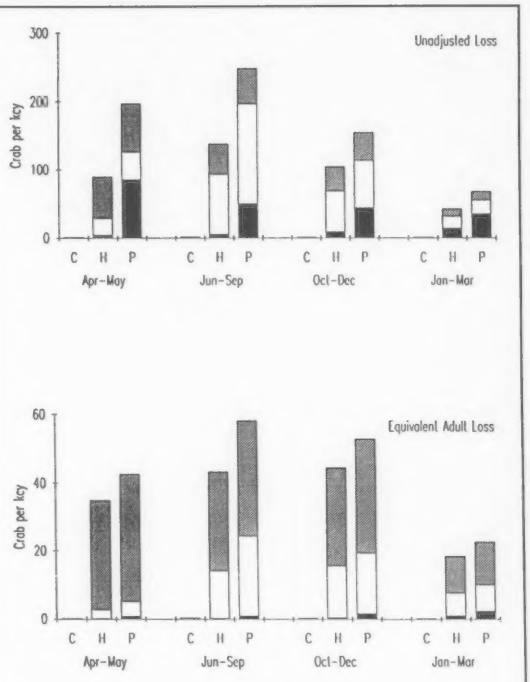

Figure 6
Entrainment rates of Dungeness crab by season and dredge type for the Outer Harbor, by age-class. (upper) Unadjusted losses; (lower) age 2+ equivalent losses. Dredge types: C = clamshell, H = hopper, P = pipeline. Age-classes as in Figure 5.

abundant in the Outer Harbor, where they reached peak densities in the summer season.

Mortality Estimated instantaneous mortality rates for age 0+ crab within Grays Harbor ranged from 1.6 to 3.5 yr^{-1}, with a mean of 2.5 yr^{-1}, corresponding to an annual survival of 8.1% (Table 4). For older crab, estimated mortality rates (Eq. 7) decreased to age 3+, then increased slightly between ages 3+ and 4+ (Table 5). These two results were combined to derive the seasonal survival schedule (Table 6) used in the model.

Gear and season comparisons

The results of gear/season comparison simulations are presented in Figures 6 and 7. These data show the strong contrast between the pipeline and clamshell dredges: the clamshell dredge has negligible impact. Comparing the unadjusted losses (Eq. 3) with age 2+ equivalent losses (Eq. 4) shows the relative unimportance of 0+ crab. Also notable are the high age 2+ equivalent losses in the Outer Harbor during summer and fall, when there are concentrations of age 1+ and older crab in this area (Fig. 5).

Impact estimates

Calculations of total age 2+ equivalent loss (Eq. 5) for the two project scenarios are shown in Figure 8. As expected, Scenario 1 (full use of the pipeline dredge with confined disposal) shows higher losses than Scenario 2. For both scenarios, a large part of the total loss occurs during the June–September season, due to large volumes being dredged in the Outer Harbor where older crab are concentrated at this time. The results indicate strong year-to-year variation in

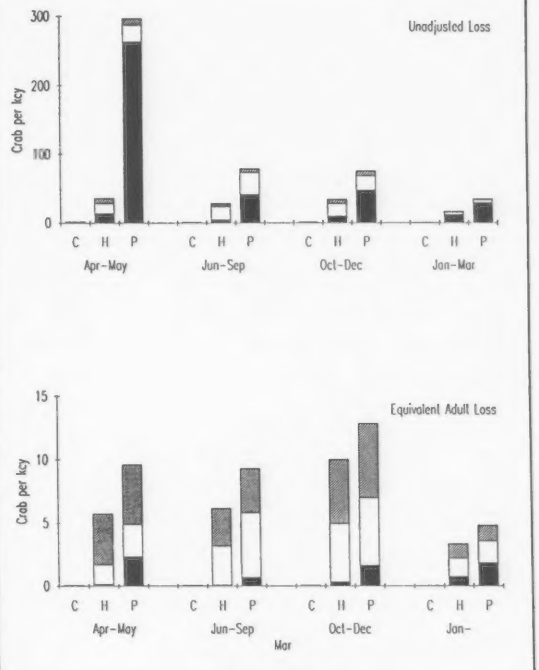

Figure 7
Entrainment rates of Dungeness crab by season and dredge type for the Inner Harbor, as in Figure 6.

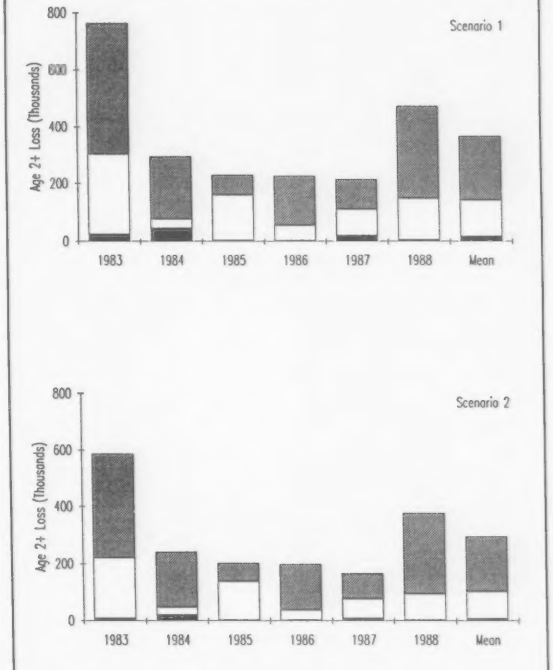

Figure 8
Total estimated age 2+ equivalent losses for hypothetical dredging in six years for two project scenarios. (upper) Full use of confined disposal; (lower) limited confined disposal. Age-classes as in Figure 5.

impacts, with 1983 construction resulting in impacts nearly three times the average for the other years. This is apparently because 1983 followed two years of strong settlement, as evidenced by the high abundance of both age 1+ and >1+ crab in that year (Fig. 5; see also Gunderson et al. 1990). This emphasizes the importance of population monitoring during construction to accurately assess impacts.

Discussion

Gear and season comparisons made with DIM provided several results which were subsequently used to schedule construction gear, season, and location combinations so as to reduce crab losses. As expected, the clamshell dredge (which moves slowly and does little mechanical damage to organisms) had insignificant impact in all seasons and areas. Comparing pipeline and hopper dredge effects, our initial impression was that, with confined disposal (resulting in 100% loss of all age-classes), the pipeline dredge would cause extremely high losses relative to the hopper dredge. This is true when one considers the unadjusted losses (Figs. 6A and 7A). However, when viewed on an equivalent adult loss basis (Figs. 6B and 7B), the pipeline dredge loss rate is only 10–50% higher than that of the hopper dredge. The equivalent adult loss viewpoint was also important in seasonal comparisons, especially in the Inner Harbor (Fig. 7) where unadjusted loss was highest in spring, but equivalent adult loss peaked in fall.

During any modeling endeavor in applied ecology, certain decisions must be made to limit the scope and applicability of the model. Many decisions are made simply on the basis of information or time available, while others reflect the biases and experiences of the authors. One of the major decisions in this project was the choice between predicting short-term losses via the equivalent adult loss approach, or accounting for potential longer-term losses due to reduction of the local reproductive stock via "production foregone" (Rago 1984) techniques. For local, short-term entrainment to have longer-term population effects requires a strong influence of current stock size on future recruitment.

For Dungeness crab, there is little evidence of stock-dependence. In fact, it is not clear whether a local stock, such as that in Grays Harbor, is self-reproducing or depends on larval drift from other areas. For this reason, we chose to use only short-term loss predictions.

The choice of slope for the regression of crab entrainment on trawl catch will strongly influence model results. We gave long consideration to the choice of regression models. Problems arise because there are few data points and large measurement errors associated with both variables. Costs of sampling (which involved simultaneous operations of a specially modified hopper dredge and a chartered trawler) prohibited any increase in data quantity or precision. Initially, we chose to use least-squares regression (LSR) with its underlying assumptions of normal errors with equal variances. There are two forms of LSR in common use: predictive LSR which assumes that all error is in measurement of the Y (dependent) variate, and functional LSR which incorporates errors in both X and Y variates. In the overall context of DIM, the entrainment regression serves the role of a calibration curve predicting entrainment from a set of observed trawl catches. For this reason, we used a predictive regression conditional on the observed trawl catches. (This implies that the result is not generalizable to any other method of crab density estimation, but such generalization is not needed here.) Two outliers were dropped from the LSR analysis; both points were from the same station in different years, and both were influenced by one or two extremely high trawl catches. Because we were not entirely satisfied with the assumptions of the LSR analysis, the data was reanalyzed using a nonparametric regression technique which is robust to non-normality, inequality of variances, and errors in measurement of the X variate. Because this analysis agreed with the final LSR model (Eq. 8), we accepted that model as the most reasonable.

Another limitation was our inability to reliably distinguish age-classes beyond 1+ and obtain mortality estimates for older age-groups. Because of this, we stopped our calculations at age 2+, but there is a strong desire to relate the results to fishery stocks with recruitment at 3–5 years of age. It is possible to perform some rough calculations of actual impact to fisheries, if we are willing to make some assumptions. Using Scenario 2 (limited confined disposal) as an example, estimated age 2+ equivalent losses ranged from 166 to 587 thousand crab (Fig. 8). The fishery harvests males only, so with a 50% sex ratio these numbers become 83–298 thousand age 2+ male crab lost. To relate these to the fishery, we need to know survival from age 2+ to recruitment. We have rough estimates of mortality from age 2+ to 3+ and from age 3+ to 4+ (Table 6) calculated from the trawl survey data set. These estimates are confounded with the decline in gear efficiency with crab size, and so are probably underestimates of true survival. They also depend on tenuous assumptions about size-at-age. Accepting these estimates and assuming the bulk of the fishery recruits at age 3+, our estimates of age 2+ loss correspond to losses to the fishery of 37–134 thousand age 3+ male crab. As exploitation rates are quite high (~70–90%; Methot and Botsford 1982), these numbers can be related directly to annual catch. The ten-year average catch for the Washington coast has been about 3000 metric tons, which corresponds to 3.3 million crab (average individual weight of 0.9 kg). So, losses for this hypothetical scenario would be on the order of 1–4% of the average annual catch by the Washington coast fishery.

The model was limited by several other factors, particularly problems of data quality and parameter estimates. Primary among these was lack of data on beam trawl efficiency and size selectivity (Gunderson and Ellis 1986). We have implicitly assumed that the trawl sampling was 100% efficient for all sizes of crab, which is certainly not the case. The gear was designed for capturing juvenile crab, and we believe it to be relatively efficient for juvenile sizes, but crab approaching legal size are able to avoid or escape the small net. For estimating absolute numbers entrained, this is not a problem because the entrainment function is essentially a calibration of entrainment against trawl catch, regardless of trawl efficiency. However, to the extent that gear efficiency is below 100%, we underestimate total populations within the estuary. Calculations of entrainment as a proportion of the local population are thus biased upward. Trawl efficiency also affects natural mortality rate estimates, to which equivalent adult loss calculations are extremely sensitive.

Overall, DIM has proved useful even with its limitations. In project planning, the model allowed scheduling gear and work seasons to reduce impacts on the crab population, and provided some quantitative predictions of loss on which to base mitigation programs. DIM is now being used in conjunction with crab survey data gathered during construction to estimate actual crab losses and to fully define levels and type of mitigation. Beyond these intended uses, the model served to focus concerns about crab impacts, which tended to be somewhat ill-defined, onto specific questions of data quality and reliability of predictions, providing all sides a common basis for argument.

Acknowledgments

This work was done under a combination of support from the Seattle District, U.S. Army Corps of Engi-

neers (#DACW67-85-C-0033), Battelle Pacific Northwest Laboratories, Sequim, Washington, and Washington Sea Grant (#NA86AA-D-SG044 Project R/F-68). We appreciate the contributions of the Corps staff, notably Fred Weinmann, Gail Arnold, James Waller, and Ann Uhrich, and the valuable comments and discussion of the Grays Harbor Crab Study Panel convened by Walter Pearson. Louis Botsford provided invaluable suggestions for the initial model design. Loveday Conquest provided analysis of the entrainment regression and other statistical advice. The project could not have been completed without the cooperation of the crews of the COE dredge YAQUINA and the fishing vessel Karelia (Vern Heikkila at the helm). We also thank those (too numerous to name) who contributed greatly to field work, data analysis, and administrative support.

Citations

Armstrong, D.A., and D.R. Gunderson
1985 The role of estuaries in Dungeness crab early life history: A case study in Grays Harbor, Washington. *In* Melteff, B.R. (ed.), Proceedings, Symposium on Dungeness crab biology and management, p. 145–170. Alaska Sea Grant Rep. 85-3, Univ. Alaska, Fairbanks.

Armstrong, D.A., B.G. Stevens, and J.C. Hoeman
1982 Distribution and abundance of Dungeness crab and *Crangon* shrimp, and dredging-related mortality of invertebrates and fish in Grays Harbor, Washington. Tech. Rep. to Wash. Dep. Fish. and U.S. Army Corps of Eng., Seattle Dist. by School of Fisheries, Univ. Wash., Seattle, 349 p.

Armstrong, D.A., T.C. Wainwright, J. Orensanz, P.A. Dinnel, and B.R. Dumbauld
1987 Model of dredging impact on Dungeness crab in Grays Harbor, Washington. Fish. Res. Inst. Rep. FRI-UW-8702, School of Fisheries, Univ. Wash., Seattle, 167 p.

Bella, D.A., and K.J. Williamson
1980 Diagnosis of chronic impacts of estuarine dredging. J. Environ. Syst. 9:289–311.

Boreman, J., C.P. Goodyear, and S.W. Christensen
1981 An empirical methodology for estimating entrainment losses at power plants sited on estuaries. Trans. Am. Fish. Soc. 110:253–260.

Botsford, L.W., D.A. Armstrong, and J.M. Shenker
1989 Oceanographic influences on the dynamics of commercially fished populations. *In* Landry, M.R., and B.M. Hickey (eds.), Coastal oceanography of Washington and Oregon, p. 511–565. Elsevier, Amsterdam.

Butler, T.H.
1960 Maturity and breeding of the Pacific edible crab, *Cancer magister* Dana. J. Fish. Res. Board Can. 17:641–646.
1961 Growth and age determination of the Pacific edible crab *Cancer magister* Dana. J. Fish. Res. Board Can. 18:873–890.

Cleaver, F.C.
1949 Preliminary results of the coastal crab (*Cancer magister*) investigation. Wash. Dep. Fish. Biol. Rep. 49A:47–82.

Cochran, W.G.
1962 Sampling techniques, 2d ed. Wiley, NY, 413 p.

Conover, W.J.
1980 Practical nonparametric statistics, 2d ed. Wiley, NY, 462 p.

Dinnel, P.A., D.A. Armstrong, B.R. Dumbauld, and T.C. Wainwright
1986 Impact of dredging on Dungeness crab, *Cancer magister*, in Grays Harbor, Washington during August 1986. Fish. Res. Inst. Rep. FRI-UW-8611, School of Fisheries, Univ. Wash., Seattle, 34 p.

Dumbauld, B.R., and D.A. Armstrong
1987 Potential mitigation of juvenile Dungeness crab loss during dredging through enhancement of intertidal shell habitat in Grays Harbor, Washington. Fish. Res. Inst. Rep. FRI-UW-8714, School of Fisheries, Univ. Wash., Seattle, 64 p.

Dumbauld, B., D. Armstrong, P. Dinnel, and T. Wainwright
1988 Impact of dredging on Dungeness crab, *Cancer magister*, in Grays Harbor, Washington during August 1987. Fish. Res. Inst. Rep. FRI-UW-8820, School of Fisheries, Univ. Wash., Seattle, 25 p.

Goodyear, C.P.
1977 Mathematical methods to evaluate entrainment of aquatic organisms by power plants. Rep. FWS/OBS-76/20.3, U.S. Fish Wildl. Serv., Wash., DC.

Gunderson, D.R., and I.E. Ellis
1986 Development of a plumb staff beam trawl for sampling demersal fauna. Fish. Res. (Amst.) 4:35–41.

Gunderson, D.R., D.A. Armstrong, Y.-B. Shi, and R.A. McConnaughey
1990 Patterns of estuarine use by juvenile English sole (*Parophrys vetulus*) and Dungeness crab (*Cancer magister*). Estuaries 13:59–71.

Hankin, D.G., N. Diamond, M.S. Mohr, and J. Ianelli
1989 Growth and reproductive dynamics of adult female Dungeness crabs (*Cancer magister*) in northern California. J. Cons. Cons. Int. Explor. Mer 46:94–108.

Hartnoll, R.G.
1982 Growth. *In* Abele, L.G. (ed.), Embryology, morphology, and genetics (The Biology of Crustacea, vol. 2), p. 111–196. Academic Press, NY.

Horst, T.J.
1975 The assessment of impact due to entrainment of ichthyoplankton. *In* Saila, S.B. (ed.), Fisheries and energy production: A symposium, p. 107–118. Lexington Books, Lexington, MA.

Jamieson, G.S., and D.A. Armstrong
1991 Spatial and temporal recruitment patterns of Dungeness crab in the northeast Pacific. Mem. Queensl. Mus. 31:365–381.

MacCall, A.D., K.R. Parker, R. Leithiser, and B. Jessee
1982 Power plant impact assessment: A simple fishery production model approach. Fish. Bull., U.S. 81:613–619.

McGraw, K.A., L.L. Conquest, J.O. Waller, P.A. Dinnel, and D.A. Armstrong
1988 Entrainment of Dungeness crabs, *Cancer magister* Dana, by hopper dredge in Grays Harbor, Washington. J. Shellfish Res. 7(2):219–231.

Methot, R.D. Jr., and L.W. Botsford
1982 Estimated preseason abundance in the California Dungeness crab (*Cancer magister*) fisheries. Can. J. Fish. Aquat. Sci. 39:1077–1083.

Morton, J.W.
1977 Ecological effects of dredging and dredge spoil disposal: A literature review. Tech. Pap. U.S. Fish Wildl. Serv. 94, Wash., DC, 33 p.

Orensanz, J.M., and V.F. Gallucci
1988 A comparative study of postlarval life history schedules in four sympatric *Cancer* species. J. Crust. Biol. 8:187–220.

Pacific Marine Fisheries Commission
1989 Data series: Crab and shrimp section (Rev. 1989). Pac. Mar. Fish. Comm., Portland.

Poiner, I.R., and R. Kennedy
1984 Complex patterns of change in the macrobenthos of a large sandbank following dredging. Mar. Biol. 78:335–352.

Rago, P.J.
1984 Production forgone: An alternative method for assessing the consequences of fish entrainment and impingement losses at power plants and other water intakes. Ecol. Modell. 24:79–111.

Simenstad, C.A. (editor)
1990 Effects of dredging on anadromous Pacific Coast fishes: Workshop proceedings, Seattle, September 8–9, 1988. Wash. Sea Grant Prog., Univ. Wash., Seattle, 160 p.

Stevens, B.G.
1981 Dredging-related mortality of Dungeness crabs associated with four dredges operating in Grays Harbor, Washington. Seattle Dist., U.S. Army Corps of Eng. DA-79-45, Seattle, 148 p.

Stevens, B.G., D.A. Armstrong, and J.C. Hoeman
1984 Diel activity of an estuarine population of Dungeness crabs, *Cancer magister*, in relation to feeding and environmental factors. J. Crust. Biol. 4:390–403.

van Winkle, W. (editor)
1977 Proceedings of the conference on assessing the effects of power-plant-induced mortality in fish populations, Gatlinburg, Tennessee, May 3–6, 1977. Pergamon Press, NY, 380 p.

Wainwright, T.C., K.A. McGraw, D.A. Armstrong, B.R. Dumbauld, and L.L. Conquest
1990 Impact of dredging on Dungeness crab, *Cancer magister*, in Grays Harbor, Washington, during August 1989. Fish. Res. Inst. Rep. UW-FRI-9005, Univ. Wash., Seattle, 18 p.

Washington Department of Fisheries
1951 Washington commercial fisheries 1951 statistics. Wash. Dep. Fish., Seattle, 46 p.

Weisberg, S.
1985 Applied linear regression, 2d ed. Wiley, NY, 324 p.

Comparison of feeding and growth of larval round herring *Etrumeus teres* and gulf menhaden *Brevoortia patronus*

Weihzong Chen
East China Sea Fisheries Research Institute
300 Jun Gong Road, Shanghai, Peoples Republic of China

John J. Govoni
Stanley M. Warlen
Beaufort Laboratory, Southeast Fisheries Science Center
National Marine Fisheries Service, NOAA, Beaufort, North Carolina 28516

The round herring *Etrumeus teres* is one of several clupeid fishes, abundant in continental shelf waters of the Gulf of Mexico, that presently is not commercially exploited by the United States, although its sibling species *E. whiteheadi* is a fishery resource for South Africa (Roel and Melo 1990). The potential annual yield of this latent resource is estimated as 3.3×10^4 to 4.2×10^5 metric tons for the eastern Gulf (Houde 1977) and 1.1×10^5 to 1.1×10^6 metric tons for the entire Gulf (Reintjes 1980). Details relevant to the distribution and population dynamics of round herring, including elements of its early life history, are presently sketchy. Houde (1977) reported that round herring in the eastern Gulf of Mexico spawn from mid-October to the end of May between the 30 and 200 m isobaths. He surmised that there is a major spawning area about 150 km west-southwest of Tampa Bay, Florida, and a minor area just north of the Dry Tortugas. Off Texas and Louisiana, spawning occurs from 50 to 200 km offshore and may extend to the edge of the continental shelf (Fore 1971). Round herring and another clupeid, the gulf menhaden *Brevoortia patronus*, are sympatric; the latter spawns in inshore waters of the northern Gulf at least as far offshore as 130 km with a focus of spawning off Mississippi between mid-October and late March (Christmas and Waller 1975).

Differences between adult round herring and gulf menhaden are so obvious that systematists once referred these two species to separate families, Dussumieriidae and Clupeidae (Whitehead 1963), but their larvae are morphologically similar with one major exception, their jaw structure. (The misperception that, unlike other clupeids, round herring larvae do not possess a swimbladder (Fahay 1983) has been perpetuated in the literature.) At hatching larvae of both species are about 3.0 mm notochord length (NL) and are slender and elongate with a straight alimentary canal and a posterior anus (Houde and Fore 1973). Transformation to the juvenile form begins at about 18 mm standard length (SL) (Houde and Fore 1973). Round herring larvae develop teeth on their long, spatulate upper and lower jaws at about 6 mm SL (Houde and Fore 1973); but gulf menhaden do not develop teeth on their shorter, less compressed jaws until they are about 10 mm SL (Hettler 1984).

The diets of the larvae of these species might reflect differences in jaw structure and dentition. In addition, differences in diet quality and quantity may register different growth between these species. While feeding and growth of gulf menhaden larvae are documented (Govoni et al. 1983, Stoecker and Govoni 1984, Warlen 1988), similar information on the early life history of round herring is unavailable. In this paper, we compare the feeding and growth of larval round herring and gulf menhaden.

Materials and methods

Round herring and gulf menhaden larvae used in this study were removed from ichthyoplankton collections obtained during two cruises (December 1980 and February 1981) using MOCNESS gear (multiple opening/closing nets and environmental sensing system). Three stations were occupied, one each at the 18, 91, and 183 m isobaths, along three transects (off Cape San Blas, FL; off the Mississippi Delta, LA; and off Galveston Bay, TX (Sogard et al. 1987)). The objective of the sampling plan was to broadly canvass the continental shelf of the northern Gulf for larval gulf menhaden and two other species (Sogard et al. 1987); larval round herring were collected incidentally. Sampling at three discrete depths (surface, in the middle of the upper mixed layer, and within or below the thermocline) assured the collection of adequate numbers of specimens. In addition, larvae from a single collection taken at the Mississippi River plume front (Govoni et al. 1989) in December 1982 were examined to augment gut content data. Larvae were preserved in 5% formalin for food analysis and in 70% ethanol for growth studies (Table 1). To provide an indication of true dietary differences between species encountering the same food assortment, only those larvae from a single vertically and horizontally discrete collection (Govoni et al. 1986) that produced both species were used for diet comparisons

Manuscript accepted 25 November 1991.
Fishery Bulletin, U.S. 90:183–189 (1992).

Table 1

Time, location, and depth of collection in the northern Gulf of Mexico of round herring *Etrumeus teres* larvae examined for diet composition and growth determination.

Date	Time	Transect	Water column depth (m)	Sample depth (m)	No. of larvae collected	No. of larvae with food
6 Dec 80[1]	0645	Mississippi Delta	183	1	2	0
8 Dec 80[2]	0013	Cape San Blas	183	1	8	
8 Dec 80[2]	0013	Cape San Blas	183	51	2	
8 Dec 80[1]	0040	Cape San Blas	183	50	6	0
8 Dec 80[1]	0056	Cape San Blas	183	1	10	0
8 Dec 80[1]	0621	Cape San Blas	183	50	3	0
8 Dec 80[2]	1800	Cape San Blas	183	1	20	
8 Dec 80[2]	1800	Cape San Blas	183	102	1	
8 Dec 80[1]	1821	Cape San Blas	183	49	3	0
8 Dec 80[1]	1834	Cape San Blas	183	1	20	1
9 Dec 80[2]	0600	Cape San Blas	91	1	7	
9 Dec 80[2]	0600	Cape San Blas	91	35	1	
9 Dec 80[2]	0600	Cape San Blas	91	74	3	
9 Dec 80[1]	0617	Cape San Blas	91	35	13	0
9 Dec 80[1]	1237	Cape San Blas	91	37	2	0
9 Dec 80[2]	1800	Cape San Blas	91	1	19	0
9 Dec 80[1]	1806	Cape San Blas	91	75	3	0
9 Dec 80[1]	1817	Cape San Blas	91	35	3	0
9 Dec 80[1]	1827	Cape San Blas	91	1	20	4
10 Dec 80[2]	0005	Cape San Blas	91	1	19	
10 Dec 80[2]	0005	Cape San Blas	91	35	1	0
10 Dec 80[2]	0010	Cape San Blas	91	12	4	0
10 Dec 80[1]	0025	Cape San Blas	91	74	6	0
10 Dec 80[1]	0025	Cape San Blas	91	1	1	0
10 Dec 80[1]	0035	Cape San Blas	91	46	16	0
10 Dec 80[1]	0045	Cape San Blas	91	1	11	0
10 Dec 80[1]	1812	Cape San Blas	18	6	2	1
10 Dec 80[1]	1821	Cape San Blas	18	1	17	2
11 Dec 80[1]	0019	Cape San Blas	18	12	11	1
11 Dec 80[1]	0031	Cape San Blas	18	1	3	0
12 Feb 81[2]	1900	Galveston Bay	18	6	2	
13 Feb 81[2]	0600	Galveston Bay	91	35	5	
14 Feb 81[1]	0033	Galveston Bay	91	61	13	1
14 Feb 81[1]	0047	Galveston Bay	91	35	20	1
14 Feb 81[1]	0100	Galveston Bay	91	1	12	0
14 Feb 81[2]	0600	Galveston Bay	91	37	13	
14 Feb 81[1]	0620	Galveston Bay	91	77	8	0
14 Feb 81[1]	0635	Galveston Bay	91	27	20	0
14 Feb 81[1]	0644	Galveston Bay	91	1	20	0
14 Feb 81[1]	1823	Galveston Bay	91	74	20	1
14 Feb 81[1]	1846	Galveston Bay	91	1	20	7
18 Feb 81[1]	0014	Mississippi Delta	91	75	2	0
18 Feb 81[1]	0025	Mississippi Delta	91	1	20	8
18 Feb 81[2]	0600	Mississippi Delta	91	25	20	0
18 Feb 81[1]	0607	Mississippi Delta	91	25	20	2
18 Feb 81[1]	0625	Mississippi Delta	91	1	4	1
18 Feb 81[2]	1800	Mississippi Delta	91	40	8	
10 Dec 82[1]	0830	Mississippi Delta	18	1	88	26

[1]Collections for examination of diet.
[2]Collections for determination of growth.

(Table 1). Adequate numbers of larvae allowed growth comparisons of larvae collected on the Cape San Blas transect in December 1980 and larvae collected on the Mississippi Delta and Galveston Bay transects in February 1981.

Larvae were measured to the nearest 0.1 mm (NL before and SL after the formation of hypural plates). Guts were dissected and all gut contents were excised, identified, and measured. Percent similarity (Schoener 1970) was used to compare the diets of larval round herring and gulf menhaden from single collections.

Sagittal otoliths were removed from larvae, cleaned in distilled water, and mounted on glass microscope slides with clear acrylic resin; no griding or sectioning was necessary to resolve daily growth increments. Otoliths of round herring were semi-opaque and similar to those of gulf menhaden. Presumed daily increments were clearly discernable as bipartite structures consisting of adjoining incremental and discontinuous zones (Campana and Neilson 1985).

In describing the growth of larval round herring, we did not experimentally verify that their first otolith increment appeared 5 days after hatching or that subsequent increments were added daily as Warlen (1988) has done for gulf menhaden. We assumed that initial and subsequent increment deposition in round herring was similar to gulf menhaden. This assumption is justified, in part, by similarities in the period of some key developmental events. Incubation takes 36 hours at 20.5°C for round herring (O'Toole and King 1974), and 40–42 hours at 19–20°C for gulf menhaden (Hettler 1984). Complete adsorption of the yolk occurs in 4 days for round her-

ing reared in the laboratory at 24–26°C (Miller et al. 1979), as well as for gulf menhaden reared at 18–22°C (Hettler 1984). Further, we used alternative empirical methods to support our assumption that otolith growth increment formation occurs daily (Hales 1987). By comparing the width of marginal increments with the width of the proximal completely-formed increment, we determined the percentage of larvae with partially-formed or completely-formed marginal increments over a 24-hour period (8–10 December 1981; Table 1). The frequency of increment formation was inferred from these percentages and from the relationship of otolith radius and larval length.

The Laird version of the Gompertz growth model was used to describe growth from the logarithm of length and the estimated age of larvae (Zweifel and Lasker 1976). Growth curves of round herring and gulf menhaden larvae were compared by using the predictive, resampling method described by Kappenman (1981). Data for gulf menhaden growth were taken from Warlen (1988) for comparisons with the growth of round herring.

Results

Distribution and co-occurrence

In all, 419 round herring larvae were identified in the present collections, four fewer than gulf menhaden (Sogard et al. 1987). Collections of the larvae of both species indicate that they co-occur infrequently. Round herring and gulf menhaden larvae occurred together at 15 of 45 locations where collections produced either species. Larval round herring were collected most frequently throughout the water column at the offshore stations in water 91 m deep, although one of the largest single collections was made at 18 m (Table 1). Larval gulf menhaden were collected mostly inshore at the 18 m stations along each transect. The larvae of these species co-occurred mainly at the 91 m stations along each transect.

Diet comparisons

Only 56 round herring larvae had food in their guts. Larval round herring had eaten primarily copepod nauplii, copepodites, and adults, with pteropods (mainly *Limacina trochiformis*), tintinnids, invertebrate eggs, and *Eucalanus* spp. nauplii contributing lesser percentages (Table 2). *Eucalanus* nauplii were considered a discrete food organism separate from other copepod nauplii, because its form and size differed markedly; *Eucalanus* spp. nauplii have long, paddle-like appendages and are more than three times larger than the other copepod nauplii observed in the guts of larvae.

Table 2
The diet composition of 56 round herring *Etrumeus teres* larvae in the northern Gulf of Mexico.

	Percent frequency of occurrence	Percent total no.
Centric diatoms	1.8	1.3
Tintinnids	3.6	5.2
Pteropods	8.9	6.5
Pelecypods	1.8	1.3
Unidentified copepod nauplii	25.0	36.4
Unidentified *Eucalanus* nauplius	3.6	3.9
Copepodid and adult copepods	21.4	16.9
Calanoid copepodites and adults	5.4	3.9
Harpacticoid copepodites and adults	1.8	1.3
Cyclopoid copepodites and adults	16.1	11.7
Invertebrate eggs	10.7	11.7

Table 3
Comparison of the percent frequency of occurrence of food organisms in the diet of 26 larval round herring and gulf menhaden larvae collected simultaneously in the northern Gulf of Mexico.

	Percent frequency of occurrence	
Food organism	Round herring	Gulf menhaden
Tintinnid	3.8	4.2
Pteropods	19.2	2.1
Unidentified copepod nauplii	7.7	5.3
Unidentified *Eucalanus* nauplius	3.8	5.3
Unidentified copepodites and adult copepods	15.4	31.6
Calanoid copepodites and adults	3.8	33.7
Harpacticoid copepodites and adults	3.8	0
Cyclopoid copepodites and adults	30.8	11.6
Invertebrate eggs	11.5	6.3

The width of food organisms ranged from 40 to 280 μm, a width range comparable to that found for gulf menhaden (Govoni et al. 1983).

Of the 88 round herring larvae collected simultaneously with gulf menhaden, 26 had food in their guts. There were differences in the gut contents of these 26 round herring and 26 randomly selected gulf menhaden larvae collected simultaneously (Table 3). Larval round herring had eaten cylopoid copepods (*Oncaea* spp. and *Corycaeus* spp.) and pteropods more frequently, but calanoid copepodites and adult copepods less frequently, than had larval gulf menhaden. Percent similarity of the diets of these larvae was 52.2, a value that indicates marginal overlap in diet (Schoener 1970).

Growth comparisons

Marginal growth increments seemed to form from evening through early morning (Table 4). The allometric relationship ($\log_{10}$ radius = 0.126 $\log_{10}$SL+ 1.413; r^2 0.91) between otolith radius and standard length of 131 larvae also suggested a daily periodicity in otolith increment formation (Hales 1987).

Estimates of the length at hatching ($L_{(0)}$) for gulf menhaden provided by the Laird-Gompertz model 3.4 mm SL (Fig. 1; Table 5), closely approximate the length-at-hatching of larvae incubated in the laboratory at a temperature of 20°C, 2.6–3.0 mm SL (Hettler 1984). Estimates of $L_{(0)}$ for round herring, about 1.2 mm SL, however, are considerably lower than the lengths reported for larvae hatched in the laboratory: 3.8–4.0 mm body length from eggs collected in the South Atlantic and incubated at 20.5°C (O'Toole and King 1974) and 6.0 mm SL from eggs collected in the Pacific and incubated at 24–26°C (Miller et al. 1979). If the interval from hatching to deposition of the first growth increment is shorter in reality than the assumed 5 days, the Laird Gompertz growth curve would shift to the left, yielding a greater value for $L_{(0)}$, but the form of the growth curve, i.e., the growth rate, would remain the same.

Round herring grew faster than gulf menhaden through the first 20–40 days; gulf menhaden exhibited faster growth than round herring thereafter (Fig. 2). The fastest growth rate (≈0.85 mm/day) for round herring larvae occurred at about 15 days. Average growth rates through 27 days for December 1980 were 0.71 and 0.46 mm/day for round herring and gulf menhaden; average rates through 50 days in February 1981 were 0.45 and 0.34 mm/day. Annual differences in larval gulf menhaden growth are discussed in Warlen (1988).

Table 4

Percentage of round herring larvae with partially formed (narrow) or completed (wide) marginal otolith growth increments collected at three different times of day.

Time of capture (h)	No. of fish	Percentage	
		Partially formed	Completed
1800	9	22	78
2400	10	40	60
0600	6	100	0

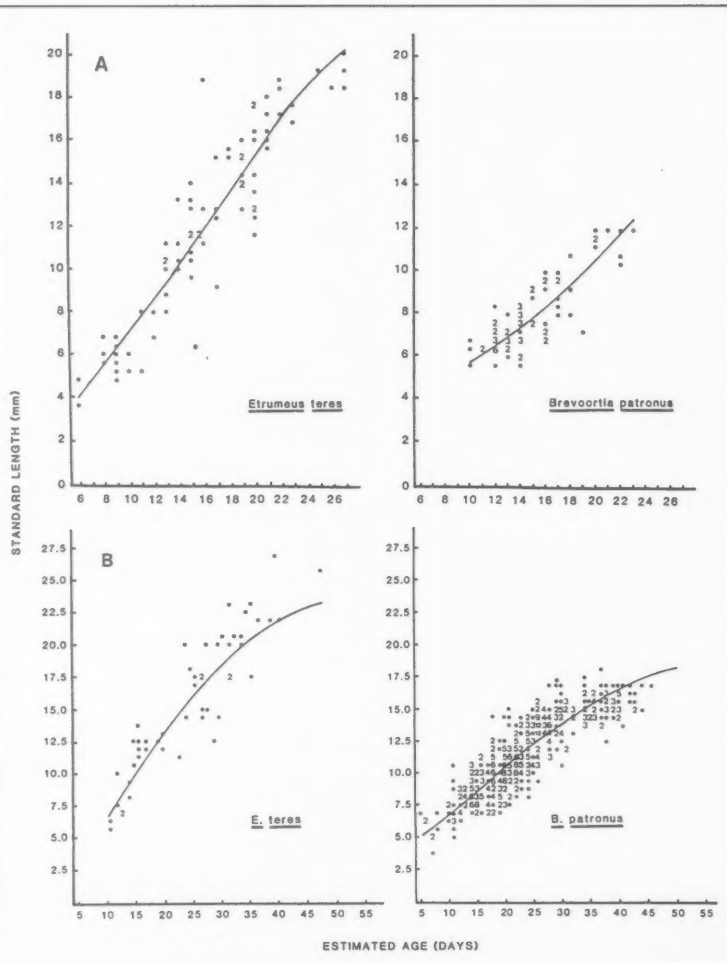

Figure 1

Growth of larval round herring *Etrumeus teres* and gulf menhaden *Brevoortia patronus* collected in December 1980 (A) and February 1981 (B) in the northern Gulf of Mexico. The log form of the Laird-Gompertz model was used to describe the growth of both species (numbers indicate location of coincident data points).

Table 5

Estimates of Laird-Gompertz growth model parameters* and mean age (d) and SL (mm) for larval round herring and gulf menhaden collected in the northern Gulf of Mexico during December 1980 and February 1981.

Date		Number of observations	Growth model parameters			Mean estimated age (d)	Mean SL (mm)
			$L_{(0)}$	$A_{(0)}$	α		
December 1980	Round herring	81	1.184	0.259	0.081	16.025	12.056
			(0.310)	(0.055)	(0.015)	(0.590)	(0.501)
	Gulf menhaden	80	3.418	0.056	<0.001	14.862	8.034
			(0.995)	(0.037)	(0.407)	(0.337)	(0.191)
February 1981	Round herring	50	1.240	0.232	0.077	25.200	15.620
			(0.710)	(0.089)	(0.018)	(1.318)	(28.871)
	Gulf menhaden	561	3.401	0.087	0.045	23.401	11.493
			(0.246)	(0.009)	(0.005)	(0.333)	(0.121)

*$L_{(0)}$ = length at hatching, $A_{(0)}$ = specific growth rate at hatching, α = exponential decay of the specific growth rate. Values in parentheses are asymptotic standard errors.

In two comparisons, the growth curves of these species differed, i.e., the sum of squares of the differences between observed and predicted lengths was greater when data for the two species were pooled than when the data were considered separately. In the comparison of larvae collected in December 1980, the sum of squares of deviations was 6.327 for pooled data and 2.736 for data considered separately (total observations = 161). In the comparison of larvae collected in February 1981, from two transects, the sum of squares of deviations was 13.255 for pooled data and 10.477 for data considered separately (total observations = 611).

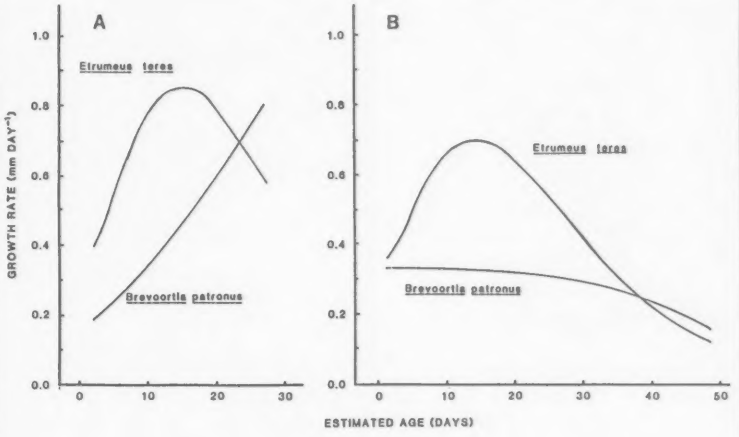

Figure 2

Age-specific growth rates of larval round herring *Etrumeus teres* and gulf menhaden *Brevoortia patronus* collected in December 1980 (A) and February 1981 (B) in the northern Gulf of Mexico. Specific growth rates-at-age were derived from the log form of the Laird-Gompertz growth model parameters.

Discussion

The large, spatulate, and toothed jaws of larval round herring might enable them to eat larger food organisms than gulf menhaden, but while the diets of larval round herring and gulf menhaden differed, the width of food organisms coincided. Diets, then, do not directly reflect differences in jaw structure and dentition. The pteropods eaten by both species were *Limacina trochiformis*, the cyclopoid copepods were primarily of the genera *Oncaea* and *Corycaeus*, and the calanoid copepods were primarily of the genera *Paracalanus* and *Acartia*. Round herring larvae ate more pteropods and cyclopoid copepods, but fewer calanoid copepods than did gulf menhaden larvae.

The more offshore distribution of larval round herring in the central and western northern Gulf of Mexico (Shaw and Drullinger 1990; present data) may explain differences in diet and growth. All of the food organisms eaten by larval round herring and gulf menhaden are broadly distributed in continental shelf waters, but some of the copepods have different patterns of distribution across the shelf in the northern

Gulf of Mexico (Ortner et al. 1989). *Acartia*, for example, occurs in greater abundance inshore, in less saline waters, whereas *Oncaea* and *Corycaeus* are more abundant in water of traditional salinities offshore (Ortner et al. 1989). Prior experience and learning can influence the capture efficiency, food selection, and ingestion rates of larval fishes (see review in Stoecker and Govoni 1984); and because larval round herring occupy more offshore waters, they may be conditioned to feed preferentially on the cyclopoids *Oncaea* and *Corycaeus*.

The difference in larval growth between these two species may reflect differences in the physical environment where these larvae grow. Offshore water in the northern Gulf of Mexico is typically warmer than inshore water during the winter. Inshore–offshore gradients in average water column temperature among the three stations along the three transects were 19.2 to 20.7 to 22.1°C for the Cape San Blas transect in December 1980; 16.1 to 15.0 to 18.1, 16.9 to 19.5 to 19.8, and 12.9 to 18.5 to 19.0°C for the Mississippi Delta, Cape San Blas, and Galveston Bay transects in February 1981. Temperature differences of this magnitude can account for intraspecific differences in growth rates among larval fish (Jones 1986, Warlen 1988) as seen here in the slower growth of round herring larvae in the cooler water of February 1981. The faster, early growth of round herring larvae, overall, probably results from the warmer waters of its offshore occurrence.

Acknowledgments

The collection of specimens examined in this paper was supported by a contract to the Beaufort Laboratory of the Southeast Fisheries Science Center, National Marine Fisheries Service, NOAA, from the Ocean Assessment Division, National Ocean Services, NOAA. This paper was developed while the senior author was a visiting scientist at the National Marine Fisheries Service, NOAA, Beaufort Laboratory.

Citations

Campana, S.E., and J.D. Neilson
1985 Microstructure of fish otoliths. Can. J. Fish. Aquat. Sci. 42:1014–1032.

Christmas, J.Y., and R.S. Waller
1975 Location and time of menhaden spawning in the Gulf of Mexico. Gulf Coast Res. Lab., Ocean Springs, MS, 20 p.

Fahay, M.P.
1983 Guide to the early stages of marine fishes occurring in the western North Atlantic Ocean, Cape Hatteras to the southern Scotian Shelf. J. Northwest Atl. Fish. Sci. 4:1–423.

Fore, P.L.
1971 The distribution of eggs and larvae of the round herring, *Etrumeus teres*, in the northern Gulf of Mexico. Am. Soc. Biol. Bull. 18, 34 p.

Govoni, J.J., D.E. Hoss, and A.J. Chester
1983 Comparative feeding of three species of larval fishes in the northern Gulf of Mexico: *Brevoortia patronus*, *Leiostomus xanthurus*, and *Micropogonias undulatus*. Mar. Ecol. Prog. Ser. 13:189–199.

Govoni, J.J., P.B. Ortner, F. Al-Yamani, and L.C. Hill
1986 Selective feeding of spot, *Leiostomus xanthurus*, and Atlantic croaker, *Micropogonias undulatus*, larvae in the northern Gulf of Mexico. Mar. Ecol. Prog. Ser. 28:175–183.

Govoni, J.J., D.E. Hoss, and D.R. Colby
1989 The spatial distribution of larval fishes about the Mississippi River plume. Limnol. Oceanogr. 34:178–187.

Hales, L.S.
1987 Distribution, abundance, reproduction, food habits, age, and growth of round scad, *Decapterus punctatus*, in the South Atlantic Bight. Fish. Bull., U.S. 85:251–268.

Hettler, W.F.
1984 Description of eggs, larvae, and early juveniles of gulf menhaden, *Brevoortia patronus*, and comparisons with Atlantic menhaden, *B. tyrannus*, and yellowfin menhaden, *B. smithi*. Fish. Bull., U.S. 82:85–95.

Houde, E.D.
1977 Abundance and potential yield of the round herring, *Etrumeus teres*, and aspects of its early history in the eastern Gulf of Mexico. Fish. Bull., U.S. 75:61–89.

Houde, E.D., and P.L. Fore
1973 Guide to identity of eggs and larvae of some Gulf of Mexico clupeid fishes. Fla. Dep. Nat. Resour., Mar. Res. Lab., Leafl. ser. IV, pt. 1, no. 23, 14 p.

Jones, C.
1986 Determining age of larval fish with the otolith increment technique. Fish. Bull., U.S. 84:91–103.

Kappenman, R.F.
1981 A method for growth curve comparisons. Fish. Bull., U.S. 79:95–101.

Miller, J.M., W. Watson, and J.M. Leis
1979 An atlas of common nearshore marine fish larvae of the Hawaiian Islands. Misc. Rep. PO-02, Univ. Hawaii Sea Grant Prog., Honolulu, 179 p.

Ortner, P.B., L.C. Hill, and S.R. Cummings
1989 Zooplankton community structure and copepod species composition in the northern Gulf of Mexico. Continental Shelf Res. 9:387-402.

O'Toole, M.J., and D.P.F. King
1974 Early development of the round herring, *Etumeus teres* (De Kay) from the south-east Atlantic. Vie Milieu 24:443-452.

Reintjes, J.W.
1980 Marine herring and sardine resources of the northern Gulf of Mexico. *In* Flandorfer, M., and L. Skuplen (eds.), Workshop for potential fishery resources of the northern Gulf of Mexico, New Orleans, 1980. Publ. MASGP-80-012, Miss.–Alabama Sea Grant Consort., 14 p.

Roel, B.A., and Y.C. Melo
1990 Reproductive biology of the round herring, *Etrumeus whiteheadi*. S. Afr. J. Mar. Sci. 9:177–187.

Schoener, T.W.
1970 Nonsynchronous spatial overlap of lizards in patchy habitats. Ecology 51:408–418.

Shaw, R.F., and D.L. Drullinger
1990 Early-life history profiles, seasonal abundance, and distribution of four species of clupeid larvae from the northern Gulf of Mexico, 1982 and 1983. NOAA Tech. Rep. NMFS 88, 60 p.

Sogard, S.M., D.E. Hoss, and J.J. Govoni
1987 Density and depth distribution of larval gulf menhaden, *Brevoortia patronus*, Atlantic croaker, *Micropogonias undulatus*, and spot, *Leiostomus xanthurus*, in the northern Gulf of Mexico. Fish. Bull., U.S. 85:601–609.

Stoecker, D.K., and J.J. Govoni
1984 Food selection by young gulf menhaden (*Brevoortia patronus*). Mar. Biol. (Berl.) 80:299–306.

Warlen, S.M.
1988 Age and growth of larval gulf menhaden, *Brevoortia patronus*, in the northern Gulf of Mexico. Fish. Bull., U.S. 86:77–90.

Whitehead, P.J.
1963 A revision of the recent round herrings (Pisces: Dussumieriidae). Bull. Br. Mus. (Nat. Hist.) Zool. 10:305–380.

Zweifel, J.R., and R. Lasker
1976 Prehatch and posthatch growth of fishes—a general model. Fish. Bull., U.S. 74:609–621.

Analytical correction for oversampled Atlantic mackerel *Scomber scombrus* eggs collected with oblique plankton tows

Denis D'Amours
Francois Grégoire

Division de la Recherche sur les Pêches
Ministère des Pêches et des Océans, Institut Maurice-Lamontagne
C.P. 1000, Mont-Joli, Québec G5H 3Z4, Canada

Atlantic mackerel *Scomber scombrus* is a pelagic species spawning on both sides of the North Atlantic ocean. In the east, mackerel spawn off the British Isles and in the North Sea (as reviewed by Lockwood 1988 and Daan et al. 1990). In the west, mackerel spawn in the Middle Atlantic Bight (Berrien 1978) and in the Gulf of St. Lawrence (Ware 1977). Atlantic mackerel is a moderately prolific species (Bigelow and Schroeder 1953); its fecundity has been estimated at 255,000 eggs for a medium-size female (30 cm FL) in the northeast Atlantic (Lockwood et al. 1981), and at 243,000 eggs for a similar-size female in the Middle Atlantic Bight (Morse 1980).

Mackerel eggs are concentrated near the surface when the water column is thermally stratified during spawning (Coombs et al. 1983, Ware and Lambert 1985). Sette's (1943) data from the Middle Atlantic Bight indicated that 80% of mackerel eggs were in the top 10 m. In the North Sea, Coombs et al. (1981) reported that 91% of mackerel eggs were above 26 m, and that more than 85% were between 0 and 16 m. In the Gulf of St. Lawrence, de Lafontaine and Gascon (1989) indicated that 89% of mackerel eggs were within 15 m of the surface. The distribution of mackerel eggs is thus characteristically non-homogeneous in the vertical plane.

In the Gulf of St. Lawrence and Middle Atlantic Bight, mackerel eggs are routinely surveyed for stock assessment purposes (e.g., Castonguay and Grégoire 1989, Berrien 1990). Surveys are carried out with oblique plankton tows, with bongo nets as described by Posgay and Marak (1980). However, accuracy of oblique plankton tows is known to be sensitive to nonhomogeneous vertical distribution of the sampled organisms (Smith and Richardson 1977). Ideally, there should be no hesitation at the surface when retrieving the net, as it would lead to a severe oversampling of the surface layer where the eggs are concentrated (Posgay and Marak 1980, Smith et al. 1985). In practice, it is difficult not to drag the plankton net at the surface for at least a few seconds; when the net is retrieved, it reaches the surface several meters behind the block, and is dragged at the surface until directly under the block, where it can be lifted out. During such dragging at the surface, the mouth of the net is typically nearly all submerged and samples the surface layer. It is usually assumed that such oversampling at the surface leads to a negligible bias in estimates of abundance.

In this paper, the bias caused by an oversampling of surface water on the calculated abundance of mackerel eggs is analyzed. An analytical correction for this bias is derived and applied to empirical data from a mackerel egg survey held in the Gulf of St. Lawrence in 1990 to reevaluate the annual production of eggs. Also, some potential effects of oversampling surface water are evaluated when computing total abundance and mortality rates of near surface organisms.

Manuscript accepted 9 December 1991.
Fishery Bulletin, U.S. 90:190–196 (1992).

Bias in computed egg abundance caused by oversampled surface water

Distribution of mackerel eggs

Concentrations of mackerel eggs are highest near the surface and decrease rapidly with depth. Sundby (1983) reported that under assumptions applicable in the present study, a negative exponential model (as Eq. 1, below) was appropriate to describe the vertical distribution of mackerel eggs. Ware and Lambert (1985) also concluded that the vertical distribution of mackerel eggs was best described by a negative exponential model. Data on the vertical distribution of mackerel eggs presented by Sette (1943) and by de Lafontaine and Gascon (1989) were fitted to negative exponential models; in both cases, over 90% of the variance in the egg distribution was explained. Therefore, a negative exponential model is appropriate to describe the distribution of mackerel eggs in the vertical plane.

Sampling mackerel eggs

Let the abundance of a population of eggs in a body of water decrease from the surface following an exponential model:

$$\frac{dN(z)}{dz} = -kN(z) \qquad (1)$$

where N(z) = concentration of eggs in number per volume at depth z, and k = rate constant. Upon integration of Eq. 1, the concentration of eggs at depth z is given by

$$N(z) = N_o\, e^{-kz}, \tag{2}$$

where N_o = concentration of eggs at the surface. When integrating Eq. 2, the total number of eggs (N_a) in number per surface area in this body of water is given by

$$N_a = \int_0^{\infty} N_o\, e^{-kz}\, dz = \frac{N_o}{k}. \tag{3}$$

If an oblique plankton tow (Fig. 1A) is made through this distribution of eggs with a net of radius a, and a centered depth of α, the total number of eggs collected (N_H) will be equal to

$$N_H = \tag{4}$$

$$\int_0^{L_1} \int_{\alpha-a}^{\alpha+a} \int_{-\sqrt{a^2-(z-\alpha)^2}}^{+\sqrt{a^2-(z-\alpha)^2}} N(z)\, dydzdx_1$$

$$+ \int_0^{L_2} \int_{\alpha-a}^{\alpha+a} \int_{-\sqrt{a^2-(z-\alpha)^2}}^{+\sqrt{a^2-(z-\alpha)^2}} N(z)\, dydzdx_2,$$

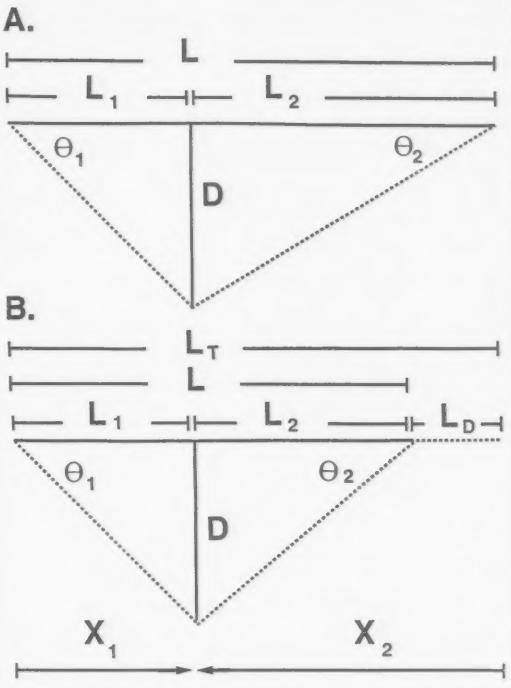

Figure 1

Path (broken line) of net during an oblique plankton tow: L's represent length components of the tow along horizontal references x_1 and x_2; D is the maximum depth of sampling, and θ's represent angles between path of net and horizon. In (A), the net is recovered upon reaching the surface; in (B), the net is dragged at the surface along L_D before recovery.

where x_1 is the horizontal distance from the start of the tow and x_2 is the horizontal distance from the end of the tow (Fig. 1A), and where z and y represent the vertical and horizontal openings of the net, respectively. Integrating Eq. 4 over the limits on z and y (as in D'Amours 1988),

$$N_H \approx \left[1 + \frac{(ka)^2}{8}\right] \left(\int_0^{L_1} N_o\, e^{-kz}\, dx_1 + \int_0^{L_2} N_o\, e^{-kz}\, dx_2 \right). \tag{5}$$

The term ka originates from the slight difference between the position of the geometric center of the net and the position of the center of abundance of the eggs within its opening (D'Amours 1988). Defining, $\tan \theta_i = \frac{D}{L_i}$, where D is the maximum depth of the tow, Eq. 5 can be rewritten as

$$N_H \approx \left[1 + \frac{(ka)^2}{8}\right] \left(\int_0^{L_1} N_o\, e^{-k \tan \theta_1 x_1}\, dx_1 + \int_0^{L_2} N_o\, e^{-k \tan \theta_2 x_2}\, dx_2 \right), \tag{6}$$

Evaluating Eq. 6 for kD>>0,

$$N_H \approx \frac{N_o}{k}\left(\frac{L}{D}\right)\left[1 + \frac{(ka)^2}{8}\right], \quad (7)$$

where $L = L_1 + L_2$, and is the total horizontal length of the tow (Fig. 1A). It can now be seen that when the number of eggs collected in an oblique plankton tow (Eq. 7) is multiplied by the ratio D/L, and when the product ka is small, an approximation of Eq. 3 is obtained, which is a measure of the local abundance of eggs in number per surface area. The procedure of multiplying the total number of eggs collected in the oblique tow (equation 7) by the ratio of its maximum depth to its total horizontal length (D/L), is equivalent to the standardization procedure described by Smith and Richardson (1977). To obtain estimates of abundance in number per surface area, the standardization procedure consists of multiplying the number of eggs collected by the ratio of the maximun depth attained during the tow to the volume of water filtered. This standardization procedure is valid if all depth strata are sampled equally.

Now assume the same population of eggs, but where the net is dragged at the surface while being readied for recovery at the end of the tow. The length of drag at the surface is represented by L_D in Figure 1B. Along L_D, the mouth of the net is centered at depth α, which is equal to its radius a; i.e., oversampling occurs in the layer of water immediately below the surface, as deeply as the diameter of the net. Over L_D, the net will collect a number of eggs (N_S) equal to

$$N_S \approx L_D \int_{\alpha-a}^{\alpha+a} \int_{-\sqrt{a^2-(z-\alpha)^2}}^{+\sqrt{a^2-(z-\alpha)^2}} N(z)\, dydz, \quad (8)$$

which is approximated by (as in D'Amours 1988)

$$N_S \approx N_o\, e^{-k\alpha} L_D\left[1 + \frac{(ka)^2}{8}\right]. \quad (9)$$

The total number of eggs (N_T) collected during an oblique tow, where the net is dragged at the surface at the end, will then be equal to the sum of N_H (Eq. 7) and N_S (Eq. 9):

$$N_T \approx \frac{N_o}{k}\left(\frac{L}{D}\right)\left[1 + \frac{(ka)^2}{8}\right] + N_o\, e^{-k\alpha} L_D\left[1 + \frac{(ka)^2}{8}\right]. \quad (10)$$

The component N_S will add to the number of eggs collected, and its inclusion in the standardization procedure will result in a systematic overestimation of the abundance of eggs per surface area. When Eq. 10 is standardized with L_D included in the total length of the tow (L_T in Fig. 1B), and the result divided by the true theoretical abundance of eggs (Eq. 3), an expression is obtained which is the ratio (B) of the biased abundance to the true abundance of eggs:

$$B \approx L + D\left(k\, e^{-k\alpha} L_D\left[1 + \frac{(ka)^2}{8}\right]\right). \quad (11)$$

Removal of bias from computed abundance of mackerel eggs

Assumption of constant filtration efficiency

In Eq. 11, L and L_D can be replaced by the proportion of the total duration of the tow they represent, under the assumption of constant filtration efficiency. This assumption is required to use tow time as a measure directly proportionnal to amount of water filtered, so as to separate L and L_D in Eq. 11. However, as pointed out by Smith and Richardson (1977), the filtration efficiency of a plankton tow declines typically with the duration of the tow, as the accumulated plankton reduces the porosity of the net. They warned that the diminishing efficiency of a net could result in an undersampling of surface water. To verify whether such undersampling of surface water occurred, which would offset oversampling at the end of the tow, the time-course of the efficiency of the plankton net must be assessed.

If filtration efficiency diminishes with time, the volume filtered per unit time will diminish with increasing tow duration. The residuals about a straight line fitted on the values of volume filtered against tow duration would then show a decreasing pattern of departure from linearity. The volumes filtered for the tows in the Gulf of St. Lawrence in 1990 were regressed against their respective total duration. The residuals of this regression did not indicate a decreasing de-

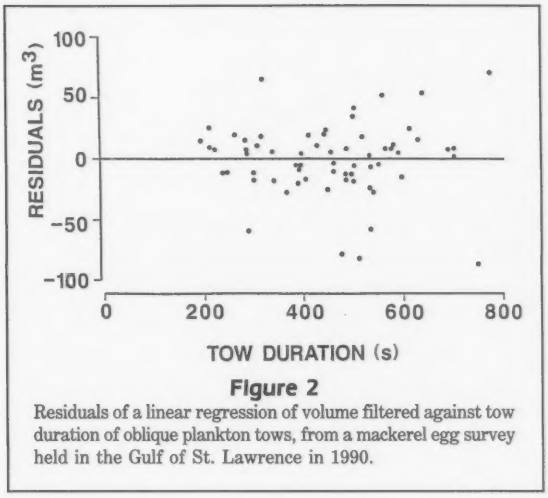

Figure 2

Residuals of a linear regression of volume filtered against tow duration of oblique plankton tows, from a mackerel egg survey held in the Gulf of St. Lawrence in 1990.

parture from linearity; somewhat unexpectedly, a tendency towards an increasing departure from linearity could be detected (Fig. 2). Therefore, it can be concluded that no surface undersampling occurred as a result of diminishing filtration efficiency. The apparent increasing departure from linearity can be explained by the fact that long tows (e.g., duration of 10 minutes) are deeper, i.e., well below the stratum where mackerel eggs are abundant. During short tows (e.g., duration of 6 minutes), the net is towed mainly in the stratum were eggs are present, and the filtration efficiency is less, though stationary, than in water devoid of eggs. During long, deep tows, more time is spent below the stratum containing mackerel eggs, and proportionally more free-flowing water is filtered there.

Correction of survey data

In Eq. 11, a rate constant k must be introduced to describe the distribution of the sampled organisms in the vertical plane. For the purpose of the demonstration, a rate constant $k = 0.15/m$ was selected as representative of all mackerel egg stages at all stations; as discussed below, this rate constant is a representative value extracted from the literature on mackerel egg distribution. During the mackerel egg survey carried out in the Gulf of St. Lawrence in late-June and early-July 1990, the total duration of each oblique tow was measured, as well as the duration of the period during which the Bongo net was dragged at the surface before recovey (F. Grégoire, unpubl. data). The period of drag at the surface started when the net was visually spotted at the surface and ended when the net was lifted out of the water. From those measurements, values of L and L_D were calculated in percent of total tow time. With a rate constant $k = 0.15/m$, a net radius $a = 0.305$ m, a centered depth $\alpha = 0.305$ m along L_D, and a measured maximum depth D, a value of the degree of bias B was calculated for each tow as per Eq. 11. The corrected abundance of eggs was obtained by multiplying the computed biased abundance by [100%/B]. Using uncorrected and corrected abundances of eggs at each station, two total annual productions of mackerel eggs were computed for the Gulf of St. Lawrence in 1990 following the procedures of Ouellet (1987). The totals were 6.77×10^{14} eggs with uncorrected abundance, and 5.63×10^{14} eggs with corrected abundance. The difference of 1.14×10^{14} eggs, with a mean fecundity of 300,000 eggs and a sex ratio of 1:1, amounted to 7.6×10^8 mature mackerel.

The parameter D used in the above calculations was measured accurately with a bathymeter mounted on the plankton net. If triangulation had been used, where D is estimated by the amount of wire paid out and the angle subtended at the block, another source of bias would have been introduced owing to the approximative nature of the method. Assume a population of mackerel eggs in a body of water where $k = 0.15$ and $N_o = 750$; if sampled to a depth D of 50 m with a net of radius $a = 0.305$ on a transect where $L = 1000$ m, a total of 100,000 eggs will be collected (Eq. 7). Standardization of this result by the ratio of D to L shows that the abundance of eggs is 5000 eggs/m^2. Had D been underestimated by 10% at 45 m, the abundance of eggs would have been underestimated also by 10% at 4500 eggs/m^2. If the same tow is repeated, but with $L_D = 75$ m and $\alpha = 0.305$ m, a total of 153,775 eggs will be collected. Standardization of this result with D correctly evaluated at 50 m indicates an abundance of 7152 eggs/m^2; with D underestimated by 10% at 45 m, standardization indicates an abundance of 6437 eggs/m^2. These examples show how an underestimation of 10% of D results in an abundance of eggs equal to 90% of the real value, and how a 7% (75 m/1075 m) oversampling at the surface results in an abundance of eggs equal to 143% of real value. Also, they show that when both an underestimation of D and an oversampling of the surface layer occur during a tow, the effects of both biases on the estimate of abundance are opposite, but not symmetrical, with the effect of the oversampling at the surface much more important than that from the underestimation in D.

A degree of bias (B in Eq. 11) was computed for various combinations of L_D (with $L = 100\% - L_D$) and rate constant k, with $a = \alpha = 0.305$ m, and $D = 50$ m (Fig. 3A). The degree of bias caused by an oversampling of surface water is a function of the time of sampling at the surface, and of the degree of contagion of the eggs near the surface, as described by the parameter k. For

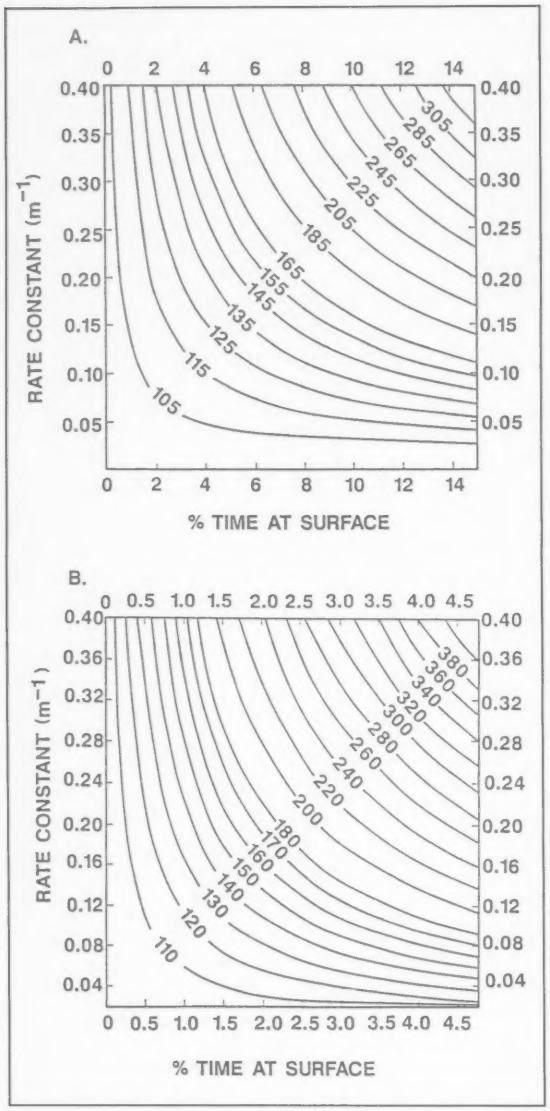

Figure 3
Isopleths (in %) of the ratio of biased abundance to true abundance per surface area of a theoretical population of fish eggs. The isopleths were computed for variable rate constants k of a negative exponential model describing the vertical distribution of the eggs, and for varying degree of oversampling surface water during an oblique plankton tow, L_D, expressed as percent of the total duration of the tow. In (A), the maximum sampling depth was set at 50 m; in (B), the maximum sampling depth was set at 200 m. All other parameters equal in (A) and (B).

example, with a sampling time at the surface representing 7% of the total duration of the tow, and with a rate constant of 0.15/m, the calculated abundance will be 140% of the real value. With eggs highly concentrated near the surface, that is with high values of k, even briefer towing times at the surface will still result in severe bias.

The degree of bias B was also computed for similarily varying k and L_D, again with $a=\alpha=0.305$ m, but with maximum depth D increased to 200 m (Fig. 3B). For a rate constant of 0.15/m as in the previous example, but with towing time at the surface representing only 2% of the total duration (e.g., 12 seconds at the surface for a total tow time of 10 minutes), the calculated abundance of eggs will again be 140% of the real value. This somewhat counterintuitive result stems from the fact that by sampling deep strata, the fraction of the tow occurring in the stratum where eggs are present is proportionally smaller. As a result, brief times of oversampling at the surface have proportionally more effect on the calculated abundances of eggs than when the tow extends only to shallow strata.

Effects of oversampling surface water on variance of total abundance and on mortality rate

Effect on variance

Since the length of dragging at the surface is likely to vary (as a function of weather, crew handling of the net, etc.), a variance will be introduced in the computation of the total abundance of eggs over the studied body of water. It was assumed that the abundance of eggs (5000 eggs/m^2) was constant over the surface of a theoretical body of water where numerical experiments were carried out. Ten oblique tows were made in this theoretical body of water, with L = 1000 m, $a=\alpha=0.564$ m, and k = 0.2/m, which are convenient values for illustrative purposes. A different length of drag at the surface (L_D) was assigned randomly to each tow; ten random numbers were multiplied by an arbitrary length of 6 m and the resulting L_D's were 6 (×2), 12, 24 (×3), 30, 36, 48, and 54 m. Ten estimates of abundance of eggs per unit surface area were calculated, and the mean was 5994 eggs/m^2, with 95% confidence intervals of 5646–6342 eggs/m^2. This illustrates that small and variable lengths of drag at the surface bias the estimated abundance over the whole body of water, and add a substantial margin of uncertainty to the estimate of local abundance.

In another numerical experiment, the abundance of eggs was again assumed constant throughout at 5000 eggs/m^2, except this time the degree of contagion

near the surface was made variable, i.e., the rate constant k varied randomly within bounds. Ten transects were carried out through these distributions of eggs, with L = 1000 m, $a = \alpha = 0.564$ m, and the length of drag at the surface (L_D) was held constant at 50 m. For each tow, a random value was assigned to the rate constant k: ten random numbers were multiplied by 0.1/m, and added to 0.15. The resulting values were 0.15, 0.16, 0.17 (×2), 0.20 (×2), 0.21 (×2), 0.22, 0.23 (×2), and the corresponding values of N_o were adjusted so that $N_o/k = 5000$ eggs/m^2. Ten estimates of abundance of eggs per unit surface area were calculated, and the mean was 6876/m^2, with 95% confidence interval of 6713–7039 eggs/m^2. This indicates that even when maintaining a constant length of drag at the surface, similar problems of bias and variance still arise when the degree of contagion of the eggs varies.

Effect on mortality rates

Again for numerical experiments, the abundance of eggs at a theoretical station was assumed to be 5000 eggs/m^2, with $N_o = 475/m^3$, and $k = 0.095$/m (i.e., 475/0.095 = 5000). An oblique tow with L = 1000 m, D = 50 m, $L_D = 50$ m, and $a = \alpha = 0.564$ m, was made through this concentration of eggs at time t_0, and the biased abundance was calculated to be 5873/m^2. For the purpose of the demonstration, it was assumed that the eggs suffered no mortality. Some time later at time t_1, the abundance of eggs was still the same, but they were closer to the surface, with $N_o = 950/m^3$ and k = 0.19/m (i.e., 950/0.19 = 5000). The same oblique tow in this slightly rearranged concentration of eggs yielded a biased estimate of abundance of 6806/m^2, a relative increase of nearly 16% compared with the value at t_0, and an absolute bias of over 36%. In real situations, then, an increase in the degree of vertical contagion of the eggs over a sampling period could lead to an underestimation of the mortality rate if the surface water is oversampled, or to an overestimation if the degree of contagion decreases.

Conclusion

The oblique tow is a convenient method to obtain an estimate of abundance of eggs over a body of water. However, in actual operating conditions, it is rarely possible to carry out an oblique tow without dragging the net at the surface for some period of time, which may introduce a large bias in the estimate of abundance. The first practical recommendation to avoid such bias is to evaluate the assumption that a brief drag time at the surface will cause only a small bias in the estimation of abundance. If eggs are equally distributed over considerable depth, or concentrated in deeper water, this assumption is valid. If not, action should be taken to avoid dragging the net at the surface. If this is impossible, a measure of the amount of oversampling at the surface, and of the rate constant k, should be used to remove the bias from the data following Eq. 11.

In this study, the percent time of the tow spent at the surface was used as a measure of the amount of oversampling at the surface; this information is readily recorded in the field. However, the constant k describing the distribution of eggs had to be approximated from data available in the literature. Ware and Lambert (1985) reported values of k ranging from 0.1 to 1.1; they further indicated that variations in k were related to the steepness of the thermal gradient in the water column, the development stage of the eggs, and the degree of wind-induced mixing. Data on mackerel egg distribution by de Lafontaine and Gascon (1989) indicated a mean value k = 0.1, with the lowest values for the most recently spawned eggs. Data on mackerel egg distribution by Sette (1943) indicated a higher mean value k = 0.17, but with the highest values for the most recently spawned eggs. Differences in mean values of k as well as development-stage specific values may result from differences in local wind conditions as well as in differences in local water density. As discussed by Sundby (1983), the shape of a vertical distribution of mackerel eggs will be determined by the difference of density between the egg and the surrounding water, and by the degree of wind-induced mixing. The relationship reported by Sundby (1983) between wind velocity and vertical eddy diffusivity coefficient of mackerel eggs indicates that the rate constant k should diminish as the state of the sea increases. The definite application of the analytical correction proposed herein will require more site-specific studies on the factors affecting the vertical distribution of mackerel eggs and determining the value of k. Nonetheless, the value k = 0.15 used in this study is representative of realistic conditions in the field, and can be considered as a conservative estimate of the degree of vertical contagion of mackerel eggs. With more reliable values of k, the simple correction procedure suggested in this study could help increase the accuracy of biological parameters based on data from fish egg surveys where the technique of the oblique plankton tow has been used.

Acknowledgments

Dr. D. Booth and Mr. P. Gagnon reviewed an early version of the manuscript. This work followed a study by D'Amours (1988) during which help was provided by

Dr. Brian Petkau and Mr. Brian Leroux of the Statistical Consulting and Research Laboratory, Department of Statistics, University of British Columbia, Vancouver. I thank an anonymous reviewer and Dr. L.L. Jones for helpful reviews and comments.

Citations

Berrien, P.L.
1978 Eggs and larvae of *Scomber scombrus* and *Scomber japonicus* in continental shelf waters between Massachusetts and Florida. Fish. Bull., U.S. 76:95–115.

Berrien, P.
1990 Atlantic mackerel egg production and spawner biomass estimates for the Gulf of St. Lawrence and Northeastern United States waters in 1987. ICES CM 1990/H:18, 17 p.

Bigelow, H.B., and W.C. Schroeder
1953 Fishes of the Gulf of Maine. U.S. Fish. Wildl. Serv., Fish. Bull. 74, vol. 53, 577 p.

Castonguay, M., and F. Grégoire
1989 Le maquereau bleu (*Scomber scombrus* Linné) du nord-ouest de l'Atlantique, sous-régions 2 à 6 de l'OPANO en 1988. CAFSAC (Can. Atl. Fish. Sci. Advis. Comm.) Res. Doc. 89/39, 25 p.

Coombs, S.H., R.K. Pipe, and C.E. Mitchell
1981 The vertical distribution of eggs and larvae of blue whiting (*Micromesistius poutassou*) and mackerel (*Scomber scombrus*) in the eastern North Atlantic and North Sea. Rapp. P.-V. Réun. Cons. Int. Explor. Mer 178:188–195.

Coombs, S.H., J.A. Lindley, and C.A. Fosh
1983 Vertical distribution of larvae of mackerel *Scomber scombrus* and microplankton, with some conclusions on feeding conditions and survey methods. FAO Fish. Rep. 291(3):939–956.

Daan, N., P.J. Bromley, J.G.R. Hislop, and N.A. Nielsen
1990 Ecology of North Sea fish. Neth. J. Sea Res. 26: 343–386.

D'Amours, D.
1988 Vertical distribution and abundance of natant harpacticoids on a vegetated tidal flat. Neth. J. Sea Res. 22:161–170.

de Lafontaine, Y., and D. Gascon
1989 Ontogenetic variation in the vertical distribution of eggs and larvae of Atlantic mackerel (*Scomber scombrus*). Rapp. P.-V. Réun. Cons. Int. Explor. Mer 191:137–145.

Lockwood, S.J.
1988 The mackerel—Its biology, assessment and the management of a fishery. Fishing News Books Ltd., Farnham, Surrey, England, 181 p.

Lockwood, S.J., I.G. Baxter, J.C. Gueguen, G. Joakimsson, R. Grainger, A. Eltink, and S.H. Coombs
1981 The western mackerel spawning stock estimate for 1980. Cons. Int. Explor. Mer, CM 1981/H:13, 20 p.

Morse, W.W.
1980 Spawning and fecundity of Atlantic mackerel, *Scomber scombrus*, in the Middle Atlantic Bight. Fish. Bull., U.S. 78: 103–108.

Ouellet, P.
1987 Mackerel (*Scomber scombrus*) egg abundance in the southern gulf of St. Lawrence from 1979 to 1986, and the use of the estimate for stock assessment. CAFSAC (Can. Atl. Fish. Sci. Advis. Comm.) Res. Doc. 87/62, 40 p.

Posgay, J.A., and R.R. Marak
1980 The MARMAP Bongo zooplankton samplers. J. Northwest Atl. Fish. Sci. 1:91–99.

Sette, O.E.
1943 Biology of the Atlantic mackerel (*Scomber scombrus*) of North America. Part 1. Early life history. Fish. Bull., U.S. 50:149–237.

Smith, P.E., and S.L. Richardson
1977 Standard techniques for pelagic fish egg and larva surveys. FAO Fish. Tech. Pap. 175, 100 p.

Smith, P.E., W. Flerx, and R.P. Hewitt
1985 The CalCOFI vertical egg tow (CalVET) net. *In* Lasker, R. (ed.), An egg production method for estimating spawning biomass of pelagic fish: Application to the northern anchovy, *Engraulis mordax*. NOAA Tech. Rep. NMFS 36.

Sundby, S.
1983 A one-dimensional model for the vertical distribution of pelagic fish eggs in the mixed layer. Deep-Sea Res. 30: 645–661.

Ware, D.
1977 Spawning time and egg size of Atlantic mackerel, *Scomber scombrus*, in relation to the plankton. J. Fish. Res. Board Can. 34:2308–2315.

Ware, D., and T.C. Lambert
1985 Early life history of Atlantic mackerel (*Scomber scombrus*) in the southern Gulf of St. Lawrence. Can. J. Fish. Aquat. Sci. 42:577–592.

Association between the sessile barnacle *Xenobalanus globicipitis* (Coronulidae) and the bottlenose dolphin *Tursiops truncatus* (Delphinidae) from the Bay of Bengal, India, with a summary of previous records from cetaceans

Arjuna Rajaguru
Gopalsamy Shantha

Systematics Laboratory, National Marine Fisheries Service, NOAA
National Museum of Natural History, Washington, DC 20560

Several instances of association between cetaceans and cirripeds have been reported in the literature. Among the barnacles, *Coronula* spp., *Conchoderma* spp., and *Xenobalanus* sp. have been reported from various species of cetaceans of both temperate and tropical waters (Mackintosh and Wheeler 1929, Mackintosh 1942). Devaraj and Bennet (1974) reported a single specimen of *Xenobalanus globicipitis* found attached to the fluke of a finless black porpoise *Neophocaena phocaenoides* caught off Karwar, west coast of India. This type of phoretic partnership (i.e., transportation by one promotes well-being of the other) between 14 specimens of a sessile barnacle *Xenobalanus globicipitis* and a host, the bottlenose dolphin *Tursiops truncatus*, is recorded here from the Bay of Bengal on the east coast of India. This is the first record of the bottlenose dolphin as a host for *Xenobalanus globicipitis* from the central and northern Indian Ocean.

Five spinner dolphins *Stenella longirostris* (Gray 1828) (113.0–177.5 cm TL) and six bottlenose dolphins *Tursiops truncatus* (Montagu 1821) (95.3–367.5 cm TL), were collected from the Bay of Bengal, off Porto Novo (11°29′N; 79°46′E), southeast coast of India, between 15 March 1982 and 1 September 1987. These specimens were entangled accidentally in bottom-set gillnets (called *Motha Valai*, in Tamil vernacular) set mainly for sharks. The net is made of thick (no. 7-12) nylon thread (monofilament). The stretched mesh size is 10–12 cm, and there are about 120 meshes from the head to the foot rope; hence the net is about 12 m deep. Total length of the net is about 800 m (~ one-half mile). Fishing operations, which were carried out mostly at night, were confined to the upper continental shelf, up to 4 km from the coast, to depths of 18–22 m. The dolphins became entangled in the nets both day and night.

All entangled dolphins were examined for external and internal parasites (several dolphins had internal parasites). No barnacles were found on the spinner dolphins. One small bottlenose dolphin (148 cm male) caught on 28 January 1985 had numerous *Xenobalanus globicipitis* attached (Fig. 1A, B). None of the four larger (>150 cm) bottlenose dolphins had any barnacles. All barnacles were collected (four from the left fluke, eight from the right fluke, and one from each flipper) and preserved in formalin. The barnacles were still alive after more than 12 hours out of water. Measurements to the nearest millimeter (Fig. 2) are given in Table 1.

In the sessile barnacles, extreme reduction of plates is found in *Xenobalanus*. The shell is thin, small, white, irregularly star-shaped, and vestigial, containing only the basal parts of the animal. Connected to this thin, star-shaped shell is a cylindrical, smooth, flexible, pedunclelike body (Fig. 3). At the distal end of this greatly elongated pseudopeduncle is a reflexed hood, which bears two stumpy outpushings or 'horns,' but terga and scuta are absent. Cirri, mouth, a probosciform penis, and associated organs project from the reflexed hood. The wall plates of this barnacle are embedded in the skin of the dolphin, with feeding appendages (cirri) and associated organs suspended by the long fleshy stalk. The body of *X. globicipitis* was dark-brown in live specimens, with a lighter colored hood; the penis was whitish.

Although belonging to the sessile group of the Cirripedia, this barnacle closely resembles stalked barnacles, especially *Conchoderma auritum* which is also found on cetaceans though never attached directly to the skin of its host. *Xenobalanus globicipitis* is always attached directly to the skin of its host (Pilsbry 1916, Barnard 1924). The resemblance is superficial, and is likely adaptive to being dragged through the water by the host. The closest affinities with *Xenobalanus* are the genera *Coronula*, *Platylepas*, and *Tubicinella* (Darwin 1854, Pope 1958).

The barnacles are found only around the rear margins of flippers and flukes. It is hypothesized that those that settle elsewhere are more easily swept off. A single immature barnacle (15 mm TL) was found attached to each flipper of the dolphin (Fig. 1A). All 12 mature barnacles (30–39 mm TL) (Table 1) were aggregated at the rear margin of the flukes (Fig. 1B). Pilsbry

Manuscript accepted 19 December 1991.
Fishery Bulletin, U.S. 90:197–202 (1992).

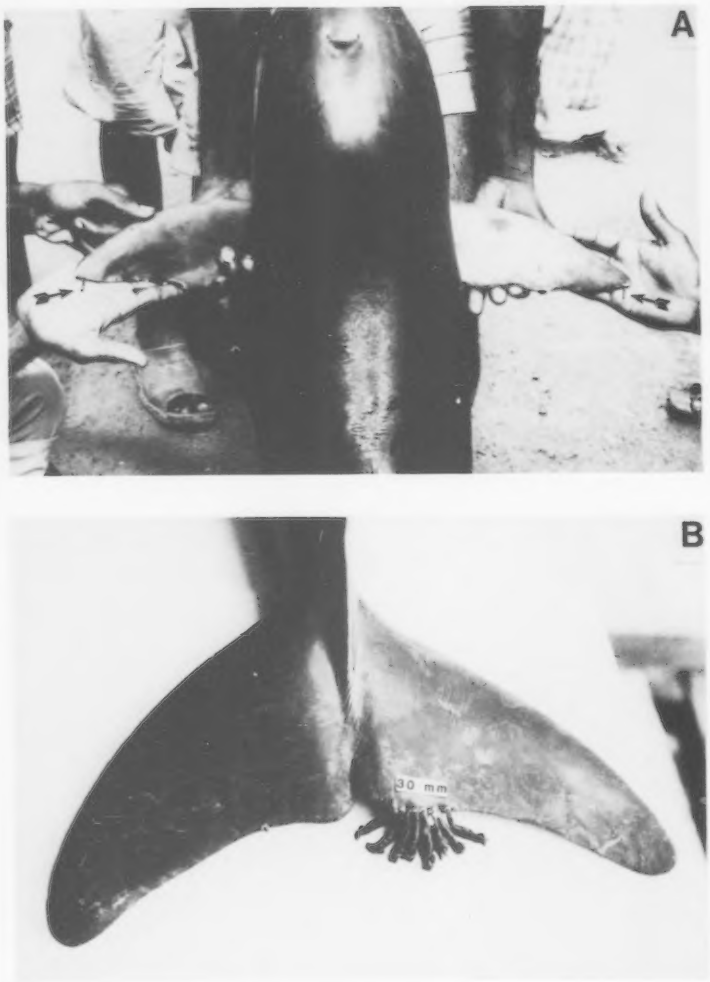

Figure 1
Sessile barnacles *Xenobalanus globicipitis* on a bottlenose dolphin *Tursiops truncatus*, caught in the Bay of Bengal, India. (A) Small barnacles on flippers. (B) Adult barnacles on tail flukes. Barnacles from the left fluke were removed prior to photographing; however, shell remnants are visible.

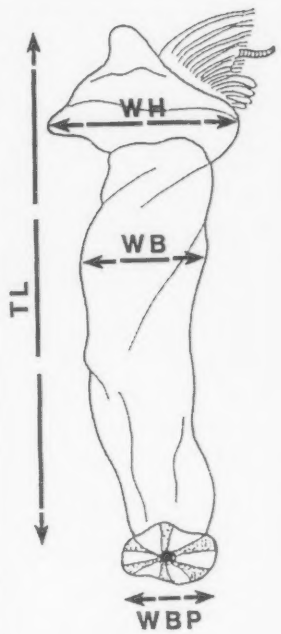

Figure 2
External measurements of the sessile barnacle *Xenobalanus globicipitis*. TL = total length, WB = width of body, WBP = width of basal plate, WH = width of hood.

(1916) reported that these barnacles grow in close groups. This aggregation permits cross-fertilization, which is common in hermaphroditic crustaceans (Barnes 1986).

Xenobalanus globicipitis occurs on about 19 species of cetaceans, from the small harbor porpoise *Phocoena phocoena* to the large blue whale *Balaenoptera musculus* (Table 2). The present record is the seventh report from a bottlenose dolphin. Six previous reports were from the central Atlantic coast of the United States (True 1891, Mead and Potter 1990), Gibraltar (Dollfus 1968, Pilleri 1970), and the east coast of South Africa (Barnard 1924, Ross 1984).

Based on a review of the literature, Rappé and Waerebeek (1988) suggested that *X. globicipitis* is an inhabitant of tropical and warm-temperate waters. They reported that occurrence of this species in the northeast Atlantic and Mediterranean is erratic, possibly related to sporadic incursions from adjacent tropical warm-temperate waters. Their information was based on only 23 reported localities. Our study shows 87 localities (Table 2) reported for *X. globicipitis*: 28 (32.2%) are located north of 40°N; 27 (31.0%) between 35° and 40°N; and 32 (36.8%) between 30°N and 30°S. From this it is clear that *X. globicipitis* is

Table 1

External measurements of the sessile barnacle *Xenobalanus globicipitis* collected from a bottlenose dolphin *Tursiops truncatus* (♂; 148 cm TL), entangled in a gillnet off Porto Novo, southeast coast of India, 28 January 1985

Attachment area	Specimen no.	TL	WH	WB	WBP
		(mm)			
Left fluke	1	37	11	7	5
	2	37	10	6	5
	3	37	11	6	5
	4	32	9	6	5
Right fluke	5	35	11	7	5
	6	30	11	7	5
	7	39	12	7	5
	8	35	12	7	5
	9	30	10	7	5
	10	34	11	8	8
	11	37	10	6	4
	12	30	9	6	5
Left flipper	13	15	5	3	3
Right flipper	14	15	4	3	3

Total length (TL): Basal plate to highest point of hood
Width of body (WB): Maximum width of elongated body
Width of basal plate (WBP): Maximum width of basal plate
Width of hood (WH): Maximum width of hood

a cosmopolitan species, occurring in temperate, warm-temperate, and tropical waters. In relation to the distribution of *X. globicipitis*, the bottlenose dolphin is distributed widely in temperate and tropical oceans. It is common from at least the north coast of Argentina to northern Norway (Kenney 1990).

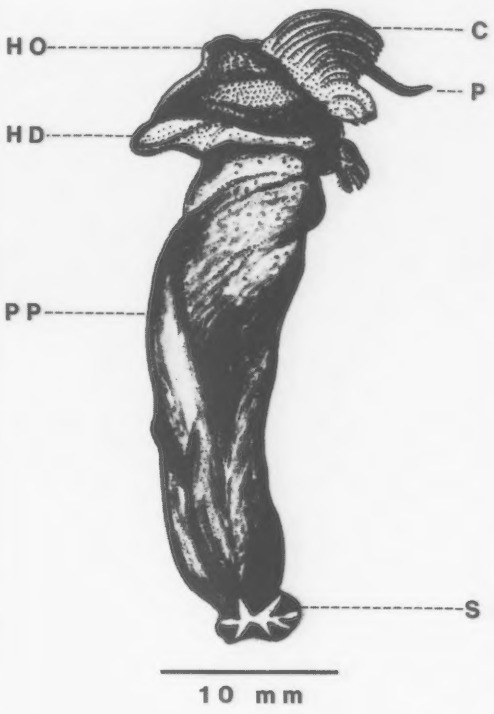

Figure 3

The sessile barnacle *Xenobalanus globicipitis*. C = cirri, HD = hood, HO = horn, P = penis, PP = pseudopeduncle, S = shell.

Table 2

Distribution and reported hosts of the sessile barnacle *Xenobalanus globicipitis*. Identification of host species names are updated.

Host	Reported by	Year	Locality
Order: Cetacea			
Suborder: Mysticeti			
Family: Balaenopteridae			
Balaenoptera borealis (Sei whale)	Broch	1924	Faröe Is., Greenland; Ingoy, Norway
	Cornwall	1927	Vancouver
	Nilsson-Cantell	1921	Faröe Is.
		1930	Saldanha Bay, S. Afr.
	Matthews	1938	Saldanha Bay
	Mackintosh	1942	Saldanha Bay
	Heldt	1950	Tunis
	Boxshall (in Rappé and Waerebeek)		Finnmark, Norway
Balaenoptera musculus (Blue whale)	Barnard	1924	Saldanha Bay
	Mackintosh and Wheeler	1929	South Africa
Balaenoptera musculus (Blue whale) (continued)	Nilsson-Cantell	1930	Saldanha Bay
	Mackintosh	1942	South Africa
	Cornwall	1955a	Pacific Canada
	Pike (in Cornwall)	1955b	No locality
	Boxshall (in Rappé and Waerebeek)		Shetland Is., Scotland
Balaenoptera physalus (Fin whale)	Calman	1920	Shetland Is.
	Barnard	1924	North Atlantic
	Barnard	1924	Antarctic
	Mackintosh and Wheeler	1929	South Africa
	Nilsson-Cantell	1930	S. Shetland Is.
	Nilsson-Cantell	1930	Saldanha Bay
	Mackintosh	1942	South Africa
	Raga and Sanpera	1986	Galicia, Spain

Table 2 (continued)

Host	Reported by	Year	Locality
Suborder: Odontoceti			
Family: Delphinidae			
Delphinus delphis (Common dolphin)	Hoek	1883	Atlantic
	Gruvel	1905	South Africa
	Gruvel	1920	South Africa
	Richard	1936	Oran, Algeria
	Stubbings	1965	Gorée, Senegal
	Pilleri	1970	W. Mediterranean
	Rappé	1988	Belgium
Grampus griseus (Risso's dolphin)	Gruvel	1920	Azores
	Richard	1936	Azores
	Richard	1936	Azores
	Pilleri and Gihr	1969	Barcelona, Spain
	Ross	1984	SE coast, S. Afr.
Sotalia sp. (Tucuxi)	Siciliano et al.	1988	Rio de Janeiro, Brazil
Stenella attenuata (Spotted dolphin)	Ross	1984	Mpelane, S. Afr.
Stenella coeruleoalba (Striped dolphin)	Raga et. al.	1982	Spanish coast, Medit. Sea
	Raga et. al.	1983	Spanish coast Medit. Sea
	Ross	1984	SE coast, S. Afr.
	Raga and Carbonell	1985	W. Mediterranean
	Boxshall (in Rappé and Waerebeek)		Mallorca
Stenella euphrosyne (Euphrosyne dolphin)	Pilleri	1970	Str. of Gilbraltar
Tursiops truncatus (Bottlenose dolphin)	True	1891	N. Carolina
	Dollfus	1968	Gibraltar
	Pilleri	1970	Gibraltar
	Present study	1985	Porto Novo, India
	Mead and Potter	1990	Central Atlantic coast, USA
	Ross	1984	Natal, S. Africa
	Barnard	1924	Natal, S. Africa
Unidentified delphinid	Pope	1958	Heron I., Queensl.
	Relini	1979	Ligurian Sea
Feresa attenuata (Pygmy killer whale)	Stubbings	1965	Yenn, Senegal
Globicephala macrorhynchus (Short-finned pilot whale)	Spivey	1977	Florida, Atlantic coast
Globicephala melas (Long-finned pilot whale)	Steenstrup	1852	Faröe Is.
	Hoek	1883	Faröe Is.
	Weltner	1897	Faröe Is.
	Gruvel	1912	Monaco
	Pilsbry	1916	Chesapeake Bay
	Gruvel	1920	Gibraltar
	Nilsson-Cantell	1921	Faröe Is.
	Richard	1936	Gibraltar
	Zullo	1963	Woods Hole
	Pilleri and Knuckey	1969	Spanish coast, Medit. Sea
	Kinze (in Rappé and Waerebeek)		Faröe Is.
	Raga et. al.	1983	Faröe Is.
	Pilsbry	1916	New England
Globicephalus sp.	Barnard	1924	North Atlantic
	Richard	1936	Mid-Atlantic
	Richard	1936	Baléares, Spain
Orcinus orca (Killer whale)	Gruvel	1920	Mediterranean
	Richard	1936	Monaco
	Richard	1936	Gibraltar
Pseudorca crassidens (False killer whale)	Gruvel	1912	Monaco
	Gruvel	1920	Miguel, Azores
	Richard	1936	Miguel, Azores
	Pilleri	1967	Spanish coast, Medit. Sea
Family: Phocoenidae			
Neophocaena phocaenoides (Finless black porpoise)	Devaraj and Bennet	1974	Karwar, India
Phocoena phocoena (Harbor porpoise)	Stubbings	1965	Hann, Senegal
Family: Ziphiidae			
Mesoplodon mirus (True's Beaked whale)	Ross	1984	SE coast, S. Afr.
Ziphius cavirostris (Goosebeaked whale [or] Cuvier's Beaked whale)	Bane and Zullo	1980	North Carolina
Unidentified whale	Broch	1924	Greenland
	Nilsson-Cantell	1930	W. Afr. (14°45′N; 18°34′W)
Unknown host	Nilsson-Cantell	1978	Bay of Biscay

Acknowledgments

Bruce B. Collette, Director, NMFS Systematics Laboratory, provided laboratory facilities and reviewed the manuscript, and the Fish Division, USNM, provided computer facilities. R. Natarajan and the authorities of Annamalai University, Tamil Nadu, India, provided facilities for this work. The senior author is grateful

to CSIR, New Delhi, for a Senior Research Fellowship for the Marine Mammal Project. William A. Newman verified the identification of *X. globicipitis*. Drafts of the manuscript were read by James G. Mead, William F. Perrin, and Austin B. Williams.

Citations

Bane, G.W., and V.A. Zullo
1980 (1981) Observations on a stranded goosebeaked whale (*Ziphius cavirostris*, Cuvier, 1823) and its ectocommensal barnacles (*Xenobalanus globicipitis*). J. Elisha Mitchell Sci. Soc. 96(1):1–3.

Barnard, K.H.
1924 Contributions to the crustacean fauna of South Africa. No. 7. Cirripedia. Ann. S. Afr. Mus. 20(1):1–103.

Barnes, R.D.
1986 Invertebrate zoology. W.B. Saunders, Philadelphia, 868 p.

Broch, Hj.
1924 Cirripedia Thoracica von Norwegen und dem norwegischen Nordmeere. Ein Systematik und biologischtiergeographische Studie. Skr. Vidensk. Selsk. Christiana, mat. naturv. KL, 17:1–121.

Calman, W.T.
1920 A whale-barnacle of the genus *Xenobalanus* from Antarctic seas. Ann. Mag. Nat. Hist., ser. 9, 6:165–166.

Cornwall, I.E.
1927 Some north Pacific whale barnacles. Contrib. Can. Biol. Fish., Toronto, new ser., 3(23):501–517.
1955a Cirripedia. Canada Pacific Fauna, Ottawa, fasc. 10C, 49 p.
1955b The barnacles of British Columbia. B.C. Prov. Mus., Handbk. 7:1–69.

Darwin, C.H.
1854 A monograph on the sub-class Cirripedia. II. The Balanidae, Verrucidae, etc. Ray Soc. Publ., 440 p.

Devaraj, M., and P.S. Bennet
1974 Occurrence of *Xenobalanus globicipitis* (Steenstrup) on the finless black porpoise, *Neomeris phocoenoides* in Indian seas. Indian J. Fish. 21(2):579–581.

Dollfus, R.Ph.
1968 *Xenobalanus globicipitis* Steenstrup (Cirripedia: Thoracica) recolté de la Côte Nord du Maroc. Bull. Inst. Pêches Marit. Maroc 16:55–60.

Gruvel, A.
1905 Monographie des Cirrhipèdes ou Thecostraces. Masson et Cie, Paris, 472 p.
1912 Sur le développement de la muraille chez le *Xenobalanus globicipitis* Steenstrup. C.R. Acad. Sci., Paris, 155: 1266–1268.
1920 Cirrhipèdes provenant des campagnes scientifiques de S.A.S. le Prince de Monaco (1885–1913). Rèsult. Campagnes Sci. accomp. sur son yacht par Albert I^{er}, Prince Souverain de Monaco, 53:1–88.

Heldt, J.H.
1950 Note au sujet de *Xenobalanus globicipitis* Steenstrup sur *Balaenoptera borealis* Lessou en Méditerranée. Bull. Soc. Hist. Nat. Tunis 3(1):25–28.

Hoek, P.P.C.
1883 Report on the Cirripedia collected by H.M.S. *Challenger* during years 1873–76. Rep. Sci. Res. Voyage H.M.S. *Challenger* 8(25):1–169.

Kenney, R.D.
1990 Bottlenose dolphins off the northeastern United States. *In* Leatherwood, S., and R.R. Reeves (eds.), The bottlenose dolphin, p. 369–386. Academic Press, San Diego.

Mackintosh, N.A.
1942 The southern stocks of whalebone whales. Discovery Rep. 22:199–298.

Mackintosh, N.A., and J.F.G. Wheeler
1929 Southern blue and fin whales. Discovery Rep. 1: 257–540.

Matthews, L.H.
1938 The sei whale, *Balaenoptera borealis*. Discovery Rep. 17:183–290.

Mead, J.G., and C.W. Potter
1990 Natural history of bottlenose dolphins along the central Atlantic coast of the United States. *In* Leatherwood, S., and R.R. Reeves (eds.), The bottlenose dolphin, p. 165–195. Academic Press, San Diego.

Nilsson-Cantell, C.A.
1921 Cirripeden-Studien. Zur Kenntnis der Biologie, Anatomie und Systematik dieser Gruppe. Zool. Bidr. Upps. 7:75–378.
1930 Thoracic cirripedes collected in 1925–27. Discovery Rep. 2:223–260.
1978 Cirripedia Thoracica and Acrothoracica. Marine Invertebrates of Scandinavia. Universistetes-forlaget, Oslo (5):1–135.

Pilleri, G.
1967 Behaviour of the *Pseudorca crassidens* (Owen) off the Spanish Mediterranean coasts. Rev. Suisse Zool. 74:679–683.
1970 *Xenobalanus globicipitis* Steenstrup on *Delphinus delphis*, *Stenella styx*, and *Tursiops truncatus* of the western Mediterranean. *In* Pilleri, G. (ed.), Investigations on cetacea, vol. II, p. 247–249. Hirnanatomisches Inst. der Univ., Berne, Switzerland.

Pilleri, G., and M. Gihr
1969 On the anatomy and behaviour of Risso's dolphin (*Grampus griseus* G. Cuvier). *In* Pilleri, G. (ed.), Investigations on cetacea, vol. I, p. 74–93. Hirnanatomisches Inst. der Univ., Berne, Switzerland.

Pilleri, G., and J. Knuckey
1969 Behaviour patterns of some Delphinidae observed in the western Mediterranean. Z. Tierpsychol. 26:48–72.

Pilsbry, H.A.
1916 The sessile barnacles (Cirripedia) contained in the collections of the U.S. National Museum, including a monograph of the American species. Bull. U.S. Nat. Mus. 93, 366 p.

Pope, E.C.
1958 The barnacle, *Xenobalanus globicipitis* Steenstrup in Australian Seas. Proc. R. Zool. Soc. N.S.W. 1956–57:159–161.

Raga, J.A., and E. Carbonell
1985 New dates about parasites on *Stenella coeruleoalba* (Meyen, 1833) (Cetacea: Delphinidae) in the western Mediterranean Sea. Invest. Cetacea 17:207–213.

Raga, J.A., and C. Sanpera
1986 Ectoparasitos y epizoitos de *Balaenoptera physalus* (L., 1758) en aguas atlanticas ibericas. Invest. Pesq. (Barcèlona) 50(4):489–498.

Raga, J.A., E. Carbonell, and M.A. Raduan
1982 Incidencias de parasitos en los cetaceos varados en las costas espanolas del Mediterraneo. Mem. Mus. Mar. Ser. Zool. 2(19):1–11.

Raga, J.A., M.A. Raduan, C. Blanco, and E. Carbonell
1983 Etude parasitologique du dauphin bleu et blanc *Stenella coeruleoalba* dans la Mediterranée occidentale. Rapp. P.-V. Reun. Comm. Int. Explor. Sci. Mer Medit. 28(5):211–212.

Rappé, G.
1988 Een vondst van *Xenobalanus globicipitis* in de Noordzee? Strandvlo 8(2):100–101.

Rappé, G., and K. van Waerebeek
1988 *Xenobalanus globicipitis* (Crustacea: Cirripedia) on cetaceans in the northeast Atlantic and the Mediterranean: A review. *In* Evans, P.G.H. (ed.), European research on cetaceans, p. 75–78. Proc., Second annual conf. European Cetacean Society, Troia, Portugal, 5–7 Feb. 1988. European Cetacean Society, Lisbon.

Relini, G.
1979 Remarks on cirripeds of Ligurian Sea. Rapp. Comm. Int. Mer. Médit. 25/26(4):131–132.

Richard, J.
1936 Notes sur les cétacés et les pinnipèdes. Result. Campagnes. Sci., Monaco 94:34–71.

Ross, G.J.B.
1984 The smaller cetaceans of the southeast coast of southern Africa. Ann. Cape Prov. Mus. Nat. Hist., 15(2):173–410.

Siciliano, S., L. Capistrano, and L. Lodi
1988 *Xenobalanus globicipitis* registrado em *Sotalia* sp. na bata de Guanabara - Rio de Janeiro - Brasil. Reunion Trabajo Especialistas Mamiferos Acuaticos, America del Sur, 25–30 de Julio. (Unpubl. Abstract #III-CL-36). Projeto Baleia, Jubarte, Rua José Higino 340, Ap. 102, Tijuca, Rio de Janiero, RJ 20520, Brazil.

Spivey, H.R.
1977 Those tenacious travelers of Florida's Atlantic coast. Fla. Nat. 50(6):6–10.

Steenstrup, J.
1852 Om *Xenobalanus globicipitis*, en ny Cirriped-Slaegt af Coronulafamilien. Vidensk. Medd. Naturhist. Foren. (1852): 62–64.

Stubbings, H.G.
1965 West African Cirripedia in the collections of the Institute Français d'Afrique Noire, Dakar, Senegal. Bull. Inst. Fr. Afr. Noire 27, ser. A (3):876–905.

True, F.W.
1891 Observations on the life history of the bottlenose porpoise. Proc. U.S. Nat. Mus. 13:197–203.

Weltner, W.
1897 Verzeichniss der bisher beschriebenen recenten Cirripeden Arten. Arch. Naturgesch. 63:227–280.

Zullo, V.A.
1963 A preliminary report on systematics and distribution of barnacles (Cirripedia) of the Cape Cod region. Publ. Mar. Biol. Lab., Woods Hole, 33 p.

Lack of biochemical genetic and morphometric evidence for discrete stocks of Northwest Atlantic herring *Clupea harengus harengus*

Susan E. Safford

U.S. Fish and Wildlife Service, P.O. Box 796 Turner's Falls, Massachusetts 01376
Present address: Graduate Center of Toxicology, 204 Funkhouser Building
University of Kentucky, Lexington, Kentucky 40506-0054

Henry Booke

U.S. Fish and Wildlife Service, P.O. Box 796, Turner's Falls, Massachusetts 01376

Historically, herring stock delineation has been based on spawning site because herring are presumed to return to their natal beds to spawn (Sindermann 1979). For example, Wheeler and Winters (1984) have estimated homing fidelity of spawning herring at 90%. Furthermore, some recognition of these historic stocks has been achieved through meristic studies (Anthony 1972, Parsons 1975, Cote et al. 1980), though these meristic differences disappear after several years, probably from environmental perturbations (Sindermann 1979). These means of defining a stock imply genetic differentiation, but do not measure it. A valid stock definition such as that in Booke (1981), "a species group, or population, of fish that maintains and sustains itself over time in a definable area," should include both genetic and geographic isolation. However, for managerial purposes it is often useful to divide large groups of a species into smaller groups, even if genetic or permanent geographic isolation cannot be demonstrated. Managerial units have sometimes been defined as stocks as in Anthony (1972), "a group of fish that remain sufficiently isolated so it can be managed as a unit separate from another one." A population can subdivide itself into discrete groups, which can be individually managed during the period of subdivision, such as a spawning season, even if these groups aren't genetically differentiated. Therefore, the goal of this study was to determine if the two spawning groups investigated constitute genetically differentiated stocks, and whether these groups could be identified either genotypically or phenotypically, regardless of stock status, outside the spawning grounds.

The first objective was to determine if herring which spawn in two geographically well-defined areas—Trinity Ledge, Nova Scotia, and Jeffries' Ledge, MA—constituted separate stocks through the demonstration of genetic differentiation by starch gel electrophoresis of enzymes. Electrophoretic studies on herring, including specimens from the two spawning grounds sampled in the present study, have been published (Kornfield et al. 1981 and 1982, Grant 1981 and 1984, King 1984). However, lack of standardization in technique, which has led to differences in the number and frequency of alleles at the same locus in different studies, makes it difficult to assess the true amount of electrophoretic differentiation among spawning groups. The second objective was to determine if these same groups of herring were separable phenotypically, whether or not genetic differences were detected. Included in this objective was the assessment of the temporal stability of a set of phenotypic characters measured over two years. This was important, as most morphometric and meristic studies which have indicated that significant phenotypic differences do exist between spawning groups of herring consist of only one year's data (Parsons 1975, Cote et al. 1980, Meng and Stocker 1984). The third and most important objective was to simultaneously measure the amount of electrophoretic and morphometric variation in the two spawning groups. Simultaneous performance of both kinds of analyses, previously done only by Ryman et al. (1984) on Northeast Atlantic herring, permits a better understanding of the level of variation between herring spawning groups.

Materials and methods

Sampling

Trinity Ledge (TL) fish were collected on 31 August 1983 and 5 September 1984, and Jeffries' Ledge (JL) fish on 1 November 1983 and 11 October 1984. All fish were taken on spawning grounds (Fig. 1) by commercial fishermen. The fish were transported frozen or packed in ice, and stored at −20°C for 1 week to 9 months until white muscle tissue samples were excised. The tissue samples were stored at −80°C until analyzed electrophoretically. A sample of 100 fish from each collection (400 total) was analyzed electrophoretically. These same fish were also analyzed morphometrically, except for 50 TL fish collected in 1983. Poor packing conditions made these 50 fish difficult

Manuscript accepted 23 September 1991.
Fishery Bulletin, U.S. 90:203–210 (1992).

to measure accurately, so an additional 50 herring were taken from the remaining TL 1983 sample for the morphometric analysis.

Morphometrics

Measurements Initially, 25 morphometric characters described by Meng and Stocker (1984) in their analysis of Pacific herring were measured on 100 Atlantic herring, 50 from each location, from the 1983 sample. The measurements followed Hubbs and Lagler (1958). Standard length (SL) was measured to the nearest 0.5 mm on a measuring board. The other measurements were taken with vernier calipers to the nearest thousandth of an inch and converted to millimeters. Multivariate analyses were used to determine if the groups were different from one another and which characters contributed to these differences. To address length bias, multiple analysis of covariance, performed under the MANOVA subroutine in the statistical package for the social sciences, was used to remove the effect of SL on the other variables (Sokal and Rohlf 1969, Steel and Torrie 1980). The results of multiple analysis of variance of the adjusted measurements versus spawning group, performed under the same subroutine, showed that the two groups were significantly different from each other and identified eight characters whose means were significantly different (Snedecor and Cochran 1967, Safford 1985) (Fig. 2). The binomial distribution predicted the probability of eight significant characters out of 25 as 1.77×10^{-5}, given a probability of 0.05 that a single character would be significantly different due to chance alone.

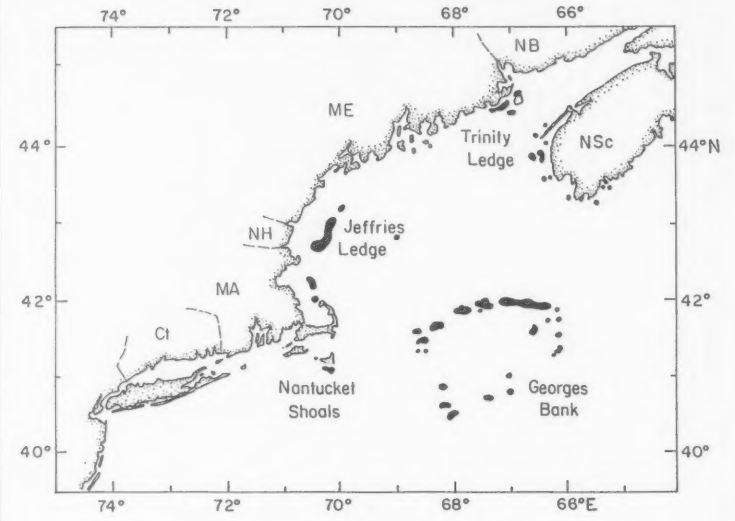

Figure 1
Atlantic herring spawning grounds in the Gulf of Maine region.

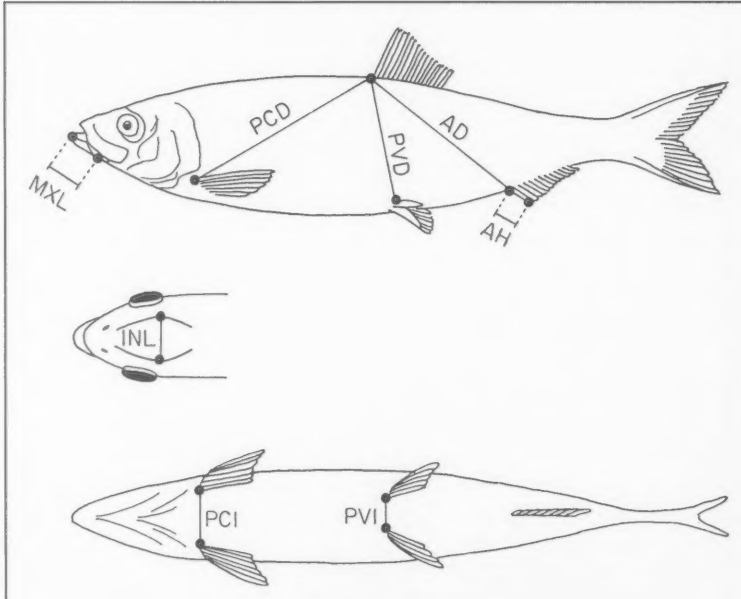

Figure 2
Eight morphometric measurements used to derive the discriminant function: MXL = maxillary length; PCD = pectoral to dorsal fin; PVD = pelvic to dorsal fin; AD = anal to dorsal fin; AH = anal fin height; INL = interorbital distance; PCI = distance between insertions of pelvic fins; PVI = distance between insertions of pectoral fins.

Discriminant function These eight characters were used to derive a discriminant function (Snedecor and Cochran 1967, Sokal and Rohlf 1969). Each measurement in subsequent samples was adjusted to the SL of the original sample to eliminate bias due to differences in the SL. Details of the construct of the discriminant function and the formulae used to adjust the subsequent measures can be found in Appendix A and Safford (1985).

The discriminant function was tested for spatial and temporal stability with additional samples from both 1983 and 1984. The additional sample data were treated as described in Appendix A to yield a z-score so the fish could be classified according to spawning group. The cut-off value for the z-score was set at zero, where fish with a z-score >0 were classified as Trinity Ledge fish and those with a z-score ≤ 0 were classified as Jeffries' Ledge fish (Norusis 1979, Safford 1985).

Table 1
Means (mm), unadjusted for standard length, and 95% confidence intervals of the eight morphometric characters used in the discriminant function derived from 100 Atlantic herring from the 1983 samples.

Character	Jeffries' Ledge (n 50)	Trinity Ledge (n 50)
Maxillary length (MXL)	27.90±0.57	31.06±0.51
Pectoral to dorsal fin (PCD)	81.46±1.98	93.44±1.82
Pelvic to dorsal fin (PVD)	48.41±1.53	59.43±1.63
Anal to dorsal fin (AD)	70.56±1.88	79.62±1.59
Height of anal fin (AH)	14.35±0.59	13.13±0.47
Interorbital distance (INL)	10.34±0.31	10.10±0.25
Distance between insertions of pectoral fins (PCI)	13.16±0.49	17.37±0.71
Distance between insertions of pelvic fins (PVI)	8.41±0.31	10.63±0.35
Standard length (SL)	233.50±18.03	251.50±14.19

Statistics A stepwise function employing the F-value of each character, ($p<0.05$), to accept or reject a character was derived to rank the variables. The distribution of phenotypic variation was measured by a nested analysis of variance (ANOVA), with years nested within groups, generated by nested procedures using PC-SAS packaged programs (SAS 1985). One-way ANOVA generated by the general linear models procedure in PC-SAS packaged programs (SAS 1985) was used to analyze differences in morphometric measurements, both between years within a spawning group and between spawning groups within a year.

Electrophoresis

Enzyme visualization Traditional starch gel electrophoresis of white muscle tissue samples as described by Utter et al. (1974), with some modifications, was used to resolve the enzymes. A detailed description of the gel composition and running conditions can be found in Safford (1985). Four polymorphic loci—phosphoglucomutase, *PGM-2** (5.4.2.2), glucose-6-phosphate isomerase, *GPI-2** (5.3.1.9), and two of lactate dehydrogenase, *LDH-1** and *LDH-2** (1.1.1.27)—were analyzed. The enzyme abbreviations and numbers follow the suggestions of Shaklee et al. (1989). Two buffer systems, Ridgway et al. (1970) and Markert and Faulhaber (1965), were used. The Ridgway gel buffer, used for LDH and GPI, was modified by doubling the amount of Tris (Sigma Chemical Co., St. Louis) in the recipe, which raised the pH to 8.5 and made the bands more distinct. The Markert-Faulhaber buffer was used for PGM because it improved band resolution. Stain recipes and techniques followed Shaw and Prasad (1970) with modifications which are detailed in Safford (1985). Photographs were taken immediately upon staining.

Statistics Allelic frequencies were compared between samples by chi-square contingency table analysis. Genotypic frequencies were tested for conformation to the Castle-Hardy-Weinberg (C-H-W) equilibrium with a chi-square goodness-of-fit test (Zar 1974). Gene diversity analyses were conducted according to Nei (1973), Chakraborty (1980), and Chakraborty et al. (1982).

Results

Morphometrics

Group means of eight morphometric characters were found to be significantly different ($p<0.01$) between samples taken from the two spawning areas in 1983. No overlap in range was found within the 95% confidence interval for seven of these variables, and overlap at the eighth variable was very small (Table 1). Therefore, it was concluded for this study that 50 fish from each sample were sufficient. The stepwise discriminant function accepted the first seven of these eight variables. Multiple analysis of variance of the eight characters versus locality for the 1984 samples revealed that only three of these characters—distance between insertions of the pelvic and dorsal fins (PVD), anal fin height (AH), and distance between the insertions of the pectoral fins (PCI)— were significantly different ($p<0.01$) between the two groups. Two of these characters, PVD and PCI, were among the three which

Table 2

Discriminant function analysis results of different Atlantic herring samples from known spawning grounds.

Sample	Number from each spawning ground classified as:		Percent from each spawning ground classified as:		Overall correct classification
	Jeffries' Ledge	Trinity Ledge	Jeffries' Ledge	Trinity Ledge	
1983 discriminant function construction sample ($N=N_1+N_2=100$)					
Jeffries' Ledge ($N_1=50$)	44	6	88%	12%	
Trinity Ledge ($N_2=50$)	7	43	14%	86%	87%
1983 Sample ($N=N_1+N_2=100$)					
Jeffries' Ledge ($N_1=50$)	38	12	76%	24%	
Trinity Ledge ($N_2=50$)	11	39	22%	78%	77%
1984 Sample ($N=N_1+N_2=198$)					
Jeffries' Ledge ($N_1=99$)	92	7	93%	7%	
Trinity Ledge ($N_2=99$)	84	15	85%	15%	54%

Table 3

Phenotypic variation of Atlantic herring in geographic and temporal hierarchies for each of eight morphometric characters. (*)$p \leq 0.01$; (+)$p \leq 0.001$. See Figure 2 for definitions of morphometric characters.

Source of variation:	Between spawning groups			Between years within a spawning group			Within samples		
Character	df	mean square	variance component (%)	df	mean square	variance component (%)	df	mean square	variance component (%)
MXL	1	120.3+	0.0	2	597.3+	59.0	390	4.2	41.0
AH	1	38.2*	0.7	2	29.0*	3.3	390	6.6	96.0
PCD	1	2136.1+	0.7	2	7778.3+	58.5	390	55.7	41.5
PVD	1	2655.8+	0.7	2	4483.7+	57.1	390	34.0	42.9
AD	1	1379.7	0.0	2	4475.3	53.4	390	41.9	46.6
INL	1	0.0	0.0	2	131.0+	63.6	390	0.6	36.4
PCI	1	282.3+	0.0	2	383.9+	46.5	390	4.4	53.5
PVI	1	45.8+	0.0	2	136.2+	46.3	390	1.6	53.7

accounted for most of the between-group variation in the 1983 sample. The percent correct classification by spawning group of three sets of samples (two from 1983, one from 1984) separated by the derived discriminant function is found in Table 2. Overall misclassification of fish collected in 1983 was 18%, while that of fish collected in 1984 was 46%.

The phenotypic variation of the unadjusted measurements was partitioned similarly within each morphometric character, except AH (Table 3). The partitioning of the phenotypic variation averaged across all characters is found in Table 4. None of the variation was explained by differences between spawning groups, while approximately one-half was partitioned within a spawning group between years. The remainder of the variation was within a sample. One-way ANOVA of between-year differences within a spawning group showed that within the TL group the means of all the characters, except AH ($p \leq 0.02$), were highly significantly different ($p \leq 0.0001$) between 1983 and 1984. In contrast, within the JL group three characters—distance between the insertions of the pelvic fins (PVI), AH, and PCI—were not significantly different between years. The remaining characters were significantly different ($p \leq .05$) between years.

Electrophoresis

Allelic frequencies within each sample for the four loci chosen for analysis are found in Table 5. Other enzyme systems were also investigated, but few specimens expressed enzyme activity at these loci (Safford 1985). We chose these loci because they had previously been shown to be polymorphic and to follow Mendelian in-

heritance in herring (Grant 1981, Kornfield et al. 1981 and 1982, King 1984). The designation of alleles is taken from Kornfield et al. (1982) and is based on direction of migration of the enzymes on the gel and their distance from the origin. *LDH** is encoded by three anodally migrating loci. The fastest locus, *LDH-3**, was present only in eye tissue and activity was found in only some of the fish, so this locus was not used in the present analysis. Each of the other two loci were represented by two alleles. *PGM** is encoded by two anodally migrating loci. The slower locus, *PGM-1**, was fixed for the same allele in all samples. The polymorphic locus, *PGM-2**, was represented by three alleles. However, the slowest allele was found in only one specimen. *GPI** is encoded by one anodally migrating locus, *GPI-2**, which was represented by five alleles in our samples.

Chi-square contingency table analysis revealed that *GPI-2** was significantly different ($p \leq 0.05$) between JL 1984 and both TL 1984 and JL 1983. This was probably due to a greater frequency of allele 150 in the JL 1984 sample. Its frequency was double (0.18) that found in the JL 1983 sample (0.09) and the TL 1984 sample (0.10). The chi-square goodness-of-fit test showed that the JL 1984 sample was not in C-H-W equilibrium at the *GPI-2** locus, which contained an excess of 150/−3 heterozygotes. The gene-diversity analysis results for the individual loci were similar within each locus, and revealed that more than 99% of the genetic diversity was found within a single sample. A comparison between the partitioning of the average gene diversity and the average phenotypic variation is shown in Table 4. The large between-year phenotypic variation is not reflected in the between-year genetic diversity index, as <1% of the gene diversity can be explained by between-year differences within a spawning group.

Discussion

In-depth discussions of the historical construct of herring stocks and the implications of recent electrophoretic findings can be found in Jorstad and Naevdal (1981), Smith and Jamieson (1986), and Kornfield and Bogdanowicz (1987). The traditional herring stock construct has not been supported by genetic stock structure analyses as none of the electrophoretic studies, including the present one, have found a large amount of genetic differentiation (Andersson et al. 1981, Grant 1981 and 1984, Jorstad and Naevdal 1981 and 1983,

Table 4

Distribution of relative gene diversity and phenotypic variation of Atlantic herring in geographic and temporal hierarchies. Gene diversity is based on four individual or pooled samples and four polymorphic loci. Phenotypic variation is averaged over 393 individuals, four individual or pooled samples, and eight morphometric characters.

	Gene diversity		Phenotypic variation		
Source of variation	Absolute	%	df	Mean square	Variance component (%)
Between spawning groups	0.00024	0.1	1	823.28	0.09
Between years within spawning groups	0.00074	0.4	2	2289.34	48.46
Within samples	0.20138	99.5	390	18.63	51.45

Table 5

Allelic frequencies of samples of Atlantic herring.

	Loci and alleles											
	LDH-1		*LDH-2*		*PGM-2*			*GPI-2*				
Location/Year	*100	0	100	72	112	100	95	150	100	40	−3	−75
Jeffries' Ledge (*N*)												
1983 (100)	0.980	0.020	0.955	0.045	0.025	0.975	0	0.090	0.630	0.140	0.120	0.020
1984 (100)	0.985	0.015	0.955	0.045	0.055	0.945	0	0.180	0.540	0.105	0.160	0.015
Trinity Ledge (*N*)												
1983 (100)	0.965	0.035	0.955	0.045	0.065	0.925	0.005	0.110	0.560	0.210	0.115	0.005
1984 (100)	1.000	0	0.945	0.055	0.025	0.975	0	0.100	0.630	0.120	0.130	0.020

* Allelic designations indicate direction of migration (+ anodal, − cathodal), and relative distance from origin (the farther away, the larger the number).

Kornfield et al. 1982, King 1984, Ryman et al. 1984). The conclusion that herring spawning groups are not discrete genetically-distinct stocks is further supported by the results of a recent study by Kornfield and Bogdanowicz (1987). They investigated the genetic relationships of ripe female herring from three locations, including Jeffries' Ledge and some of the 1983 Trinity Ledge samples analyzed in this study, by restriction endonuclease analysis of mitochondrial DNA (mtDNA). In other species, this technique has revealed genetic differentiation not uncovered by traditional enzyme electrophoresis (Avise et al. 1986). Kornfield and Bogdanowicz (1987) found that these spawning groups were not completely distinguished by the composite mtDNA digestion patterns generated, and no consistent geographic patterns were found for the unique composites. Therefore, they concluded that this approach also provided no evidence for the existence of genetically distinct stocks in the Gulf of Maine.

The significant departures from C-H-W equilibrium found in this and previous studies (Grant 1981, Ryman et al. 1984) may be considered contradictory to the hypothesis of the existence of a genetically homogenous herring population. However, these departures seem to be a feature of pelagic fish stocks (Smith et al. 1989). These disequilibria have been variously attributed to chance due to the low frequency of occurrence (Grant 1981, Ryman et al. 1984) and assortative mating (Smith et al. 1989). The significant departure in the present data has derived from an excess number of heterozygotes of one particular allelic combination in the JL 1984 data. One significant departure in 16 tests is slightly higher than would be expected by chance alone at the 5% probability level. An excess of heterozygotes can result from negative assortative mating; however, the data are not sufficient to support that hypothesis. Importantly, the C-H-W equilibrium applies to all generations in a population, thus significant departures may occur if sampling does not measure all generations in the same proportion in which they occur in the population. Based on SL, few immature and old fish were included, so this sample bias may have contributed to the significance level. Thus, the departure from C-H-W equilibrium is probably due to chance and perhaps some sampling bias. However, the distribution of alleles across generations within a population may warrant further investigation as disequilibrium, though explicable, is a feature of herring populations and some age-based selection may be occurring.

Although the genetic evidence argues for a single population of herring, significant phenotypic differences between spawning groups have been demonstrated (Parrish and Saville 1965, Burd 1969, Anthony 1972, Cote et al. 1980, Ryman et al. 1984). Morphometric and meristic characters, which have a complex underlying genetic structure, are believed to be greatly influenced by environmental parameters (Sindermann 1979, Ryman et al. 1984). Thus phenotypic differences may not reflect genetic differentiation, and small but detectable genetic differences may not significantly alter phenotypic characters. Differences in biochemical genetic and phenotypic variation can best be demonstrated when genetic and phenotypic analyses are performed on the same specimens. In their study, Ryman et al. (1984) screened 17 loci from herring caught in 17 locations ranging from the Gulf of Bothnia to the northeast Atlantic off Norway's western coast, and found significant allelic heterogeneity at only 4 loci. They concluded that the results resembled those of samples drawn from a single breeding population, as both the genetic diversity index and genetic distances were very small. They chose numbers of vertebrae and keeled scales as morphological characters. Morphological distances were used to construct a dendogram which differentiated herring in central Baltic fall spawning groups from a spring spawning Baltic group and the other fall spawning groups. Thus these meristic characters differed to some extent despite genetic similarities. Morphologic variation was partitioned by nested ANOVA with localities nested within larger geographic areas, and genetic variation was partitioned by genetic diversity analysis. They found over 99% of the gene diversity within a locality, compared with 50% of the phenotypic variation. Most important, $<1\%$ of the gene diversity was explained by between-geographic-group differences, while these differences explained 40% of the phenotypic variation.

The partitioning of variance in our samples was similar in many respects to that of Ryman et al. (1984). Over 99% of the genetic variance in our samples also occurred within a locality within a year, compared with approximately 50% of the morphometric variance component. However, the percent of the morphometric variance component explained by differences between spawning groups was similar for both the genetic and morphometric components (0.1%), in contrast to the large between-group morphometric variation found by Ryman et al. (1984). Results from both these studies demonstrate that most genetic diversity lies within a single locality at one point in time, further supporting the hypothesis that herring form a single panmictic population. Thus the current situation seems to be that despite the existence of discrete, defined spawning groups and apparent high homing fidelity, enough gene flow exists between spawning groups to prevent Northwest Atlantic herring from evolving into genetically distinct stocks. Alternatively, herring may have begun this process in recent geographic time, so that genetic differences have not had time to evolve. This lack of genetic differentiation also means that observed

phenotypic differences are most likely due primarily to differences in environmental conditions during development, and therefore will not be reliable indicators of stock identity. Further, if all measurable phenotypic characters are distributed similarly to those in the present study and Ryman et al. (1984), then the use of phenotypic characters to distinguish herring groups may be proscribed, as the large within-group variation would mask the subtler between-group differences.

These ideas need to be incorporated into current herring management policy. The results show that individuals from discrete spawning groups can not be reliably identified off the spawning grounds. Therefore, the contribution of each spawning group to various fisheries cannot be estimated. These results also suggest that the demise of a single spawning ground will not adversely affect the underlying genetic structure of the herring population, as few unique genes should be found exclusively within a spawning location. However, small discrete spawning grounds are apparently necessary to support a large population. Small spawning grounds may be necessary for appropriate spawning behavior or to ensure proper conditions for the larvae. Therefore, until the relationship between discrete spawning grounds and a healthy herring population is understood, management policy should include the maintenance of existing spawning grounds.

Acknowledgments

The authors thank Pamela Mace (Fisheries and Oceans, Canada) and the captain and crew of the FV *Barnegat* (Gloucester, MA) for field collection assistance, as well as three anonymous reviewers whose comments strengthened the paper. This work was supported by a two-year stipend to S. Safford from the Massachusetts Division of Marine Fisheries and additional funds from the Massachusetts Division of Fisheries and Wildlife and The Masssachusetts Co-operative Research Unit of Fisheries and Wildlife Biology.

Citations

Andersson, L., N. Ryman, R. Rosenberg, and G. Stahl
1981 Genetic variability in Atlantic herring (*Clupea harengus harengus*): Description of protein loci and population data. Hereditas 95:69–73.

Anthony, V.
1972 Population dynamics of the Atlantic herring in the Gulf of Maine. Ph.D. diss., Univ. Wash., Seattle, 266 p.

Avise, J.C., G.S. Helfman, N.C. Saunders, and L.S. Hales
1986 Mitochondrial DNA differentiation in North Atlantic eels: Population consequences of an unusual life history pattern. Proc. Natl. Acad. Sci. 83:4350–4354.

Booke, H.E.
1981 The conundrum of the stock concept—Are nature and nurture definable in fishery science? Can. J. Fish. Aquat. Sci. 38:1479–1480.

Burd, A.C.
1969 Trials with principal component analysis for herring racial studies. Int. Counc. Explor. Sea CM 1969/30, Pelagic Fish Comm., 11 p.

Chakraborty, R.
1980 Gene-diversity analysis in nested subdivided populations. Genetics 96:721–726.

Chakraborty, R., M. Haag, N. Ryman, and G. Stahl
1982 Hierarchical gene diversity analysis and its application to brown trout population data. Hereditas 97:17–21.

Cote, G., P. Lamoureux, J. Boulva, and G. Lacroix
1980 Separation des populations de hareng de l'Atlantique (*Clupea harengus harengus*) de l'estuaire du Saint-Laurent et de la peninsule gaspienne. Can. J. Fish. Aquat. Sci. 37:66–71.

Grant, W.S.
1981 Biochemical genetic variation, population structure, and evolution of Atlantic and Pacific herring. Ph.D. diss., Univ. Wash., Seattle, 135 p.
1984 Biochemical population genetics of Atlantic herring, *Clupea harengus*. Copeia 1984(2):357–364.

Hubbs, C., and K. Lagler
1958 Fishes of the Great Lakes region. Bull. 26, Cranbrook Inst. Sci., Bloomfield Hills, MI, 186 p.

Jorstad, K., and G. Naevdal
1981 Significance of population genetics on management of herring stocks. Int. Counc. Explor. Sea CM 1981/4:64.

Jorstad, K.E., and G. Naevdal
1983 Genetically distinct populations of herring. Contrib. XV Int. Cong. Genetics, New Delhi, India.

King, D.P.F.
1984 Genetic analysis of enzyme polymorphisms in herring. Heredity 52:121–131.

Kornfield, I., and S.M. Bogdanowicz
1987 Differentiation of mitochondrial DNA in Atlantic herring, *Clupea harengus*. Fish. Bull., U.S. 85(3):561–568.

Kornfield, I., P. Gagnon, and B. Sidell
1981 Inheritance of allozymes in Atlantic herring. Can. J. Genet. Cytol. 23:715–720.

Kornfield, I., B. Sidell, and P. Gagnon
1982 Stock definition in Atlantic herring: Genetic evidence for discrete fall and spring spawning populations. Can. J. Fish. Aquat. Sci. 39:1610–1621.

Markert, C.L., and I. Faulhaber
1965 Lactate dehydrogenase patterns in fish. J. Exp. Zool. 159:319–332.

Meng, H.J., and M. Stocker
1984 An evaluation of morphometrics and meristics for stock separation of Pacific herring (*Clupea harengus pallasi*). Can. J. Fish. Aquat. Sci. 41:414–422.

Nei, M.
1973 Analysis of gene diversity in subdivided populations. Proc. Natl. Acad. Sci. 70(12)Pt. I:3321–3323.

Norusis, M.J.
1979 SPSS. Statistical algorithms. Release 8.0. SPSS, Inc., Chicago.

Parrish, B.B., and A. Saville
1965 The biology of the Northeast Atlantic herring populations. Oceanogr. Mar. Biol. Annu. Rev. 3:323–373.

Parsons, L.S.
1975 Morphometric variation in Atlantic herring from Newfoundland and adjacent waters. Int. Comm. Northwest Atl. Fish. Res. Doc. 11:73–92.

Ridgway, G.J., S.W. Sherburne, and R.P. Lewis
1970 Polymorphism in the esterases of Atlantic herring. Trans. Am. Fish. Soc. 99(1):147–151.
Ryman, N., U. Lagercrantz, I. Andersson, R. Chakraborty, and R. Rosenberg
1984 Lack of correspondence between genetic and morphological variability patterns in Atlantic herring (*Clupea harengus*). Heredity (53)3:687–704.
Safford, S.E.
1985 Stock identification through electrophoretic and morphometric analyses of two spawning populations of Northwest Atlantic herring (*Clupea harengus harengus*, Linnaeus). Master's thesis, Univ. Mass., Amherst, 111 p.
SAS
1985 SAS/STAT guide for personal computers, Version 6 Ed. SAS Inst., Inc., Cary, NC.
Shaklee, J.B., F.W. Allendorf, D.C. Morizot, and G.S. Whitt
1989 Genetic nomenclature for protein-coding loci in fish: Proposed guidelines. Trans. Am. Fish. Soc. 118:218–227.
Shaw, C.R., and R. Prasad
1970 Starch gel electrophoresis of enzymes: A compilation of recipes. Biochem. Genet. 4:297–320.
Sindermann, C.J.
1979 Status of Northwest Atlantic herring stocks of concern to the United States. Tech. Ser. Rep. 23, Sandy Hook Lab., NMFS, NOAA, Highlands, NJ, 449 p.
Smith, P.J., and A. Jamieson
1986 Stock discreteness in herrings: A conceptual revolution. Fish. Res. 4:223–234.
Smith, P.J., A.J. Birley, and A. Jamieson
1989 Electrophoretic studies and the stock concept in marine fishes. J. Fish. Biol. 35(Suppl. A):345–346.
Snedecor, G.W., and W.G. Cochran
1967 Statistical methods, 6th ed. Iowa State Univ. Press, Ames, 593 p.
Sokal, R.R., and F.J. Rohlf
1969 Biometry. W.H. Freeman, San Francisco, 776 p.
Steel, R.G.D., and J.H. Torrie
1980 Principles and procedures of statistics, biometrical approach, 2d ed. McGraw-Hill, NY.
Utter, F.M., H.O. Hodgins, and F.W. Allendorf
1974 Biochemical genetic studies of fishes: Potentialities and limitations. *In* Malins, D.C., and J.R. Sargent (eds.), Biochemical and biophysical perspectives in marine biology, Vol. 1, p. 213–238. Academic Press, NY.
Wheeler, J.P., and G.H. Winters
1984 Homing of Atlantic herring in Newfoundland waters as indicated by tagging data. Can. J. Fish. Aquat. Sci. 41: 108–117.
Zar, J.H.
1974 Biostatistical analysis. Prentice-Hall, Englewood Cliffs, NJ, 620 p.

Appendix A

The values of the eight morphometric characters were linearly combined to form a single value, a z-score, which was used to classify an individual into a group (Sokal and Rohlf 1969, Norusis 1979). The general formula for a z-score is

$$Z = C1X1 + C2X2 + \ldots + CnXn + e$$

where each C is the unstandardized canonical discriminant function coefficient for each character (Norusis 1979).

The general formula used to adjust each measurement was

$$R_v = Vn - b_o - b_i * SL$$

where R_v = adjusted measure,
V_n = original measure,
b_o = intercept,
b_i = slope of the univariate covariance equation, with
SL = 242.5 (mean SL of original sample).

Variability of monthly catches of anchovy *Engraulis encrasicolus* in the Aegean Sea

Konstantinos I. Stergiou
National Centre for Marine Research
Agios Kosmas, Hellinikon, Athens 16604, Hellas

In a recent paper, Stergiou (1990a) showed that the autoregressive terms of an ARIMA model describing the monthly fishery of the anchovy *Engraulis encrasicolus* in Hellenic waters indicated a 2- to 3-year periodicity in catches. A similar cycle has also been shown for anchovy in the Azov (Dementʼeva 1987) and Adriatic Seas (S. Regner 1985). In comparison, long-term periodicities have been shown for *Engraulis mordax* off California (Soutar and Isaacs 1974). In this present study, I examined the variability of the Hellenic monthly catches of anchovy during the period 1964–87 using spectral analysis.

The purse-seine fishery landed 51,282 t of fish which comprised 49% of the total Hellenic catch in 1987 (Stergiou 1990b). Anchovy comprised 46.6% of the 1987 purse-seine catch; the remainder included sardine *Sardina pilchardus*, horse mackerel *Trachurus* sp., bogue *Boops boops*, chub mackerel *Scomber japonicus*, and bonito *Sarda sarda* (Stergiou 1990b). Ninety percent of the mean annual anchovy catch (1964–85) was caught in the northern, northwestern, and western Aegean Sea (Stergiou unpubl. data; no data are available for monthly catches per major fishing area). A recent study of genetic distances, based on electrophoretic variation, and of morphometric and meristic characters using multivariate analysis does not indicate separate stocks of anchovy (or sardine) in the Aegean Sea (Spanakis et al. 1989).

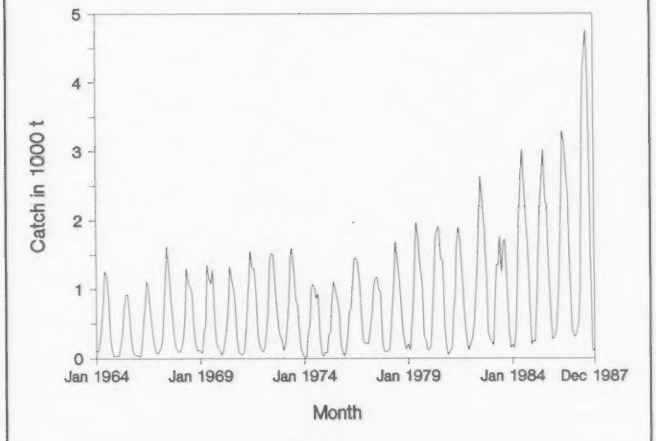

Figure 1
Monthly commercial catches (in 1000 tons) of anchovy *Engraulis encrasicolus* in Hellenic waters, 1964–87.

Monthly catches of anchovy (1964–87, 288 data points) and annual fishing effort (in horsepower, HP) of pelagic seiners were gathered from the Bulletins of the Hellenic National Statistical Service (1968–89). The monthly series was log-transformed and detrended to become stationary. The seasonal component was removed by differencing with lag = 12 (Chatfield 1984). To avoid a discontinuity at the end of the data, the resulting series was tapered by 20%. The Fast Fourier Transform was used to compute power spectral estimates, and smoothed (5 moving averages) squared amplitudes of the sinusoids were plotted.

Anchovy catches show a marked seasonal pattern (Fig. 1) and an increasing trend for the years following 1980. The increased trend in catch in recent years has raised concern about whether these high catches are sustainable. Due to higher prices of anchovy since the late 1970s, purse-seine fishing in Hellenic waters is anchovy-oriented rather than sardine-oriented (Stergiou 1986a, 1990a, b). Monthly fishing effort by pelagic seiners is not available. However, annual fishing effort of pelagic seiners increased considerably between 1964 and 1987 (from 363 boats, 20,316 HP, and 6152 tonnage of boats, to 502 boats, 112,310 HP, and 18,922 tonnage of boats; Hellenic Natl. Stat. Serv., 1968–89). Annual catches of anchovy are highly positively correlated with annual horsepower of the pelagic seiners [Ln(annual catch) = 8.25 + 0.000013HP; n 24, r + 0.89, $p < 0.001$) (Fig. 2), indicating that the highly significant linear

Manuscript accepted 26 July 1991.
Fishery Bulletin, U.S. 90:211–215 (1992).

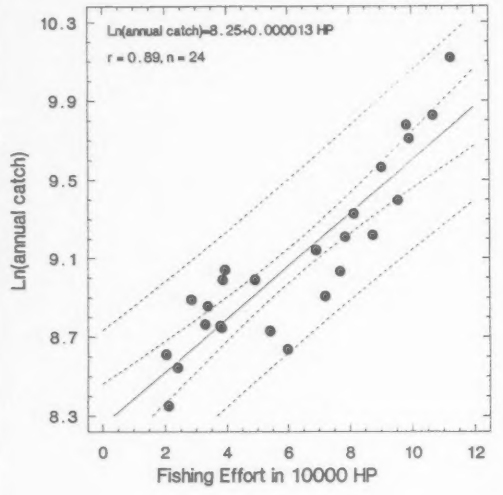

Figure 2
Regression line (solid) and 95% and 99% confidence limits (dotted) of the log annual commercial catch of anchovy and fishing effort in horsepower (HP), in Hellenic waters, 1964–87.

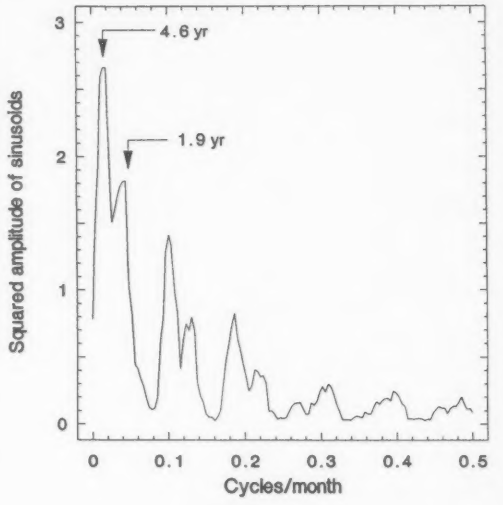

Figure 3
Spectrum of logged/detrended seasonally corrected monthly anchovy catches.

trend in monthly catches [Ln(monthly catch) = 5.38 + 0.0053T, n 288, r 0.38, $p<0.01$, where T = 1–288] is most likely attributed to increased fishing effort.

The spectrum of the resulting series (not shown here), which may be postulated to be free of any annual changes in effort, revealed a large major peak at 12 months (frequency 0.0833). This marked seasonal pattern is most likely related to the seasonal offshore-inshore migrations of anchovy and the nature of the purse-seine fishery (Stergiou 1990a). Purse-seine fishing in Hellenic waters does not occur in the open sea but is mainly restricted to coastal areas where schools of anchovy migrate seasonally. The anchovy starts its inshore migration in early spring, but peak abundance occurs in coastal waters in May–August. Offshore migration probably occurs in late summer–fall.

The smoothed spectrum of the seasonally corrected and detrended series (Fig. 3) reveals a prominent peak at 4.6 years (frequency 0.018) and a probable secondary peak at 1.9 years (frequency 0.043) (95% confidence intervals of the spectrum for 10 df: 0.4882–3.0798 squared amplitude of sinusoids). In contrast, non-sinusoidal periodic variability generates harmonics with periods of less than 1 year (Fig. 3).

Cycles of 2–3 and 4–5 years have also been identified in the air temperature in the northern (Thessaloniki) and western Aegean (Athens) (Table 1) and in different biotic (zooplankton, phytoplankton, fish eggs/larvae, fish) and abiotic variables (air temperature/pressure, sea temperature/salinity) in different areas of the Mediterranean, Black, and Azov Seas (Table 1). These cycles have also been suggested for annual anchovy catches and eggs/larvae, temperature, salinity, and zooplankton in the Adriatic Sea but the data set is limited (annual, 1962–76) and the cycles may not be statistically significant (D. Regner 1985). Correlations have been found between biotic/abiotic variables (primary production, zooplankton biomass, winds, river flow, air/sea temperature, salinity) and various abundance indices of the Mediterranean anchovy (Azov–Black Sea: Dement'eva 1987, Dekhnik and Rass 1988, Porumb and Marinescu 1979; Hellenic waters: Stergiou 1986b; Adriatic Sea: S. Regner 1985; western Mediterranean: Palomera and Lleonart 1989) and other species of *Engraulis* (see Bakun 1985).

Cycles with periods of 2–4 and 4–7 years have also been identified in the physical environment and marine populations in other areas of the world (e.g., Kort 1970, Shuntov et al. 1981, Colebrook and Taylor 1984, Mysak 1986). Such cycles have frequently been related to short-term ocean-atmosphere interactions (e.g., surface heat-exchange phenomena: Zupanovich 1968, Colebrook and Taylor 1984; advection: Kort 1970, Mysak 1986).

A comprehensive discussion of the mechanisms underlying such variability requires adequate biological

Table 1

Cycles identified in the variability of various climatic and biological parameters in the Mediterranean–Black Sea ecosystem. T = type of data (A = annual, M = monthly, D = daily); P = time period of available data; Me = method of analysis of data (sa = spectral analysis, acf = autocorrelation function, cgm = composite graphic method, i.e., comparison of graphs; see Dement'eva 1987).

Variable	Area	T	P	Me	Cycles, in years			Source
Sardine catch*	Adriatic	A	1853–1960	sa	2.3	3–3.5		Zupanovic 1968 Regner and Gacic 1974
Sardine catch	Hellas	M	1964–1982	sa		3.3		Stergiou 1988
Anchovy catch	Hellas	M	1964–1987	sa	1.9	3.3	4.6	This study
Anchovy catch*	Azov Sea	A	1955–1981	cgm	2–3			Dement'eva 1987
Carp catch*	Hellas[a]	A	1947–1983	sa		3–4		Economidis et al. 1988
Perch catch*	Hellas[a]	A	1947–1983	sa		3–4		Economidis et al. 1988
Copepods	Adriatic	M	1970–1974	acf	2–3			D. Regner 1985
Fish larvae	Adriatic	M	1971–1977	acf	3			S. Regner 1982
Fish eggs	Adriatic	M	1970–1974	acf	2–3			D. Regner 1985
Primary production	Adriatic	M	1970–1974	acf	2–3			D. Regner 1985
Diatoms*	Black Sea	A	1954–1987	sa	2.9		4.5	Petrova-Karadjova and Apostolov 1988
Air temp.*	Hellas[b]	A	1892–1981	sa	2.2–2.3		4	Flocas and Giles 1984
Air temp.*	Hellas[c]	A	1859–1981	sa	2.2–2.3		4	Flocas and Giles 1984
Air temp.*	Trieste	A	*	sa	2–2.9		4	Polli 1955
Air pressure*	Trieste	A	*	sa	2.3		4	Polli 1955
Air pressure*	Venice	A	*	sa	2.1–2.8		4	Polli 1955
Sea surface temp.	Adriatic	M	1970–1974	acf	2–3			D. Regner 1985
Sea surface temp.	Monaco	D	1946–1961	sa	1.8		4.4	Bethoux and Ibanez 1979
Sea surface salinity	Adriatic	M	1970–1974	acf	2–3			D. Regner 1985

*Together with cycles of 8–12 years (frequently related to the 11-year cycle in sunspot number, e.g., Gnevyshen and Ol' 1977).
[a] Lake Koronia, [b]Thessaloniki in summer, [c]Athens in summer.

and physical oceanographic information, probably on time scales of a few days and spatial scales of <1km (*sensu* Leggett 1986). This information is not currently available. The distribution and biology of larval, juvenile, and adult anchovy and larval dispersal patterns have not been studied in Hellenic waters. However, some preliminary, conjectural discussion is presented here.

The anchovy spawning season in the eastern Mediterranean extends from April to September with a peak in the summer months (Demir 1965, S. Regner 1985). Anchovy larvae and postlarvae occur in the plankton between May and September with a peak in July–September (S. Regner 1985). This corresponds to the predictable period of the etesians winds. These dry northern, northeastern, and eastern winds blow each year over the Aegean Sea from the end of May until the end of October with a maximum frequency in July–August (Fig. 4; Carapiperis 1962, Mariopoulos 1961). Since anchovy spawning in the eastern Mediterranean does not seem to be affected by abiotic factors such as temperature or salinity (Demir 1965, S. Regner 1985), the summer spawning habit of anchovy may represent an important adaptation to the highly oligotrophic conditions of the stratified coastal Aegean waters in summer. By spawning in summer, anchovy larvae (1) do not compete with sardine larvae which occur in the plankton mainly in winter and spring (Yannopoulos 1977, Daoulas and Economou 1986, Regner et al. 1987), and (2) are released in a relatively food-rich environment due to the effect of the etesians winds. The increased frequency and intensity of the etesians winds

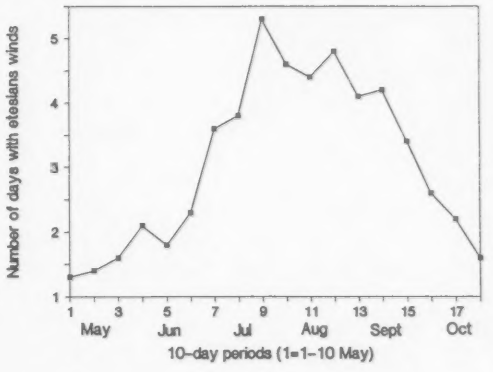

Figure 4

Mean number of days with etesians winds in Athens for May–October, 1893–1960 (data from Carapiperis 1962).

over the Aegean Sea in July–August when they frequently reach gale force (Carapiperis 1962) would probably deepen the mixed layer, and hence entrain nutrient-rich water from below the thermocline. Mullin et al. (1985) have shown that microzooplankton biomass and chlorophyll *a* levels can be doubled after wind-related events. In addition, an increase in the frequency and intensity of etesians winds may also result in an intensification of upwelling in the northern, northeastern, and eastern part of the Aegean Sea (Metaxas 1973, Theocharis et al. 1988). Hence, periods dominated by higher-than-average frequency of etesians in July–August may be associated with favorable feeding conditions for anchovy larvae which may be subject to lesser mortalities through starvation and predation, the main factors affecting larval mortality in Mediterranean anchovy (Azov–Black Sea: see Dekhnik and Rass 1988 for a review; Adriatic Sea: see S. Regner 1985 for a review; western Mediterranean: Palomera and Lleonart 1989).

Other factors may also affect variability in the anchovy abundance. For example, climatically-mediated long-term changes in production and plankton species composition in the eastern Mediterranean, changes in larval dispersion due to changing patterns of currents, as well as other factors, intrinsic or extrinsic, may affect the egg/larval/postlarval/juvenile phases. It has been maintained that in periods of increased air pressure gradient over the eastern Mediterranean, the water exchange between its basins intensifies (Pucher-Petkovic et al. 1971, Vucetic 1981). As a result, the salinity, nutrient content, temperature, and primary productivity of the Adriatic Sea and of the eastern Mediterranean basin rise, and the species composition of the phytoplankton community changes. These changes were accompanied by changes in the total biomass of small pelagic fish (sardine, anchovy, horse mackerel, etc). Such climate-plankton-small pelagic fish interactions in the eastern Mediterranean involve time lags of 2–3 years (Pucher-Petkovic et al. 1971). Lastly, cycles in anchovy catches may also be the result of social-economic factors (Stergiou 1991) and/or a change in the anchovy availability to purse seiners (changes in the distribution and/or density of schools as a response to changes in atmospheric and/or marine climatic patterns) rather than to changes in the abundance of anchovy itself.

Incorporation into management schemes of these cycles in abundance (e.g., Taylor and Prochaska 1984) is particularly important for anchovy and other small pelagic fish which are prone to collapse under intense fishing pressure and poor recruitment.

Acknowledgments

The author wishes to thank two anonymous reviewers for their constructive criticisms.

Citations

Bakun, A.
1985 Comparative studies and the recruitment problem: Searching for generalizations. Calif. Coop. Oceanic Fish. Invest. Rep. 26:30–40.

Bethoux, N., and F. Ibanez
1979 Analyse temporelle de la temperature de surface de la mer dans la baie de Monaco: Relation avec la temperature de l'air. Rapp. Comm. Int. Mer Medit. 25/26:47–49.

Carapiperis, L.N.
1962 The etesian winds II. On the frequency of the etesian winds. Notes, Natl. Observatory of Athens, Greece, Ser. II, Meteorologia 10:1–16 [Engl.].

Chatfield, C.
1984 The analysis of time series: An introduction. Chapman and Hall, NY.

Colebrook, J.M., and A.H. Taylor
1984 Significant time scales of long-term variability in the plankton and the environment. Rapp. P.-V. Reun. Cons. Int. Explor. Mer 183:20–26.

Daoulas, Ch., and A.N. Economou
1986 Seasonal variation of egg size in the sardine, *Sardina pilchardus* Walb., of the Saronikos Gulf: Causes and a probable explanation. J. Fish Biol. 28:449–457.

Dekhnik, T.V., and T.S. Rass
1988 Main aspects of the study on icthyoplankton. J. Ichthyol. 28:51–57.

Dement'eva, T.F.
1987 A method for correlation of environmental factors and year-class strength of fishes. J. Ichthyol. 27:55–59.

Demir, N.
1965 Synopsis of biological data on anchovy, *Engraulis encrasicolus*, (Linnaeus) 1758 (Mediterranean and adjacent seas). FAO Fish. Synop. 26, Rev. 1, 48 p.

Flocas, A.A., and B.D. Giles
1984 Air temperature variations in Greece. Pt. 2. Spectral analysis. J. Climatol. 4:541–546.

Economidis, P.S., A. Sinis, and G.P. Stamou
1988 Spectral analysis of exploited fish populations in lake Koronia (Macedonia, Greece) during the years 1947–1983. Cybium 12:151–159.

Gnevyshen, M.N., and A.I. Ol' (editors)
1977 Effects of solar activity on the earth's atmosphere and biosphere. Israel Prog. Sci. Transl., Jerusalem, 290 p.

Hellenic National Statistical Service
1968–1989 Results of the sea fishery survey by motor vessels. Sect. G, 20 issues (for years 1964–1987), Athens, Hellas.

Kort, V.G.
1970 Large-scale interaction between the ocean and the atmosphere using the North Pacific as an example. Oceanology 10:171–183.

Leggett, W.C.
1986 The dependence of fish larval survival on food and predator densities. *In* Skreslet, S. (ed.), The role of freshwater outflow in coastal marine ecosystems. NATO ASI Ser. G7: 117–137.

Mariopoulos, E.G.
1961 An outline of the climate of Greece. Publ. Meteor. Inst. Univ. Athens (Greece) 6:1–51 [Engl.].

Metaxas, D.A.
1973 Air-sea interaction in the Greek seas and resulted etesian wind characteristics. Tech. Rep. 5, Univ. Ioannina, Greece, School of Physics and Math., p. 1–32 [Engl.].

Mullin, M.M., E.R. Brooks, F.M.H. Reid, J. Napp, and E.F. Stewart
1985 Vertical structure of nearshore plankton off southern California: A storm and a larval fish food web. Fish. Bull., U.S. 83:151–167.

Mysak, L.A.
1986 El Niño, interannual variability and fisheries in the northwest Pacific Ocean. Can. J. Fish. Aquat. Sci. 43:464–497.

Palomera, I., and J. Lleonart
1989 Field mortality estimates of anchovy larvae, *Engraulis encrasicolus*, in the western Mediterranean. J. Fish. Biol. 35 (Suppl.):133–138.

Petrova-Karadjova, V.J., and E.M. Apostolov
1988 Influence of solar activity upon the diatoms of Black Sea plankton. Rapp. Comm. Int. Mer Medit. 31:224.

Polli, S.
1955 I cicli climatici di 5.6 e 8 anni e la loro realta' fisca. Riv. Meteor. Aueronaut. 2:1–12 [not seen, from Regner and Gacic 1974].

Porumb, I.I., and F. Marinescu
1979 Influence du facteur nourriture sur la formation des agglomerations d'anchois dans la zone neritique roumaine de la Mer Noire. Rapp. Comm. Int. Mer Medit. 25/26:47–48.

Pucher-Petkovic, T., M. Zore-Armanda, and I. Kacic
1971 Primary and secondary production of the Middle Adriatic in relation to climatic factors. Thallasia Jugosl. 7:301–311.

Regner, D.
1985 Seasonal and multiannual dynamics of copepods in the middle Adriatic Sea. Acta Adriat. 26:11–99.

Regner, S.
1982 Investigations of qualitative and quantitative composition of the larval fish stages in the plankton at the high sea of the central Adriatic. Stud. Mar. Fauna 11/12:45–60.
1985 Ecology of planktonic stages of anchovy, *Engraulis encrasicolus* (Linnaus, 1758), in the central Adriatic. Acta Adriat. 26:5–113.

Regner, S., and J. Gacic
1974 The fluctuation of sardine catch along the eastern Adriatic coast and solar activity. Acta Adriat. 15:1–15.

Regner, S., D. Regner, I. Marasovic, and F. Krsinic
1987 Spawning of sardine, *Sardina pilchardus* (Walbaum, 1792), in the Adriatic under upwelling conditions. Acta Adriat. 28:161–198.

Shuntov, B.P., N.A. Shurunov, and V.P. Vasil'kov
1981 Periodicity in the reproduction of fish from the New Zealand plateau based on data from commercial statistics. J. Ichthyol. 22:32–43.

Soutar, A., and J.D. Isaacs
1974 Abundance of pelagic fish during the 19th and 20th centuries as recorded in anaerobic sediments off California. Fish. Bull., U.S. 72:257–275.

Spanakis, E., N. Tsimenidis, and E. Zouros
1989 Genetic differences between populations of sardine, *Sardina pilchardus*, and anchovy, *Engraulis encrasicolus*, in the Aegean and Ionian seas. J. Fish. Biol. 35:417–437.

Stergiou, K.I.
1986a On the anchovy and sardine fishery in Greek waters, 1964–1982. Rapp. Comm. Int. Mer Medit. 30:241.
1986b Pre-war changes in the abundance of *Pagellus erythrinus*, *Merluccius merluccius*, and *Engraulis encrasicolus* in Greek waters and climatic change. FAO Fish. Rep. 361: 99–105.
1988 Spectral analysis of sardine fishery in Greek waters, 1964–1982. Rapp. Comm. Int. Explor. Mer Medit. 31:282.
1990a An autoregressive model of the anchovy *Engraulis encrasicolus* fishery in the eastern Mediterranean. Fish. Bull., U.S. 88:411–414.
1990b On the Greek fishery production. Greek Fish. News. 103:31–38 [in Greek].
1991 Describing and forecasting the sardine-anchovy complex in the eastern Mediterranean using vector autoregressions. Fish. Res. (Amst.) 11:127–141.

Taylor, G.T., and F.J. Prochaska
1984 Incorporating unobserved cyclical stock movements in fishery catch equations: An application to the Florida blue crab fishery. N. Am. J. Fish. Manage. 4:67–74.

Theocharis, A., D. Georgopoulos, Y. Krestenitis, and C. Koutitas
1988 Observations and modelling of upwelling in the Aegean Sea. Rapp. Comm. Int. Mer Medit. 31:212.

Vucetic, T.
1981 Biological production of the Adriatic plankton. FAO Fish. Rep. 253:65–71.

Yannopoulos, C.
1977 The reproduction and the egg size variations of *Sardina pilchardus* Walb. in the Thermaikos Gulf, Aegean Sea. Rapp. Comm. Int. Mer Medit. 24:73–75.

Zupanovic, S.
1968 Causes of fluctuations in sardine catches along the eastern coast of the Adriatic Sea. Anali Jandranskog Inst. 4:401–489.

Superintendent of Documents **Subscriptions** Order Form

Order Processing Code:
* 5178

☐ **YES,** enter my subscription as follows:

Charge your order. It's Easy! MasterCard VISA

To fax your orders (202) 512–2233

____ subscriptions to **FISHERY BULLETIN (FB)** for $24.00 per year ($30.00 foreign).

The total cost of my order is $_____. Price includes regular domestic postage and handling and is subject to change.

(Company or Personal Name) (Please type or print)

(Additional address/attention line)

(Street address)

(City, State, ZIP Code)

(Daytime phone including area code)

(Purchase Order No.)

May we make your name/address available to other mailers? YES ☐ NO ☐

Please Choose Method of Payment:

☐ Check Payable to the Superintendent of Documents

☐ GPO Deposit Account ☐☐☐☐☐☐-☐

☐ VISA or MasterCard Account

☐☐☐☐☐☐☐☐☐☐☐☐☐☐☐☐

☐☐☐☐ (Credit card expiration date)

Thank you for your order!

(Authorizing Signature) 11/91

Mail To: New Orders, Superintendent of Documents
P.O. Box 371954, Pittsburgh, PA 15250–7954

The National Marine Fisheries Service (NMFS) does not approve, recommend or endorse any proprietary product or proprietary material mentioned in this publication. No reference shall be made to NMFS, or to this publication furnished by NMFS, in any advertising or sales promotion which would indicate or imply that NMFS approves, recommends or endorses any proprietary product or proprietary material mentioned herein, or which has as its purpose an intent to cause directly or indirectly the advertised product to be used or purchased because of this NMFS publication.

Fishery Bulletin

Guidelines for Contributors

Form of manuscript

The document should be in the following sequence: Title Page, Abstract (not required for Note), Text, Acknowledgments, Citations, Text footnotes, Appendices, Tables, Figure legends, and Figures.

Title page should include authors' full names and mailing addresses and the senior author's telephone and FAX numbers.

Abstract Not to exceed one double-spaced typed page. Should include a sentence or two explaining to the general reader why the research was undertaken and why the results should be viewed as important. Abstract should convey the main point of the paper and outline the results or conclusions. No footnotes or references.

Text A brief introduction should portray the broad significance of the paper. The entire text should be intelligible to readers from different disciplines. All technical terms should be defined, as well as all abbreviations, acronyms, and symbols in text, equations, or formulae. Abbreviate units of measure only when used with numerals or in tables and figures to conserve space. Measurements should be expressed in metric units, with other equivalent units given in parentheses. Follow the *U.S. Government Printing Office Style Manual*, 1984 ed., and the *CBE Style Manual*, 5th ed. Fishery and invertebrate nomenclature should follow the *American Fisheries Society Special Publication 12* (for fishes), *16* (for mollusks), and *17* (for decapod crustaceans).

Text footnotes should be numbered in Arabic numerals and typed on a separate sheet from the text. Footnotes are not used for reference material or personal communications, but rather to explain or define terms in the text and for contribution numbers on the title page.

Informal sources Personal communications, unpublished data, and untitled manuscripts in preparation are noted parenthetically in the text (full name, affiliation, brief address including zip code, and month and year when appropriate).

Acknowledgments Gather all acknowledgments into a brief statement at the end of the text. Give credit only for exceptional contributions and not to those whose contributions are part of their normal duties.

Citations All titled sources should be listed in the Citations section, including unpublished and processed material. In text, cite as Smith and Jones (1977) or (Smith and Jones 1977); if more than one citation, list chronologically (Smith 1936, Jones 1975, Doe In press). All sources cited in the text should be listed alphabetically by the senior authors' surnames under the heading CITATIONS. Abbreviations of periodicals and serials should conform to *Serial Sources for the BIOSIS Data Base*™. Indicate whether sources are in a language other than English. For informal literature, include address of author or publisher. Authors are responsible for the accuracy of all citations.

Tables should supplement, not duplicate, the text. Each table should be numbered and cited consecutively, with headings short but amply descriptive so that the reader need not refer to the text. For values less than one, zeros should precede all decimal points. Indicate units of measure in column headings; do not deviate from the unit of measure within a column. Table footnotes should be noted consecutively in Roman letters across the page from left to right and then down. Since all tables are typeset, they need not be submitted camera-ready.

Figures Photographs and line drawings should be of professional quality—clear and concise—and reducible to 42 picas for full-page width or to 20 picas for a single-column width, and to a maximum 55 picas high. All graphic elements in illustrations must be proportioned to insure legibility when reduced to fit the page format. Line weight and lettering should be sharp and even. Lettering should be upper and lower case, and vertical lettering should be avoided whenever possible (except for vertical, y, axis). Zeros should precede all decimal points for values less than one. Reproductions of line artwork are accepted in the form of high-quality photographic prints from negatives or photomechanical transfer (PMT). Halftones should be sharply focused with good contrast. Micron rules should be inserted on electron micrographs, even when magnification is included in the figure legend. There should be clear distinction between identifying letters (press-on or overlay) and background of photograph. Label each figure in pencil on the back. Send only xerox copies of figures to the Scientific Editor; originals or photographic prints will be requested later when the manuscript is accepted for publication.

Copyright Government publications are in the public domain, i.e., they are not protected by copyright.

Submission of manuscript

Disks Authors are encouraged to retain manuscripts on word-processing storage media (diskettes, floppy disks) and submit a double-spaced hardcopy run from the storage media. Submit disks as MS-DOS "print" or "nondocument" files (often called "ASCII files"). If a disk cannot be converted to an ASCII file, the author should indicate on the disk the source computer and software language along with the file name. Either 5¼-inch or 3½-inch disks from IBM-compatible or Apple/MacIntosh systems (non-graphics only) can be submitted, double-sided/double-density or high-density, limiting each file to 300 kilobytes. All 8-inch word-processing disks (e.g., Wang or NBI) must be converted onto 5¼- or 3½-inch MS-DOS print disks.

Send original hardcopy and two duplicated copies to:

Dr. Linda L. Jones, Scientific Editor
National Marine Mammal Laboratory
F/AKC3
National Marine Fisheries Service,
NOAA
7600 Sand Point Way NE
Seattle, WA 98115-0070
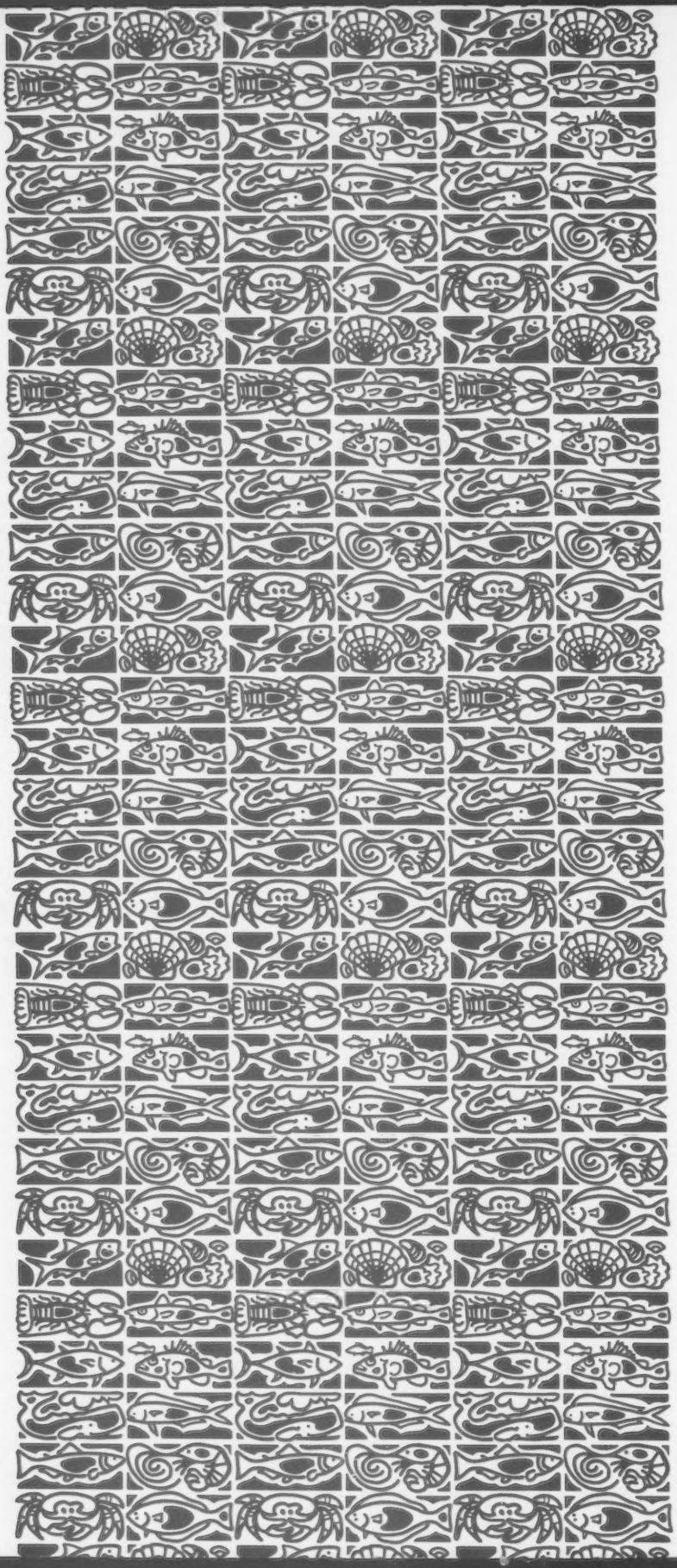
Copies of published articles and notes
The senior author and his/her organization each receive 50 separates free-of-charge. Additional copies may be purchased in lots of 100.